NASA/CR–20210017185

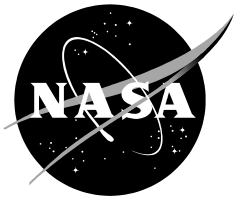

Reliability and Safety Assessment of Urban Air Mobility Concept Vehicles

Cedric Justin, Srujal Patel, Etienne Demers Bouchard, Jonathan Gladin, Johannes Verberne, Eddie Li, Metin Ozcan, Dushhyanth Rajaram, and Dimitri Mavris
Aerospace System Design Laboratory, School of Aerospace Engineer, Georgia Institute of Technology, Atlanta, Georgia

Matilde D'Arpino, Tunc Aldemir, Giorgio Rizzoni, Gülçin Sarıcı Türkmen
Ohio State University, Columbus, Ohio

Michael Mayo, Court Bivens
Aerospace, Transportation and Advanced Systems Lab, Georgia Tech Research Institute, Atlanta, Georgia

Prepared for:
Technical Monitor: Curtis Hanson
NASA Armstrong Flight Research Center

Contract Officer: Robert Kufeld
NASA Ames Research Center

Under Contract No. 80ARC020F0055

March 2021

NASA STI Program Report Series

The NASA STI Program collects, organizes, provides for archiving, and disseminates NASA's STI. The NASA STI program provides access to the NTRS Registered and its public interface, the NASA Technical Reports Server, thus providing one of the largest collections of aeronautical and space science STI in the world. Results are published in both non-NASA channels and by NASA in the NASA STI Report Series, which includes the following report types:

- TECHNICAL PUBLICATION. Reports of completed research or a major significant phase of research that present the results of NASA Programs and include extensive data or theoretical analysis. Includes compilations of significant scientific and technical data and information deemed to be of continuing reference value. NASA counter-part of peer-reviewed formal professional papers but has less stringent limitations on manuscript length and extent of graphic presentations.

- TECHNICAL MEMORANDUM. Scientific and technical findings that are preliminary or of specialized interest, e.g., quick release reports, working papers, and bibliographies that contain minimal annotation. Does not contain extensive analysis.

- CONTRACTOR REPORT. Scientific and technical findings by NASA-sponsored contractors and grantees.

- CONFERENCE PUBLICATION. Collected papers from scientific and technical conferences, symposia, seminars, or other meetings sponsored or co-sponsored by NASA.

- SPECIAL PUBLICATION. Scientific, technical, or historical information from NASA programs, projects, and missions, often concerned with subjects having substantial public interest.

- TECHNICAL TRANSLATION. English-language translations of foreign scientific and technical material pertinent to NASA's mission.

Specialized services also include organizing and publishing research results, distributing specialized research announcements and feeds, providing information desk and personal search support, and enabling data exchange services.

For more information about the NASA STI program, see the following:

- Access the NASA STI program home page at http://www.sti.nasa.gov

- Help desk contact information:

https://www.sti.nasa.gov/sti-contact-form/ and select the "General" help request type.

NASA/CR–20210017185

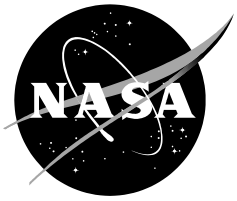

Reliability and Safety Assessment of Urban Air Mobility Concept Vehicles

Cedric Justin, Srujal Patel, Etienne Demers Bouchard, Jonathan Gladin, Johannes Verberne, Eddie Li, Metin Ozcan, Dushhyanth Rajaram, and Dimitri Mavris
Aerospace System Design Laboratory, School of Aerospace Engineer, Georgia Institute of Technology, Atlanta, Georgia

Matilde D'Arpino, Tunc Aldemir, Giorgio Rizzoni, Gülçin Sarıcı Türkmen
The Ohio State University, Columbus, Ohio

Michael Mayo, Court Bivens
Aerospace, Transportation and Advanced Systems Lab, Georgia Tech Research Institute, Atlanta, Georgia

Prepared for:
Technical Monitor: Curtis Hanson
NASA Armstrong Flight Research Center

Contract Officer: Robert Kufeld
NASA Ames Research Center

Under Contract No. 80ARC020F0055

National Aeronautics and
Space Administration

Ames Research Center
Moffett Field, California 94035-1000

March 2021

Available from:

NASA STI Support Services
Mail Stop 148
NASA Langley Research Center
Hampton, VA 23681-2199
757-864-9658

National Technical Information Service
5301 Shawnee Road
Alexandria, VA 22312
webmail@ntis.gov
703-605-6000

This report is also available in electronic form at

http://ntrs.nasa.gov

This page intentionally left blank.

Revision Record

Revision	Date	Revised by	Description
2	12th April 2021	C. Justin	Initial Release

ABSTRACT

The primary objective of this research effort is to identify failure modes and hazards associated with several configurations of multicopter concept vehicles supplied by NASA. Functional hazard analyses (FHA) and failure modes and effects criticality analyses (FMECA) are performed for each of the eight vehicle configurations under review. Conceptual design of notional powertrain configurations (turboshaft, electric, hybrid electric), notional thrust control systems (rpm control and collective control), and navigation control systems for the concept vehicles were to support the reliability and safety analysis and to assess whether a mission can be completed safely. Two kinds of analyses are performed: static safety analysis which enable the quantification of the likelihood of individual events, and dynamic safety analyses which allows the investigation of multiple time-dependent failures. Their objective is to quantify the likelihood of catastrophic failures.

Table of Contents

1 Introduction 15
1.1 Background 15
1.2 Research Objectives 17
1.3 Vehicle Configurations 19
1.3.1 Quadrotor Vehicles 20
1.3.2 Hexacopter Vehicle 21
1.3.3 Octocopter Vehicle 23
1.4 Mission Description 23

2 Methodology and Common Assumptions 25
2.1 Overall safety assessment approach 25
2.2 Probability Calculations 28
2.2.1 Hazard Classification 28
2.2.2 One Engine Inoperative (OEI) Condition 29
2.2.3 DET Scenario Design 29
2.3 Configuration Assumptions 32
2.3.1 Electric drive and energy storage system assumptions 32
2.3.2 Vehicle modeling and control assumptions 34
2.3.3 Safety analysis assumptions 34
2.4 Modeling environment 40
2.5 Component/System Reliability 42
2.5.1 Components and Component Failure Rates (FR) 42
2.5.2 System Reliability Assessment 43
2.5.2.1 Electric drive (ED) system 44
2.5.2.2 Rotor actuation system (ACT) failures 45
2.5.2.3 Transmission system (TS) failures 45
2.5.2.4 Gas turbine engine (GTE) and Generator (GEN) failures 46
2.5.3 Failure rate model of electric components 47

3 Vehicle Architecture overview 49
3.1 Electric Quadcopter 49
3.2 Hybrid Electric Quadcopter 51
3.3 Turboshaft Quadcopter 52
3.4 Hexacopter with Collective Control 54
3.5 Hexacopter with RPM Control 55
3.6 Octocopter 56

4 Vehicle and system Modeling 57
4.1 Airframe dynamics 57
4.1.1 Review of NASA Linear Dynamics Model 57
4.1.1.1 States 60
4.1.2 Mission 61
4.1.3 Reduced Order Dynamic Model 61
4.1.4 Modification of the linear models for OEI purposes 61

4.1.4.1 Conversion to individual rotor collective pitch 62
4.1.4.2 Limit on Inoperative Rotor RPM 62
4.1.4.3 Rotor inoperative and Pitch Control Allocation 63
4.1.5 Assessment of Airframe Characteristics 63
4.1.5.1 Trim 63
4.1.5.2 Observations on Trim Results with One Motor Inoperative 64
4.1.6 Wind Model 65
4.2 Powertrain 65
4.2.1 Electric Drive Modeling 65
4.2.1.1 Electric motor model 66
4.2.1.2 Electronic speed controller model 66
4.2.1.3 Battery Pack model 67
4.2.1.4 Thermal Management System model 67
4.2.1.5 Model calibration 68
4.2.2 Powertrain Control 70
4.2.3 Transmission Modeling 72
4.2.4 Turboshaft Transient Model 73
4.2.4.1 Quadrotor with Turboshaft – Implementation 74
4.2.4.2 Hybrid Electric Quadrotor – Implementation 74
4.3 Guidance and Navigation 74
4.3.1 Accelerating/Decelerating from/to Hover 76
4.3.2 Emergency Landing Maneuver 77
4.4 Flight Control Architecture 78
4.4.1 Variable Pitch Vehicle LQI 79
4.4.2 Variable RPM Vehicle LQI 80
4.4.3 One Motor Inoperative (OMI) LQI 81
4.5 Fault models 83
4.5.1 Electric Powertrain modeling 83
4.5.2 Transmission Faults 85
4.5.3 Actuator Faults 85
4.5.4 Turboshaft Engine Faults 85
4.5.5 Turbine-generator Faults 85
4.6 Vehicle Performance Verification 86

5 Results 87
5.1 Static Safety and Reliability Assessment Results 87
5.1.1 Functional Hazard Analysis (FHA) 87
5.1.2 Failure Modes, Effects and Criticality Analysis (FMECA) 87
5.1.3 Fault Tree Analysis (FTA) 87
5.1.4 Reliability impact of Turbine-Generator Interface Design Choice: Direct-drive versus Gearbox 90
5.1.5 Reliability comparison between Cross-shafting System and Redundant Motors 90
5.1.6 Reliability Comparison between Additional Rotors and Redundant Motors 92
5.2 Dynamic Safety and Reliability Assessment Results 95
5.2.1 Overall Architecture Comparison using DET Analysis 95
5.2.2 Impact of power profile and duty cycle on motor reliability 100
Impact of Control Strategy 101

Impact of Number of Rotors 102
5.2.3 Impact of battery sizing on Hybrid Quadcopter Reliability 103
Nominal Operation: No use of the battery 104
Battery Use to Supplement Turbogenerator 105
Observations 107
Alternative Operating Modes 108
5.2.4 Impacts of voltage and current levels on reliability (C2, A6, B5) 110
5.2.5 Impacts of liquid cooled vs. air cooled motors and motor controllers (C5, A7, B6) 116
5.2.6 Impact on reliability associated with repeated overcharging and excessive discharging, repeated high-rate discharging on battery (C7, A8, B7) 119
5.2.7 Impact of sensor placement and redundancy (B4, A4) 121

6 conclusions and Recommendations for future work 124
6.1 Comparison of architectures 124
6.2 Possible extensions for future work 125

7 References 128

Meet the Authors 135

List of Figures

Figure 1: Wheel of fortune for e-vtol vehicle concepts [7] 16
Figure 2: Quadcopter electric vehicle 20
Figure 3: Quadcopter hybrid vehicle 20
Figure 4: Quadcopter turboshaft vehicle 21
Figure 5: Hexacopter Variable Pitch Vehicle 22
Figure 6: Hexacopter variable RPM vehicle 22
Figure 7: Octocopter vehicle 23
Figure 8: NDARC UAM Design Mission 24
Figure 9: Overview of the Technical Approach 25
Figure 10: An example DET with branching probabilities quantified by FTs 27
Figure 11: Mission schematic with the failure injection points 30
Figure 12: DET faults grouped by the subsystems 31
Figure 13: An example of the DET execution in a two-fault injection scenario 32
Figure 14: Quad-Hybrid emergency landing maneuver 38
Figure 15: Reliability/Safety Assessment Workflow 41
Figure 16: DET analysis info chart 41
Figure 17: Overview of the Systems and Components considered in the Safety Analysis 42
Figure 18: Example of failure rate model of electric motor and electronic speed controller 47
Figure 19 Rotating components diagram for the electric quadrotor concept with collective control 50
Figure 20 Flight control system diagram for the electric quadrotor concept with collective control 50
Figure 21 Rotating components diagram for the series-hybrid quadrotor concept with collective control 51
Figure 22 Flight control system diagram for the series-hybrid quadrotor concept with collective control 52
Figure 23 Rotating components diagram for the turboshaft quadrotor concept with collective control 53
Figure 24 Flight control system diagram for the turboshaft quadrotor concept with collective control 53
Figure 25 Rotating component diagram for the hexacopter concept with collective control 54
Figure 26 Flight control system diagram for the hexacopter concept with collective control 54
Figure 27 Rotating component diagram for the hexacopter concept with RPM control 55
Figure 28 Flight control system diagram for the hexacopter concept with RPM control 55
Figure 29 Rotating component diagram for the octocopter concept with RPM control 56
Figure 30 Flight control system diagram for the octocopter concept with RPM control 56
Figure 31 Schematic Representation of the Dynamic Simulation Environment 57
Figure 32 Schematic representation of the airframe dynamics 58
Figure 33 Translational and angular velocity definition in the vehicle body frame 59
Figure 34 Quadcopter Vehicles Motor Definition and Rotor Spin Direction 59
Figure 35 Hexacopter Vehicles Motor Definition and Rotor Spin Direction 60
Figure 36 Octocopter Vehicles Motor Definition and Rotor Spin Direction 60
Figure 37 Limit on Inoperative Rotor RPM 62
Figure 38 Wind gust example 65
Figure 39 Block Diagram of the Dynamic Model of the electric propulsion system 66
Figure 40 Example of electric motor efficiency map 70
Figure 41 Speed Control Loop 70
Figure 42 Inner Loop: Current Control Loop 70
Figure 43 Master-Follower Approach 71
Figure 44 Master assignment when motor 1 has a malfunction. 71

Figure 45 Master control assignment after isolation of motor *n* 72
Figure 46 Reference Frame Definition 75
Figure 47 Guidance and Navigation Module 75
Figure 48 Guidance and Navigation Model algorithm 76
Figure 49: Waypoint hover algorithm 77
Figure 50 Acceleration Algorithm 77
Figure 51: Emergency Landing Maneuver Algorithm 78
Figure 52 LQI Control Architecture Applied to Variable Pitch Vehicle 80
Figure 53 LQI Control Architecture Applied to Variable RPM Vehicle 81
Figure 54: Block Diagram of the Dynamic Model of the electric propulsion system including fault injection points. 83
Figure 55 Electric Drive fault modes applied at $\boldsymbol{t = 2s}$ 85
Figure 56: Fault Tree of a Single Rotor with dual electric motors (Quadcopter with No Cross-Shafting) .. 91
Figure 57: Top level fault tree of the dual-motor quadcopter design. 92
Figure 58: Fault tree for a rotor in the dual-motor Hexacopter design. 93
Figure 59: Top level fault tree of the dual-motor Hexacopter design. 93
Figure 60 Hexacopter collective Low Torque (SL1) Motor 1 Torque Balance (LEFT) and Hexacopter collective Low Torque (SL3) Motor 1 Torque Balance (RIGHT) 98
Figure 61 Hexacopter collective Low Torque (SL1) Motor RPM (LEFT) and Hexacopter collective Low Torque (SL3) Motor RPM (RIGHT) 98
Figure 62 Sum of power required by the 4 electric rotors as a function of time for the hybrid aircraft . 104
Figure 63: Power output of the turbogenerator as a function of time 105
Figure 64: RPM of the high pressure and low pressure spools of the turbogenerator (left) and expanded view of the high pressure spool transient behavior during climb (right) 105
Figure 65 Power schedule from the turbogenerator as a function of time 106
Figure 66: RPM of the high pressure and low pressure spools of the turbogenerator (left) and expanded view of the high pressure spool transient behavior during climb (right) 106
Figure 67: Scheduled power from the turbogenerator 107
Figure 68: Battery usage throughout mission showing peak voltage, depth of discharge, and C-rate 107
Figure 69 Alternative operating mode of the hybrid system: include a maximum value for the turbogenerator 109
Figure 70 Temperature profile of EM and ESC considering air and liquid cooling 119
Figure 71: Roots of the linear dynamic model of the electric quadrotor in hover in the complex plane: complete dynamic system (circles) and reduced order model (asterix). On the right is a “zoom” on the origin of the complex plane where some of the roots are present. 312
Figure 72 Power to operate with rotor 1 inoperative compared to nominal power 316
Figure 73 Power to operate with rotor 1 inoperative compared to nominal power 319
Figure 74 Rotor angular velocity for the hexacopter with rpm control to trim with rotor 1 inoperative 319
Figure 75 Power to operate with rotor 1 inoperative compared to nominal power 322
Figure 76 Rotor angular velocity for the octocopter with rpm control to trim with rotor 1 inoperative 322
Figure 77 Quad Electric Nominal Translational Velocity Profile (LEFT) and Translational Displacement Profile (RIGHT) 324
Figure 78 Quad Electric Nominal Angular Velocity Profile (LEFT) and Angular Displacement Profile (RIGHT) 325
Figure 79 Quad Electric Nominal Rotor Angular Velocity (LEFT) and Electric Machine Power Profile (RIGHT) 325
Figure 80 Quad Electric Heat Map (LEFT) and Battery Profile (RIGHT) 326

Figure 81 Quad with Turboshaft Nominal Translational Velocity Profile (LEFT) and Translational Displacement Profile (RIGHT) 327
Figure 82 Quad with Turboshaft Nominal Angular Velocity Profile (LEFT) and Angular Displacement Profile (RIGHT) 327
Figure 83 Quad with Turboshaft Turbine Power Output (LEFT) and Turbine Spool Speeds (RIGHT) 328
Figure 84 Quad Hybrid Nominal Translational Velocity Profile (LEFT) and Translational Displacement Profile (RIGHT) 328
Figure 85 Quad Hybrid Nominal Angular Velocity Profile (LEFT) and Angular Displacement Profile (RIGHT) 329
Figure 86 Turbine power output 329
Figure 87 Quad Hybrid Nominal Rotor Angular Velocity (LEFT) and Electric Machine Power Profile (RIGHT) 330
Figure 88 Quad Hybrid Heat Map (LEFT) and Battery Profile (RIGHT) 330
Figure 89 Hexacopter Variable Pitch Nominal Translational Velocity Profile (LEFT) and Translational Displacement Profile (RIGHT) 331
Figure 90 Hexacopter Variable Pitch Angular Velocity Profile (LEFT) and Angular Displacement Profile (RIGHT) 331
Figure 91 Hexacopter Variable Pitch Nominal Rotor Angular Velocity (LEFT) and Electric Machine Power Profile (RIGHT) 332
Figure 92 Hexacopter Variable Pitch Heat Map (LEFT) and Battery Profile (RIGHT) 332
Figure 93 Hexacopter Variable RPM Nominal Translational Velocity Profile (LEFT) and Translational Displacement Profile (RIGHT) 333
Figure 94 Hexacopter Variable RPM Angular Velocity Profile (LEFT) and Angular Displacement Profile (RIGHT) 333
Figure 95 Hexacopter Variable RPM Nominal Rotor Angular Velocity (LEFT) and Electric Machine Power Profile (RIGHT) 334
Figure 96 Hexacopter Variable RPM Heat Map (LEFT) and Battery Profile (RIGHT) 334
Figure 97 Octocopter Variable RPM Nominal Translational Velocity Profile (LEFT) and Translational Displacement Profile (RIGHT) 335
Figure 98 Octocopter Variable RPM Angular Velocity Profile (LEFT) and Angular Displacement Profile (RIGHT) 335
Figure 99 Octocopter Variable RPM Nominal Rotor Angular Velocity (LEFT) and Electric Machine Power Profile (RIGHT) 336
Figure 100 Octocopter Variable RPM Heat Map (LEFT) and Battery Profile (RIGHT) 336
Figure 101 Quad Electric Emergency Maneuver Translational Velocity Profile (LEFT) and Translational Displacement Profile (RIGHT) 338
Figure 102 Quad Electric Emergency Maneuver Angular Velocity Profile (LEFT) and Angular Displacement Profile (RIGHT) 338
Figure 103 Quad Electric Emergency Maneuver Rotor Angular Velocity (LEFT) and Electric Machine Power Profile (RIGHT) 339
Figure 104 Quad Electric Emergency Maneuver Heat Map (LEFT) and Battery Profile (RIGHT) 339
Figure 105 Quadrotor Electric OMI Translational Velocity Profile (LEFT) and Translational Displacement Profile (RIGHT) 341
Figure 106 Quad Electric OMI Angular Velocity Profile (LEFT) and Angular Displacement Profile (RIGHT) 341
Figure 107 Quad Electric OMI Rotor Angular Velocity (LEFT) and Electric Machine Power Profile (RIGHT) 342
Figure 108 Quad Electric OMI Heat Map (LEFT) and Battery Profile (RIGHT) 342

Figure 109 Spool dynamics after engine fault at t=200s 343
Figure 110 Hexacopter Variable Pitch OMI Translational Velocity Profile (LEFT) and Translational Displacement Profile (RIGHT) 344
Figure 111 Hexacopter Variable Pitch OMI Angular Velocity Profile (LEFT) and Angular Displacement Profile (RIGHT) 344
Figure 112 Hexacopter Variable Pitch OMI Rotor Angular Velocity (LEFT) and Electric Machine Power Profile (RIGHT) 345
Figure 113 Hexacopter Variable Pitch OMI Heat Map (LEFT) and Battery Profile (RIGHT) 345
Figure 114 Hexacopter Variable RPM OMI Translational Velocity Profile (LEFT) and Translational Displacement Profile (RIGHT) 346
Figure 115 Hexacopter Variable RPM OMI Angular Velocity Profile (LEFT) and Angular Displacement Profile (RIGHT) 346
Figure 116 Hexacopter Variable RPM OMI Rotor Angular Velocity (LEFT) and Electric Machine Power Profile (RIGHT) 347
Figure 117 Hexacopter Variable RPM OMI Heat Map (LEFT) and Battery Profile (RIGHT) 347
Figure 118 Octocopter Variable RPM OMI Translational Velocity Profile (LEFT) and Translational Displacement Profile (RIGHT) 348
Figure 119: Octocopter Variable RPM OMI Angular Velocity Profile (LEFT) and Angular Displacement Profile (RIGHT) 348
Figure 120: Octocopter Variable RPM OMI Rotor Angular Velocity (LEFT) and Electric Machine Power Profile (RIGHT) 349
Figure 121: Octocopter Variable RPM OMI Heat Map (LEFT) and Battery Profile (RIGHT) 349
Figure 122: Hexacopter with pitch control during takeoff, acceleration and climb: Power as a function of time and power bucket distribution 351
Figure 123: Hexacopter with pitch control during cruise: Power as a function of time and power bucket distribution 351
Figure 124: Hexacopter with pitch control descent and landing: Power as a function of time and power bucket distribution 352
Figure 125: Hexacopter with pitch control during takeoff, acceleration and climb: Power as a function of time and power bucket distribution 352
Figure 126: Hexacopter with pitch control during cruise: Power as a function of time and power bucket distribution 353
Figure 127: Hexacopter with pitch control descent and landing: Power as a function of time and power bucket distribution 353
Figure 128: Hexacopter with pitch control: Power as a function of time and power bucket distribution 354
Figure 129: Hexacopter with RPM control during takeoff, acceleration and climb: Power as a function of time and power bucket distribution 355
Figure 130: Hexacopter with RPM control during cruise: Power as a function of time and power bucket distribution 355
Figure 131: Hexacopter with RPM control descent and landing: Power as a function of time and power bucket distribution 356
Figure 132: Hexacopter with RPM control during takeoff, acceleration and climb: Power as a function of time and power bucket distribution 357
Figure 133: Hexacopter with RPM control during cruise: Power as a function of time and power bucket distribution 357
Figure 134: Hexacopter with RPM control descent and landing: Power as a function of time and power bucket distribution 358

Figure 135: Hexacopter with RPM control: Power as a function of time and power bucket distribution358
Figure 136: Octocopter with RPM control during takeoff, acceleration and climb: Power as a function of time and power bucket distribution 359
Figure 137: Octocopter with RPM control during cruise: Power as a function of time and power bucket distribution..... 359
Figure 138: Octocopter with RPM control descent and landing: Power as a function of time and power bucket distribution..... 360
Figure 139: Octocopter with RPM control during takeoff, acceleration and climb: Power as a function of time and power bucket distribution 360
Figure 140: Octocopter with RPM control during cruise: Power as a function of time and power bucket distribution..... 361
Figure 141: Octocopter with RPM control descent and landing: Power as a function of time and power bucket distribution..... 361
Figure 142: Hexacopter with RPM control: Power as a function of time and power bucket distribution362
Figure 143 Hexacopter RPM Low Torque (SL2) GT-OSU Motors Translational Velocity Profile (LEFT) and Attitude Angle Profile (RIGHT) 367
Figure 144 Hexacopter RPM Low Torque (SL2) GT-OSU Motors RPM Profile (LEFT) and Electric Machine Profile (RIGHT) 367
Figure 145 Hexacopter RPM Low Torque (SL2) GT-OSU Motors Heat Map (LEFT) and Battery Profile (RIGHT) 368
Figure 146 Hexacopter RPM Low Torque (SL2) GT-OSU OMI Motors Translational Velocity Profile (LEFT) and Attitude Angle Profile (RIGHT) 368
Figure 147 Hexacopter RPM Low Torque (SL2) GT-OSU OMI Motors RPM Profile (LEFT) and Electric Machine Profile (RIGHT) 369
Figure 148 Hexacopter RPM Low Torque (SL2) GT-OSU OMI Motors Heat Map (LEFT) and Battery Profile (RIGHT)..... 369
Figure 149 Octocopter RPM Low Torque (SL3) GT-OSU Motors Translational Velocity Profile (LEFT) and Attitude Angle Profile (RIGHT) 370
Figure 150 Octocopter RPM Low Torque (SL3) GT-OSU Motors RPM Profile (LEFT) and Electric Machine Profile (RIGHT) 370
Figure 151 Octocopter RPM Low Torque (SL3) GT-OSU Motors Heat Map (LEFT) and Battery Profile (RIGHT) 371
Figure 152 Octocopter RPM Low Torque (SL3) GT-OSU OMI Motors Translational Velocity Profile (LEFT) and Attitude Angle Profile (RIGHT) 371
Figure 153 Octocopter RPM Low Torque (SL3) GT-OSU OMI Motors RPM Profile (LEFT) and Electric Machine Profile (RIGHT) 372
Figure 154 Octocopter RPM Low Torque (SL3) GT-OSU OMI Motors Heat Map (LEFT) and Battery Profile (RIGHT)..... 372

List of Tables

Table 1: Table 'A' 18
Table 2: Table 'B' 18
Table 3: Table 'C' 18
Table 4: Summary of all vehicle configurations under review 19
Table 5: Quadcopter Power and Gross Weight per Configuration as provided by NDARC 21
Table 6: Hexacopter Power and Gross Weight per Configuration as provided by NDARC 22
Table 7: Octocopter Power and Gross Weight per Configuration as provided by NDARC 23
Table 8: Climb, Cruise and Reserve Velocities of Vehicle Configurations 24
Table 9: Hazard Severity Classification used in FMECA and DET analyses 29
Table 10: Electric drives and battery pack components for the different architectures 32
Table 11: A summary of DET fault scenarios 39
Table 12: Electric Drive Double-Fault Injection Matrix (same driveline) 40
Table 13: Failure rate and related sources used for the analysis 43
Table 14: Dynamic Event Tree Analysis Failure Effects and Failure Rates 46
Table 15 A summary of the states, control inputs and external disturbances 58
Table 16 EM, ESC, and BP model parameters 68
Table 17 Thermal model of EM and ESC 69
Table 18 Electric drive model calibration parameters (SLS = Sea Level Standard) 69
Table 19. Quadcopter electric FTA summary 88
Table 20. Quadcopter hybrid FTA summary 88
Table 21. Quadcopter Turboshaft FTA summary 88
Table 22. Hexacopter collective FTA summary 89
Table 23. Hexacopter RPM FTA summary 89
Table 24. Octocopter RPM FTA summary 89
Table 25. Comparison of Direct-drive and Geared Hybrid Quadcopter 90
Table 26. Comparison of RPM-Control Hexacopter and Octocopter configurations ignoring effects of the RGB 94
Table 27. Comparison of RPM-Control Hexacopter and Octocopter configurations ignoring effects of the RGB and Common Cause Failure Modes. 94
Table 28. Quadcopter Electric Dynamic Event Tree (DET) Summary 95
Table 29 Peak Power vs Power to Cruise for the hexacopter with pitch control and hexacopter with RPM Control 102
Table 30 Peak Power vs Power to Cruise for the hexacopter with pitch control and hexacopter with RPM Control with one motor inoperative 102
Table 31 Peak Power vs Power to Cruise for the hexacopter and octocopter with rpm control 103
Table 32 Peak Power vs Power to Cruise for the hexacopter and octocopter with rpm control with one motor inoperative 103
Table 33: Calculation of the stress factors ($\boldsymbol{\pi U}$ and $\boldsymbol{\pi I}$) and component failure rate for the Quadcopter Electric 112
Table 34: Electric drive failure rate per failure mode considering the impact of voltage and current level 113
Table 35: Impact of voltage and current rating on powertrain architecture (electric vs hybrid) 114
Table 36: Impact of voltage and current rating on vehicle control strategy (collective pitch vs RPM) 114
Table 37: Impact of voltage and current rating on number of rotor (Hexavopter vs Octocopter) 115
Table 38: Comparison of air and liquid cooling. 117
Table 39 Failure rate and failure modes for air and liquid cooling 117

Table 40 Impact of cooling method on electric drive failure rate 117
Table 41: Failure modes and Effects due to overcharge, over-discharge and operation at high c-rate of lithium-ion batteries 120
Table 42: Traditional and proposed sensor set for electric aircraft. 123
Table 43: FMEA summary for electric machines 300
Table 44: FMEA summary for electronic speed controller 301
Table 45: FMEA summary for electronic power distribution 302
Table 46: FMEA summary for energy storage system 302
Table 47: Failure modes and causes defined for all the main components of the electric system. ESC: electronic speed controller; BMS: battery management system; EM: electric motor; BP: battery pack. 303
Table 48: Trim and control authority of the Hexacopter Pitch 314
Table 49: Trim and control authority of the Hexacopter Pitch with motor 1 inoperative 315
Table 50: Trim and control authority of the Hexacopter RPM 317
Table 51: Trim and control authority of the Hexacopter RPM with motor 1 inoperative 318
Table 52: Trim and control authority of the Octocopter RPM 320
Table 53 Trim and control authority of the Octocopter RPM with Motor 1 inoperative 321

List of Acronyms

Acronym	Description
BMS	Battery Management System
DEP	Distributed Electric Propulsion
DET	Dynamic Event Tree
EASA	European Aviation Safety Agency
ED	Electric Drive
EM	Electric Motor
ESC	Electronic Speed Controller
ESS	Energy Storage System
FHA	Functional Hazard Assessment
FIP	Fault Injection Point
FMEA	Failure Mode and Effects Analysis
FMECA	Failure Mode, Effects & Criticality Analysis
FTA	Fault Tree Analysis
HV	High Voltage
IRP	Intermediate Rated Power
LQI	Linear Quadratic Integral
LQR	Linear Quadratic Regulator
LV	Low Voltage
MCP	Maximum Continuous Power
NASA	National Aeronautics and Space Administration
NDARC	NASA Design and Analysis of Rotorcraft
ODM	On-Demand Mobility
OEI	One Engine Inoperative
OMI	One Motor Inoperative
PMSM	Permanent Magnet Synchronous Machine
RGB	Rotor Gear Box
RPM	Revolutions per Minute
RVLT	Revolutionary Vertical Lift Technology
SOC	State of Charge
SL	Severity Level
SLS	Sea Level Standard
STOL	Short Take Off and Landing
TMS	Thermal Management System
UAM	Urban Air Mobility
VTOL	Vertical Takeoff and Landing

1 INTRODUCTION

Increasing urban sprawl and increasing population around the globe exacerbate urban and suburban mobility challenges. Traffic congestion in and around urban centers have increased steadily over the years and have significantly slowed down daily commutes [1]. This increase has led to a renewed interest in Urban Air Mobility as a means to alleviate and bypass congestion on the ground. Urban Air Mobility (UAM) is typically defined as the transportation of passengers aboard small capacity vehicles within large metropolitan areas. These new operations aim at reducing commuting times by flying over road traffic. Vertical Takeoff and Landing (VTOL) aircraft have been investigated extensively for these operations and many VTOL-capable configurations have been proposed by the industry. It is however unclear how these various configurations compare to each other in terms of safety, and how challenging their respective path to certification will be.

In Section 1, we provide some background information about Urban Air Mobility, the objectives of this research, and the vehicle configurations chosen for investigations. In Section 2, we present the methodologies and assumptions. In Section 3, we provide an overview of the vehicle and system architecture. In Section 4, we go over the details of the modeling of vehicle flight dynamics, the powertrain, the guidance and navigation system, as well as the faults. In Section 5, we present the results of the static and dynamic safety and reliability assessments. Finally, in Section 6 we present our conclusions and recommendations for the future work.

1.1 Background

As urban populations increase all over the world, the strain placed on the existing transportation infrastructures leads to increasing traffic congestion and significant increases in commute times. Traffic congestion on roads stifle economic growth and adversely impact the environment. Yet, few options seem available to alleviate road congestion and a paradigm shift is needed to yield faster, cheaper, and more environmentally responsible forms of inter-urban and intra-urban transportation. As many land-based solutions designed to reduce congestion are hampered by combination of regulatory concerns and land availability related issues, UAM is proposed as one promising solution with the potential to mitigate some of those challenges. UAM operations currently envisioned require a limited ground infrastructure and a small ground footprint—provided that the safety and regulatory requirements as well as environment concerns regarding noise due to flight over congested areas can be satisfied.

Personal Air Vehicles for urban and suburban air mobility operations have been investigated for many decades [2] [3] and have been on-going for several years in cities such as Sao Paulo, Mexico City, and New York. The recent convergence of seemingly unrelated technologies in electric propulsion, supervised automation, autonomy, navigation, as well as the establishment of new On-Demand Mobility (ODM) paradigms for urban mobility stemming from the proliferation of ridesharing services worldwide have the potential to significantly speed up the development of Urban Air Mobility operations. A whitepaper from 2016 [4] highlighting the possibilities of UAM had a catalyst effect on the industry. Significant capital investments in startups and established companies alike have followed with the intent to accelerate the development and certification of new vehicles fulfilling the requirements of these operations.

The potential of urban air mobility is best illustrated by the Cambrian explosion of new vehicle architectures and new vehicle concepts that have been proposed during the past decade. These are currently at various stages of development: some designs are at the preliminary design stage, some designs are already flying, and some are nearing certification [5]. While some aircraft designers have focused on super Short Take-Off and Landing (STOL)-capable vehicles, a majority of designers have devised Vertical Take-Off and Landing (VTOL)-capable concepts in order to minimize the footprint of the supporting ground infrastructure. Many such concepts have been proposed to satisfy the emerging market of point-to-point air taxi operations. Within the subset of VTOL-capable aircraft, a variety of configurations exist, as illustrated by the wheel of fortune of Hirshberg [6] [7].

Figure 1: Wheel of fortune for e-vtol vehicle concepts [7]

To aid in research pertaining to these vehicle concepts, NASA developed four concept vehicles as part of the Revolutionary Vertical Lift Technology (RVLT) project to identify crucial technologies, define research requirements, and explore a range of propulsion systems. Among these four concepts, there exists a wide range of possible propulsive architectures. In recent work, Boeing examined failure modes and effects associated with the powertrains of the four RVLT concepts [8]. In the conclusion of this study, the recommendations were made to perform more pointed safety and reliability analysis for a subset of the configurations. Based on those suggestions, NASA has elected to focus on multirotor configurations for a subsequent research effort. The present research explores the safety and reliability impact of three major vehicle configuration decisions impacting these multirotor vehicles, namely the number of rotors, the selection of control strategy, and the propulsion architecture.

March 2021 Final Report, Reliability and Safety Assessment of Urban Air Mobility Concept Vehicles, Contract No. 80ARC020F0055, GTRI Document No. D9015A001R2, April 2021

The safety assessment carried out in this report follows the European Union Aviation Safety Agency (EASA) guidelines titled "*Special Condition, Vertical Take Off and Landing (VTOL) Aircraft*" [9]. This special condition details tailored specifications addressing the unique characteristics of these vehicles and their operations. It prescribes airworthiness standards for the issuance of the type certificate for a person-carrying VTOL-aircraft in the small category, with lift and thrust units used to generate powered lift and control. This document is used as a guideline for the classification of the severity of failures and the maximum likelihood targets associated with the various severities of failures. This classification helps benchmark the safety-related strengths and weaknesses of the various configurations of multirotor systems, and highlights where additional research is warranted to meet expected certification requirements.

1.2 Research Objectives

The objective of the research presented in this report is to identify failure modes and hazards associated with the six different configurations of multirotor under review, to perform functional hazard analyses (FHA), and to perform failure modes and effects criticality analyses (FMECA) with the intent to highlight the safety implications of major design differences related to the vehicle architecture, its propulsion system, and its flight dynamics and control. This research also recognizes the time dependencies associated with some failures and thus emphasizes the investigation of transient behaviors and the timing of failures. More specifically, this research aimed to accomplish following objectives:

- Perform a conceptual design of powertrain configurations for each of the multirotor configuration under review, starting from the NDARC design [10], in as much detail as necessary to perform subsequent elements of this research and respond to a series of technical questions raised by NASA.

- Based on the process outlined in the previous RVLT Boeing study [8], perform propulsion subsystem-centric reliability assessment of each of the proposed configurations. Compare and contrast various architecture choices based on the reliability assessment.

- Develop physics-based flight dynamic simulation models for each concept aircraft and its propulsion and control subsystems

- Using the dynamic behavior simulation models, perform a dynamic safety assessment to analyze the impact of various component and system failures on overall aircraft safety. Various combinations of the failure types, their magnitudes, orders and injection times are considered to understand the complex flight behavior and subsequent safety implications are noted in terms of safety level achieved.

- Based on the static and dynamic safety/reliability assessment, weak points of the architectures are highlighted and recommendations are made in terms of reliability improvements in the aircraft component and /or features needed to meet the required safety likelihood of 10^{-9} or less per flight hour for failures deemed catastrophic, as recommended in the EASA Special Condition for small-category VTOL aircraft [9].

The first set of analyses aims at assessing the impact of the choice of number of rotors on the safety of the vehicle and a configuration featuring six rotors is compared to a configuration featuring eight rotors. Questions related to the comparative assessment of the number of rotors are related to Table 'A'.

Table 1: Table 'A'

General Configuration	Number of Rotors	Number of Motors	Cross-Shafting (YES/NO)	Propulsion	Collective or RPM-Control?
Hexacopter	6	1 or more per rotor	NO	Electric	RPM
Octocopter	8	1 or more per rotor	NO	Electric	RPM

The second set of analyses aims at assessing the impact of the thrust control choice. Thrust control for electrically driven multirotors can be achieved via controlling the rotational speed at which the rotors are spinning or via actuation which changes the collective pitch of the blades. Questions referring to the comparative assessment of the thrust control systems are related to Table 'B'.

Table 2: Table 'B'

General Configuration	Number of Rotors	Number of Motors	Cross-Shafting (YES/NO)	Propulsion	Collective or RPM-Control?
Hexacopter	6	1 or more per rotor	NO	Electric	RPM
Hexacopter	6	1 or more per rotor	NO	Electric	Collective

The third set of analyses aims at assessing the impact of the powertrain configurations and its associated energy storage for a quadcopter design. In the first option, fuel provides energy to one or two turboshaft engines (the NDARC model supplied by NASA and used as a blueprint to model the vehicles features two turboshaft engines for redundancy) that are supplying mechanical power to the rotors via the cross-shaft system. In the second option, fuel provides energy to a single gas turbine which supplies mechanical power to a generator which supplies electric power to the various electric motors powering the four rotors of the quadcopter. A backup battery is also present to provide emergency power for a limited amount of time. The battery is sized to provide energy and power during an emergency landing in case the single gas turbine fails. In the third option, a battery-array provides electric power to the electric motors powering each rotor of the quadcopter. For all configurations, a cross-shaft system is used to ensure that a failure to supply mechanical power to any of the four rotors does not immediately lead to a catastrophic event. Questions referring to the comparative assessment of the powertrain systems are related to Table 'C'.

Table 3: Table 'C'

General Configuration	Number of Rotors	Number of Motors	Cross-Shafting (YES/NO)	Propulsion	Collective or RPM-Control?
Quadcopter	4	1 or more per rotor	YES	Electric	Collective
Quadcopter	4	1 or more per rotor	YES	Hybrid electric	Collective
Quadcopter	4	1/2[1] turboshaft engine(s)	YES	Turboshaft	Collective

[1] NASA-supplied NDARC file had two turboshafts for the fuel-powered quadcopter

Besides these comparisons across architectures, several design considerations, and their impacts on the reliability of components, are investigated as part of this research which include:

- Impact of voltage and current levels on the reliability of the electric powertrain components
- Impact of liquid versus air cooling on the reliability of electric motors and their controllers
- Impact of repeated overcharging and excessive discharge rates on the longevity of the battery
- Impact of the power profile and related duty cycle on electric components
- Impact of the Hybridization strategy

1.3 Vehicle Configurations

For this study, six configurations were chosen, as shown in the Table 4. As per the number of rotors, each configuration was identified as either a quadcopter (4 rotors), a hexacopter (6 rotors) or an octocopter (8 rotors). All quadcopter architectures include interconnecting shafts, also known as cross-shafting for emergency conditions. These are controlled by an actuator-based collective control system that varies the pitch angle of all rotor blades collectively (at the same time). There are three variants of quadcopter configurations based on the propulsion system choice: all electric (which contains one or more electric motors per rotor), hybrid-electric (which contains a gas turbine, a generator and one or more motors per rotor) and twin-turboshaft engine configuration. On the other hand, hexacopter and octocopter configurations are all driven by a fully electric powertrain. The hexacopter configuration has two variants: one features a collective control while the other features a RPM-based control. Octocopter is configured with RPM-based control. Each vehicle is designed to carry 6 passengers bringing the total payload to 1200 lbs and a design range of 75 nm.

Table 4: Summary of all vehicle configurations under review

Configuration	No. of Rotors	Cross-shafting	Propulsion	Control type
Hexacopter	6	No	Electric Motor*	RPM
Octocopter	8	No	Electric Motor*	RPM
Hexacopter	6	No	Electric Motor*	Collective
Quadcopter	4	Yes	Electric Motor*	Collective
Quadcopter	4	Yes	Hybrid-electric with Turbine, Generator and Electric Motor	Collective
Quadcopter	4	Yes	2 Turboshaft Engines	Collective

*One or more motors per rotor

1.3.1 Quadrotor Vehicles

Figure 2 through Figure 4 show the quadcopter vehicles with their overall sizing dimensions. Depending on the type of propulsion system, there are three variants: quadcopter electric configuration or quad-electric, quadcopter hybrid configuration or quad-hybrid and quadcopter turboshaft configuration or quad-turboshaft. All quadcopter configurations are equipped with interconnecting shafting or cross-shafting, which allows for a redistribution of mechanical power in case of emergency. The tip speed of all three configurations is set at 550 ft/s, and the rotor radius is 9.2 ft which results in the rotor speed of 571 RPM. Table 5 shows the engine/motor power and gross weight for the three configurations. The quad-electric is configured with four 112 hp electric motors which are driven by a battery pack which results in higher gross weight as compared to other configurations. The quad-hybrid contains one turboshaft engine with an Maximum Continuous Power (MCP) rating of 737hp coupled to an electric generator that provides electric power to four electric motors with a MCP rating of 106 hp. The vehicle also contains a battery for storage in case of emergency. Finally, the quadcopter turboshaft is equipped with two turboshaft engines that provide the power to the four rotors.

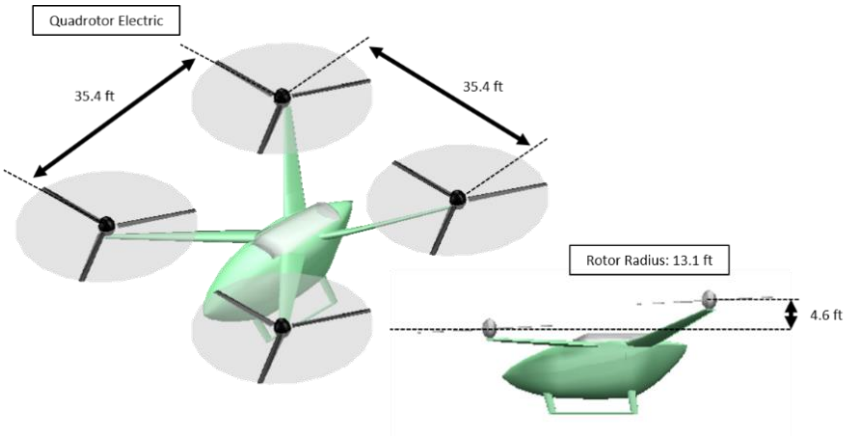

Figure 2: Quadcopter electric vehicle

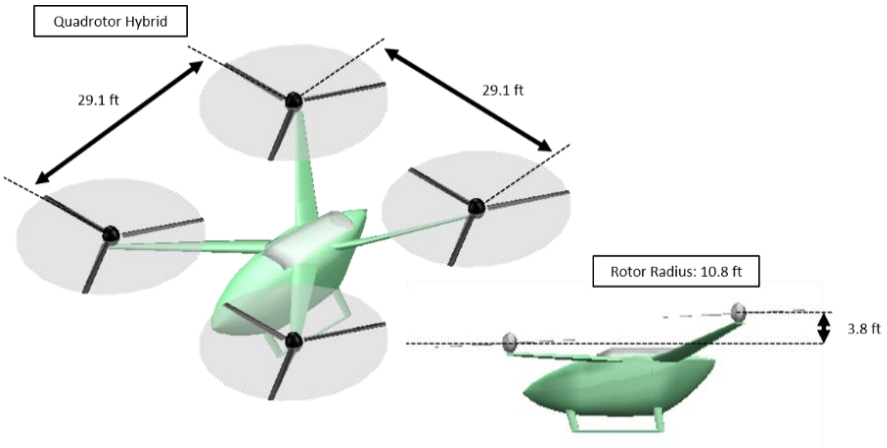

Figure 3: Quadcopter hybrid vehicle

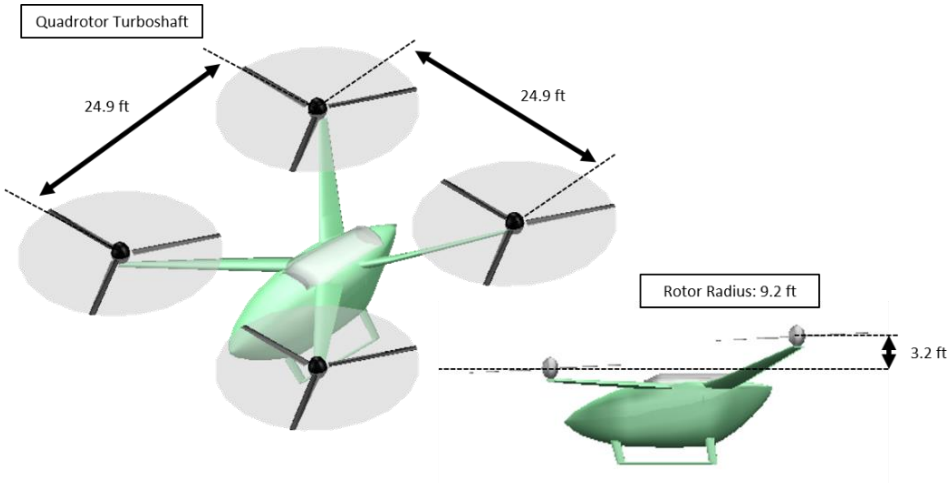

Figure 4: Quadcopter turboshaft vehicle

Table 5: Quadcopter Power and Gross Weight per Configuration as provided by NDARC

Configuration	Engine/Motor Power	Gross Vehicle Weight
Quad Electric	112 hp	6,469 lb
Quad Hybrid	107 hp	5,115 lb
Quad Turboshaft	240 hp	3,734 lb

1.3.2 Hexacopter Vehicle

The hexacopter vehicles are shown in Figure 5 & Figure 6 for the two variant configurations based on their control strategy: variable pitch control and variable RPM control. The hexacopter has evenly spaced rotors in a grid where the front motors are lower than the rear motors. The hexacopter vehicle configurations are fully electric, with six electric motors powered by batteries. The tip speed of both hexacopter configurations is set at 550 ft/s and their rotor radius is 11.9 ft which results in the rotor speed of 441 RPM. As shown in Table 6, differently sized motors are installed on the hexacopter; less powerful motors are in the front and motors with higher power rating are in the aft. As will be shown in this study, more power in the rear motors is required for vehicle trim during transient maneuvers and especially during cruise operations.

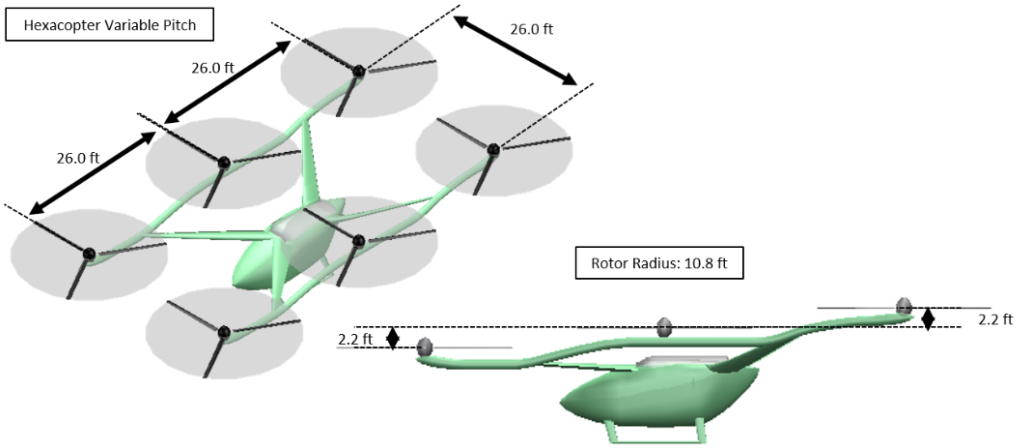

Figure 5: Hexacopter Variable Pitch Vehicle

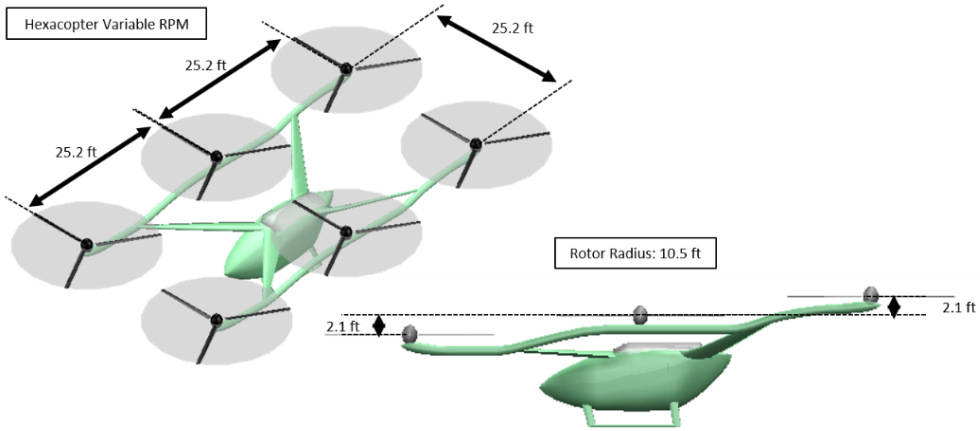

Figure 6: Hexacopter variable RPM vehicle

Table 6: Hexacopter Power and Gross Weight per Configuration as provided by NDARC

Configuration	Motor Power	Gross Vehicle Weight
Hexacopter Variable Pitch	Motor 1 and 2: 74 hp Motor 3 and 4: 82 hp Motor 5 and 6: 91 hp	6,655 lb
Hexacopter Variable RPM	Motor 1 and 2:68 hp Motor 3 and 4: 77 hp Motor 5 and 6: 83 hp	6,211 lb

1.3.3 Octocopter Vehicle

The final configuration is the octocopter vehicle shown in Figure 7 with a variable RPM control strategy. The octocopter vehicle is fully electric with power provided to the motors by battery system. As shown in the Figure 7, the front rotors are located at the lowest vertical distance on the vehicle while the rear motors are located at the highest vertical distance on the vehicle. The eight motors are configured evenly in a rectangular pattern. Table 7 shows the electric motor power and gross weight for the octocopter. Similar to the hexacopter configuration, the lower powered motors are located at the front while the higher power motors are located at the aft. The tip speed of both octocopter configuration is set at 550 ft/s and their rotor radius is 9.5 ft which results in the rotor speed of 553 RPM. Again, more power in the rear motors is required for vehicle trim during transient maneuvers and especially during cruise operations.

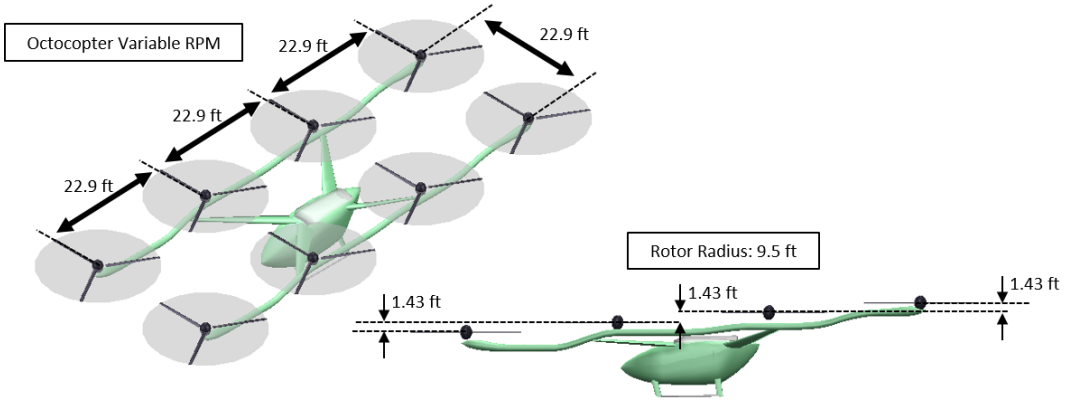

Figure 7: Octocopter vehicle

Table 7: Octocopter Power and Gross Weight per Configuration as provided by NDARC

Configuration	Motor Power	Gross Vehicle Weight
Octocopter Variable RPM	Motor 1 and 2: 58 hp Motor 3 and 4: 64hp Motor 5 and 6: 67hp Motor 7 and 8: 75hp	6,846 lb

1.4 Mission Description

The UAM mission for the safety assessment follows the design mission described in the NASA-supplied NDARC (NASA Design and Analysis of Rotorcraft) [11] materials. The vehicles are sized for a design mission consisting of two back and forth segments (without energy recharge at the first destination) shown in Figure 8. Each segment of the mission is 37.5 nm (43mi) long for all vehicle configurations. At the end of the second segment, an added reserve mission of 18.8 nm (21.6mi) is included for the diversion. For comparison, San Francisco Central Business District (CBD) to San Jose CBD distance is about 41mi; Denver International Airport (DEN) to Denver CBD distance is 21mi; Denver International Airport to Boulder is 31mi, and New York John Fitzgerald Kennedy Airport (JFK) to Wall Street in Manhattan is 13mi. The origin

and destination are at an elevation of 6,000 ft which is slightly higher than the elevation of Denver. The main cruise segments are at 10,000 ft (4,000 ft above the ground). The final reserve segment is performed at 6,000 ft. Standard atmospheric conditions assumed throughout the mission. Since various vehicles configurations climb and cruise at different velocities, the distance covered during the climb and the time necessary to complete the overall mission varies. Various climb and cruise velocities for the vehicle configurations are provided in Table 8. These velocities are not always consistent with the specification of the NDARC files, but they result from adjustments needed based on the limitations of the linear simulation models provided by NASA.

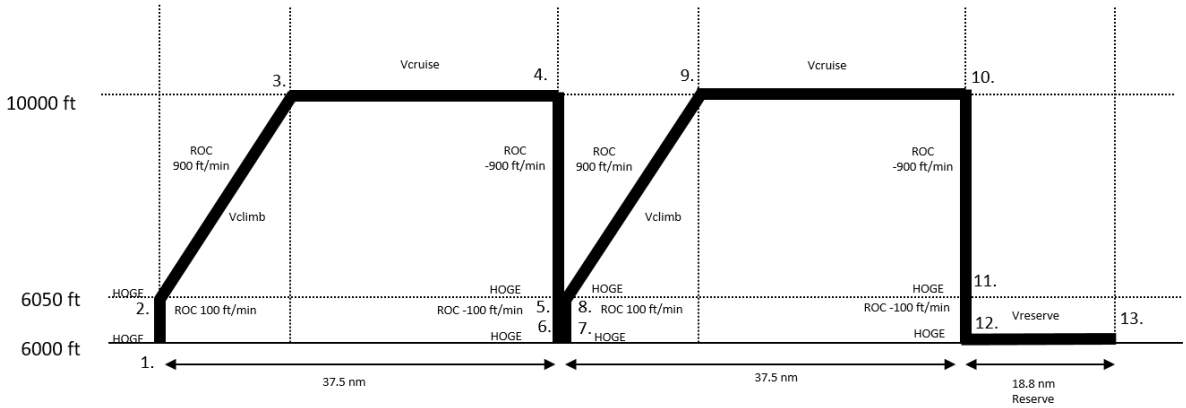

Figure 8: NDARC UAM Design Mission

Table 8: Climb, Cruise and Reserve Velocities of Vehicle Configurations

Configurations	Quad Electric	Quad Hybrid	Quad Turbo	Hexa Collective	Hexa RPM	Octo RPM
Vcruise	102* kts	120 kts	120 kts	102* kts	92* kts	92* kts
Vclimb	102* kts	120 kts	120 kts	102* kts	92* kts	92* kts
Vreserve	56.5 kts	57.3 kts	57.3 kts	56.5 kts	56.5 kts	56.5 kts

* These values were slightly adjusted to overcome the limitations of the linear models provided by the NASA

2 METHODOLOGY AND COMMON ASSUMPTIONS

The purpose of this section is to detail an overall approach and the assumptions made during the safety assessment. We first describe the techniques and methods used, then we describe how the quantification of likelihood is made, next we define the criticality of failures, and finally we describe the type of failures considered.

2.1 Overall safety assessment approach

In order to accomplish the noted research objectives, this research was divided into six tasks, shown in Figure 9.

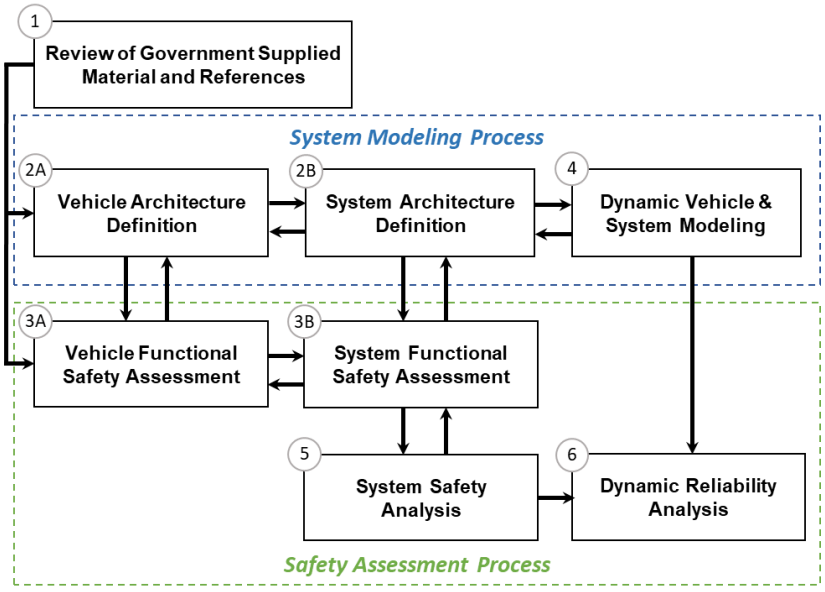

Figure 9: Overview of the Technical Approach

1. **Literature Review**: The study began with the review of technical publications provided by NASA. In particular, first phase RVLT conceptual design related publications and safety assessment reports were studied [8] [12] [13]. The proposed concept aircrafts for this research (see Section 1.3) were designed using a NASA conceptual design and sizing tool for vertical lift, NASA design and analysis of rotorcraft (NDARC) [10] [11] [12] [14] [15]. NASA provided the NDARC models and linearized stability & control derivative models of the bare-airframe dynamics for the proposed aircraft configurations. Thorough review of the models helped the team identify additional sub-models needed to simulate the dynamic response of the vehicle configurations to various failure effects.

2. **Vehicle (2A) and System Architecture (2B) Definition**: For each of the six proposed configurations, conceptual powertrain configurations are developed with enough detail to support the safety and reliability assessment. Architecture drawings or stick diagrams are created to identify major components (e.g., motors, gearboxes, etc.) in the drivetrain system, to define required component

models, and to establish major modeling assumptions. Functional block diagrams (FBD) are generated to support safety analyses in the future. For more information on stick diagrams and functional block diagrams, please refer to the RVLT Boeing safety analysis report [8]. Stick diagrams and functional block diagrams for all six configurations are detailed in Section 3.

3. **Vehicle (3A) and System Functional (3B) Safety Assessment:** The functional hazard assessment (FHA) is performed to identify the conditions that may result in the functional failures and then to classify those according to their severity. By using functional block diagrams as the basis, the failure modes, effects and criticality analysis (FMECA) is performed to further identify the component failure modes and their subsequent effects at the system, and ultimately at the aircraft level. Based on the effects identified in FMECA, it is determined whether a transient analysis is required to model a component failure. For example, the response time of an electrical cable may be fast enough that a detailed transient model is not required; however, the failure of an energy storage device may require a transient model of the gas turbine generator due to the time required to throttle up and replace the power loss. For more information on the FHA and FMECA approach and terminology, the reader is referred to the RVLT Boeing safety analysis report [8]. The results of FHA and FMECA for all six configurations are discussed in Section 5.

4. **Dynamic Vehicle and System Modeling:** A dynamic vehicle model and associated propulsion system models are developed for the simulation of all six proposed vehicle configurations. Additionally, the models allow the simulation of aircraft response to various powertrain component failures. The outcome of this task resulted in a flight dynamic behavior simulation environment compatible with the dynamic event tree framework described under Task 6. The dynamic behavior models are developed in MATLAB programming language, and the modeling approach is described in detail in Section 4.

5. **Vehicle and System Reliability Analysis:** In this task, fault tree analysis (FTA) is performed to predict overall reliability of the aircraft. Using Reliability Workbench® software [16] , the fault trees are built with a top-down, deductive approach that uses Boolean logic to identify a series of low-level events that may result in the top event, usually an undesired system state also known as *system failure condition*. For this study, loss of power transmission is considered as the top-level failure condition for the aircraft. The outcome of this process is an overall reliability assessment for the power transmission of all vehicle configurations. The analysis also helps identify key components that impact overall aircraft power transmission reliability. A thorough literature review is performed to identify and substantiate the failure rates of all the components considered safety-critical for the FTA analysis. Alterations to the system architecture design (for example, in the form of redundancy) are explored to identify any reliability gains. Using FTAs, many of the configuration-specific questions posed by NASA are addressed (see Sections 5.1.4 to 5.1.6). The failure rates are also propagated to the Dynamic Safety Assessment framework (Task 6) to calculate the outcome probabilities or likelihood values (for more details, see Section 2.2). For more information on the FTA methodology, please refer to the RVLT Boeing safety analysis report [8]. The results of FTA are discussed in the Section 5.1.3.

6. **Dynamic Safety Assessment:** While static reliability/safety analysis (e.g. FTA) describes the fault topology, it does not account for the timing of the relationship between faults and their propagation in time. For example, a single motor failure may or may not result in catastrophic outcome (depending

on whether aircraft is flying in OEI avoid region). However, due to common cause failures, such faults may occur in more than one motors at a time, which may result in multiple hard or soft failures of the components simultaneously. In such cases, it is not certain how the system-level malfunction may affect overall aircraft behavior. Also depending on the flight phase at which such component failures occur may dictate the nature and severity of the final outcome of the scenario at the aircraft level. A way to capture these transient relationships between the faults and their propagation is by using Dynamic Event Trees (DETs) approach [17] [18] . In principle, DETs are similar to the traditional event trees (ETs) except that unlike ETs, where the sequence of system responses following initiating events is predetermined by the analyst, both the timing and sequence of system responses with DETs are determined by a time-dependent model of system evolution (simulator) and branching conditions selected by the analyst (e.g. motor in normal operation, motor in degraded operation, motor failed etc.). In addition to allowing the consideration of both the epistemic and aleatory uncertainties within the same phenomenological and probabilistic framework, the use of DETs also lead to a more comprehensive and systematic coverage of possible event sequences than the traditional Event Tree/Fault Tree approach and allow consideration of hardware / process / software / human interactions in a consistent manner [19].

Figure 10 illustrates the DET approach for a three-stage process. The DET generation starts with an initiating event (e.g. vehicle takes off) and follows the evolution of each event sequence (scenario) under consideration using the simulator. When system conditions as reflected by the simulator are appropriate for a branching condition to occur (fault injection, for example), the simulator is stopped, and a new set of inputs are generated for each possible scenario. The collection of the possible scenarios forms the DET. The probability of branch occurrence is either input data or quantified using the failure rates of an FTA. The output of DET is a set of possible sequences of events with their hazard severity classification and their probabilities.

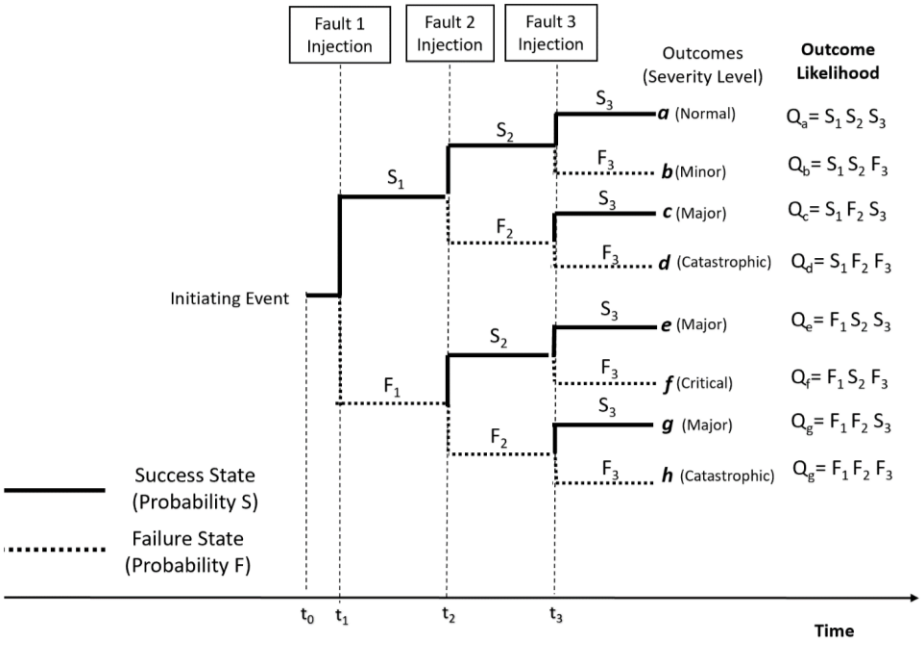

Figure 10: An example DET with branching probabilities quantified by FTs

2.2 Probability Calculations

All component failure rates (λ) are assumed constant for this study, (i.e., the equipment is operating in the flat portions of the reliability "Bathtub Curve"). Failure probability or unreliability for constant failure rates is calculated using the following equation:

$$Q = 1 - e^{-\lambda t} \quad (1)$$

When $\lambda t << 0.1$ (applicable to all component failures in this study), Equation (1) above can be simplified and yields Equation (2):

$$Q = \lambda t \quad (2)$$

For the FTA, to be consistent with the previous study performed by Boeing [8], the mission time is assumed as one hour. For the DET calculations, the time at which the fault is injected in the simulation is used to calculate the branch probabilities. When two faults are injected, the injection is done randomly and the failures are assumed to be independent events. Therefore, the final conditional probability values for any branch is calculated by multiplying the failure probabilities of all events that occurred on that branch. For example, if two faults with failure rates λ_1 and λ_2 are injected at time t_1 and t_2 and these two failures result in a catastrophic outcome, then the final conditional probability value of the catastrophic event is defined by Equation (3):

$$Q = Q_1 \cdot Q_2 = \lambda_1 t_1 \cdot \lambda_2 t_2 \quad (3)$$

A cutoff probability value of 10^{-11} is set in order to exclude all possible fault scenarios for which the simulations are not needed due to the very low likelihood of the event. The likelihood of events resulting in catastrophic outcomes is compared against the benchmark catastrophic outcome likelihood value of 10^{-9} set forth for enhanced category vehicles in EASA special condition for small-category VTOL aircraft [9].

2.2.1 Hazard Classification

Severity is divided into four categories as defined in MIL-STD-1629A [20]. Severity category is assigned to provide a qualitative measure of the worst potential consequences resulting from design error or item failure. The hazard severity classifications are described in Table 9.

During the DET simulation, the aircraft behavior is monitored at each time step. In cases when there is a deviation from the nominal flight behavior, based on the severity of the observed behavior, a hazard condition flag (Minor, Major, Critical, and Catastrophic) is assigned to the simulation branch. The assignment automatically occurs when one of the observed flight parameters reaches a certain threshold value. For example, if the rotor RPM drops below a prescribed cutoff value, then "RPM too low" flag is triggered and based on the RPM value, a hazard condition flag is assigned to the event. In subsequent time steps, if the severity level increases, the flag variable is over-written by the new assignment of the appropriate hazard condition. A list of all hazard condition flags with their severity classification based on the flight parameters is provided in the APPENDIX O.

Table 9: Hazard Severity Classification used in FMECA and DET analyses

Category	Severity of Effect
I	**Catastrophic:** A failure which can cause a loss of aircraft and/or death of its occupants.
II	**Critical/Hazardous:** A failure which can cause severe injury, major property damage, or major aircraft damage which will result in mission loss.
III	**Marginal/Major:** A failure which may cause minor injury, minor property damage, or minor aircraft damage which will result in delay or loss of availability or mission degradation.
IV	**Minor:** A failure not serious enough to cause injury, property damage, or system damage, but which will result in unscheduled maintenance or repair.

2.2.2 One Engine Inoperative (OEI) Condition

For the safety certification of the aircrafts with conventional twin gas turbine engine propulsions systems, One Engine Inoperative (OEI) condition signifies the performance requirements of the aircraft in case of single gas turbine engine failure which results in reduced safe-flight envelope. For the sake of simplicity and consistency with the previous research performed by Boeing, such performance requirement for all configurations is identified as *OEI Condition*. The condition means that the combination of one or more critical powertrain related failures—e.g. single motor failure, also known as One Motor Inoperative (OMI), Rotor Gear Box (RGB) failure etc...— may result in loss of lift necessary to continue the flight in certain flight envelope or *OEI Avoid Region*. Therefore, in this report, OEI signifies a condition, it does not necessarily describe what physically occurs to an aircraft engine which may or may not be present in the architecture under consideration. On the other hand, OMI signifies single motor failure which is a physical fault related to the electric drive of an aircraft with distributed electric propulsion (DEP). The aircrafts are uniformly assumed to spend 25% of their flight time within the OEI avoid region, in which function loss of single rotor will result in power required exceeding power available and a hard landing sufficient to cause catastrophic damage to the aircraft or its occupants.

2.2.3 DET Scenario Design

In DET analysis, the scenarios are generated by introducing component faults (or failures) at discrete points in time during the mission. In this report, each such point will be called fault injection point (FIP). For this study, four discrete injection points per mission segment (total 8) are chosen (see Figure 11). *Takeoff* and *climb* phases are deemed as the two most challenging flight phases for all vehicles due to their stringent power requirements; therefore, one FIP is allocated to each flight phase. Remaining two FIPs are chosen for the *cruise* phase and *descent & land* flight phase respectively. Since the mission contains two identical segments, in order to optimize the DET simulation runs, the flight simulator code is modified to simulate only second segment of the mission. The FIPs for the second segment are numbered 5 through 8 (see Figure 11). For electric vehicles, appropriate adjustments to the initial conditions and states are made to account for the energy utilized during the first segment of the mission.

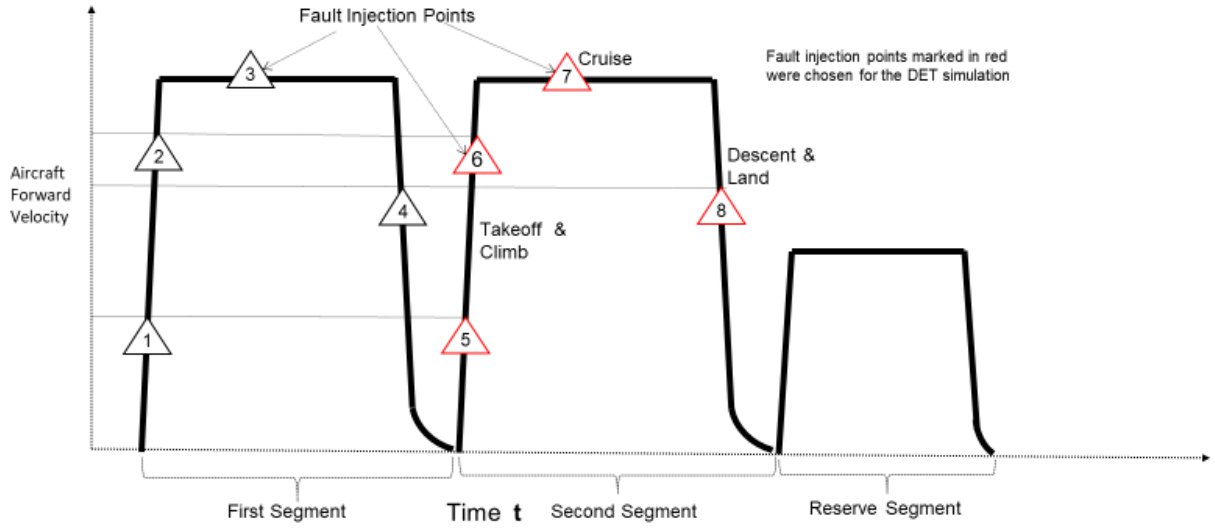

Figure 11: Mission schematic with the failure injection points

As explained in the Section 2.1.1, all single-fault probability values calculated at the four FIPs are greater than the simulation cutoff probability of 10^{-11}. Therefore, DET simulation scenarios include all single fault injection-based simulations.

For two-fault scenarios, the faults are injected for following three combinations:

a. First fault in *takeoff* phase (FIP5) & second fault in *climb* phase (FIP 6)
b. First fault in *takeoff* phase (FIP 5) and second fault in *cruise* phase (FIP 7)
c. First fault in *cruise* phase (FIP 7) and second fault in *descent & land* phase (FIP 8).

Based on these chosen FIPs, DET simulations are performed for various two-fault scenarios for which the calculated conditional probability values are higher than the cutoff probability. Scenarios with three or more faults are not considered due to their extremely low conditional probability values (of the order 10^{-18} or less).

For the DET analysis, the faults are grouped by the subsystems, as shown in Figure 12. The faults within each group and their simulated effects are explained in detail in the Section 2.4.

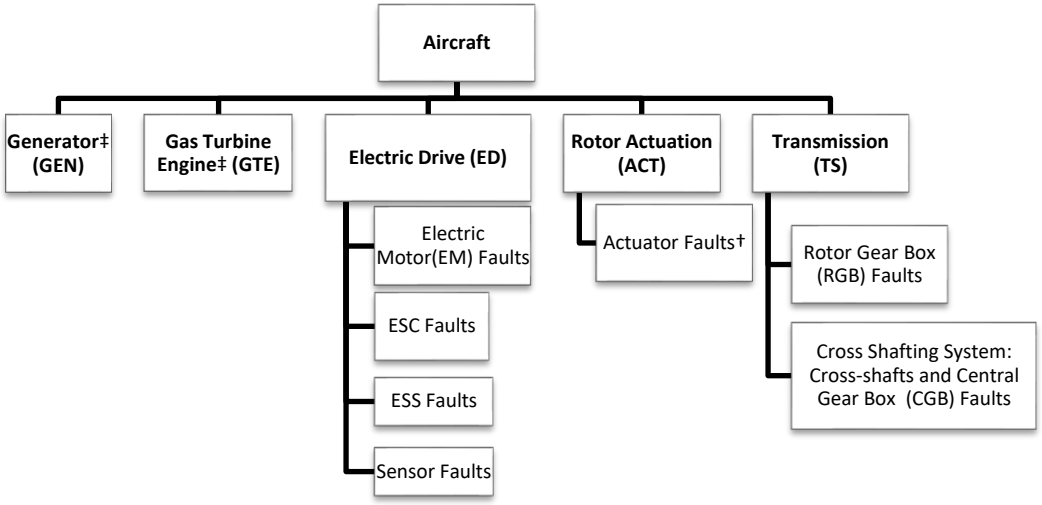

Figure 12: DET faults grouped by the subsystems

Figure 13describes example DET simulation scenario for electric quadcopter with two faults injected during the second mission segment. The faults are injected during the *takeoff* (FIP 5) and *cruise* (FIP 7) phases of the mission segment. First fault injection occurs in the electric drive (ED). Two different fault types or more precisely, two different end-effect types, *torque ripple* and *low torque* are shown as individual branches at time t_5. In an actual DET, all possible electric drive faults are introduced at time t_5, however, for the simplicity, only two electric drive faults are shown in the figure. The DET simulation uses two input vectors for the electric drive fault injection: state vector describing fault type for each of the four electric drive and the fault vector describing the fault magnitudes. Similarly, for other system faults (for example, for the rotor actuation system), state and fault vectors are prescribed as the DET inputs. As shown in Figure 13, the second fault occurs in the transmission system at time t_7. Six different transmission faults (or end-effects) are considered for the DET simulation. Combination of the *torque ripple* fault of magnitude 0.3 and all six possible transmission fault states generates six DET simulation branches, outcome of each is determined by the dynamic vehicle simulation based on the physics-based vehicle response to the faults injected while performing the mission. At each time-step, DET simulation is continuously monitoring the vehicle flight parameters to check for any deviations from nominal mission. In case a deviation occurs, the DET simulation assigns the branch a hazard condition flag (as explained in Section 2.2.1). The likelihood values of each branch are calculated a priori since the fault injection times are predetermined for the simulation. This ensures that only the scenarios which have final branch conditional probability value greater than the cutoff probability are simulated.

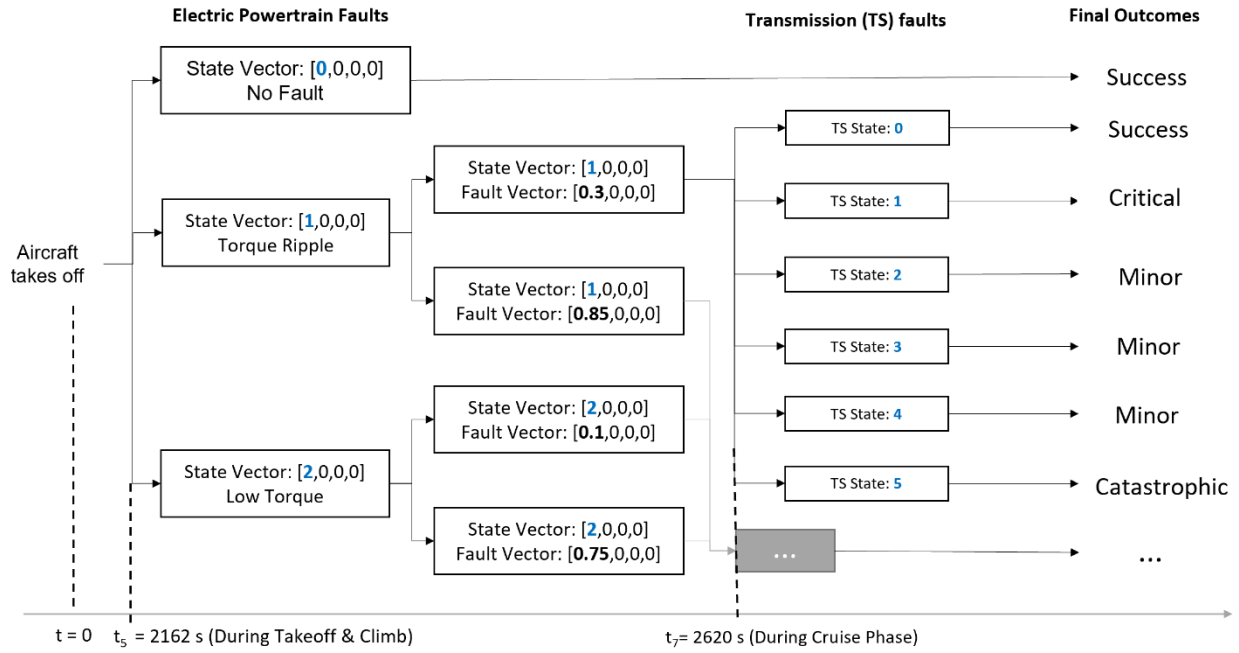

Figure 13: An example of the DET execution in a two-fault injection scenario.

2.3 Configuration Assumptions

Assumptions related to vehicle design, powertrain design, and safety assessment are reported in this section. Some of the assumptions have been made considering discussion with NASA, information carried over from NDARC [10], the previous study performed by Boeing [8], and experience of the team.

2.3.1 Electric drive and energy storage system assumptions

Each vehicle with electric propulsion or hybrid-electric propulsion is equipped with several electric drives (EDs) and lithium-ion battery packs (BP) as shown in Table 10.

Table 10: Electric drives and battery pack components for the different architectures

Vehicle	Number of electric drives	Number of battery packs
Quadcopter electric	4	4
Quadcopter hybrid	4	1
Quadcopter turboshaft	-	-
Hexacopter	6	6
Octocopter	8	8

Each electric drive consists of an electric motor (EM), an electronic speed controller (ESC) and a related thermal management system (TMS). Many design options are available for EM and ESC depending on the torque/speed requirements, overload capabilities, power density, dynamic response, efficiency, noise, reliability, failure modes, and cost [21]. In this work, permanent magnet synchronous motors (PMSMs) are considered due to their high energy density and low inertia compared to other electric machines while the ESC is based on a three-phase voltage-source inverter. Each BP consists of lithium-ion battery cells arranged in series and parallel (to achieve the desired voltage, power and energy level), a battery management system (BMS) and a vapor cycle refrigeration system [8].

The ESC oversees the following functions:

1. Measure three phase currents, EM rotor speed, DC link voltage, EM temperature, ESC temperature
2. Provide the electric motor with the proper voltage to achieve the desired torque reference through PI controllers
3. Enforce the power limits of the electric motor, ESC (continuous and peak operation) and battery pack—ensuring the operation of the system within the components' safe operating range
4. Diagnose and prognose faults in the ED

While the BMS is in charge of:

1. Measuring cell voltages, BP current, and BP temperature
2. Calculating the state of charge (SoC) and the power limits
3. Enforcing voltage, current, and state of charge limits
4. Providing the ESC with the dynamic maximum power available from the BP for discharge or charge
5. Diagnosing and prognosing faults in the BP

Considering the state of the art of thermal management system for EDs [22], this work considers the following:

1. The cooling loop of EM and ESC are not interconnected with the aim of increasing the reliability
2. Each EM is equipped with a forced liquid TMS connected to the transmission cooling loop (medium transmission oil)
3. Each ESP has an independent liquid cooling system (medium water-glycol)
4. BPs are equipped with a vapor cycle refrigeration system
5. The cooling system is shared among all battery packs, and hence the failure of the BP cooling system will lead to the failure of the battery packs
6. BP does not share cooling loop with the ESC (less risk of overheating the battery due to ESC overheating, reduced weight and reduced piping losses)
7. Cooling loop control and operating temperature can be optimized for the specific component;
8. Because of their higher reliability, accessory gear drives (for pumps / fans, etc.) are chosen over the electrical drives
9. Option of air cooling of EM and ESC is considered for the comparison purposes.

Each liquid cooling system includes a pump, a radiator, a fan, pipes, and filters. The air cooling includes a double-fan system and filters.

When possible, the electric components are sized by following the NDARC specifications [11]. However, a few adjustments had to be made and are reported in the Section 4.2. For the electric drive, upsizing the system is often required to account for the system (in)-efficiencies. This electric drive design is named GT-OSU ED. Additionally, the NDARC design does not consider the power required in case of a motor failure. In some cases, the NDARC electric drive design is able to fulfill the mission requirements even during a single motor failure, i.e. an OMI case; while in other cases, depending on the control strategy and specific location of the faulty motor, the vehicle is not able to safely continue the mission. An additional design strategy is proposed for this study, in which the electric machines are sized to supply enough power for the OMI case. This electric machine design strategy is named GT-OSU OMI.

2.3.2 Vehicle modeling and control assumptions

The dynamic modeling assumptions provide some perspectives on the dynamic analysis of the vehicle. First, the aircraft dynamic models consider the piecewise linear dynamic models provided by NASA for the aircraft flight dynamics. Consequently, the models use the weight of the aircraft provided by NASA, and are not affected by the different hypotheses relative to subsystem sizing, such as battery, electric machine, etc., i.e. there is no sizing impact on the vehicle dynamics. Moreover, for the aircraft powered by turbine (turboshaft and turbogenerator), the effect of fuel burn does not propagate on the vehicle dynamics. The set of states of interest is also kept to the order provided by the NASA linear dynamic models, and do not include other airframe states such as inflow states, structural vibrations, etc. There is also no ground effect considered in the analysis of the aircraft behavior.

The mission is assumed to be mainly longitudinal, going from the starting location, climbing, accelerating, decelerating and landing on a straight line. For the aircraft where no wind analyses are reported, the longitudinal dynamics alone is considered.

For the controller, the aircraft has a perfect control feedback loop with no delay and sensor noise or uncertainty. The only delays in the feedback loop are the delays inherent to the actuation mechanism, such as the pitch actuator rate and the acceleration of the of the rotor for the RPM-control aircraft.

2.3.3 Safety analysis assumptions

The assumptions are classified according to the nature of analysis performed:

i. Assumptions for static safety and reliability analysis which encompasses the FHA, FMECA and FTA are described in the Section 2.2.4.1.
ii. Assumptions related to the dynamic safety assessment using DET analysis are listed in the Section 2.2.4.2.

2.3.3.1 Static safety and reliability analysis assumptions

The Static Safety and Reliability Analysis in this study follows the guidelines of Society of Automotive Engineers (SAE) Aerospace Recommended Practice (ARP) 4761 [23]. As in the previous Boeing study [8],

the scope of the static safety and reliability analysis is to encompass the propulsion system for each air vehicle concept. Therefore, many of the assumptions made in the Boeing study are included in this section when applicable.

A separate FHA/FMECA/FTA is generated for each concept vehicle which combines aircraft level and system level analyses. Systems aligned with, but not directly tied into providing propulsion for the air vehicle are addressed to the extent that they affect the function of propulsion and rotating systems.

Typical component failures that result in the loss of propulsion are engine failures or individual/dual motor failures, electrical (battery, low and high-power supply) failures, transmission related failures, cooling failures (both liquid-cooling and forced air-cooling as applicable), actuator failures, and generator failures.

One major contrast from previous Boeing study is inclusion of the hardware related flight control system failures in the safety analysis. In order to compare the reliability of two different control strategies considered in this study, loss of control due to actuator malfunction (in case of pitch-control aircraft) and loss of control due to loss of a propulsor (in case of RPM-control aircraft)—both are considered.

The following safety related assumptions apply to all the configurations in this study:

- The UAM mission is intended to be flown over major cities to reduce congestion and travel time; therefore, risk considered while classifying the functional failure related hazards includes the assumption of flight over highly dense urban areas.

- Ground based hazards such as overheating during charging, arcing, and fuel leaks are not considered for the safety analysis. Environmental systems, or other sub-systems that are unaffected by the change from conventional propulsion to all-electric or hybrid-electric propulsion are not generally assessed because the reliability and safety of such systems are adequately addressed by existing regulations and known best practices. Those systems will only be assessed to the extent that they uniquely interface into the propulsion system.

- Hazards for this study are limited to powered mission segments only. Autorotation flight is not examined in this work. The ability to autorotate or maintain an intended flight path with primary power turned off requires complex analysis and/or test, which is out of the scope of both the static reliability analysis and the dynamic safety assessment.

- It is assumed that the aircraft starter system, whether electric or conventional APU starting, is isolated from the primary propulsion system and hence is not included in the reliability/safety analysis.

- For all electric and hybrid configurations, the low voltage battery which powers the ESC and the FCC is necessary for speed control of the propulsor RPM. Loss of either of those components is assumed to result in the loss of all propulsors.

- Single propulsor failures are assumed to include following components that are critical for the propulsor function: an overrunning clutch (OVR), electric motor (EM), ESC, low voltage (LV) ESC Power, and high voltage motor power—HV battery power.

- Single rotor function loss may occur due to a combination of failures (depending on the configuration type):
    - All electric and hybrid Configurations:
        - Loss of single propulsor and cross-shafting, or
        - Loss of single rotor gear box (RGB), or
        - Loss of rotor actuation (ACT) system (for collective-control vehicles)
    - Quadcopter Turboshaft:
        - Loss of single rotor gear box, or
        - Loss of rotor actuation system

- Impact of multiple propulsor failures on the controllability of an electric or hybrid-electric vehicle varies depending on whether the faulty propulsors are diagonal to each other or not. For all non-diagonal cases in architectures with no cross-shafting, dual propulsor failure is assumed catastrophic in all flight conditions.

Cross-shafting related assumptions

In the cross-shafted configurations (all quadcopter vehicles), all four (4) rotors are interconnected via a common collector gearbox and associated drive-shafts. A loss of a single propulsor is minor at altitude, and only potentially catastrophic when the air vehicle is being operated in the OEI avoid region. In case of a failure of a cross-shaft, a switch in the controller logic will allow continuation of the desired operation of the isolated rotor. However, failure of a single gearbox will result in the total loss of torque to the connected rotor and is assumed as catastrophic due to lack of thrust and due to controllability issues. Also, loss of dual propulsors will result in inadequate thrust, and hence is considered catastrophic. For the aircrafts without cross-shafting, either dual rotor loss (in case of hexacopter vehicles) or triple rotor loss (in case of octocopter vehicle) will result in the total loss of the aircraft.

All-electric configuration assumptions

The all-electric vehicle configurations contain energy storage system (ESS) which includes battery packs, battery cooling system and battery management system. Each battery pack is assumed to operate between 20-100% State of Charge (SoC) range including in the reserve mission.

The battery packs are assumed to be distributed and isolated from one-another inside the fuselage for each rotor. Although the packs are represented as a single block of high voltage batteries in the configuration diagrams, it is assumed that those include fail-safe switching and will be physically isolated from one-another so that a failure in one module does not propagate to all modules. The battery packs are conceptualized to be placed near each electric motor and ESC; the safety analysis assumes a common battery cooling system with two (2) pumps acting in parallel, either one capable of supplying adequate flow and pressure. Every battery pack includes an independent BMS.

Every ESC has a separate cooling system, based on water cooling. Every electric machine is cooled using the transmission oil cooling available for the mechanical components. The cooling system of electric machine and transmission of every rotor is independent.

In addition:

- Severe failures of the motor/ESC cooling system (e.g. loss of a component) will lead to complete loss of the powertrain (no torque)
- Partial operation of the thermal management of motor/ESC will cause overheating, so a derating will be applied (low torque)
- EM warning and fault temperature: 130 and 160 °C
- ESC warning and fault temperature: 80 and 100 °C

Hybrid-electric configuration assumptions

Hazards and FTA will assume the fuel system meets reliability requirements regardless of propulsion system. Both conventional (turboshaft engine burning fossil fuels turning rotors) and series hybrid propulsion (turboshaft engine burning fossil fuels turning generator) will require effectively the same fuel system. The turboshaft engine and associated Planetary Axis Gearbox (PAG), Clutch, AC Generator, and AC/DC convertor are grouped together so that the loss of any of those components will result in the air vehicle relying on battery power alone for continued flight. The batteries are assumed to last 10 minutes, and the air vehicle is assumed to be within 5 minutes of a suitable landing vertiport. Since UAM missions are expected to be conducted in environments with high geo-density of vertiports [24], the UAM vehicles will rarely be farther than a few minutes (miles) away from a potential landing site. Therefore, for hybrid configuration, an emergency landing maneuver is added as an additional consideration for contingencies once the vehicle battery SoC reaches 50% of its full capacity.

The hybrid configuration emergency landing maneuver is conceptually described in Figure 14. The maneuver consists of a vertical descent at 900 ft/min to reach a close-by vertiport. The forward velocity decreases linearly from the forward velocity at the time of failure to a null forward velocity once the vehicle reaches the ground. Touching down at 900 ft/min is not realistic to achieve a safe landing but the emphasis of this simulation is to check whether attempting to divert to an emergency vertiport in case of significant failure can mitigate an outcome likely to be catastrophic otherwise. The details of the actual touchdown are not considered in this evaluation.

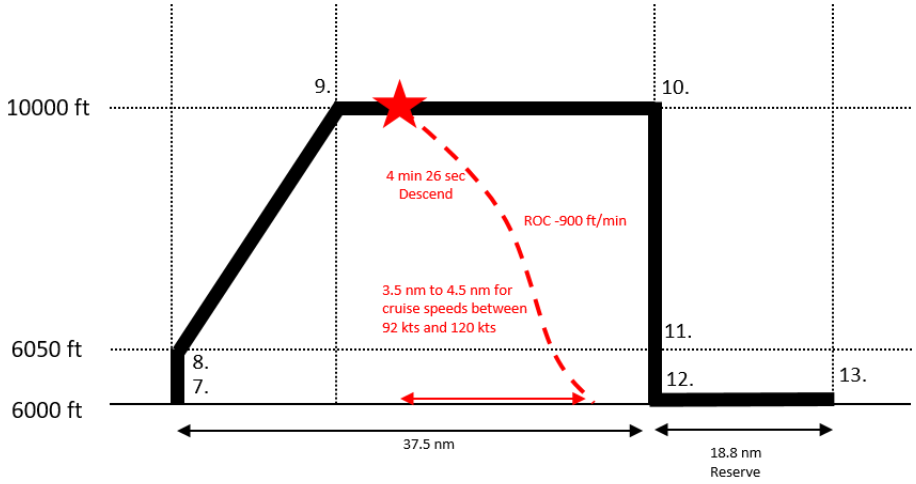

Figure 14: Quad-Hybrid emergency landing maneuver.

2.3.3.2 DET analysis assumptions

Task 6 in the Section 3.1 described the DET analysis in detail. Following are the main assumptions of DET analysis for this study:

- Only hardware faults are considered (no software errors related scenarios are studied). Also, no human interaction with the system or fly-by-wire type of mitigation scenarios are included.

- Only discrete fault injections points (FIPs) and fault magnitudes are considered in order to limit the total number of computations to an acceptable feasible number that is necessary to gain sufficient insights into the overall performance of each vehicle architecture.

- The component/system faults that are assumed to result in catastrophic outcomes in static analysis are not simulated.

- For special cases, where scenarios are assumed to provide safe outcome are not simulated. For example, for the quadcopter hybrid configuration, OEI condition for turbine engine is assumed to trigger emergency landing using reserve battery which will be performed by following a standard emergency landing procedure and hence the condition is assumed safe and hence is not simulated. However, in case of a generator fault in combination with other faults, it is uncertain how the battery SoC may vary which may depend on the state of the vehicle at the time of fault injection and severity of the generator fault. Hence such fault scenarios are simulated to gain more insights.

- All single faults scenario branches have outcome likelihood values above the simulation cutoff of 10^{-11}, hence all the single-fault cases are simulated. For the double-faults scenarios that have the branch outcome likelihood values less than the simulation cutoff probability are not simulated.

- All double faults are injected to same rotor electric driveline, except for the case of quad-electric and quad-hybrid configurations which include electric drive faults scenarios for two different

drivelines as well, since those configurations have higher fault tolerance due to the cross-shafting system. Double faults cases in two drivelines are not considered for configurations without cross-shafting which require more advanced control laws for fault tolerance, and hence those considerations are out of the scope of this work. In the Table 11, all the faults scenarios for DET analysis are summarized. The simulated fault injection scenarios are shown with checkmarks. If a component is not part of the architecture, the corresponding component failure scenarios are marked as not applicable (NA). For special cases, where scenarios are assumed to provide safe outcome are marked as SAFE and hence are not simulated. All single faults scenarios have outcome likelihood probabilities above the simulation cutoff probability of 10^{-11}, so all applicable cases are simulated. The double-faults scenarios marked with cross-mark symbol signify the scenarios that are not simulated due to their final branch outcome likelihood values falling below the simulation cutoff probability of 10^{-11}.

Table 11: A summary of DET fault scenarios

	Single Faults					Double Faults					
Configuration	**ED**	**TS**	**ACT**	**GTE**	**GEN**	**ED-ED**	**ED-TS**	**ED-ACT**	**TS-ACT**	**GTE-ACT**	**GTE-TS**
Quad Electric	✓	✓	✓	NA	NA	✓▪	✓	✓	✓	NA	NA
Quad Hybrid	✓	✓	✓	SAFE	✓	✓▪	✓	✓	✓	☒	☒
Quad Turboshaft	NA	✓	✓	✓	NA	NA	NA	NA	✓	☒	☒
Hex Collective	✓	✓	✓	NA	NA	✓	☒	✓	✓	NA	NA
Hex RPM	✓	✓	NA	NA	NA	✓	☒	NA	NA	NA	NA
Oct RPM	✓	✓	NA	NA	NA	✓	☒	NA	NA	NA	NA

✓ Fault scenario simulated
▪ Scenario is considered for same as well as two different electric drives
NA Fault scenario is not applicable
SAFE Fault scenario is not simulated; Safe outcome is assumed
☒ Fault scenario is not simulated due to low conditional probabilities

ED Electric Drive
TS Transmission System
ACT Rotor Actuation System
GTE Gas Turbine Engine
TG Turbogenerator

- For the double faults in the same electric driveline (or in other words, electric driveline of a given rotor), the faults are injected at two discrete failure injection points (in time). However, due to nature of fault-physics, not all two fault combinations are possible for the same electric drive. For example, it is assumed that if the first injected fault is *no torque*, then the second injected fault cannot be *low torque* and hence is not considered. Table 12 shows all possible valid combinations that are chosen for the double faults in same electric drive.

- For the electric drive double faults in two different drivelines (or in other words, for electric drivelines of two different rotors), all fault combinations are considered as independent events and hence are simulated. However, due to limitations in linearized control models, the faults are only introduced in diagonally opposite rotors. For quadcopter, the faults are introduced in the

electric drive pair (ED1, ED4) which is equivalent to introducing the faults in the electric drive pair (ED2, ED3). Any faults injected in two non-diagonal motors are assumed to result in catastrophic outcomes and hence such combinations are not considered for the DET analysis.

Table 12: Electric Drive Double-Fault Injection Matrix (same driveline)

		Second Fault Injections						
		No Torque	Low Torque	High Torque	Torque Ripple	Short Circuit 1	Short Circuit 2	Short Circuit 3
First Fault Injections	No Torque	X	X	X	X	✓	✓	✓
	Low Torque	✓	X	X	X	✓	✓	✓
	High Torque	✓	✓	X	✓	✓	✓	✓
	Torque Ripple	✓	✓	✓	X	✓	✓	✓
	Short Circuit 1	✓	✓	✓	✓	X	✓	✓
	Short Circuit 2	✓	✓	✓	✓	✓	X	✓
	Short Circuit 3	✓	✓	✓	✓	✓	✓	X

- If the two double faults are injected in two different subsystems, then the faults are injected at the two injections points in both orders, since the vehicle dynamics may differ depending on the order of the fault injection. For example, if the first fault is injected during the *takeoff* (FIP5) and second during the *cruise* (FIP7) phase, and if the two subsystems under consideration are rotor actuation system (ACT) and electric drive (ED) respectively, following two combinations are considered for each fault pairing: (ACT fault during *takeoff*, ED fault during *cruise*) and (ED fault during *takeoff*, ACT fault during *cruise*).

2.4 Modeling environment

Figure 15 describes the safety assessment workflow and the software used for each task. Architecture diagrams were developed using Inkscape, FHA tables were generated in MS Excel. Isograph Reliability Workbench® software and its accompanying failure databases were used for failure rate calculations, and to perform FMECA and FTA analyses. The component failure rate data was exported in MS Excel format, and post-processed further in MS Excel to apply the revised failure rate values calculated for a group of component failures which all result in the same end effects. The end-effect based failure rates were then imported by the DET analysis MATLAB framework. Dynamic simulation models were also developed in MATLAB which allowed easy interface of Dynamic behavior models with the DET framework (described in detail in an info-chart within Figure 16)

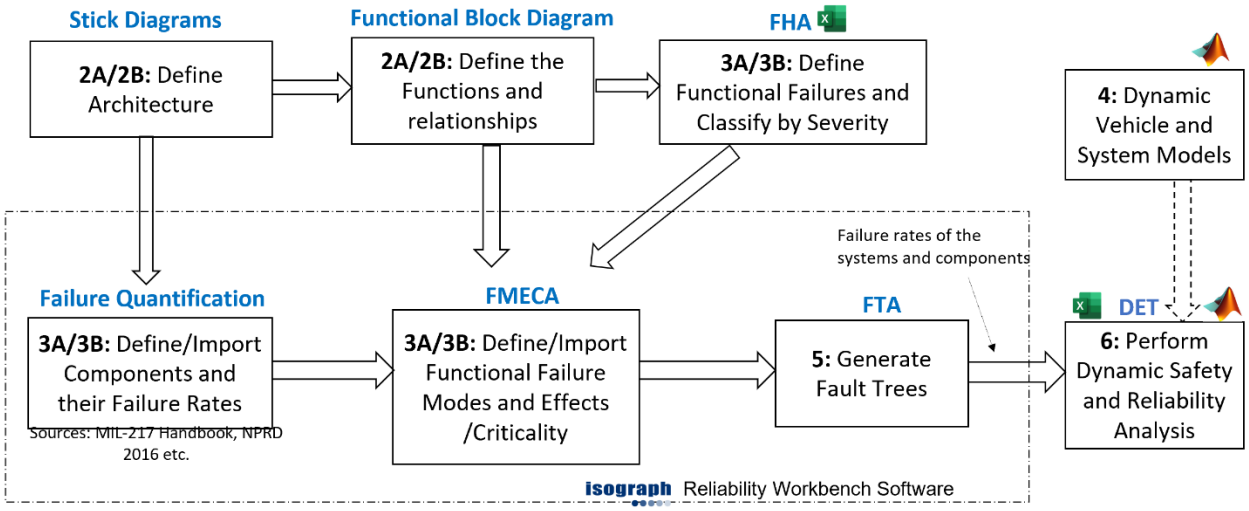

Figure 15: Reliability/Safety Assessment Workflow

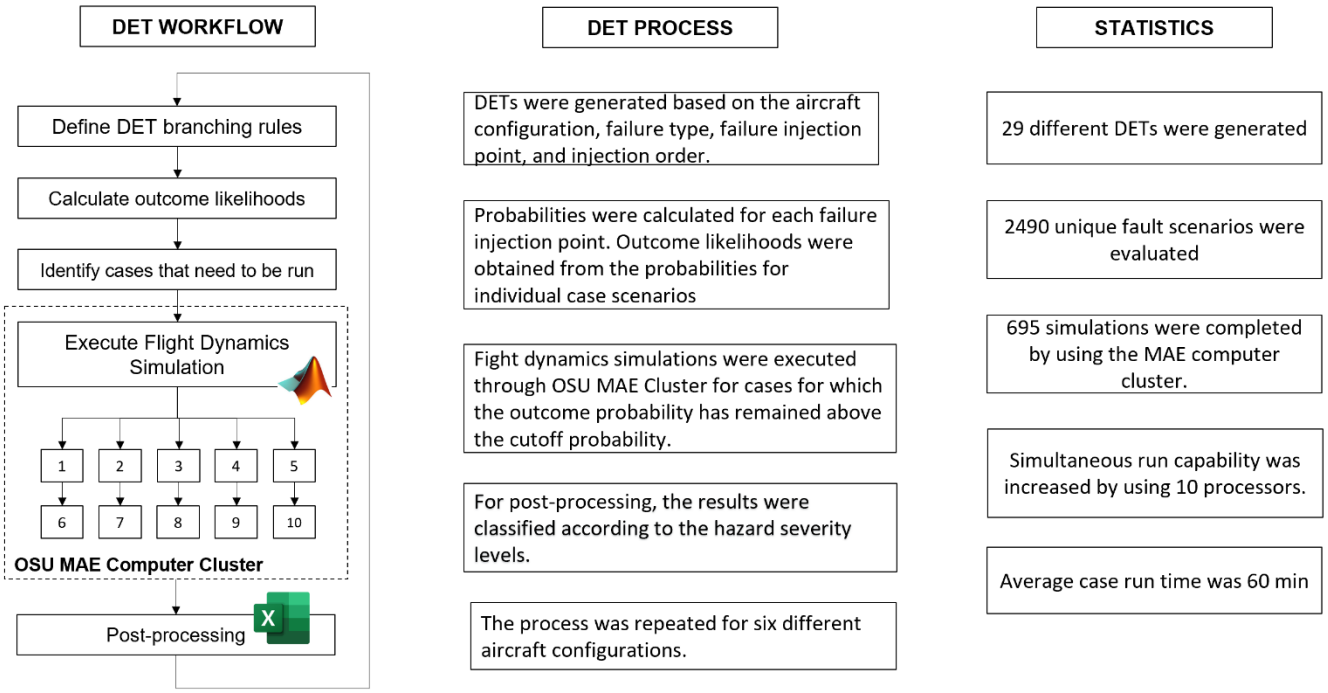

Figure 16: DET analysis info chart

2.5 Component/System Reliability

This section will review all the systems and components that are included in the safety analyses. Subsection 2.5.1 will summarize all the major components and their failure rates. Also, the summary will highlight various data sources used to determine the component failure rates. In the Section 2.5.2, the components and their failure modes for static and dynamic safety assessment will be identified for the aircraft systems considered. In particular, for the dynamic event tree analysis, the component failure modes are grouped by their system-level end effects. Therefore, the failure rates are recalculated for the end-effect based component fault groups, the process will be discussed in detail.

2.5.1 Components and Component Failure Rates (FR)

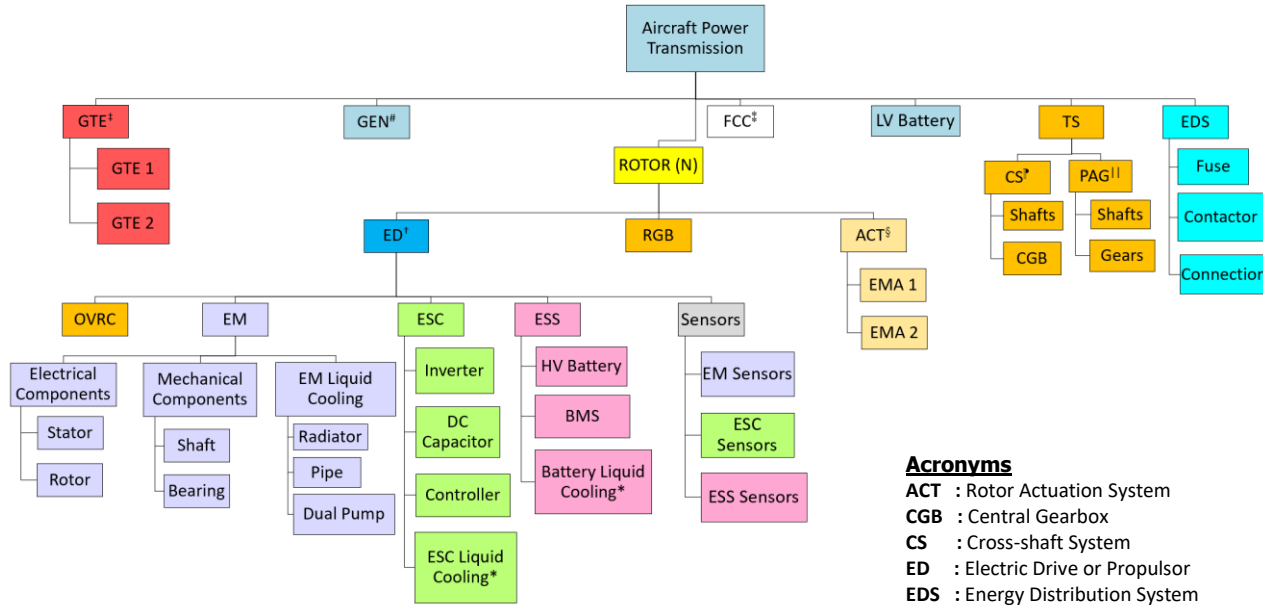

Symbols

‖ All Quadcopter vehicles (Electric, Hybrid & Turboshaft)
\# Quadcopter Hybrid vehicle only
‡ Quadcopter Hybrid (1 unit) and Turboshaft (2 units) vehicles
§ All Collective Control vehicles only
† All Electric or Hybrid-Electric vehicles
|| Quadcopter Turboshaft vehicle only
* For Cooling System components, see EM Liquid Cooling
‡‡ Not included in vehicle failure-rate calculations

Acronyms

ACT : Rotor Actuation System
CGB : Central Gearbox
CS : Cross-shaft System
ED : Electric Drive or Propulsor
EDS : Energy Distribution System
EM : Electric Motor
EMA : Electromechanical Actuator
ESC : Electronic Speed Controller
FCC : Flight Control Computer
GEN : Generator
GTE : Gas Turbine Engine
N : Total number of units (4, 6 or 8)
OVRC : Overrunning Clutch
PAG : Parallel Axis Gearbox
RGB : Rotor Gearbox
TS : Transmission System

Figure 17: Overview of the Systems and Components considered in the Safety Analysis

Failure rates of electrical and mechanical components for this study (Figure 17) are taken from the Nonelectronic Parts Reliability Data publication (NPRD-2016) [25], RVLT Boeing study [8], and other similar sources in the literature. NPRD-2016 database provides historical reliability data to augment reliability prediction. The NPRD dataset was collected from the early 1970's through 2014 from sources including published reports and papers, government-sponsored studies, military maintenance data collection systems, commercial warranty repair systems and maintenance databases, and other failure databases

maintained [25] by commercial or military organizations. While there are numerous entries for each type of part or assembly within the NPRD-2016 database, the most applicable part summary is chosen whenever possible to be used in the analysis. The summary failure rates (as reported in) were derived by combining failure rates on similar parts/assembled from various sources. Almost all the part summaries chosen represented parts of military quality level described in NPRD-2016 as being procured in accordance with MIL-217 handbook specifications [26]. In addition, the application-based operating environment was also considered. Whenever possible, parts identified as being used in rotorcraft were chosen and failing that, parts identified as being used in an aircraft were chosen. The NPRD-2016 database also reports total population and operating time for each entry. In some of the part summaries chosen, the dataset includes no recorded failures. In these instances, the failure rate is estimated by assuming one failure for the sum of the total operating hours as a worse case failure rate. Table 13 summarizes the component failure rates and their sources.

Table 13: Failure rate and related sources used for the analysis

Component	Base failure rate (1/hr)	Source
Actuator (EMA)	5.49E-5	[25]
Gas Turbine Engine (GTE)	6.48E-6	[27]
AC generator (GEN)	4.30E-6	[25]
Gearbox (RGB, CGB, PAG)	4.23E-7	[25]
Clutch (OVRC)	4.23E-7	[25]
Cross-shaft (CS)	7.15E-7	[25]
Lithium-Ion battery*	5.61E-6	[28, 29, 8]
Low Voltage battery	1.01E-5	[8]
Electronic Sensors	1.76E-7	[30]
Electric Motor* (EM)	9.24E-7	[8], [25]
Electronic Speed Controller (ESC)	5.40E-6	[8], [25]
Contactor, fuse	1.49E-7	[25], [30]
Connection failure	1.39E-7	[25]
Liquid cooling	4.30E-6	[25]
Air cooling	1.03E-6	[25]

2.5.2 System Reliability Assessment

In this section, we will discuss system safety assessment performed to supplement the static fault Tree analysis and dynamic event tree analysis. For the FTA, component failures that result in loss of function of the relevant system are considered. An aircraft system usually includes hundreds and sometimes thousands of components, each exhibiting its own complex failure modes. From the transient vehicle analysis perspective, it is beneficial to group the failure modes by their system-level effects, since the vehicle simulator only uses overall system-level inputs to predict the aircraft behavior. FME(C)A tables

were used to identify system level effect of the failure modes and to calculate failure rates based on those effects. In following subsections, failure modes and their effects will be considered the systems of interest.

2.5.2.1 Electric drive (ED) system

For this study, a detailed safety assessment has been developed for the electric drive components, such as electric machine (or motor), electronic speed controller, electronic power distribution and energy storage system. Multiple literature sources, including handbooks and manuals have been analyzed for this purpose [31, 32, 33, 34, 35, 36, 37, 38, 28, 39] [40, 8]. The summary of the literature review is provided in the 0. For example, a failure rate of 9.24e-7 per hour is defined for the electric and mechanical failures of the electric machine [8]. For each failure type, multiple causes of failure are identified (e.g. high voltage, overcurrent, voltage transient, etc.). For each cause of failure, the higher-level effects in the component are postulated as well (e.g. stator short circuit, stator open circuit, rotor demagnetization, etc.). Probability is assigned to each higher-level failure effect. Two failure modes of the cooling system are identified: complete failure resulting in the failure of the electric machine and partial failure of the cooling system corresponding to the failure of the stator, rotor or core. Similar approach is used for other components of the electric drive.

From the provided summary of the electronic component faults, it is clear that a multitude of faults can happen in electric machines (EM), electronic speed controller (ESC), electronic power distribution (EPD) and lithium-ion battery pack (BP). The development of accurate models of all the possible faults that may occur in an electric propulsion system can be sometimes necessary, however for the scope of this work and considering the computational requirements of DET simulations, the team decided to categorize the component-level faults on the basis of the effect at the electric drive (ED) level under different categories as reported in 0:

1. **No torque** – For example, this condition can be observed in case of complete failure of the cooling system for ESC, EM, or battery pack with shutdown due to overtemperature, which causes no torque output for the ED.
2. **Low torque** - Internal battery failure (such as cell short circuit) is one such example case, that can lead to a low torque output for the ED due to lower voltage or capacity. Fault severity levels (SLs) of 1, 2 and 3 are considered which result in the low torque magnitude of 85%, 30% and 10% of reference torque respectively.
3. **Torque ripple** – A fault in the current or speed sensor of the powertrain can lead to oscillation in the torque output while the average torque still meeting the torque request. Fault severity levels of 1, 2 and 3 are considered..
4. **High torque** – An electric distribution failure due to failure-to-open of a contactor can cause a high torque output for the ED. Fault magnitude of 0.85 has been considered.
5. **Short circuits modes:** Three short circuit modes are considered to take into account for single phase, two-phase, three-phase short circuits and including the response of the ESC.
    - **Mode 1 - Torque transient** – After a short circuit, the ESC or the vehicle supervisory control may turn-off the ED causing the high torque condition to be eliminated. Severity level 1.5 has been considered.

- **Mode 2 - High torque oscillations** - This condition is observed when short circuit occurs in EM winding or ESC. Severity levels 1.5 and 2.5 have been considered.
- **Mode 3 – Dumped torque oscillations** - This condition is observed when short circuit occur in EM winding or ESC. Severity level 1.5 has been considered.

2.5.2.2 Rotor actuation system (ACT) failures

Due to the growing trend in more electrified aircraft, electromechanical actuators (EMA) are becoming more popular in aerospace applications. Without the need for hydraulic plumbing, EMAs are less maintenance intensive and costly compared to hydraulic actuators [41].

Using data from the NPRD library for each component within an EMA, the average failure rate of commercial off-the-shelf EMAs can be estimated to be approximately 54.96 failures per million hours. Existing work studying failure of EMAs on small UAVs lead to the identification of six failure modes: bias, stuck surface, hard-over, floating surface, oscillations, and increased dead-band [42]. These different failure modes are used for static reliability (FMECA and FTA) analysis.

However, not all of the identified failure modes of EMA are included in the DET analysis. Only the failure modes which are within the bounds of the simulation models and/or the modes that impact the transient vehicle response are considered. The behavior of EMA caused by bias can vary based on whether the bias causes a constant or drifting error and the magnitude of the bias itself. A comprehensive simulation of bias is out of the scope of this work. Similarly, the oscillations caused by hardware or software related issues also vary in their behavior and no concrete characterization of such behavior would be sufficiently representative of typical EMAs. Hard-over and stuck surface failures are not included since the total inability to control rotor pitch can be assumed to cause catastrophic failure for multirotor configurations and hence transient analysis is not necessary for such failure modes. Two actuator failure modes (or end-effects) are considered for the DET analysis: floating surface and increased dead-band. The details of the implementation of each failure mode is described in Section 4.5.

2.5.2.3 Transmission system (TS) failures

The transmission failures are attributed to following three components:

i) Gear failures
ii) Shafts and Shaft bearings related failures
iii) Overrunning Clutch failures

A detailed literature review [43] [44] [45] [46] [47] [48] [49] [50] resulted in the classification of transmission related failures by one of the following two main causes:

a) Overload or fatigue related failures
b) End of life/wear related failures

A study [51] based on the historical data of the helicopter transmission related accidents also identified overload or fatigue related failures as the primary cause of accidents. These fatigue failures usually are attributed to inadequate maintenance or vehicle operation in overload conditions due to pilot error. Such catastrophic failures are considered for static reliability analysis. Various modes of failure of the transmission components are described in detail in the FMECA tables in Appendix B.

For the DET analysis, wear related soft failures of the transmission components that result in efficiency losses are considered, since transient analysis of such failures can provide more interesting insights into their effect on overall vehicle dynamics. Only exception to this rule is made while considering the cross-shafting failures; a fatigue or overloading related failure of a bearing or shaft is considered since such failure will cause a rotor to isolate from the cross-shafting system, but may not necessarily result in the catastrophic outcome as long as there are no severe faults occurring simultaneously in the isolated rotor driveline. The soft failures related to the transmission are analyzed in isolation as well and as in combination with other systems faults (e.g. ED or ACT faults).

2.5.2.4 Gas turbine engine (GTE) and Generator (GEN) failures

A complex system like gas turbine engine has hundreds of failure modes. There are extensive studies that provide insights into the critical components of a gas turbine engine and their failure modes and effects [52]. However, for this study, only complete loss of function of the engine is considered to compare and contrast the quadcopter turboshaft and hybrid vehicles' response to the OEI condition. Similarly, the literature review suggests that despite the many root causes of turbine generator failures, the primary end-effect of such failures is a loss of power production efficiency [53] [54]. For the DET analysis, this effect is simulated by reducing overall generator efficiency by introducing 10%, 30% and 85% losses with respect to the reference power output; the faults are assigned three severity levels SL1, SL2 and SL3 respectively.

Table 14 summarizes all system level failure effects and their failure rates derived from FME(C)A tables.

Table 14: Dynamic Event Tree Analysis Failure Effects and Failure Rates

System/Component	Effect Type	FR (1/hr)
Electric Drive (ED)	ED - No Torque	9.39E-06
	ED - Low Torque **[SL-1, SL-2, SL-3]**	5.34E-06
	ED - High Torque **[SL-3]**	3.05E-07
	ED - Torque Ripple **[SL-1, SL-2, SL-3]**	2.15E-06
	ED - Short Circuit **[SL-2, SL-3]**	2.05E-06
Transmission System*(TS) (includes Cross-shaft System & RGB)	CS - Isolated Motor	3.57E-07
	TS - Soft failure **[SL-1, SL-2, SL-3]**	4.28E-06
Transmission System‡ (TS) (includes RGB)	TS - Soft failure **[SL-1, SL-2, SL-3]**	1.41E-07
Rotor Actuation System (ACT)	ACT-1 (Rate limit)	2.19E-05
	ACT-2 (Deflection limit)	1.20E-10
Gas Turbine Engine (GTE)	No Torque (OEI)	3.03E-07
Generator (GEN)	GEN **[SL-1, SL-2, SL-3]**	5.26E-07

* Applicable to all quadcopter vehicles
‡ Applicable to all hexacopter and octocopter vehicles
SL Failure Severity Level
RGB Rotor Gear Box
CGB Central Gear Box
CS Cross-shafting System

2.5.3 Failure rate model of electric components

The failure rate λ of an electric component (electric machine, power electronics, actuators), which does not operate under the reference (nominal) conditions, can be calculated as following [55, 56]:

$$\lambda = \lambda_{ref} \cdot \pi_U \cdot \pi_I \cdot \pi_T \quad (4)$$

where λ_{ref}=reference failure rate at nominal conditions, π_U=voltage dependent factor, π_I=current dependent factor, π_T=temperature dependent factor.

This stress model allows extrapolation of failure rates from reference conditions to other operating conditions considering voltage, temperature and current stresses. This model is especially helpful to compare the system level reliability considering different design choices and the related impact on the component's failure rate. As example, this model can be helpful to predict the failure rate of a 600V powertrain versus a 300V powertrain in which the same components are operated.

Some models are reported in literature for the stress factors, however these models are usually empirical and derive from the fitting of experimental data. IEC 61709 and MIL-217 report some examples and related calibrations. As an example, the failure rate model used for the electric machines and power electronics is illustrated in Figure 18 [57, 58, 59].

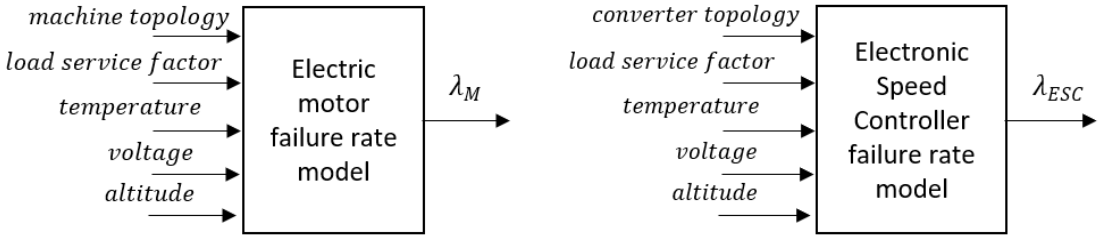

Figure 18: Example of failure rate model of electric motor and electronic speed controller

The total motor system failure rate (λ_M) is the sum of the failure rates of each of the parts in the motor:

$$\lambda_M = (\lambda_{Stat} + \lambda_{Rotor} + \lambda_{Mech} + \lambda_{Cool}) \cdot \pi_U \cdot \pi_I \cdot \pi_T \quad (5)$$

where λ_{Stat} = Failure rate of electric motor windings and core; λ_{Rotor} = Failure rate of permanent magnets; λ_{Mech} = Failure rate of the mechanical system (bearing, shafts, eccentricity, vibrations, defects); λ_{Cool} = Failure rate of the cooling system.

The total electronic speed controller (ESC) failure rate (λ_{ESC}) is the sum of the failure rates of each of the parts in the ESC:

$$\lambda_{ESC} = (\lambda_{Inverter} + \lambda_{DC\,cap} + \lambda_{Control} + \lambda_{Cool}) \cdot \pi_U \cdot \pi_I \cdot \pi_T \quad (6)$$

Where $\lambda_{Inverter}$= Failure rate of power semiconductors; $\lambda_{DC\ cap}$= Failure rate of DC capacitors; $\lambda_{control}$= Failure rate of ESC controller (including sensors).

The total energy storage system (ESS) failure rate (λ_{ESS}) is the sum of the failure rates of each of the parts in the ESS:

$$\lambda_{ESS} = (\lambda_{cell} + \lambda_{BMS} + \lambda_{Cool}) \cdot \pi_U \cdot \pi_I \cdot \pi_T \quad (7)$$

where λ_{cell} = Failure rate of lithium-ion cells; λ_{BMS} = Failure rate of the battery management system (BMS); λ_{Cool} = Failure rate of the cooling system.

The total electronic distribution system (EDS) failure rate (λ_{EDS}) is the sum of the failure rates of each of the parts in the ESS:

$$\lambda_{EDS} = (\lambda_{fuse} + \lambda_{contactor} + \lambda_{connection}) \cdot \pi_U \cdot \pi_I \cdot \pi_T \quad (8)$$

where λ_{fuse} = Failure rate of fuses; $\lambda_{contactor}$ = Failure rate of contactors; $\lambda_{connection}$ = Failure rate of connections.

3 VEHICLE ARCHITECTURE OVERVIEW

Analyzing an UAM vehicle's safety requires more information than what is provided by a general vehicle configuration description. Information on significant components and how the components interact with each other is necessary. In general, such information is not available in a vehicle configuration description. For example, the information on the components and their connections is needed TO calculate the vehicle's overall static safety. Moreover, the same information outlines what is necessary in a transient simulation environment to be developed for analyzing the vehicle's safety in transient operation. Necessary vehicle architecture details for static and transient safety analysis are provided with two diagrams: a rotating component diagram and a flight control system diagrams. Both are provided for each of the six concepts covered in this report.

The rotating component diagram includes two types of the components. One type of component converts a source of energy into kinetic energy like an electric motor or gas turbine whereas the other component type is a link of the chain which transmits the generated kinetic energy to the vehicle rotors like gears and shafts. On the other hand, the flight control system diagrams integrate the rotating component diagrams with the flight controller, actuators, sensors, and other important nonrotating components like batteries. The rest of this section introduces and discusses the rotating component and flight control system diagrams for each one of the six concepts in separate subsections starting with the electric quadcopter.

3.1 Electric Quadcopter

Figure 19 provides the rotating component diagram for an electric quadrotor concept which uses collective control. The planetary gears between the electric motors and rotors reduce the rotational speed at the electric motor exit to the rotor rotational speed. This speed reduction is one of the two purposes of mechanical power train as stated earlier. The bevel gears between the electric motors and the planetary gears direct some of the electric motor power to a cross-shafting system which provides an alternative power supply path for all the rotors when one of the electric motors fails. This is the second listed purpose of a mechanical powertrain system. If a quadcopter rotor stops spinning in flight, such an event causes a catastrophic failure due to loss of control. Therefore, the cross-shafting system in Figure 19 is proposed to keep all the rotors powered when an electric motor fails.

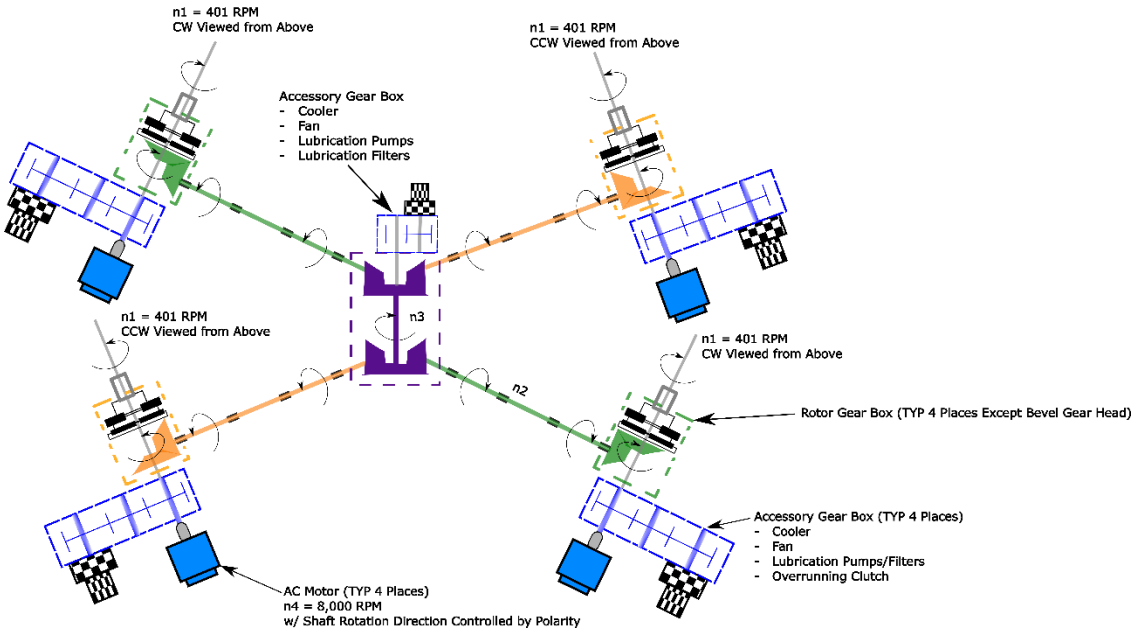

Figure 19 Rotating components diagram for the electric quadrotor concept with collective control

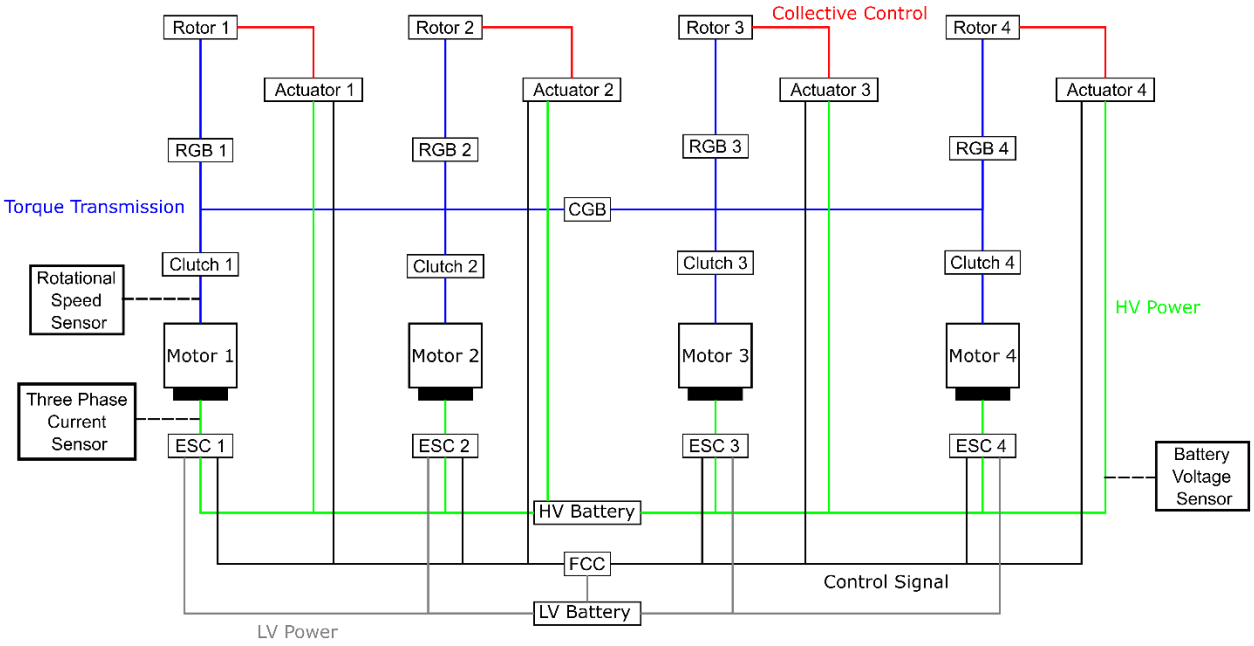

Figure 20 Flight control system diagram for the electric quadrotor concept with collective control

3.2 Hybrid Electric Quadcopter

Figure 21 shows the rotating components diagram for a series hybrid quadrotor with collective control. The mechanical powertrain in Figure 21 reduces the electric motor rotational speed to the rotor rotational speed with planetary gearboxes like the electric quadcopter in Figure 19. Moreover, the cross-shafting system is the same as the system and ready to provide alternative power paths when needed. The only difference between the quadrotor concepts is the turboshaft engine and the electric generator attached to the turboshaft. The series hybrid concept replaces most of the batteries in the electric quadrotor concept with the turboshaft and generator couple for electricity production.

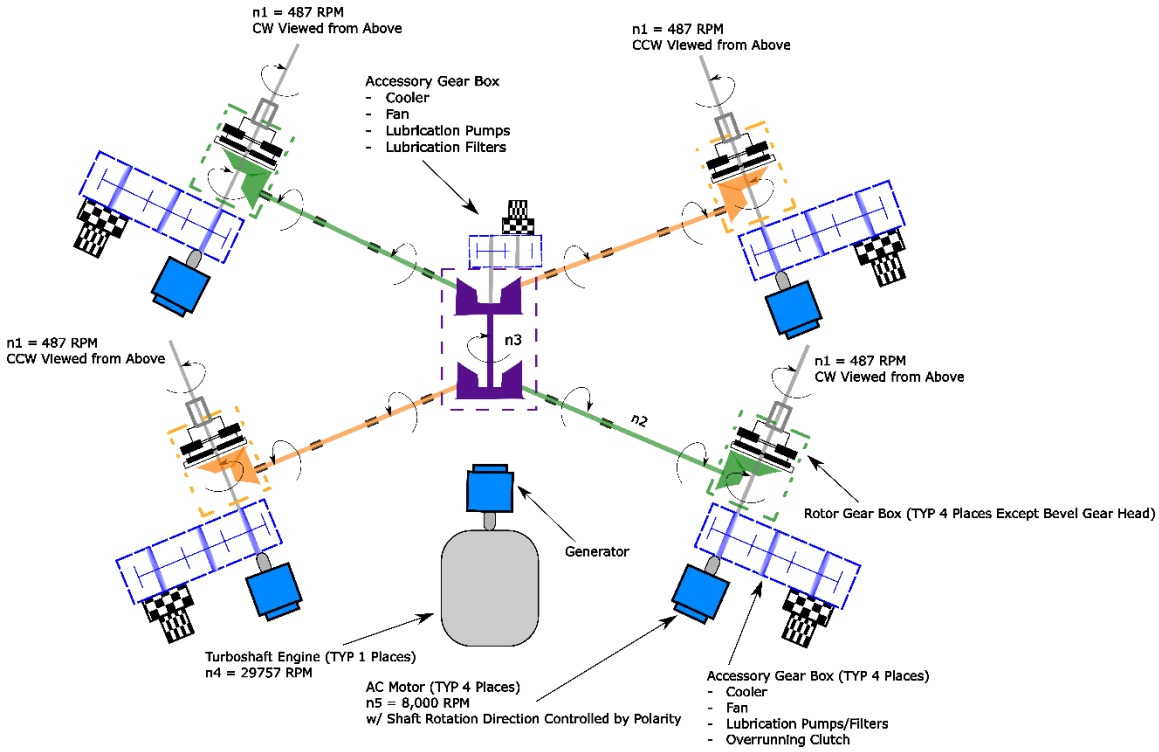

Figure 21 Rotating components diagram for the series-hybrid quadrotor concept with collective control

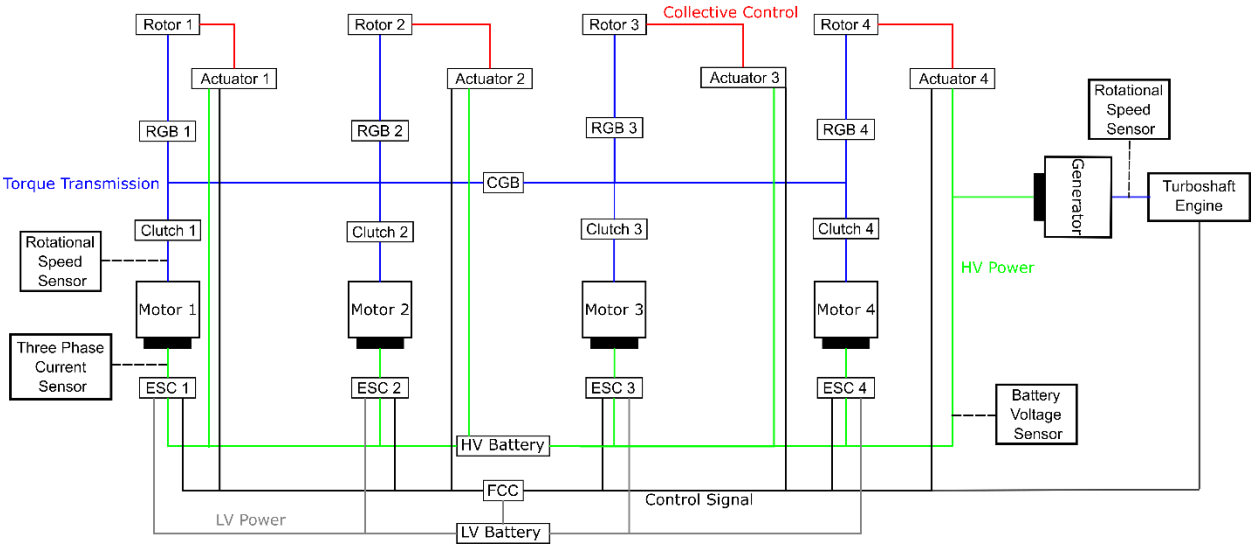

Figure 22 Flight control system diagram for the series-hybrid quadrotor concept with collective control

3.3 Turboshaft Quadcopter

In contrast, Figure 23 introduces a different quadrotor concept with respect to the concepts in Figure 19 and Figure 21. The rotating components diagram in Figure 23 is for a collective control quadrotor with two turboshaft engines. The electric motors in the previous two concepts were replaced with two turboshafts. The power generated by the two gas turbines are blended with a series of gears. Then, the blended power is provided to each rotor through the central gearbox and the cross-shafts attached to the central gearbox. As the generated power is blended and transmitted, the rotational speed is reduced from the turboshaft value to the rotor value. If a power source fails, the failed gas turbine is disengaged from the powertrain with an overrunning clutch and the remaining gas turbine powers all the four rotors.

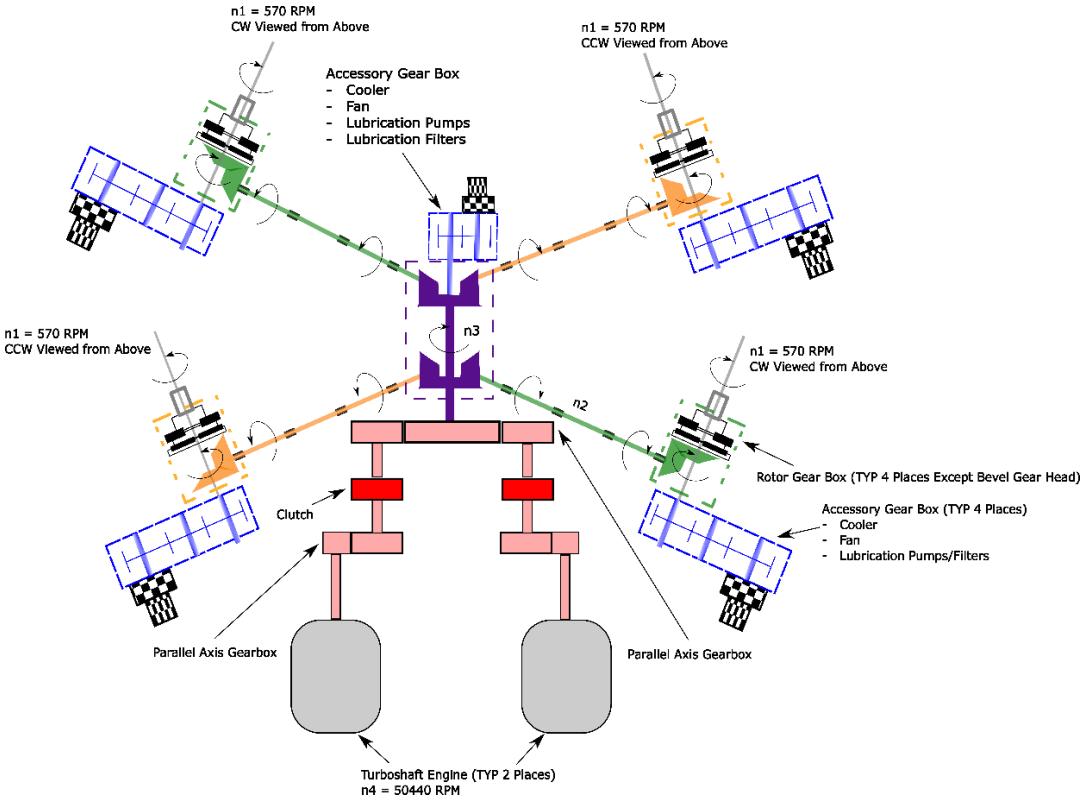

Figure 23 Rotating components diagram for the turboshaft quadrotor concept with collective control

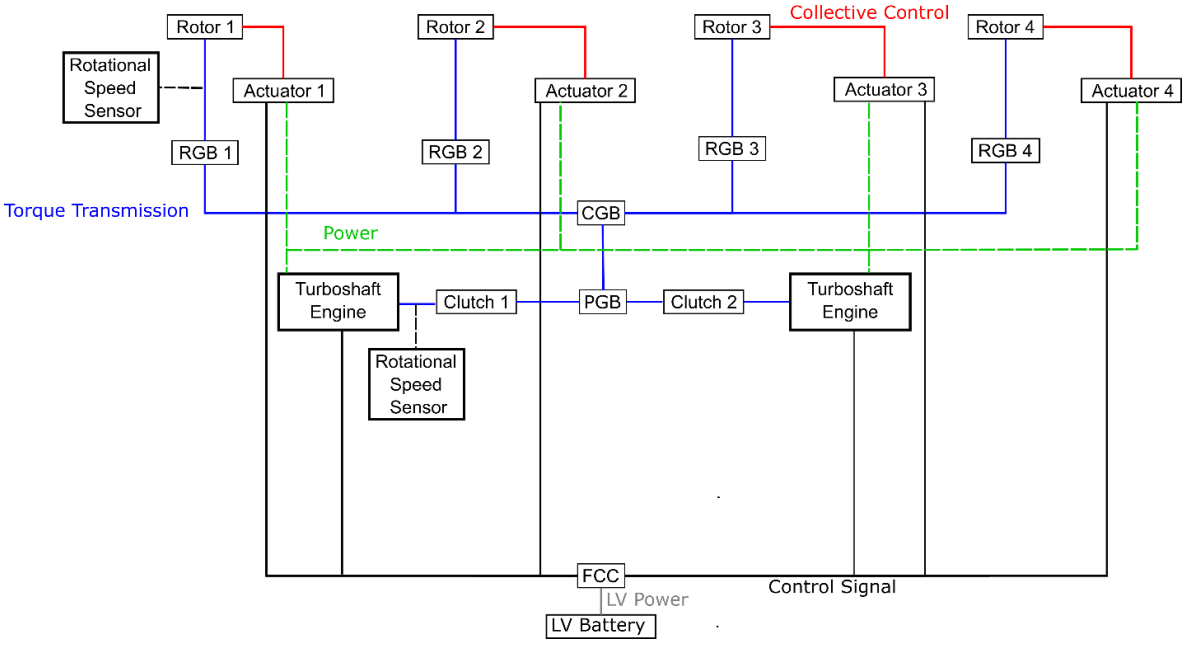

Figure 24 Flight control system diagram for the turboshaft quadrotor concept with collective control

3.4 Hexacopter with Collective Control

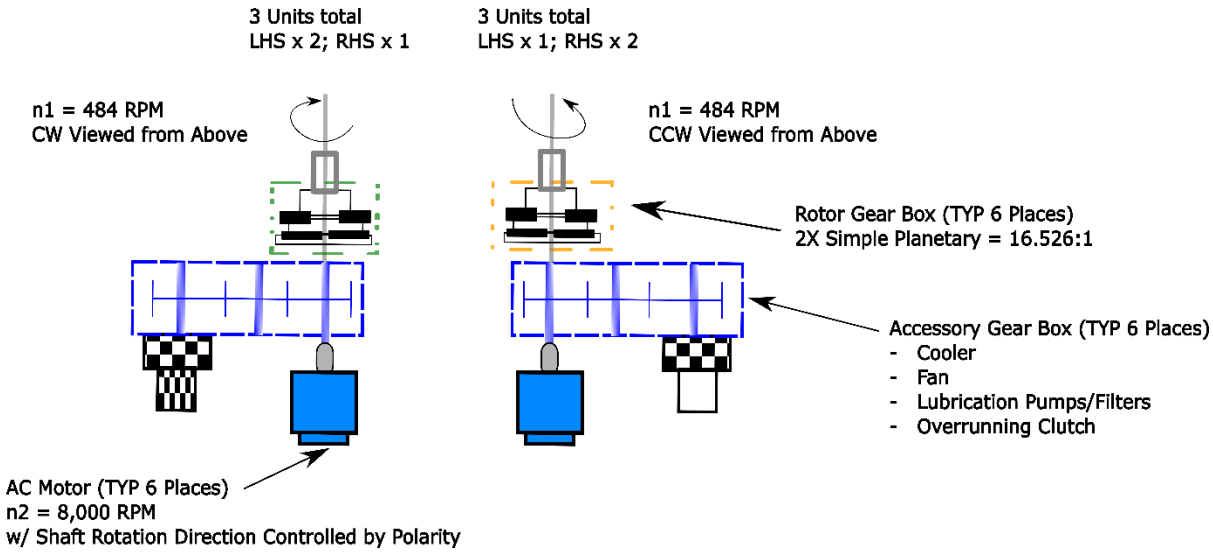

Figure 25 Rotating component diagram for the hexacopter concept with collective control

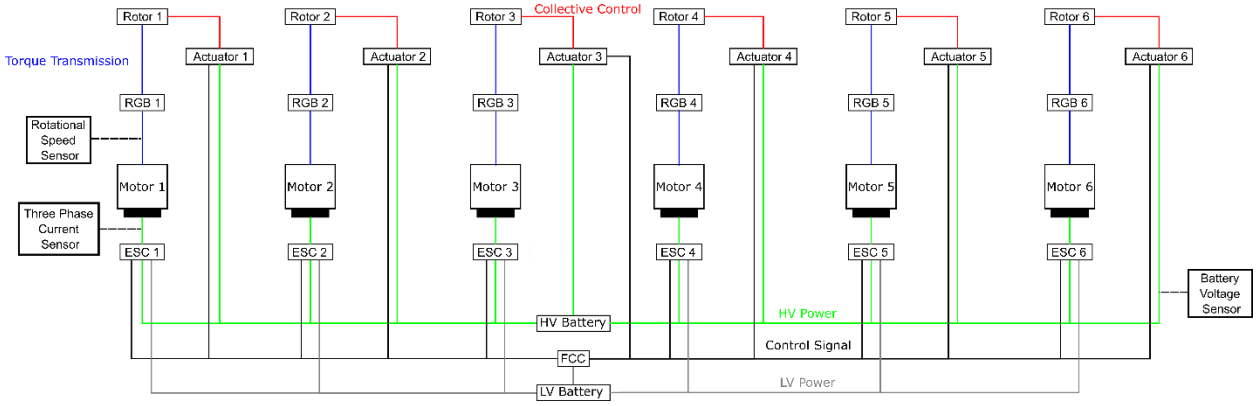

Figure 26 Flight control system diagram for the hexacopter concept with collective control

3.5 Hexacopter with RPM Control

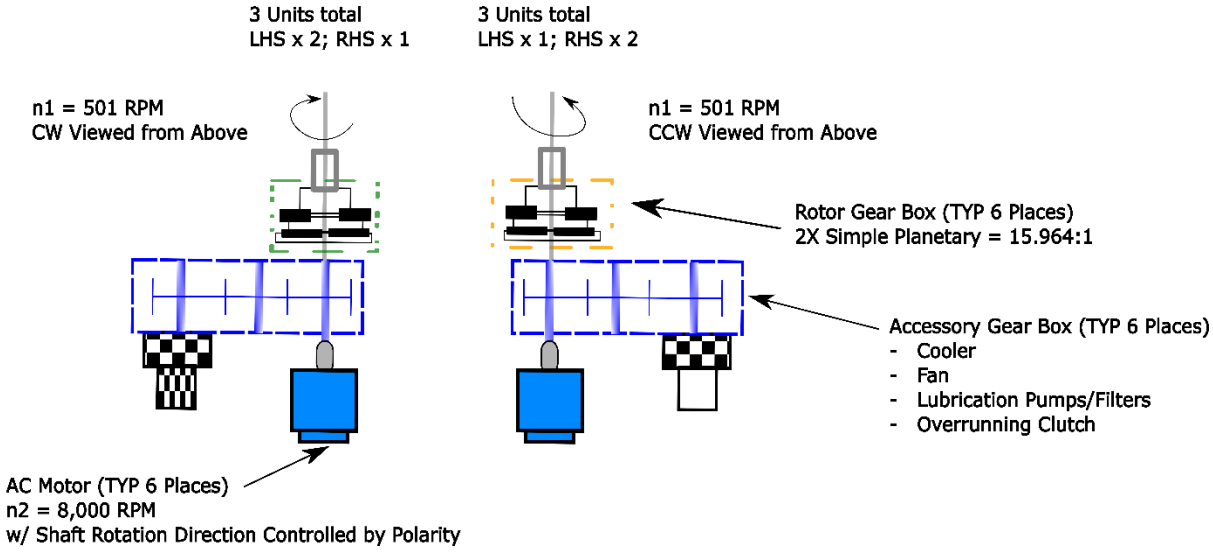

Figure 27 Rotating component diagram for the hexacopter concept with RPM control

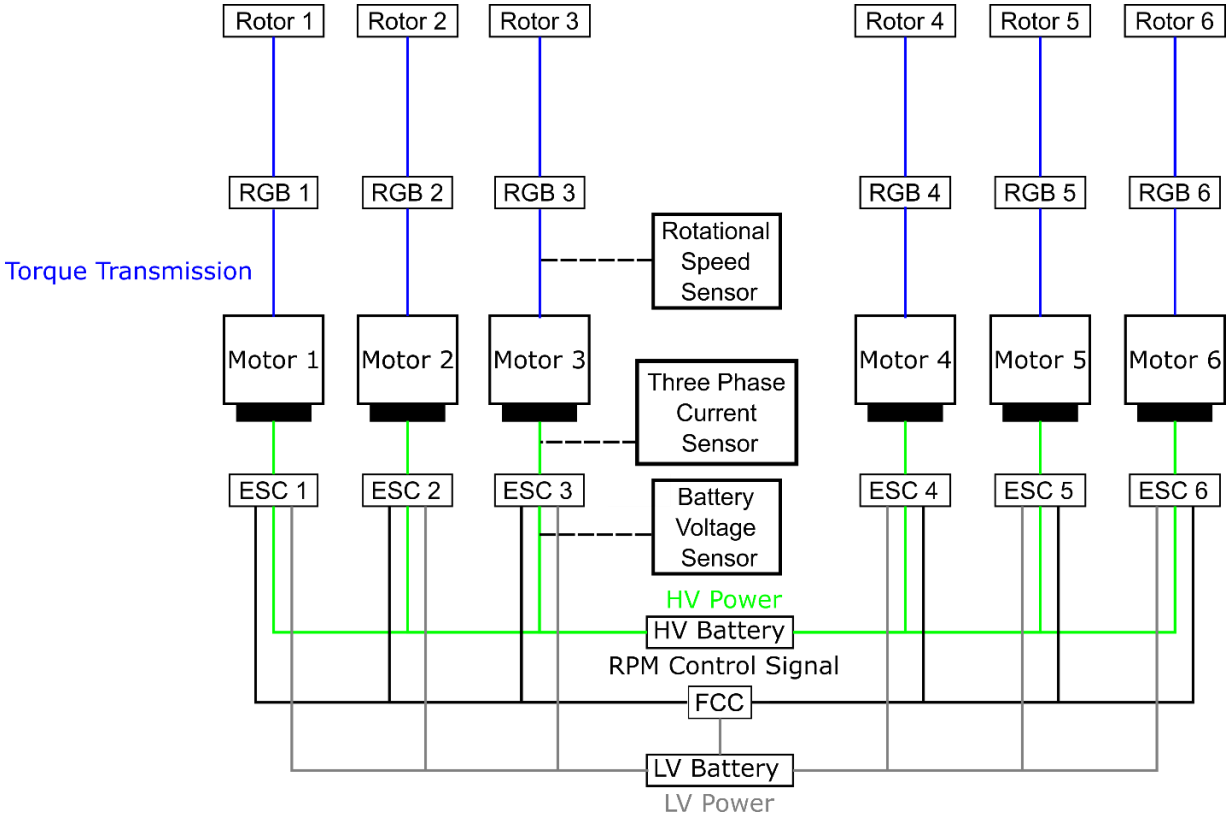

Figure 28 Flight control system diagram for the hexacopter concept with RPM control

3.6 Octocopter

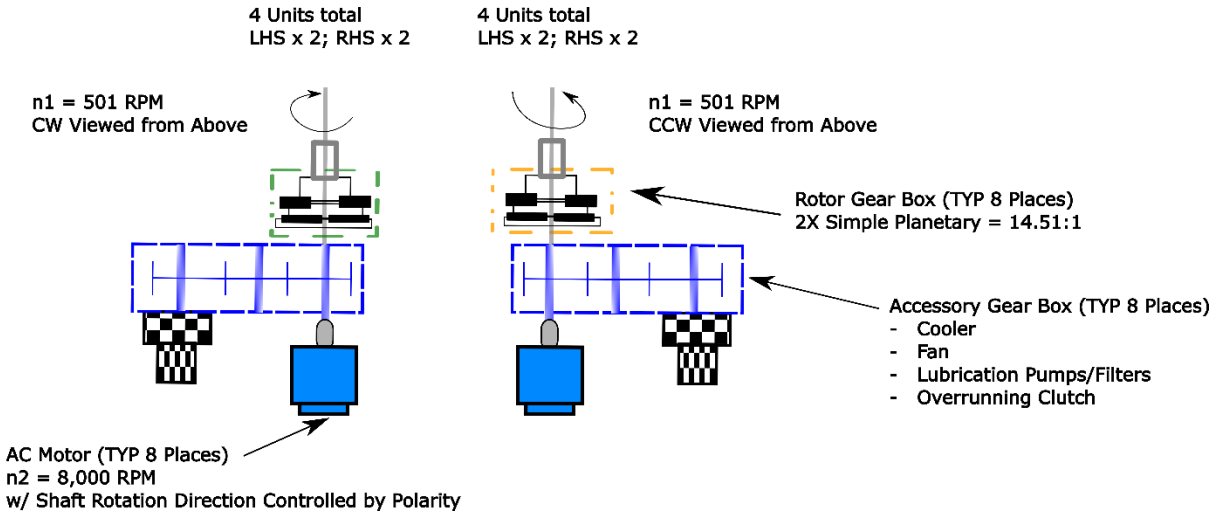

Figure 29 Rotating component diagram for the octocopter concept with RPM control

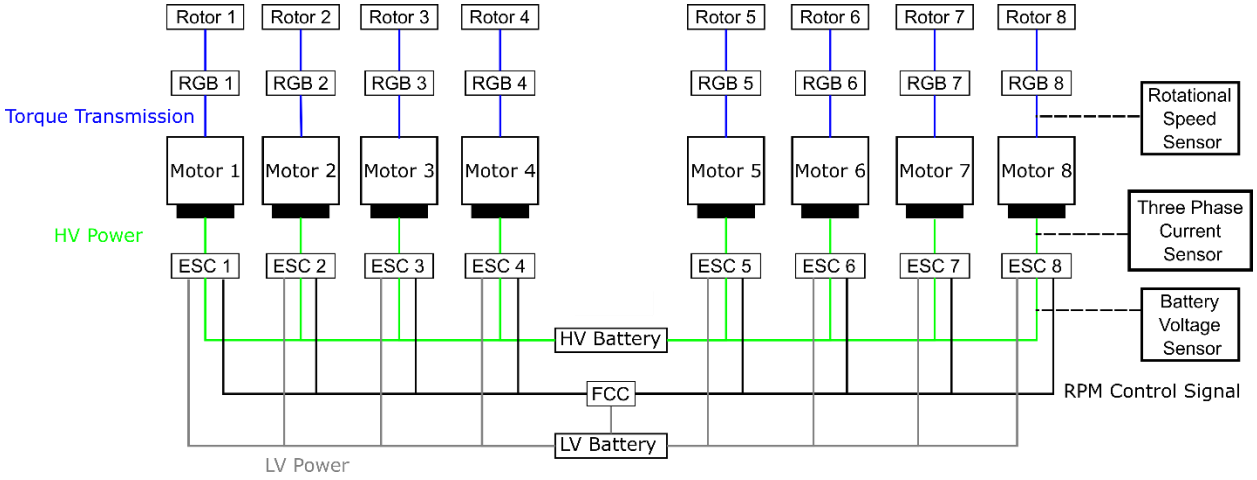

Figure 30 Flight control system diagram for the octocopter concept with RPM control

4 VEHICLE AND SYSTEM MODELING

This section presents details of the simulation model developed to complete the DET. As shown on Figure 31, the dynamic simulation environment include a wind model, a guidance and navigation module, a controller, and the aircraft dynamic include airframe dynamics, a transmission model, electric drives, batteries and turbine model.

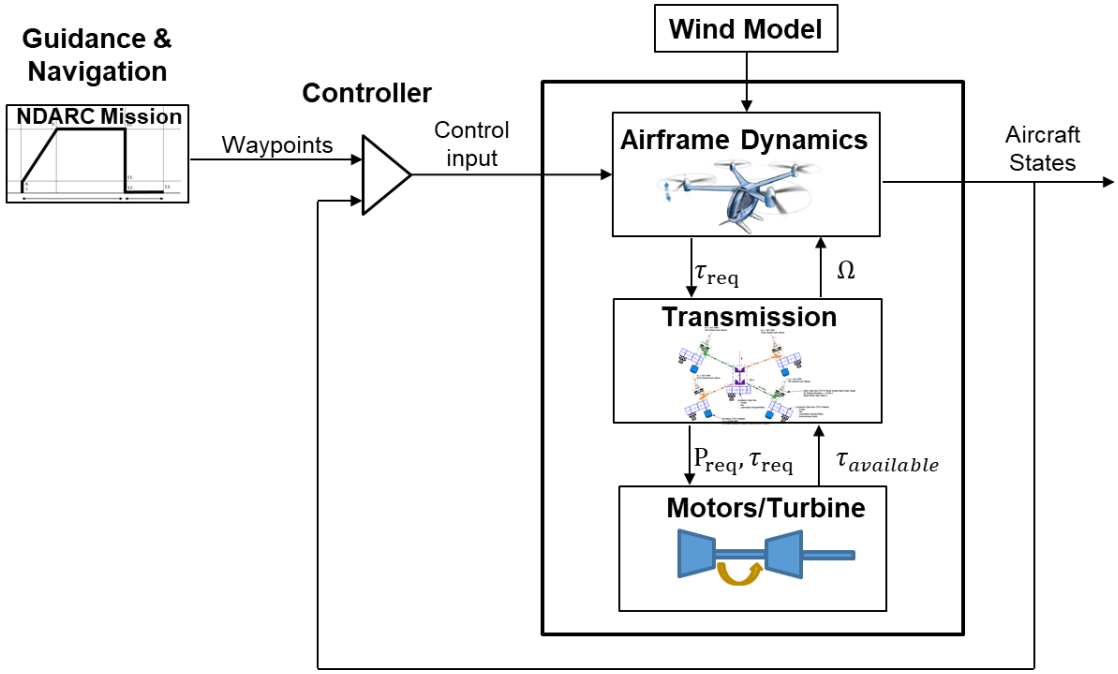

Figure 31 Schematic Representation of the Dynamic Simulation Environment

4.1 Airframe dynamics

The airframe dynamics model provides the dynamics of the airframe and the flapping angles. The following sections describes the use of the NASA provided linear dynamic models, the description of the mission modeled by the aircraft, the trim analysis and the wind profile used for the analysis.

4.1.1 Review of NASA Linear Dynamics Model

The starting point for the vehicle model is the airframe dynamic model. The model is based on the SIMPLI-FLYD ('SIMPLIfied FLight dynamics for conceptual Design') dynamic models provided by NASA [60]. A schematic representation of the dynamic model is illustrated on Figure 32: the dynamic response of the aircraft is provided as a function of the current states, control input, torque input at the rotor and wind condition. The dynamic model is provided as piecewise with advancing velocity linear coefficient about the trimmed conditions.

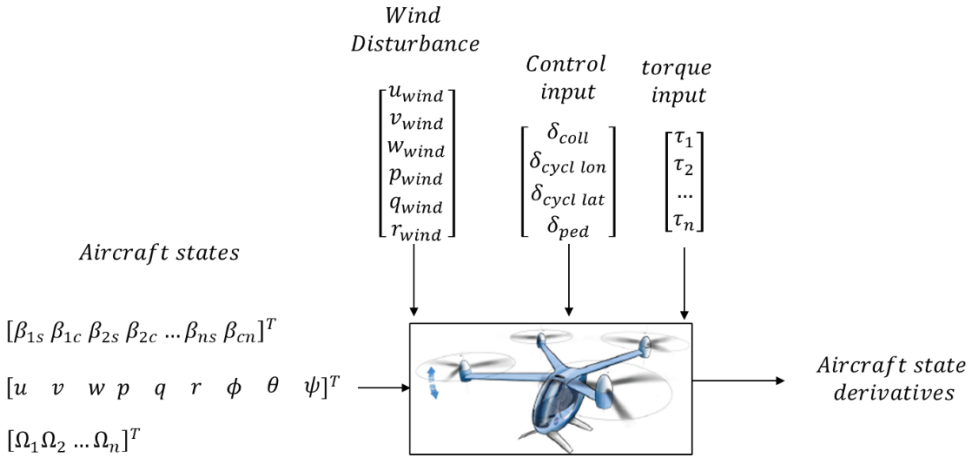

Figure 32 Schematic representation of the airframe dynamics

The models are in state-space form:

$$\dot{\boldsymbol{x}} = \boldsymbol{A}\boldsymbol{x} + \boldsymbol{B_1}\boldsymbol{u} + \boldsymbol{B_2}\boldsymbol{w} \quad \textbf{(9)}$$

With $\boldsymbol{x}$, the state vector, $\boldsymbol{u}$, the control input and $\boldsymbol{w}$, the external disturbance. With $\boldsymbol{A}$, the system dynamics matrix, $\boldsymbol{B_1}$, the input matrix and $\boldsymbol{B_2}$, the external disturbance matrix. A summary of the states and control input is provided in Table 15 where n is the number of rotors.

Table 15 A summary of the states, control inputs and external disturbances

Symbol	Definition	Symbol	Definition
u	Horizontal velocity body frame	$\beta_{1s}, \beta_{1c}, \beta_{2s}, \beta_{2c}, \dots, \beta_{ns}, \beta_{nc}$	Blade flapping coefficients
v	Sideways velocity body frame	$\Omega_1, \Omega_2, \dots, \Omega_n$	Angular rotor velocity
w	Vertical velocity body frame	$\tau_1, \tau_2, \dots, \tau_n$	Rotor input torque
p	Roll rate	$u_{wind}, v_{wind}, w_{wind}$	Wind velocity in u, v, w direction
q	Pitch rate	$p_{wind}, q_{wind}, r_{wind}$	Wind angular velocity in p, q, r direction
r	Yaw rate	δ_{coll} (u_0)	Collective pitch input
ϕ	Roll angle	$\delta_{cycl\ lon}$ (u_c)	Cyclic longitudinal pitch input
θ	Pitch angle	$\delta_{cycl\ lat}$ (u_s)	Cyclic lateral pitch input
ψ	Yaw angle	δ_{ped} (u_{ped})	Anti-torque pedal input

A coordinate frame definition for the translational and angular velocities in the vehicle body frame can be seen in Figure 33.

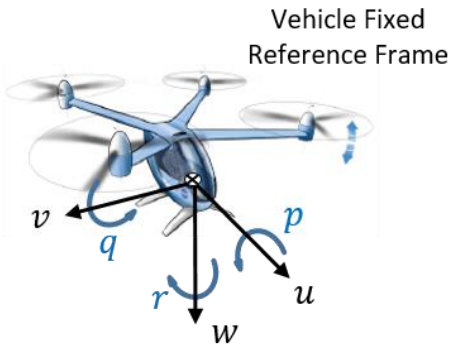

Figure 33 Translational and angular velocity definition in the vehicle body frame

The motor definition and rotor spin direction are defined for the quadrotor vehicles, hexacopter vehicles and octocopter vehicle can be seen in Figure 34, Figure 35 and Figure 36 respectively. The torque direction at the rotor level is in the opposite direction of the rotor spin.

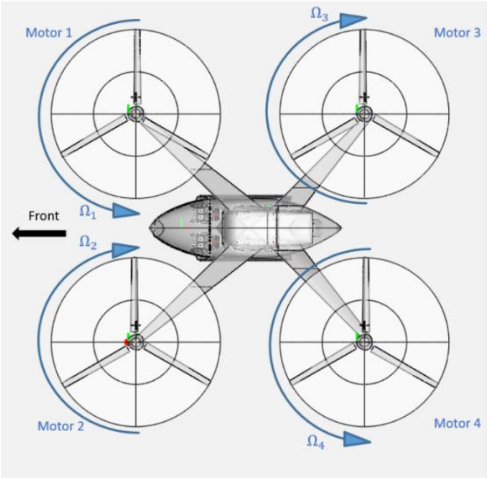

Figure 34 Quadcopter Vehicles Motor Definition and Rotor Spin Direction

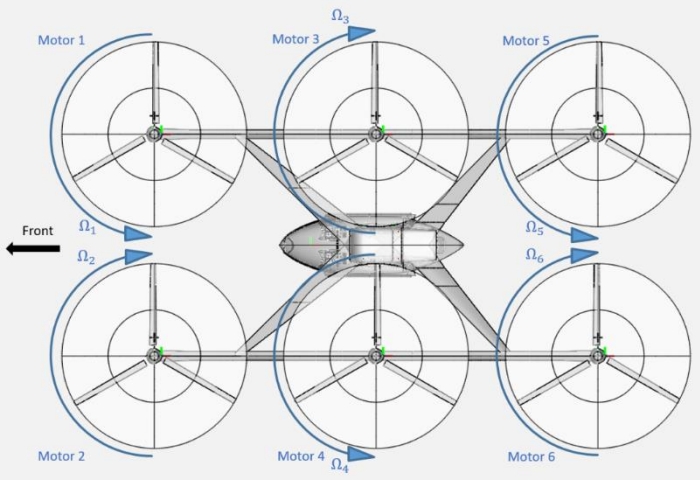

Figure 35 Hexacopter Vehicles Motor Definition and Rotor Spin Direction

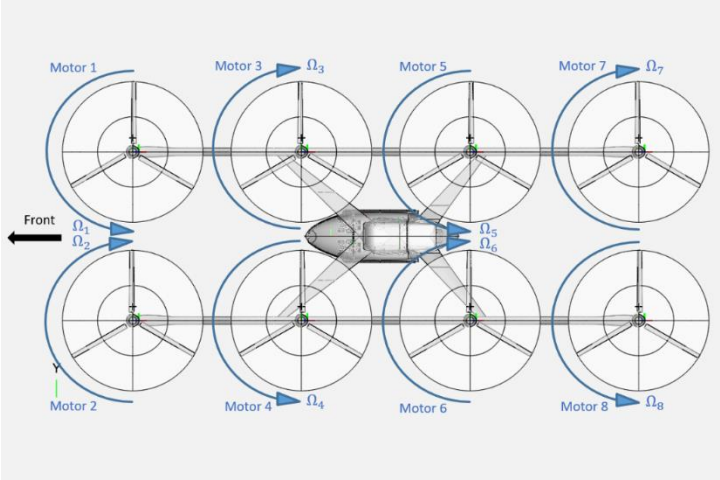

Figure 36 Octocopter Vehicles Motor Definition and Rotor Spin Direction

4.1.1.1 States

The previous section introduced the NASA provided linear dynamic models. The state and control input vectors are defined differently for the various vehicle configurations. An overview of the state vector, control input vector and wind vector for the various vehicles is shown below.

Quadrotors:

$$x = \begin{bmatrix} \beta_{1s}, \beta_{1c}, \beta_{2s}, \beta_{2c}, \beta_{3s}, \beta_{3c}, \beta_{4s}, \beta_{4c}, \\ \Omega_1, \Omega_2, \Omega_{,3}, \Omega_4, u, v, w, p, q, r, \phi, \theta, \psi \end{bmatrix}^T \quad (10)$$

$$u = \left[u_0, u_c, u_s, u_{ped}, \tau_1, \tau_2, \tau_3, \tau_4\right]^T \quad (11)$$

$$w = [u_{wind}, v_{wind}, w_{wind}, p_{wind}, q_{wind}, r_{wind}]^T \quad (12)$$

Hexacopter Pitch Control:

$$x = \begin{bmatrix} \beta_{1s}, \beta_{1c}, \beta_{2s}, \beta_{2c}, \beta_{3s}, \beta_{3c}, \beta_{4s}, \beta_{4c}\ \beta_{5s}, \beta_{5c}, \beta_{6s}, \beta_{6c} \\ \Omega_1, \Omega_2, \Omega_{,3}\ , \Omega_4, \Omega_{,5}\ , \Omega_6, \\ u, v, w, p, q, r, \phi, \theta, \psi \end{bmatrix}^T \quad (13)$$

$$u = \left[u_0, u_c, u_s, u_{ped}, \tau_1, \tau_2, \tau_3, \tau_4, \tau_5, \tau_6\right]^T \quad (14)$$

$$w = [u_{wind}, v_{wind}, w_{wind}, p_{wind}, q_{wind}, r_{wind}]^T \quad (15)$$

Hexacopter RPM Control:

$$x = \begin{bmatrix} \beta_{1s}, \beta_{1c}, \beta_{2s}, \beta_{2c}, \beta_{3s}, \beta_{3c}, \beta_{4s}, \beta_{4c}\ \beta_{5s}, \beta_{5c}, \beta_{6s}, \beta_{6c} \\ \Omega_1, \Omega_2, \Omega_{,3}\ , \Omega_4, \Omega_{,5}\ , \Omega_6, \\ u, v, w, p, q, r, \phi, \theta, \psi \end{bmatrix}^T \quad (16)$$

$$u = [\tau_1, \tau_2, \tau_3, \tau_4, \tau_5, \tau_6]^T \quad (17)$$

$$w = [u_{wind}, v_{wind}, w_{wind}, p_{wind}, q_{wind}, r_{wind}]^T \quad (18)$$

Octocopter RPM Control:

$$x = \begin{bmatrix} \beta_{1s}, \beta_{1c}, \beta_{2s}, \beta_{2c}, \beta_{3s}, \beta_{3c}, \beta_{4s}, \beta_{4c}\ \beta_{5s}, \beta_{5c}, \beta_{6s}, \beta_{6c}, \beta_{7s}, \beta_{7c}, \beta_{8s}, \beta_{8c} \\ \Omega_1, \Omega_2, \Omega_{,3}\ , \Omega_4, \Omega_{,5}\ , \Omega_6, \Omega_{,7}\ , \Omega_8, \\ u, v, w, p, q, r, \phi, \theta, \psi \end{bmatrix}^T \quad (19)$$

$$u = [\tau_1, \tau_2, \tau_3, \tau_4, \tau_5, \tau_6, \tau_7, \tau_8]^T \quad (20)$$

$$w = [u_{wind}, v_{wind}, w_{wind}, p_{wind}, q_{wind}, r_{wind}]^T \quad (21)$$

4.1.2 Mission

The NDARC design mission is introduced in Section 1.4 . In order to simulate this mission in the simulation environment, the mission profile can be divided into waypoints of altitude and forward distance covered. The NDARC design mission specifies the rate of climb (ROC) and forward velocity between these defined waypoints and so these will be used to specify the position and velocities the vehicle is required to track in the simulation. Additionally, at certain waypoints a timed hover is required.

4.1.3 Reduced Order Dynamic Model

The dynamic models presented in the previous sections show that some modifications are needed in order to provide useful for vehicle control synthesis. Details about the creation of inverse models, and reduced order dynamic models are shown in Appendix H. [61]

4.1.4 Modification of the linear models for OEI purposes

In order to use the linear dynamic models for conditions with engine inoperative, some additional modules were created.

4.1.4.1 Conversion to individual rotor collective pitch

The linear dynamic models include pitch effect in typical "cockpit" input: collective, cyclic (longitudinal and lateral) and pedal input. In order to include the effect of individual pitch actuators, there is a need to convert the input to individual rotor pitch $\boldsymbol{\theta_i}$.

$$[\theta_1,\ \theta_2, \ldots \theta_n]' = T_1[u_0, u_c, u_s, u_{ped}]' \tag{22}$$

$$[u_0, u_c, u_s, u_{ped}]' = T_2[\ \theta_1,\ \theta_2, \ldots \theta_n]' \tag{23}$$

The conversion matrices are formulated as follows derived from the NASA provided linear model by using the partial derivatives for angular velocity and control input, $\frac{\partial \Omega}{\partial u}$, and are shown in Appendix G.

4.1.4.2 Limit on Inoperative Rotor RPM

One inherent limitation of using linearized models is the inaccuracy that presents itself when the operating point moves away from the model linearization point. This short coming can be seen in this analysis when simulating an inoperative motor. Figure 37 shows the comparison for the typical helicopter thrust calculation where T is the thrust, C_T is the thrust coefficient, ρ is the air density, Ω is the rotor angular velocity, R is the radius of the rotor and A is the rotor disk area, versus the thrust calculation that stems from the application of the linearized models where the relationship between angular velocity and thrust is approximated at the linearization point using a straight line. Comparing these two models highlights a region of negative thrust below $\Omega_0\ /2$. This observation is supported by analyzing the vertical acceleration $\frac{\delta w}{\delta \Omega}$ coefficients in the models. In order to limit the impact of the One Engine Inoperative (OEI), no contribution to the vehicle dynamic is assumed below a rotor speed of $\Omega_0\ /2$. This will prevent the additional penalization in thrust that would exist when setting $\Omega = 0$.

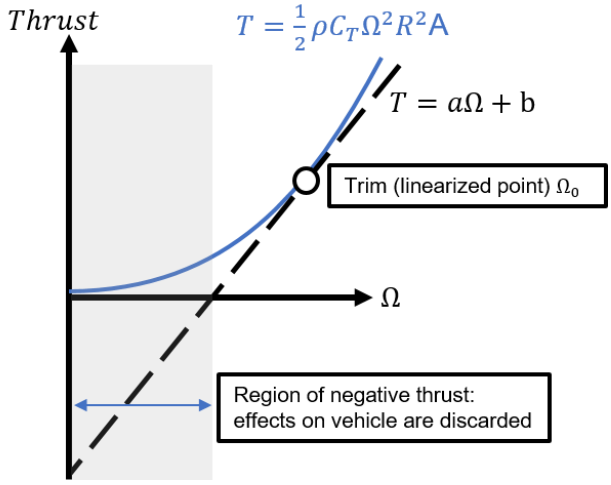

Figure 37 Limit on Inoperative Rotor RPM

4.1.4.3 Rotor inoperative and Pitch Control Allocation

One of the additional limitations of the linear dynamic model is the absence of coupling between the rotor RPM and the pitch control authority. A typical expression for a helicopter rotor thrust is as follows:

$$\boldsymbol{T = \frac{1}{2}\rho C_T \Omega^2 R^2 A} \tag{24}$$

It is apparent in this expression that if $\boldsymbol{\Omega}$ is 0, (no rotation), regardless of the thrust coefficient, the thrust will also be zero. However, in the linear models, there is no coupling between the angular velocity and the rotor pitch which results in the vehicle preserving its pitch control on a rotor even when it is not spinning through $B_1 u$ as seen in Equation (9).

Since the conditions of stopped rotors are of interest for this analysis, there is a need to include a correction for the loss of thrust, and loss of pitch control authority with loss of RPM. The correction can be seen below where the effective pitch angle of the individual rotor, $\theta_{i_{effective}}$, is defined in terms of the trim pitch angle of the individual rotor, $\theta_{i_{trim}}$, the minimum value between the current angular velocity of the rotor and the nominal trim angular velocity of the rotor, Ω_{i}, the nominal trim angular velocity of the rotor, $\Omega_{nominal}$, and the pitch angle of the individual rotor, θ_i.

$$\boldsymbol{\theta_{i_{effective}} = \theta_{i_{trim}} + \frac{\Omega_{\mathrm{i}}}{\Omega_{nominal}} * (\theta_i - \theta_{i_{trim}})} \tag{25}$$

Analyzing Equation (25) shows that for normal operations the division between the angular velocity terms is equal to one which results in $\theta_{i_{effective}} = \theta_i$. However, when the rotor spin slows down and ultimately stops, Equation (25) simplifies to $\theta_{i_{effective}} = \theta_{i_{trim}}$ which results in the desired loss of pitch control authority for the stopped rotor.

4.1.5 Assessment of Airframe Characteristics

4.1.5.1 Trim

In this section, the condition for nominal operation and operation with one motor out are detailed. NASA linear dynamic model provided the nominal operations including the control input and torque required for steady-state operation at various advancing velocity.

The Appendix H presents the trim conditions for the hexacopter with pitch control, as well as the maximum axial control authority. The maximal control authority is defined as the maximal acceleration of the vehicle in the z axis, as well as the maximal rotational accelerations. The values reported in the table for the column “w” are the results of the following optimization routine:

$$\begin{aligned} \text{Max:} \quad & \dot{w} \\ \text{w.r.t.:} \quad & control\ input: \theta_{1,}\theta_2 \dots \theta_n \\ \text{s.t.:} \quad & [\dot{p}, \dot{q}, \dot{r}] = 0 \\ & -15^o < \theta_{1,}\theta_2 \dots \theta_n < 45^o \end{aligned} \tag{26}$$

This process attempts to find the maximal acceleration in one axis, without influencing the other ones (no cross-coupling). The routine is repeated for the other axes (p, q and r) by changing the axis along which the acceleration is maximized, and which is kept to 0.

The Appendix I also presents similar results for the case of Motor 1 inoperative motor. The nominal torque and pitch angles describe the trimmed operation with a motor inoperative. The trimmed conditions are the results of another optimization routine, which aims at finding the control input that lead to no acceleration:

$$\begin{aligned} \text{Min:} \quad & [\theta_2 \dots \theta_n]^T [\theta_2 \dots \theta_n] \\ \text{w.r.t.:} \quad & control\ input: \theta_2 \dots \theta_n \\ \text{s.t.:} \quad & [\dot{w}, \dot{p}, \dot{q}, \dot{r}] = 0 \\ & -15^o < \theta_2 \dots \theta_n < 45^o \end{aligned} \tag{27}$$

For the operation with one motor inoperative, it is assumed that :

$$\Omega_1 = \frac{\Omega_{nominal}}{2} \tag{28}$$

$$\theta_1 = trimmed\ \theta_1 \tag{29}$$

4.1.5.2 Observations on Trim Results with One Motor Inoperative

A few observations can be drawn from the trim condition and from the maximum control authority assessment:

- All 3 aircraft can be trimmed with motor 1 inoperative, and they can maintain control authority over the 4 axes presented in the tables, under these assumptions;
- In both nominal and motor 1 inoperative condition, both RPM-control vehicles have a much smaller control authority in yaw ($\dot{r}$);
- Both hexacopter aircraft see a large reduction of the contribution of the rotor 6 to the trim operation (very small pitch angle or RPM);
- The hexacopter with RPM control sees a larger power ratio penalty (P/P nominal) than the hexacopter with pitch control
- The octocopter sees a larger power ratio penalty than the hexacopter with RPM control. This result comes as counter intuitive given that the octocopter has more rotors on which to redistribute the thrust. Other objective functions (minimize max power for example) with similar outcomes.

- While roll pitch and yaw control authority is almost symmetric (positive or negative), after the loss of a motor, there is an asymmetric control authority, due to one of the rotor being out, as expected. For example, in hover, the maximum roll acceleration $\dot{p}$ is 10.4 rad/s^2, while the minimum one is -10.4 rad/s^2. For the condition of rotor 1 inoperative, this observation is not true anymore, as expected due to the limit on pitch deflections. For example, in hover, the maximum roll acceleration $\dot{p}$ is 9 rad/s^2, while the minimum one is -6.2 rad/s^2.

- All three aircraft see reduced control authority on all 4 axes with one motor out, and among them:

    - The hexacopter with pitch control sees a greater reduction in pitch rate ($\dot{q}$) than along its other axes;

    - The hexacopter with rpm control sees a greater reduction of control authority in most of its axes when motor 1 becomes inoperative than the hexacopter with pitch control;

4.1.6 Wind Model

A wind gust model is created for the dynamic simulations. The model generates trapezoidal-shape wind gusts in u,v and w based on atitude, building height and aircraft velocity [62] [63] [64] [65]. Angular rates are introduced based on a filtering post-processing of the u, v and w components of the velocity, similar to Dryden turbulence model [66]. An example of 20s for the wind model is shown on Figure 38.

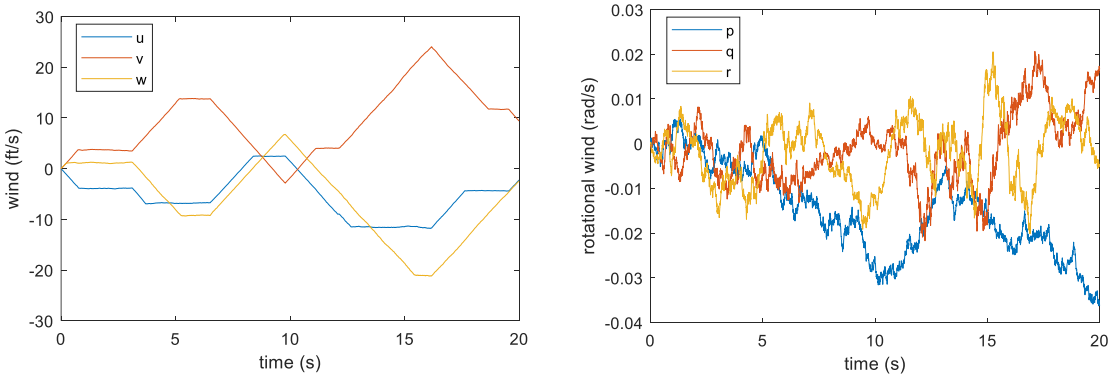

Figure 38 Wind gust example

4.2 Powertrain

4.2.1 Electric Drive Modeling

Considering the system assumption reported in section 2.3, Figure 39 shows the block diagram of the dynamic model of the electric drive system, in which all the main components have been modeled and the control strategy has been illustrated. The model is composed in several sections: electric motor, electronic speed controller, battery and thermal management system.

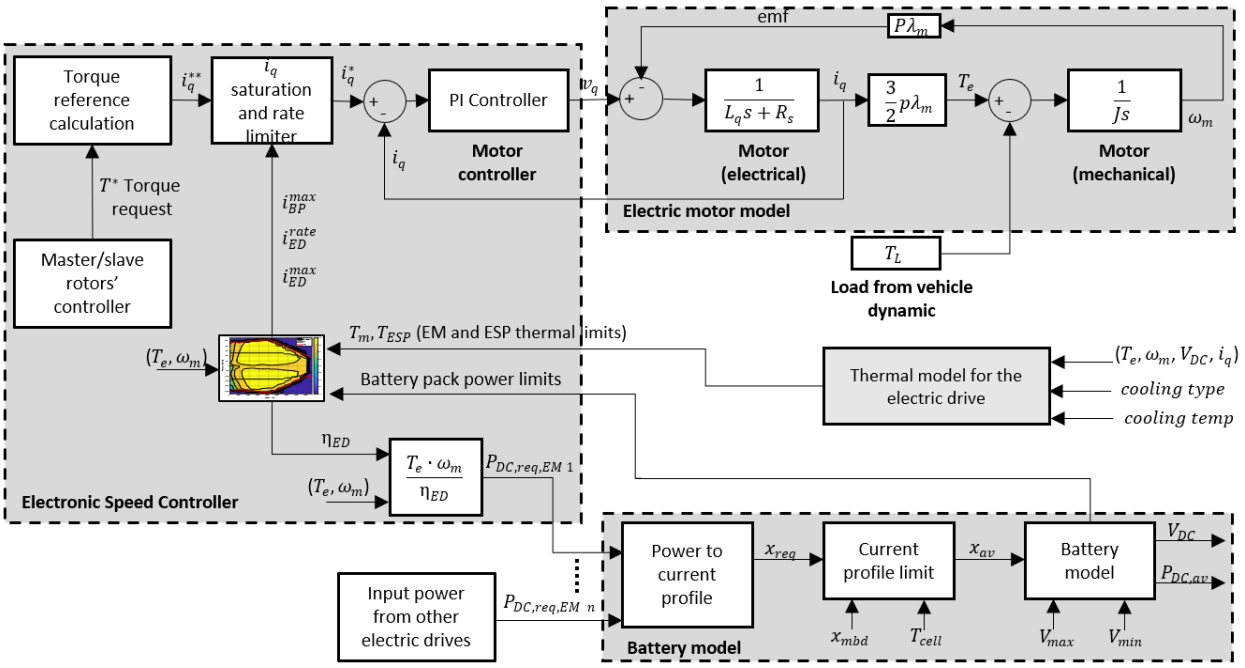

Figure 39 Block Diagram of the Dynamic Model of the electric propulsion system

4.2.1.1 Electric motor model

The PMSM has been modeled using a *d-q model* in which the dynamic of the *d*-axis has been ignored for simplicity. This is a good approximation for system level analysis and when surface mounted PMSM are considered, with the advantage of reducing the computational effort of the model. Moreover, this approximation ignores the flux dynamic during the field-weakening operation. This approximation will not affect torque availability, efficiency, and fault modes. In addition, it is worth mentioning that the considered d-q model neglects field saturation, eddy currents and hysteresis losses of EM, considers sinusoidal induced electromotive force (EMF), no field current dynamics and damper winding [67]. Moreover, an efficiency map has been included to model the EM heat generation.

4.2.1.2 Electronic speed controller model

The ESC power electronics has been modelled using an efficiency map. The voltage dynamic due to the modulation technique has been here ignored due to the fast time constant when compared to the overall vehicle simulation. The ESC control strategy is based on a d-q Field Oriented control (FOC), where the torque request (T^*) is defined by the motor speed controller with the aim of achieving the desired vehicle speed and position. The torque request T^* is converted to q-axis current request (i_q^{**}) as following:

$$i_q^{**} = \frac{T^*}{\frac{3}{2}p\lambda_m} \tag{30}$$

Then i_q^{**} is processed considering:

1. **ED power limits (i_{ED}^{max})**: i_q^{**} is saturated considering the peak (Intermediate rated power IRP maximum application 30 minutes) and the maximum continuous power limit (MCP) defined for each torque-speed combination, as shown in the example of Figure 40.

$$i_{ED}^{max} = \begin{cases} IRP & for\ 30\ minutes \\ MCP & otherwise \end{cases} \quad (31)$$

2. **ED power rate limiter (i_{ED}^{rate})**: is also applied to constrain the rate of change of i_q^{**}.
3. **BP power limits (i_{BP}^{max})**: the battery pack provide a dynamic power limit considering the current state of charge and temperature of the pack.

The control reference q-axis current i_q^* is then evaluated as:

$$i_q^* = min(i_q^{**}, i_{ED}^{max}, i_{ED}^{rate}, i_{BP}^{max}) \quad (32)$$

A PI controller is then used for deriving the q-axis voltage (v_q) for the EM, given the saturated i_q^* and the actual q-axis current (i_q).

4.2.1.3 Battery Pack model

The battery pack is modelled using a zero-order equivalent circuit model according to the specifications reported on the NASA Design and Analysis of Rotorcraft (NDARC) [68, 69]. This model takes into account for both current and temperature effects on the battery pack parameters (resistance and open circuit voltage). For simplicity the battery packs in every architecture are modelled as a unique battery pack, to limit the number of states of the simulator. The total battery pack power request is calculated as the summation of all the requests from the EDs, as function of i_q, motor speed, EM and ESC efficiencies. The battery pack power limits are calculated considering the maximum C-rate allowable and applied to constrain the electric motor power consumption as well [70].

4.2.1.4 Thermal Management System model

Heat rejection and temperature significantly affect the performance of and degradation phenomena in EM, ESC, and BP. The TMS is in charge of ensuring that these components operate efficiently, safely, and with limited degradation [71, 72]. A lumped-parameter thermal model with simplified heat transfer is developed to estimate the temperature T of the EM and ESC during cycling and is presented in (33):

$$mc_p \frac{dT}{dt} = \dot{Q}_{gen} - hA(T - T_{c,in}) \quad (33)$$

where m is the EM or ESC mass, c_p is the EM or ESC specific heat, A is the EM or ESC surface cooling area, h is the convection coefficient between the EM or ESC and the TMS, $T_{c,in}$ is the coolant temperature, and $\dot{Q}_{gen}$ is the heat generation rate of EM or ESC as function of operating voltage, current, torque and speed. The simulation framework allows for air or liquid cooling option considering the following relations [72].

$$\frac{hA_{(liquid)}}{hA_{(air)}} \approx 3 \; ; \frac{mc_{p(liquid)}}{mc_{p(air)}} \approx 9 \tag{34}$$

4.2.1.5 Model calibration

The proposed model is then calibrated using the NDARC specification [10] and considering the vehicle specifications (e.g. one motor inoperative condition). Table 16, Table 17, and Table 18 reports the summary of the system parameters.

Assumptions:

1. within every vehicle architecture, all the EDs have the same rating power regardless of their location in the vehicle (different form NDARC);
2. every ED is equipped with a BP, however the model is considering a combined BP for simplicity;
3. EM and ESC design starting from NDARC specs (MCP and IRP requirements);
4. efficiency map of ED (combined EM and ESC) obtained by scaling an automotive PMSM map [73];
5. BP needs oversizing compared to NDARC model to take into account the system efficiency (~+50%, $K_{BP,eff}$) and to fulfill the mission requirements, including a reserve (at end of the mission SoC=20%);
6. For some architectures the OMI condition would bring the electric machine in saturation, limiting the available bandwidth in case of disturbances, or not have enough power – an additional design option is included to avoid saturation during OMI (this is achieved by oversizing the ED), named GT-OSU OMI design. Note, in case of the Hexacopter and Octocopter with RPM control, the OMI condition brings the motor to operates at completely different RPMs, so to ensure the proper speed and torque range for both nominal and faulty conditions, the EM needs to be highly oversized.

Note, 8krpm is the base speed of the electric machines designed by NDARC, for the OMI condition, some designed needed a higher base speed.

Table 16 EM, ESC, and BP model parameters

Symbol	Description	value
λ_m	Permanent magnets flux	0.057 Wb
p	Number of pole pairs	6
R_s	Winding resistance	0.0048 Ω
L_s	Winding inductance in d-q domain	0.64 mH
-	ESC rate limiter	200A/s
$V_{dc,n}$	Nominal DC link voltage	400 V
-	SoC range	20-100%
	EM warning and fault temperature	130 and 160 °C
	ESC warning and fault temperature	80 and 100 °C

Table 17 Thermal model of EM and ESC

Cooling method	Parameter	Unit	EM	ESC
	A	$[m^2]$	0.5	0.15
Air cooling	type	-	enclosed fan cooled motor	Fan
	h_m, h_{EPS}	$[W/m^2K]$	500	600
	mc_p	$[J/K]$	200	100
	$T_{c,in}$	$[K]$	300 (26.85°C)	300 (26.85°C)
Liquid cooling	type	-	Transmission oil cooling	Water cooling
	h_m, h_{EPS}	$[W/m^2K]$	1550	2050
	mc_p	$[J/K]$	1800	900
	$T_{c,in}$	$[K]$	350 (76.85°C)	320 (46.85°C)

Table 18 Electric drive model calibration parameters (SLS = Sea Level Standard)

Architecture	Design	SLS MCP @8krpm	SLS IRP @8krpm	ESS sizing
Quadcopter electric Collective control	NDARC	112hp 83kW	168hp 125.3kW	368· $K_{BP,eff}$kWh $K_{BP,eff}$=1.5
	GT-OSU	88.5kW	137kW	
	GT-OSU OMI	129kW	193kW	
Quadcopter hybrid	NDARC	66.6 hp 50kW	100 hp 75kW	27.8· $K_{BP,eff}$ · $K_{BP,land}$ kWh $K_{BP,eff}$=1.5 $K_{BP,land}$=2
	GT-OSU	64kW	99kW	
	GT-OSU OMI	87kW	133kW	
	NDARC generator	472.78hp 352.55kW	709.18hp 528.83kW	
Hexacopter electric Collective control	NDARC	Motor 1 and 2 : 74hp (IRP 111hp) Motor 3 and 4 : 82hp (IRP 124hp) Motor 5 and 6 : 91hp (IRP 137hp)		413· $K_{BP,eff}$ kWh $K_{BP,eff}$=1.5
	GT-OSU	70kW	114kW	
	GT-OSU OMI	85kW	128kW	
Hexacopter electric RPM control	NDARC	Motor 1 and 2 :68hp (IRP 101hp) Motor 3 and 4 : 77hp (IRP 116hp) Motor 5 and 6 : 83hp (IRP 125hp)		386· $K_{BP,eff}$ kWh $K_{BP,eff}$=1.48
	GT-OSU	69kW	114kW	

	GT-OSU OMI	100kW (@1.2krpm)	150kW (@1.2krpm)	
Octocopter electric RPM control	NDARC	Motor 1 and 2 : 58hp (IRP 86hp) Motor 3 and 4 : 64hp (IRP 96hp) Motor 5 and 6 : 67hp (IRP 101hp) Motor 7 and 8 : 75hp (IRP 113hp)		454· $K_{BP,eff}$ kWh $K_{BP,eff}$=1.44
	GT-OSU	61kW	97kW	
	GT-OSU OMI	84kW (@1.2krpm)	134kW (@1.2krpm)	

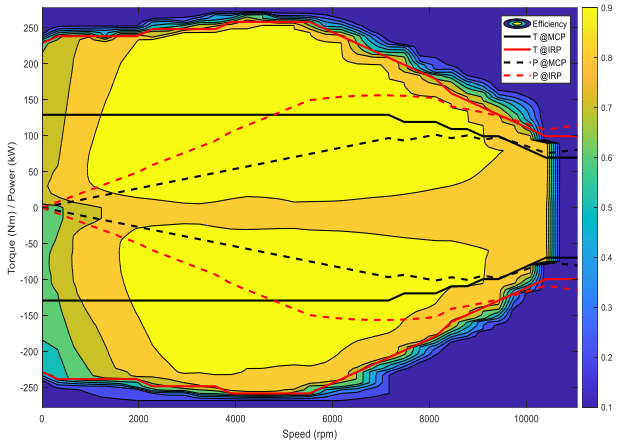

Figure 40 Example of electric motor efficiency map

4.2.2 Powertrain Control

For the other hexacopter with pitch control and for the hexacopter and octocopter with RPM control, each motor operates on an individual speed control loop. For each motor, a PI loop on speed control is used to generate the current desired through each motor, as described in the previous section. The nominal individual speed control is shown on Figure 41 and Figure 42.

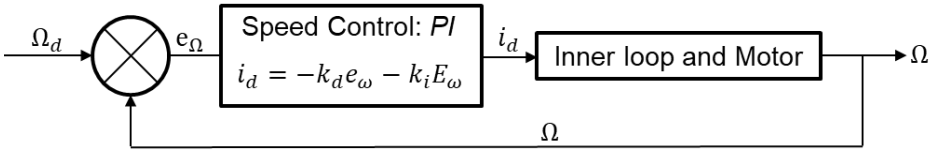

Figure 41 Speed Control Loop

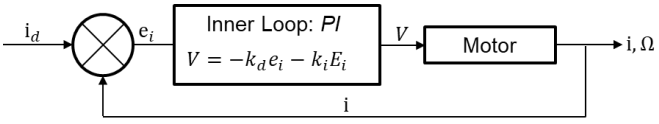

Figure 42 Inner Loop: Current Control Loop

For the configurations with mechanical links between the rotors, it is not possible to apply individual speed control approach. Consequently, a master-follower controller is used to control the multiple electric motors of the electric and hybrid quadrotor vehicles. This approach consists in having one motor operating in speed control (master), and the other motors (followers) are matching the current of the master motor. The current desired is an output of the speed control PI loop of the master motor. It is used by all of the motors, as shown on Figure 43. Because the motors are attempting to operate with the same current, they provide the same torque, which leads to a uniform use of the different motors. In the nominal configuration, no logic is used to select the master motor, and the master motor is motor number 1.

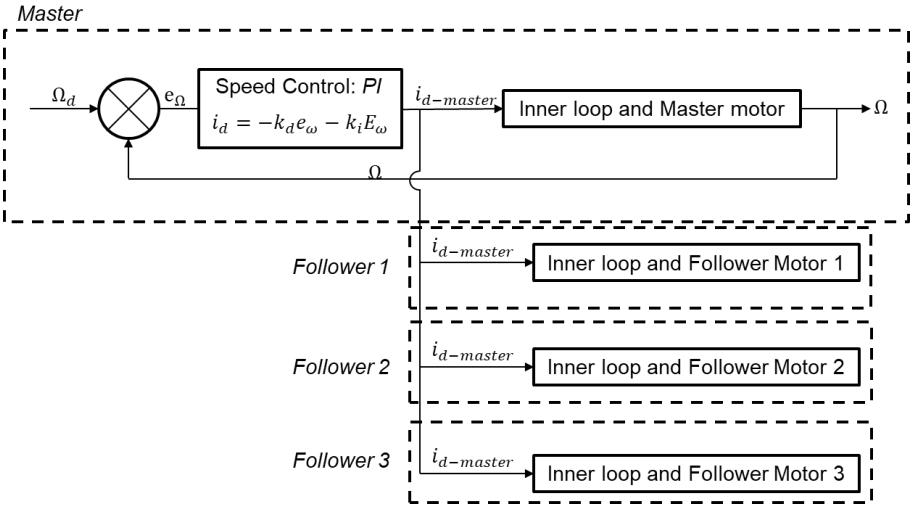

Figure 43 Master-Follower Approach

In a case of motor or transmission malfunction, the Master-Follower approach is modified. First, if the motor 1 has a malfunction, the Master control is assigned to another motor, typically motor 2, as shown in Figure 44. It is important to note that this implementation requires that it is possible to diagnose a motor malfunction.

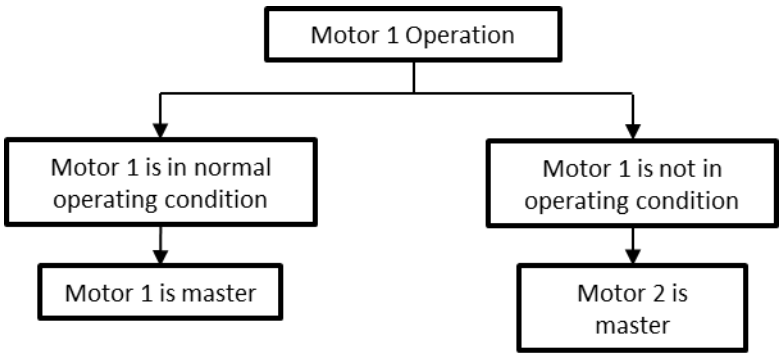

Figure 44 Master assignment when motor 1 has a malfunction.

Second, if the transmission (cross shafting) fails and a rotor is isolated, this motor will operate on its own speed control loop. The other motors are kept in master-follower control, as shown on Figure 45. Once again, it is important to note that this implementation requires that it is possible to diagnose a transmission and motor malfunction.

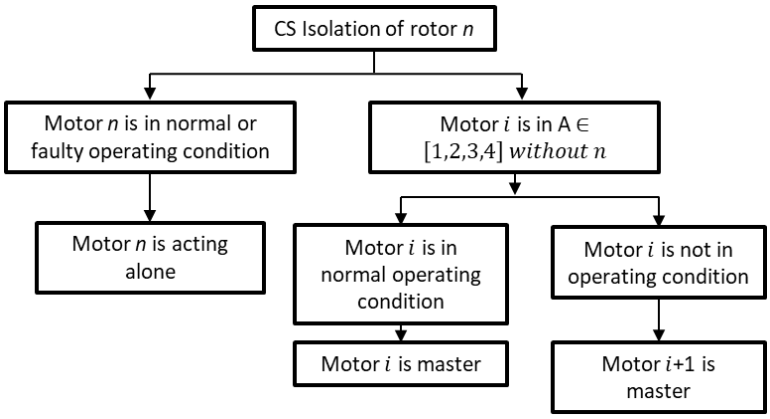

Figure 45 Master control assignment after isolation of motor *n*

4.2.3 Transmission Modeling

The transmission system serves two purposes: reducing the higher rotational speeds of power generating components like electric motors or gas turbines to the lower rotor rotational speed and provide alternative power supply paths for safe flight if one of the power generating components fails.

When the mechanical powertrain components are listed, it becomes apparent that there are only a few types of components. The types of mechanical components are shafts, bearings, gears and clutches.

The dominant transient mechanical components are the shafts with their associated rotational inertias, speeds and net torque calculations. The bearing inertias can be added to the shaft inertias and the frictional losses in the bearings can be represented through shaft transmission efficiency changes. The shafts are modeled as the only mechanical component with dynamic behavior in this work. The inertias of bearings are neglected but bearing losses are included in the transmission efficiency. The mechanical powertrain analysis assumes rigid components.

Gear inertias can also be added to the shaft inertias. Gears are important for dynamic mechanical simulations because they relate the gearbox inlet and outlet rotational speeds, acceleration and torque values through their gear ratio. The gear inertias are also neglected in this study, but the gear ratio-based speed, acceleration and torque relations are included.

Lastly, the clutch disengages the failed power generators like electric motors or gas turbines from the powertrain. The dynamic aspects of clutch engagement or disengagement are neglected but the effects of a disengaged clutch are modeled by setting the power input of an electric motor or gas turbine equal to zero.

4.2.4 Turboshaft Transient Model

Two transient turboshaft Numerical Propulsion System Simulation (NPSS) models were developed for the simulation environment. The turboshaft model for the series hybrid quadrotor concept generates a Maximum Rated Power (MRP) of about 950 hp at Sea Level Static (SLS), whereas the MRP of the turboshaft model developed for the conventional quadrotor concept is 450 hp at SLS. Also, the conventional and series hybrid quadcopter concepts have different numbers of turboshafts. The conventional quadcopter concept has two gas turbines, whereas the series hybrid quadcopter concept has one gas turbine.

The two developed transient turboshaft models have only spool dynamics. Spool dynamics is the fundamental gas turbine dynamics because the spool dynamics captures the interactions among the power consuming and producing gas turbine components on a spool. Without the net power calculation for a spool, the transient gas turbine model cannot even predict steady state performance let alone transient performance. Therefore, every transient gas turbine model has spool dynamics.

Modeling spool dynamics require spool rotational inertia values. It is outside the scope of this paper to develop a gas turbine weight prediction model like a WATE++ model. Therefore, the spool rotational inertia values are determined by calibrating for the typical spool dynamics time constant values provided in the literature. The typical time constant value for spool dynamics is about one second.

The other gas turbine dynamics are volume dynamics, heat soak effects and tip clearance effects. Volume dynamics is the accumulation of gas mass inside the cavities in the gas turbine components. Volume dynamics is the fastest dynamics in a gas turbine but modeling volume dynamics is necessary if the goal is to analyze high frequency events like stall or the gas turbine model has a large enough volume that can slow down volume dynamics enough to affect spool dynamics. In this paper, the goal is not to study stall or the modeled turboshaft engines do not have a large internal volume. Therefore, volume dynamics is not simulated in the developed models.

Heat soak effects are the heat transfers between a component's material and the flow going through the component during operation. Simulating heat soak effects require a basic component geometry and weight information, but such information was not available because it was outside the scope of this paper to develop a weight model like WATE++. Therefore, heat soak effects were not included in the developed transient turboshaft models either.

Tip clearance effects depend on the spool dynamics and heat soak effects. The spool dynamics determines the pull forces on the turbomachinery blades as a function of spool speed. The blade strains change as the spool speed changes. On the other hand, heat soak effects provide the component material temperature changes which are necessary to calculate the subcomponent thermal expansions or contractions. Tip clearances are computed from the blade strains and overall thermal size changes. The developed model does not include tip clearance effects because heat soak effects are not included as a result of unavailable basic component weight and geometry.

Although nonlinear transient turboshaft NPSS models were developed, the linear models were generated from the developed NPSS models across the flight envelope. The generated turboshaft linear models were integrated with the simulation environment in Matlab. Using the linear models prevents the computation overhead of integrating the Matlab environment with NPSS. Moreover, the imported linear

models can be used with the functionality in Matlab unlike an external function call to NPSS. In particular, the generated linear models can be used with the control functions in Matlab.

The created linear turboshaft models were scheduled across the flight envelope based on the flight condition and power setting. To control the power turbine rotational speed, a Linear Quadratic Regulator (LQR) controller design was used as the turboshaft speed governor. The scheduled linear turboshaft models represented the turboshaft dynamics for the LQR process.

4.2.4.1 Quadrotor with Turboshaft – Implementation

The turboshaft quadrotor is equipped with two turboshaft engines coupled together. For the purpose of dynamic analysis, a single turboshaft is modeled. In normal operation, the turboshaft provides half the torque required by the four 4 rotors, and the angular velocity of the rotors are dictated by the angular velocity of the turboshaft and the transmission ratio. In the case of an inoperative turbine, the full torque of the four rotors is provided by the single modeled turbine.

4.2.4.2 Hybrid Electric Quadrotor – Implementation

The quadrotor with hybrid electric propulsion is equipped with a an electric turbogenerator and a battery. The generator has been modeled as mechanical to electric conversion unit with a constant efficiency of 90%. The electric motors, the battery and the electric generators are all connected and share the same voltage.

Two modes of operations for the turbine have been modeled: all generator and battery-generator.

1. All generator
   In this mode of operation, the generator is providing all the power required by the electric motors. Consequently, in this mode, the battery is not used, unless a fault occurs.

2. Battery-Generator
   In this mode of operation, the turbine is prescribed a power schedule as a function of the mission segment, and the battery provides the difference between the power required and the power produced by the gas turbine.

4.3 Guidance and Navigation

Sections 1.4 and 4.1.2 presented the NDARC design mission as a set of waypoints and velocities, while sections 1.3 and 4.1.1 presented the various vehicles included in this research. In order for the vehicles to fly the NDARC design mission, a guidance and navigation module together with a vehicle control module is required. This section will discuss the guidance and navigation module. As seen in Section 4.1.2, the NDARC Design mission can be divided into inertial reference frame waypoints (X, Z) together with the velocity between sub sequential waypoints for which a reference frame definition can be seen in Figure 46.

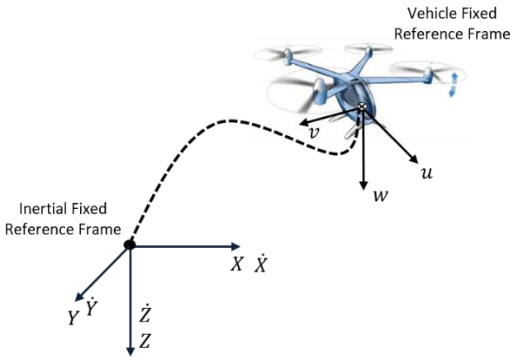

Figure 46 Reference Frame Definition

A high-level overview of the closed-loop simulation can be seen in Figure 47. The closed-loop simulation consists of four fundamental pieces; the NDARC mission profile, the guidance and navigation module, the vehicle control module and the airframe dynamics module. The vehicle control architecture will be discussed in the next section. The NDARC mission profile is loaded into the guidance and navigation module as a set of desired inertial reference waypoints and velocities. Current inertial reference coordinates are being continuously sent from the airframe dynamics module and are used by the guidance and navigation module to determine where the vehicle is currently located with respect to the NDARC mission profile. The guidance and navigation module will output a desired forward velocity and rate of climb defined in the inertial reference frame per the NDARC mission profile and as determined based on the location of the vehicle with respect to the next waypoint in the X and Z direction as defined in Figure 46. Motion in the Y direction is not of interest as an output of the guidance and navigation module since this motion is not specified by the NDARC design mission and can therefore be regulated by the vehicle controller as will be discussed in the subsequent section. Tasks for the guidance and navigation module include accelerating/decelerating from/to hover, a timed hover maneuver and an emergency landing.

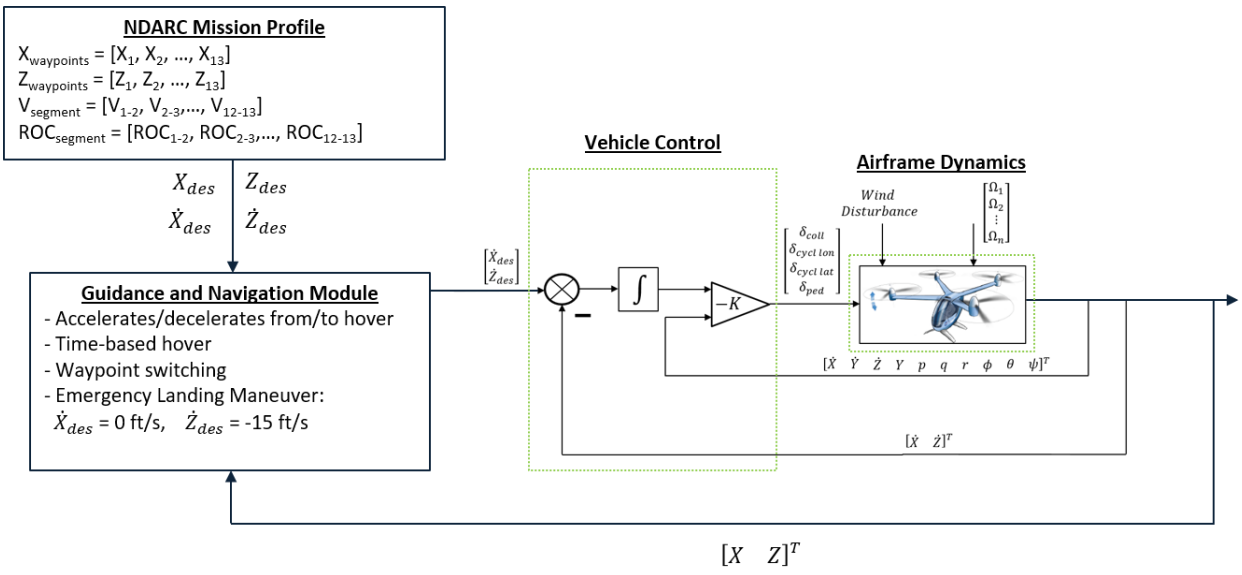

Figure 47 Guidance and Navigation Module

4.3.1 Accelerating/Decelerating from/to Hover

For deceleration to hover, an example of the output determination can be seen in Figure 48. The vehicle is currently in a steady-state cruise climb to Waypoint 2 where a hover is required. If the vehicle is relatively far from the waypoint, that is the distance to the waypoint is larger than $r_{waypoint}$, then the guidance and navigation module will command the desired vertical and horizontal velocity as referenced from the NDARC mission profile for this flight phase. When the distance between the vehicle and the waypoint is smaller than $r_{waypoint}$, the guidance and navigation module will determine the desired output velocities by linearly interpolating the desired velocities using the cruise velocity at $r_{waypoint}$ and zero velocity at the waypoint based on the distance from the waypoint. This ensures that zero velocity is commanded when the vehicle is located at the waypoint.

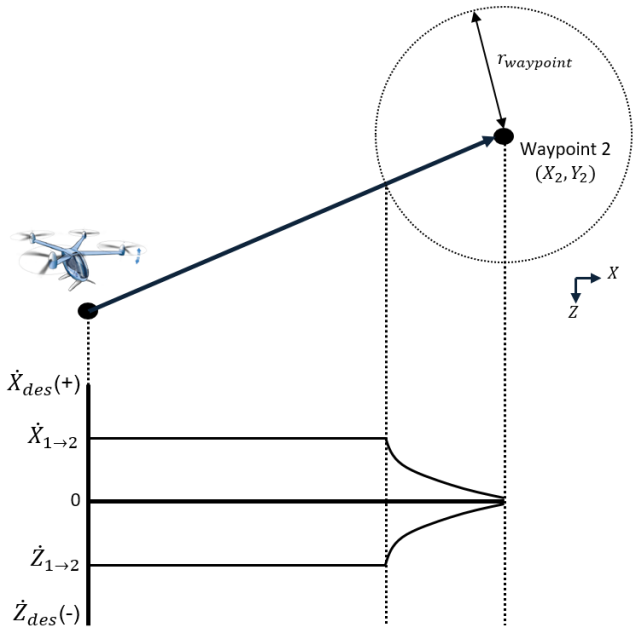

Figure 48 Guidance and Navigation Model algorithm

Once the vehicle is 'captured' by the waypoint, the guidance and navigation module will switch modes to keep the vehicle at the waypoint location for a duration of time specified by the NDARC mission profile. The concept for the waypoint hover algorithm can be seen in Figure 49. In essence, the vehicle is considered to be located at the waypoint of interest when the vehicle is within the sphere around the waypoint defined by $r_{capture}$. The commanded velocities by the guidance and navigation module are zero. Once the vehicle moves outside the sphere defined by $r_{capture}$, the guidance and navigation module will determine the desired velocities by linearly interpolating from zero velocity at $r_{capture}$ to a maximum velocity magnitude defined at $r_{waypoint}$. This will ensure that the guidance and navigation module will command an appropriate adjustment desired velocity to keep the vehicle at the waypoint.

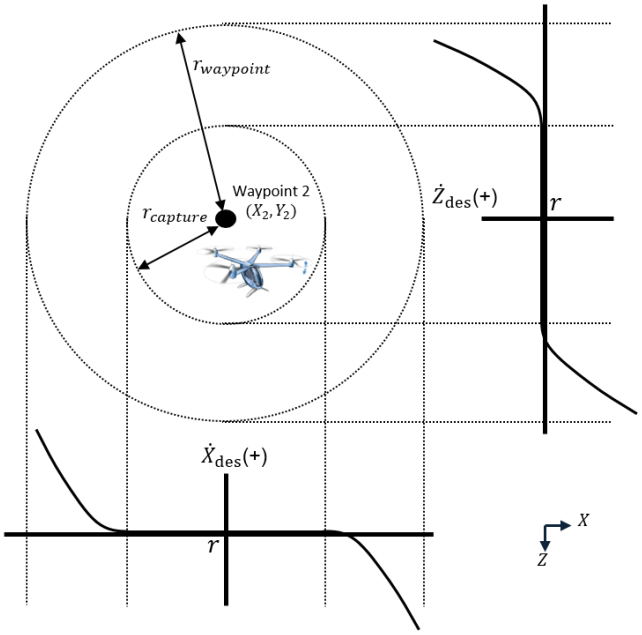

Figure 49: Waypoint hover algorithm

When accelerating from hover, the guidance and navigation module will command the increase in both the vertical and horizontal velocity as a function of time as can be seen in Figure 50. For the horizontal acceleration, the guidance and navigation module will linearly increase the desired velocity to the final cruise velocity over 60 seconds. This in part to ensure the vehicle does not lose significant altitude when acceleration, to ensure the load factor is realistic for a simulated acceleration and to ensure the power transient is not unrealistically large. The desired vertical velocity is linearly increased over 10 seconds to ensure a realistic power transient.

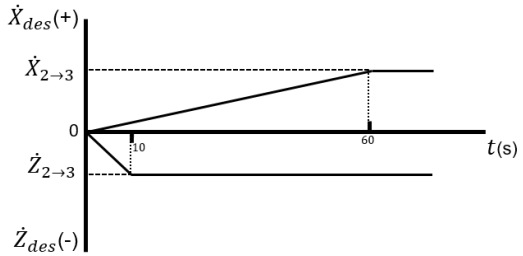

Figure 50 Acceleration Algorithm

4.3.2 Emergency Landing Maneuver

In the case of an emergency during flight, an emergency landing maneuver is triggered. The guidance and navigation module will switch modes to bring the vehicle to the ground in a safe and fast manner. The emergency landing maneuver algorithm can be seen in Figure 51. When an emergency is declared, the mission manager will switch to command a downward velocity of 15 ft/s for the remainder of the flight. The horizontal velocity is linearly interpolated through altitude starting from the initial velocity at the

beginning of the maneuver at the current flight altitude to zero velocity on the ground in order to slow the vehicle down horizontally before the landing. As motivated in Section 1.4, a downward velocity of 15 ft/s is chosen to ensure a vertiport can be reached within five minutes from the maximum cruise altitude. Again, a touchdown velocity of 15 ft/s is in reality too high to ensure a safe landing. However, the emphasize here is on evaluating whether the vehicle could get close to the ground for the pilot to attempt to make a landing in the first place or if the magnitude of the emergency prevents this.

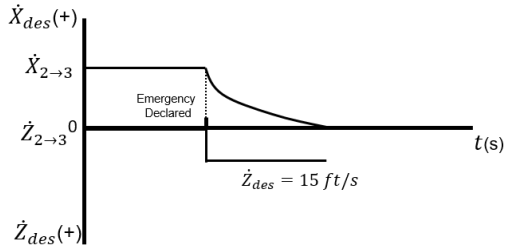

Figure 51: Emergency Landing Maneuver Algorithm

4.4 Flight Control Architecture

The previous section showed how the guidance and navigation module provides desired horizontal and vertical velocities such that the vehicle follows the NDARC design mission, or in the case for an emergency landing, towards a landing. A stabilizing and robust vehicle controller is required to follow these commands being sent from the guidance and navigation module. Referencing Figure 47, while the previous section outlined the guidance and navigation module, this section will focus on the derivation of the vehicle control. The Linear Quadratic Integral (LQI) control architecture was chosen as the baseline flight controller for both the variable propeller pitch and variable RPM control vehicle architectures [74]. Given the diverse range of considered vehicle configurations, control architectures and overall flight envelope in this research, the application of a linear optimal control architecture is considered a good match. The LQI architecture, as will be discussed later in this section, is relatively straightforward to implement and facilities the tuning process to allow for a robust performance in diverse operating conditions.

Some background on the LQI control can be provided. The LQI control architecture is an extension of the more popular Linear Quadratic Regulator (LQR) problem where traditionally an optimal state-feedback gain is determined that will achieve guaranteed robustness while minimizing energy spent [75]. The guaranteed robustness is achieved in the LQR problem by minimizing a quadratic cost function to regulate the states back to their equilibrium, that is x(t) = 0. However, state regulation will not be desired in the case of the application as a baseline flight controller in this application which requires robust tracking of non-zero states. Therefore, the LQR control architecture will not suffice. In order to combat this inherent shortcoming of the LQR, the theorem can be extended to allow for integral based state tracking which gives rise to the LQI problem. The availability and observability of all states is a necessary requirement in order to apply linear quadratic control. This assumption in the simulation environment is deemed acceptable given that the emphasis of this research task is on providing an environment to

perform a reliability assessment. This can be achieved with any stabilizing and robust baseline controller, but the LQI control was selected for its optimality characteristics and low tuning requirements.

The LQI problem can be defined as follows [2]. Consider a linear, state-space dynamic system model:

$$\dot{x} = Ax + Bu \qquad (35)$$
$$y = Cx$$

Where, $x \in \mathbb{R}^n$ is the state vector, $y \in \mathbb{R}^q$ is the output vector, $u \in \mathbb{R}^m$ is the control input vector, $A \in \mathbb{R}^{n\times n}$ represent the system dynamics, $B \in \mathbb{R}^{n\times m}$ is the input matrix and $C \in \mathbb{R}^{q\times n}$ is the output matrix. Tracking states of interest can be concatenated to the state vector x:

$$z = \begin{bmatrix} x \\ \tilde{x} \end{bmatrix} \qquad (36)$$

Where, $\tilde{x} \in \mathbb{R}^p$ is the integrated error signal between desired tracking state reference values, $r \in \mathbb{R}^p$, and desired tracking state outputs, $y \in \mathbb{R}^p$:

$$\tilde{x}(t) = \int (r - y)dt \qquad (37)$$

Which can be written for implementation in a discrete simulation environment as:

$$\tilde{x}_{i+1} = \tilde{x}_i + (r_i - y_i)dt \qquad (38)$$

As shown in [2], an optimal state-feedback control gain matrix $K \in \mathbb{R}^{m\times(n+p)}$ can be synthesized such that state-feedback control law:

$$u = -K \begin{bmatrix} x \\ \tilde{x} \end{bmatrix} \qquad (39)$$

minimizes the following cost function:

$$\boldsymbol{J(u) = \int_0^\infty [z^T Q z + u^T R u] dt} \qquad (40)$$

Where, $Q \in \mathbb{R}^{(n+p)\times(n+p)}$ is a diagonal matrix where the terms represent a weighting factor for state diversion of vector *z,* and $R \in \mathbb{R}^{m\times m}$ is a diagonal matrix where the terms represent a penalization of control action in *u*. Matrix Q and R are considered tuning matrices to influence the transient and steady-state performance of the LQI controller.

The proposed LQI control architecture will be used both for the variable pitch and variable RPM vehicles.

4.4.1 Variable Pitch Vehicle LQI

The LQI control architecture for the variable pitch vehicle can be seen in Figure 52.

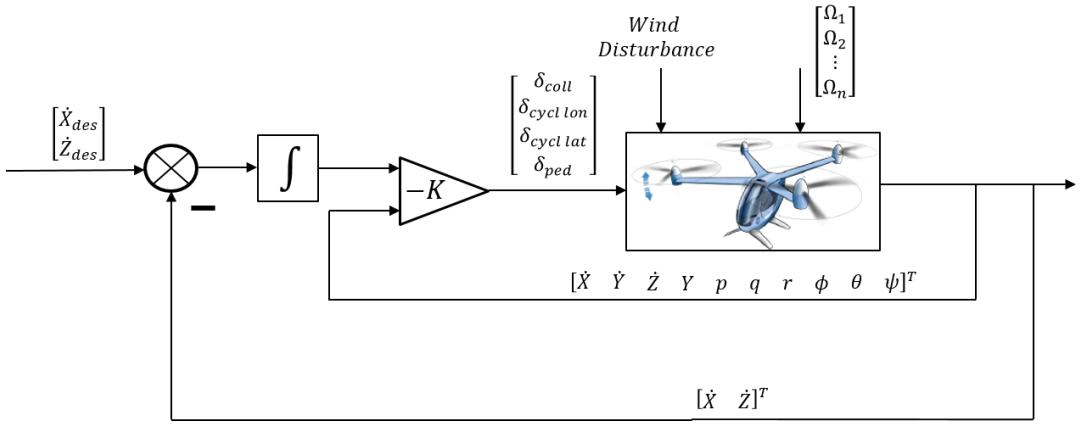

Figure 52 LQI Control Architecture Applied to Variable Pitch Vehicle

The reference tracking states of interest for the LQI collective pitch controller are the forward velocity in the inertial reference frame, $\dot{X}_{des}$, and the rate of climb in the inertial reference frame, $\dot{Z}_{des}$, both provided by the NDARC mission profile. All other states, that is the side velocity in the inertial reference frame (Y), the angular rates in the body reference frame (p, q, r), and the attitude angles (ϕ, θ, ψ), are regulated in steady-state, except for the pitch angle (θ) which in practice settles at a non-zero value during non-hover operations. Ω represents the motor RPM value for the n motors. The powertrain attempts to keep the RPM value constant between the motors in the collective pitch control vehicle. The wind disturbance acts as an external unknown disturbance to the system.

The dynamic model used for the variable pitch vehicle LQI is defined as followed and was obtained through the reduced order modeling presented in Section 4.1.3.

$$\begin{bmatrix}\dot{p}\\ \dot{q}\\ \dot{r}\\ \dot{u}\\ \dot{v}\\ \dot{w}\\ \dot{\phi}\\ \dot{\theta}\\ \dot{\psi}\end{bmatrix} = A\begin{bmatrix}p\\ q\\ r\\ u\\ u\\ w\\ \phi\\ \theta\\ \psi\end{bmatrix} + B\begin{bmatrix}u_0\\ u_c\\ u_s\\ u_{ped}\end{bmatrix} \tag{41}$$

4.4.2 Variable RPM Vehicle LQI

The LQI control architecture for the variable RPM vehicle can be seen in Figure 53.

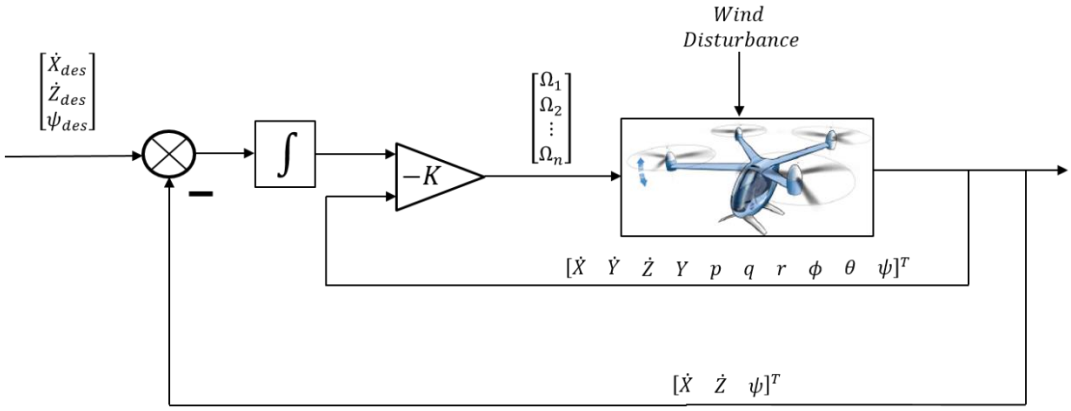

Figure 53 LQI Control Architecture Applied to Variable RPM Vehicle

The reference tracking states of interest for the LQI RPM controller are the forward velocity in the inertial reference frame, $\dot{X}_{des}$, the rate of climb in the inertial reference frame, $\dot{Z}_{des}$, both provided by the NDARC mission profile. Different from the LQI for the variable pitch vehicle, the heading angle (ψ) is added as a reference tracking state to improve the stability of the system. All other states are regulated by the LQI. Ω represents the motor RPM value for the n motors which acts as the control input to the vehicle. The wind disturbance acts as an external unknown disturbance to the system.

The dynamic model used for the variable RPM vehicle LQI is defined as followed and was obtained through the reduced order modeling presented in Section 4.1.3.

$$\begin{bmatrix} \dot{p} \\ \dot{q} \\ \dot{r} \\ \dot{u} \\ \dot{v} \\ \dot{w} \\ \dot{\phi} \\ \dot{\theta} \\ \dot{\psi} \end{bmatrix} = A \begin{bmatrix} p \\ q \\ r \\ u \\ u \\ w \\ \phi \\ \theta \\ \psi \end{bmatrix} + B \begin{bmatrix} \Omega_1 \\ \dots \\ \Omega_n \end{bmatrix} \tag{42}$$

An important observation on the control development and the dynamic models used for its synthesis is the fact that the rotor acceleration and its reaction on the vehicle is not considered as part of the yaw dynamics: only the reaction associated with the increased drag on the rotor.

4.4.3 One Motor Inoperative (OMI) LQI

It was found that in order to evaluate the one motor inoperative (OMI) condition for the hexacopter and octocopter variable RPM vehicles, the LQI controller required a modification such that a trim condition could be found. This is due to the fact that the linear models provided are not linearized around OMI conditions and so some modifications are required to allow for this analysis. In comparison, the hexacopter with pitch control did not exhibit this problem, and for this configuration, the nominal controller is used during the OMI condition.

Equation (35) shows the linear, state-space dynamic system model used in the control synthesis of the LQI controller. The input matrix, B, models the effect of individual rotor RPM on the state vector. In the case that one motor is out, one column in the B matrix effectively becomes zero. A new definition for the input matrix is required at this point due to the reconfiguration of control power.

For the purpose of the assessment of the dynamic response to a motor fault, a series of new controllers were defined for the hexacopter RPM and octocopter RPM vehicle. Each controller is assigned to an individual OMI condition (Controller "A" for the case of Motor 1 out, Controller "B" for the case of Motor 2 out, etc). The consequence to this configuration is that there is a need to assume that a fault in the powertrain can be diagnosed and recognized.

The controller for the OMI condition is a modified version of the LQI formulated in the previous section. Rather than considering the individual rotor angular velocities as the control input as expressed in Equation (42), the controller considers independent axes effectors. The linear dynamic model is re-casted as follows:

$$\begin{bmatrix} \dot{p} \\ \dot{q} \\ \dot{r} \\ \dot{u} \\ \dot{v} \\ \dot{w} \\ \dot{\phi} \\ \dot{\theta} \\ \dot{\psi} \end{bmatrix} = A \begin{bmatrix} p \\ q \\ r \\ u \\ u \\ w \\ \phi \\ \theta \\ \psi \end{bmatrix} + B \begin{bmatrix} 1 & 0 & 0 & 0 \\ 0 & 1 & 0 & 0 \\ 0 & 0 & 1 & 0 \\ 0 & 0 & 0 & 0 \\ 0 & 0 & 0 & 0 \\ 0 & 0 & 0 & 1 \\ 0 & 0 & 0 & 0 \\ 0 & 0 & 0 & 0 \\ 0 & 0 & 0 & 0 \end{bmatrix} \begin{bmatrix} \delta_p \\ \delta_q \\ \delta_r \\ \delta_w \end{bmatrix} \tag{43}$$

The symbols δ_i represent the contribution of individual vector, defined offline, as vector of angular velocities that only affect a single axis "i".

The vectors representing the control input to achieve a unit acceleration along one axis were defined as the result of an optimization routine. For the case of motor 1 inoperative, the control input to provide a unit acceleration along the z-axis, $\dot{w}$, was found by solving:

$$\begin{aligned} \text{Min:} \quad & [\Omega_2 \dots \Omega_6]^T [\Omega_2 \dots \Omega_6] \\ \text{w.r.t.:} \quad & control\ input: \Omega_2 \dots \Omega_6 \\ \text{s.t.:} \quad & [\dot{p}, \dot{q}, \dot{r}] = 0 \\ & \dot{w} = 1 \end{aligned} \tag{44}$$

The vectors found for the 4 axes are then used to populate the matrix $T_{[\delta \to u]}$ which can transform the axial effectors to individual angular velocities:

$$u = T_{[\delta \to u]} \begin{bmatrix} \delta_p \\ \delta_q \\ \delta_r \\ \delta_w \end{bmatrix} \tag{45}$$

For the hexacopter RPM-control aircraft in hover, the transformation $T_{[\delta \to u]}$ is as follows:

$$T_{[\delta \to u]} = \begin{bmatrix} 0 & 0 & 0 & 0 \\ -1.38 & 0.95 & 6.9 & -44.9 \\ -1.32 & -4.96 & 2.2 & -144 \\ -1.28 & 2.9 & 2.1 & 239 \\ -1.35 & -2.9 & -2.2 & 146 \\ 0.07 & 3.96 & -9.4 & -193 \end{bmatrix} \quad (46)$$

The same approach is implemented for the octocopter aircraft.

As discussed in the previous section, it is assumed that the rotor fault detection is immediate. Once the detection occurred, the transition from the nominal to the OMI controller happens over 10 seconds, with a gradual linear mixing between the generated two control inputs.

4.5 Fault models

4.5.1 Electric Powertrain modeling

The model described in section 4.2.1 is then equipped with dynamic models of the electric drive system faults with the aim of evaluating the overall system reliability using Dynamic Event Tree (DET). Considering the FTA and FMECA process proposed in section 2.4 the fault models have been integrated in the electric powertrain model, as shown in Figure 54. Figure 55 shows the different torque and q-axis current profiles that can be achieved by injecting faults in the electric powertrain model, highlighting the corresponding class of effect, including no torque, low torque, high torque, torque transient, torque ripple and high torque oscillations due to short circuit. In the reported cases, the faults have been injected at the time instant of 2s, but both the magnitude and the time injection can be set as desired.

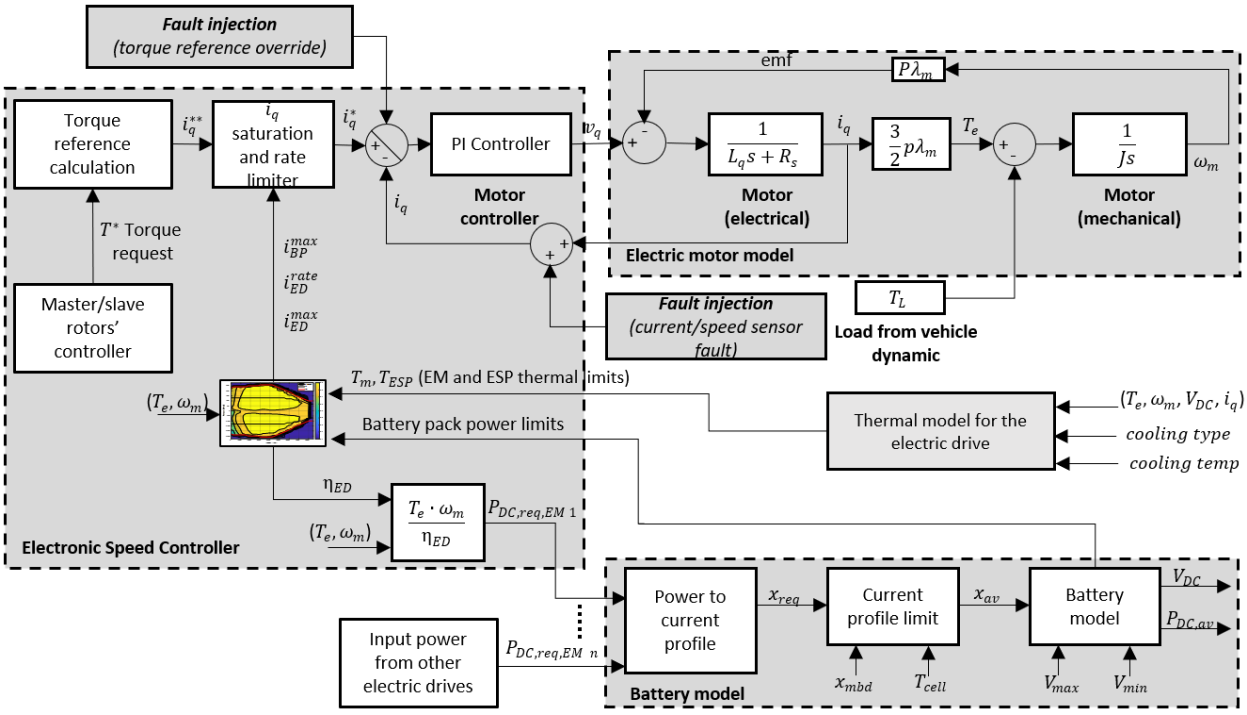

Figure 54: Block Diagram of the Dynamic Model of the electric propulsion system including fault injection points.

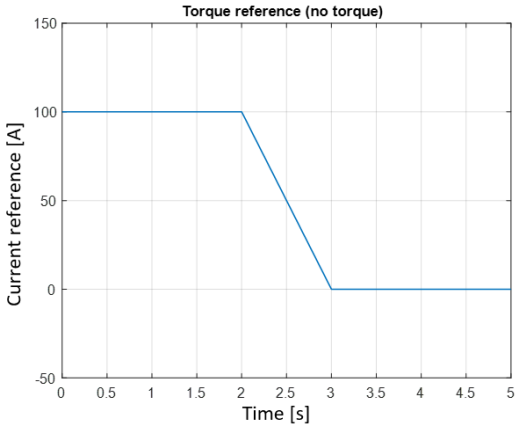

Fault mode: No Torque

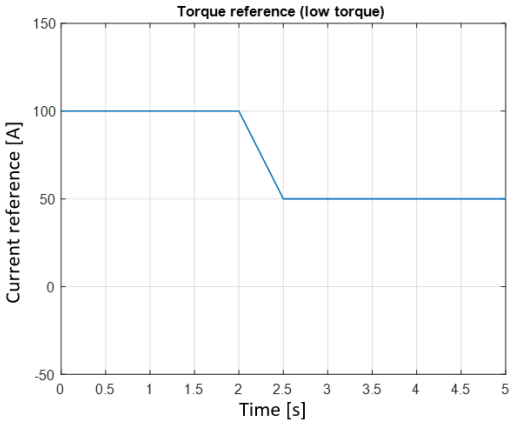

Fault mode: Low Torque

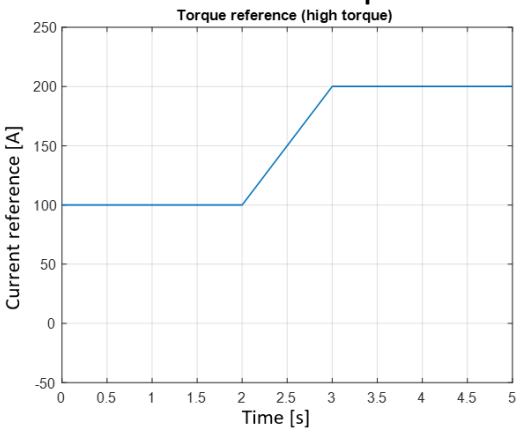

Fault mode: High Torque

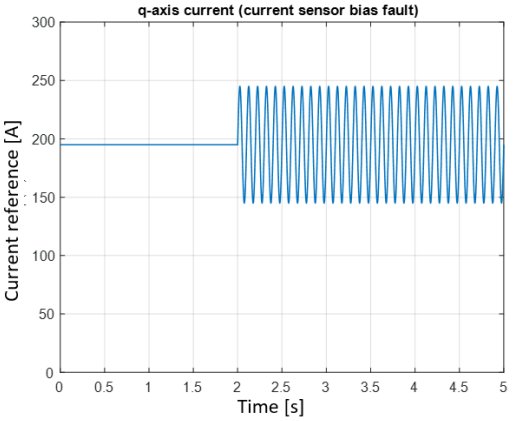

Fault mode: Torque Ripple

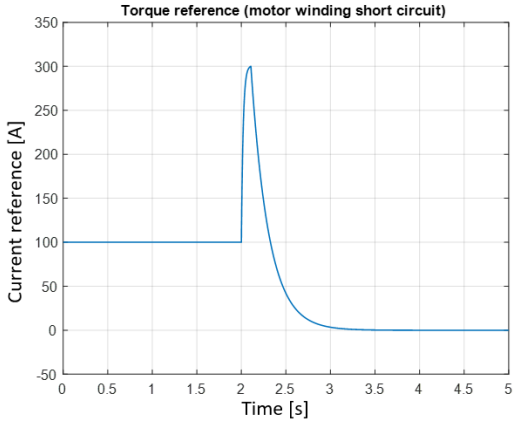

Fault mode: Short circuit 1

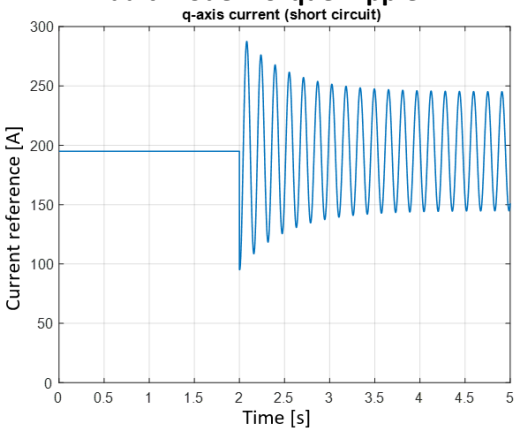

Fault mode: Short circuit 2

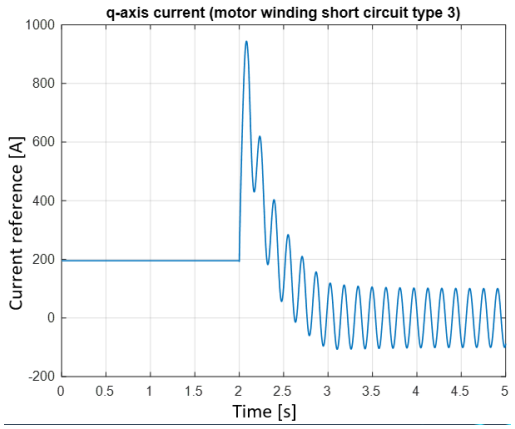

Fault mode: Short circuit 3

Figure 55 Electric Drive fault modes applied at $t = 2s$

4.5.2 Transmission Faults

For the cross shafting transmission model, two faults are included in the model: the isolation of one rotor and the loss of transmitted power. For the condition with rotor isolation, the dynamics of the individual rotor is calculated on its own and the other rotors are assumed as still connected. The loss of transmitted power is modeled as an extra power required at the rotor, in percentage of the nominal power.

4.5.3 Actuator Faults

Two types of actuator failure modes are considered for transient analysis of the system: i) Actuator floating and ii) Increased deadband. With two actuators per rotor allocated to all collective-control configurations, the effect of one actuator floating was simulated simply as a decrease of overall actuation rate by a factor of 50%. The increased dead band failure effect is simulated by a decrease in the range of actuator motion by 50%. Both of the simulated scenarios are reflective of EMA failure behavior in general for the associated failure modes and would require dynamic simulation to determine the resulting effects at the aircraft level.

4.5.4 Turboshaft Engine Faults

The turboshaft aircraft has a model for the one engine inoperative and for a transmission loss. Since the aircraft is equipped with two turbines, the engine inoperative condition leads to the transfer of the full power required on a single turbine. The transmission loss fault is represented as an additional torque required on one of the turbines.

4.5.5 Turbine-generator Faults

Similarly, the turbogenerator has a model for the one engine inoperative and for a transmission loss. Since there is a single turbine in the turbogenerator, the engine out condition leads to no electric power available from the turbine. The transmission loss is expressed as an additional torque required on the turbine.

4.6 Vehicle Performance Verification

Before analyzing specific fault cases, it is valuable to analyze the nominal behavior of the quadcopter, hexacopter and octocopter vehicles and compare the results with the steady state operating point provided by NDARC [11]. For all configurations, the nominal NDARC design mission has been shortened to only simulate the second segment without the reserve mission. This decision was taken to decrease the total simulation runtime. To still capture the effect of the first segment of the mission profile, the battery model depth of discharge has been calibrated such that the battery model is initialized in the simulation as if the first segment has been completed.

The details of the nominal flight profile are shown in the Appendix J:

- Nominal flight of the quadrotor with an electric powertrain;
- Nominal flight of the quadrotor with a hybrid electric powertrain;
- Nominal flight of the quadrotor with a turboshaft;
- Nominal flight of the hexacopter with pitch control;
- Nominal flight of the hexacopter with RPM control;
- Nominal flight of the octocopter with RPM control.

The nominal flight results show the vehicle and powertrain states during the second leg of the mission. All aircraft successfully complete this flight.

Appendix K also shows a representation of an emergency landing for the electric quadrotor. The emergency landing maneuver is triggered while the aircraft is in cruise-climb to illustrate the trajectory during this diversion maneuver. The electric quadrotor successfully lands and completes the emergency landing.

The Appendix L presents the results of the operation with one motor inoperative or one engine inoperative for the various aircraft. For the various aircraft, a fault is introduced at time t=200s, and the aircraft attempt to fly the nominal mission. The simulations illustrate the following results:

The electric quadcopter is able to complete the mission with one motor inoperative.

- The quadcopter with a turboshaft powertrain has one of its two turboshaft turned off at t=200s. The remaining turboshaft sees an increased load, but the aircraft is able to complete the whole mission.

The hexacopter with pitch control is able to complete the mission with one motor inoperative.

- For the RPM-Control aircraft (hexacopter and octocopter), the aircraft are not able to complete the mission due to the inability to keep the aircraft on a controlled stable path.

The hybrid quadcopter is not modeled with its turbogenerator inoperative, as this would automatically trigger an emergency landing.

The results of the nominal missions illustrate that the environment is ready to be used for more in-depth analyses case studies.

5 RESULTS

5.1 Static Safety and Reliability Assessment Results

The purpose of this section is to review the results of the static safety and reliability assessment process, which primarily includes the FHA, FMECA and FTA results.

5.1.1 Functional Hazard Analysis (FHA)

The safety analysis process for this study began with a functional hazard analysis. First step of FHA is to identify primary functions of the aircraft and its major systems (e.g. convert electrical energy to torque) and their failure conditions (e.g. single propulsor fail, dual ESC fail etc.). For each failure condition, an aircraft level end-effect is postulated considering the loss of the function, incorrect operation of the function, or inadvertent occurrence of the function when not desired. Using hazard classification guidelinesTable 9: Hazard Severity Classification used in FMECA and DET analyses, each failure condition is given a severity classification (as detailed in Section 2.2.1, Table 9). The FHAs for six configurations may be found in the Appendix A.

5.1.2 Failure Modes, Effects and Criticality Analysis (FMECA)

The FMECA analysis for each of the six configurations may be found in the Appendix B. It details all the major system and component level failure modes, their immediate effect at the system level and end effects at the aircraft level. Failure rates calculated for the failure modes with their probabilities (Beta values) are used in the FTA analysis, as described in detail in Section 2.5.2

5.1.3 Fault Tree Analysis (FTA)

The FTA diagrams for each of the six configurations may be found in the Appendix C Table 19, Table 20, Table 21, Table 22, Table 23, Table 24 summarize the FTA for six configurations. As per NASA's request, The FTA results include overall aircraft reliability with and without Rotor Gear Box failure considerations, to gain further insights into the impact of design choices related to the propulsion and control systems on the aircraft reliability with and without the RGB which is a common single-point-of-failure (SPOF) among all configurations. All six configurations are assumed to be flying in 25% OEI Avoid Region.

Comparison by propulsion-system choice: All-electric, Hybrid-electric and Turboshaft

The quadcopter FTAs are detailed in the APPENDIX C, Figures C1, C2 and C3. For all quadcopter configurations, loss of single rotor (with or without a propulsor loss) is considered catastrophic. For the Quadcopter electric and hybrid configurations, dual electric motor loss outside of the OEI avoid region will result in insufficient power to sustain the flight and hence is considered catastrophic. Similarly, dual turboshaft engine loss outside of the OEI avoid region for quadcopter turboshaft configuration is considered catastrophic. As shown in the Table 19, Table 20, and Table 21, higher failure rates related to ED components compared to twin-turboshaft engine seem to suggest that the electric propulsion technology requires significant improvements in the component reliability across the board to be comparable with the proven higher reliability systems in the aircraft industry. Overall low aircraft reliability can be attributed to the common cause failures related to the cooling systems of the electric drive components which include EM cooling, ESC cooling and ESS cooling. All cooling systems use same

set of basic components and so those have same fault topology (and hence similar reliability). Such common cause failures offset the benefits of modular battery packs allocated to each propulsor. Significant design improvements of the liquid cooling systems are required to improve their component reliability. Additionally, A single LV battery, is another SPOF which may result in the complete failure of all ESCs and FCC, in turn resulting in catastrophic outcome for the aircraft. Therefore, by increasing the redundancy in the form of multiple LV power sources and/or backup battery cooling, incremental improvements in the aircraft reliability can be made. However, such exercise in redundancy has limitations due to overall sizing constraints. Therefore, reliability allocation must be performed with the vehicle sizing in the loop to ensure that only feasible design choices are considered. Additionally, the comparison of the FTA results with and without considerations of RGB related failures suggest that overall impact of the ED common cause failures is substantial and so there are no reliability improvements noticed despite considering a hypothetical aircraft architecture that does not include RGB as a SPOF.

Table 19. Quadcopter electric FTA summary

Description	Failure Rate per Flight Hour (RGB Considered)	Failure Rate per Flight Hour (RGB not considered)
Overall	**4.90E-05**	**4.88E-05**
Dual Propulsor (EM) Failure	2.68E-05	2.68E-05
Single Rotor Loss	1.65E-07	1.33E-08
OEI Propulsion Loss	2.18E-05	2.18E-05

Table 20. Quadcopter hybrid FTA summary

Description	Failure Rate per Flight Hour (RGB Considered)	Failure Rate per Flight Hour (RGB not considered)
Overall	**1.55E-05**	**1.54E-05**
Dual Propulsor Failure	1.01E-05	1.01E-05
Single Rotor Loss	1.64E-07	1.32E-08
OEI propulsion Loss	1.42E-05	1.42E-05

Table 21. Quadcopter Turboshaft FTA summary

Description	Failure Rate per Flight Hour (RGB Considered)	Failure Rate per Flight Hour (RGB not considered)
Overall	**3.93E-06**	**3.78E-06**
Dual Turboshaft Fail	9.21E-14	9.21E-14
Single Rotor Loss	1.64E-07	1.30E-08
OEI Propulsion Loss	1.52E-07	1.52E-07

Comparison by Flight Control Method: Collective and RPM-Control

The hexacopter FTAs are described in detail in the 210APPENDIX C, Figures C4 and C5. For both six rotor configurations, dual rotor failure is considered catastrophic, due to resultant loss of power and control authority. The fault trees for the collective and RPM-control hexacopter differ only by the addition of dual actuators per rotor for collective-Control hexacopter. Table 22 and Table 23show the FTA results for hexacopter with collective and RPM control. Due to very high reliability of the dual actuator

configuration compared to the rest of the systems, there is no noticeable difference in overall reliability of the two configurations. Also as with the quadcopter electric/hybrid configurations, consideration of RGB failures does not impact overall aircraft reliability, again substantiating the multilayered reliability weaknesses in the electric drive system.

Table 22. Hexacopter collective FTA summary

Description	Failure Rate per Flight Hour (RGB Considered)	Failure Rate per Flight Hour (RGB not considered)
Overall	**9.84E-05**	**9.83E-05**
Dual Rotor Failure	6.55E-05	6.55E-05
OEI Propulsion Loss	3.26E-05	3.26E-05

Table 23. Hexacopter RPM FTA summary

Description	Failure Rate per Flight Hour (RGB Considered)	Failure Rate per Flight Hour (RGB not considered)
Overall	**9.84E-05**	**9.83E-05**
Dual Rotor Failure	6.55E-05	6.55E-05
OEI Propulsion Loss	3.26E-05	3.26E-05

Comparison by Number of Rotors: Six vs Eight Rotor (RPM-control) Configuration

The hexacopter RPM-control and octocopter RPM-control FTAs are described in detail in the APPENDIX C, Figures C5 and C6. Table 23 and Table 24show the results of the static safety assessment for hexacopter and octocopter with RPM control. For RPM-Control octocopter, triple rotor failure is considered catastrophic. Even though each rotor has isolated battery packs for the motor, the HV battery cooling system and LV battery (for ESC control and FCC power) is shared by all the rotor electric drives, just as for the other electric and hybrid propulsion architectures. For octocopter, these common cause failures offset the benefits of additional rotors and result in overall lower reliability numbers compared to RPM-Control hexacopter. Therefore, purely from the static reliability perspective, for the RPM-control configurations, increasing the number of rotors negatively impact the overall reliability of the aircraft.

Table 24. Octocopter RPM FTA summary

Description	Failure Rate per Flight Hour (RGB Considered)	Failure Rate per Flight Hour (RGB not considered)
Overall	**2.72E-04**	**2.72E-04**
Triple Rotor Failure	2.42E-04	2.42E-04
OEI Propulsion Loss	3.04E-05	3.04E-05

5.1.4 Reliability impact of Turbine-Generator Interface Design Choice: Direct-drive versus Gearbox

The Quadcopter Hybrid architecture uses a direct-drive turbogenerator. An alternate geared turbogenerator design would include an additional reduction gearbox between the turboshaft engine and the electric generator. Adding more components to the vehicle increases the failure rate calculated by the FTA, but in this case the impact on the overall failure rate of the vehicle is insignificant, as shown in Table 25. From previous studies on reported annual wind turbine generators, the failure rate of a generator gearbox was assumed to be approximately 4.289E-06 per hour assuming 90% operational up-time during the year [76]. The addition of the gearbox increases the failure rate of the turbine-generator system and the hybrid power system by one order of magnitude. However, compared to the rest of the vehicle component failure rates, the hybrid power system failure rate is lower by several orders of magnitude. Thus, the impact of the additional gearbox on failure rates is greatly diminished at the vehicle level.

Table 25. Comparison of Direct-drive and Geared Hybrid Quadcopter

Architecture	Turbine-generator Failure Rate per Flight Hour	Power System Failure Rate per Flight Hour	Overall Vehicle Failure Rate per Flight Hour
Direct Drive	4.508E-06	3.538E-11	1.553E-05
Geared	3.132E-05	2.458E-10	1.553E-05

5.1.5 Reliability comparison between Cross-shafting System and Redundant Motors

The cross-shafting system adds a degree of redundancy for the quadcopter electric and hybrid architectures. When an electric propulsor fails, the rotor can continue spinning with the help of remaining electric propulsors connected through the cross-shafting system.

A theoretical dual-motor design for the quad-electric was analyzed to determine the feasibility of replacing the cross-shafting system with a redundant electric propulsor for each rotor. As with all other quadcopter configurations, all electric propulsors share the same LV power source; the two motors on each rotor share a single cooling loop and the two ESCs share the same cooling loop as well. The sizing of the vehicle was assumed to not change for the dual-motor design, i.e. both electric propulsors on each rotor combined produce the same amount of power as the single propulsor in the base quad-electric configuration design.

Without the cross-shafting system, the fault tree of the dual-motor quadcopter configuration resembles the fault tree of hexacopter collective-control configuration. Figure 56 shows the fault tree of a single rotor in the dual-motor quadcopter. Failure of either the reduction gearbox, collective actuators, the battery pack with the associated energy distribution components, or both electric propulsors result in catastrophic loss of rotor function. Figure 57 shows the top level of the dual-motor quadcopter fault tree. Compared to the base quad-electric design, OEI propulsion loss for the dual-motor configuration involves failure of any two electric propulsors which is the same loss of 25% of total propulsive power; catastrophic loss of propulsive power is triggered by loss of any three electric propulsors resulting in greater than 25% loss of propulsive power. Failure of a single rotor on the dual-motor quadcopter is considered catastrophic just as in the base quad-electric design.

Table 26 shows the failure rates of several major catastrophic events as well as the overall catastrophic failure rate of the overall vehicle architectures. Compared to the base quad-electric configuration, the dual-motor quadcopter has a lower failure rate for insufficient propulsive power both in and out of the OEI avoid region. However, the failure rate of catastrophic loss of function for a single rotor is significantly increased and offsets the benefits of the redundant electric propulsor at the overall vehicle level for the dual-motor design. In summary, the cross-shafting system is beneficial in case of the single propulsor failure, allowing for the uninterrupted power supply to the rotor with faulty propulsor. On the other hand, the redundant electric propulsors provide gains in terms of additional propulsive power that proves beneficial in OEI scenarios.

An additional comparison can be made between the base quad-electric configuration and the hexacopter collective-control configuration. In place of the cross-shafting system, the Hexacopter has two additional rotors. The addition of two extra rotors does not provide benefits when compared against the cross-shafting system as the additional rotors reduce overall reliability due to the ED common cause failures already mentioned earlier, thus not providing the vehicle with enough redundancy to match the reliability of the cross-shafting system.

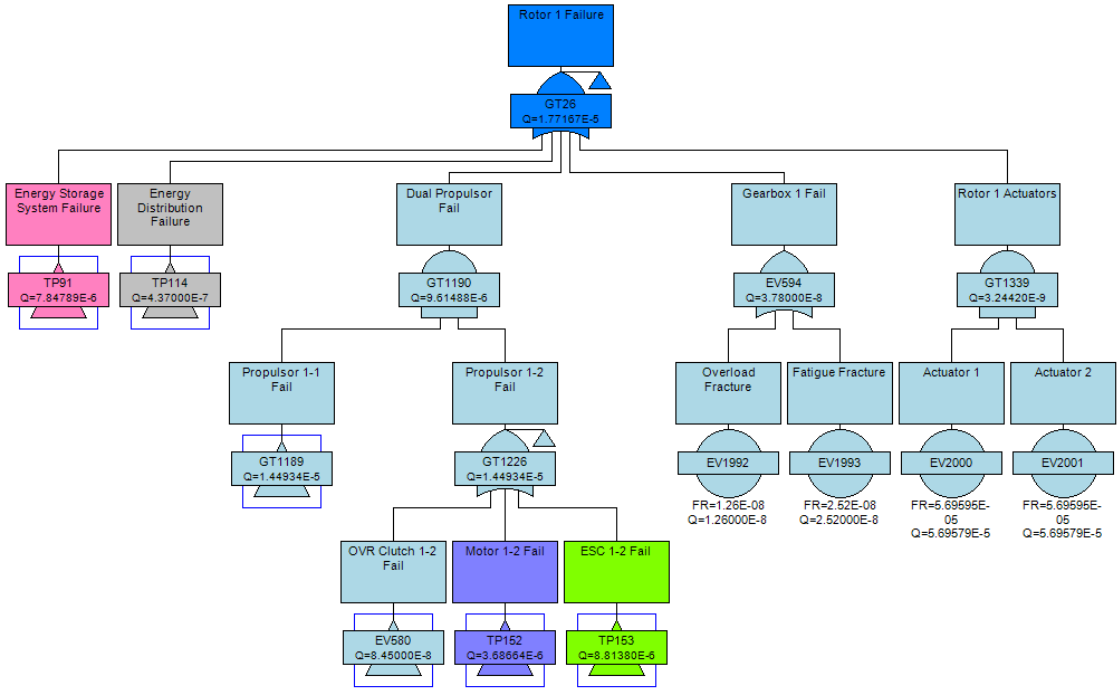

Figure 56: Fault Tree of a Single Rotor with dual electric motors (Quadcopter with No Cross-Shafting)

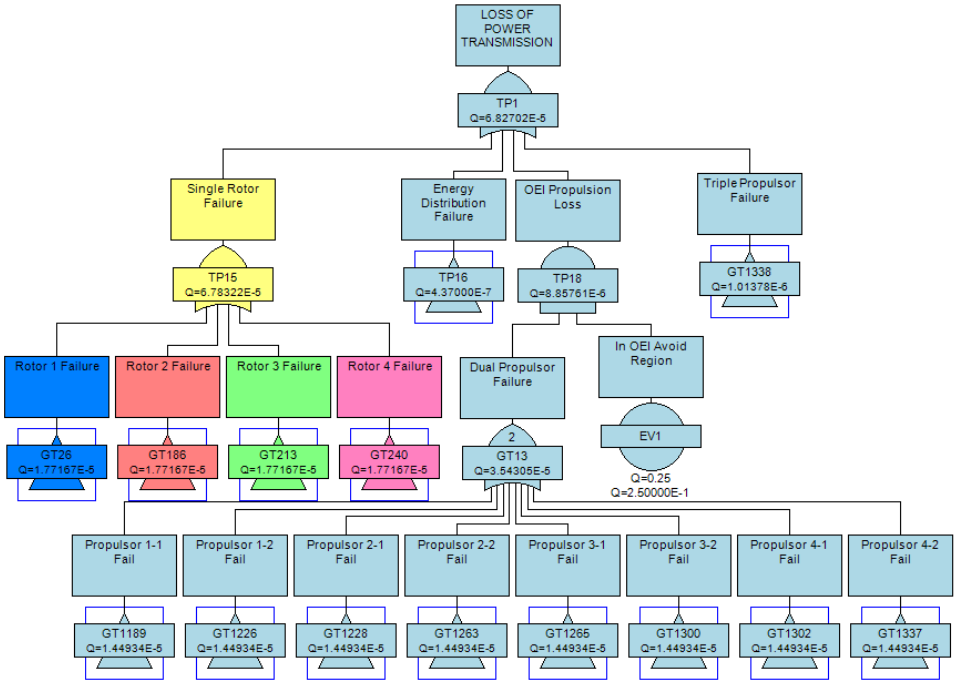

Figure 57: Top level fault tree of the dual-motor quadcopter design.

5.1.6 Reliability Comparison between Additional Rotors and Redundant Motors

A theoretical dual-motor configuration for the RPM-control Hexacopter was created to compare the reliability of the hexacopter and octocopter configurations. Figure 58 shows the fault tree of a single rotor for the dual-motor configuration of the hexacopter. Compared to the base RPM-control hexacopter, each rotor on the dual-motor configuration has an extra motor, ESC, and clutch. The two motors share a single cooling loop and both ESCs also share the same cooling loop.

Figure 59 shows the top level of the fault tree for the dual-motor hexacopter configuration. Just as for the base RPM-control hexacopter, loss of two rotors is considered catastrophic compared to loss of three rotors on the octocopter. Out of the twelve (12) electric propulsors (consisting of a motor, ESC, and clutch), loss of three (3) propulsors in the OEI avoid region (resulting in loss of 25% propulsive power) is considered catastrophic while loss of four (4) propulsors in the region away from OEI avoid region (loss of >25% propulsive power) is considered catastrophic. Table 27 shows the comparison of the top-level failure modes for both hexacopter configurations and the octocopter RPM-control configuration, ignoring the effects of the mechanical RGB to better isolate the effects of the number of rotors and propulsors. Due to the effect of ED related common cause failures in both vehicles, overall system reliability scales poorly with the increase of rotors. The dual-motor configuration has a lower failure rate for a catastrophic loss of propulsive power in the OEI avoid region, while the new failure mode (loss of propulsive power out of the OEI avoid region) has a very low failure rate. The Octocopter has higher overall catastrophic failure rate due to the significant increase in the catastrophic rotor failure (loss of three rotors).

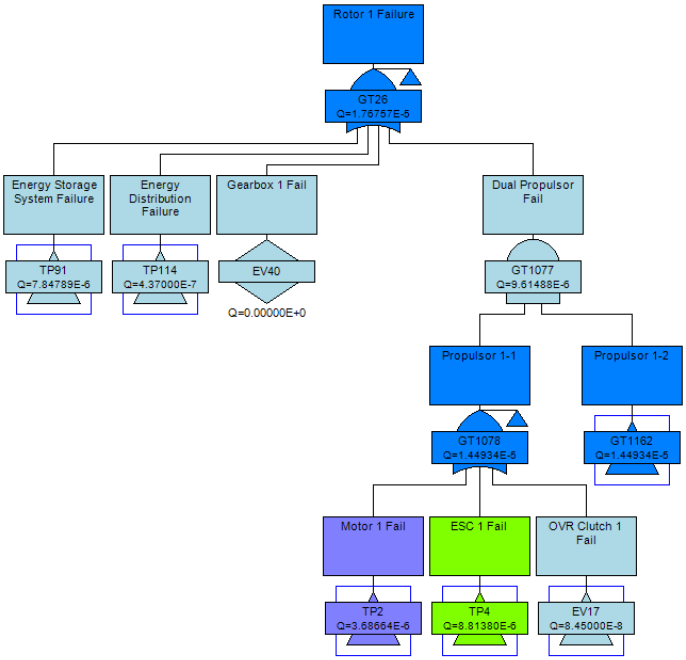

Figure 58: Fault tree for a rotor in the dual-motor Hexacopter design.

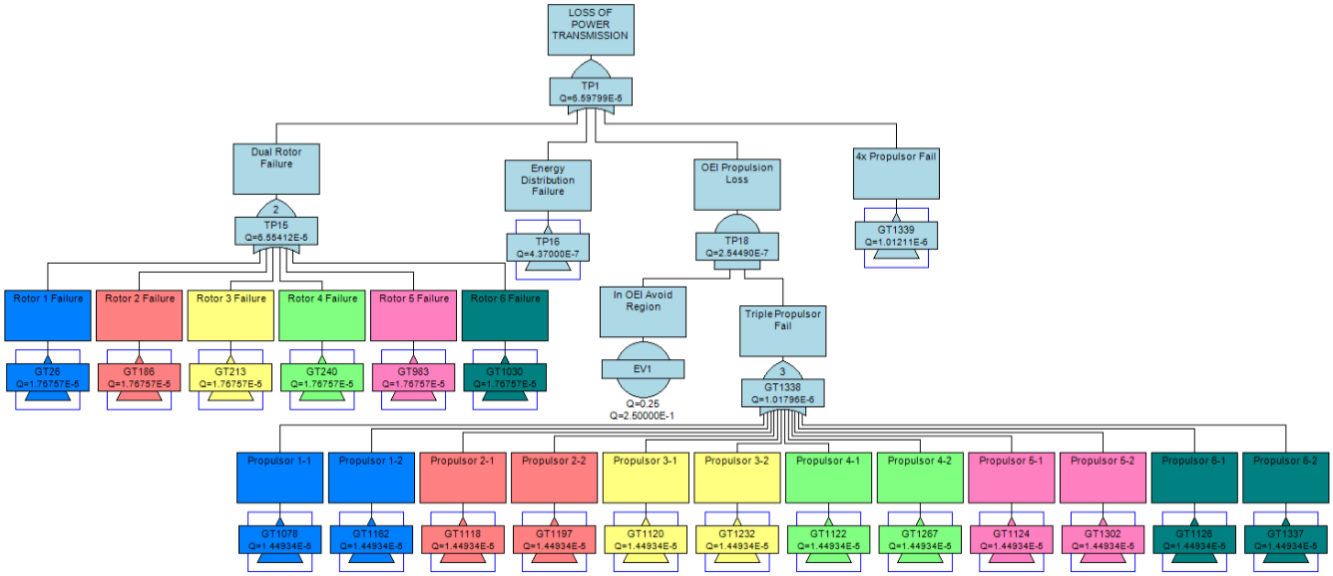

Figure 59: Top level fault tree of the dual-motor Hexacopter design.

Table 26. Comparison of RPM-Control Hexacopter and Octocopter configurations ignoring effects of the RGB.

Architecture	**Catastrophic Rotor** Failure Rate per Flight Hour	**Propulsion Loss in OEI Avoid Region** Failure Rate per Flight Hour	**Propulsion Loss away from OEI Avoid Region** Failure Rate per Flight Hour	**Overall** Catastrophic Failure Rate per Flight Hour
Hexacopter RPM-Control (without RGB)	6.554E-05	3.257E-05	N/A	9.829E-05
Hexacopter Dual-motors (without RGB)	6.554E-05	2.545E-07	1.012E-06	6.598E-05
Octocopter RPM-Control (without RGB)	2.419E-04	3.037E-05	N/A	2.724E-04

Since the base configurations are severely limited by common cause failure modes, the results do not reflect the full potential of the vehicle architectures. While the analysis was not conducted, it is feasible that the hexacopters and octocopter could be redesigned with more redundancy. Thus, the FTA analysis was again performed for the same three configurations without any common cause failure modes. Each propulsor component would have its own independent LV power source and cooling system, such that failure of one would not trigger failure in any other propulsors. In addition, the HV battery pack for each rotor has an independent cooling system as well. Table 27 shows the comparison of top-level failure modes for the more redundant designs. Without the detrimental effects of common cause failures, the octocopter is much more reliable than the hexacopter; every major top-level failure mode is improved for the octocopter. The dual-motor hexacopter design has a lower overall catastrophic failure rate than the octocopter. Compared to the octocopter, the dual-motor hexacopter has a higher failure rate for catastrophic rotor failure (dual rotor failure for the hexacopter and triple-rotor failure for the octocopter) but it is compensated by the lower failure rate for the OEI propulsion loss. Without common cause failure modes, the reliability gap between the octocopter and the more redundant dual-motor hexacopter design is much closer. In the absence of such common cause failures, electric distribution system component failures prove as the most significant contributor to the overall catastrophic failure rate for both configurations.

Table 27. Comparison of RPM-Control Hexacopter and Octocopter configurations ignoring effects of the RGB and Common Cause Failure Modes.

Architecture	**Catastrophic Rotor Failure Rate per Flight Hour**	**OEI Propulsion Loss Failure Rate per Flight Hour**	**Out of OEI Propulsion Loss Failure Rate per Flight Hour**	**Overall Catastrophic Failure Rate per Flight Hour**
Hexacopter RPM-Control (Without RGB)	7.630E-09	3.383E-05	N/A	3.428E-05

Hexacopter Dual-motors (Without RGB)	1.235E-09	2.083E-10	1.533E-11	4.387E-07
Octocopter RPM-Control (Without RGB)	6.404E-13	3.561E-09	N/A	4.405E-07

5.2 Dynamic Safety and Reliability Assessment Results

In this section, we will contrast and compare various configurations and technologies which require transient analysis of the aircraft and its subsystems.

5.2.1 Overall Architecture Comparison using DET Analysis

Comparison by Choice of Propulsion Systems: Quadcopter Electric, Hybrid and Turboshaft

Tables A summarize the DET results for quadcopter turboshaft vehicle (detailed DET results in Appendix D, Tables D1.1-D1.6).

Table 28. Quadcopter Electric Dynamic Event Tree (DET) Summary

Outcome Type	Single Faults			Double Faults			
	ED	TS	ACT	ED-ED	ED-TS	ED-ACT	TS-ACT
Catastrophic (> 10^{-9})	0	6	0	0	0	0	0
Critical (> 10^{-7})	0	0	0	0	0	0	0
Catastrophic (≤10^{-9})	0	0	0	9	19	0	9
Critical (≤10^{-7})	0	0	0	0	0	0	0
Major	3	0	0	0	0	0	0
Minor	0	0	0	0	0	0	0

Quadcopter Electric configuration single faults result (Appendix D, Table D1.1) show that the vehicle is able to handle all ED faults (including OMI) and is able to continue its mission without any critical or catastrophic outcomes. However, high torque and torque ripple faults in a single motor during takeoff/climb and landing phases respectively trigger *power limit state error* flag suggesting that the additional power demanded from the remaining motors exceeds the MCP rating of single or multiple motors during the demanding flight phases. Quadcopter electric configuration is also able to handle two actuator faults (floating surface and increased deadband) on a single rotor without any undesirable outcomes. In case of failure of one of the four cross-shafts, the respective motor is isolated. In such cases, controller reconfigures the motor operation, allowing for the isolated motor to function independently. The outcomes of *TS- Front left motor isolated* fault scenario confirms this outcome. However, severe transmission related soft failures (TS SL-3) result in catastrophic outcomes for the aircraft. Such cases, for example could be due to severe damage in Rotor Gear Box (RGB) which is the last component in the driveline connected to the rotor, so in absence of any redundant options, a severe damage in component could result in drop in RPM of the affected rotor, indicated by *RPM too low* flag in the simulation.

For quadcopter electric or hybrid configurations, any two ED-related faults in same motor do not cause any severe perturbations from the nominal behavior since remaining motors in combination with the cross-shafting are successfully able to smooth out any torque/RPM related errors for the rotor which is connected to a faulted motor. Therefore, this scenario for the quadcopter electric (and hybrid) provides safe outcomes for all cases (Appendix D, Table D1.2). Similarly, any two ED-ACT related faults in same driveline do not cause any undesirable outcomes (Appendix D, Table D1.3). However, as it occurs for single TS fault scenarios, TS SL-3 faults injected in combination with ACT faults (Appendix D, Table D1.4) or ED faults (Appendix D, Table D1.5) result in catastrophic outcomes due to loss of power and subsequent loss of RPM (as indicated by *RPM too low* flag) and complete loss of vehicle control (as indicated by *Over-G* flags). Although the frequency of such outcomes is high, all double fault scenarios that result in catastrophic outcomes have likelihood values that are less than EASA threshold of 10^{-9} and hence are not critical in nature.

For quadcopter electric (or hybrid configuration), any two ED-related faults in two different motors (Appendix D, Table D1.6) result in some cases with catastrophic outcomes (however likelihood of such outcomes is less than EASA threshold). All failures have *RPM too low* flag, suggesting limitations of current motors which are sized for OMI but are not able to match the power deficit in case some severe faults occur in two out of four motors.

Tables B summarizes the DET results for quadcopter hybrid vehicle (detailed DET results in Appendix D, Tables D2.1 & D1.2-D1.6). Quadcopter hybrid architecture only differs from the quadcopter electric architecture in the way energy is generated and/or supplied to the electric motors. For electric case, battery is the source of energy while for hybrid case, turbo-generator is the main source and battery functions as auxiliary unit, in case of emergency use. Therefore, all common single faults for the two configurations have identical results (Appendix D, Table D2.1) It is important to note that for the hybrid system, the power available from the battery and generator are combined and the power limit has not been reached for this aircraft. Only additional fault scenarios considered for the hybrid vehicle are concerned with the turbine-generator related faults. Some very low efficiency cases for the turbine generator result in catastrophic outcomes for the aircraft where instability occurs during the emergency landing.

Table B. Quadcopter Hybrid Dynamic Event Tree (DET) Summary

Outcome Type	**Single Faults**				**Double Faults**			
	ED	TS	ACT	TG	ED-ED	ED-TS	ED-ACT	TS-ACT
Catastrophic (> 10^{-9})	0	6	0	2	0	0	0	0
Critical (> 10^{-7})	0	0	0	0	0	0	0	0
Catastrophic (≤10^{-9})	0	0	0	0	0	19	0	9
Critical (≤10^{-7})	0	0	0	0	0	0	0	0
Major	3	0	0	0	0	0	0	0
Minor	0	0	0	3	0	0	0	0

Tables C summarizes the DET results for quadcopter turboshaft vehicle (detailed DET results in Appendix D, Tables D3.1-D3.2). The vehicle shows very reliable dynamic response to all the single faults cases (including OEI case) at all four FIPs (Appendix D, Table D3.1), assuring that second operating engine is sized to handle the power demand at all four FIPs in case of faulty conditions. Also, unlike quadcopter electric or hybrid configurations, for the transmission fault scenarios where the transmission efficiency

drops severely, the turboshaft engine is able to compensate for the required power deficits, indicating stark contrast between the power sizing of turboshaft configuration and electric/hybrid configurations provided by NDARC.

TABLE C. Quadcopter Turboshaft Dynamic Event Tree (DET) Summary

Outcome Type	Single Faults			Double Faults
	Engine-OEI	ACT	TS	TS-ACT
Catastrophic (> 10^{-9})	0	0	0	0
Critical (> 10^{-7})	0	0	0	0
Catastrophic (≤10^{-9})	0	0	0	0
Critical (≤10^{-7})	0	0	0	0
Major	0	0	0	0
Minor	0	0	0	0

Comparison by Flight Control Method: Hexacopter Collective and RPM-Control

Tables D summarizes the DET results for hexacopter Collective-Control vehicle (detailed DET results in Appendix D, Tables D4.1-D4.3).

TABLE D. Hexacopter Collective-control Dynamic Event Tree (DET) Summary

Outcome Type	Single Faults			Double Faults	
	ED	TS	ACT	ED-ED	ED-ACT
Catastrophic (> 10^{-9})	0	0	0	0	0
Critical (> 10^{-7})	3	0	0	0	0
Catastrophic (≤**10^{-9}**)	0	0	0	0	0
Critical (≤10^{-7})	0	0	0	0	3
Major	0	0	0	0	0
Minor	0	0	0	0	0

Hexacopter collective control configuration single faults results (Appendix D, Table D4.1) show that critical outcomes for ED faults trigger *Motor temperature too hot* condition in the case for a low torque and high torque fault. Upon closer inspection, the *Motor temperature too hot* is showing for Low Torque (SL1) (least severe) while this low torque (SL3)(most severe) is not resulting in any off nominal outcomes. This somewhat counterintuitive result can be understood by analyzing the specific motor that overheats at the time of the fault. Figure 60 and Figure 61 show a comparison between the two cases for torque available and required for motor 1 and the RPM value for each motor respectively. By failing motor 1 with low torque, the speed control loop is bypassed and a constant torque available is provided by the motor. This results in the RPM values for motor 1 to be different than for the remaining non-failed motors. It can be seen that for both cases a decrease in required torque for motor 1 increases the RPM value for the failed motor 1. In the case of the failed motor 1 (SL1), the RPM value increases more significantly than for the

failed motor 1 (SL3). This increase in failed motor 1 (SL1) eventually overheats motor 1 which triggers the fault seen in TABLE D.

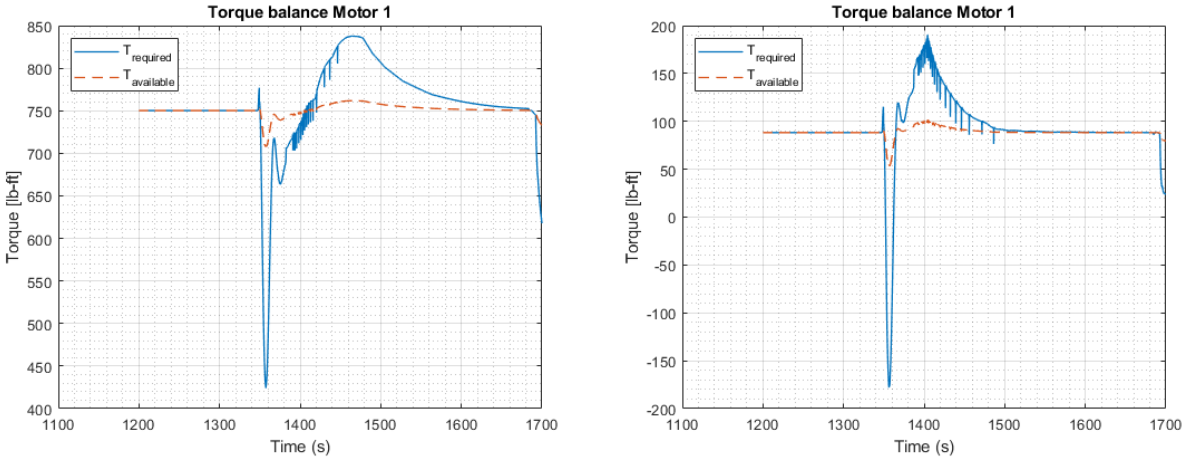

Figure 60 Hexacopter collective Low Torque (SL1) Motor 1 Torque Balance (LEFT) and Hexacopter collective Low Torque (SL3) Motor 1 Torque Balance (RIGHT)

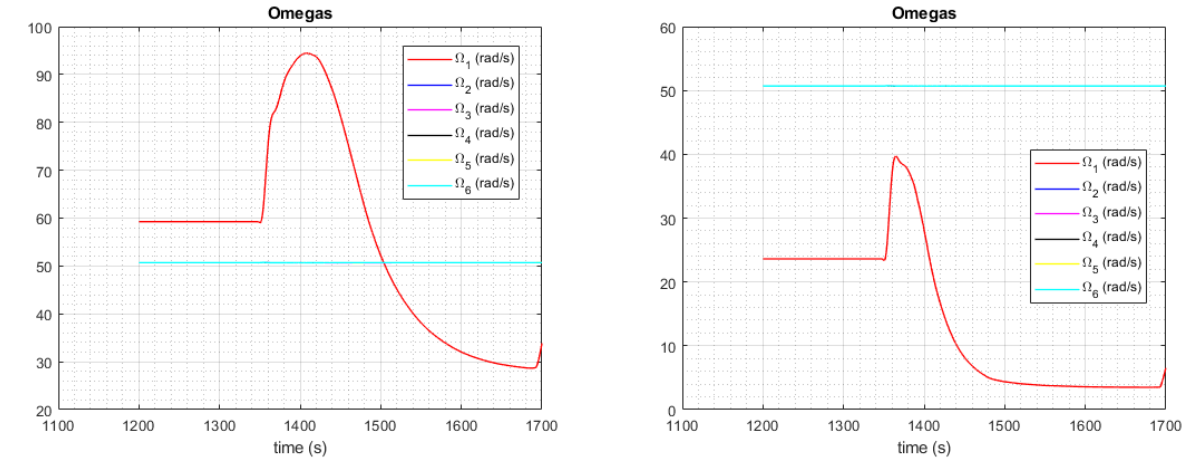

Figure 61 Hexacopter collective Low Torque (SL1) Motor RPM (LEFT) and Hexacopter collective Low Torque (SL3) Motor RPM (RIGHT)

For all other single faults, the hexacopter collective control vehicle was able to continue its mission and complete it without further incidents. The hexacopter collective control vehicle shows a particularly reliable dynamic response to the OMI (no torque) case during all flight phases. Just like in quadcopter cases, for the hexacopter collective control configuration, any two ED-related faults in same motor (Appendix D, Table D4.2) do not result in severe outcomes. In this perspective, the addition of more rotors provides the same benefits as are provided by cross-shafting in the quadcopter vehicles. Hexacopter collective double ED-ACT faults in same motor/rotor (Appendix D, Table D4.3) show the same counterintuitive outcomes for the low torque (0.85) fault as could be seen for the single faults (Appendix

D, Table D4.1). Again, these can be considered as an outlier and are most likely the result of certain assumptions made in the simulation environment.

Tables E summarizes the DET results for hexacopter RPM-Control vehicle (detailed DET results in Appendix D, Tables D5.1-D5.2).

TABLE E. Hexacopter RPM-control Dynamic Event Tree (DET) Summary

Outcome Type	Single Faults	
	ED	TS
Catastrophic (> 10^{-9})	24†	-
Critical (> 10^{-7})	4†	-
Catastrophic (≤10^{-9})	-	-
Critical (≤10^{-7})	10†	-
Major	6†	-
Minor	7†	-

†Inconclusive results

Hexacopter RPM control configuration single faults result (Appendix D, Table D5.1) show that all triggered conditions are shown as inconclusive. An abnormal flight response occurred for these faults which originally flagged the condition. However, due to the complexity of these flight phases and existing limitations of the applied control system, no accurate prediction can be made about the vehicle response after the abnormal condition. Hence, these results are categorized as inconclusive. The majority of these inconclusively marked flights showed an abnormal variation in the heading angle after the fault which can be traced back to the interaction between the dynamics of the vehicle and the vehicle controller. Improvements to the vehicle controller in an effort to mitigate these effects were deemed beyond the scope of this research. Therefore, an inconclusive marking of these cases is deemed appropriate due to potential improvements of the control system and not necessarily the inherent shortcoming of the variable RPM control vehicle architecture as compared to the variable pitch control vehicle.

Comparison by Number of Rotors: Hexacopter vs Octocopter (RPM-control)

Tables F summarizes the DET results for octocopter RPM-Control vehicle (detailed DET results in Appendix D, Tables D6.1-D6.2).

TABLE F. Octocopter RPM-control Dynamic Event Tree (DET) Summary

Outcome Type	Single Faults	
	ED	TS
Catastrophic (> 10^{-9})	25†	-
Critical (> 10^{-7})	5†	-
Catastrophic (≤10^{-9})	-	-
Critical (≤10^{-7})	11†	-
Major	8†	-
Minor	1†	-

†Inconclusive results

Similarly to the hexacopter RPM vehicle, all outcomes under single faults (Appendix D, Table D6.1) are marked inconclusive since a similar behavior was seen in the flight phases after single fault injection for the octocopter vehicle. Again, abnormal flight conditions occur that are being registered as catastrophic, critical, major or minor outcome, but no real conclusion can be drawn from the results given there is potential to improve the interaction between vehicle dynamics and control system.

5.2.2 Impact of power profile and duty cycle on motor reliability

The availability of multiple vehicle architectures provides an opportunity to analyze the impact of the configuration on the power profile and stress on the components. The analysis of the power profile of the hexacopter pitch control, the hexacopter rpm control and the octocopter are reported in this section.

The objectives of the analysis are to quantify the impact of the architecture on the power required to trim, the peak power required during the maneuvers, the power required induced by wind disturbances and the implications of operating with one motor inoperative. The following analyses have been performed on the hexacopter with pitch control, hexacopter with RPM control and octocopter with RPM control:

- Nominal mission with results reported in the Appendix M;
- Nominal mission with wind disturbances, with results reported in the Appendix M;
- Mission analysis with loss of electric motor at the beginning of the mission to assess the performance during the whole mission with results reported in the Appendix M;
- Nominal trim condition (provided by NASA) and trim condition with one motor out reported in section 4.1.5.1 with results in the Appendix M ;

For each aircraft, the power of the individual motors as a function of time in the different phases of the mission are displayed, as well as a distribution of the power in which the motors operate. The nominal conditions, the aircraft operating in wind and operating with one motor out are compared.

The cases with one motor inoperative are modeled as a no torque condition applied on the motor 1 in the first few seconds of flight. This allows to simulate the whole mission with one engine inoperative. For every aircraft, the motor 1 is selected as the inoperative motor, one of the rotors at the front of the aircraft. This selection is based on the fact that the rotor 1 and 2 have the smallest nominal power rating, and that the thrust lost by rotor 1 has to be partially reassigned to rotor 2. This leads to a large ratio of power to operate vs. nominal power for the rotor 2.

In order to simulate the whole mission for the cases with one motor out, there is a need to have a system that can successfully complete the whole mission. Consequently, the motors for the RPM-Control aircraft (hexacopter with rpm control and octocopter) are upsized, according to the GT-OSU OMI guidelines detailed in a previous section.

Some of the general observations from the scenarios shown in Appendix:

- With the larger electric machines, all 3 aircrafts are able to complete the mission segment under nominal, wind and OMI conditions;

- As expected, the takeoff and climb are the most demanding segments, and the cruise is the least demanding segment for all three aircrafts;
- The peak power occurs during the acceleration phase, and the maximum value happens on the rear rotors;
- Under wind conditions, the power distributions of all three vehicles during all three flight phases approaches a normal distribution;
- OMI operations significantly increase the peak power demand per rotor;
- The presence of wind affects the power requirement of the aircraft in a similar fashion: The ratios of 95% percentile of motor power requirements during wind operation vs. no wind condition are the same for all three aircraft: increase of about 8% in takeoff and acceleration, 35% in cruise and 8-10% during deceleration and landing;
- Similarly, there is a not a large differentiating factor in the ratio of peak to nominal power for the three aircraft in case of wind disturbance;

Impact of Control Strategy

As outlined in the previous paragraph, there are some similarities between the power transients, and power transient ratios for the hexacopter with rpm or pitch control. However, some output provide some insight into the differences of operating conditions.

In Table 29, the ratios of mean power required during cruise are compare to the peak power of each rotor for the hexacopter with pitch control and hexacopter with RPM control. For both aircraft, the general trend is that the front rotors (1 and 2) require less power to cruise and experience a smaller peak power than the rear rotors (5 and 6), as expected due to the rotor placement, However, given that the RPM control aircraft sees a large gradient of thrust required between the front and rear rotors during cruise, the ratio of peak/cruise power is not uniform through the aircraft.

Finally, an important observation is on the ratio of peak power with one motor inoperative (rotor 1) vs. the nominal power in cruise as shown on Table 30. The maximal peak power to power to cruise in nominal condition is 2.74 for the hexacopter with pitch control and 5.24 for the hexacopter with rpm control. This comparison indicates a large penalty for peak power with loss of a rotor for the system with rpm control, consistent with the trim analysis for one motor inoperative.

Table 29 Peak Power vs Power to Cruise for the hexacopter with pitch control and hexacopter with RPM Control

	Hexa pitch			Hexa rpm		
Rotor number	Mean Power in Cruise (hp)	Peak Power (hp)	Peak/Mean Cruise Power	Mean Power in Cruise (hp)	Peak Power	Peak/Mean Cruise Power
1	54.3	110.3	2.03	38.7	96.2	2.49
2	54.3	110.3	2.03	38.7	96.2	2.49
3	61.4	120.6	1.96	51.7	106.9	2.07
4	61.4	120.6	1.96	51.7	106.9	2.07
5	69.0	133.2	1.93	59.2	106.9	1.81
6	69.0	133.2	1.93	59.2	106.9	1.81

Table 30 Peak Power vs Power to Cruise for the hexacopter with pitch control and hexacopter with RPM Control with one motor inoperative

	Hexa pitch			Hexa rpm		
Rotor Number	Mean Power in Cruise (hp)- Nominal	Peak Power (hp)	Peak/Mean Cruise Power	Mean Power in Cruise (hp) - Nominal	Peak Power	Peak/Mean Cruise Power
1	54.3	N/A	N/A	38.7	N/A	N/A
2	54.3	138.8	2.56	38.7	181.8	4.70
3	61.4	168.2	2.74	51.7	211.3	4.09
4	61.4	114.8	1.87	51.7	271.1	5.24
5	69.0	130.2	1.89	59.2	232.1	3.92
6	69.0	142.5	2.07	59.2	67.1	1.13

Impact of Number of Rotors

The analysis of the hexacopter and octocopter with RPM control provides an opportunity to compare the effect of the number of rotors on the power levels.

The ratio of peak power to power to cruise is shown in Table 31. For both architectures, the ratios are a function of the longitudinal position of the rotors on the aircraft. Similarly, the ratio of peak power for the OEI to power to cruise is expressed on Table 32. It is possible to observe that there is a larger peak value for the octocopter vehicle on rotor 3, the rotor located behind the failed rotor 1.

In the trim analysis, it can also be observed that the octocopter has rotors with higher power required increased in steady-state conditions compared to the hexacopter with rpm control. It is understood that minimizing the change in rpm squared as the objective to the trim problem will not yield the minimum power requirement, but it allows to keep some actuation power.

Table 31 Peak Power vs Power to Cruise for the hexacopter and octocopter with rpm control

	Hexa rpm			Octo rpm		
Rotor number	Mean Power in Cruise (hp)	Peak Power (hp)	Peak/Mean Cruise Power	Mean Power in Cruise (hp)	Peak Power	Peak/Mean Cruise Power
1	38.7	96.2	2.49	34.1	78.3	2.30
2	38.7	96.2	2.49	33.6	78.3	2.33
3	51.7	106.9	2.07	42.2	90.0	2.13
4	51.7	106.9	2.07	43.5	90.0	2.07
5	59.2	106.9	1.81	47.4	90.4	1.91
6	59.2	106.9	1.81	46.7	90.4	1.94
7	N/A	N/A	N/A	57.3	103.1	1.80
8	N/A	N/A	N/A	58.7	103.1	1.76

Table 32 Peak Power vs Power to Cruise for the hexacopter and octocopter with rpm control with one motor inoperative

	Hexa pitch			Octo rpm		
Rotor Number	Mean Power in Cruise (hp)	Peak Power (hp)	Peak/Mean Cruise Power	Mean Power in Cruise (hp)	Peak Power	Peak/Mean Cruise Power
1	38.7	N/A	N/A	34.1	N/A	N/A
2	38.7	181.8	4.70	33.6	183.3	5.46
3	51.7	211.3	4.09	42.2	269.7	6.39
4	51.7	271.1	5.24	43.5	158.2	3.64
5	59.2	232.1	3.92	47.4	241.0	5.08
6	59.2	67.1	1.13	46.7	96.6	2.07
7	N/A	N/A	N/A	57.3	150.1	2.62
8	N/A	N/A	N/A	58.7	59.0	1.01

5.2.3 Impact of battery sizing on Hybrid Quadcopter Reliability

Collective control changes on the rotors leads to fluctuations in the power required from the turbo-generator, increasing its duty cycle and likelihood of failure. The presence of a battery in the hybrid systems provides new operating degrees of freedom. This section explores the use of 2 hybrid-electric operating modes and the impact on the reliability of the system: battery usage only after a turbine-generator failure and battery usage throughout the mission to support the transient power requirement.

In the NDARC models provided, the battery was sized to provide a 10-minutes hover. During the nominal operation, it is assumed that the turbine provides all of the power, except during short low-power

taxi segments, during which the turbine-generator is turned off and the battery becomes the only power source. However, these taxi segment do not have a significant impact on the battery charge state.

In the dynamic simulation of the hybrid aircraft, in the case of a turbine-generator failure, the controller redirects the aircraft to the ground through the emergency diversion maneuver. It is observed that the nominal battery sized by NDARC is not able to provide enough power to allow the aircraft to land. Consequently, the battery size is doubled, and this assumption is consistent through the different operating modes. [10]

The sum of the power required by the 4 electric motors is shown on Figure 62. It can be observed that there are large peaks of power required at the beginning and the end of the climb. The maximum peak has the value of 604hp, and the power required in cruise is 300hp, illustrating that the magnitude of the peaks are considerable. A second observation is that there is a very low power dip at the end of the cruise segment, with a predicted negative power required.

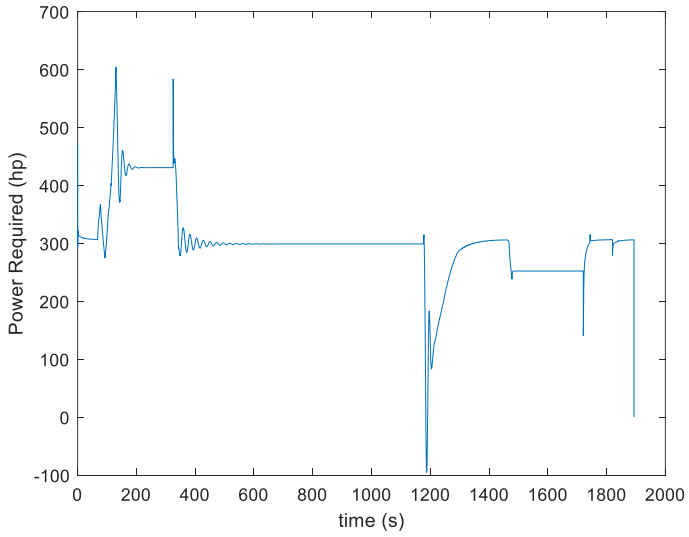

Figure 62 Sum of power required by the 4 electric rotors as a function of time for the hybrid aircraft

Nominal Operation: No use of the battery

The nominal operating mode, discussed previously in the report, uses only the turbogenerator to provide electric power to the electric motors. The results from the nominal mission without wind are shown in the following figures. It is important to note that the turbine has a minimal power required of 175hp in order to stay within the bounds of the turboshaft model.

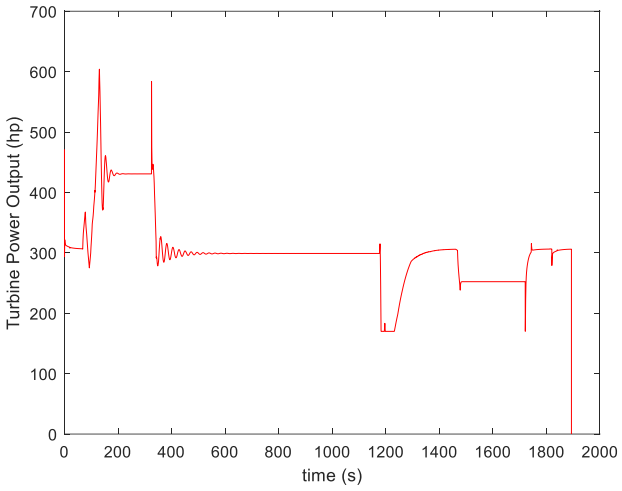

Figure 63: Power output of the turbogenerator as a function of time

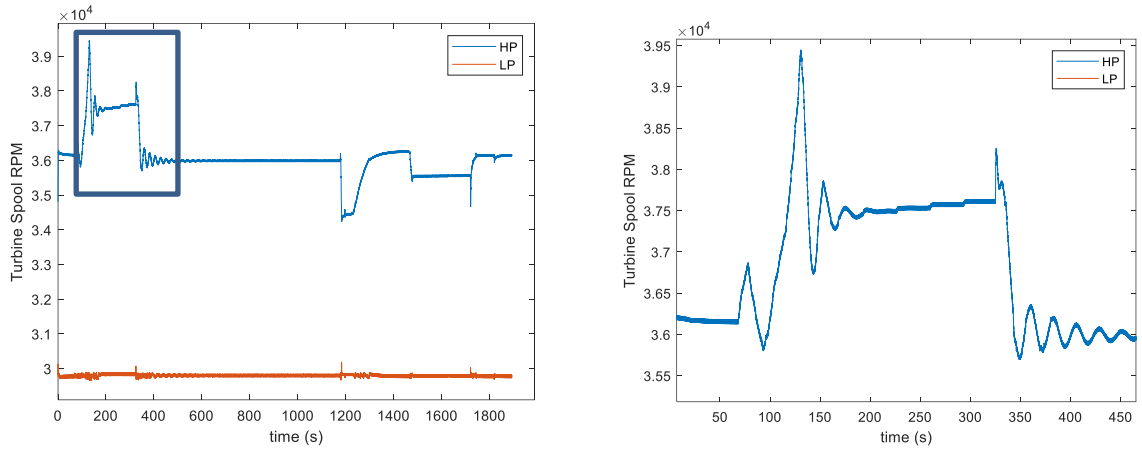

Figure 64: RPM of the high pressure and low pressure spools of the turbogenerator (left) and expanded view of the high pressure spool transient behavior during climb (right)

The turbogenerator is capable of matching the power required at any point in the operation. Conceptually, the generator increases the torque required on the turbine instantaneously which reduces the RPM of the low pressure spool. The turbine reacts to the loss of RPM of the low pressure spool by increasing the fuel flow.

This operating mode introduces important sharp variations of power and spool speed of the turbine due to the power required change with mission segment.

Battery Use to Supplement Turbogenerator

A second operating mode is to use the battery to supplement the turbogenerator power. This could allow to potentially smooth out the transient power demands.

The power request from the turbine, rather than being driven by the immediate power request from the electric motors, comes from a power schedule, which has been coded as a function of time. In the future, it could be envisioned that the schedule would be as a function of the mission segment.

The power schedule is defined offline based on the power profile. Manually, the power schedule is created to attempt the least amount of variations or smooth variation, and a 5% power margin during the steady-state operating conditions to reduce the chances of having to throttle down the turbine. As mentioned in the previous sections, at the end of the cruise there is a negative power required segment. The power schedule assumes that the power required stays positive during this portion.

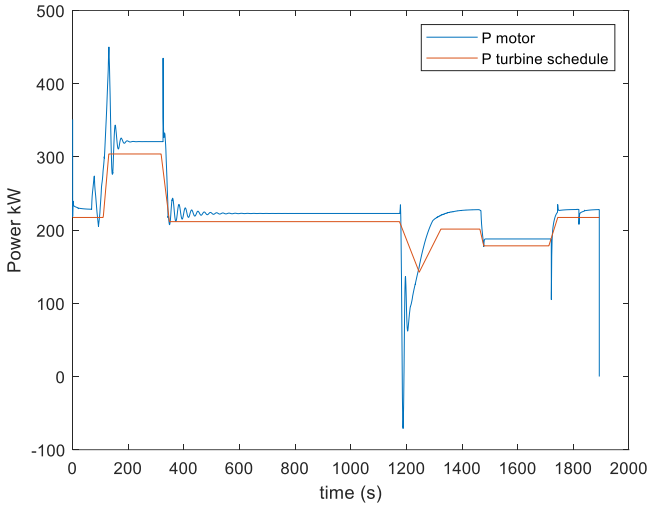

Figure 65 Power schedule from the turbogenerator as a function of time

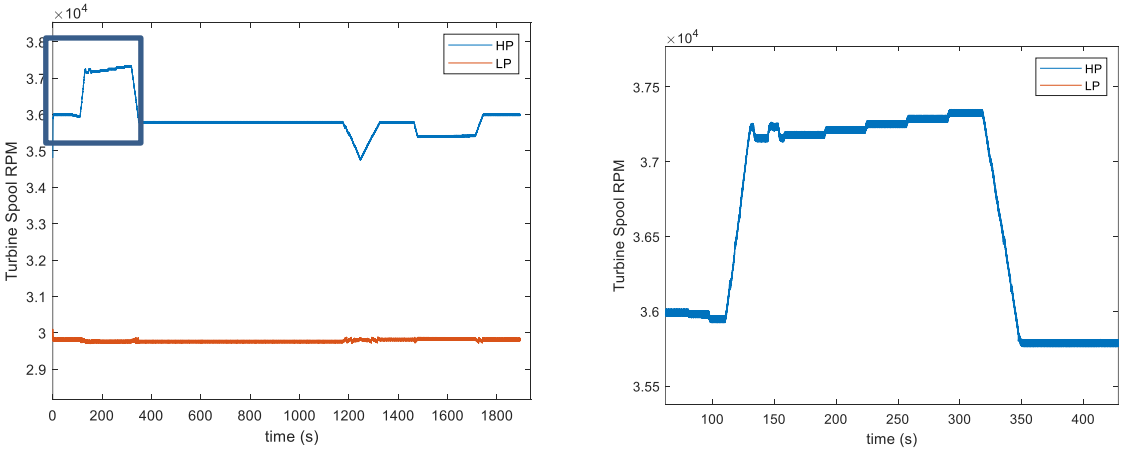

Figure 66: RPM of the high pressure and low pressure spools of the turbogenerator (left) and expanded view of the high pressure spool transient behavior during climb (right)

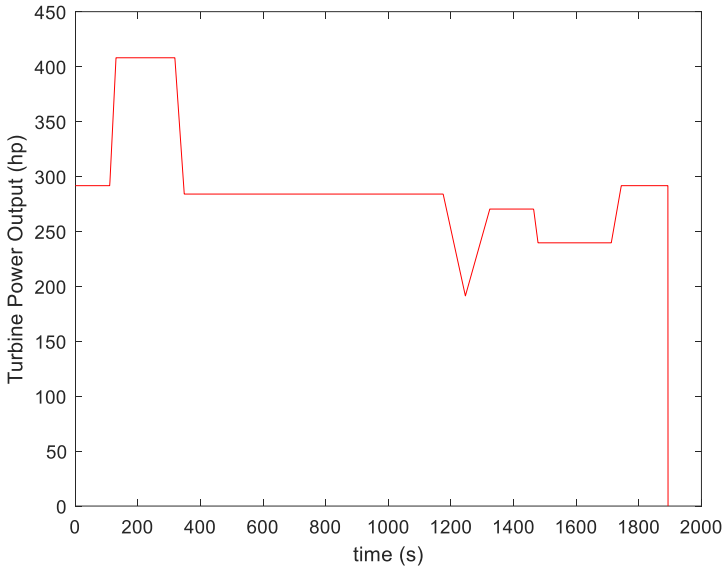

Figure 67: Scheduled power from the turbogenerator

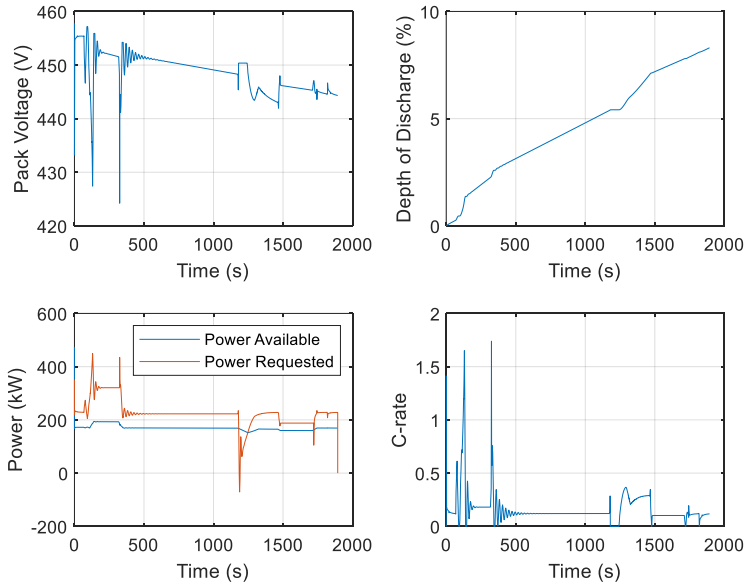

Figure 68: Battery usage throughout mission showing peak voltage, depth of discharge, and C-rate

Observations

The operating mode of the hybrid powertrain can have an impact on the transient response of the turbogenerator. In nominal operation, if the battery contributes to 5% of the nominal power and the transient can be predicted, the power demands on the generator can be smoothed out considerably. This

operating mode lead to the use of the battery of about only 8% of its depth of discharge. It is important to note that the wind was not considered for this analysis. Also, the nominal battery capacity was twice the capacity of the NDARC prescribed capacity, dictated by the power required to perform the emergency landing rather than capacity. In this operating mode, there is an increase in the c-rate due to the fact that the battery provides peak power: the c-rate is relatively large (1.5-1.75) compared to the nominal operation of the all-electric aircraft, which sees a max C-rate of about 1. This does not brings any concern given that the upper limit assed on c-rate is 5.

Finally, the change in transient level can affect the reliability and durability of the turbogenerator. While the model does not include a quantitative approximation of the reliability, some cause and effects can be outlined. The model provides an insight in the dynamic response at the spool level. For the case where no battery is used, there is an overshoot in high pressure spool rpm of about 2,300 RPM, or about 6% at the beginning of the acceleration phase for a very small amount time. This can introduce variations of temperature and this short duty cycle can possibly reduce the life of the turbine.

It is important to note that with the hypotheses used for the model, the battery discharge rate during operation without the turbogenerator constraints the size of the battery. For this condition, the battery can be used during the nominal operation without affecting the ability to fill the 10-minute hover requirement.

Alternative Operating Modes

Another important assumption of the analysis was that the battery is not charged in flight. If the battery was to be charged in flight, this could lead to an additional smoothing out of the turbine power required, and a very small impact on the battery capacity. As an example, if the turbine was operated at the average power required over the last 30 seconds, the peaks and valley of motor power required could be filled with the battery with relatively low impact on its capacity.

An extreme case of this hybrid operation would be to use the generator at a single power setting, the average of the power required for the whole mission. This operating mode would introduce the least amount of transient on the turbine, but would require the largest battery.

A simpler operating mode of the turbine could be to define a maximal power required for the turbogenerator, as shown on Figure 69. The battery would be used only for 2 very small portions of the mission during which the power required exceeds the maximal turbine power limit, , without affecting the capacity of the battery significantly.

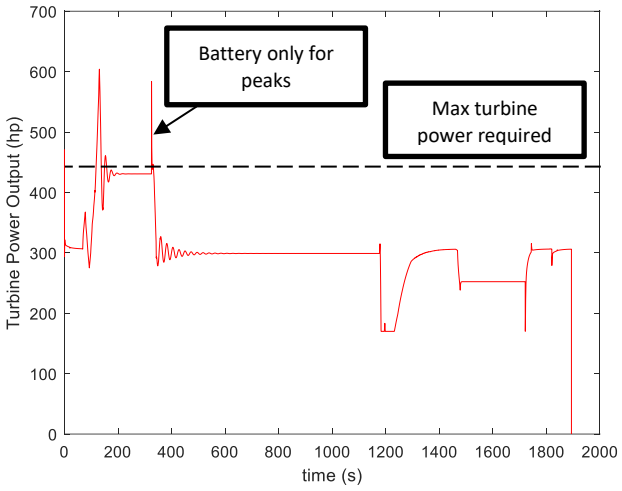

Figure 69 Alternative operating mode of the hybrid system: include a maximum value for the turbogenerator

5.2.4 Impacts of voltage and current levels on reliability (C2, A6, B5)

Voltage and current levels are important design parameters for electric drive. They affect efficiency, dynamic response, size, electromagnetic compatibility and emissions, and life of components and systems. In recent years, industry and academia have been investigating and demonstrating powertrain components for traction application with voltage higher than 700V with the aim of developing high power density drive. However, limitations have been encountered due to availability and reliability of capacitors and semiconductor devices at high voltage. In general, an electric component is designed to withstand a certain max voltage and current level, then an isolation voltage is defined as well.

Operating a component at a low voltage, compared to nominal, usually correspond to higher current for the same power, this is usually not a problem if the current does not overcome the current rating. On the contrary, operating a component at high voltage, compared to nominal, can correspond to a higher magnetic flux can cause partial saturation, demagnetization of the permanent magnets for electric machines, reduce life of the winding insulation, reduce life of the semiconductor devices, and quickly introduce severe failures such as short circuit.

On the other side, there are in general no mayor issues in operating a component at a low current compared to nominal, this can correspond to a reduced power request from the load. While high current compared to nominal usually correspond to higher thermal stress of the components.

In this section, the impact of different design strategies has been analyzed. A nominal 600V electric drive is here compared with a 300V and 900V system.

The electric drive failure rate models proposed have been adapted to take into account the design specification of voltage/current levels and the related stress factors [56]:

$$\begin{aligned} \lambda_M &= \lambda_{Stat} \cdot \pi_U \cdot \pi_I + \lambda_{Rotor} \cdot \pi_U \cdot \pi_I + \lambda_{Mech} \cdot \pi_U \cdot \pi_I + \lambda_{Cool} \\ \lambda_{ESC} &= \lambda_{Inverter} \cdot \pi_U \cdot \pi_I + \lambda_{DC\,cap} \cdot \pi_U \cdot \pi_I + \lambda_{Control} \cdot \pi_U + \lambda_{Cool} \\ \lambda_{ESS} &= \lambda_{cell} + \lambda_{BMS} \cdot \pi_U + \lambda_{Cool} \\ \lambda_{EDS} &= \lambda_{fuse} \cdot \pi_U \cdot \pi_I + \lambda_{contactor} \cdot \pi_U \cdot \pi_I + \lambda_{connection} \end{aligned} \quad (47)$$

In detail from the FTA analysis of these components it has been noted that:

- Cooling systems are not directly affected by the voltage current level, since the function of the cooling is to dissipate a certain amount of heat independently from the source;
- Control unit of the ESC and BMS are mainly affected by the voltage level due to EMI/C;
- Connections of the EDS are minimally affected by voltage and current levels, if a proper design strategy is adopted.

The π-factors are represented with the following empirical models to describe the voltage and current dependence of failure rates.

$$\pi_U = exp\left(C_3 \cdot \left(\frac{V_{op}}{V_{rat}}\right)^{C_2} - \left(\frac{V_{ref}}{V_{rat}}\right)^{C_2}\right)$$
$$\pi_I = exp\left(C_4 \cdot \left(\frac{I_{op}}{I_{rat}}\right)^{C_5} - \left(\frac{I_{ref}}{I_{rat}}\right)^{C_5}\right) \quad (48)$$

Where X_{op}= average operating (e.g. 900V or 300V); X_{ref}= system reference (e.g. 600V); X_{rat}= system rating (e.g. 1kV); C_2, C_3, C_4, C_5 = calibration constant.

Considering the powertrain of the quadcopter electric defined in section 1.3.1:

- reference vehicle is designed for 600V;
- two electric systems rated for 300V (corresponds to high current) and 900V (corresponds to high voltage) have been designed;
- Component insulation rating 1-kV.
- MCP = 136hp=88.5kW (continuous power)
- IRP = 233hp=137kW (intermediate power)
- PF=0.9 (power factor)
- Stress factor calibration: (C_2, C_3, C_4, C_5)= (0.5, 1.2, 0.5, 1.2) [58]

Note: in the following tables percentage increase/decrease of failure rate is calculated compared to the nominal condition.

Table 33 shows the impact of current and voltage level on the components of the Quadcopter Electric. In detail, electric machine, electronic speed controller and electronic power distribution are highly affected by both the stress factors. Voltage stress seems to have a larger impact, considering the current model calibration. Energy storage system is lightly impacted by high voltage/current design and in particular the 300V design corresponds to a decrease of the failure rate.

It can be demonstrated that Table 33 is valid for the electric drive of all the different configurations, due to the constant ratio between current and voltage levels when designing systems having the same nominal power. Then, this failure rates will be applied to all the different architectures.

At the electric drive level (subsystem), higher failure rate is shown for high voltage system design compared to the high current solution, as shown in Table 34.

Table 33: Calculation of the stress factors (π_U and π_I) and component failure rate for the Quadcopter Electric

	Reference system (600V)		High Current system (300V)		High Voltage system (900V)	
	MCP	**IRP**	**MCP**	**IRP**	**MCP**	**IRP**
Power [kW]	88.5	137	88.5	137	88.5	137
Rated voltage [V]	1000	1000	1000	1000	1000	1000
Operating [V]	600	600	300	300	600	600
Current [A]	83.00	128.49	166.00	256.97	83.00	128.49
Stress factors calculations	$\pi_U = 1$ $\pi_I = 1$		$\boldsymbol{\pi_U = 0.889}$ $\boldsymbol{\pi_I = 1.486}$		$\boldsymbol{\pi_U = 1.439}$ $\boldsymbol{\pi_I = 0.980}$	
Electric machine						
λ_{Stat}	$\pi_U = 1$ $\pi_I = 1$	1.45E-06	$\pi_U = 0.889$ $\pi_I = 1.486$	1.92E-06	$\pi_U = 1.439$ $\pi_I = 0.980$	2.05E-06
λ_{Rotor}		1.24E-06		1.64E-06		1.75E-06
λ_{Mech}		2.13E-07		2.81E-07		3.00E-07
λ_{Cool}		2.15E-06		2.15E-06		2.15E-06
Common cause		-1.37E-06		-1.37E-06		-1.37E-06
$\boldsymbol{\lambda_M}$	**total**	**3.69E-06**	**total**	**4.62E-06**	**total**	**4.88E-06**
				(+25%)		**(+32%)**
Electronic speed controller						
$\lambda_{Inverter}$	$\pi_U = 1$ $\pi_I = 1$	4.02E-06	$\pi_U = 0.889$ $\pi_I = 1.486$	5.31E-06	$\pi_U = 1.439$ $\pi_I = 0.980$	5.67E-06
$\lambda_{DC\ cap}$		2.71E-06		3.58E-06		3.82E-06
$\lambda_{Control}$		1.72E-06		2.27E-06		2.42E-06
λ_{Cool}		2.15E-06		2.15E-06		2.15E-06
Common cause		-1.78E-06		-1.78E-06		-1.78E-06
$\boldsymbol{\lambda_{ESC}}$	**total**	**8.81E-06**	**total**	**1.15E-05**	**total**	**1.23E-05**
				(+31%)		**(+39%)**
Energy storage system						
λ_{cell}	$\pi_U = 1$ $\pi_I = 1$	5.61E-06	$\pi_U = 0.889$ $\pi_I = 1.486$	5.61E-06	$\pi_U = 1.439$ $\pi_I = 0.980$	5.61E-06
λ_{BMS}		1.28E-06		1.13E-06		1.83E-06
λ_{Cool}		2.15E-06		2.15E-06		2.15E-06
Common cause		-1.19E-06		-1.19E-06		-1.19E-06
$\boldsymbol{\lambda_{ESS}}$	**total**	**7.85E-06**	**total**	**7.71E-05**	**Total**	**8.41E-05**
				(-2%)		**(+7%)**
Electronic power distribution						
λ_{fuse}	$\pi_U = 1$ $\pi_I = 1$	1.49E-07	$\pi_U = 0.889$ $\pi_I = 1.486$	1.97E-07	$\pi_U = 1.439$ $\pi_I = 0.980$	2.10E-07
$\lambda_{contactor}$		1.49E-07		1.97E-07		2.10E-07
$\lambda_{connection}$		1.39E-07		1.39E-07		1.39E-07
$\boldsymbol{\lambda_{EDS}}$	**total**	**4.37E-07**	**total**	**5.33E-07**	**Total**	**5.59E-07**
				(+22%)		**(+28%)**

Table 34: Electric drive failure rate per failure mode considering the impact of voltage and current level

Failure mode of the Electric Drive	FTA reliability Reference (1/hr) (600V)	FTA reliability High Current (1/hr) (300V)	FTA reliability High Voltage (1/hr) (900V)
No torque	9.398E-6	9.479E-6 **(+1%)**	9.524E-6 **(+1%)**
Low torque	5.340E-6	5.538E-6 **(+4%)**	5.646E-6 **(+6%)**
High torque	3.059E-7	3.732E-7 **(+22%)**	3.915E-7 **(+28%)**
Torque ripple	2.158E-6	2.170E-6 **(+1%)**	2.173E-6 **(+1%)**
Short circuit 1	2.056E-6	2.405E-6 **(+17%)**	2.496E-6 **(+21%)**
Short circuit 2	2.056E-6	2.405E-6 **(+17%)**	2.496E-6 **(+21%)**
Short circuit 3	2.063E-6	2.412E-6 **(+17%)**	2.504E-6 **(+21%)**
Total	**2.34E-05**	**2.48E-05 (+6%)**	**2.52E-05 (+8%)**

Table 35, Table 36, and Table 37 shows the comparison of failure rate for the different architectures and control strategies when he different voltage/current ratings are considered.

The high voltage system is less reliable of the high current system for all the architectures. This depends on the impact of the high voltage on the components, then electric drive, then effect on the vehicle (Table 34). At the electric driveline level, High Voltage system has a FTA reliability 2% higher than High Current system, even if at the component level up to 12% difference was shown.

- Effect of powertrain architecture (electric vs hybrid)

The High Voltage system and High Current system have a greater impact on the Quadcopter hybrid when compared to the Quadcopter electric due to the lack of crosshafting.

- Effect of control technique (collective pitch vs RPM)

No specific impact has been found between the reported with reference to the vehicle control strategy.

March 2021 Final Report, Reliability and Safety Assessment of Urban Air Mobility Concept Vehicles, Contract No. 80ARC020F0055, GTRI Document No. D9015A001R2, April 2021

- Effect of number of rotors (Hexacopter vs Octocopter)

The effect of High Voltage and High Current system design becomes less important when the number of rotors increases.

Table 35: Impact of voltage and current rating on powertrain architecture (electric vs hybrid)

Architecture		FTA Reliability Reference (1/hr)	FTA Reliability High Current (1/hr) (300V)	FTA Reliability High voltage (1/hr) (900V)
Quadcopter Electric collective	Single Rotor Loss	1.645E-7	1.645E-7	1.645E-7
	Dual Electric Motor Failure	2.682E-5	2.683E-5	2.683E-5
	OEI Propulsion Loss	2.180E-5	2.307E-5	2.358E-5
	Energy Storage Failure	7.848E-6	7.908E-6	8.096E-6
	Energy Distribution Failure	4.37E-7	5.331E-7	5.593E-7
	Total Failure rate of the architecture	**4.897E-5**	**5.034E-5 (+3%)**	**5.088E-5 (+4%)**
Quadcopter Hybrid	Single Rotor Loss	1.644E-7	1.644E-7	1.644E-7
	Dual Electric Motor Failure	1.012E-6	1.012E-6	1.012E-6
	OEI Propulsion Loss	1.417E-5	1.548E-5	1.583E-5
	Energy Storage Failure	3.538E-11	3.565E-11	3.650E-11
	Energy Distribution Failure	4.370E-7	5.331E-7	5.594E-7
	Total Failure rate of the architecture	**1.553E-5**	**1.694E-5 (+9%)**	**1.731E-5 (+11%)**

Table 36: Impact of voltage and current rating on vehicle control strategy (collective pitch vs RPM)

Architecture		FTA reliability Reference	FTA reliability High Current	FTA reliability High voltage

		(1/hr)	(1/hr) (300V)	(1/hr) (900V)
Hexacopter Electric Collective	Single Rotor Loss	2.260E-5	2.376E-5	2.438E-5
	Dual Electric Motor Failure	6.554E-5	6.554E-5	6.555E-5
	OEI Propulsion Loss	3.263E-5	3.437E-5	3.530E-5
	Energy Storage Failure	7.848E-6	7.908E-6	8.096E-6
	Energy Distribution Failure	4.370E-7	5.331E-7	5.594E-7
	Total Failure rate of the architecture	**9.835E-5**	**1.002E-4 (+2%)**	**1.012E-5 (+3%)**
Hexacopter Electric RPM	Single Rotor Loss	2.259E-5	2.387E-5	2.438E-5
	Dual Rotor Failure	6.554E-5	6.554E-5	6.554E-5
	OEI Propulsion Loss	3.262E-5	3.454E-5	3.5230E-5
	Energy Storage Failure	7.848E-6	7.908E-6	8.096E-6
	Energy Distribution Failure	4.370E-7	5.331E-7	5.594E-7
	Total Failure rate of the architecture	**9.835E-5**	**1.004E-4 (+2%)**	**1.011E-4 (+3%)**

Table 37: Impact of voltage and current rating on number of rotor (Hexavopter vs Octocopter)

Architecture		FTA reliability Reference (1/hr)	FTA reliability High Current (1/hr) (300V)	FTA reliability High voltage (1/hr) (900V)
Hexacopter RPM	Single Rotor Loss	2.259E-5	2.387E-5	2.438E-5
	Dual Rotor Failure	6.554E-5	6.554E-5	6.554E-5
	OEI Propulsion Loss	3.262E-5	3.454E-5	3.5230E-5
	Energy Storage Failure	7.848E-6	7.908E-6	8.096E-6

	Energy Distribution Failure	4.37E-7	5.331E-7	5.594E-7
	Total Failure rate of the architecture	**9.835E-5**	**1.004E-4 (+2%)**	**1.011E-4 (+3%)**
Octocopter RPM	Single Rotor Loss	2.259E-5	N/A	N/A
	Triple Rotor Fail	2.419E-4	2.419E-4	2.419E-4
	OEI Propulsion Loss (Dual Rotor Loss)	3.037E-5	3.037E-5	3.037E-5
	Energy Storage Failure	7.848E-6	7.908E-6	8.096E-6
	Energy Distribution Failure	4.37E-7	5.331E-7	5.594E-7
	Total Failure rate of the architecture	**2.724E-4**	**2.725E-4 (+0%)**	**2.726E-4 (+0%)**

5.2.5 Impacts of liquid cooled vs. air cooled motors and motor controllers (C5, A7, B6)

Operating life and performance of electronic and electromechanical components are highly affected by operating temperature and temperature variation that occur due to mission profile or malfunction of the cooling system. Many cooling systems options are considered for the components of the electric drive [22, 77, 78]. The selection and design of the optimal thermal management for electric machines and power electronics is a big task and requires consideration of weight/volume, capability of responding to high transients, cooling power requirement, cost, and reliability. It is known that liquid cooling is very effective in removing heat when compared to air cooling with the same fluid rate. However, air cooling is simpler to implement, lighter and easy to maintain. In [72] a comparative analysis between liquid and air cooling for lithium-ion batteries has been reported. However, there are no many literature contributes comparing liquid and air cooling for electric drive and related safety assessment. Table 38 provides a comparison between air and liquid cooling.

The specifications of the cooling system design are reported in section 4.2.1, then additional assumptions are defined for this analysis:

- Natural air convection heat transfer won't be enough to cool the system
- Failures of the gear box won't affect the failure of the electric machine
- Filters and other components will be replaced as stated by the manufacturers

Table 38: Comparison of air and liquid cooling.

	Air Cooling	Liquid cooling
Pro.s	simpler, lighter, and easier to maintain.	very effective in removing substantial amounts of heat with relatively low flow rates
Con.s	lower heat capacity; for achieving similar cooling performance of liquid cooling, a much higher volumetric air flow rate is required	potential leaks, weight, and its complexity
Sys components	Electric fans (double electric fan considered in this work)	Pump Radiator with fan Pipes

Table 39 reports the failure rate and the related failure modes considered in this analysis for the comparison between air and liquid cooling. In detail the failure rate of air cooling is 40% lower than the liquid cooling due to the number of components involved in the system. Detailed FTA and failure rate are reported in section 2.4. Then the impact at the sub-system level has been evaluated by assessing the failure rate of the electric drive considering both cooling methods (Table 40). In detail the cooling method will impact most of the electric drive failure modes (except sensor failures and electric distribution failure). At the electric drive level, air cooling is 15% more reliable.

Table 39 Failure rate and failure modes for air and liquid cooling

Failure rate of the thermal management system	SEVERE failure	PARTIAL failure
$\boldsymbol{\lambda_{liq} = 4.30E-6}$	50% SEVERE failures of the motor/ESC cooling system (e.g. loss of a component) will lead to complete loss of the powertrain (No Torque)	50% PARTIAL operation of the thermal management of motor/ESC will cause overheating
$\boldsymbol{\lambda_{air} = 2.58\,\mathrm{E}-6}$ (-40%)		

Table 40 Impact of cooling method on electric drive failure rate

Failure mode of the Electric Drive	FTA reliability Liquid cooling (1/hr)	FTA reliability Air cooling (1/hr)

No torque	9.398E-6	7.547E-6 (-20%)
Low torque	5.340E-6	4.694E-6 (-12%)
High torque	3.059E-7	3.059E-07 (0%)
Torque ripple	2.158E-6	2.1585E-6 (0%)
Short circuit 1	2.056E-6	1.7124E-6 (-17%)
Short circuit 2	2.056E-6	1.7124E-6 (-17%)
Short circuit 3	2.063E-6	1.7124E-6 (-17%)
Total	**2.34E-05**	**1.986E-05 (-15%)**

The developed dynamic model of the Quadcopter electric (section 4.2.1) has been used in conjunction with the mission profile define in section 1.4 for assessing the dynamic response of the two cooling systems (air and liquid) included in the simulation framework (Table 17). In particular, the first 200s of climb are here analyzed to compare the steady state and transient temperature of electric machine and electronic speed control (Figure 70).

- Air cooling has a lower average temperature due to the direct exchange with the ambient;
- Liquid cooling for the electric machine is combined with the transmission cooling, so works at higher temperature;
- The temperature dynamic of the air cooling is heavier affected by the power request when compared to liquid cooling.

While the liquid cooling is showing higher temperature of operation, it is also able to guarantee a steadier temperature during heavy transient. The effect on the motor and power electronics reliability needs to be assessed in real world case scenarios through experiments.

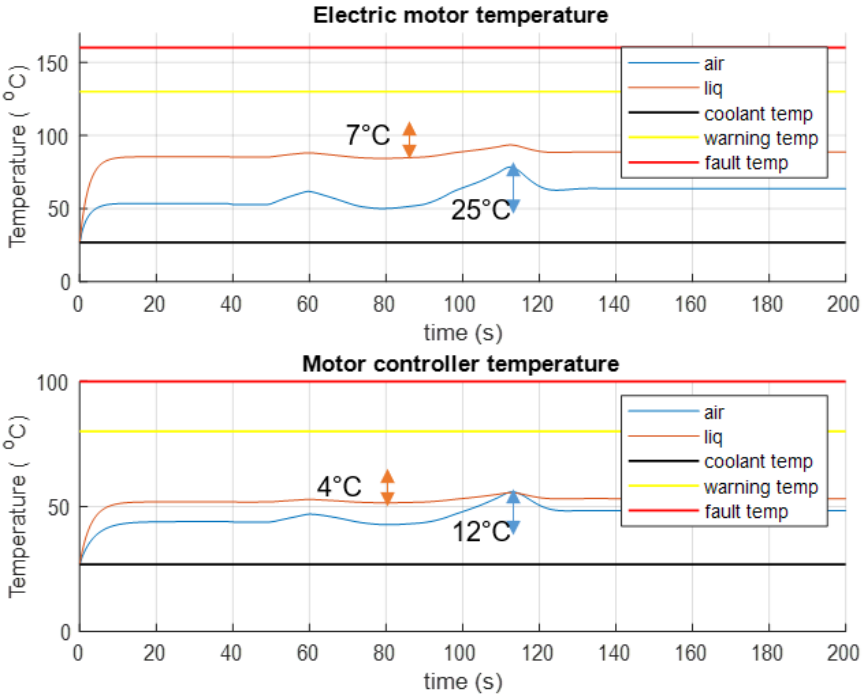

Figure 70 Temperature profile of EM and ESC considering air and liquid cooling

5.2.6 Impact on reliability associated with repeated overcharging and excessive discharging, repeated high-rate discharging on battery (C7, A8, B7)

Lithium-ion batteries are becoming an accepted component in aircraft systems; in fact, they represent one of the key enablers for low-impact propulsion systems (hybrid or electric). Lithium-ion batteries demonstrate several benefits in terms of specific energy/power density and efficiency when compared to traditional lead acid and nickel-cadmium battery technology. There are still several challenges to be addressed before lithium-ion batteries will be widely adopted in aircraft systems, such as cell reliability and safety [79].

A complete literature review of the failure modes of lithium-ion battery packs has been conducted and the results are reported in Table 41 [40, 80, 81]. This analysis has focused on the impact of overcharge, over-discharge and high c-rate and how the repeated occurrence of these events may cause a failure of the energy storage system. All of these events can potentially lead to thermal runaway. Note that Table 41 reports typical sequences of occurrence, but the order can strongly depend on the cell operating conditions and the cell-to-cell variations due to manufacturing defects. Failure rates cannot be defined a priori without considering the specific chemistry, cell format, pack design and without experimental testing. The assumptions made for these analyses are summarized below:

- The battery pack is divided in multiple isolated modules those include BMS, each module is connected to a powertrain/rotor subsystem
- The TMS is shared between the battery packs
- In case of failure of a battery module, the rotor connected to the module will fail as well.

March 2021 Final Report, Reliability and Safety Assessment of Urban Air Mobility Concept Vehicles, Contract No. 80ARC020F0055, GTRI Document No. D9015A001R2, April 2021

- Effect of powertrain architecture (electric vs hybrid)

No specific impact has been found between the reported battery failure modes and the vehicle powertrain architecture.

- Effect of numbers of rotors (Hexacopter vs Octocopter)

The increase of number of rotors increases the failure rate of the pack. However, at the system level the increase in number of rotors can bring benefits in terms of capability of surviving to the fault.

$\lambda_{ESS-module} = 7.85e-6; \lambda_{ESS-Hexa} = 6 \times 7.85e-6; \lambda_{ESS-Octo} = 8 \times 7.85e-6$

- Effect of control technique (collective pitch vs RPM)

No specific impact has been found between the reported battery failure modes and the vehicle control strategy.

Table 41: Failure modes and Effects due to overcharge, over-discharge and operation at high c-rate of lithium-ion batteries

Fault Type	Failure Modes & Effects at ED level
Overcharge	1. **Overheating: (**Low Torque failure mode**)** ▪ The cathode is susceptible to thermally driven decomposition. ▪ The electrolyte becomes unstable, which leads to reactions between the electrolyte and cathode that can raise the cell temperature and release oxygen gas. 2. **Capacity/Power Fade:** ▪ Gas from graphite exfoliation induces crack of SEI and loss of active area. ▪ The aluminium can corrode → this can lead to a reduction of power or increased resistance. 3. **Internal Short Circuit (**No Torque failure mode**)** ▪ Lithium plating and dendrite growth on anode surface 4. **Thermal Runaway**
Overdischarge	1. **Capacity/Power Fade:** ▪ Excessive delithiation of anode causes SEI decomposition and loss of active area. ▪ Copper plating. 2. **Overheating: (**Low Torque failure mode**)** ▪ Changes of thermal stability → repeated overdischarge can lead to undesired cell temperature increase. 3. **Internal Short Circuit (**No Torque failure mode**)** ▪ The copper can dissolve → this can lead to free copper particles suspended in the electrolyte and potentially internal short circuit. 4. **Thermal Runaway**

High C-rates	**1. Overheating:** ▪ Higher power consumption across the same internal resistor → accelerates the internal temperature increase. ▪ Sometimes only locally in the correspondence of high impedance locations (tab connections, electrodes, etc.). ▪ Powertrain level: Reduced Torque Output due to battery power limitations → increase probability of Low Torque failure mode **2. Capacity/Power Fade:** ▪ Ions are not fully de-intercalated which results in capacity loss and lithium dendrite. ▪ Accelerated aging ▪ Powertrain level: Reduced Torque Output and Available Energy due to battery power limits and capacity fade→ increase probability of Low Torque failure mode or Emergency Landing due to limited SOC **3. Internal Short Circuit:** ▪ Lithium metal can deposit on the surface of the anode → over time, these deposits can develop into dendritic structures that may puncture the separator and initiate internal short circuits. ▪ Electrode particle fracture ▪ Powertrain level: battery pack fuse will blow or open contactors → increase probability of No Torque failure mode **4. Thermal Runaway -** Catastrophic event

5.2.7 Impact of sensor placement and redundancy (B4, A4)

Sensors are used to measure variable that cannot be accurately estimated or observed [82]. Every sensor installation can potentially increase the diagnostic capability of the system, however it generates a new point of failure. So, it is important to study the reliability of the sensor and evaluate redundancy.

The electric drive of the considered vehicles has several safety-critical feedbacks that support the motor control and the flight control. Electric drive based on PMSM are usually equipped with the following set of sensors:

- shaft speed sensor
  - single speed measurement is included in an electric drive for control purposes and flight control (RPM control);
  - Resolver or incremental encoder are usually adopted;
  - In traditional aircraft a governor is used to measure the rotor speed, electrified architectures are still exacted to have a rotor speed sensor to monitor rotor speed;
  - Redundancy of speed measurement is demonstrated to increase system reliability [83];
  - Double shaft speed measurements in an electric drive is usually very difficult to implement due to space and cost;
  - Rotor speed sensor can increase reliability of the electric drive itself;
  - Sensorless controls for PMSM have done great improvement in the last decade, however they are still not fully accepted by industry (especially due to the error at low speed) [84].

Sensorless control can be utilized in case of failure of the speed sensor to bring the vehicles to a safe operating condition.

- Voltage sensor
  - Voltage sensors are utilized to measure the three-phase voltage input of the machine;
  - These measurements are always in conjunction with current sensors to perform diagnostic functions;
  - Consider that electric drives are supplied by switching voltages, so the voltage acquisition is usually affected by filtering and averaging error;
  - The presence of voltage sensors can for sure help to increase diagnosis capability of the PMSM drive, however due to the sensor accuracy and performance, the redundancy of these sensors may not be effective for increasing reliability.

- Current sensor
  - Two phase current sensors are required in an electric drive for control purposes;
  - Redundancy can be included in the system by:
    - third sensor may be installed to increase reliability (sum of the three phase currents is equal to zero);
    - DC link current measurement can be used to estimated faults in electric drive;
    - Include more phase current measurements.

- Temperature sensor
  - Electric machine winding temperature sensors (one per phase) and switches temperature sensors (one for IGBT) are usually included in an electric drive;
  - Redundancy on switches temperature measurement (junction temperature) can be useful for increasing reliability, but it is very impractical due to cost, volume, manufacturing issues, and fats dynamic of the temperature response of these components;
  - Redundancy of winding temperature sensors are often included in electric machine for increasing reliability in estimating possible degradations;
  - Not very useful for failure caused by fast dynamic, due to thermal inertia and speed of the acquisition system.

In summary the traditional and proposed sensor set for an electric drive for UAM application is reported in Table 42. The failure rate reported in Table 42 are provided by NPRD-2016. Systematic methodologies can be used for the analytical definition of the intrinsic redundancy of a system and the related needs of sensors for improving diagnosability, isolability, observability and reliability [85].

- Effect of number of rotors (Hexacopter vs Octocopter)

In these architectures the rotors are independent from each other. Every rotor is potentially equipped with different speed and current sensors. The increase of number of rotors increases the number of sensors in the system (increases failure rate) and the possibility of utilizing the sensors in the other rotors to detect failures or issues in one of the rotors (increase diagnosability).

Table 42: Traditional and proposed sensor set for electric aircraft.

Sensor type	Traditional powertrain	Failure rate (1/hr) NPRD-2016	Redundancy requirement	Note
Shaft speed	1	7.34E-06 (resolver) 2.32E-07 (resolver)	none	Gearbox speed sensor is used to measure rotor speed (failure rate 4.2280E-07) Sensorless control can implemented to increase reliability
Voltage	Not always present	1.74E-07 (AC)	none	These sensors are used to increase diagnostic capabilities Redundancy of these sensors may not be effective for increasing reliability, due to the switching voltage
Current	2	1.92E-06 2.14E-06 6.97E-07	+1 or more	Used for control purposes, one additional sensor can increase reliability
Winding temperature	3	1.49E-06 1.96E-06 (thermocouple) 2.14E-07 (thermocouple) 3.48E-07 4.21E-07	-	Mainly to estimate degradation Not very useful for failure caused by fast dynamic, due to thermal inertia and speed of the acquisition system.
IGBT temperature	3		-	

6 CONCLUSIONS AND RECOMMENDATIONS FOR FUTURE WORK

This section reports a summary of the results of this study including both the static and dynamic analyses performed.

6.1 Comparison of architectures

Of all the propulsion architectures considered for the static safety analysis, the quadcopter with twin turboshafts is the most reliable. The high reliability of the turboshaft architecture is due to its dependence on fewer critical systems and the redundancy in the twin-turboshaft system. In comparison, the Quad Electric configuration only has redundancy in the form of cross-shafting. The failure of either the electric motor, electronic speed controller, HV battery or clutch on a rotor results in a loss of power. Furthermore, both the LV battery and HV battery packs, which supply power to every propulsor and control of the vehicle, are susceptible to single point failures. The Quad Hybrid configuration has two sources of power for the electric propulsors (engine and batteries) which alleviates the problem of the single point failure of the Quad Electric configuration. Replacing the cross-shafting system with an additional electric propulsor on each rotor trades a decrease in the probability of catastrophic power loss at the expense of an increase in the probability of catastrophic rotor loss and does not improve the overall reliability of the architecture.

The analysis of electric hexacopter and octocopter demonstrated that for these architectures the loss of electric propulsion on any rotor cannot be compensated by the remaining electric propulsors, due to the removal of the cross-shafting. Combining this with the same issues of common cause failures present in the Quad Electric configuration means that the additional rotors do not make up for the loss of redundancy provided by the cross-shafting system. If these problems were resolved by redesigning the electric propulsors to be independent, additional rotors would then provide more reliability (e.g. octocopter would be more reliable then hexacopter). Finally, an octocopter would have similar reliability as a hexacopter with dual electric drives on each rotor.

The choice of RPM vs. collective control has little impact on the reliability of the architectures analyzed. This is due to the redundant collective actuator configuration being much more reliable than other components necessary for rotor function such as the single RGB. The choice of a direct drive turbogenerator vs. a geared turbogenerator for the Quad Hybrid configuration also has little impact on reliability at the vehicle level as the redundancy provided by the battery reduces the impact of adding an additional critical component to the turbogenerator.

From a dynamic perspective, the electric quadcopter is capable of operating and reacting to the loss of an electric motor with little to no impact on the aircraft flight due to the presence of cross shafting and a dynamic reconfiguration of the master-follower control of the multiple electric drives.

The modeled reduction of actuator rate and travel range do not have an impact on the behavior of the aircraft. Some faults in two different motors or in a motor and in the transmission can have a catastrophic impact on the vehicle, but the probability of such events to occur is below the threshold of interest.

The hybrid electric configuration presents similar behavior as the electric quadcopter, with the exception of faults occurring on the turbogenerator. For the cases with faulty turbogenerator, the battery is used to power the aircraft down to a safe landing. Finally, given that the turbine has a relatively high power rating, it is capable of operating even with an important transmission loss or low conversion efficiency. Alternate modes of operation of the hybrid powertrain were investigated which lead to reduction in the turbine transients with limited impact on the battery capacity.

The quadcopter with a dual turboshaft powertrain is able to sustain the flight after any considered single faults. Moreover, since the aircraft is equipped with two turboshafts, the powertrain has plenty of excess power, and can overcome severe loss of efficiency in the transmission.

The hexacopter with pitch control is also capable of operating with one rotor inoperative. However, the absence of cross shafting highlights the impact of individual electric machine faults, malfunctions and power limitation. This is the case for a low torque condition for example, , and can lead to large RPM excursion throughout the mission.

The RPM-control aircrafts (hexacopter and octocopter) present complex behavior after fault injection, which lead to some inconclusive scenarios. For the RPM-control vehicles, the nominal controller is not successful at stabilizing the aircraft after the loss of a rotor. Consequently, an alternate control structure is implemented once an electric motor fails. This control structure is able to stabilize the aircraft, but is not able to perform the acceleration or deceleration profiles imposed by the nominal mission. Given the relatively low complexity of the controller, it is unknown if the aircraft's inability to fly the whole mission with one motor inoperative is due to the controller limitations or to the aircraft configuration and sizing.

More powerful electric motors were implemented on the RPM-Control aircraft such that the aircraft can fly the whole mission with one motor inoperative. Both RPM-Control aircraft have a larger power increase when operating with one motor inoperative compared to the hexacopter with pitch control. However, the difference between the RPM-Control hexacopter and octocopter is less significant.An assessment of the sensor required for the effective diagnoses of fault in the different architectures is provided. In general, the phase current sensors are of fundamental important, redundancy on these sensor is going to increase the diagnostic capability of the system and potentially improve reliability. Having separate sensors for rotor RPM monitoring can provide the additional redundancy to the motor speed controller.

Powertrain design specifications, as voltage rating and cooling design, will impact the overall vehicle reliability. High voltage systems have potential of increase efficiency; however, the failure rate of the electric dive may increase and can highly impacting solutions without cross-shafting. Air cooling thermal management is more reliable of liquid cooling (due to a smaller number of components), however it corresponds to higher temperature variation during transient.

6.2 Possible extensions for future work

There are multiple avenues for future work with potential to increase the understanding of the vehicles' behavior and performance potentialities. Among them, there is a possibility to include higher order fidelity analyses for rotor performance, especially for cases far from the linearized conditions, such as one engine out considerations. There is also the possibility to include controllers with a more advanced architecture for operation with one engine out. Moreover, the simulation assumed that it is possible to

identify a fault and reconfigure the flight controller and the centralized electric motor controller. It could be of interest to assess the feasibility of identifying those faults and the time response of those processes. Finally, the controller aimed at following the prescribed path regardless of the condition of the aircraft. It could be interesting to analyze the possibility of reducing the performance such as speed, rate of climb in case of a fault recognition.

More generally, the evaluated hexacopter and octocopter configurations consist of the motors configured in a rectangular orientation. It could be of interesting to analyze additional orientations of the hexacopter and octocopter electric motors to evaluate if this strongly influences the safety analysis. We also recommend that the electric motors be sized for one motor inoperative scenario for all vehicles in order to provide a more consistent benchmark for each configuration.

The DET analysis was performed for six different vehicle concepts within the scope of the dynamic probabilistic risk assessment (DPRA) study, but the analysis could benefit from a more extensive DPRA with entirely randomized fault injection points. In that respect, this study does not include the effect of changing weather conditions and environmental conditions such as wind. In future studies, all environmental factors that have an impact on the vehicle can be evaluated using the DET methodology.

Within the scope of the DET analysis, the FIPs on the vehicle trajectory were determined based on the main segments of the mission. Due to time limitations, the DET analysis could not be repeated for refined FIPs to observe convergence in the figure of merit (i.e. probability of successful completion/failure of mission). In a future comprehensive DET analysis, such a target of convergence can be achieved by further refinement of FIPs.

A cutoff probability for DETs needs to be defined to prevent the DETs from expanding in an uncontrollable manner. The cutoff probability for this study was defined as 10^{-11}. In future studies, the cutoff probability could be reduced to detect weak points of the system that can lead to failure even if the probability of occurrence is small.

In this study, it was assumed that the failure probabilities used in the DET analysis do not change over time and that all subsystem components were new. In addition, it was also assumed that the control mechanisms of the vehicles function without failures and that no software errors occur the design phase and during the missions. A more comprehensive study can be done by re-evaluating these assumptions, as well as accounting for model uncertainties that have not been included in this study due to time limitations.

In summary, the team is here proposing the following aspects to be considered in future studies:

- LV control system architecture: analyze strategies for improving LV reliability considering traditional aviation approaches, as well as ring network configurations.
- HV bus architecture: as mentioned in this report every rotor is served by a battery pack, the failure of the battery pack will cause a failure of the rotor drive. Fail safe interconnection/isolation and reconfiguration of the battery packs can increase reliability by sharing the available resources with the faulty unit with the aim of maximizing vehicle controllability and stability. Ring network configuration can be considered for these systems.

- Sensor placement for diagnostic and prognostic – in the current work multiple sensors are considered, but their location in the system in not considered. Methodologies like Structural Analysis can help to analytically define the sensor placement considering the required reliability specifications.
- Optimal sizing of electrical motor and thermal management for the different multi-rotors configurations and control considering OMI conditions.
- Understand the impact of advance vehicle control for the management of multi-rotor vehicles in case of failure of 1 or 1+ rotors.
- Study the impact of components level redundancy versus in-component redundancy (e.g. double winding machines versus redundant electric machine), their impact on the safety assessment and vehicle weight.

7 REFERENCES

[1] T. Lomax, D. Schrank and B. Eisele, "2019 Urban Mobility Report - Congestion data for your city," Texas A&M Transportation Institute, College Station, TX, 2015.

[2] Y. Li, D. DeLaurentis and D. Mavris, "Advanced Rotorcraft Concept Development and Selection Using a Probabilistic Methodology," in *AIAA 3rd Annual Aviation Technology, Integration, and Operations Forum*, Denver, CO, 2003.

[3] M. Moore, "NASA Personal Air Transportation Technologies," in *General Aviation Technology Conference & Exhibition*, Wichita, KS, 2006.

[4] Uber Elevate, "Fast-Forwarding to a Future of On Demand Urban Air Transportation," Uber, San Francisco, CA, 2016.

[5] B. Garrett-Glaser, "Joby Aviation receives first airworthiness approval from U.S. military for electric VTOL aircraft," Verticalmag, 10 12 2020. [Online]. Available: https://verticalmag.com/news/joby-aviation-receives-first-airworthiness-approval-electric-vtol-aircraft/. [Accessed 3 2021].

[6] M. Hirschberg, "V/STOL: The First Half-Century," *Vertiflight,* March/April 1997.

[7] M. Hirschberg, "Electric VTOL Wheel of Fortune," *Vertiflite,* March/April 2017.

[8] P. Darmstadt, R. Catanese, A. Beiderman, F. Dones, E. Chen, M. Mistry, B. Babie, M. Beckman and R. Preator, "Hazards Analysis and Failure Modes and Effects Criticality Analysis (FMECA) of Four Concept Vehicle Propulsion Systems," NASA, 2019.

[9] EASA, "Special Condition for Small-Category VTOL Aircraft," EASA, Cologne, Germany, 2019.

[10] W. Johnson, "NDARC —NASA Design and Analysis of Rotorcraft. Theoretical Basis and Architecture," in *AHS Specialists' Conference on Aeromechanics*, San Francisco, CA, 2010.

[11] W. Johnson, "NASA Design and Analysis of Rotorcraft (NDARC) - Theory," NASA Ames Research Center, Moffet Field, 2019.

[12] W. Johnson, "Propulson System Models for Rotorcraft Conceptual Design," in *AHS 5th Decennial Aeromechanics Specialist's Conference*, San Francisco, CA, 2014.

[13] W. Johnson and C. a. S. E. Silva, "Concept Vehicles for Air Taxi Operations," in *AHS Aeromechanics Design for Transformative Vertical Lift*, San Fransisco, 2018.

[14] NASA, "NDARC Input Manual Release 1.8," NASA, 2014.

[15] NASA, "NDARC Theory Manual Release 1.8," NASA, 2014.

[16] Isograph Ltd, *Reliability Workbench,* Alpine, UT, 2021.

[17] U. Catalyurek, B. Rutt, K. Metzroth, A. Hakobyan, T. Aldemir, R. Denning, S. Dunagan and D. Kunsman, "Development of a code-agnostic computational infrastructure for the dynamic generation of accident progression event trees," *Reliability Engineering & System Safety,* pp. 95, 278-294, 2010.

[18] G. Cojazzi, "The DYLAM approach for the dynamic reliability analysis of systems," *Reliability Engineering & System Safety,* pp. 52, 279-296, 1996.

[19] T. Aldemir, "A survey of dynamic methodologies for probabilistic safety assessment of nuclear power plants," *Annals of Nuclear Energy,* pp. 52, 113-124, 2013.

[20] Department of Defense, "MIL-STD-1629A, Military Standard: Procedures for Performing a Failure Mode, Effects and Criticality Analysis," Department of Defense, Washington, 1980.

[21] J. De Santiago, H. Bernhoff, B. Ekergård, S. Eriksson, S. Ferhatovic, R. Waters and M. Leijon, "Electrical motor drivelines in commercial all-electric vehicles: A review. ," *IEEE Transactions on vehicular technology,,* pp. 475-484., 2011.

[22] Y. Gai, M. Kimiabeigi, Y. C. Chong, J. D. Widmer, X. Deng, M. Popescu and A. Steven, " Cooling of automotive traction motors: schemes, examples, and computation methods.," *IEEE Transactions on Industrial Electronics,* vol. 66, no. 3, 2018.

[23] S. International, *Guidelines and Methods for Conducting the Safety Assessment Process on Civil Airborne Systems and Equipment,* 1996.

[24] Crown Consulting Inc., "Urban Air Mobility (UAM) Market Study," NASA, Washington, DC, 2019.

[25] Quanterion Solutions Incorporated, "Nonelectronic Parts Reliability Data, NPRD-16," Quanterion Solutions Incorporated, 2016.

[26] U. D. o. Defense, Reliability prediction of electronic equipment, Military Handbook, 1991.

[27] R. A. DeLucia, B. C. Fenton and J. Blake, "Statistics on Aircraft Gas Turbine Engine Rotor Failures that Occured in U.S. Commercial Aviation During 1987," 1991.

[28] R. K. R. S. C. G. J. &. W. M. Abdallah, " Fault tree analysis for the communication of a fleet formation flight of UAVs," *In 2017 2nd International Conference on System Reliability and Safety (ICSRS) IEEE,* pp. (pp. 202-206), (2017, December)..

[29] R. M. O.Manuel Uy, "Fault tree safety analysis of a large Li/SOCl2 spacecraft battery," *Journal of Power Sources, ,* no. Volume 21, Issues 3–4, Pages 207-225, ISSN 0378-7753., 1987.

[30] W. Y. Y. G. K. W. B. Q. G. Z. Xiong Shu, "A reliability study of electric vehicle battery from the perspective of power supply system," *Journal of Power Sources,* vol. Volume 451, no. 227805, ISSN 0378-7753, 2020.

[31] J. D. Neely, " Fault types and reliability estimates in permanent magnet AC motors.," *Michigan State University. Department of Electrical and Computer Engineering,* 2005.

[32] P. Kadanik, "A brief survey of AC Drive Fault Diagnosis and Detection," *Prague,* pp. 1-24, 1998.

[33] B. T. G. L. Y. &. Q. T. Wang, "Reliability modeling and evaluation of electric vehicle motor by using fault tree and extended stochastic Petri nets," *Journal of Applied Mathematics,* 2014.

[34] X. Shu, Y. Guo, W. Yang, K. Z. Y. Wei and H. Zou, "A Detailed Reliability Study of the Motor System in Pure Electric Vans by the Approach of Fault Tree Analysis.," *IEEE Access,* pp. 5295-5307., 2019.

[35] S. B. A. M. P. X. D. R. L. &. T. P. Yang, "An industry-based survey of reliability in power electronic converters.," *IEEE transactions on Industry Applications,* pp. 47(3), 1441-1451, 2011.

[36] S. W. Z. &. B. F. Peyghami, "Reliability modeling of power electronic converters: A general approach," *In 2019 20th Workshop on Control and Modeling for Power Electronics (COMPEL) (pp. 1-7). IEEE.,* (2019, June)..

[37] M. P. Ciappa, "Some reliability aspects of IGBT modules for high-power applications," *(Doctoral dissertation, ETH Zurich).,* 2020.

[38] Y. &. W. B. Song, "Survey on reliability of power electronic systems.," *IEEE transactions on power electronics, 28(1), 591-604.,* 2012.

[39] C. W. N. M. S. &. P. M. Hendricks, "A failure modes, mechanisms, and effects analysis (FMMEA) of lithium-ion batteries.," *Journal of Power Sources, ,* pp. 297, 113-120., 2015.

[40] R. G. V. &. M. C. Bubbico, "Hazardous scenarios identification for Li-ion secondary batteries.," *Safety science,* pp. 108, 72-88., 2018.

[41] J. Weiss, "Control Acutation Reliability and Redundancy for Long Duration Underwater Vehicle Missions with High Value Payloads," in *Underwater Intervention*, New Orleans, 2014.

[42] P. Freeman and G. J. Balas, "Actuation Failure Modes and Effects Analysis for a Small UAV," in *American Control Conference*, Portland, 2014.

[43] D. J. Wulpi, Failures of Shafts, ASM Handbook, Volume 11: Failure Analysis and Prevention p. 459-482, 1986.

[44] L. Rexnord Industries, Failure Analysis: Gears-Shafts-Bearings-Seals,108-010, 1978.

[45] A. H. Bonnett, Cause, Analysis and Prevention of Motor Shaft Failures, IEEE, 1998.

[46] R. L. Widner, "Failures of Rolling-Element Bearings," *Failure Analysis and Prevention,* vol. 11, pp. 490 - 513, 1986.

[47] L. E. Alban, Systematic Analysis of Gear Failures,, Russell Township, OH: ASM international, 1985.

[48] A. G. M. S. C. P. Lynwander, "Sprag Overriding Aircraft Clutch, USAAMRDL Technical Report-72-49," AVRADCOM, 1972.

[49] J. G. Kish, "Advanced Overrunning Clutch Technology, USAAMRDL-TR-77-16," AVRADCOM, 1977.

[50] Sikorsky Aircraft, "Helicopter Freewheel Unit Design Guide USAAMRDL-TR-77-18,," AVRADCOM, 1977.

[51] D. G. Astridge, "Helicopter transmissions—Design for safety and reliability: Proceedings of the Institution of Mechanical Engineers," *Journal of Aerospace Engineering,* vol. 203, no. 2, pp. 123-138, 1989.

[52] F. Carazas and G. De Souza, "Availability analysis of gas turbines used in power plants.," *International Journal of Thermodynamics,* vol. 12, no. 1, pp. 28-37, 20098.

[53] H. Arabian-Hoseynabadi, O. H. and P. Tavner, "Failure modes and effects analysis (FMEA) for wind turbines," *International Journal of Electrical Power & Energy Systems,* vol. 32, no. 7, pp. 817-824, 2010.

[54] P. Tavner, A. Higgins, H. Arabian and Y. Feng, "Using an FMEA method to compare prospective wind turbine design reliabilities," *European Wind Energy Conference and Exhibition, EWEC 2010,* vol. 4, pp. 2501-2537, 2010.

[55] E. P. S. M. Association, " Reliability Guidelines to understanding reliability prediction.," *Wellingborough EPSMA ,* pp. 1-29., 2005.

[56] I.-I. E. Commission, " IEC 61709 'Electric components – Reliability – Reference conditions for failure rates and stress models for conversion'," 2017.

[57] E. P. Anderson, "Electric Motors Handbook," Bobbs-Merrill Co., Inc., New York, 1983.

[58] Department of Defense, "MIL-HDBK-217: Reliability Prediction of Electronic Equipment," Department of Defense, Washington, DC, 1991.

[59] NSWC-11, "Handbook of Reliability Prediction Procedures for Mechanical Equipment, Logistics Technology Support," Naval Surface Warfare Center, 2011.

[60] B. Lawrence, B. Lawrence, M. B. Tischler, C. R. Theodore, J. Elmore, A. Gallaher and E. L. Tobias, "Integrating Flight Dynamics & Control Analysis and Simulation in Rotorcraft Conceptual Design," in *AHS 72ndAnnual Forum*, West Palm Beach, 2016.

[61] K. Fernndo and H. Nicholson, "Singular perturbational model reduction in the frequency domain," *International Journal of Control,* vol. 15, no. 5, pp. 961-979, 1972.

[62] J. Barlwo, "Progress in observing and modeling the urban boundary layer," *Urban Climate,* vol. 10, no. 2, pp. 216-240, 2014.

[63] T. Bentahm and R. Britter, "Spatially averaged flow within obstacle arrays," *Atmospheric Environment,* vol. 37, no. 15, pp. 2037-2043, 2003.

[64] R. Macdonald, "Modeling the Mean Velocity Profile in the Urban Canopy Layer," *Boundary-Layer Meteorology,* vol. 97, no. 1, pp. 25-45, 2000.

[65] D. Zajic, H. Fernando, M. Brown and E. Pardyjak, "On Flows in Simulated Urban Canopies," *Environment Fluid Mechanics,* 2015.

[66] Department of Defense, "Flying Qualities of Piloted Aircraft," Washington D.C., 2012.

[67] M. D. M. a. G. &. T. C. Attaianese, ""Multi-source traction drive for axial flux permanent magnet in-wheel synchronous motor.","," *in IEEE International Electric Machines & Drives Conference,* 2011.

[68] W. Johnson, "NDARC - NASA Design and Analysis of Rotorcraft," NASA, 2009.

[69] M. D. a. M. C. D. Freudiger, " A generalized equivalent circuit model for design exploration of li-ion battery packs using data analytics," *IFAC-PapersOnLine, ,* pp. vol. 52, no. 5, pp. 568-573,, 2019.

[70] M. C. A. S. M. C. a. C. P. M. D'Arpino, "A simulation tool for battery life prediction of a Turbo-Hybrid-Electric Regional Jet for the NASA ULI Program," *in AIAA Propulsion and Energy 2019 Forum ,* p. 2019.

[71] M. D'Arpino, M. Cancian, A. Sergent, M. Canova and C. Perullo, "A simulation tool for battery life prediction of a Turbo-Hybrid-Electric Regional Jet for the NASA ULI Program," in *AIAA Propulsion and Energy 2019 Forum* , 2019.

[72] T. K. B. Y. E. C. &. K. S. Han, "Li-ion battery pack thermal management: liquid versus air cooling.," *Journal of Thermal Science and Engineering Applications, ,* no. 11(2)., 2019.

[73] G. Rizzoni, L. Guzzella and B. M. Baumann, "Unified modeling of hybrid electric vehicle drivetrains," *IEEE/ASME transactions on mechatronics,* vol. 4, no. 3, 1999.

[74] P. Young and J. Willems, An approach to the linear multivariable servomechanism problem., 1972.

[75] W. S. Levine, The Control Handbook; Control system Advanced Method, Boca Raton: CRC press, 2011.

[76] K. Smolders, H. Long, Y. Feng and P. J. Tavner, "Reliabilty Analysis and Prediction of Wind Turbine Gearboxes," in *European Wind Energy Conference*, Warsaw, 2010.

[77] S. L. Schnulo, J. Chin, A. Smith and A. Paul-Dubois-Taine, "Steady state thermal analyses of SCEPTOR X-57 wingtip propulsion.," *In 17th AIAA Aviation Technology, Integration, and Operations Conference,* p. p. 3783, 2017.

[78] S. L. S. a. A. S. Jeff Chin, "Transient Thermal Analyses of Passive Systems on SCEPTOR X-57," *In 17th AIAA Aviation Technology, Integration, and Operations Conference ,* p. p. 3784, 2017.

[79] L. H. Saw, Y. Ye and A. A. Tay, "“Integration issues of lithium-ion battery into electric vehicles battery pack,”," *Journal of Cleaner Production,,* no. Vol. 113, 2016, pp. 1032–1045.

[80] C. Hendricks, N. Williard, S. Mathew and M. Pecht, "A failure modes, mechanisms, and effects analysis (FMMEA) of lithium-ion batteries," *Journal of Power Sources,* vol. 297, pp. 113-120, 2015.

[81] X. &. Z. K. &. L. K. &. L. X. &. D. S. &. O. S. Hu, "Advanced Fault Diagnosis for Lithium-Ion Battery Systems.," 2020.

[82] J. Zhang, H. Yao and G. Rizzoni, "Fault diagnosis for electric drive systems of electrified vehicles based on structural analysis.," *IEEE Transactions on Vehicular Technology,* no. 66(2), 1027-1039., 2016.

[83] J. Zhang, A. Amodio, T. Li, B. Aksun-Güvenç and G. Rizzoni, "Fault diagnosis and fault mitigation for torque safety of drive-by-wire systems.," *IEEE Transactions on Vehicular Technology,* no. 67(9), 8041-8054, 2018.

[84] Q. W. S. &. C. C. Wang, "Review of sensorless control techniques for PMSM drives," *IEEJ Transactions on Electrical and Electronic Engineering,* no. 14(10), 1543-1552, 2019.

[85] Y. D. M. &. R. G. Cheng, "Structural Analysis for Fault Diagnosis and Sensor Placement in Battery Packs.," *arXiv preprint arXiv:2008.10533.,* 2021.

[86] C. Attaianese, M. Di Monaco and G. & Tomasso, "Multi-source traction drive for axial flux permanent magnet in-wheel synchronous motor.," in *IEEE International Electric Machines & Drives Conference*, 2011.

[87] D. Freudiger, M. D’Arpino and M. Canova, "A generalized equivalent circuit model for design exploration of li-ion battery packs using data analytics," *IFAC-PapersOnLine,* vol. 52, no. 5, pp. 568-573, 2019.

[88] X. Shu, Y. Guo, W. Yang, K. Wei, Y. Zhu and H. Zou, "A Detailed Reliability Study of the Motor System in Pure Electric Vans by the Approach of Fault Tree Analysis," *IEEE Access,* vol. 8, pp. 5295-5307, 2020.

[89] L. Wei, C. Justin, S. Briceno and D. Mavris, "Door-to-Door Travel Time Comparative Assessment for Conventional Transportation Methods and Short Takeoff and Landing On Demand Mobility Concepts," in *AIAA Aviation Technology, Integration, and Operations Conference*, Atlanta, GA, 2018.

[90] W. Johnson, "NASA Design and Analysis of Rotorcraft. Validation and Demonstration," in *AHS Specialists' COnference on Aeromechanics*, San Francisco, CA, 2010.

[91] C. Z. C. G. Y. &. Z. Y. Wu, "A review on fault mechanism and diagnosis approach for Li-ion batteries.," *Journal of Nanomaterials,* 2015.

[92] C. Silva, W. Johnson, K. R. Antcliff and M. and Patterson, "VTOL Urban Air Mobility Concept Vehicles for Technology Development, AIAA Aviation Forum, AIAA 2018-3847," in *2018 Aviation Technology, Integration, and Operations Conference*, Dallas, 2018.

MEET THE AUTHORS

Dr. Courtand Bivens

Courtland has over 30 years of experience in aviation engineering and currently serves as the Chief of Engineering for GTRI's Aerospace, Transportation, and Advanced Systems (ATAS) Laboratory. Mr. Bivens holds a BS in Mechanical Engineering from the U.S. Military Academy, and an MS in Aerospace Engineering from the U.S. Naval Postgraduate School. In addition, he is a graduate of the U.S. Naval Test Pilot School (Class 105) and has two NASA sponsored patents relating to improving handling qualities in helicopter Air-to-air combat

Dr. Matilde D'Arpino

Research Scientist at OSU-CAR. 10 years of experience in design and control of energy storage for automotive, aerospace and grid-connected systems; battery management systems and balancing circuits design; modeling and control of dynamic systems.

Dr. Etienne Demers-Bouchard

Etienne's experience focuses on systems design and engineering of complex mechanical and aeromechanical systems. He has been working on modeling and simulation of aerospace vehicles, with an emphasis on dynamics-driven decisions for novel rotorcraft concepts.

Dr. Jon Gladin

Jon is the lab's propulsion and energy division chief and is the electric and hybrid electric propulsion lead for the lab. His research is heavily focused in the area of advanced propulsion system concepts

Dr. Cedric Justin

Cedric's interest lies at the crossroad of engineering and economics with a keen interest in civil commercial aviation and general aviation. Over the years, Cedric's research led to the investigation of challenges related to the construction and evaluation of technology portfolios, to the modeling of competitive forces in the aerospace industry, and to the evaluation of new concepts of operations pertaining to future on-demand air mobility paradigms. Recently, he focused his research on the supporting ground infrastructure for urban air mobility and thin haul air transportation. One common aspect across these diverse topics is the development of methods and tools to analyze complex systems of systems. Cedric graduated with a MS in Quantitative and Computational Finance in 2012, and a PhD in Aerospace Engineering in 2015.

Mr. Eddie Li

Eddie has previously worked on modeling of UAM concepts doing mission analysis. He also has experience building and testing small scale eVTOL aircraft

Prof. Dimitri Mavris

Dimitri Mavris is a Regents' Professor, Boeing Professor of Advanced Aerospace Systems Analysis, and an S.P. Langley Distinguished Professor. He also serves as the director of the Aerospace Systems Design Laboratory (ASDL) and executive director of the Professional Master's in Applied Systems Engineering (PMASE). Dr. Mavris received his B.S., M.S., and Ph.D. in aerospace engineering from the Georgia Institute of Technology. His primary areas of research interest include: advanced design methods, aircraft conceptual and preliminary design, air-breathing propulsion design, multi-disciplinary analysis, design and optimization, system of systems, and non-deterministic design theory. Dr. Mavris has actively pursued closer ties between the academic and industrial communities in order to foster research opportunities and tailor the aerospace engineering curriculum towards meeting the future needs of the US aerospace industry.

Dr. Michael Mayo

Michael is a Research Engineer at GTRI and specializes in experimental aerodynamics and acoustics. He has over 8 years of experience in aerodynamic testing and analysis and has experience on multiple projects involving the measurement of rotor noise. Mr. Mayo has also managed multiple projects involving aerodynamic and acoustic measurements. He is an instructor in the Georgia Tech Vertical Integrated Projects Department, an associate member of the AIAA Aerodynamic Measurement Technology technical committee, and a graduate of the NASA Ames Aeronautics Academy program

Mr. Metin Ozcan

Metin has been working on gas turbine transient modeling for the last nine years. His work includes developing different types of transient models and using the developed transient models for transient technology evaluation and real-time modeling

Mr. Srujal Patel

Srujal's research is focused on conceptual and preliminary design of the novel aircrafts, with an emphasis on the application of Safety-by-Design principles to the novel architectures. Srujal has also recently contributed to the research in performance-based safety certification of unconventional electric-propulsion based aircrafts.

Prof. Giorgio Rizzoni

The Ford Motor Company Chair in Electromechanical Systems, director of OSU-CAR, has dedicated his career to the discipline of dynamic systems and control multi-domain (electrical, mechanical, fluid, thermal, and chemical) systems with the aim of developing physics-based models that can be used to create control and diagnostic strategies and algorithms for application to complex systems including xEV propulsion systems, ICEs and transmissions, battery systems, and larger-scale energy systems.

Prof. Tunc Aldemir

Professor in the Department of Mechanical and Aerospace Engineering. Specializes in the reliability and probabilistic risk assessment of dynamic systems which may be difficult to model using conventional techniques, such as those with significant hardware/software/human/process interactions.

Ms. Gülçin Sarıcı Türkmen

Gülçin has experience in system modeling and deterministic safety analysis for nuclear reactors. She has been currently working on probabilistic risk assessment of dynamic systems.

Mr. Johannes (Juan) Verberne

Juan is a current PhD student at ASDL. He has previous experience with the design, development and implementation of guidance, navigation and control techniques in unmanned systems. He graduated with a B.S. and M.S. degree in Aerospace Engineering from Embry-Riddle Aeronautical University in Daytona Beach, FL. His interests lay in flight dynamics and control for both aerial and space systems.

APPENDIX A : FUNCTIONAL HAZARD ANALYSIS (FHA) TABLES

Appendix A - Table 1: Quadcopter Electric FHA

Function	Failure Condition	Phase of Operation	Effect of Failure	Classification
Convert Electrical Energy to Torque	Loss of single propulsor	Away from OEI Avoid Region	Aircrew detects failure and compensates with remaining thrust to continue flight. Cross-shafting results in all rotors continuing to spin.	Minor
		In OEI Avoid Region	Failure is detected. Power Required is greater than Power available (Pr > Pa). Hard landing with potential loss of aircraft/occupants.	Catastrophic
	Dual Propulsor Fail	All	Failures are detected. Cross-shafting ensures all rotors are still spinning. Controllability still present. Reduced power available. Insufficient power to maintain level fight. Autorotative approach requires suitable landing area. Worst case feasible outcome is loss of air vehicle/occupant.	Catastrophic
	Single ESC Fail	High, away from OEI Avoid Region	Failures are detected. Cross shafting ensures all rotors are still spinning. Controllability still present. Pilots will need to manually modulate engine power to a hover landing or a no hover landing with some forward speed to maximize Effective Translational Lift (ETL). Pilot workload issue.	Minor
		Low, away from OEI Avoid Region	Failures are detected. Cross shafting ensures all rotors are still spinning. Controllability still present. Pilots will need to manually modulate engine power to a hover landing or a no hover landing with some forward speed to maximize Effective Translational Lift (ETL). Pilot workload issue.	Minor
		Low, In OEI Avoid Region	Failure is detected. Cross shafting ensures controllability. Power Required is greater than Power available (Pr > Pa). Hard landing with potential loss of aircraft/crew.	Catastrophic

(Continued)

Function	Failure Condition	Phase of Operation	Effect of Failure	Classification
Provide Control Signals to Rotors and ESC	FCC Fail	All	ECS loses RPM loop closure commands from FCC. Additionally, collective control of rotor is lost. Catastrophic outcome due to loss of flight path control	Catastrophic
Transfer Torque to Rotors	Single Gearbox Fail	All	Failures detected and annunciated to aircrew (chip light, temp/ pressure indications). Loss of ability to spin rotor associated with that gearbox. Loss of flight-path control and subsequent catastrophic loss of air vehicle/occupants	Catastrophic
Provide HV Power to ESC (to drive the motor)	Complete HV Battery Fail	All	Complete loss of all High Voltage Power to motors. Complete loss of propulsion. Autorotative landing required. Worst case feasible outcome is loss of air-vehicle/occupant.	Catastrophic
	Individual portions of HV Battery Fail	In OEI Avoid Region	Failure is detected. Power Required is greater than Power available (Pr > Pa). Hard landing with potential loss of aircraft/occupants.	Catastrophic
		Away from OEI Avoid Region	Aircrew detects failure and compensates with remaining thrust to continue flight	Minor
Provide LV Power for FCC	LV Battery Fail	All	Loss of power to all 4 ESC and FCC. Collective control of rotor lost. Loss of flight Path Control and air vehicle with remaining thrust to continue flight	Catastrophic
Distribute Torque amongst Rotors	Cross Shaft Fail	All	Annunciated to pilot. Need proper anti-flail in place on driveshaft. Possible minor handling qualities impact, lack of redundancy available for follow-on propulsion single or dual failures. This fail in and of itself is not Catastrophic.	Minor
Control Rotor Pitch	Actuator Fail	All	Aircraft response becomes sluggish. Extreme cases lead to complete loss of aircraft control if FCC is unable to compensate.	Catastrophic

Appendix A - Table 2: Quadcopter Hybrid FHA

Function	Failure Condition	Phase of Operation	Effect of Failure	Classification
Convert Electrical Energy to Torque	Loss of single propulsor	Away from OEI Avoid Region	Aircrew detects failure and compensates with remaining thrust to continue flight. Cross-shafting results in all rotors continuing to spin.	Minor
		In OEI Avoid Region	Failure is detected. Power Required is greater than Power available (Pr > Pa). Hard landing with potential loss of aircraft/occupants.	Catastrophic
	Dual Propulsor Fail	All	Failures are detected. Cross-shafting ensures all rotors are still spinning. Controllability still present. Reduced power available. Insufficient power to maintain level fight. Autorotative approach requires suitable landing area. Worst case feasible outcome is loss of air-vehicle/occupant.	Catastrophic
	Single ESC Fail	High, away from OEI Avoid Region	Failures are detected. Cross shafting ensures all rotors are still spinning. Controllability still present. Pilots will need to manually modulate engine power to a hover landing or a no hover landing with some forward speed to maximize Effective Translational Lift (ETL). Pilot workload issue.	Minor
		Low, away from OEI Avoid Region	Failures are detected. Cross shafting ensures all rotors are still spinning. Controllability still present. Pilots will need to manually modulate engine power to a hover landing or a no hover landing with some forward speed to maximize Effective Translational Lift (ETL). Pilot workload issue.	Minor
		Low, In OEI Avoid Region	Failure is detected. Cross shafting ensures controllability. Power Required is greater than Power available (Pr > Pa). Hard landing with potential loss of aircraft/crew.	Catastrophic

(Continued)

Function	Failure Condition	Phase of Operation	Effect of Failure	Classification
Provide Control Signals to Rotors and ESC	FCC Fail	All	ECS loses RPM loop closure commands from FCC. Additionally, collective control of rotor is lost. Catastrophic outcome due to loss of flight path control	Catastrophic
Transfer Torque to Rotors	Single Gearbox Fail	All	Failures detected and annunciated to aircrew (chip light, temp/ pressure indications). Loss of ability to spin rotor associated with that gearbox. Loss of flight-path control and subsequent catastrophic loss of air vehicle/occupants	Catastrophic
Provide HV Power to ESC (to drive the motor)	Complete HV Battery Fail	All	Turbo-generator needs to provide enough power for any transient power requirement. Possible reduction in range.	Critical
	Turbo-generator Fail	All	Aircraft switches to reserve HV battery power. Crew must attempt emergency landing using the remaining battery reserve power.	Critical
Provide LV Power for FCC	LV Battery Fail	All	Loss of power to all 4 ESC and FCC. Collective control of rotor lost. Loss of flight Path Control and air vehicle with remaining thrust to continue flight	Catastrophic
Distribute Torque amongst Rotors	Cross Shaft Fail	All	Annunciated to pilot. Need proper anti-flail in place on driveshaft. Possible minor handling qualities impact, lack of redundancy available for follow-on propulsion single or dual failures. This fail in and of itself is not Catastrophic.	Minor
Control Rotor Pitch	Actuator Fail	All	Aircraft response becomes sluggish. Extreme cases lead to complete loss of aircraft control if FCC is unable to compensate.	Catastrophic

Appendix A - Table 3: Quadcopter Turboshaft FHA

Function	Failure Condition	Phase of Operation	Effect of Failure	Classification
Provide Control Signals to Rotors	FCC Fail	All	Collective control of rotor is lost. Catastrophic outcome due to loss of aircraft control.	Catastrophic
Transfer Torque to Rotors	Single Gearbox Fail	All	Failures detected and annunciated to aircrew (chip light, temp/ pressure indications). Loss of ability to spin rotor associated with that gearbox. Loss of flight-path control and subsequent catastrophic loss of air vehicle/occupants	Catastrophic
Provide LV Power for FCC	LV Battery Fail	All	Loss of power to all 4 ESC and FCC. Collective control of rotor lost. Loss of flight Path Control and air vehicle with remaining thrust to continue flight	Catastrophic
Distribute Torque amongst Rotors	Cross Shaft Fail	All	Loss of torque to rotors. Aircraft becomes unbalanced, loss of control ensues. Catastrophic outcome due to both loss of control and propulsion.	Catastrophic
Control Rotor Pitch	Actuator Fail	All	Aircraft response become sluggish. Extreme cases lead to complete loss of aircraft control if FCC is unable to compensate.	Catastrophic
Generate Mechanical Power	Single Turboshaft Fail	Low, away from OEI Avoid Region	Due to sudden loss of power, aircraft initially loses altitude, pilot skills required to safely continue the flight or emergency land the aircraft with one engine operating. Pilot workload issue.	Critical
	Single Turboshaft Fail	Low, in OEI Avoid Region	Aircraft loses propulsive power necessary to continue flight. Autorotative landing is required.	Catastrophic
	Dual Turboshaft Fail	All	Aircraft loses all propulsive power. Autorotative landing is required.	Catastrophic

Appendix A - Table 4: Hexacopter Collective Control FHA

Function	Failure Condition	Phase of Operation	Effect of Failure	Classification
Convert Electrical Energy to Torque	Single Propulsor Fail	Away from OEI Avoid Region	Failures are detected. Controllability is reduced. Pilots will need to manually modulate engine power to a hover landing or a no hover landing with some forward speed to maximize Effective Translational Lift (ETL). Pilot workload issue.	Critical
		In OEI Avoid Region	Failure is detected. Controllability is reduced. Power Required is greater than Power available (Pr > Pa). Hard landing with potential loss of aircraft/crew.	Catastrophic
	Dual Propulsor Fail	All	Insufficient power and control to maintain level fight. Autorotative landing required. Worst case feasible outcome is loss of air-vehicle/occupant. Hazard classification is the same whether OEI or out of OEI avoid region.	Catastrophic
	Dual ESC Fail	All	Insufficient power and control to maintain level fight. Autorotative landing required. Worst case feasible outcome is loss of air-vehicle/occupant. Hazard classification is the same whether OEI or out of OEI avoid region.	Catastrophic
	Single ESC Fail	Away from OEI Avoid Region	Failures are detected. Controllability is reduced. Pilots will need to manually modulate engine power to a hover landing or a no hover landing with some forward speed to maximize Effective Translational Lift (ETL). Pilot workload issue.	Critical
		In OEI Avoid Region	Failure is detected. Controllability is reduced. Power Required is greater than Power available (Pr > Pa). Hard landing with potential loss of aircraft/crew.	Catastrophic
Provide Control Signals to Rotors and ESC	FCC Fail	All	ECS loses RPM loop closure commands from FCC. Additionally, collective control of rotor is lost. Catastrophic outcome due to loss of flight path control.	Catastrophic

Function	Failure Condition	Phase of Operation	Effect of Failure	Classification
Transfer Torque to Rotors	Single Gearbox Fail	Away from OEI Avoid Region	Failures are detected. Controllability is reduced. Pilots will need to manually modulate engine power to a hover landing or a no hover landing with some forward speed to maximize Effective Translational Lift (ETL). Pilot workload issue.	Critical
		In OEI Avoid Region	Failure is detected. Controllability is reduced. Power Required is greater than Power available (Pr > Pa). Hard landing with potential loss of aircraft/crew.	Catastrophic
	Dual Gearbox Fail	All	Insufficient power and control to maintain level fight. Autorotative landing required. Worst case feasible outcome is loss of air-vehicle/occupant. Hazard classification is the same whether OEI or out of OEI avoid region.	Catastrophic
Provide HV Power to ESC (to drive the motor)	Complete HV Battery Fail	All	Complete loss of all High Voltage Power to motors. Complete loss of propulsion. Autorotative landing required. Worst case feasible outcome is loss of air-vehicle/occupant.	Catastrophic
	Individual Portions of HV Battery Fail	In OEI Avoid Region	Failure is detected. Power Required is greater than Power available (Pr > Pa). Hard landing with potential loss of aircraft/occupants.	Catastrophic
		Away from OEI Avoid Region	Aircrew detects failure and compensates with remaining thrust to continue to emergency landing.	Major
Provide LV Power for FCC	LV Battery Fail	All	Loss of power to all 4 ESC and FCC. Collective control of rotor lost. Loss of flight Path Control and air vehicle with remaining thrust to continue flight.	Catastrophic
Control Rotor Pitch	Actuator Fail	All	Aircraft response become sluggish. Extreme cases lead to complete loss of aircraft control if FCC is unable to compensate.	Catastrophic

Appendix A - Table 5: Hexacopter RPM Control FHA

Function	Failure Condition	Phase of Operation	Effect of Failure	Classification
Convert Electrical Energy to Torque	Single Propulsor Fail	Away from OEI Avoid Region	Failures are detected. Controllability is reduced. Pilots will need to manually modulate engine power to a hover landing or a no hover landing with some forward speed to maximize Effective Translational Lift (ETL). Pilot workload issue.	Critical
		In OEI Avoid Region	Failure is detected. Controllability is reduced. Power Required is greater than Power available (Pr > Pa). Hard landing with potential loss of aircraft/crew.	Catastrophic
	Dual Propulsor Fail	All	Insufficient power and control to maintain level fight. Autorotative landing required. Worst case feasible outcome is loss of air-vehicle/occupant. Hazard classification is the same whether OEI or out of OEI avoid region.	Catastrophic
	Dual ESC Fail	All	Insufficient power and control to maintain level fight. Autorotative landing required. Worst case feasible outcome is loss of air-vehicle/occupant. Hazard classification is the same whether OEI or out of OEI avoid region.	Catastrophic
	Single ESC Fail	Away from OEI Avoid Region	Failures are detected. Controllability is reduced. Pilots will need to manually modulate engine power to a hover landing or a no hover landing with some forward speed to maximize Effective Translational Lift (ETL). Pilot workload issue.	Critical
		In OEI Avoid Region	Failure is detected. Controllability is reduced. Power Required is greater than Power available (Pr > Pa). Hard landing with potential loss of aircraft/crew.	Catastrophic
Provide Control Signals to Rotors and ESC	FCC Fail	All	ECS loses RPM loop closure commands from FCC. Additionally, collective control of rotor is lost. Catastrophic outcome due to loss of flight path control.	Catastrophic

Function	Failure Condition	Phase of Operation	Effect of Failure	Classification
Transfer Torque to Rotors	Single Gearbox Fail	Away from OEI Avoid Region	Failures are detected. Controllability is reduced. Pilots will need to manually modulate engine power to a hover landing or a no hover landing with some forward speed to maximize Effective Translational Lift (ETL). Pilot workload issue.	Critical
		In OEI Avoid Region	Failure is detected. Controllability is reduced. Power Required is greater than Power available (Pr > Pa). Hard landing with potential loss of aircraft/crew.	Catastrophic
	Dual Gearbox Fail	All	Insufficient power and control to maintain level fight. Autorotative landing required. Worst case feasible outcome is loss of air-vehicle/occupant. Hazard classification is the same whether OEI or out of OEI avoid region.	Catastrophic
Provide HV Power to ESC (to drive the motor)	Complete HV Battery Fail	All	Complete loss of all High Voltage Power to motors. Complete loss of propulsion. Autorotative landing required. Worst case feasible outcome is loss of air-vehicle/occupant.	Catastrophic
	Individual Portions of HV Battery Fail	In OEI Avoid Region	Failure is detected. Power Required is greater than Power available (Pr > Pa). Hard landing with potential loss of aircraft/occupants.	Catastrophic
		Away from OEI Avoid Region	Aircrew detects failure and compensates with remaining thrust to continue to emergency landing.	Major
Provide LV Power for FCC	LV Battery Fail	All	Loss of power to all 4 ESC and FCC. Collective control of rotor lost. Loss of flightpath Control and air vehicle with remaining thrust to continue flight.	Catastrophic

Appendix A - Table 6: Octocopter RPM Control FHA

Function	Failure Condition	Phase of Operation	Effect of Failure	Classification
Convert Electrical Energy to Torque	Dual/Single Propulsor Fail	Away from OEI Avoid Region	Failures are detected. Controllability is reduced. Pilots will need to manually modulate engine power to a hover landing or a no hover landing with some forward speed to maximize Effective Translational Lift (ETL). Pilot workload issue.	Critical
		In OEI Avoid Region	Failure is detected. Controllability is reduced. Power Required is greater than Power available (Pr > Pa). Hard landing with potential loss of aircraft/crew.	Catastrophic
	Triple Propulsor Fail	All	Insufficient power and control to maintain level fight. Autorotative landing required. Worst case feasible outcome is loss of air-vehicle/occupant. Hazard classification is the same whether OEI or out of OEI avoid region.	Catastrophic
	Triple ESC Fail	All	Insufficient power and control to maintain level fight. Autorotative landing required. Worst case feasible outcome is loss of air-vehicle/occupant. Hazard classification is the same whether OEI or out of OEI avoid region.	Catastrophic
	Dual/Single ESC Fail	Away from OEI Avoid Region	Failures are detected. Controllability is reduced. Pilots will need to manually modulate engine power to a hover landing or a no hover landing with some forward speed to maximize Effective Translational Lift (ETL). Pilot workload issue.	Critical
		In OEI Avoid Region	Failure is detected. Controllability is reduced. Power Required is greater than Power available (Pr > Pa). Hard landing with potential loss of aircraft/crew.	Catastrophic
Provide Control Signals to Rotors and ESC	FCC Fail	All	ECS loses RPM loop closure commands from FCC. Additionally, collective control of rotor is lost. Catastrophic outcome due to loss of flight path control.	Catastrophic

Function	Failure Condition	Phase of Operation	Effect of Failure	Classification
Transfer Torque to Rotors	Dual/Single Gearbox Fail	Away from OEI Avoid Region	Failures are detected. Controllability is reduced. Pilots will need to manually modulate engine power to a hover landing or a no hover landing with some forward speed to maximize Effective Translational Lift (ETL). Pilot workload issue.	Critical
		In OEI Avoid Region	Failure is detected. Controllability is reduced. Power Required is greater than Power available (Pr > Pa). Hard landing with potential loss of aircraft/crew.	Catastrophic
	Triple Gearbox Fail	All	Insufficient power and control to maintain level fight. Autorotative landing required. Worst case feasible outcome is loss of air-vehicle/occupant. Hazard classification is the same whether OEI or out of OEI avoid region.	Catastrophic
Provide HV Power to ESC (to drive the motor)	Complete HV Battery Fail	All	Complete loss of all High Voltage Power to motors. Complete loss of propulsion. Autorotative landing required. Worst case feasible outcome is loss of air-vehicle/occupant.	Catastrophic
	Individual Portions of HV Battery Fail	In OEI Avoid Region	Failure is detected. Power Required is greater than Power available (Pr > Pa). Hard landing with potential loss of aircraft/occupants.	Catastrophic
		Away from OEI Avoid Region	Aircrew detects failure and compensates with remaining thrust to continue to emergency landing.	Major
Provide LV Power for FCC	LV Battery Fail	All	Loss of power to all 4 ESC and FCC. Collective control of rotor lost. Loss of flightpath Control and air vehicle with remaining thrust to continue flight.	Catastrophic

APPENDIX B : FAILURE MODES, EFFECTS AND CRITICALITY ANALYSIS (FMECA) TABLES

Appendix B - Table 1: Quadcopter Electric FMECA

Function	Component	Failure Rate	Failure Mode	Mission Phase	Local Failure Effect	Next Higher Effect	End Effect	Severity	Alpha	Beta
Convert Electrical Energy to Torque	Electronic Speed Controller	8.08E-06	ESC High Voltage	All	Rotor Torque Ripple	Rotor experiences torque oscillations. Torque from other motors are transferred through cross-shaft system.	Available power reduced. Possible aircraft instability.	Critical	20%	100.0%
Convert Electrical Energy to Torque	Electronic Speed Controller	8.08E-06	ESC Overcurrent	All	High Torque Ripple	Rotor experiences torque oscillations. Current draw from the battery is increased. Possible battery thermal runaway.	Reduced aircraft range. Possible aircraft instability.	Critical	20%	100.0%
Convert Electrical Energy to Torque	Electronic Speed Controller	8.08E-06	ESC Voltage Transient	All	Rotor Torque Ripple	Rotor experiences torque oscillations. Torque from other motors are transferred through cross-shaft system.	Available power reduced. Possible aircraft instability.	Critical	10%	100.0%
Convert Electrical Energy to Torque	Electronic Speed Controller	8.08E-06	ESC Vibrations	All	High Torque Ripple	Rotor experiences torque oscillations. Current draw from the battery is increased. Possible battery thermal runaway.	Reduced aircraft range. Possible aircraft instability.	Critical	10%	100.0%
Convert Electrical Energy to Torque	Electronic Speed Controller	8.08E-06	Manufacturing Defects	All	Rotor Torque Ripple	Rotor experiences torque oscillations. Torque from other motors are transferred through cross-shaft system.	Available power reduced. Possible aircraft instability.	Critical	7%	100.0%

Function	Component	Failure Rate	Failure Mode	Mission Phase	Local Failure Effect	Next Higher Effect	End Effect	Severity	Alpha	Beta
Convert Electrical Energy to Torque	Electronic Speed Controller	8.08E-06	ESC Current Sensor Fault	All	Rotor Torque Ripple	Rotor experiences torque oscillations. Torque from other motors are transferred through cross-shaft system.	Available power reduced. Possible aircraft instability.	Critical	2%	100.0%
Convert Electrical Energy to Torque	Electronic Speed Controller	8.08E-06	ESC Resolver Fault	All	Rotor Torque Ripple	Rotor experiences torque oscillations. Torque from other motors are transferred through cross-shaft system.	Available power reduced. Possible aircraft instability.	Critical	2%	100.0%
Convert Electrical Energy to Torque	Electronic Speed Controller	8.08E-06	ESC Temperature Sensor Fail	All	ESC fails, motor produces no torque	Torque from other motors are transferred through cross-shaft system.	Available power reduced. Limited flight envelope.	Critical	2%	100.0%
Convert Electrical Energy to Torque	Electronic Speed Controller	8.08E-06	ESC High Temperature	All	ESC fails, motor produces no torque	Torque from other motors are transferred through cross-shaft system.	Available power reduced. Limited flight envelope.	Critical	27%	40.0%
Convert Electrical Energy to Torque	Electronic Speed Controller	8.08E-06	ESC High Temperature	All	Rotor Low Torque	Torque from other motors are transferred through cross-shaft system.	Available power reduced. Limited flight envelope.	Critical	27%	30.0%
Convert Electrical Energy to Torque	Electronic Speed Controller	8.08E-06	ESC High Temperature	All	Rotor Torque Ripple	Rotor experiences torque oscillations. Torque from other motors are transferred through cross-shaft system.	Available power reduced. Possible aircraft instability.	Critical	27%	30.0%
Convert Electrical Energy to Torque	Electric Motor	5.10E-06	Motor High Voltage	All	Motor Short Circuit	Rotor experiences torque oscillations. Torque from other motors are transferred through cross-shaft system.	Available power reduced. Possible aircraft instability.	Critical	6%	100.0%

Function	Component	Failure Rate	Failure Mode	Mission Phase	Local Failure Effect	Next Higher Effect	End Effect	Severity	Alpha	Beta
Convert Electrical Energy to Torque	Electric Motor	5.10E-06	Motor Overcurrent	All	Motor Short Circuit	Rotor experiences torque oscillations. Torque from other motors are transferred through cross-shaft system.	Available power reduced. Possible aircraft instability.	Critical	6%	20.0%
Convert Electrical Energy to Torque	Electric Motor	5.10E-06	Motor Overcurrent	All	Rotor Torque Ripple	Torque from other motors are transferred through cross-shaft system.	Available power reduced. Possible aircraft instability.	Critical	6%	10.0%
Convert Electrical Energy to Torque	Electric Motor	5.10E-06	Motor Overcurrent	All	Low/No Torque	Torque from other motors are transferred through cross-shaft system.	Available power reduced. Possible aircraft instability.	Critical	6%	60.0%
Convert Electrical Energy to Torque	Electric Motor	5.10E-06	Motor Voltage Transient	All	Rotor Low Torque; Torque Ripple	Rotor experiences torque oscillations. Torque from other motors are transferred through cross-shaft system.	Available power reduced. Possible aircraft instability.	Critical	3%	100.0%
Convert Electrical Energy to Torque	Electric Motor	5.10E-06	Motor Eccentricity	All	Rotor Low/No Torque;	Torque from other motors are transferred through cross-shaft system.	Available power reduced. Possible aircraft instability.	Critical	0%	100.0%
Convert Electrical Energy to Torque	Electric Motor	5.10E-06	Motor Shaft Failure	All	Rotor Low/No Torque;	Torque from other motors are transferred through cross-shaft system.	Available power reduced. Possible aircraft instability.	Critical	0%	100.0%
Convert Electrical Energy to Torque	Electric Motor	5.10E-06	Motor High Temperature	All	Rotor No Torque	Torque from other motors are transferred through cross-shaft system.	Available power reduced. Possible aircraft instability.	Critical	84%	50.0%

Function	Component	Failure Rate	Failure Mode	Mission Phase	Local Failure Effect	Next Higher Effect	End Effect	Severity	Alpha	Beta
Convert Electrical Energy to Torque	Electric Motor	5.10E-06	Motor High Temperature	All	Rotor Short Circuit	Rotor experiences torque oscillations. Torque from other motors are transferred through cross-shaft system.	Available power reduced. Possible aircraft instability.	Critical	84%	20.0%
Convert Electrical Energy to Torque	Electric Motor	5.10E-06	Motor High Temperature	All Emergency Maneuver	Rotor Low Torque	Torque from other motors are transferred through cross-shaft system.	Available power reduced. Possible aircraft instability.	Critical	84%	30.0%
Provide LVDC Power for Control	LV Battery	1.01E-06	LV Battery Fail	All	Loss of function of FCC and all ESC	No torque produced by all ESC, No control signals provided to actuators	Loss of all propulsion and control. Aircraft descends to ground.	Catastrophic	100%	100.0%
Provide HV Power to ESC (to drive the motor)	HV Battery	8.07E-06	Battery Current Sensor Fault	All	Low/No Torque for the connected rotor	Torque from other motors are transferred through cross-shaft system.	Available power reduced. Possible aircraft instability.	Critical	22%	100.0%
Provide HV Power to ESC (to drive the motor)	HV Battery	8.07E-06	Battery Voltage Sensor Fault	All	Low/No Torque for the connected rotor	Torque from other motors are transferred through cross-shaft system.	Available power reduced. Possible aircraft instability.	Critical	22%	100.0%
Provide HV Power to ESC (to drive the motor)	HV Battery	8.07E-06	Battery Temperature Sensor Fault	All	Low/No Torque for the connected rotor	Torque from other motors are transferred through cross-shaft system.	Available power reduced. Possible aircraft instability.	Critical	22%	100.0%
Provide HV Power to ESC (to drive the motor)	HV Battery	8.07E-06	Battery External Short Circuit	All	Low/No Torque for the connected rotor	Torque from other motors are transferred through cross-shaft system.	Available power reduced. Possible aircraft instability.	Critical	6%	100.0%

Function	Component	Failure Rate	Failure Mode	Mission Phase	Local Failure Effect	Next Higher Effect	End Effect	Severity	Alpha	Beta
Provide HV Power to ESC (to drive the motor)	HV Battery	8.07E-06	Battery Physical Damage	All	Low/No Torque for the connected rotor	Torque from other motors are transferred through cross-shaft system.	Available power reduced. Possible aircraft instability.	Critical	4%	100.0%
Provide HV Power to ESC (to drive the motor)	HV Battery	8.07E-06	Battery Manufacturing Defects	All	Low/No Torque for the connected rotor	Torque from other motors are transferred through cross-shaft system.	Available power reduced. Possible aircraft instability.	Critical	12%	100.0%
Provide HV Power to ESC (to drive the motor)	HV Battery	8.07E-06	Battery External Overheating	All	Low/No Torque for the connected rotor	Torque from other motors are transferred through cross-shaft system.	Available power reduced. Possible aircraft instability.	Critical	12%	100.0%
Provide HV Power to ESC (to drive the motor)	HV Battery Cooling	4.30E-06	Battery Cooling Failure	All	Low/No Torque for the connected rotor	Torque from other motors are transferred through cross-shaft system.	Available power reduced. Possible aircraft instability.	Critical	100%	100.0%
Provide HV Power to ESC (to drive the motor)	Electric Distribution System	5.96E-08	Fuse High Temperature	All	No Torque for the connected rotor	Torque from other motors are transferred through cross-shaft system.	Available power reduced. Possible aircraft instability.	Critical	40.0%	70.0%
Provide HV Power to ESC (to drive the motor)	Electric Distribution System	5.96E-08	Fuse High Temperature	All	High Torque for the connected rotor	Torque is transferred to other rotors through cross-shaft system. Controls must compensate for high torque error.	Possible aircraft instability	Major	40.0%	30.0%
Provide HV Power to ESC (to drive the motor)	Electric Distribution System	4.47E-08	Fuse Overcurrent	All	No Torque for the connected rotor	Torque from other motors are transferred through cross-shaft system.	Available power reduced. Possible aircraft instability.	Critical	30.0%	70.0%

Function	Component	Failure Rate	Failure Mode	Mission Phase	Local Failure Effect	Next Higher Effect	End Effect	Severity	Alpha	Beta
Provide HV Power to ESC (to drive the motor)	Electric Distribution System	4.47E-08	Fuse Overcurrent	All	High Torque for the connected rotor	Torque is transferred to other rotors through cross-shaft system. Controls must compensate for high torque error.	Possible aircraft instability	Major	30.0%	30.0%
Provide HV Power to ESC (to drive the motor)	Electric Distribution System	4.47E-08	Fuse High Voltage	All	No Torque for the connected rotor	Torque from other motors are transferred through cross-shaft system.	Available power reduced. Possible aircraft instability.	Critical	30.0%	70.0%
Provide HV Power to ESC (to drive the motor)	Electric Distribution System	4.47E-08	Fuse High Voltage	All	High Torque for the connected rotor	Torque is transferred to other rotors through cross-shaft system. Controls must compensate for high torque error.	Possible aircraft instability	Major	30.0%	30.0%
Provide HV Power to ESC (to drive the motor)	Electric Distribution System	5.96E-08	Contactor High Temperature	All	No Torque for the connected rotor	Torque from other motors are transferred through cross-shaft system.	Available power reduced. Possible aircraft instability.	Critical	40.0%	70.0%
Provide HV Power to ESC (to drive the motor)	Electric Distribution System	5.96E-08	Contactor High Temperature	All	High Torque for the connected rotor	Torque is transferred to other rotors through cross-shaft system. Controls must compensate for high torque error.	Possible aircraft instability	Major	40.0%	30.0%
Provide HV Power to ESC (to drive the motor)	Electric Distribution System	4.47E-08	Contactor Overcurrent	All	No Torque for the connected rotor	Torque from other motors are transferred through cross-shaft system.	Available power reduced. Possible aircraft instability.	Critical	30.0%	70.0%

Function	Component	Failure Rate	Failure Mode	Mission Phase	Local Failure Effect	Next Higher Effect	End Effect	Severity	Alpha	Beta
Provide HV Power to ESC (to drive the motor)	Electric Distribution System	4.47E-08	Contactor Overcurrent	All	High Torque for the connected rotor	Torque is transferred to other rotors through cross-shaft system. Controls must compensate for high torque error.	Possible aircraft instability	Major	30.0%	30.0%
Provide HV Power to ESC (to drive the motor)	Electric Distribution System	4.47E-08	Contactor High Voltage	All	No Torque for the connected rotor	Torque from other motors are transferred through cross-shaft system.	Available power reduced. Possible aircraft instability.	Critical	30.0%	70.0%
Provide HV Power to ESC (to drive the motor)	Electric Distribution System	4.47E-08	Contactor High Voltage	All	High Torque for the connected rotor	Torque is transferred to other rotors through cross-shaft system. Controls must compensate for high torque error.	Possible aircraft instability	Major	30.0%	30.0%
Provide HV Power to ESC (to drive the motor)	Electric Distribution System	1.39E-07	Connection Failure	All	No Torque for the connected rotor	Torque from other motors are transferred through cross-shaft system.	Available power reduced. Possible aircraft instability.	Critical	100.0%	70.0%
Provide HV Power to ESC (to drive the motor)	Electric Distribution System	1.39E-07	Connection Failure	All	High Torque for the connected rotor	Torque is transferred to other rotors through cross-shaft system. Controls must compensate for high torque error.	Possible aircraft instability	Major	100.0%	30.0%
Distribute Torque amongst Rotors	Central Gearbox Shaft	7.15E-07	Shaft Overload Breakage	Emergency maneuver	Not transmitting power between the two halves of the cross-shafting system and unexpected rotor speed derivatives	An unexpected maneuver ensues due to the power transmission disturbance. The electric motor power outputs should be readjusted to trim.	Available power reduced. Possible aircraft instability.	Critical	10.0%	100.0%

Function	Component	Failure Rate	Failure Mode	Mission Phase	Local Failure Effect	Next Higher Effect	End Effect	Severity	Alpha	Beta
Distribute Torque amongst Rotors	Central Gearbox Shaft	7.15E-07	Shaft Fatigue Breakage	All	Not transmitting power between the two halves of the cross-shafting system and unexpected rotor speed derivatives	An unexpected maneuver ensues due to the power transmission disturbance. The electric motor power outputs should be readjusted to trim.	Available power reduced. Possible aircraft instability.	Critical	90.0%	100.0%
Distribute Torque amongst Rotors	Central Gearbox Shaft	4.29E-06	Bearing Spalling	All	Bearing creates more vibration and spins with more friction	The central shaft transmits power less efficiently among the electric motor-rotor pairs.	Available power reduced. Possible aircraft instability.	Major	90.0%	100.0%
Distribute Torque amongst Rotors	Central Gearbox Shaft	4.26E-06	Bearing Fracture	Emergency maneuver	Bearing carries significantly less or no load and vibrates violently	Imminent sequential component failures such as central shaft dislocation which isolates the electric motors	Available power reduced. Possible aircraft instability.	Critical	10.0%	100.0%
Distribute Torque amongst Rotors	Central Gearbox Bevel Gear	2.52E-07	Teeth Surface Fatigue	Emergency maneuver	Gear power transmission efficiency goes down due to more friction and the experienced vibration in operation increases	More power generation becomes necessary to make up for the increase in inefficiency	Available power reduced. Possible aircraft instability.	Major	85.0%	100.0%
Distribute Torque amongst Rotors	Central Gearbox Bevel Gear	2.52E-07	Teeth Overload Fracture	Emergency maneuver	The broken tooth reduces the transmission efficiency. In addition, vibrations increase.	The electric motors need to compensate for the reduction in efficiency to provide the same performance	Available power reduced. Possible aircraft instability.	Critical	5.0%	100.0%

Function	Component	Failure Rate	Failure Mode	Mission Phase	Local Failure Effect	Next Higher Effect	End Effect	Severity	Alpha	Beta
Distribute Torque amongst Rotors	Central Gearbox Bevel Gear	2.52E-07	Teeth Fatigue Fracture	All	The broken tooth reduces the transmission efficiency. In addition, vibrations increase.	The electric motors need to compensate for the reduction in efficiency to provide the same performance	Available power reduced. Possible aircraft instability.	Critical	10.0%	100.0%
Distribute Torque amongst Rotors	Central Gearbox Auxiliary	3.48E-07	Teeth Surface Fatigue	Emergency maneuver	Gear power transmission efficiency goes down due to more friction and the experienced vibration in operation increases	The central gearbox transmits less power among the electric motors due to the decrease in the auxiliary gearbox's transmission efficiency.	Available power reduced. Possible aircraft instability.	Major	85.0%	100.0%
Distribute Torque amongst Rotors	Central Gearbox Auxiliary	3.48E-07	Teeth Overload Fracture	Emergency maneuver	The broken tooth reduces the transmission efficiency. In addition, vibrations increase.	The power transmission through the central gearbox is less efficient	Available power reduced. Possible aircraft instability.	Critical	5.0%	100.0%
Distribute Torque amongst Rotors	Central Gearbox Auxiliary	3.48E-07	Teeth Fatigue Fracture	All	The broken tooth reduces the transmission efficiency. In addition, vibrations increase.	The power transmission through the central gearbox is less efficient	Available power reduced. Possible aircraft instability.	Critical	10.0%	100.0%

Function	Component	Failure Rate	Failure Mode	Mission Phase	Local Failure Effect	Next Higher Effect	End Effect	Severity	Alpha	Beta
Distribute Torque amongst Rotors	Cross-Shafting Shafts	7.15E-07	Overload Breakage	Emergency maneuver	Not transmitting power between the electric motor-rotor combination and the central gearbox resulting in unexpected rotor speed derivatives	An unexpected maneuver ensues due to the power transmission disturbance. The electric motor power outputs should be readjusted to trim.	Available power reduced. Possible aircraft instability.	Critical	10.0%	100.0%
Distribute Torque amongst Rotors	Cross-Shafting Shafts	7.15E-07	Fatigue Breakage	All	Not transmitting power between the electric motor-rotor combination and the central gearbox resulting in unexpected rotor speed derivatives	An unexpected maneuver ensues due to the power transmission disturbance. The electric motor power outputs should be readjusted to trim.	Available power reduced. Possible aircraft instability.	Critical	90.0%	100.0%
Distribute Torque amongst Rotors	Cross-Shafting Bearings	4.29E-06	Bearing Spalling	All	Bearing creates more vibration and spins with more friction	The cross-shafting system transmits power less efficiently to and from the central gearbox due to the increased friction	Available power reduced. Possible aircraft instability.	Major	90.0%	100.0%
Distribute Torque amongst Rotors	Cross-Shafting Bearings	4.29E-06	Bearing Fracture	Emergency maneuver	Bearing carries significantly less or no load and vibrates violently	Imminent sequential component failures such as cross-shaft dislocation which isolates the connected electric motor from the other electric motors	Available power reduced. Possible aircraft instability.	Critical	10.0%	100.0%

Function	Component	Failure Rate	Failure Mode	Mission Phase	Local Failure Effect	Next Higher Effect	End Effect	Severity	Alpha	Beta
Distribute Torque amongst Rotors	Cross-Shafting Bevel Gears	2.52E-07	Teeth Surface Fatigue	Emergency maneuver	Gear power transmission efficiency goes down due to more friction and the experienced vibration in operation increases	The electric motors need to generate more power to provide the same performance	Available power reduced. Possible aircraft instability.	Major	85.0%	100.0%
Distribute Torque amongst Rotors	Cross-Shafting Bevel Gears	2.52E-07	Teeth Overload Fracture	Emergency maneuver	The broken tooth reduces the gear efficiency and the vibrations increase	The same performance requires an increase in electric motor power generation	Available power reduced. Possible aircraft instability.	Critical	5.0%	100.0%
Distribute Torque amongst Rotors	Cross-Shafting Bevel Gears	2.52E-07	Teeth Fatigue Fracture	All	The broken tooth reduces the gear efficiency and the vibrations increase	The same performance requires an increase in electric motor power generation	Available power reduced. Possible aircraft instability.	Critical	10.0%	100.0%
Transfer Torque to Rotors	Reduction Gearbox	4.23E-07	Teeth Surface Fatigue	Emergency maneuver	Gear power transmission efficiency goes down due to more friction and the experienced vibration in operation increases	More power is necessary to spin the rotor attached to the gearbox at the same speed and pitch angle	Available power reduced. Possible aircraft instability. Range is reduced.	Major	85.0%	100.0%
Transfer Torque to Rotors	Reduction Gearbox	4.23E-07	Teeth Overload Fracture	Emergency maneuver	The broken tooth reduces the gear efficiency and the vibrations increase	The same performance level requires an increase in power generation	Available power reduced. Possible aircraft instability. Range is reduced.	Critical	5.0%	100.0%

Function	Component	Failure Rate	Failure Mode	Mission Phase	Local Failure Effect	Next Higher Effect	End Effect	Severity	Alpha	Beta
Transfer Torque to Rotors	Reduction Gearbox	4.23E-07	Teeth Fatigue Fracture	All	The broken tooth reduces the gear efficiency and the vibrations increase	The same performance level requires an increase in power generation	Available power reduced. Possible aircraft instability. Range is reduced.	Critical	10.0%	100.0%
Convert Electrical Energy to Torque	Motor Auxiliary Gearbox	3.48E-07	Teeth Surface Fatigue	Emergency maneuver	Gear power transmission efficiency goes down due to more friction and the experienced vibration in operation increases	The power required for the same auxiliary system performance increases	Available Power Reduced. Range is reduced.	Major	85.0%	100.0%
Convert Electrical Energy to Torque	Motor Auxiliary Gearbox	3.48E-07	Teeth Overload Fracture	Emergency maneuver	The broken tooth reduces the gear efficiency and the vibrations increase.	The power required for the same auxiliary system performance increases	Available Power Reduced. Range is reduced.	Critical	5.0%	100.0%
Convert Electrical Energy to Torque	Motor Auxiliary Gearbox	3.48E-07	Teeth Fatigue Fracture	All	The broken tooth reduces the gear efficiency and the vibrations increase.	The power required for the same auxiliary system performance increases	Available Power Reduced. Range is reduced.	Critical	10.0%	100.0%
Transfer Torque to Rotors	Rotor Overruning Clutch	4.23E-07	Overload Fracture	Emergency maneuver	The clutch fails to engage	The remaining three connected motors must power the four rotors	Available power reduced. Possible aircraft instability. Range is reduced.	Critical	5.0%	100.0%
Transfer Torque to Rotors	Rotor Overruning Clutch	4.23E-07	Fatigue Fracture	All	The clutch fails to engage	The remaining three connected motors must power the four rotors	Available power reduced. Possible aircraft instability. Range is reduced.	Critical	15.0%	100.0%

Function	Component	Failure Rate	Failure Mode	Mission Phase	Local Failure Effect	Next Higher Effect	End Effect	Severity	Alpha	Beta
Transfer Torque to Rotors	Rotor Overruning Clutch	4.23E-07	Degradation	All	The clutch efficiency is lower	The electric motor power generation increases	Available power reduced. Range is reduced.	Critical	80.0%	100.0%
Control Rotor Pitch	Collective Actuators	5.50E-05	Bias	All	Rotor pitch differs from desired position.	If FCC is not able to compensate for error, aircraft loses control.	Loss of control.	Catastrophic	25.0%	100.0%
Control Rotor Pitch	Collective Actuators	5.50E-05	Stuck Surface	All	Unable to change rotor pitch.	Loss of control is inevitable.	Loss of control.	Catastrophic	15.0%	100.0%
Control Rotor Pitch	Collective Actuators	5.50E-05	Hardover	All	Rotor pitch is stuck at one extreme	Loss of control is inevitable.	Loss of control.	Catastrophic	10.0%	100.0%
Control Rotor Pitch	Collective Actuators	5.50E-05	Floating Surface	All	Unable to control rotor pitch	Loss of control is inevitable.	Loss of control.	Catastrophic	20.0%	100.0%
Control Rotor Pitch	Collective Actuators	5.50E-05	Oscillations	All	Rotor pitch changes erratically.	Loss of control is inevitable.	Loss of control.	Catastrophic	10.0%	100.0%
Control Rotor Pitch	Collective Actuators	5.50E-05	Increased Deadband	All	Reduced range of motor pitch.	Aircraft maneuvering becomes sluggish.	Possible aircraft instability	Critical	20.0%	100.0%

Appendix B - Table 2: Quadcopter Hybrid FMECA

Function	Component	Failure Rate	Failure Mode	Mission Phase	Local Failure Effect	Next Higher Effect	End Effect	Severity	Alpha	Beta
Convert Electrical Energy to Torque	Electronic Speed Controller	8.08E-06	ESC High Voltage	All	Rotor Torque Ripple	Rotor experiences torque oscillations. Torque from other motors are transferred through cross-shaft system.	Available power reduced. Possible aircraft instability.	Critical	20%	100.0%
Convert Electrical Energy to Torque	Electronic Speed Controller	8.08E-06	ESC Overcurrent	All	High Torque Ripple	Rotor experiences torque oscillations. Current draw from the battery is increased. Possible battery thermal runaway.	Reduced aircraft range. Possible aircraft instability.	Critical	20%	100.0%
Convert Electrical Energy to Torque	Electronic Speed Controller	8.08E-06	ESC Voltage Transient	All	Rotor Torque Ripple	Rotor experiences torque oscillations. Torque from other motors are transferred through cross-shaft system.	Available power reduced. Possible aircraft instability.	Critical	10%	100.0%
Convert Electrical Energy to Torque	Electronic Speed Controller	8.08E-06	ESC Vibrations	All	High Torque Ripple	Rotor experiences torque oscillations. Current draw from the battery is increased. Possible battery thermal runaway.	Reduced aircraft range. Possible aircraft instability.	Critical	10%	100.0%
Convert Electrical Energy to Torque	Electronic Speed Controller	8.08E-06	Manufacturing Defects	All	Rotor Torque Ripple	Rotor experiences torque oscillations. Torque from other motors are transferred through cross-shaft system.	Available power reduced. Possible aircraft instability.	Critical	7%	100.0%

Function	Component	Failure Rate	Failure Mode	Mission Phase	Local Failure Effect	Next Higher Effect	End Effect	Severity	Alpha	Beta
Convert Electrical Energy to Torque	Electronic Speed Controller	8.08E-06	ESC Current Sensor Fault	All	Rotor Torque Ripple	Rotor experiences torque oscillations. Torque from other motors are transferred through cross-shaft system.	Available power reduced. Possible aircraft instability.	Critical	2%	100.0%
Convert Electrical Energy to Torque	Electronic Speed Controller	8.08E-06	ESC Resolver Fault	All	Rotor Torque Ripple	Rotor experiences torque oscillations. Torque from other motors are transferred through cross-shaft system.	Available power reduced. Possible aircraft instability.	Critical	2%	100.0%
Convert Electrical Energy to Torque	Electronic Speed Controller	8.08E-06	ESC Temperature Sensor Fail	All	ESC fails, motor produces no torque	Torque from other motors are transferred through cross-shaft system.	Available power reduced. Limited flight envelope.	Critical	2%	100.0%
Convert Electrical Energy to Torque	Electronic Speed Controller	8.08E-06	ESC High Temperature	All	ESC fails, motor produces no torque	Torque from other motors are transferred through cross-shaft system.	Available power reduced. Limited flight envelope.	Critical	27%	40.0%
Convert Electrical Energy to Torque	Electronic Speed Controller	8.08E-06	ESC High Temperature	All	Rotor Low Torque	Torque from other motors are transferred through cross-shaft system.	Available power reduced. Limited flight envelope.	Critical	27%	30.0%
Convert Electrical Energy to Torque	Electronic Speed Controller	8.08E-06	ESC High Temperature	All	Rotor Torque Ripple	Rotor experiences torque oscillations. Torque from other motors are transferred through cross-shaft system.	Available power reduced. Possible aircraft instability.	Critical	27%	30.0%
Convert Electrical Energy to Torque	Electric Motor	5.10E-06	Motor High Voltage	All	Motor Short Circuit	Rotor experiences torque oscillations. Torque from other motors are transferred through cross-shaft system.	Available power reduced. Possible aircraft instability.	Critical	6%	100.0%

Function	Component	Failure Rate	Failure Mode	Mission Phase	Local Failure Effect	Next Higher Effect	End Effect	Severity	Alpha	Beta
Convert Electrical Energy to Torque	Electric Motor	5.10E-06	Motor Overcurrent	All	Motor Short Circuit	Rotor experiences torque oscillations. Torque from other motors are transferred through cross-shaft system.	Available power reduced. Possible aircraft instability.	Critical	6%	20.0%
Convert Electrical Energy to Torque	Electric Motor	5.10E-06	Motor Overcurrent	All	Rotor Torque Ripple	Torque from other motors are transferred through cross-shaft system.	Available power reduced. Possible aircraft instability.	Critical	6%	10.0%
Convert Electrical Energy to Torque	Electric Motor	5.10E-06	Motor Overcurrent	All	Low/No Torque	Torque from other motors are transferred through cross-shaft system.	Available power reduced. Possible aircraft instability.	Critical	6%	60.0%
Convert Electrical Energy to Torque	Electric Motor	5.10E-06	Motor Voltage Transient	All	Rotor Low Torque; Torque Ripple	Rotor experiences torque oscillations. Torque from other motors are transferred through cross-shaft system.	Available power reduced. Possible aircraft instability.	Critical	3%	100.0%
Convert Electrical Energy to Torque	Electric Motor	5.10E-06	Motor Eccentricity	All	Rotor Low/No Torque;	Torque from other motors are transferred through cross-shaft system.	Available power reduced. Possible aircraft instability.	Critical	0%	100.0%
Convert Electrical Energy to Torque	Electric Motor	5.10E-06	Motor Shaft Failure	All	Rotor Low/No Torque;	Torque from other motors are transferred through cross-shaft system.	Available power reduced. Possible aircraft instability.	Critical	0%	100.0%
Convert Electrical Energy to Torque	Electric Motor	5.10E-06	Motor High Temperature	All	Rotor No Torque	Torque from other motors are transferred through cross-shaft system.	Available power reduced. Possible aircraft instability.	Critical	84%	50.0%

Function	Component	Failure Rate	Failure Mode	Mission Phase	Local Failure Effect	Next Higher Effect	End Effect	Severity	Alpha	Beta
Convert Electrical Energy to Torque	Electric Motor	5.10E-06	Motor High Temperatur e	All	Rotor Short Circuit	Rotor experiences torque oscillations. Torque from other motors are transferred through cross-shaft system.	Available power reduced. Possible aircraft instability.	Critical	84%	20.0%
Convert Electrical Energy to Torque	Electric Motor	5.10E-06	Motor High Temperatur e	All	Rotor Low Torque	Torque from other motors are transferred through cross-shaft system.	Available power reduced. Possible aircraft instability.	Critical	84%	30.0%
Provide LVDC Power for Control	LV Battery	1.01E-06	LV Battery Fail	All	Loss of function of FCC and all ESC	No torque produced by all ESC, No control signals provided to actuators	Loss of all propulsion and control. Aircraft descends to ground.	Catastrophic	100%	100.0%
Provide HV Power to ESC (to drive the motor)	HV Battery	8.07E-06	Battery Current Sensor Fault	All	Low/No Torque when battery power is used	If only battery power is available, rotors may not receive sufficient power for desired maneuvers.	Available Power Reduced. Range is reduced.	Critical	22%	100.0%
Provide HV Power to ESC (to drive the motor)	HV Battery	8.07E-06	Battery Voltage Sensor Fault	All	Low/No Torque when battery power is used	If only battery power is available, rotors may not receive sufficient power for desired maneuvers.	Available Power Reduced. Range is reduced.	Critical	22%	100.0%
Provide HV Power to ESC (to drive the motor)	HV Battery	8.07E-06	Battery Temperatur e Sensor Fault	All	Low/No Torque when battery power is used	If only battery power is available, rotors may not receive sufficient power for desired maneuvers.	Available Power Reduced. Range is reduced.	Critical	22%	100.0%
Provide HV Power to ESC (to drive the motor)	HV Battery	8.07E-06	Battery External Short Circuit	All	Low/No Torque when battery power is used	If only battery power is available, rotors may not receive sufficient power for desired maneuvers.	Available Power Reduced. Range is reduced.	Critical	6%	100.0%

Function	Component	Failure Rate	Failure Mode	Mission Phase	Local Failure Effect	Next Higher Effect	End Effect	Severity	Alpha	Beta
Provide HV Power to ESC (to drive the motor)	HV Battery	8.07E-06	Battery Physical Damage	All	Low/No Torque when battery power is used	If only battery power is available, rotors may not receive sufficient power for desired maneuvers.	Available Power Reduced. Range is reduced.	Critical	4%	100.0%
Provide HV Power to ESC (to drive the motor)	HV Battery	8.07E-06	Battery Manufacturing Defects	All	Low/No Torque when battery power is used	If only battery power is available, rotors may not receive sufficient power for desired maneuvers.	Available Power Reduced. Range is reduced.	Critical	12%	100.0%
Provide HV Power to ESC (to drive the motor)	HV Battery	8.07E-06	Battery External Overheating	All	Low/No Torque when battery power is used	If only battery power is available, rotors may not receive sufficient power for desired maneuvers.	Available Power Reduced. Range is reduced.	Critical	12%	100.0%
Provide HV Power to ESC (to drive the motor)	HV Battery Cooling	4.30E-06	Battery Cooling Failure	All	Low/No Torque when battery power is used	If only battery power is available, rotors may not receive sufficient power for desired maneuvers.	Available Power Reduced. Range is reduced.	Critical	100%	100.0%
Provide HV Power to ESC (to drive the motor)	Electric Distribution System	5.96E-08	Fuse High Temperature	All	No Torque for the connected rotor	Torque from other motors are transferred through cross-shaft system.	Available power reduced. Possible aircraft instability.	Critical	40.0%	70.0%
Provide HV Power to ESC (to drive the motor)	Electric Distribution System	5.96E-08	Fuse High Temperature	All	High Torque for the connected rotor	Torque is transferred to other rotors through cross-shaft system. Controls must compensate for high torque error.	Possible aircraft instability	Major	40.0%	30.0%
Provide HV Power to ESC (to drive the motor)	Electric Distribution System	4.47E-08	Fuse Overcurrent	All	No Torque for the connected rotor	Torque from other motors are transferred through cross-shaft system.	Available power reduced. Possible aircraft instability.	Critical	30.0%	70.0%

Function	Component	Failure Rate	Failure Mode	Mission Phase	Local Failure Effect	Next Higher Effect	End Effect	Severity	Alpha	Beta
Provide HV Power to ESC (to drive the motor)	Electric Distribution System	4.47E-08	Fuse Overcurrent	All	High Torque for the connected rotor	Torque is transferred to other rotors through cross-shaft system. Controls must compensate for high torque error.	Possible aircraft instability	Major	30.0%	30.0%
Provide HV Power to ESC (to drive the motor)	Electric Distribution System	4.47E-08	Fuse High Voltage	All	No Torque for the connected rotor	Torque from other motors are transferred through cross-shaft system.	Available power reduced. Possible aircraft instability.	Critical	30.0%	70.0%
Provide HV Power to ESC (to drive the motor)	Electric Distribution System	4.47E-08	Fuse High Voltage	All	High Torque for the connected rotor	Torque is transferred to other rotors through cross-shaft system. Controls must compensate for high torque error.	Possible aircraft instability	Major	30.0%	30.0%
Provide HV Power to ESC (to drive the motor)	Electric Distribution System	5.96E-08	Contactor High Temperatur e	All	No Torque for the connected rotor	Torque from other motors are transferred through cross-shaft system.	Available power reduced. Possible aircraft instability.	Critical	40.0%	70.0%
Provide HV Power to ESC (to drive the motor)	Electric Distribution System	5.96E-08	Contactor High Temperatur e	All	High Torque for the connected rotor	Torque is transferred to other rotors through cross-shaft system. Controls must compensate for high torque error.	Possible aircraft instability	Major	40.0%	30.0%
Provide HV Power to ESC (to drive the motor)	Electric Distribution System	4.47E-08	Contactor Overcurrent	All	No Torque for the connected rotor	Torque from other motors are transferred through cross-shaft system.	Available power reduced. Possible aircraft instability.	Critical	30.0%	70.0%

Function	Component	Failure Rate	Failure Mode	Mission Phase	Local Failure Effect	Next Higher Effect	End Effect	Severity	Alpha	Beta
Provide HV Power to ESC (to drive the motor)	Electric Distribution System	4.47E-08	Contactor Overcurrent	All	High Torque for the connected rotor	Torque is transferred to other rotors through cross-shaft system. Controls must compensate for high torque error.	Possible aircraft instability	Major	30.0%	30.0%
Provide HV Power to ESC (to drive the motor)	Electric Distribution System	4.47E-08	Contactor High Voltage	All	No Torque for the connected rotor	Torque from other motors are transferred through cross-shaft system.	Available power reduced. Possible aircraft instability.	Critical	30.0%	70.0%
Provide HV Power to ESC (to drive the motor)	Electric Distribution System	4.47E-08	Contactor High Voltage	All	High Torque for the connected rotor	Torque is transferred to other rotors through cross-shaft system. Controls must compensate for high torque error.	Possible aircraft instability	Major	30.0%	30.0%
Provide HV Power to ESC (to drive the motor)	Electric Distribution System	1.39E-07	Connection Failure	All	No Torque for the connected rotor	Torque from other motors are transferred through cross-shaft system.	Available power reduced. Possible aircraft instability.	Critical	100.0%	70.0%
Provide HV Power to ESC (to drive the motor)	Electric Distribution System	1.39E-07	Connection Failure	All	High Torque for the connected rotor	Torque is transferred to other rotors through cross-shaft system. Controls must compensate for high torque error.	Possible aircraft instability	Major	100.0%	30.0%
Distribute Torque amongst Rotors	Central Gearbox Shaft	7.15E-07	Shaft Overload Breakage	Emergency maneuver	Not transmitting power between the two halves of the cross-shafting system and unexpected rotor speed derivatives	An unexpected maneuver ensues due to the power transmission disturbance. The electric motor power outputs should be readjusted to trim.	Available power reduced. Possible aircraft instability.	Critical	10.0%	100.0%

Function	Component	Failure Rate	Failure Mode	Mission Phase	Local Failure Effect	Next Higher Effect	End Effect	Severity	Alpha	Beta
Distribute Torque amongst Rotors	Central Gearbox Shaft	7.15E-07	Shaft Fatigue Breakage	All	Not transmitting power between the two halves of the cross-shafting system and unexpected rotor speed derivatives	An unexpected maneuver ensues due to the power transmission disturbance. The electric motor power outputs should be readjusted to trim.	Available power reduced. Possible aircraft instability.	Critical	90.0%	100.0%
Distribute Torque amongst Rotors	Central Gearbox Shaft	4.29E-06	Bearing Spalling	All	Bearing creates more vibration and spins with more friction	The central shaft transmits power less efficiently among the electric motor-rotor pairs.	Available power reduced. Possible aircraft instability.	Major	90.0%	100.0%
Distribute Torque amongst Rotors	Central Gearbox Shaft	4.26E-06	Bearing Fracture	Emergency maneuver	Bearing carries significantly less or no load and vibrates violently	Imminent sequential component failures such as central shaft dislocation which isolates the electric motors	Available power reduced. Possible aircraft instability.	Critical	10.0%	100.0%
Distribute Torque amongst Rotors	Central Gearbox Bevel Gear	2.52E-07	Teeth Surface Fatigue	Emergency maneuver	Gear power transmission efficiency goes down due to more friction and the experienced vibration in operation increases	More power generation becomes necessary to make up for the increase in inefficiency	Available power reduced. Possible aircraft instability.	Major	85.0%	100.0%
Distribute Torque amongst Rotors	Central Gearbox Bevel Gear	2.52E-07	Teeth Overload Fracture	Emergency maneuver	The broken tooth reduces the transmission efficiency. In addition, vibrations increase.	The electric motors need to compensate for the reduction in efficiency to provide the same performance	Available power reduced. Possible aircraft instability.	Critical	5.0%	100.0%

Function	Component	Failure Rate	Failure Mode	Mission Phase	Local Failure Effect	Next Higher Effect	End Effect	Severity	Alpha	Beta
Distribute Torque amongst Rotors	Central Gearbox Bevel Gear	2.52E-07	Teeth Fatigue Fracture	All	The broken tooth reduces the transmission efficiency. In addition, vibrations increase.	The electric motors need to compensate for the reduction in efficiency to provide the same performance	Available power reduced. Possible aircraft instability.	Critical	10.0%	100.0%
Distribute Torque amongst Rotors	Central Gearbox Auxiliary	3.48E-07	Teeth Surface Fatigue	Emergency maneuver	Gear power transmission efficiency goes down due to more friction and the experienced vibration in operation increases	The central gearbox transmits less power among the electric motors due to the decrease in the auxiliary gearbox's transmission efficiency.	Available power reduced. Possible aircraft instability.	Major	85.0%	100.0%
Distribute Torque amongst Rotors	Central Gearbox Auxiliary	3.48E-07	Teeth Overload Fracture	Emergency maneuver	The broken tooth reduces the transmission efficiency. In addition, vibrations increase.	The power transmission through the central gearbox is less efficient	Available power reduced. Possible aircraft instability.	Critical	5.0%	100.0%
Distribute Torque amongst Rotors	Central Gearbox Auxiliary	3.48E-07	Teeth Fatigue Fracture	All	The broken tooth reduces the transmission efficiency. In addition, vibrations increase.	The power transmission through the central gearbox is less efficient	Available power reduced. Possible aircraft instability.	Critical	10.0%	100.0%
Distribute Torque amongst Rotors	Cross-Shafting Shafts	7.15E-07	Overload Breakage	Emergency maneuver	Not transmitting power between the electric motor-rotor combination and the central gearbox resulting in unexpected rotor speed derivatives	An unexpected maneuver ensues due to the power transmission disturbance. The electric motor power outputs should be readjusted to trim.	Available power reduced. Possible aircraft instability.	Critical	10.0%	100.0%

Function	Component	Failure Rate	Failure Mode	Mission Phase	Local Failure Effect	Next Higher Effect	End Effect	Severity	Alpha	Beta
Distribute Torque amongst Rotors	Cross-Shafting Shafts	7.15E-07	Fatigue Breakage	All	Not transmitting power between the electric motor-rotor combination and the central gearbox resulting in unexpected rotor speed derivatives	An unexpected maneuver ensues due to the power transmission disturbance. The electric motor power outputs should be readjusted to trim.	Available power reduced. Possible aircraft instability.	Critical	90.0%	100.0%
Distribute Torque amongst Rotors	Cross-Shafting Bearings	4.29E-06	Bearing Spalling	All	Bearing creates more vibration and spins with more friction	The cross-shafting system transmits power less efficiently to and from the central gearbox due to the increased friction	Available power reduced. Possible aircraft instability.	Major	90.0%	100.0%
Distribute Torque amongst Rotors	Cross-Shafting Bearings	4.29E-06	Bearing Fracture	Emergency maneuver	Bearing carries significantly less or no load and vibrates violently	Imminent sequential component failures such as cross-shaft dislocation which isolates the connected electric motor from the other electric motors	Available power reduced. Possible aircraft instability.	Critical	10.0%	100.0%
Distribute Torque amongst Rotors	Cross-Shafting Bevel Gears	2.52E-07	Teeth Surface Fatigue	Emergency maneuver	Gear power transmission efficiency goes down due to more friction and the experienced vibration in operation increases	The electric motors need to generate more power to provide the same performance	Available power reduced. Possible aircraft instability.	Major	85.0%	100.0%
Distribute Torque amongst Rotors	Cross-Shafting Bevel Gears	2.52E-07	Teeth Overload Fracture	Emergency maneuver	The broken tooth reduces the gear efficiency and the vibrations increase	The same performance requires an increase in electric motor power generation	Available power reduced. Possible aircraft instability.	Critical	5.0%	100.0%

Function	Component	Failure Rate	Failure Mode	Mission Phase	Local Failure Effect	Next Higher Effect	End Effect	Severity	Alpha	Beta
Distribute Torque amongst Rotors	Cross-Shafting Bevel Gears	2.52E-07	Teeth Fatigue Fracture	All	The broken tooth reduces the gear efficiency and the vibrations increase	The same performance requires an increase in electric motor power generation	Available power reduced. Possible aircraft instability.	Critical	10.0%	100.0%
Transfer Torque to Rotors	Reduction Gearbox	4.23E-07	Teeth Surface Fatigue	Emergency maneuver	Gear power transmission efficiency goes down due to more friction and the experienced vibration in operation increases	More power is necessary to spin the rotor attached to the gearbox at the same speed and pitch angle	Available power reduced. Possible aircraft instability. Range is reduced.	Major	85.0%	100.0%
Transfer Torque to Rotors	Reduction Gearbox	4.23E-07	Teeth Overload Fracture	Emergency maneuver	The broken tooth reduces the gear efficiency and the vibrations increase	The same performance level requires an increase in power generation	Available power reduced. Possible aircraft instability. Range is reduced.	Critical	5.0%	100.0%
Transfer Torque to Rotors	Reduction Gearbox	4.23E-07	Teeth Fatigue Fracture	All	The broken tooth reduces the gear efficiency and the vibrations increase	The same performance level requires an increase in power generation	Available power reduced. Possible aircraft instability. Range is reduced.	Critical	10.0%	100.0%
Convert Electrical Energy to Torque	Motor Auxiliary Gearbox	3.48E-07	Teeth Surface Fatigue	Emergency maneuver	Gear power transmission efficiency goes down due to more friction and the experienced vibration in operation increases	The power required for the same auxiliary system performance increases	Available Power Reduced. Range is reduced.	Major	85.0%	100.0%
Convert Electrical Energy to Torque	Motor Auxiliary Gearbox	3.48E-07	Teeth Overload Fracture	Emergency maneuver	The broken tooth reduces the gear efficiency and the vibrations increase.	The power required for the same auxiliary system performance increases	Available Power Reduced. Range is reduced.	Critical	5.0%	100.0%
Convert Electrical Energy to Torque	Motor Auxiliary Gearbox	3.48E-07	Teeth Fatigue Fracture	All	The broken tooth reduces the gear efficiency and the vibrations increase.	The power required for the same auxiliary system performance increases	Available Power Reduced. Range is reduced.	Critical	10.0%	100.0%

Function	Component	Failure Rate	Failure Mode	Mission Phase	Local Failure Effect	Next Higher Effect	End Effect	Severity	Alpha	Beta
Transfer Torque to Rotors	Rotor Overruning Clutch	4.23E-07	Overload Fracture	Emergency maneuver	The clutch fails to engage	The remaining three connected motors must power the four rotors	Available power reduced. Possible aircraft instability. Range is reduced.	Critical	5.0%	100.0%
Transfer Torque to Rotors	Rotor Overruning Clutch	4.23E-07	Fatigue Fracture	All	The clutch fails to engage	The remaining three connected motors must power the four rotors	Available power reduced. Possible aircraft instability. Range is reduced.	Critical	15.0%	100.0%
Transfer Torque to Rotors	Rotor Overruning Clutch	4.23E-07	Degradation	All	The clutch efficiency is lower	The electric motor power generation increases	Available power reduced. Range is reduced.	Critical	80.0%	100.0%
Provide HV Power to ESC (to drive the motor)	Turboshaft	6.48E-06	Non-Recoverable Failures (Surge, Flameout, FOD, etc.)	All	Turboshaft cannot provide any power to the generator for the rest of the flight	The flight crew must attempt an emergency landing within the time window provided by the capacity of the reserve battery	Aircraft descends to ground rapidly. Emergency landing required.	Catastrophic	10.0%	100.0%
Provide HV Power to ESC (to drive the motor)	Turboshaft	6.48E-06	Recoverable Failures	All	The power provided by the turboshaft is lost temporarily	The flight crew must attempt to recover or try an emergency landing while the battery power is still available.	If crew is unable to recover, aircraft descends to ground rapidly. Emergency landing required.	Catastrophic	90.0%	100.0%
Provide HV Power to ESC (to drive the motor)	Generator	4.30E-06	Generator Failure	All	HVDC power generation stops, aircraft switches to HVDC battery power.	The flight crew must attempt an emergency landing within the time window provided by the capacity of the reserve battery	Aircraft descends to ground rapidly. Emergency landing required.	Catastrophic	100.0%	100.0%
Control Rotor Pitch	Collective Actuators	5.50E-05	Bias	All	Rotor pitch differs from desired position.	If FCC is not able to compensate for error, aircraft loses control.	Loss of control.	Catastrophic	25.0%	100.0%

Function	Component	Failure Rate	Failure Mode	Mission Phase	Local Failure Effect	Next Higher Effect	End Effect	Severity	Alpha	Beta
Control Rotor Pitch	Collective Actuators	5.50E-05	Stuck Surface	All	Unable to change rotor pitch.	Loss of control is inevitable.	Loss of control.	Catastrophic	15.0%	100.0%
Control Rotor Pitch	Collective Actuators	5.50E-05	Hardover	All	Rotor pitch is stuck at one extreme	Loss of control is inevitable.	Loss of control.	Catastrophic	10.0%	100.0%
Control Rotor Pitch	Collective Actuators	5.50E-05	Floating Surface	All	Unable to control rotor pitch	Loss of control is inevitable.	Loss of control.	Catastrophic	20.0%	100.0%
Control Rotor Pitch	Collective Actuators	5.50E-05	Oscillations	All	Rotor pitch changes erratically.	Loss of control is inevitable.	Loss of control.	Catastrophic	10.0%	100.0%
Control Rotor Pitch	Collective Actuators	5.50E-05	Increased Deadband	All	Reduced range of motor pitch.	Aircraft maneuvering becomes sluggish.	Possible aircraft instability	Critical	20.0%	100.0%

Appendix B - Table 3: Quadcopter Turboshaft FMECA

Function	Component	Failure Rate	Failure Mode	Mission Phase	Local Failure Effect	Next Higher Effect	End Effect	Severity	Alpha	Beta
Provide LV Power for FCC	LV Battery	1.01E-06	LV Battery Fail	All	Loss of function of FCC.	No control signals provided to actuators and Turboshaft.	Loss of control. Aircraft descends to ground.	Catastrophic	100%	100.0%
Distribute Torque amongst Rotors	Central Gearbox Shaft	7.15E-07	Shaft Overload Breakage	Emergency maneuver	Not transmitting power to the two rotors on the opposite side of the gas turbines on the shaft	Catastrophic failure due to two unpowered rotors	Loss of control. Aircraft descends to ground.	Catastrophic	10.0%	100.0%
Distribute Torque amongst Rotors	Central Gearbox Shaft	7.15E-07	Shaft Fatigue Breakage	All	Not transmitting power to the two rotors on the opposite side of the gas turbines on the shaft	Catastrophic failure due to two unpowered rotors	Loss of control. Aircraft descends to ground.	Catastrophic	90.0%	100.0%
Distribute Torque amongst Rotors	Central Gearbox Shaft	4.29E-06	Bearing Spalling	All	Bearing creates more vibration and spins with more friction	More gas turbine power generation is necessary to provide the same performance	Available power reduced. Possible aircraft instability.	Major	90.0%	100.0%
Distribute Torque amongst Rotors	Central Gearbox Shaft	4.26E-06	Bearing Fracture	Emergency maneuver	Bearing carries significantly less or no load and vibrates violently	Imminent subsequent component failure like central shaft dislocation which may lead to loss of power for every rotor	Emergency landing required. Aircraft descends to ground quickly.	Catastrophic	10.0%	100.0%

Function	Component	Failure Rate	Failure Mode	Mission Phase	Local Failure Effect	Next Higher Effect	End Effect	Severity	Alpha	Beta
Distribute Torque amongst Rotors	Central Gearbox Bevel Gear	2.52E-07	Teeth Surface Fatigue	Emergency maneuver	Gear power transmission efficiency goes down due to more friction and the experienced vibration in operation increases	The power production in the gas turbines increases to make up for the increase in the transmission loss	Available power reduced. Possible aircraft instability.	Major	85.0%	100.0%
Distribute Torque amongst Rotors	Central Gearbox Bevel Gear	2.52E-07	Teeth Overload Fracture	Emergency maneuver	The broken tooth reduces the transmission efficiency and vibrations increase	Gas turbine power production increases to mitigate the effects of the efficiency drop	Available power reduced. Possible aircraft instability.	Critical	5.0%	100.0%
Distribute Torque amongst Rotors	Central Gearbox Bevel Gear	2.52E-07	Teeth Fatigue Fracture	All	The broken tooth reduces the transmission efficiency and vibrations increase	Gas turbine power production increases to mitigate the effects of the efficiency drop	Available power reduced. Possible aircraft instability.	Critical	10.0%	100.0%
Distribute Torque amongst Rotors	Central Gearbox Auxiliary	3.48E-07	Teeth Surface Fatigue	Emergency maneuver	Gear power transmission efficiency goes down due to more friction and the experienced vibration in operation increases	The gas turbines generate more power to compensate the drop in the transmission efficiency	Available power reduced. Possible aircraft instability.	Major	85.0%	100.0%
Distribute Torque amongst Rotors	Central Gearbox Auxiliary	3.48E-07	Teeth Overload Fracture	Emergency maneuver	The broken tooth can reduce the transmission efficiency and vibrations increase	Power supplied to the auxiliary gearbox increases to keep the auxiliary systems operating	Available power reduced. Possible aircraft instability.	Critical	5.0%	100.0%

Function	Component	Failure Rate	Failure Mode	Mission Phase	Local Failure Effect	Next Higher Effect	End Effect	Severity	Alpha	Beta
Distribute Torque amongst Rotors	Central Gearbox Auxiliary	3.48E-07	Teeth Fatigue Fracture	All	The broken tooth can reduce the transmission efficiency and vibrations increase	Power supplied to the auxiliary gearbox increases to keep the auxiliary systems operating	Available power reduced. Possible aircraft instability.	Critical	10.0%	100.0%
Distribute Torque amongst Rotors	Cross-Shafting Shafts	7.15E-07	Overload Breakage	Emergency maneuver	Power transmission to the rotor connected to the failed shaft stops	Catastrophic failure due to an unpowered rotor	Loss of control. Aircraft descends to ground.	Catastrophic	10.0%	100.0%
Distribute Torque amongst Rotors	Cross-Shafting Shafts	7.15E-07	Fatigue Breakage	All	Power transmission to the rotor connected to the failed shaft stops	Catastrophic failure due to an unpowered rotor	Loss of control. Aircraft descends to ground.	Catastrophic	90.0%	100.0%
Distribute Torque amongst Rotors	Cross-Shafting Bearings	4.29E-06	Bearing Spalling	All	Bearing creates more vibration and spins with more friction	The gas turbines generate more power to compensate the drop in the transmission efficiency	Available power reduced. Possible aircraft instability.	Major	90.0%	100.0%
Distribute Torque amongst Rotors	Cross-Shafting Bearings	4.29E-06	Bearing Fracture	Emergency maneuver	Bearing carries significantly less or no load and vibrates violently	Imminent subsequent component failures like cross-shaft dislocation which prevents power transmission to a rotor and cause a catastrophic failure	Emergency landing required. Aircraft descends to ground quickly.	Catastrophic	10.0%	100.0%
Distribute Torque amongst Rotors	Cross-Shafting Bevel Gears	2.52E-07	Teeth Surface Fatigue	Emergency maneuver	Gear power transmission efficiency goes down due to more friction and the experienced vibration in operation increases	The gas turbines generate more power to compensate the drop in the transmission efficiency	Available power reduced. Possible aircraft instability.	Major	85.0%	100.0%

Function	Component	Failure Rate	Failure Mode	Mission Phase	Local Failure Effect	Next Higher Effect	End Effect	Severity	Alpha	Beta
Distribute Torque amongst Rotors	Cross-Shafting Bevel Gears	2.52E-07	Teeth Overload Fracture	Emergency maneuver	The broken tooth reduces the gear efficiency and the vibrations increase	The gas turbines generate more power to provide the same performance	Available power reduced. Possible aircraft instability.	Critical	5.0%	100.0%
Distribute Torque amongst Rotors	Cross-Shafting Bevel Gears	2.52E-07	Teeth Fatigue Fracture	All	The broken tooth reduces the gear efficiency and the vibrations increase	The gas turbines generate more power to provide the same performance	Available power reduced. Possible aircraft instability.	Critical	10.0%	100.0%
Transfer Torque to Rotors	Reduction Gearbox	4.23E-07	Teeth Surface Fatigue	Emergency maneuver	Gear power transmission efficiency goes down due to more friction and the experienced vibration in operation increases	The gas turbines generate more power to make up for the transmission efficiency loss	Available power reduced. Possible aircraft instability. Range is reduced.	Major	85.0%	100.0%
Transfer Torque to Rotors	Reduction Gearbox	4.23E-07	Teeth Overload Fracture	Emergency maneuver	The broken tooth reduces the gear efficiency and the vibrations increase	The gas turbine power generation increases to provide the same performance	Available power reduced. Possible aircraft instability. Range is reduced.	Critical	5.0%	100.0%
Transfer Torque to Rotors	Reduction Gearbox	4.23E-07	Teeth Fatigue Fracture	All	The broken tooth reduces the gear efficiency and the vibrations increase	The gas turbine power generation increases to provide the same performance	Available power reduced. Possible aircraft instability. Range is reduced.	Critical	10.0%	100.0%
Transfer Torque to Rotors	Turboshaft Overruning Clutch	4.23E-07	Overload Fracture	Emergency maneuver	The clutch fails to engage	The remaining gas turbine needs to power all of the rotors	Available power reduced. Emergency landing may be required.	Catastrophic	5.0%	100.0%

Function	Component	Failure Rate	Failure Mode	Mission Phase	Local Failure Effect	Next Higher Effect	End Effect	Severity	Alpha	Beta
Transfer Torque to Rotors	Turboshaft Overruning Clutch	4.23E-07	Fatigue Fracture	All	The clutch fails to engage	The remaining gas turbine needs to power all of the rotors	Available power reduced. Emergency landing may be required.	Catastrophic	15.0%	100.0%
Transfer Torque to Rotors	Turboshaft Overruning Clutch	4.23E-07	Degradation	All	The power transmission efficiency of the clutch is lower and the clutch experiences more heat generation due to the degradation.	The gas turbines generate more power to provide the same performance	Available power reduced. Range is reduced.	Critical	80.0%	100.0%
Generate Mechanical Power	Turboshaft	6.48E-06	Non-Recoverable Failures (Surge, Flameout, FOD, etc.)	All	The failed turboshaft cannot provide any power to the mechanical powertrain for the rest of the flight	The flight crew must determine if an emergency landing is necessary or it is possible to continue the mission with one engine	Available power reduced. Emergency landing may be required.	Catastrophic	10.0%	100.0%
Generate Mechanical Power	Turboshaft	6.48E-06	Recoverable Failures	All	The power provided by the failed turboshaft is lost temporarily	The flight continues with limited available power. The flight crew must determine if an emergency landing is necessary or it is possible to continue the mission with one engine.	If crew is unable to recover, aircraft descends to ground rapidly. Emergency landing may be required.	Catastrophic	90.0%	100.0%
Control Rotor Pitch	Collective Actuators	5.50E-05	Bias	All	Rotor pitch differs from desired position.	If FCC is not able to compensate for error, aircraft loses control.	Loss of control.	Catastrophic	25.0%	100.0%
Control Rotor Pitch	Collective Actuators	5.50E-05	Stuck Surface	All	Unable to change rotor pitch.	Loss of control is inevitable.	Loss of control.	Catastrophic	15.0%	100.0%

Function	Component	Failure Rate	Failure Mode	Mission Phase	Local Failure Effect	Next Higher Effect	End Effect	Severity	Alpha	Beta
Control Rotor Pitch	Collective Actuators	5.50E-05	Hardover	All	Rotor pitch is stuck at one extreme	Loss of control is inevitable.	Loss of control.	Catastrophic	10.0%	100.0%
Control Rotor Pitch	Collective Actuators	5.50E-05	Floating Surface	All	Unable to control rotor pitch	Loss of control is inevitable.	Loss of control.	Catastrophic	20.0%	100.0%
Control Rotor Pitch	Collective Actuators	5.50E-05	Oscillations	All	Rotor pitch changes erratically.	Loss of control is inevitable.	Loss of control.	Catastrophic	10.0%	100.0%
Control Rotor Pitch	Collective Actuators	5.50E-05	Increased Deadband	All	Reduced range of motor pitch.	Aircraft maneuvering becomes sluggish.	Possible aircraft instability	Critical	20.0%	100.0%

Appendix B - Table 4: Hexacopter Collective-control FMECA

Function	Component	Failure Rate	Failure Mode	Mission Phase	Local Failure Effect	Next Higher Effect	End Effect	Severity	Alpha	Beta
Convert HVDC Power for Motors	Electronic Speed Controller	8.08E-06	ESC High Voltage	All	Rotor Torque Ripple	Rotor experiences torque oscillations. In extreme cases, rotor may be switched off.	Available power reduced. Possible aircraft instability.	Critical	20%	100.0%
Convert HVDC Power for Motors	Electronic Speed Controller	8.08E-06	ESC Overcurrent	All	High Torque Ripple	Rotor experiences torque oscillations. Current draw from the battery is increased. Possible battery thermal runaway. In extreme cases, rotor may be switched off.	Reduced aircraft range. Possible aircraft instability.	Critical	20%	100.0%
Convert HVDC Power for Motors	Electronic Speed Controller	8.08E-06	ESC Voltage Transient	All	Rotor Torque Ripple	Rotor experiences torque oscillations. In extreme cases, rotor may be switched off.	Available power reduced. Possible aircraft instability.	Critical	10%	100.0%
Convert HVDC Power for Motors	Electronic Speed Controller	8.08E-06	ESC Vibrations	All	High Torque Ripple	Rotor experiences torque oscillations. In extreme cases, rotor may be switched off.	Reduced aircraft range. Possible aircraft instability.	Critical	10%	100.0%
Convert HVDC Power for Motors	Electronic Speed Controller	8.08E-06	Manufacturing Defects	All	Rotor Torque Ripple	Rotor experiences torque oscillations. In extreme cases, rotor may be switched off.	Available power reduced. Possible aircraft instability.	Critical	7%	100.0%
Convert HVDC Power for Motors	Electronic Speed Controller	8.08E-06	ESC Current Sensor Fault	All	Rotor Torque Ripple	Rotor experiences torque oscillations. In extreme cases, rotor may be switched off.	Available power reduced. Possible aircraft instability.	Critical	2%	100.0%
Convert HVDC Power for Motors	Electronic Speed Controller	8.08E-06	ESC Resolver Fault	All	Rotor Torque Ripple	Rotor experiences torque oscillations. In extreme cases, rotor may be switched off.	Available power reduced. Possible aircraft instability.	Critical	2%	100.0%

Function	Component	Failure Rate	Failure Mode	Mission Phase	Local Failure Effect	Next Higher Effect	End Effect	Severity	Alpha	Beta
Convert HVDC Power for Motors	Electronic Speed Controller	8.08E-06	ESC Temperature Sensor Fail	All	ESC fails, motor produces no torque	Rotor fails, aircraft becomes unbalanced. FCC may be able to compensate.	Available power reduced. Limited flight envelope. Emergency landing may be required.	Critical	2%	100.0%
Convert HVDC Power for Motors	Electronic Speed Controller	8.08E-06	ESC High Temperature	All	ESC fails, motor produces no torque	Rotor fails, aircraft becomes unbalanced. FCC may be able to compensate.	Available power reduced. Limited flight envelope. Emergency landing may be required.	Critical	27%	40.0%
Convert HVDC Power for Motors	Electronic Speed Controller	8.08E-06	ESC High Temperature	All	Rotor Low Torque	Rotor fails, aircraft becomes unbalanced. FCC may be able to compensate.	Available power reduced. Limited flight envelope. Emergency landing may be required.	Critical	27%	30.0%
Convert HVDC Power for Motors	Electronic Speed Controller	8.08E-06	ESC High Temperature	All	Rotor Torque Ripple	Rotor experiences torque oscillations. In extreme cases, rotor may be switched off.	Available power reduced. Possible aircraft instability.	Critical	27%	30.0%
Convert HVDC Power to Torque	Electric Motor	5.10E-06	Motor High Voltage	All	Motor Short Circuit	Rotor experiences torque oscillations. In extreme cases, rotor may be switched off.	Available power reduced. Possible aircraft instability.	Critical	6%	100.0%
Convert HVDC Power to Torque	Electric Motor	5.10E-06	Motor Overcurrent	All	Motor Short Circuit	Rotor experiences torque oscillations. In extreme cases, rotor may be switched off.	Available power reduced. Possible aircraft instability.	Critical	6%	20.0%
Convert HVDC Power to Torque	Electric Motor	5.10E-06	Motor Overcurrent	All	Rotor Torque Ripple	Rotor experiences torque oscillations. In extreme cases, rotor may be switched off.	Available power reduced. Possible aircraft instability.	Critical	6%	10.0%

Function	Component	Failure Rate	Failure Mode	Mission Phase	Local Failure Effect	Next Higher Effect	End Effect	Severity	Alpha	Beta
Convert HVDC Power to Torque	Electric Motor	5.10E-06	Motor Overcurrent	All	Low/No Torque	Aircraft becomes unbalanced. FCC may be able to compensate.	Available power reduced. Limited flight envelope. Emergency landing may be required.	Critical	6%	60.0%
Convert HVDC Power to Torque	Electric Motor	5.10E-06	Motor Voltage Transient	All	Rotor Low Torque; Torque Ripple	Rotor experiences torque oscillations. In extreme cases, rotor may be switched off.	Available power reduced. Possible aircraft instability.	Critical	3%	100.0%
Convert HVDC Power to Torque	Electric Motor	5.10E-06	Motor Eccentricity	All	Rotor Low/No Torque;	Aircraft becomes unbalanced. FCC may be able to compensate.	Available power reduced. Limited flight envelope. Emergency landing may be required.	Critical	0%	100.0%
Convert HVDC Power to Torque	Electric Motor	5.10E-06	Motor Shaft Failure	All	Rotor Low/No Torque;	Aircraft becomes unbalanced. FCC may be able to compensate.	Available power reduced. Limited flight envelope. Emergency landing may be required.	Critical	0%	100.0%
Convert HVDC Power to Torque	Electric Motor	5.10E-06	Motor High Temperature	All	Rotor No Torque	Rotor fails, aircraft becomes unbalanced. FCC may be able to compensate.	Available power reduced. Limited flight envelope. Emergency landing may be required.	Critical	84%	50.0%
Convert HVDC Power to Torque	Electric Motor	5.10E-06	Motor High Temperature	All	Rotor Short Circuit	Rotor experiences torque oscillations. In extreme cases, rotor may be switched off.	Available power reduced. Possible aircraft instability.	Critical	84%	20.0%

Function	Component	Failure Rate	Failure Mode	Mission Phase	Local Failure Effect	Next Higher Effect	End Effect	Severity	Alpha	Beta
Convert HVDC Power to Torque	Electric Motor	5.10E-06	Motor High Temperature	All	Rotor Low Torque	Rotor fails, aircraft becomes unbalanced. FCC may be able to compensate.	Available power reduced. Limited flight envelope. Emergency landing may be required.	Critical	84%	30.0%
Provide LVDC Power for Control	LV Battery	1.01E-06	LV Battery Fail	All	Loss of function of FCC and all ESC	No torque produced by all ESC, No control signals provided to actuators	Loss of all propulsion and control. Aircraft descends to ground.	Catastrophic	100%	100.0%
Provide HVDC Power for Motors	HV Battery	8.07E-06	Battery Current Sensor Fault	All	Low/No Torque for the connected rotor	Aircraft becomes unbalanced. FCC may be able to compensate.	Available power reduced. Limited flight envelope. Emergency landing may be required.	Critical	22%	100.0%
Provide HVDC Power for Motors	HV Battery	8.07E-06	Battery Voltage Sensor Fault	All	Low/No Torque for the connected rotor	Aircraft becomes unbalanced. FCC may be able to compensate.	Available power reduced. Limited flight envelope. Emergency landing may be required.	Critical	22%	100.0%
Provide HVDC Power for Motors	HV Battery	8.07E-06	Battery Temperature Sensor Fault	All	Low/No Torque for the connected rotor	Aircraft becomes unbalanced. FCC may be able to compensate.	Available power reduced. Limited flight envelope. Emergency landing may be required.	Critical	22%	100.0%
Provide HVDC Power for Motors	HV Battery	8.07E-06	Battery External Short Circuit	All	Low/No Torque for the connected rotor	Aircraft becomes unbalanced. FCC may be able to compensate.	Available power reduced. Limited flight envelope. Emergency landing may be required.	Critical	6%	100.0%

Function	Component	Failure Rate	Failure Mode	Mission Phase	Local Failure Effect	Next Higher Effect	End Effect	Severity	Alpha	Beta
Provide HVDC Power for Motors	HV Battery	8.07E-06	Battery Physical Damage	All	Low/No Torque for the connected rotor	Aircraft becomes unbalanced. FCC may be able to compensate.	Available power reduced. Limited flight envelope. Emergency landing may be required.	Critical	4%	100.0%
Provide HVDC Power for Motors	HV Battery	8.07E-06	Battery Manufacturing Defects	All	Low/No Torque for the connected rotor	Aircraft becomes unbalanced. FCC may be able to compensate.	Available power reduced. Limited flight envelope. Emergency landing may be required.	Critical	12%	100.0%
Provide HVDC Power for Motors	HV Battery	8.07E-06	Battery External Overheating	All	Low/No Torque for the connected rotor	Aircraft becomes unbalanced. FCC may be able to compensate.	Available power reduced. Limited flight envelope. Emergency landing may be required.	Critical	12%	100.0%
Provide HVDC Power for Motors	HV Battery Cooling	4.30E-06	Battery Cooling Failure	All	Low/No Torque for the connected rotor	Aircraft becomes unbalanced. FCC may be able to compensate.	Available power reduced. Limited flight envelope. Emergency landing may be required.	Critical	100%	100.0%
Distribute HVDC Power	Electric Distribution System	5.96E-08	Fuse High Temperature	All	No Torque for the connected rotor	Rotor fails, aircraft becomes unbalanced. FCC may be able to compensate.	Available power reduced. Limited flight envelope. Emergency landing may be required.	Critical	40.0%	70.0%
Distribute HVDC Power	Electric Distribution System	5.96E-08	Fuse High Temperature	All	High Torque for the connected rotor	Aircraft becomes unbalanced. FCC may be able to compensate.	Available power reduced. Limited flight envelope. Emergency landing may be required.	Critical	40.0%	30.0%

Function	Component	Failure Rate	Failure Mode	Mission Phase	Local Failure Effect	Next Higher Effect	End Effect	Severity	Alpha	Beta
Distribute HVDC Power	Electric Distribution System	4.47E-08	Fuse Overcurrent	All	No Torque for the connected rotor	Rotor fails, aircraft becomes unbalanced. FCC may be able to compensate.	Available power reduced. Limited flight envelope. Emergency landing may be required.	Critical	30.0%	70.0%
Distribute HVDC Power	Electric Distribution System	4.47E-08	Fuse Overcurrent	All	High Torque for the connected rotor	Aircraft becomes unbalanced. FCC may be able to compensate.	Available power reduced. Limited flight envelope. Emergency landing may be required.	Critical	30.0%	30.0%
Distribute HVDC Power	Electric Distribution System	4.47E-08	Fuse High Voltage	All	No Torque for the connected rotor	Rotor fails, aircraft becomes unbalanced. FCC may be able to compensate.	Available power reduced. Limited flight envelope. Emergency landing may be required.	Critical	30.0%	70.0%
Distribute HVDC Power	Electric Distribution System	4.47E-08	Fuse High Voltage	All	High Torque for the connected rotor	Aircraft becomes unbalanced. FCC may be able to compensate.	Available power reduced. Limited flight envelope. Emergency landing may be required.	Critical	30.0%	30.0%
Distribute HVDC Power	Electric Distribution System	5.96E-08	Contactor High Temperature	All	No Torque for the connected rotor	Rotor fails, aircraft becomes unbalanced. FCC may be able to compensate.	Available power reduced. Limited flight envelope. Emergency landing may be required.	Critical	40.0%	70.0%
Distribute HVDC Power	Electric Distribution System	5.96E-08	Contactor High Temperature	All	High Torque for the connected rotor	Aircraft becomes unbalanced. FCC may be able to compensate.	Available power reduced. Limited flight envelope. Emergency landing may be required.	Critical	40.0%	30.0%

Function	Component	Failure Rate	Failure Mode	Mission Phase	Local Failure Effect	Next Higher Effect	End Effect	Severity	Alpha	Beta
Distribute HVDC Power	Electric Distribution System	4.47E-08	Contactor Overcurrent	All	No Torque for the connected rotor	Rotor fails, aircraft becomes unbalanced. FCC may be able to compensate.	Available power reduced. Limited flight envelope. Emergency landing may be required.	Critical	30.0%	70.0%
Distribute HVDC Power	Electric Distribution System	4.47E-08	Contactor Overcurrent	All	High Torque for the connected rotor	Aircraft becomes unbalanced. FCC may be able to compensate.	Available power reduced. Limited flight envelope. Emergency landing may be required.	Critical	30.0%	30.0%
Distribute HVDC Power	Electric Distribution System	4.47E-08	Contactor High Voltage	All	No Torque for the connected rotor	Rotor fails, aircraft becomes unbalanced. FCC may be able to compensate.	Available power reduced. Limited flight envelope. Emergency landing may be required.	Critical	30.0%	70.0%
Distribute HVDC Power	Electric Distribution System	4.47E-08	Contactor High Voltage	All	High Torque for the connected rotor	Aircraft becomes unbalanced. FCC may be able to compensate.	Available power reduced. Limited flight envelope. Emergency landing may be required.	Critical	30.0%	30.0%
Distribute HVDC Power	Electric Distribution System	1.39E-07	Connection Failure	All	No Torque for the connected rotor	Rotor fails, aircraft becomes unbalanced. FCC may be able to compensate.	Available power reduced. Limited flight envelope. Emergency landing may be required.	Critical	100.0%	70.0%
Distribute HVDC Power	Electric Distribution System	1.39E-07	Connection Failure	All	High Torque for the connected rotor	Aircraft becomes unbalanced. FCC may be able to compensate.	Available power reduced. Limited flight envelope. Emergency landing may be required.	Critical	100.0%	30.0%

Function	Component	Failure Rate	Failure Mode	Mission Phase	Local Failure Effect	Next Higher Effect	End Effect	Severity	Alpha	Beta
Transfer Torque to Rotors	Reduction Gearbox	4.23E-07	Teeth Surface Fatigue	Emergency maneuver	Gear power transmission efficiency goes down due to more friction and the experienced vibration in operation increases	More power is necessary to spin the rotor attached to the gearbox at the same speed and pitch angle	Available power reduced. Possible aircraft instability. Range is reduced.	Major	85.0%	100.0%
Transfer Torque to Rotors	Reduction Gearbox	4.23E-07	Teeth Overload Fracture	Emergency maneuver	The broken tooth reduces the gear efficiency and the vibrations increase	The same performance level requires an increase in power generation	Available power reduced. Possible aircraft instability. Range is reduced.	Critical	5.0%	100.0%
Transfer Torque to Rotors	Reduction Gearbox	4.23E-07	Teeth Fatigue Fracture	All	The broken tooth reduces the gear efficiency and the vibrations increase	The same performance level requires an increase in power generation	Available power reduced. Possible aircraft instability. Range is reduced.	Critical	10.0%	100.0%
Drive Rotor Accessories	Motor Auxiliary Gearbox	3.48E-07	Teeth Surface Fatigue	Emergency maneuver	Gear power transmission efficiency goes down due to more friction and the experienced vibration in operation increases	The power required for the same auxiliary system performance increases	Available Power Reduced. Range is reduced.	Major	85.0%	100.0%
Drive Rotor Accessories	Motor Auxiliary Gearbox	3.48E-07	Teeth Overload Fracture	Emergency maneuver	The broken tooth reduces the gear efficiency and the vibrations increase.	The power required for the same auxiliary system performance increases	Available Power Reduced. Range is reduced.	Critical	5.0%	100.0%

Function	Component	Failure Rate	Failure Mode	Mission Phase	Local Failure Effect	Next Higher Effect	End Effect	Severity	Alpha	Beta
Drive Rotor Accessories	Motor Auxiliary Gearbox	3.48E-07	Teeth Fatigue Fracture	All	The broken tooth reduces the gear efficiency and the vibrations increase.	The power required for the same auxiliary system performance increases	Available Power Reduced. Range is reduced.	Critical	10.0%	100.0%
Transfer Torque to Rotors	Rotor Overruning Clutch	4.23E-07	Overload Fracture	Emergency maneuver	The clutch fails to engage	The remaining three connected motors must power the four rotors	Available power reduced. Possible aircraft instability. Range is reduced.	Critical	5.0%	100.0%
Transfer Torque to Rotors	Rotor Overruning Clutch	4.23E-07	Fatigue Fracture	All	The clutch fails to engage	The remaining three connected motors must power the four rotors	Available power reduced. Possible aircraft instability. Range is reduced.	Critical	15.0%	100.0%
Transfer Torque to Rotors	Rotor Overruning Clutch	4.23E-07	Degradation	All	The clutch efficiency is lower	The electric motor power generation increases	Available power reduced. Range is reduced.	Critical	80.0%	100.0%
Control Rotor Pitch	Collective Actuators	5.50E-05	Bias	All	Rotor pitch differs from desired position.	If FCC is not able to compensate for error, aircraft loses control.	Loss of control.	Catastrophic	25.0%	100.0%
Control Rotor Pitch	Collective Actuators	5.50E-05	Stuck Surface	All	Unable to change rotor pitch.	Loss of control is inevitable.	Loss of control.	Catastrophic	15.0%	100.0%
Control Rotor Pitch	Collective Actuators	5.50E-05	Hardover	All	Rotor pitch is stuck at one extreme	Loss of control is inevitable.	Loss of control.	Catastrophic	10.0%	100.0%
Control Rotor Pitch	Collective Actuators	5.50E-05	Floating Surface	All	Unable to control rotor pitch	Loss of control is inevitable.	Loss of control.	Catastrophic	20.0%	100.0%
Control Rotor Pitch	Collective Actuators	5.50E-05	Oscillations	All	Rotor pitch changes erratically.	Loss of control is inevitable.	Loss of control.	Catastrophic	10.0%	100.0%
Control Rotor Pitch	Collective Actuators	5.50E-05	Increased Deadband	All	Reduced range of motor pitch.	Aircraft maneuvering becomes sluggish.	Possible aircraft instability	Critical	20.0%	100.0%

Appendix B - Table 5: Hexacopter RPM-control FMECA

Function	Component	Failure Rate	Failure Mode	Mission Phase	Local Failure Effect	Next Higher Effect	End Effect	Severity	Alpha	Beta
Convert Electrical Energy to Torque	Electronic Speed Controller	8.08E-06	ESC High Voltage	All	Rotor Torque Ripple	Rotor experiences torque oscillations. In extreme cases, rotor may be switched off.	Available power reduced. Possible aircraft instability.	Critical	20%	100.0%
Convert Electrical Energy to Torque	Electronic Speed Controller	8.08E-06	ESC Overcurrent	All	High Torque Ripple	Rotor experiences torque oscillations. Current draw from the battery is increased. Possible battery thermal runaway. In extreme cases, rotor may be switched off.	Reduced aircraft range. Possible aircraft instability.	Critical	20%	100.0%
Convert Electrical Energy to Torque	Electronic Speed Controller	8.08E-06	ESC Voltage Transient	All	Rotor Torque Ripple	Rotor experiences torque oscillations. In extreme cases, rotor may be switched off.	Available power reduced. Possible aircraft instability.	Critical	10%	100.0%
Convert Electrical Energy to Torque	Electronic Speed Controller	8.08E-06	ESC Vibrations	All	High Torque Ripple	Rotor experiences torque oscillations. In extreme cases, rotor may be switched off.	Reduced aircraft range. Possible aircraft instability.	Critical	10%	100.0%
Convert Electrical Energy to Torque	Electronic Speed Controller	8.08E-06	Manufacturing Defects	All	Rotor Torque Ripple	Rotor experiences torque oscillations. In extreme cases, rotor may be switched off.	Available power reduced. Possible aircraft instability.	Critical	7%	100.0%
Convert Electrical Energy to Torque	Electronic Speed Controller	8.08E-06	ESC Current Sensor Fault	All	Rotor Torque Ripple	Rotor experiences torque oscillations. In extreme cases, rotor may be switched off.	Available power reduced. Possible aircraft instability.	Critical	2%	100.0%

Function	Component	Failure Rate	Failure Mode	Mission Phase	Local Failure Effect	Next Higher Effect	End Effect	Severity	Alpha	Beta
Convert Electrical Energy to Torque	Electronic Speed Controller	8.08E-06	ESC Resolver Fault	All	Rotor Torque Ripple	Rotor experiences torque oscillations. In extreme cases, rotor may be switched off.	Available power reduced. Possible aircraft instability.	Critical	2%	100.0%
Convert Electrical Energy to Torque	Electronic Speed Controller	8.08E-06	ESC Temperature Sensor Fail	All	ESC fails, motor produces no torque	Rotor fails, aircraft becomes unbalanced. FCC may be able to compensate.	Available power reduced. Limited flight envelope. Emergency landing may be required.	Critical	2%	100.0%
Convert Electrical Energy to Torque	Electronic Speed Controller	8.08E-06	ESC High Temperature	All	ESC fails, motor produces no torque	Rotor fails, aircraft becomes unbalanced. FCC may be able to compensate.	Available power reduced. Limited flight envelope. Emergency landing may be required.	Critical	27%	40.0%
Convert Electrical Energy to Torque	Electronic Speed Controller	8.08E-06	ESC High Temperature	All	Rotor Low Torque	Rotor fails, aircraft becomes unbalanced. FCC may be able to compensate.	Available power reduced. Limited flight envelope. Emergency landing may be required.	Critical	27%	30.0%
Convert Electrical Energy to Torque	Electronic Speed Controller	8.08E-06	ESC High Temperature	All	Rotor Torque Ripple	Rotor experiences torque oscillations. In extreme cases, rotor may be switched off.	Available power reduced. Possible aircraft instability.	Critical	27%	30.0%
Convert Electrical Energy to Torque	Electric Motor	5.10E-06	Motor High Voltage	All	Motor Short Circuit	Rotor experiences torque oscillations. In extreme cases, rotor may be switched off.	Available power reduced. Possible aircraft instability.	Critical	6%	100.0%
Convert Electrical Energy to Torque	Electric Motor	5.10E-06	Motor Overcurrent	All	Motor Short Circuit	Rotor experiences torque oscillations. In extreme cases, rotor may be switched off.	Available power reduced. Possible aircraft instability.	Critical	6%	20.0%

Function	Component	Failure Rate	Failure Mode	Mission Phase	Local Failure Effect	Next Higher Effect	End Effect	Severity	Alpha	Beta
Convert Electrical Energy to Torque	Electric Motor	5.10E-06	Motor Overcurrent	All	Rotor Torque Ripple	Rotor experiences torque oscillations. In extreme cases, rotor may be switched off.	Available power reduced. Possible aircraft instability.	Critical	6%	10.0%
Convert Electrical Energy to Torque	Electric Motor	5.10E-06	Motor Overcurrent	All	Low/No Torque	Aircraft becomes unbalanced. FCC may be able to compensate.	Available power reduced. Limited flight envelope. Emergency landing may be required.	Critical	6%	60.0%
Convert Electrical Energy to Torque	Electric Motor	5.10E-06	Motor Voltage Transient	All	Rotor Low Torque; Torque Ripple	Rotor experiences torque oscillations. In extreme cases, rotor may be switched off.	Available power reduced. Possible aircraft instability.	Critical	3%	100.0%
Convert Electrical Energy to Torque	Electric Motor	5.10E-06	Motor Eccentricity	All	Rotor Low/No Torque;	Aircraft becomes unbalanced. FCC may be able to compensate.	Available power reduced. Limited flight envelope. Emergency landing may be required.	Critical	0%	100.0%
Convert Electrical Energy to Torque	Electric Motor	5.10E-06	Motor Shaft Failure	All	Rotor Low/No Torque;	Aircraft becomes unbalanced. FCC may be able to compensate.	Available power reduced. Limited flight envelope. Emergency landing may be required.	Critical	0%	100.0%
Convert Electrical Energy to Torque	Electric Motor	5.10E-06	Motor High Temperature	All	Rotor No Torque	Rotor fails, aircraft becomes unbalanced. FCC may be able to compensate.	Available power reduced. Limited flight envelope. Emergency landing may be required.	Critical	84%	50.0%
Convert Electrical Energy to Torque	Electric Motor	5.10E-06	Motor High Temperature	All	Rotor Short Circuit	Rotor experiences torque oscillations. In extreme cases, rotor may be switched off.	Available power reduced. Possible aircraft instability.	Critical	84%	20.0%

Function	Component	Failure Rate	Failure Mode	Mission Phase	Local Failure Effect	Next Higher Effect	End Effect	Severity	Alpha	Beta
Convert Electrical Energy to Torque	Electric Motor	5.10E-06	Motor High Temperature	All	Rotor Low Torque	Rotor fails, aircraft becomes unbalanced. FCC may be able to compensate.	Available power reduced. Limited flight envelope. Emergency landing may be required.	Critical	84%	30.0%
Provide LVDC Power for Control	LV Battery	1.01E-06	LV Battery Fail	All	Loss of function of FCC and all ESC	No torque produced by all ESC, No control signals provided to actuators	Loss of all propulsion and control. Aircraft descends to ground.	Catastrophic	100%	100.0%
Provide HV Power to ESC (to drive the motor)	HV Battery	8.07E-06	Battery Current Sensor Fault	All	Low/No Torque for the connected rotor	Aircraft becomes unbalanced. FCC may be able to compensate.	Available power reduced. Limited flight envelope. Emergency landing may be required.	Critical	22%	100.0%
Provide HV Power to ESC (to drive the motor)	HV Battery	8.07E-06	Battery Voltage Sensor Fault	All	Low/No Torque for the connected rotor	Aircraft becomes unbalanced. FCC may be able to compensate.	Available power reduced. Limited flight envelope. Emergency landing may be required.	Critical	22%	100.0%
Provide HV Power to ESC (to drive the motor)	HV Battery	8.07E-06	Battery Temperature Sesnor Fault	All	Low/No Torque for the connected rotor	Aircraft becomes unbalanced. FCC may be able to compensate.	Available power reduced. Limited flight envelope. Emergency landing may be required.	Critical	22%	100.0%
Provide HV Power to ESC (to drive the motor)	HV Battery	8.07E-06	Battery External Short Circuit	All	Low/No Torque for the connected rotor	Aircraft becomes unbalanced. FCC may be able to compensate.	Available power reduced. Limited flight envelope. Emergency landing may be required.	Critical	6%	100.0%

Function	Component	Failure Rate	Failure Mode	Mission Phase	Local Failure Effect	Next Higher Effect	End Effect	Severity	Alpha	Beta
Provide HV Power to ESC (to drive the motor)	HV Battery	8.07E-06	Battery Physical Damage	All	Low/No Torque for the connected rotor	Aircraft becomes unbalanced. FCC may be able to compensate.	Available power reduced. Limited flight envelope. Emergency landing may be required.	Critical	4%	100.0%
Provide HV Power to ESC (to drive the motor)	HV Battery	8.07E-06	Battery Manufacutring Defects	All	Low/No Torque for the connected rotor	Aircraft becomes unbalanced. FCC may be able to compensate.	Available power reduced. Limited flight envelope. Emergency landing may be required.	Critical	12%	100.0%
Provide HV Power to ESC (to drive the motor)	HV Battery	8.07E-06	Battery External Overheating	All	Low/No Torque for the connected rotor	Aircraft becomes unbalanced. FCC may be able to compensate.	Available power reduced. Limited flight envelope. Emergency landing may be required.	Critical	12%	100.0%
Provide HV Power to ESC (to drive the motor)	HV Battery Cooling	4.30E-06	Battery Cooling Failure	All	Low/No Torque for the connected rotor	Aircraft becomes unbalanced. FCC may be able to compensate.	Available power reduced. Limited flight envelope. Emergency landing may be required.	Critical	100%	100.0%
Provide HV Power to ESC (to drive the motor)	Electric Distribution System	5.96E-08	Fuse High Temperature	All	No Torque for the connected rotor	Rotor fails, aircraft becomes unbalanced. FCC may be able to compensate.	Available power reduced. Limited flight envelope. Emergency landing may be required.	Critical	40.0%	70.0%
Provide HV Power to ESC (to drive the motor)	Electric Distribution System	5.96E-08	Fuse High Temperature	All	High Torque for the connected rotor	Aircraft becomes unbalanced. FCC may be able to compensate.	Available power reduced. Limited flight envelope. Emergency landing may be required.	Critical	40.0%	30.0%

Function	Component	Failure Rate	Failure Mode	Mission Phase	Local Failure Effect	Next Higher Effect	End Effect	Severity	Alpha	Beta
Provide HV Power to ESC (to drive the motor)	Electric Distribution System	4.47E-08	Fuse Overcurrent	All	No Torque for the connected rotor	Rotor fails, aircraft becomes unbalanced. FCC may be able to compensate.	Available power reduced. Limited flight envelope. Emergency landing may be required.	Critical	30.0%	70.0%
Provide HV Power to ESC (to drive the motor)	Electric Distribution System	4.47E-08	Fuse Overcurrent	All	High Torque for the connected rotor	Aircraft becomes unbalanced. FCC may be able to compensate.	Available power reduced. Limited flight envelope. Emergency landing may be required.	Critical	30.0%	30.0%
Provide HV Power to ESC (to drive the motor)	Electric Distribution System	4.47E-08	Fuse High Voltage	All	No Torque for the connected rotor	Rotor fails, aircraft becomes unbalanced. FCC may be able to compensate.	Available power reduced. Limited flight envelope. Emergency landing may be required.	Critical	30.0%	70.0%
Provide HV Power to ESC (to drive the motor)	Electric Distribution System	4.47E-08	Fuse High Voltage	All	High Torque for the connected rotor	Aircraft becomes unbalanced. FCC may be able to compensate.	Available power reduced. Limited flight envelope. Emergency landing may be required.	Critical	30.0%	30.0%
Provide HV Power to ESC (to drive the motor)	Electric Distribution System	5.96E-08	Contactor High Temperature	All	No Torque for the connected rotor	Rotor fails, aircraft becomes unbalanced. FCC may be able to compensate.	Available power reduced. Limited flight envelope. Emergency landing may be required.	Critical	40.0%	70.0%
Provide HV Power to ESC (to drive the motor)	Electric Distribution System	5.96E-08	Contactor High Temperature	All	High Torque for the connected rotor	Aircraft becomes unbalanced. FCC may be able to compensate.	Available power reduced. Limited flight envelope. Emergency landing may be required.	Critical	40.0%	30.0%

Function	Component	Failure Rate	Failure Mode	Mission Phase	Local Failure Effect	Next Higher Effect	End Effect	Severity	Alpha	Beta
Provide HV Power to ESC (to drive the motor)	Electric Distribution System	4.47E-08	Contactor Overcurrent	All	No Torque for the connected rotor	Rotor fails, aircraft becomes unbalanced. FCC may be able to compensate.	Available power reduced. Limited flight envelope. Emergency landing may be required.	Critical	30.0%	70.0%
Provide HV Power to ESC (to drive the motor)	Electric Distribution System	4.47E-08	Contactor Overcurrent	All	High Torque for the connected rotor	Aircraft becomes unbalanced. FCC may be able to compensate.	Available power reduced. Limited flight envelope. Emergency landing may be required.	Critical	30.0%	30.0%
Provide HV Power to ESC (to drive the motor)	Electric Distribution System	4.47E-08	Contactor High Voltage	All	No Torque for the connected rotor	Rotor fails, aircraft becomes unbalanced. FCC may be able to compensate.	Available power reduced. Limited flight envelope. Emergency landing may be required.	Critical	30.0%	70.0%
Provide HV Power to ESC (to drive the motor)	Electric Distribution System	4.47E-08	Contactor High Voltage	All	High Torque for the connected rotor	Aircraft becomes unbalanced. FCC may be able to compensate.	Available power reduced. Limited flight envelope. Emergency landing may be required.	Critical	30.0%	30.0%
Provide HV Power to ESC (to drive the motor)	Electric Distribution System	1.39E-07	Connection Failure	All	No Torque for the connected rotor	Rotor fails, aircraft becomes unbalanced. FCC may be able to compensate.	Available power reduced. Limited flight envelope. Emergency landing may be required.	Critical	100.0%	70.0%
Provide HV Power to ESC (to drive the motor)	Electric Distribution System	1.39E-07	Connection Failure	All	High Torque for the connected rotor	Aircraft becomes unbalanced. FCC may be able to compensate.	Available power reduced. Limited flight envelope. Emergency landing may be required.	Critical	100.0%	30.0%

Function	Component	Failure Rate	Failure Mode	Mission Phase	Local Failure Effect	Next Higher Effect	End Effect	Severity	Alpha	Beta
Transfer Torque to Rotors	Reduction Gearbox	4.23E-07	Teeth Surface Fatigue	Emergency maneuver	Gear power transmission efficiency goes down due to more friction and the experienced vibration in operation increases	More power is necessary to spin the rotor attached to the gearbox at the same speed and pitch angle	Available power reduced. Possible aircraft instability. Range is reduced.	Major	85.0%	100.0%
Transfer Torque to Rotors	Reduction Gearbox	4.23E-07	Teeth Overload Fracture	Emergency maneuver	The broken tooth reduces the gear efficiency and the vibrations increase	The same performance level requires an increase in power generation	Available power reduced. Possible aircraft instability. Range is reduced.	Critical	5.0%	100.0%
Transfer Torque to Rotors	Reduction Gearbox	4.23E-07	Teeth Fatigue Fracture	All	The broken tooth reduces the gear efficiency and the vibrations increase	The same performance level requires an increase in power generation	Available power reduced. Possible aircraft instability. Range is reduced.	Critical	10.0%	100.0%
Convert Electrical Energy to Torque	Motor Auxilliary Gearbox	3.48E-07	Teeth Surface Fatigue	Emergency maneuver	Gear power transmission efficiency goes down due to more friction and the experienced vibration in operation increases	The power required for the same auxiliary system performance increases	Available Power Reduced. Range is reduced.	Major	85.0%	100.0%
Convert Electrical Energy to Torque	Motor Auxilliary Gearbox	3.48E-07	Teeth Overload Fracture	Emergency maneuver	The broken tooth reduces the gear efficiency and the vibrations increase.	The power required for the same auxiliary system performance increases	Available Power Reduced. Range is reduced.	Critical	5.0%	100.0%

Function	Component	Failure Rate	Failure Mode	Mission Phase	Local Failure Effect	Next Higher Effect	End Effect	Severity	Alpha	Beta
Convert Electrical Energy to Torque	Motor Auxilliary Gearbox	3.48E-07	Teeth Fatigue Fracture	All	The broken tooth reduces the gear efficiency and the vibrations increase.	The power required for the same auxiliary system performance increases	Available Power Reduced. Range is reduced.	Critical	10.0%	100.0%
Transfer Torque to Rotors	Rotor Overruning Clutch	4.23E-07	Overload Fracture	Emergency maneuver	The clutch fails to engage	The remaining three connected motors must power the four rotors	Available power reduced. Possible aircraft instability. Range is reduced.	Critical	5.0%	100.0%
Transfer Torque to Rotors	Rotor Overruning Clutch	4.23E-07	Fatigue Fracture	All	The clutch fails to engage	The remaining three connected motors must power the four rotors	Available power reduced. Possible aircraft instability. Range is reduced.	Critical	15.0%	100.0%
Transfer Torque to Rotors	Rotor Overruning Clutch	4.23E-07	Degredation	All	The clutch efficiency is lower	The electric motor power generation increases	Available power reduced. Range is reduced.	Critical	80.0%	100.0%

Appendix B - Table 6: Octocopter RPM-control FMECA

Function	Component	Failure Rate	Failure Mode	Mission Phase	Local Failure Effect	Next Higher Effect	End Effect	Severity	Alpha	Beta
Convert Electrical Energy to Torque	Electronic Speed Controller	8.08E-06	ESC High Voltage	All	Rotor Torque Ripple	Rotor experiences torque oscillations. In extreme cases, rotor may be switched off.	Available power reduced. Possible aircraft instability.	Critical	20%	100.0%
Convert Electrical Energy to Torque	Electronic Speed Controller	8.08E-06	ESC Overcurrent	All	High Torque Ripple	Rotor experiences torque oscillations. Current draw from the battery is increased. Possible battery thermal runaway. In extreme cases, rotor may be switched off.	Reduced aircraft range. Possible aircraft instability.	Critical	20%	100.0%
Convert Electrical Energy to Torque	Electronic Speed Controller	8.08E-06	ESC Voltage Transient	All	Rotor Torque Ripple	Rotor experiences torque oscillations. In extreme cases, rotor may be switched off.	Available power reduced. Possible aircraft instability.	Critical	10%	100.0%
Convert Electrical Energy to Torque	Electronic Speed Controller	8.08E-06	ESC Vibrations	All	High Torque Ripple	Rotor experiences torque oscillations. In extreme cases, rotor may be switched off.	Reduced aircraft range. Possible aircraft instability.	Critical	10%	100.0%
Convert Electrical Energy to Torque	Electronic Speed Controller	8.08E-06	Manufacturing Defects	All	Rotor Torque Ripple	Rotor experiences torque oscillations. In extreme cases, rotor may be switched off.	Available power reduced. Possible aircraft instability.	Critical	7%	100.0%
Convert Electrical Energy to Torque	Electronic Speed Controller	8.08E-06	ESC Current Sensor Fault	All	Rotor Torque Ripple	Rotor experiences torque oscillations. In extreme cases, rotor may be switched off.	Available power reduced. Possible aircraft instability.	Critical	2%	100.0%
Convert Electrical Energy to Torque	Electronic Speed Controller	8.08E-06	ESC Resolver Fault	All	Rotor Torque Ripple	Rotor experiences torque oscillations. In extreme cases, rotor may be switched off.	Available power reduced. Possible aircraft instability.	Critical	2%	100.0%

Function	Component	Failure Rate	Failure Mode	Mission Phase	Local Failure Effect	Next Higher Effect	End Effect	Severity	Alpha	Beta
Convert Electrical Energy to Torque	Electronic Speed Controller	8.08E-06	ESC Temperature Sensor Fail	All	ESC fails, motor produces no torque	Rotor fails, aircraft becomes unbalanced. FCC may be able to compensate.	Available power reduced. Limited flight envelope. Emergency landing may be required.	Critical	2%	100.0%
Convert Electrical Energy to Torque	Electronic Speed Controller	8.08E-06	ESC High Temperature	All	ESC fails, motor produces no torque	Rotor fails, aircraft becomes unbalanced. FCC may be able to compensate.	Available power reduced. Limited flight envelope. Emergency landing may be required.	Critical	27%	40.0%
Convert Electrical Energy to Torque	Electronic Speed Controller	8.08E-06	ESC High Temperature	All	Rotor Low Torque	Rotor fails, aircraft becomes unbalanced. FCC may be able to compensate.	Available power reduced. Limited flight envelope. Emergency landing may be required.	Critical	27%	30.0%
Convert Electrical Energy to Torque	Electronic Speed Controller	8.08E-06	ESC High Temperature	All	Rotor Torque Ripple	Rotor experiences torque oscillations. In extreme cases, rotor may be switched off.	Available power reduced. Possible aircraft instability.	Critical	27%	30.0%
Convert Electrical Energy to Torque	Electric Motor	5.10E-06	Motor High Voltage	All	Motor Short Circuit	Rotor experiences torque oscillations. In extreme cases, rotor may be switched off.	Available power reduced. Possible aircraft instability.	Critical	6%	100.0%
Convert Electrical Energy to Torque	Electric Motor	5.10E-06	Motor Overcurrent	All	Motor Short Circuit	Rotor experiences torque oscillations. In extreme cases, rotor may be switched off.	Available power reduced. Possible aircraft instability.	Critical	6%	20.0%
Convert Electrical Energy to Torque	Electric Motor	5.10E-06	Motor Overcurrent	All	Rotor Torque Ripple	Rotor experiences torque oscillations. In extreme cases, rotor may be switched off.	Available power reduced. Possible aircraft instability.	Critical	6%	10.0%

Function	Component	Failure Rate	Failure Mode	Mission Phase	Local Failure Effect	Next Higher Effect	End Effect	Severity	Alpha	Beta
Convert Electrical Energy to Torque	Electric Motor	5.10E-06	Motor Overcurrent	All	Low/No Torque	Aircraft becomes unbalanced. FCC may be able to compensate.	Available power reduced. Limited flight envelope. Emergency landing may be required.	Critical	6%	60.0%
Convert Electrical Energy to Torque	Electric Motor	5.10E-06	Motor Voltage Transient	All	Rotor Low Torque; Torque Ripple	Rotor experiences torque oscillations. In extreme cases, rotor may be switched off.	Available power reduced. Possible aircraft instability.	Critical	3%	100.0%
Convert Electrical Energy to Torque	Electric Motor	5.10E-06	Motor Eccentricity	All	Rotor Low/No Torque;	Aircraft becomes unbalanced. FCC may be able to compensate.	Available power reduced. Limited flight envelope. Emergency landing may be required.	Critical	0%	100.0%
Convert Electrical Energy to Torque	Electric Motor	5.10E-06	Motor Shaft Failure	All	Rotor Low/No Torque;	Aircraft becomes unbalanced. FCC may be able to compensate.	Available power reduced. Limited flight envelope. Emergency landing may be required.	Critical	0%	100.0%
Convert Electrical Energy to Torque	Electric Motor	5.10E-06	Motor High Temperature	All	Rotor No Torque	Rotor fails, aircraft becomes unbalanced. FCC may be able to compensate.	Available power reduced. Limited flight envelope. Emergency landing may be required.	Critical	84%	50.0%
Convert Electrical Energy to Torque	Electric Motor	5.10E-06	Motor High Temperature	All	Rotor Short Circuit	Rotor experiences torque oscillations. In extreme cases, rotor may be switched off.	Available power reduced. Possible aircraft instability.	Critical	84%	20.0%

Function	Component	Failure Rate	Failure Mode	Mission Phase	Local Failure Effect	Next Higher Effect	End Effect	Severity	Alpha	Beta
Convert Electrical Energy to Torque	Electric Motor	5.10E-06	Motor High Temperature	All	Rotor Low Torque	Rotor fails, aircraft becomes unbalanced. FCC may be able to compensate.	Available power reduced. Limited flight envelope. Emergency landing may be required.	Critical	84%	30.0%
Provide LVDC Power for Control	LV Battery	1.01E-06	LV Battery Fail	All	Loss of function of FCC and all ESC	No torque produced by all ESC, No control signals provided to actuators	Loss of all propulsion and control. Aircraft descends to ground.	Catastrophic	100%	100.0%
Provide HV Power to ESC (to drive the motor)	HV Battery	8.07E-06	Battery Current Sensor Fault	All	Low/No Torque for the connected rotor	Aircraft becomes unbalanced. FCC may be able to compensate.	Available power reduced. Limited flight envelope. Emergency landing may be required.	Critical	22%	100.0%
Provide HV Power to ESC (to drive the motor)	HV Battery	8.07E-06	Battery Voltage Sensor Fault	All	Low/No Torque for the connected rotor	Aircraft becomes unbalanced. FCC may be able to compensate.	Available power reduced. Limited flight envelope. Emergency landing may be required.	Critical	22%	100.0%
Provide HV Power to ESC (to drive the motor)	HV Battery	8.07E-06	Battery Temperature Sesnor Fault	All	Low/No Torque for the connected rotor	Aircraft becomes unbalanced. FCC may be able to compensate.	Available power reduced. Limited flight envelope. Emergency landing may be required.	Critical	22%	100.0%
Provide HV Power to ESC (to drive the motor)	HV Battery	8.07E-06	Battery External Short Circuit	All	Low/No Torque for the connected rotor	Aircraft becomes unbalanced. FCC may be able to compensate.	Available power reduced. Limited flight envelope. Emergency landing may be required.	Critical	6%	100.0%

Function	Component	Failure Rate	Failure Mode	Mission Phase	Local Failure Effect	Next Higher Effect	End Effect	Severity	Alpha	Beta
Provide HV Power to ESC (to drive the motor)	HV Battery	8.07E-06	Battery Physical Damage	All	Low/No Torque for the connected rotor	Aircraft becomes unbalanced. FCC may be able to compensate.	Available power reduced. Limited flight envelope. Emergency landing may be required.	Critical	4%	100.0%
Provide HV Power to ESC (to drive the motor)	HV Battery	8.07E-06	Battery Manufacutring Defects	All	Low/No Torque for the connected rotor	Aircraft becomes unbalanced. FCC may be able to compensate.	Available power reduced. Limited flight envelope. Emergency landing may be required.	Critical	12%	100.0%
Provide HV Power to ESC (to drive the motor)	HV Battery	8.07E-06	Battery External Overheating	All	Low/No Torque for the connected rotor	Aircraft becomes unbalanced. FCC may be able to compensate.	Available power reduced. Limited flight envelope. Emergency landing may be required.	Critical	12%	100.0%
Provide HV Power to ESC (to drive the motor)	HV Battery Cooling	4.30E-06	Battery Cooling Failure	All	Low/No Torque for the connected rotor	Aircraft becomes unbalanced. FCC may be able to compensate.	Available power reduced. Limited flight envelope. Emergency landing may be required.	Critical	100%	100.0%
Provide HV Power to ESC (to drive the motor)	Electric Distribution System	5.96E-08	Fuse High Temperature	All	No Torque for the connected rotor	Rotor fails, aircraft becomes unbalanced. FCC may be able to compensate.	Available power reduced. Limited flight envelope. Emergency landing may be required.	Critical	40.0%	70.0%
Provide HV Power to ESC (to drive the motor)	Electric Distribution System	5.96E-08	Fuse High Temperature	All	High Torque for the connected rotor	Aircraft becomes unbalanced. FCC may be able to compensate.	Available power reduced. Limited flight envelope. Emergency landing may be required.	Critical	40.0%	30.0%

Function	Component	Failure Rate	Failure Mode	Mission Phase	Local Failure Effect	Next Higher Effect	End Effect	Severity	Alpha	Beta
Provide HV Power to ESC (to drive the motor)	Electric Distribution System	4.47E-08	Fuse Overcurrent	All	No Torque for the connected rotor	Rotor fails, aircraft becomes unbalanced. FCC may be able to compensate.	Available power reduced. Limited flight envelope. Emergency landing may be required.	Critical	30.0%	70.0%
Provide HV Power to ESC (to drive the motor)	Electric Distribution System	4.47E-08	Fuse Overcurrent	All	High Torque for the connected rotor	Aircraft becomes unbalanced. FCC may be able to compensate.	Available power reduced. Limited flight envelope. Emergency landing may be required.	Critical	30.0%	30.0%
Provide HV Power to ESC (to drive the motor)	Electric Distribution System	4.47E-08	Fuse High Voltage	All	No Torque for the connected rotor	Rotor fails, aircraft becomes unbalanced. FCC may be able to compensate.	Available power reduced. Limited flight envelope. Emergency landing may be required.	Critical	30.0%	70.0%
Provide HV Power to ESC (to drive the motor)	Electric Distribution System	4.47E-08	Fuse High Voltage	All	High Torque for the connected rotor	Aircraft becomes unbalanced. FCC may be able to compensate.	Available power reduced. Limited flight envelope. Emergency landing may be required.	Critical	30.0%	30.0%
Provide HV Power to ESC (to drive the motor)	Electric Distribution System	5.96E-08	Contactor High Temperature	All	No Torque for the connected rotor	Rotor fails, aircraft becomes unbalanced. FCC may be able to compensate.	Available power reduced. Limited flight envelope. Emergency landing may be required.	Critical	40.0%	70.0%
Provide HV Power to ESC (to drive the motor)	Electric Distribution System	5.96E-08	Contactor High Temperature	All	High Torque for the connected rotor	Aircraft becomes unbalanced. FCC may be able to compensate.	Available power reduced. Limited flight envelope. Emergency landing may be required.	Critical	40.0%	30.0%

Function	Component	Failure Rate	Failure Mode	Mission Phase	Local Failure Effect	Next Higher Effect	End Effect	Severity	Alpha	Beta
Provide HV Power to ESC (to drive the motor)	Electric Distribution System	4.47E-08	Contactor Overcurrent	All	No Torque for the connected rotor	Rotor fails, aircraft becomes unbalanced. FCC may be able to compensate.	Available power reduced. Limited flight envelope. Emergency landing may be required.	Critical	30.0%	70.0%
Provide HV Power to ESC (to drive the motor)	Electric Distribution System	4.47E-08	Contactor Overcurrent	All	High Torque for the connected rotor	Aircraft becomes unbalanced. FCC may be able to compensate.	Available power reduced. Limited flight envelope. Emergency landing may be required.	Critical	30.0%	30.0%
Provide HV Power to ESC (to drive the motor)	Electric Distribution System	4.47E-08	Contactor High Voltage	All	No Torque for the connected rotor	Rotor fails, aircraft becomes unbalanced. FCC may be able to compensate.	Available power reduced. Limited flight envelope. Emergency landing may be required.	Critical	30.0%	70.0%
Provide HV Power to ESC (to drive the motor)	Electric Distribution System	4.47E-08	Contactor High Voltage	All	High Torque for the connected rotor	Aircraft becomes unbalanced. FCC may be able to compensate.	Available power reduced. Limited flight envelope. Emergency landing may be required.	Critical	30.0%	30.0%
Provide HV Power to ESC (to drive the motor)	Electric Distribution System	1.39E-07	Connection Failure	All	No Torque for the connected rotor	Rotor fails, aircraft becomes unbalanced. FCC may be able to compensate.	Available power reduced. Limited flight envelope. Emergency landing may be required.	Critical	100.0%	70.0%
Provide HV Power to ESC (to drive the motor)	Electric Distribution System	1.39E-07	Connection Failure	All	High Torque for the connected rotor	Aircraft becomes unbalanced. FCC may be able to compensate.	Available power reduced. Limited flight envelope. Emergency landing may be required.	Critical	100.0%	30.0%

Function	Component	Failure Rate	Failure Mode	Mission Phase	Local Failure Effect	Next Higher Effect	End Effect	Severity	Alpha	Beta
Transfer Torque to Rotors	Reduction Gearbox	4.23E-07	Teeth Surface Fatigue	Emergency maneuver	Gear power transmission efficiency goes down due to more friction and the experienced vibration in operation increases	More power is necessary to spin the rotor attached to the gearbox at the same speed and pitch angle	Available power reduced. Possible aircraft instability. Range is reduced.	Major	85.0%	100.0%
Transfer Torque to Rotors	Reduction Gearbox	4.23E-07	Teeth Overload Fracture	Emergency maneuver	The broken tooth reduces the gear efficiency and the vibrations increase	The same performance level requires an increase in power generation	Available power reduced. Possible aircraft instability. Range is reduced.	Critical	5.0%	100.0%
Transfer Torque to Rotors	Reduction Gearbox	4.23E-07	Teeth Fatigue Fracture	All	The broken tooth reduces the gear efficiency and the vibrations increase	The same performance level requires an increase in power generation	Available power reduced. Possible aircraft instability. Range is reduced.	Critical	10.0%	100.0%
Convert Electrical Energy to Torque	Motor Auxilliary Gearbox	3.48E-07	Teeth Surface Fatigue	Emergency maneuver	Gear power transmission efficiency goes down due to more friction and the experienced vibration in operation increases	The power required for the same auxiliary system performance increases	Available Power Reduced. Range is reduced.	Major	85.0%	100.0%
Convert Electrical Energy to Torque	Motor Auxilliary Gearbox	3.48E-07	Teeth Overload Fracture	Emergency maneuver	The broken tooth reduces the gear efficiency and the vibrations increase.	The power required for the same auxiliary system performance increases	Available Power Reduced. Range is reduced.	Critical	5.0%	100.0%

Function	Component	Failure Rate	Failure Mode	Mission Phase	Local Failure Effect	Next Higher Effect	End Effect	Severity	Alpha	Beta
Convert Electrical Energy to Torque	Motor Auxilliary Gearbox	3.48E-07	Teeth Fatigue Fracture	All	The broken tooth reduces the gear efficiency and the vibrations increase.	The power required for the same auxiliary system performance increases	Available Power Reduced. Range is reduced.	Critical	10.0%	100.0%
Transfer Torque to Rotors	Rotor Overruning Clutch	4.23E-07	Overload Fracture	Emergency maneuver	The clutch fails to engage	The remaining three connected motors must power the four rotors	Available power reduced. Possible aircraft instability. Range is reduced.	Critical	5.0%	100.0%
Transfer Torque to Rotors	Rotor Overruning Clutch	4.23E-07	Fatigue Fracture	All	The clutch fails to engage	The remaining three connected motors must power the four rotors	Available power reduced. Possible aircraft instability. Range is reduced.	Critical	15.0%	100.0%
Transfer Torque to Rotors	Rotor Overruning Clutch	4.23E-07	Degredation	All	The clutch efficiency is lower	The electric motor power generation increases	Available power reduced. Range is reduced.	Critical	80.0%	100.0%

APPENDIX C : FAULT TREE ANALYSIS (FTA) DIAGRAMS

Appendix C - Figure 1: Quadcopter Electric FTA

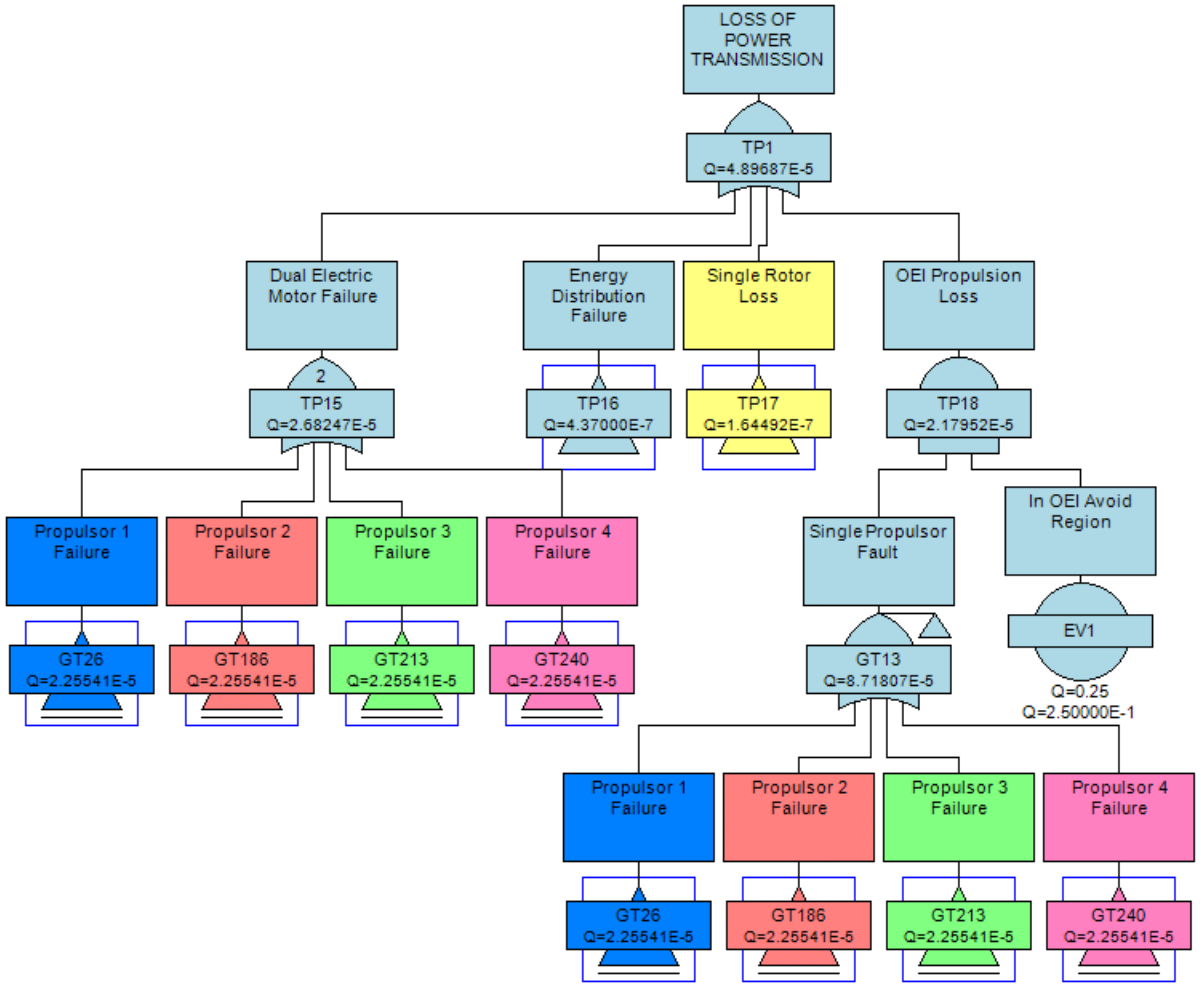

(Continued)

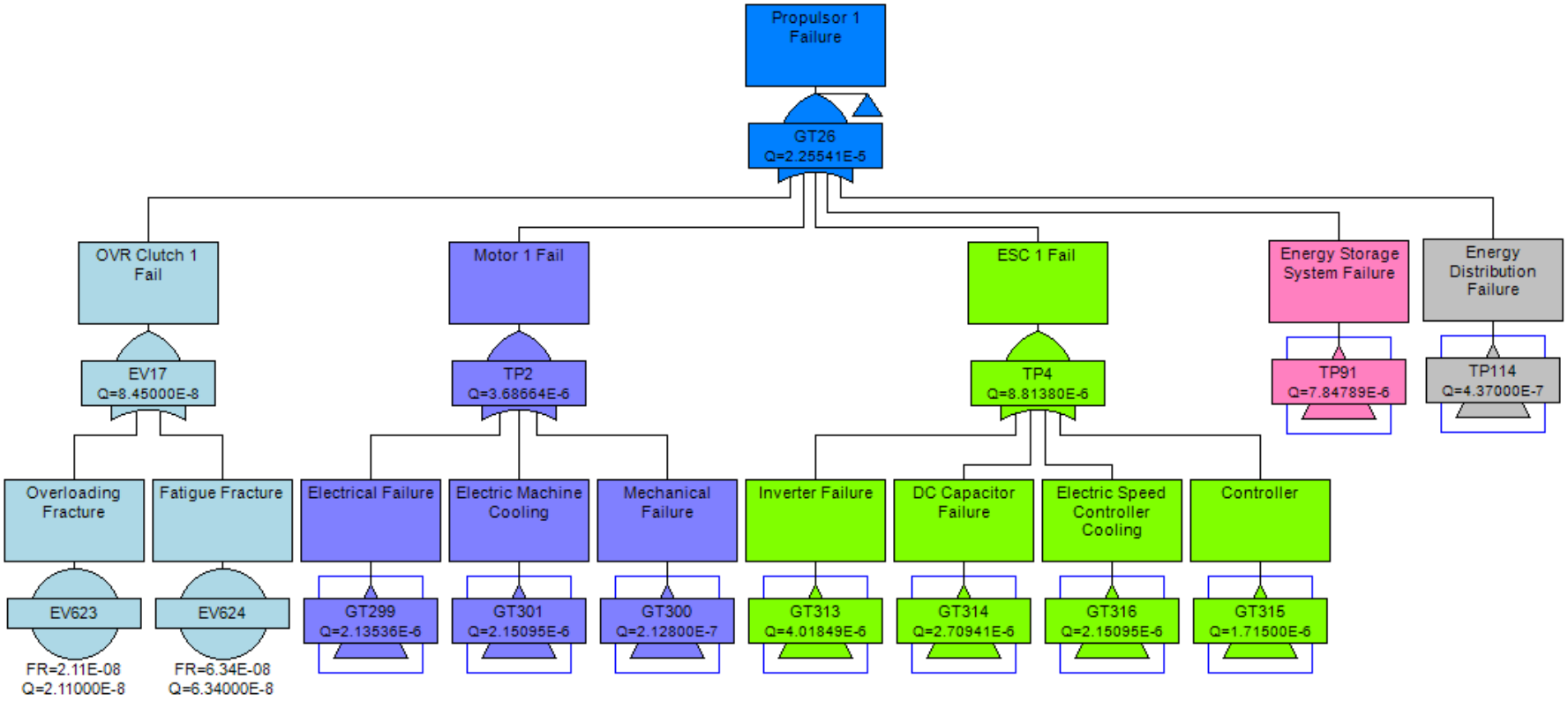
Propulsor 1 Failure
GT26
Q=2.25541E-5
OVR Clutch 1 Fail
Motor 1 Fail
ESC 1 Fail
Energy Storage System Failure
Energy Distribution Failure
EV17
Q=8.45000E-8
TP2
Q=3.68664E-6
TP4
Q=8.81380E-6
TP91
Q=7.84789E-6
TP114
Q=4.37000E-7
Overloading Fracture
Fatigue Fracture
Electrical Failure
Electric Machine Cooling
Mechanical Failure
Inverter Failure
DC Capacitor Failure
Electric Speed Controller Cooling
Controller
EV623
EV624
GT299
Q=2.13536E-6
GT301
Q=2.15095E-6
GT300
Q=2.12800E-7
GT313
Q=4.01849E-6
GT314
Q=2.70941E-6
GT316
Q=2.15095E-6
GT315
Q=1.71500E-6
FR=2.11E-08
Q=2.11000E-8
FR=6.34E-08
Q=6.34000E-8

(Continued)

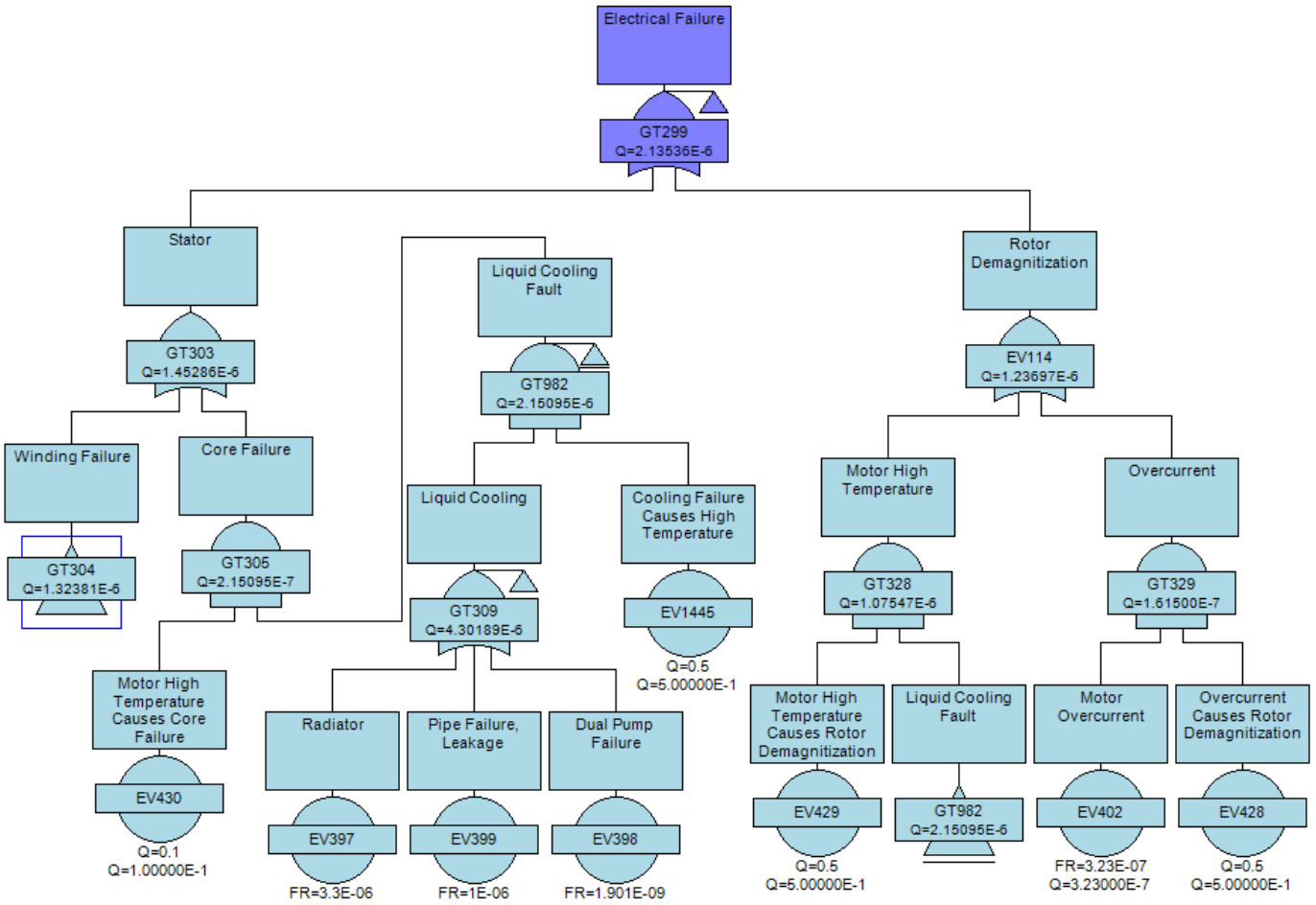
Electrical Failure
GT299
Q=2.13536E-6
Stator
GT303
Q=1.45286E-6
Winding Failure
GT304
Q=1.32381E-6
Core Failure
GT305
Q=2.15095E-7
Motor High Temperature Causes Core Failure
EV430
Q=0.1
Q=1.00000E-1
Liquid Cooling Fault
GT982
Q=2.15095E-6
Liquid Cooling
GT309
Q=4.30189E-6
Radiator
EV397
FR=3.3E-06
Pipe Failure, Leakage
EV399
FR=1E-06
Dual Pump Failure
EV398
FR=1.901E-09
Cooling Failure Causes High Temperature
EV1445
Q=0.5
Q=5.00000E-1
Rotor Demagnitization
EV114
Q=1.23697E-6
Motor High Temperature
GT328
Q=1.07547E-6
Motor High Temperature Causes Rotor Demagnitization
EV429
Q=0.5
Q=5.00000E-1
Liquid Cooling Fault
GT982
Q=2.15095E-6
Overcurrent
GT329
Q=1.61500E-7
Motor Overcurrent
EV402
FR=3.23E-07
Q=3.23000E-7
Overcurrent Causes Rotor Demagnitization
EV428
Q=0.5
Q=5.00000E-1

(Continued)

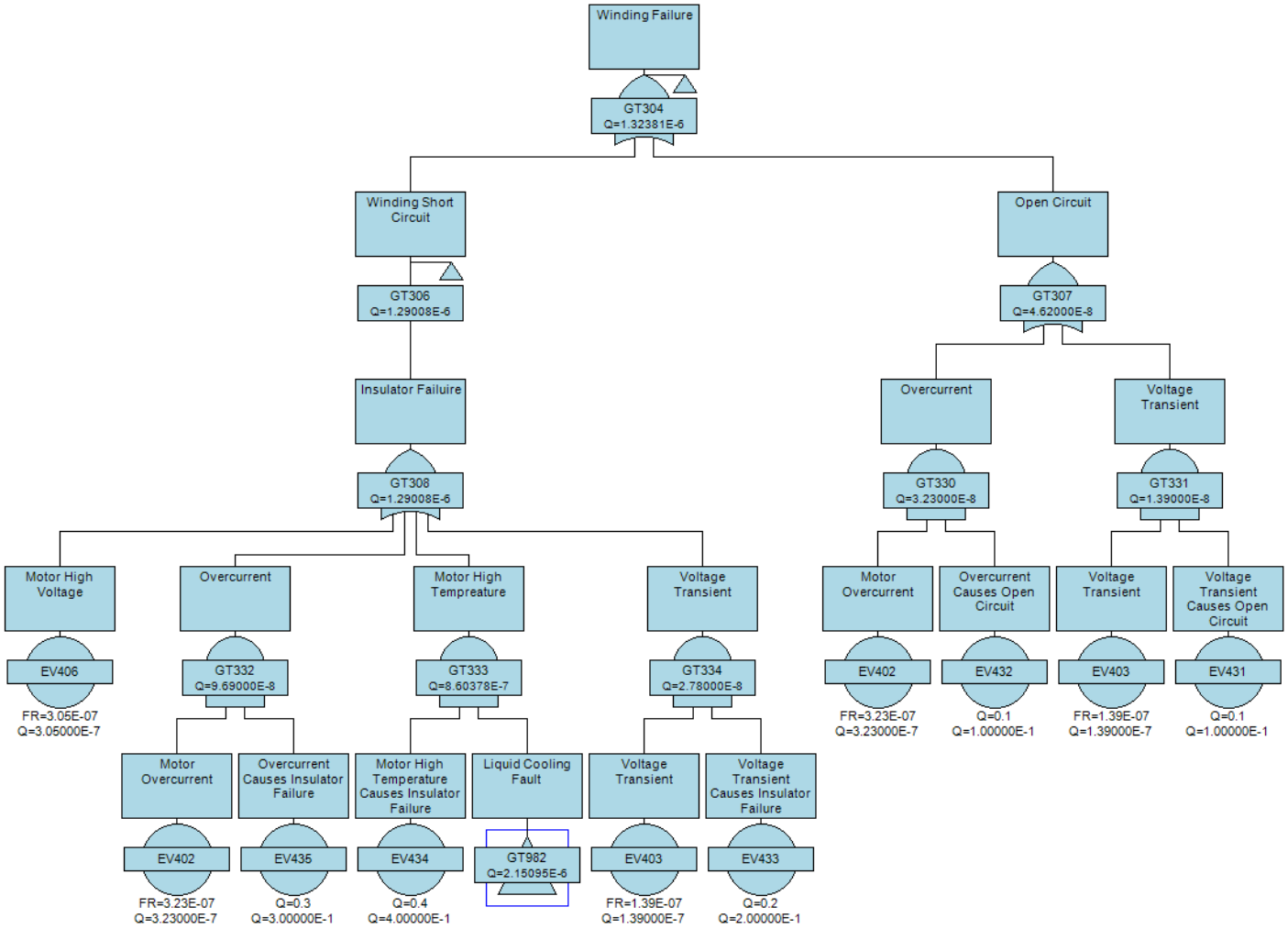
Winding Failure
GT304
Q=1.32381E-6
Winding Short Circuit
Open Circuit
GT306
Q=1.29008E-6
GT307
Q=4.62000E-8
Insulator Failuire
Overcurrent
Voltage Transient
GT308
Q=1.29008E-6
GT330
Q=3.23000E-8
GT331
Q=1.39000E-8
Motor High Voltage
Overcurrent
Motor High Tempreature
Voltage Transient
Motor Overcurrent
Overcurrent Causes Open Circuit
Voltage Transient
Voltage Transient Causes Open Circuit
EV406
GT332
Q=9.69000E-8
GT333
Q=8.60378E-7
GT334
Q=2.78000E-8
EV402
EV432
EV403
EV431
FR=3.05E-07
Q=3.05000E-7
FR=3.23E-07
Q=3.23000E-7
Q=0.1
Q=1.00000E-1
FR=1.39E-07
Q=1.39000E-7
Q=0.1
Q=1.00000E-1
Motor Overcurrent
Overcurrent Causes Insulator Failure
Motor High Temperature Causes Insulator Failure
Liquid Cooling Fault
Voltage Transient
Voltage Transient Causes Insulator Failure
EV402
EV435
EV434
GT982
Q=2.15095E-6
EV403
EV433
FR=3.23E-07
Q=3.23000E-7
Q=0.3
Q=3.00000E-1
Q=0.4
Q=4.00000E-1
FR=1.39E-07
Q=1.39000E-7
Q=0.2
Q=2.00000E-1

(Continued)

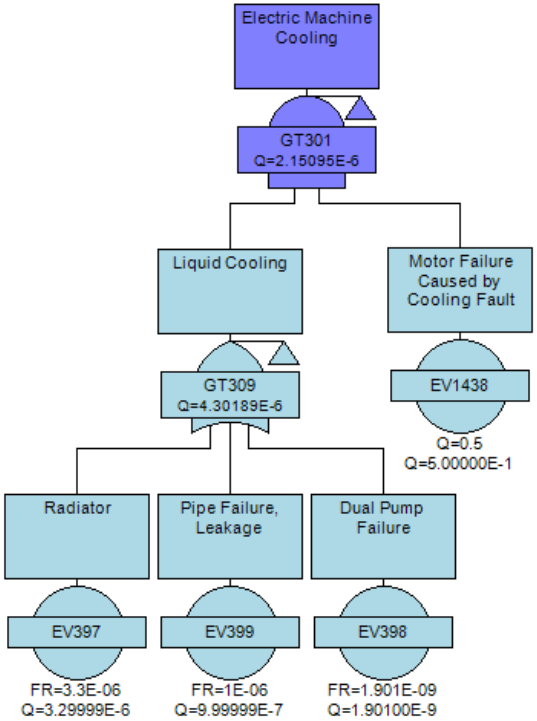
Electric Machine Cooling
GT301
Q=2.15095E-6
Liquid Cooling
Motor Failure Caused by Cooling Fault
GT309
Q=4.30189E-6
EV1438
Q=0.5
Q=5.00000E-1
Radiator
Pipe Failure, Leakage
Dual Pump Failure
EV397
EV399
EV398
FR=3.3E-06
Q=3.29999E-6
FR=1E-06
Q=9.99999E-7
FR=1.901E-09
Q=1.90100E-9

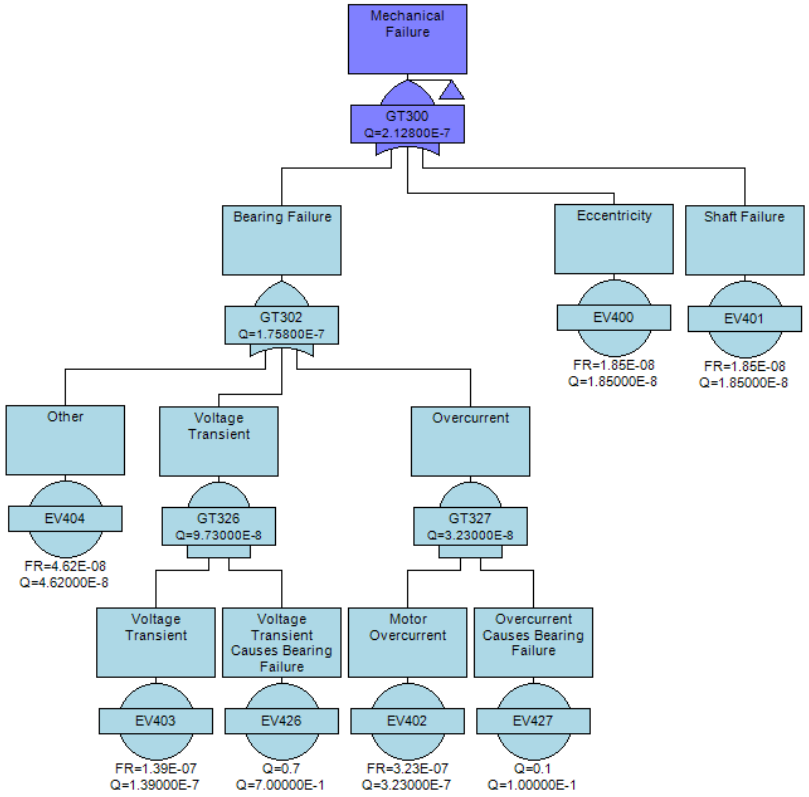
Mechanical Failure
GT300
Q=2.12800E-7
Bearing Failure
Eccentricity
Shaft Failure
GT302
Q=1.75800E-7
EV400
EV401
FR=1.85E-08
Q=1.85000E-8
FR=1.85E-08
Q=1.85000E-8
Other
Voltage Transient
Overcurrent
EV404
GT326
Q=9.73000E-8
GT327
Q=3.23000E-8
FR=4.62E-08
Q=4.62000E-8
Voltage Transient
Voltage Transient Causes Bearing Failure
Motor Overcurrent
Overcurrent Causes Bearing Failure
EV403
EV426
EV402
EV427
FR=1.39E-07
Q=1.39000E-7
Q=0.7
Q=7.00000E-1
FR=3.23E-07
Q=3.23000E-7
Q=0.1
Q=1.00000E-1

(Continued)

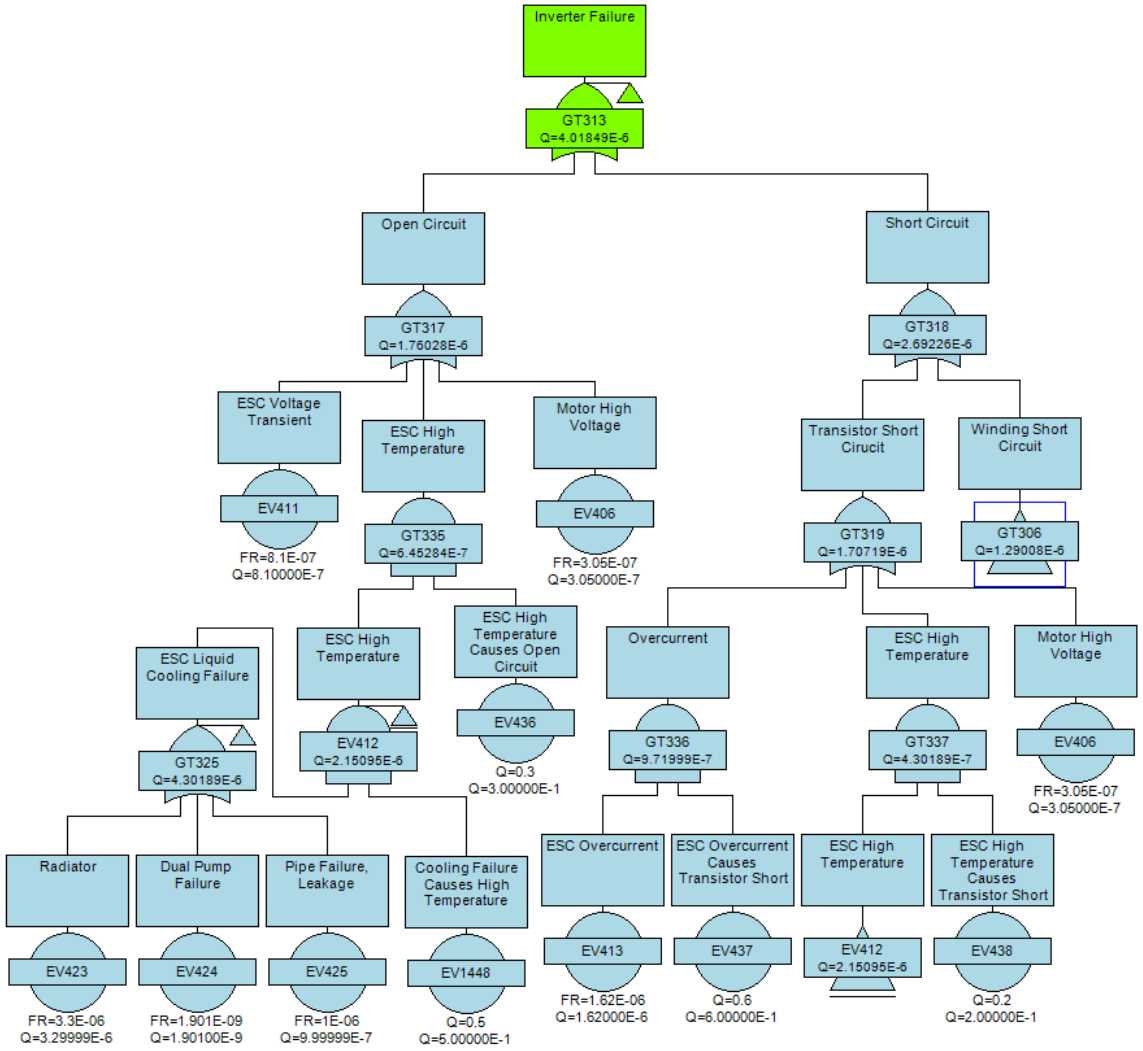
Inverter Failure
GT313
Q=4.01849E-6
Open Circuit
Short Circuit
GT317
Q=1.76028E-6
GT318
Q=2.69226E-6
ESC Voltage Transient
ESC High Temperature
Motor High Voltage
Transistor Short Cirucit
Winding Short Circuit
EV411
FR=8.1E-07
Q=8.10000E-7
GT335
Q=6.45284E-7
EV406
FR=3.05E-07
Q=3.05000E-7
GT319
Q=1.70719E-6
GT306
Q=1.29008E-6
ESC Liquid Cooling Failure
ESC High Temperature
ESC High Temperature Causes Open Circuit
Overcurrent
ESC High Temperature
Motor High Voltage
GT325
Q=4.30189E-6
EV412
Q=2.15095E-6
EV436
Q=0.3
Q=3.00000E-1
GT336
Q=9.71999E-7
GT337
Q=4.30189E-7
EV406
FR=3.05E-07
Q=3.05000E-7
Radiator
Dual Pump Failure
Pipe Failure, Leakage
Cooling Failure Causes High Temperature
ESC Overcurrent
ESC Overcurrent Causes Transistor Short
ESC High Temperature
ESC High Temperature Causes Transistor Short
EV423
FR=3.3E-06
Q=3.29999E-6
EV424
FR=1.901E-09
Q=1.90100E-9
EV425
FR=1E-06
Q=9.99999E-7
EV1448
Q=0.5
Q=5.00000E-1
EV413
FR=1.62E-06
Q=1.62000E-6
EV437
Q=0.6
Q=6.00000E-1
EV412
Q=2.15095E-6
EV438
Q=0.2
Q=2.00000E-1

(Continued)

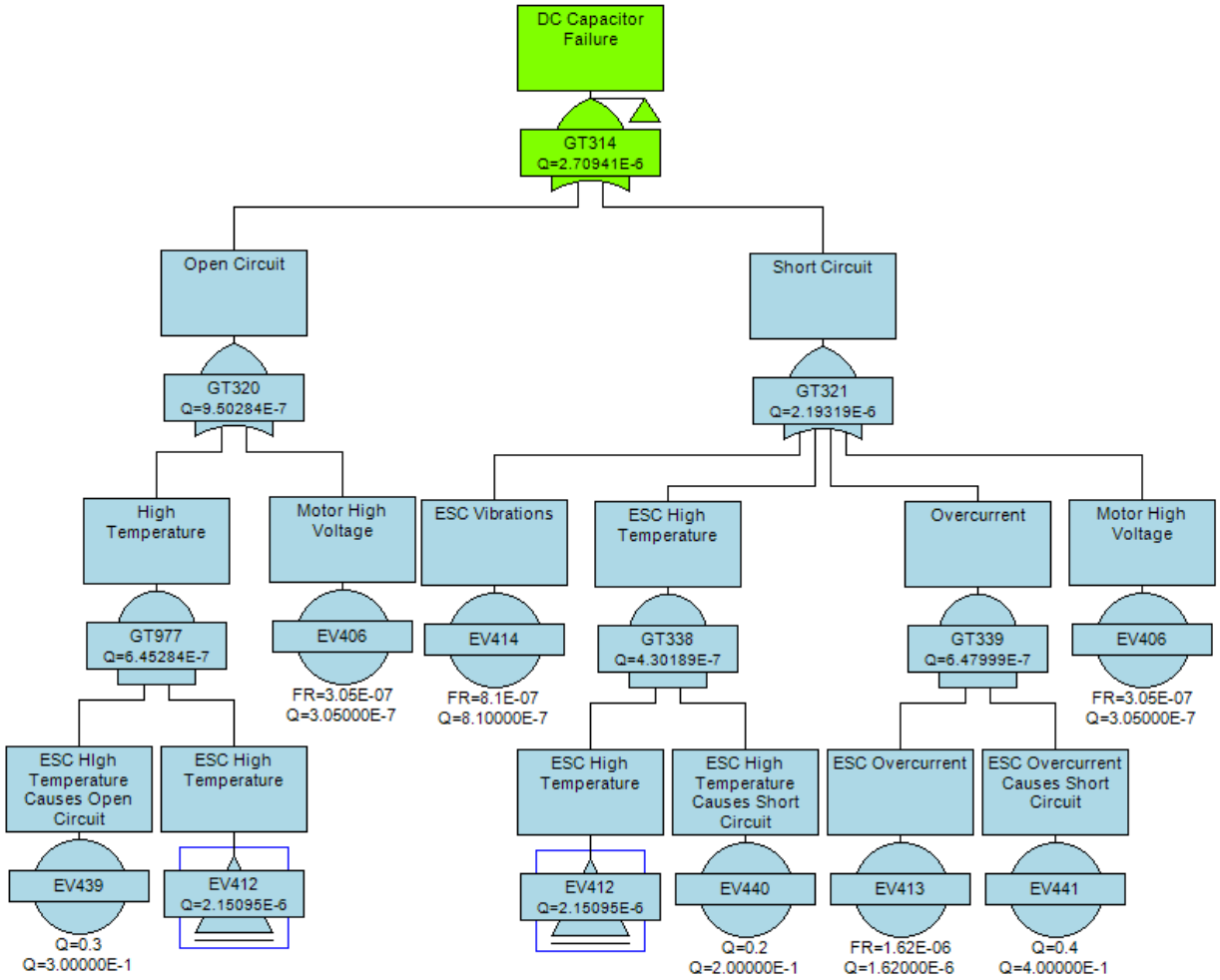
DC Capacitor Failure
GT314
Q=2.70941E-6
Open Circuit
Short Circuit
GT320
Q=9.50284E-7
GT321
Q=2.19319E-6
High Temperature
Motor High Voltage
ESC Vibrations
ESC High Temperature
Overcurrent
Motor High Voltage
GT977
Q=6.45284E-7
EV406
FR=3.05E-07
Q=3.05000E-7
EV414
FR=8.1E-07
Q=8.10000E-7
GT338
Q=4.30189E-7
GT339
Q=6.47999E-7
EV406
FR=3.05E-07
Q=3.05000E-7
ESC HIgh Temperature Causes Open Circuit
ESC High Temperature
ESC High Temperature
ESC High Temperature Causes Short Circuit
ESC Overcurrent
ESC Overcurrent Causes Short Circuit
EV439
Q=0.3
Q=3.00000E-1
EV412
Q=2.15095E-6
EV412
Q=2.15095E-6
EV440
Q=0.2
Q=2.00000E-1
EV413
FR=1.62E-06
Q=1.62000E-6
EV441
Q=0.4
Q=4.00000E-1

(Continued)

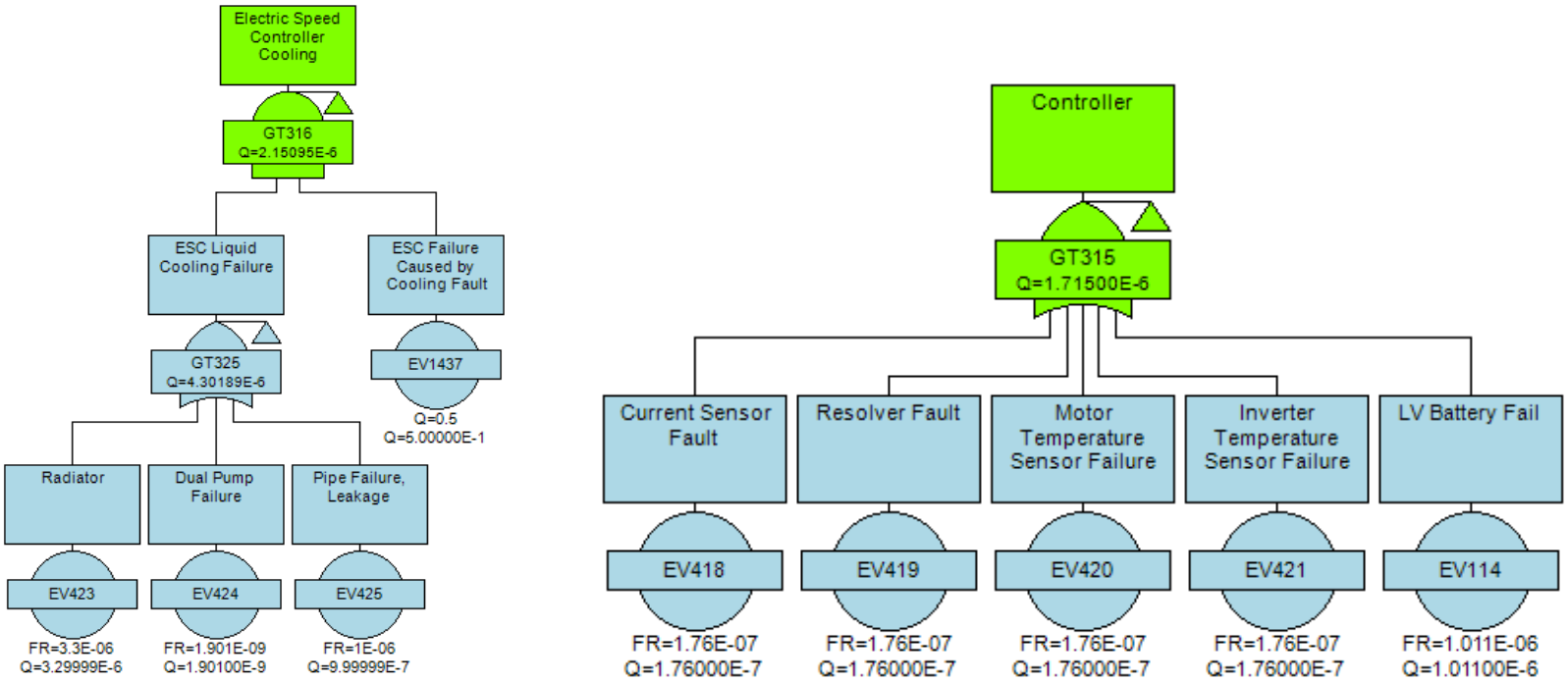
Electric Speed Controller Cooling
GT316
Q=2.15095E-6
ESC Liquid Cooling Failure
ESC Failure Caused by Cooling Fault
GT325
Q=4.30189E-6
EV1437
Q=0.5
Q=5.00000E-1
Radiator
Dual Pump Failure
Pipe Failure, Leakage
EV423
EV424
EV425
FR=3.3E-06
Q=3.29999E-6
FR=1.901E-09
Q=1.90100E-9
FR=1E-06
Q=9.99999E-7
Controller
GT315
Q=1.71500E-6
Current Sensor Fault
Resolver Fault
Motor Temperature Sensor Failure
Inverter Temperature Sensor Failure
LV Battery Fail
EV418
EV419
EV420
EV421
EV114
FR=1.76E-07
Q=1.76000E-7
FR=1.76E-07
Q=1.76000E-7
FR=1.76E-07
Q=1.76000E-7
FR=1.76E-07
Q=1.76000E-7
FR=1.011E-06
Q=1.01100E-6

(Continued)

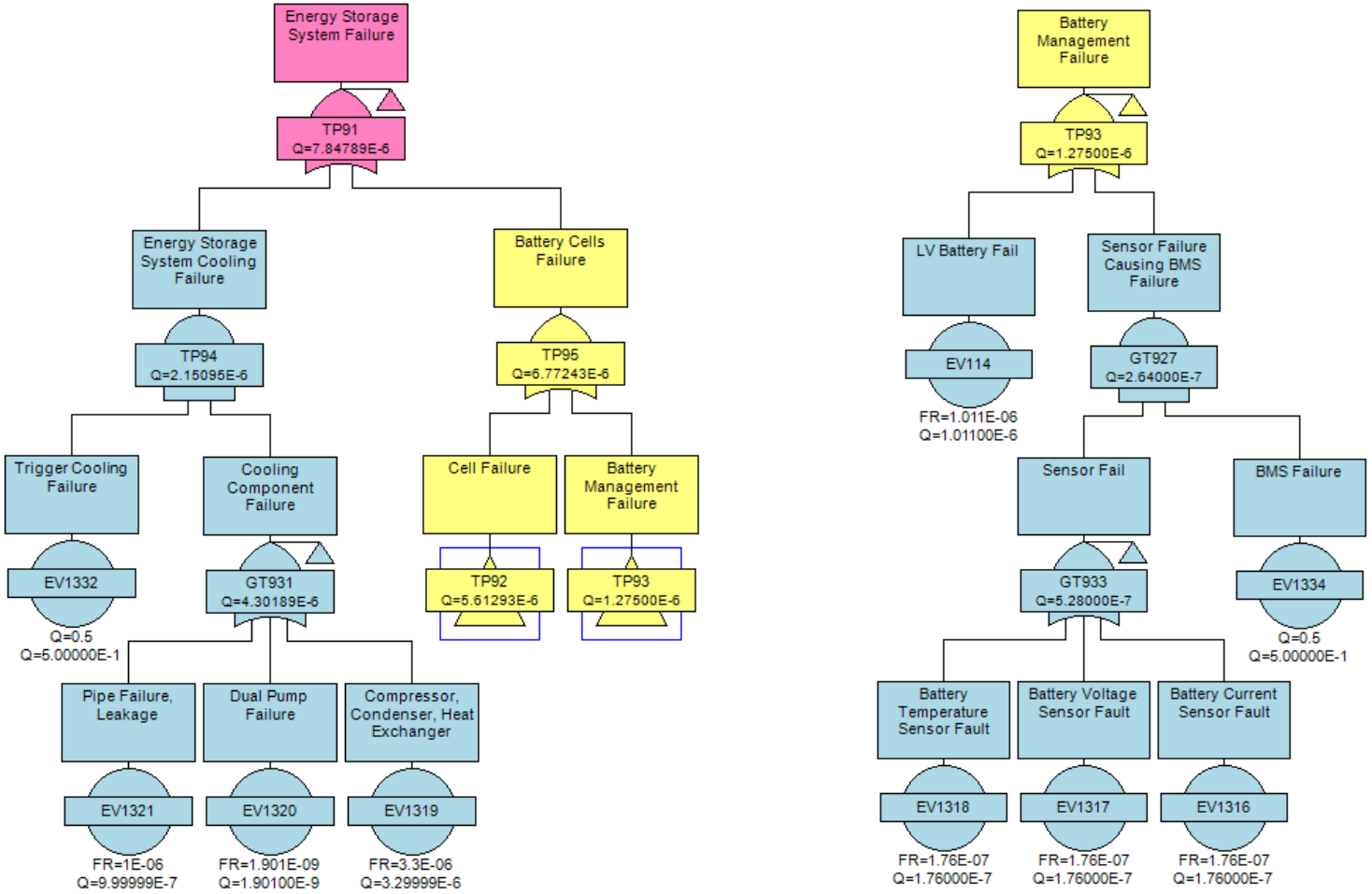
Energy Storage System Failure
TP91
Q=7.84789E-6
Energy Storage System Cooling Failure
Battery Cells Failure
TP94
Q=2.15095E-6
TP95
Q=6.77243E-6
Trigger Cooling Failure
Cooling Component Failure
Cell Failure
Battery Management Failure
EV1332
Q=0.5
Q=5.00000E-1
GT931
Q=4.30189E-6
TP92
Q=5.61293E-6
TP93
Q=1.27500E-6
Pipe Failure, Leakage
Dual Pump Failure
Compressor, Condenser, Heat Exchanger
EV1321
EV1320
EV1319
FR=1E-06
Q=9.99999E-7
FR=1.901E-09
Q=1.90100E-9
FR=3.3E-06
Q=3.29999E-6
Battery Management Failure
TP93
Q=1.27500E-6
LV Battery Fail
Sensor Failure Causing BMS Failure
EV114
FR=1.011E-06
Q=1.01100E-6
GT927
Q=2.64000E-7
Sensor Fail
BMS Failure
GT933
Q=5.28000E-7
EV1334
Q=0.5
Q=5.00000E-1
Battery Temperature Sensor Fault
Battery Voltage Sensor Fault
Battery Current Sensor Fault
EV1318
EV1317
EV1316
FR=1.76E-07
Q=1.76000E-7
FR=1.76E-07
Q=1.76000E-7
FR=1.76E-07
Q=1.76000E-7

(Continued)

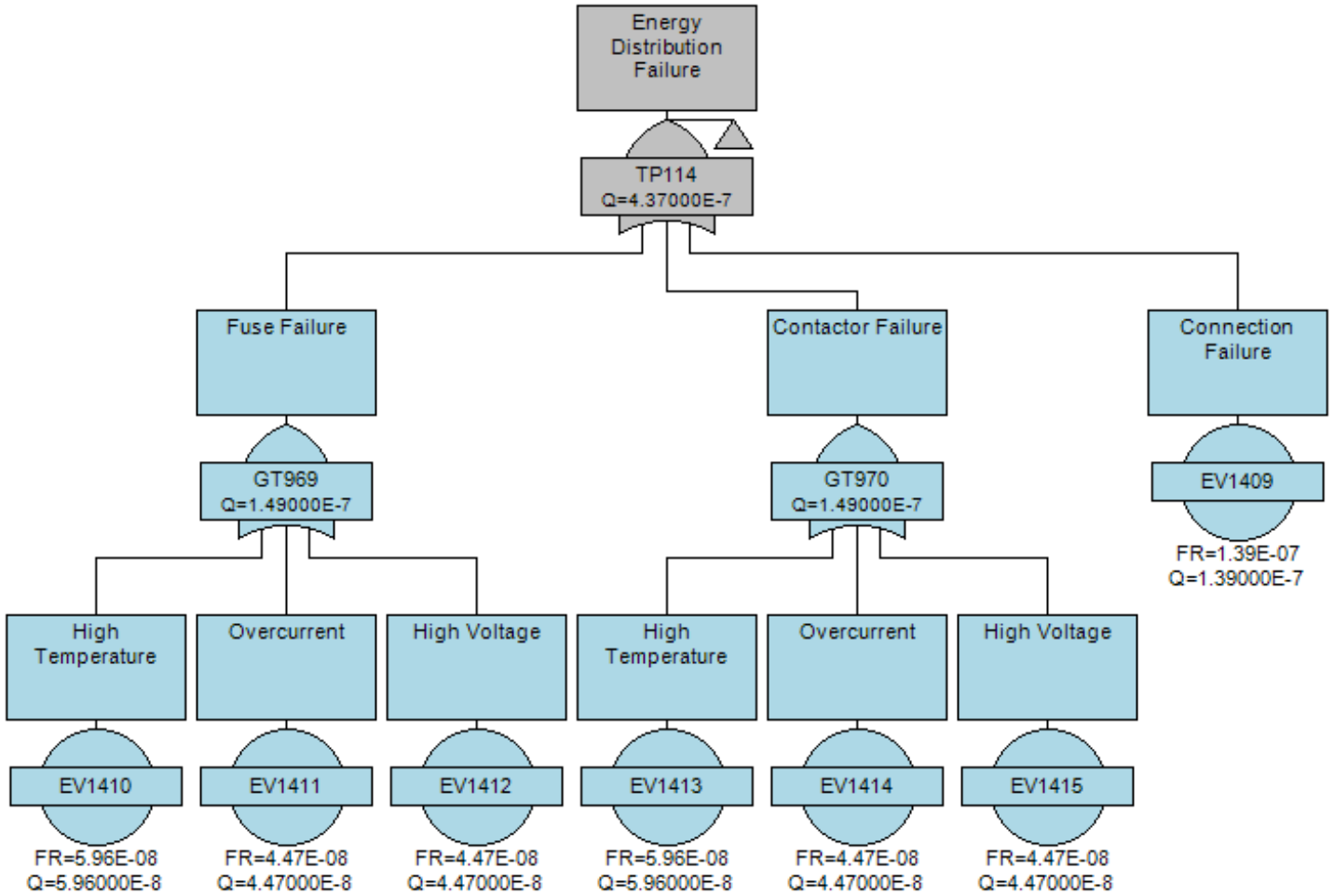
Energy Distribution Failure
TP114
Q=4.37000E-7
Fuse Failure
Contactor Failure
Connection Failure
GT969
Q=1.49000E-7
GT970
Q=1.49000E-7
EV1409
FR=1.39E-07
Q=1.39000E-7
High Temperature
Overcurrent
High Voltage
High Temperature
Overcurrent
High Voltage
EV1410
EV1411
EV1412
EV1413
EV1414
EV1415
FR=5.96E-08
Q=5.96000E-8
FR=4.47E-08
Q=4.47000E-8
FR=4.47E-08
Q=4.47000E-8
FR=5.96E-08
Q=5.96000E-8
FR=4.47E-08
Q=4.47000E-8
FR=4.47E-08
Q=4.47000E-8

(Continued)

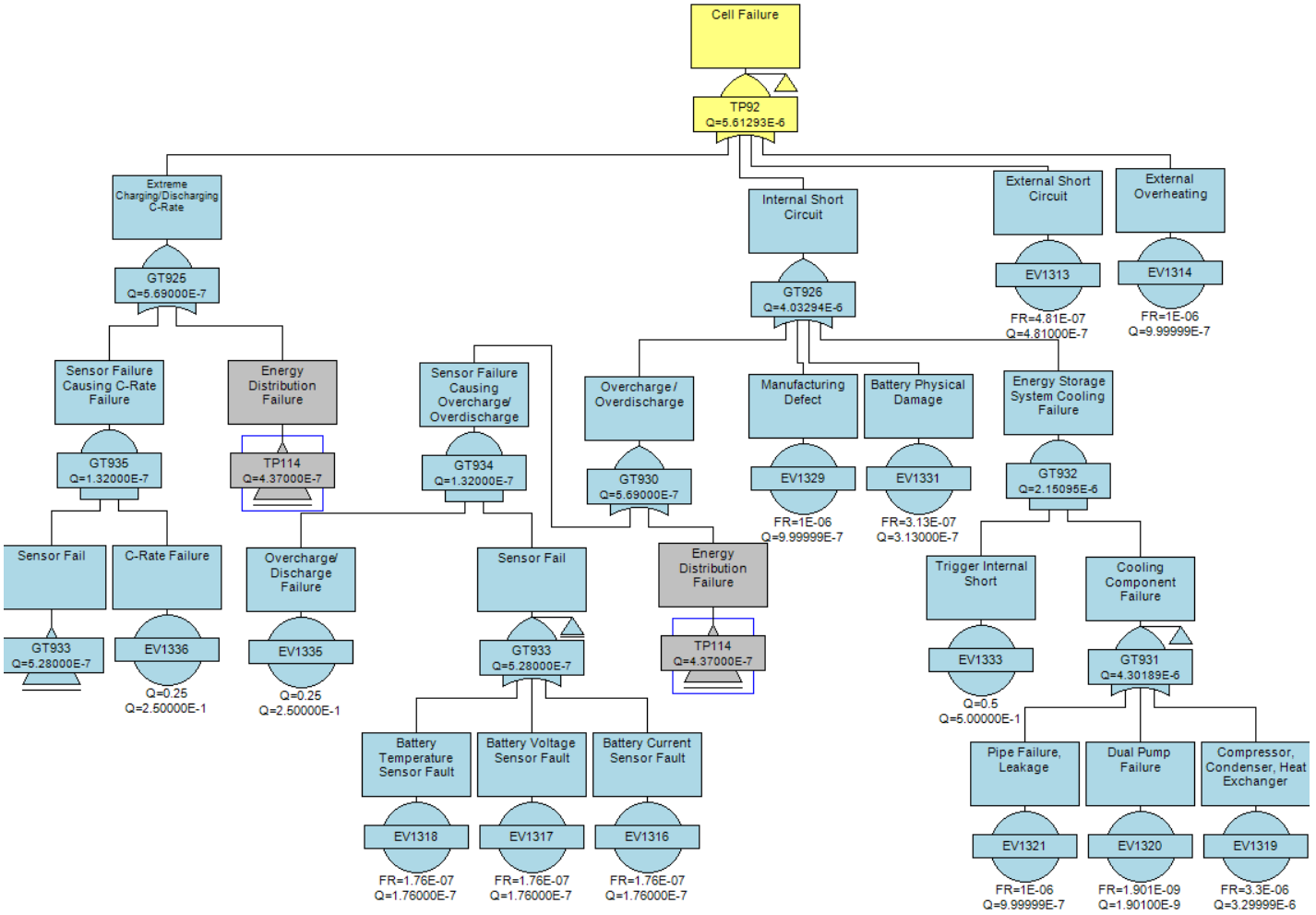
Cell Failure
TP92
Q=5.61293E-6
Extreme Charging/Discharging C-Rate
GT925
Q=5.69000E-7
Sensor Failure Causing C-Rate Failure
GT935
Q=1.32000E-7
Sensor Fail
GT933
Q=5.28000E-7
C-Rate Failure
EV1336
Q=0.25
Q=2.50000E-1
Energy Distribution Failure
TP114
Q=4.37000E-7
Overcharge/ Discharge Failure
EV1335
Q=0.25
Q=2.50000E-1
Sensor Failure Causing Overcharge/ Overdischarge
GT934
Q=1.32000E-7
Sensor Fail
GT933
Q=5.28000E-7
Battery Temperature Sensor Fault
EV1318
FR=1.76E-07
Q=1.76000E-7
Battery Voltage Sensor Fault
EV1317
FR=1.76E-07
Q=1.76000E-7
Battery Current Sensor Fault
EV1316
FR=1.76E-07
Q=1.76000E-7
Internal Short Circuit
GT926
Q=4.03294E-6
Overcharge/ Overdischarge
GT930
Q=5.69000E-7
Energy Distribution Failure
TP114
Q=4.37000E-7
Manufacturing Defect
EV1329
FR=1E-06
Q=9.99999E-7
Battery Physical Damage
EV1331
FR=3.13E-07
Q=3.13000E-7
Energy Storage System Cooling Failure
GT932
Q=2.15095E-6
Trigger Internal Short
EV1333
Q=0.5
Q=5.00000E-1
Cooling Component Failure
GT931
Q=4.30189E-6
Pipe Failure, Leakage
EV1321
FR=1E-06
Q=9.99999E-7
Dual Pump Failure
EV1320
FR=1.901E-09
Q=1.90100E-9
Compressor, Condenser, Heat Exchanger
EV1319
FR=3.3E-06
Q=3.29999E-6
External Short Circuit
EV1313
FR=4.81E-07
Q=4.81000E-7
External Overheating
EV1314
FR=1E-06
Q=9.99999E-7

(Continued)

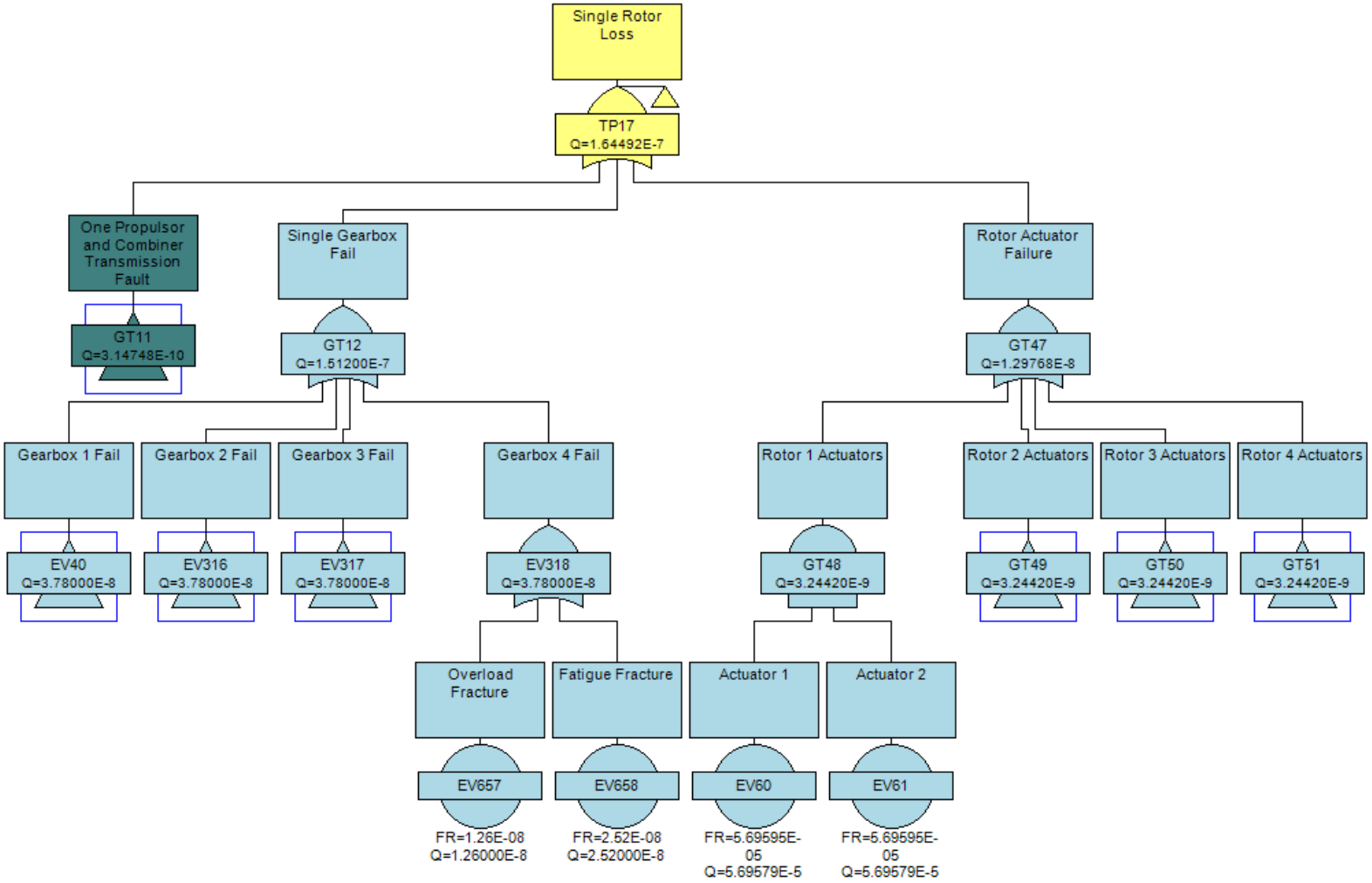
Single Rotor Loss
TP17
Q=1.64492E-7
One Propulsor and Combiner Transmission Fault
Single Gearbox Fail
Rotor Actuator Failure
GT11
Q=3.14748E-10
GT12
Q=1.51200E-7
GT47
Q=1.29768E-8
Gearbox 1 Fail
Gearbox 2 Fail
Gearbox 3 Fail
Gearbox 4 Fail
Rotor 1 Actuators
Rotor 2 Actuators
Rotor 3 Actuators
Rotor 4 Actuators
EV40
Q=3.78000E-8
EV316
Q=3.78000E-8
EV317
Q=3.78000E-8
EV318
Q=3.78000E-8
GT48
Q=3.24420E-9
GT49
Q=3.24420E-9
GT50
Q=3.24420E-9
GT51
Q=3.24420E-9
Overload Fracture
Fatigue Fracture
Actuator 1
Actuator 2
EV657
EV658
EV60
EV61
FR=1.26E-08
Q=1.26000E-8
FR=2.52E-08
Q=2.52000E-8
FR=5.69595E-05
Q=5.69579E-5
FR=5.69595E-05
Q=5.69579E-5

(Continued)

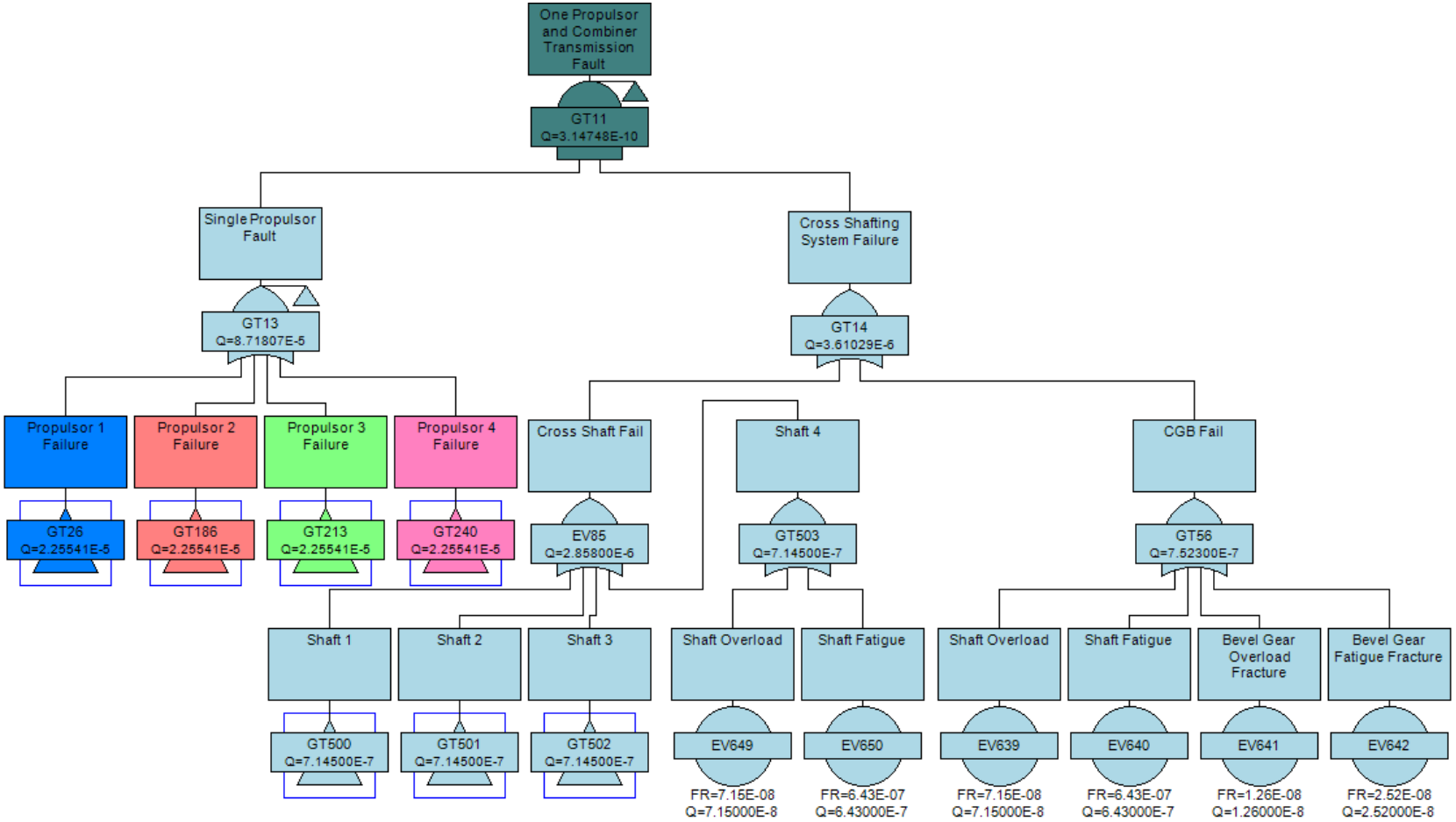
One Propulsor and Combiner Transmission Fault
GT11
Q=3.14748E-10
Single Propulsor Fault
Cross Shafting System Failure
GT13
Q=8.71807E-5
GT14
Q=3.61029E-6
Propulsor 1 Failure
Propulsor 2 Failure
Propulsor 3 Failure
Propulsor 4 Failure
Cross Shaft Fail
Shaft 4
CGB Fail
GT26
Q=2.25541E-5
GT186
Q=2.25541E-5
GT213
Q=2.25541E-5
GT240
Q=2.25541E-5
EV85
Q=2.85800E-6
GT503
Q=7.14500E-7
GT56
Q=7.52300E-7
Shaft 1
Shaft 2
Shaft 3
Shaft Overload
Shaft Fatigue
Shaft Overload
Shaft Fatigue
Bevel Gear Overload Fracture
Bevel Gear Fatigue Fracture
GT500
Q=7.14500E-7
GT501
Q=7.14500E-7
GT502
Q=7.14500E-7
EV649
EV650
EV639
EV640
EV641
EV642
FR=7.15E-08
Q=7.15000E-8
FR=6.43E-07
Q=6.43000E-7
FR=7.15E-08
Q=7.15000E-8
FR=6.43E-07
Q=6.43000E-7
FR=1.26E-08
Q=1.26000E-8
FR=2.52E-08
Q=2.52000E-8

Appendix C - Figure 2: Quadcopter Hybrid FTA

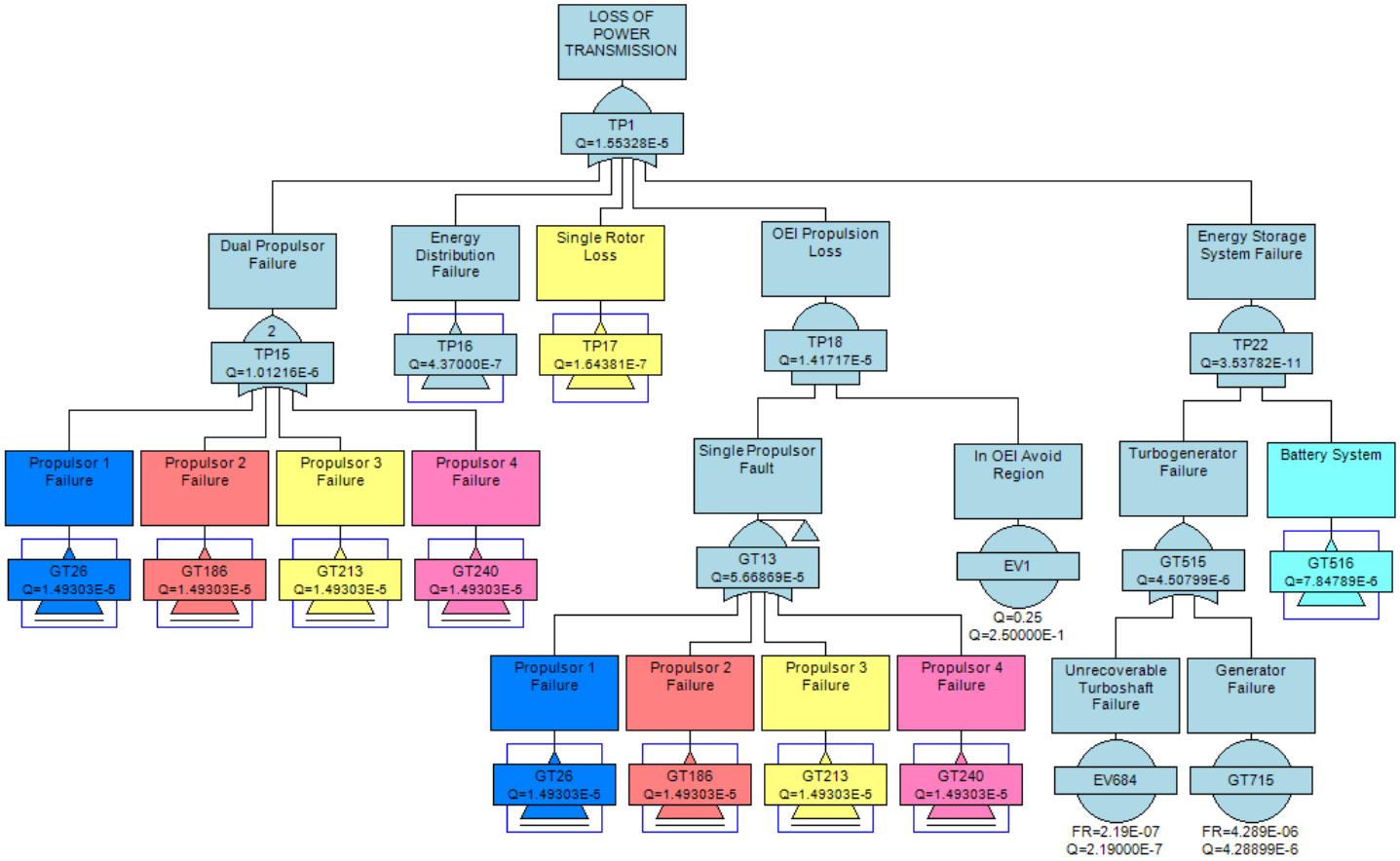

(Quadcopter Hybrid FTA Continued)

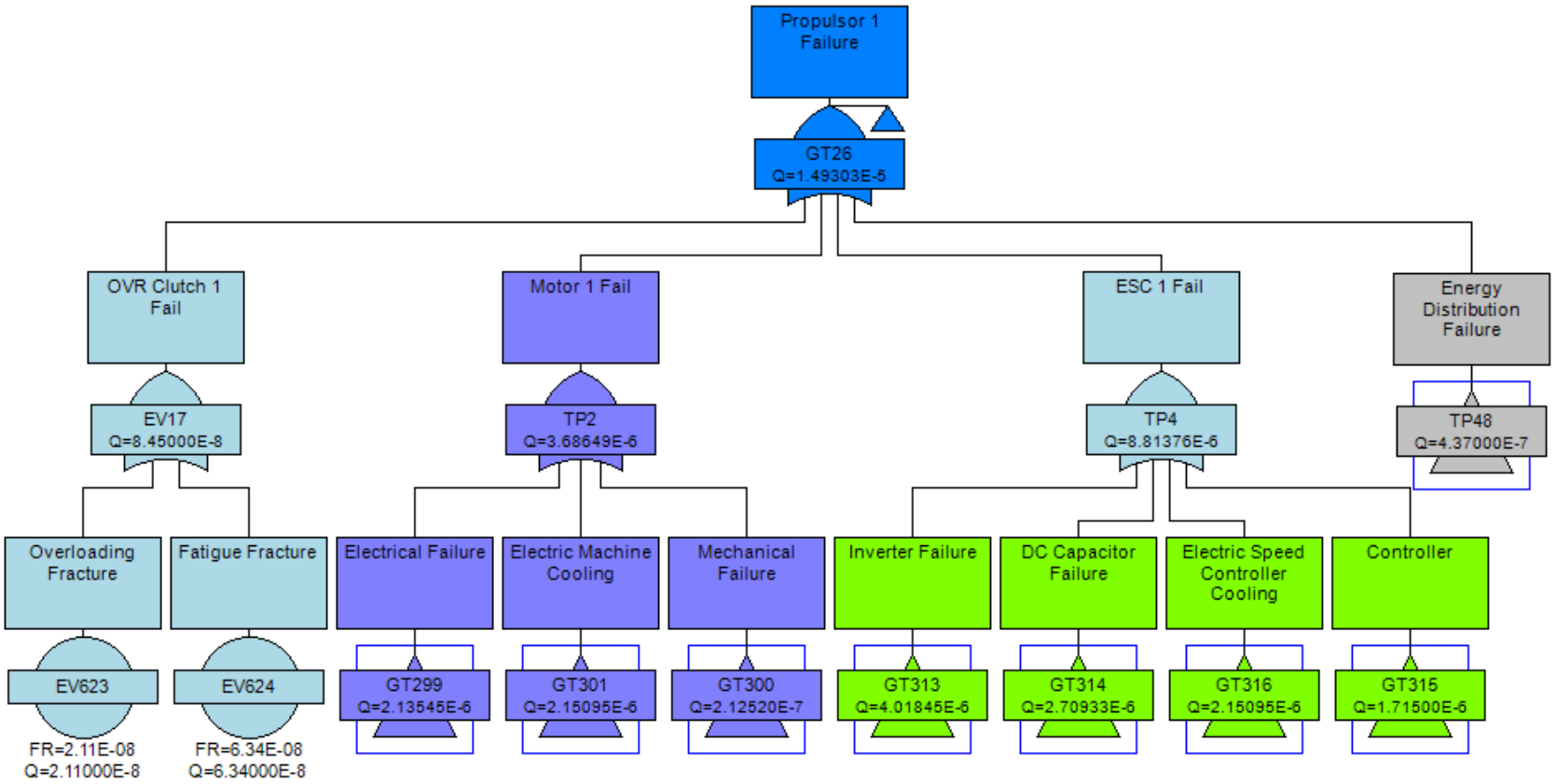

(Quadcopter Hybrid FTA Continued)

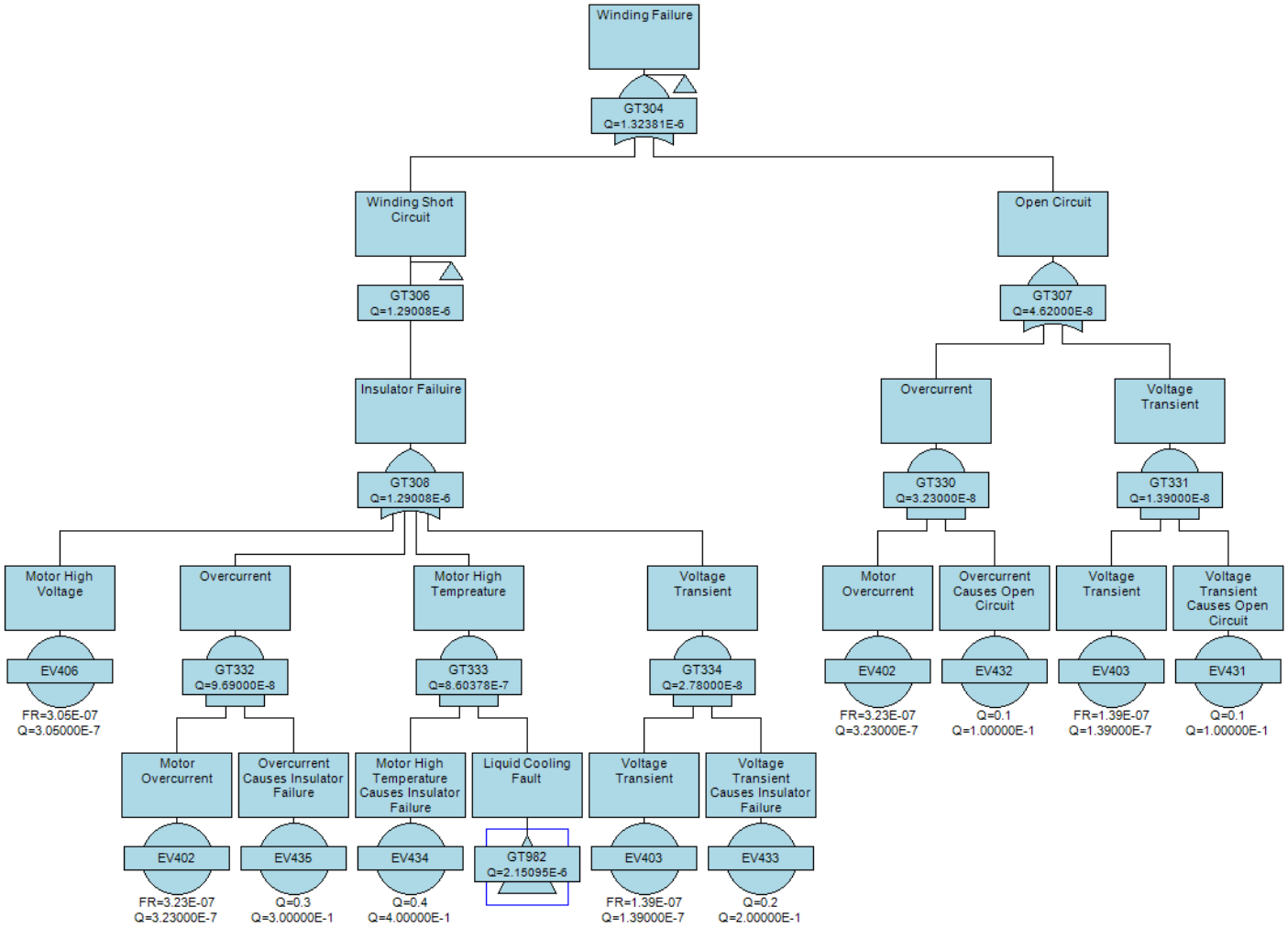

(Quadcopter Hybrid FTA Continued)

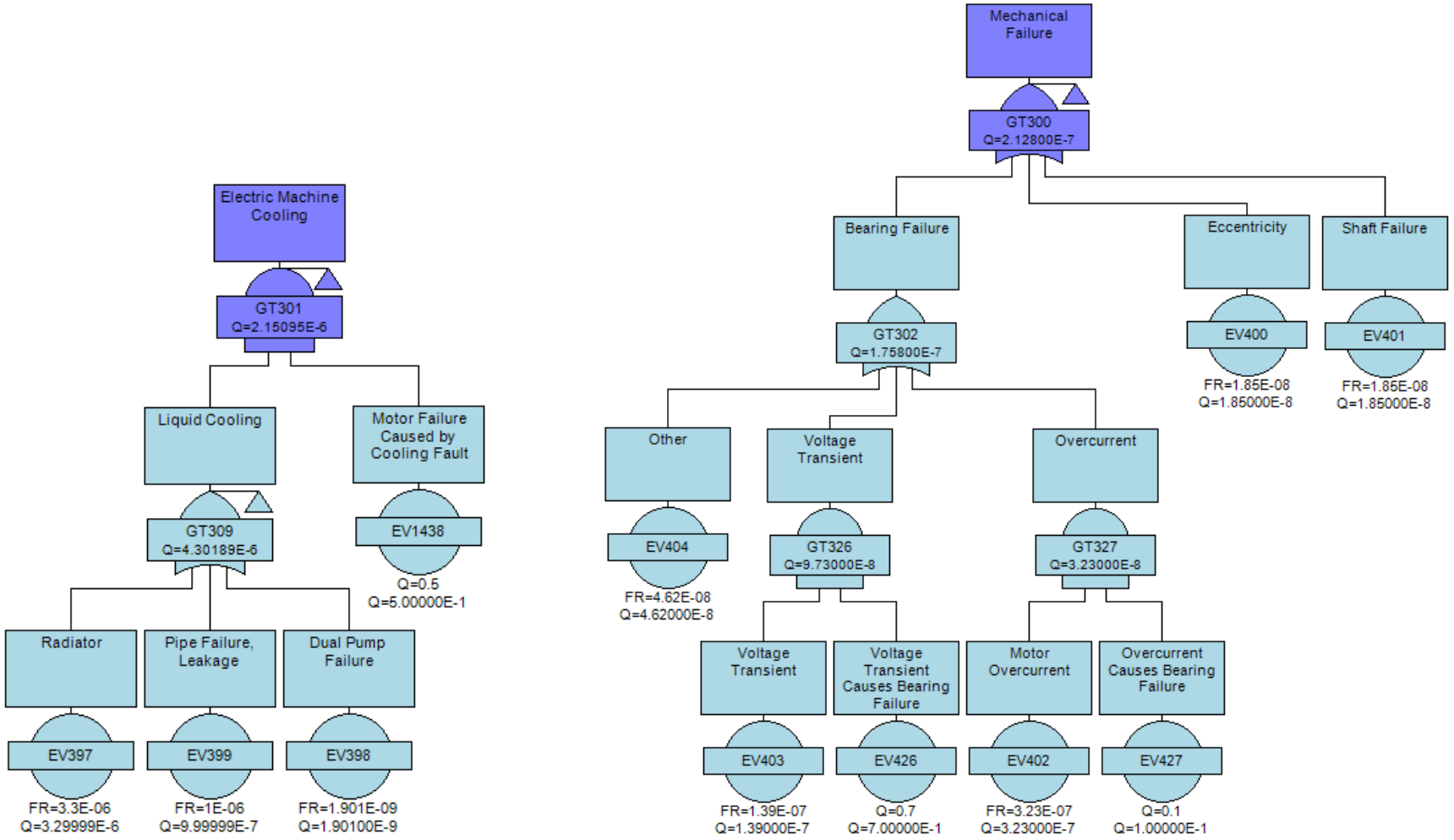

(Quadcopter Hybrid FTA Continued)

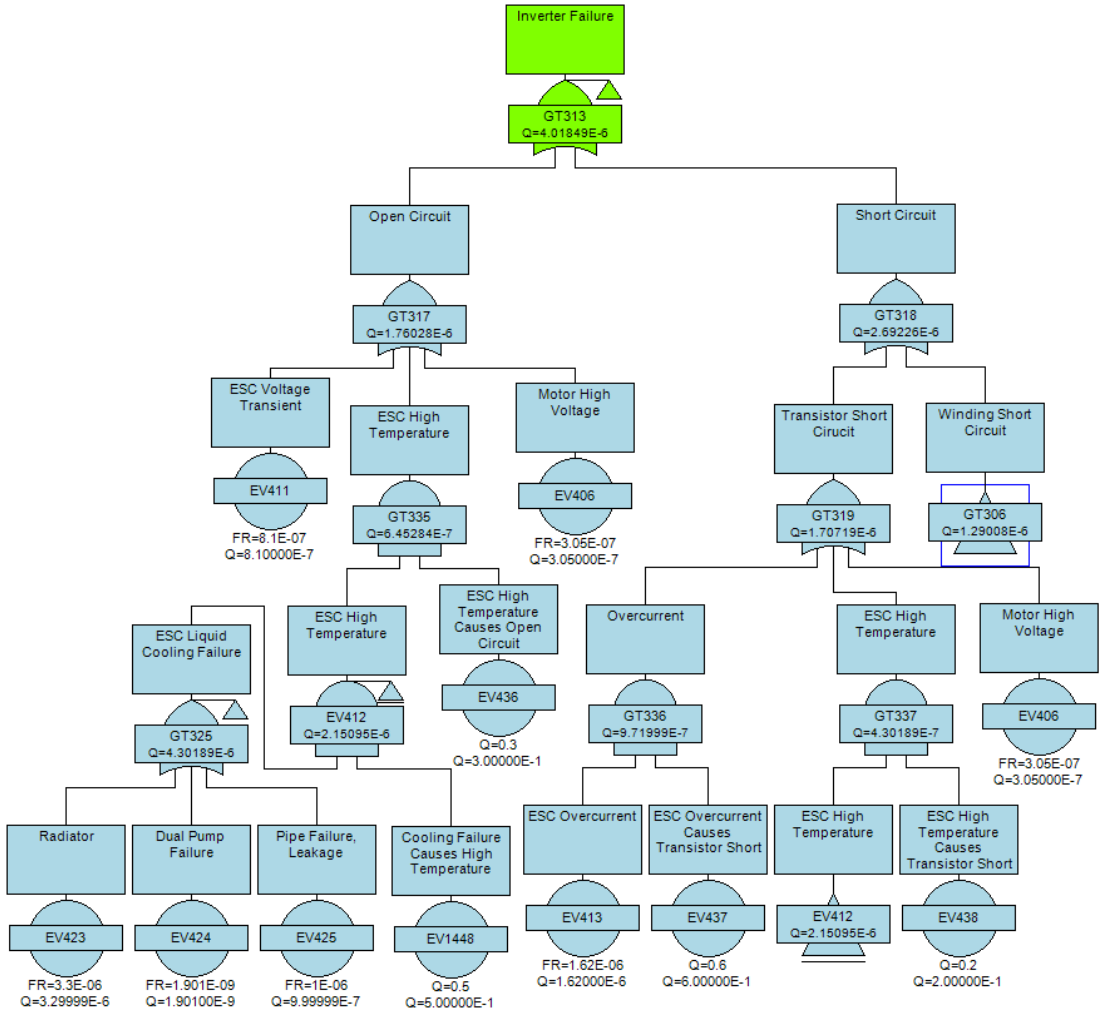

(Quadcopter Hybrid FTA Continued)

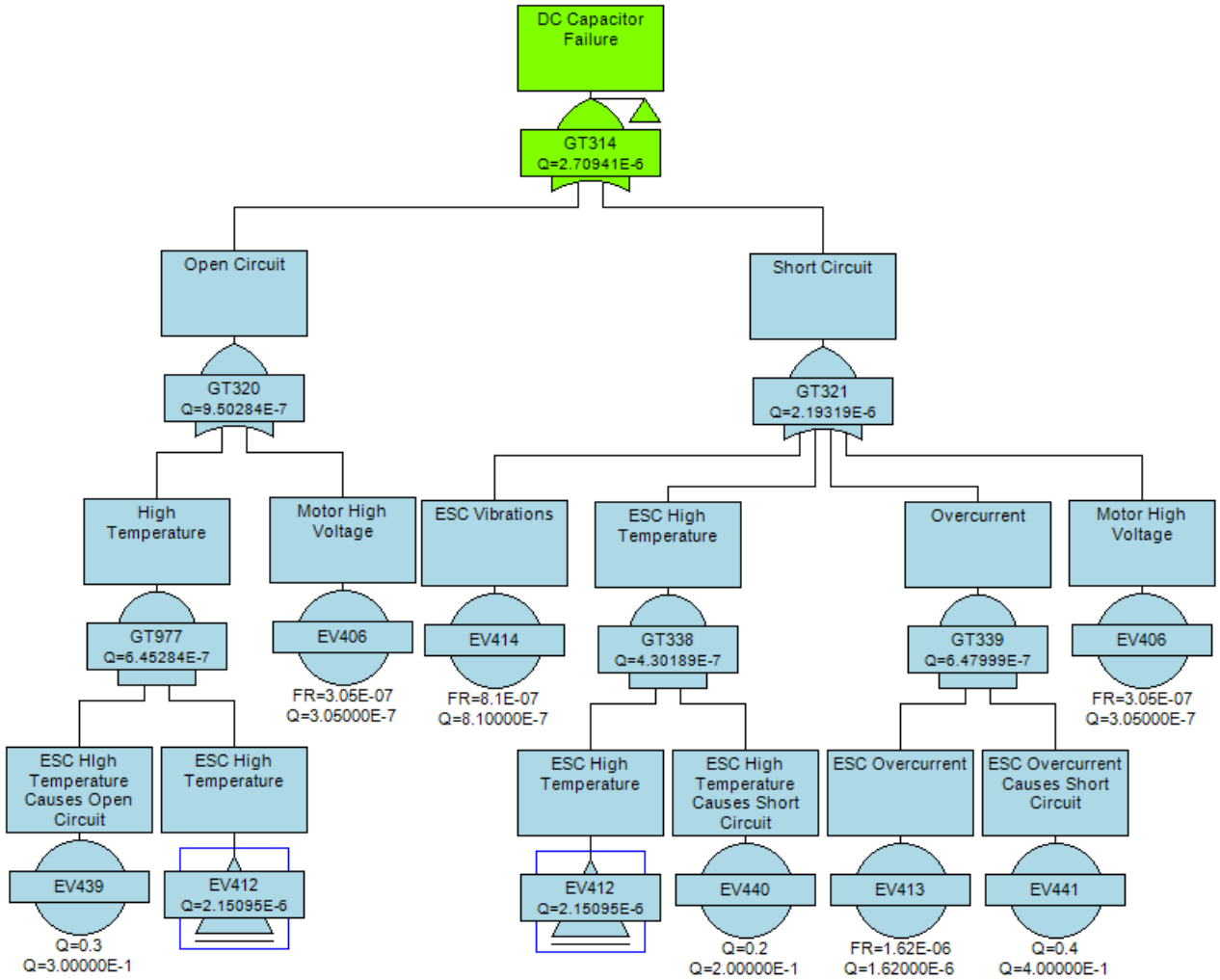

(Quadcopter Hybrid FTA Continued)

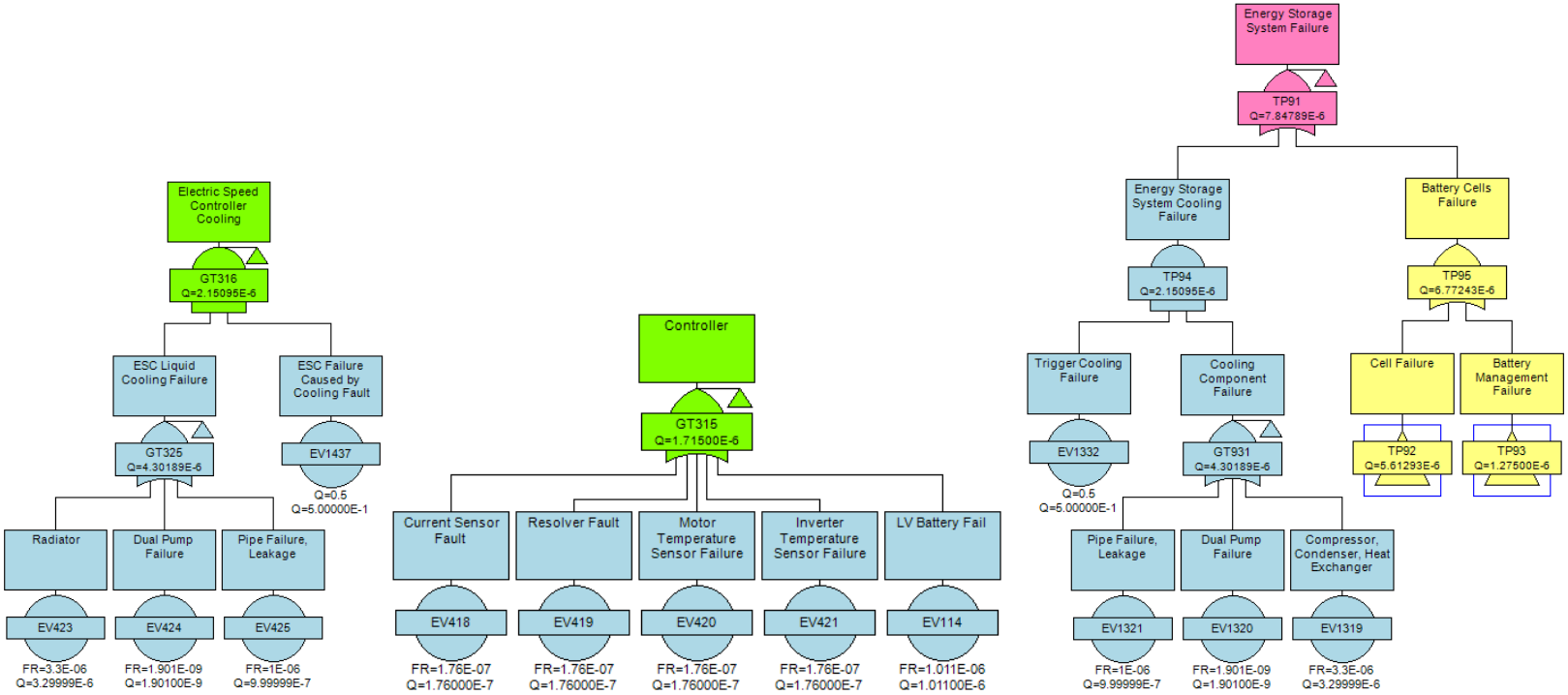

(Quadcopter Hybrid FTA Continued)

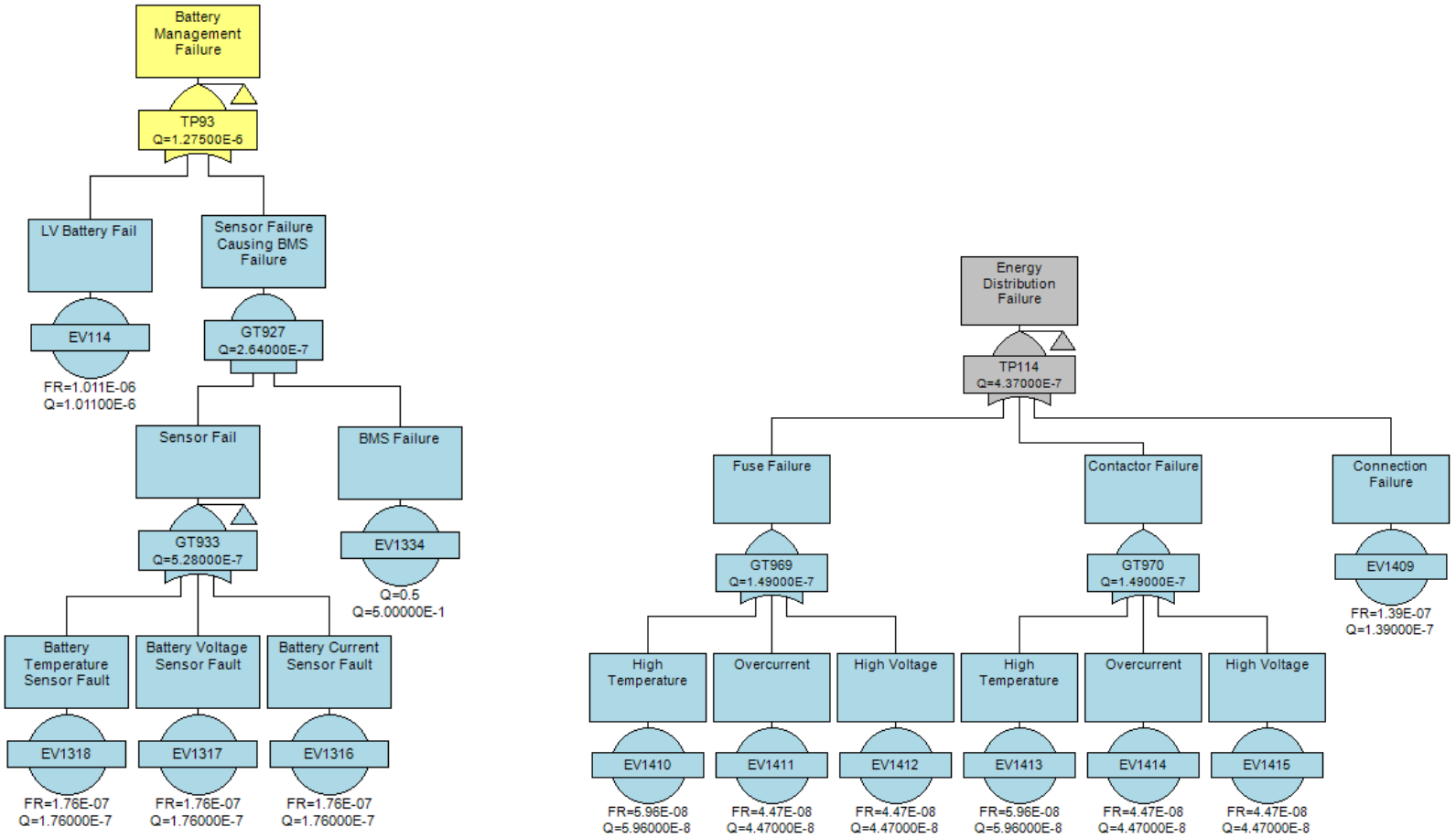

(Quadcopter Hybrid FTA Continued)

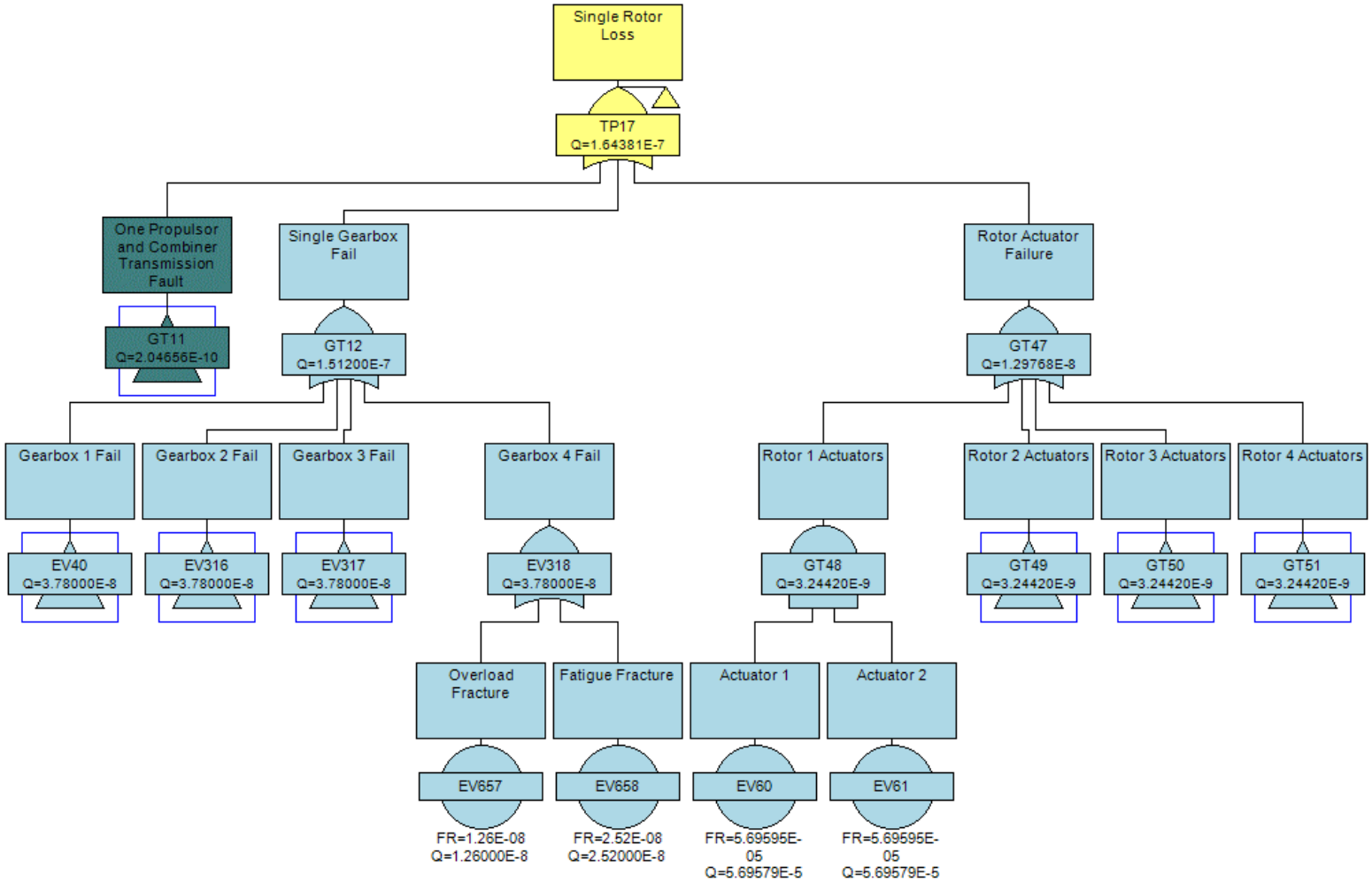

(Quadcopter Hybrid FTA Continued)

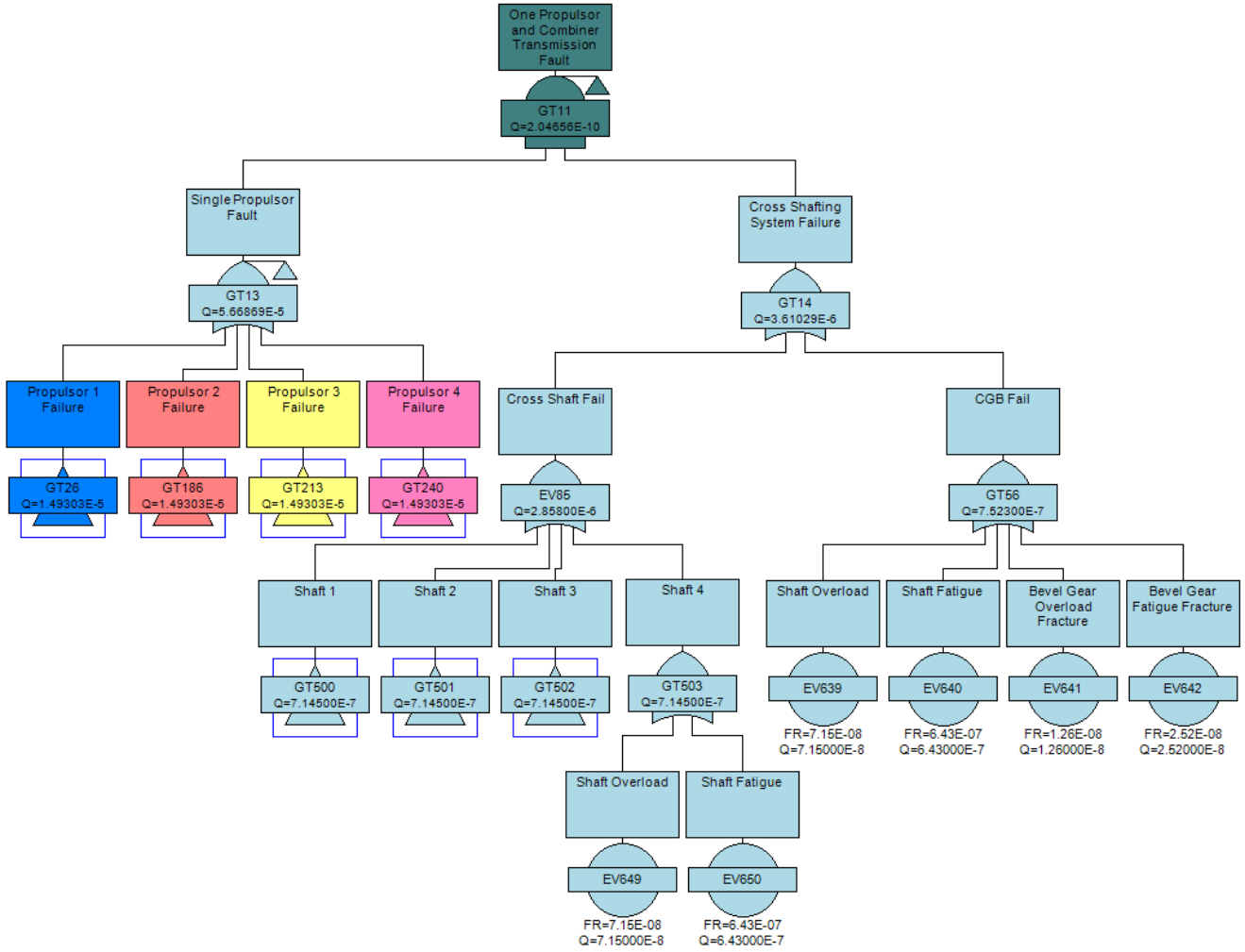

(Quadcopter Hybrid FTA Continued)

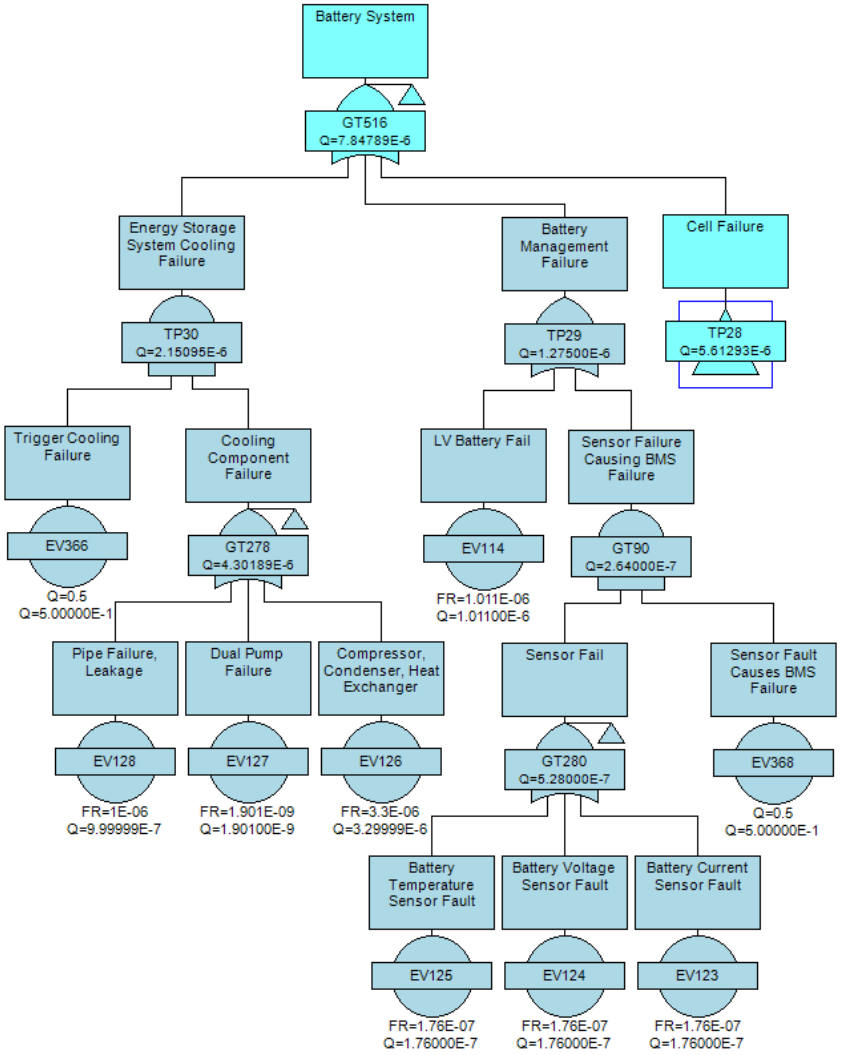

(Quadcopter Hybrid FTA Continued)

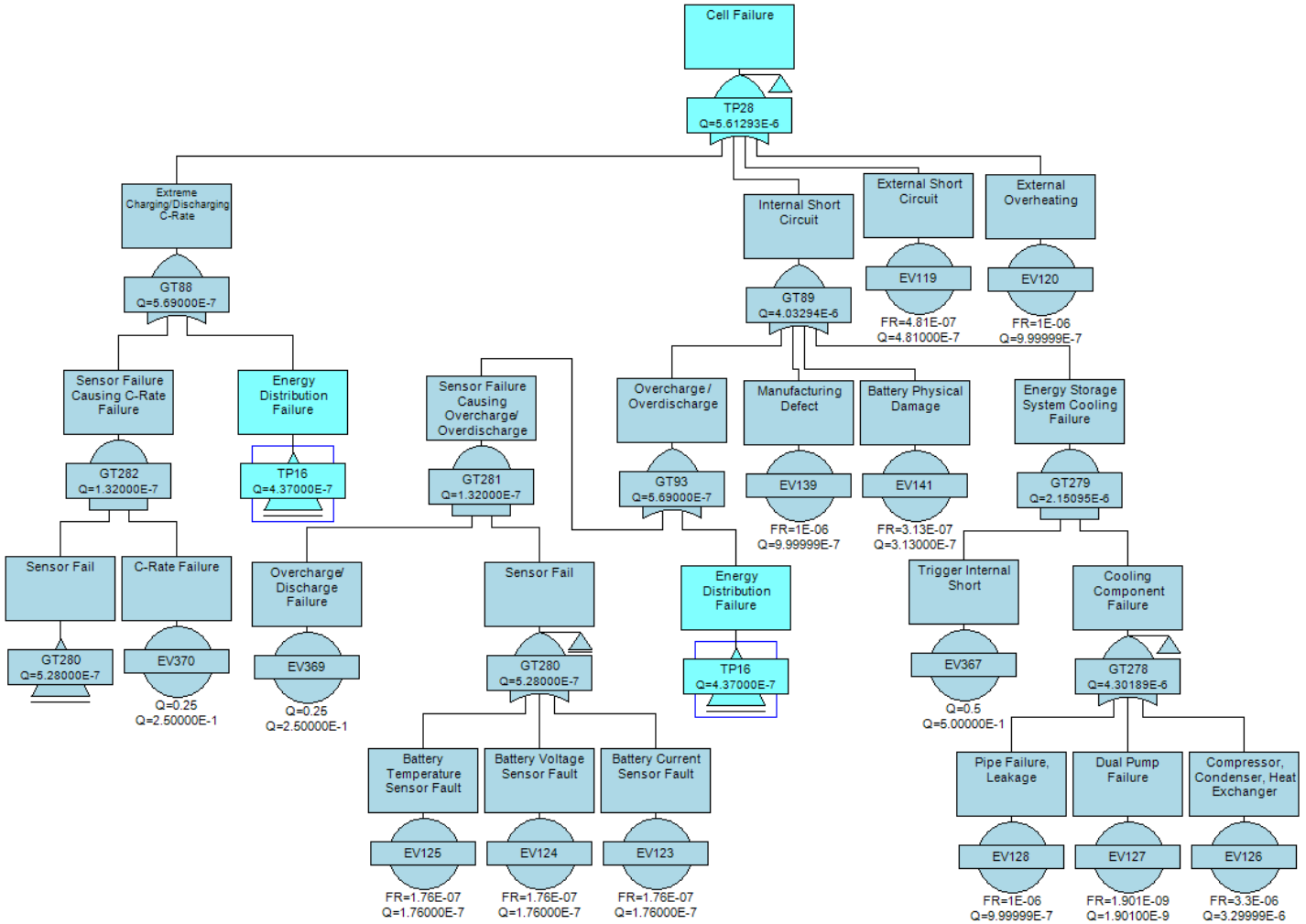

Appendix C - Figure 3: Quadcopter Turboshaft FTA

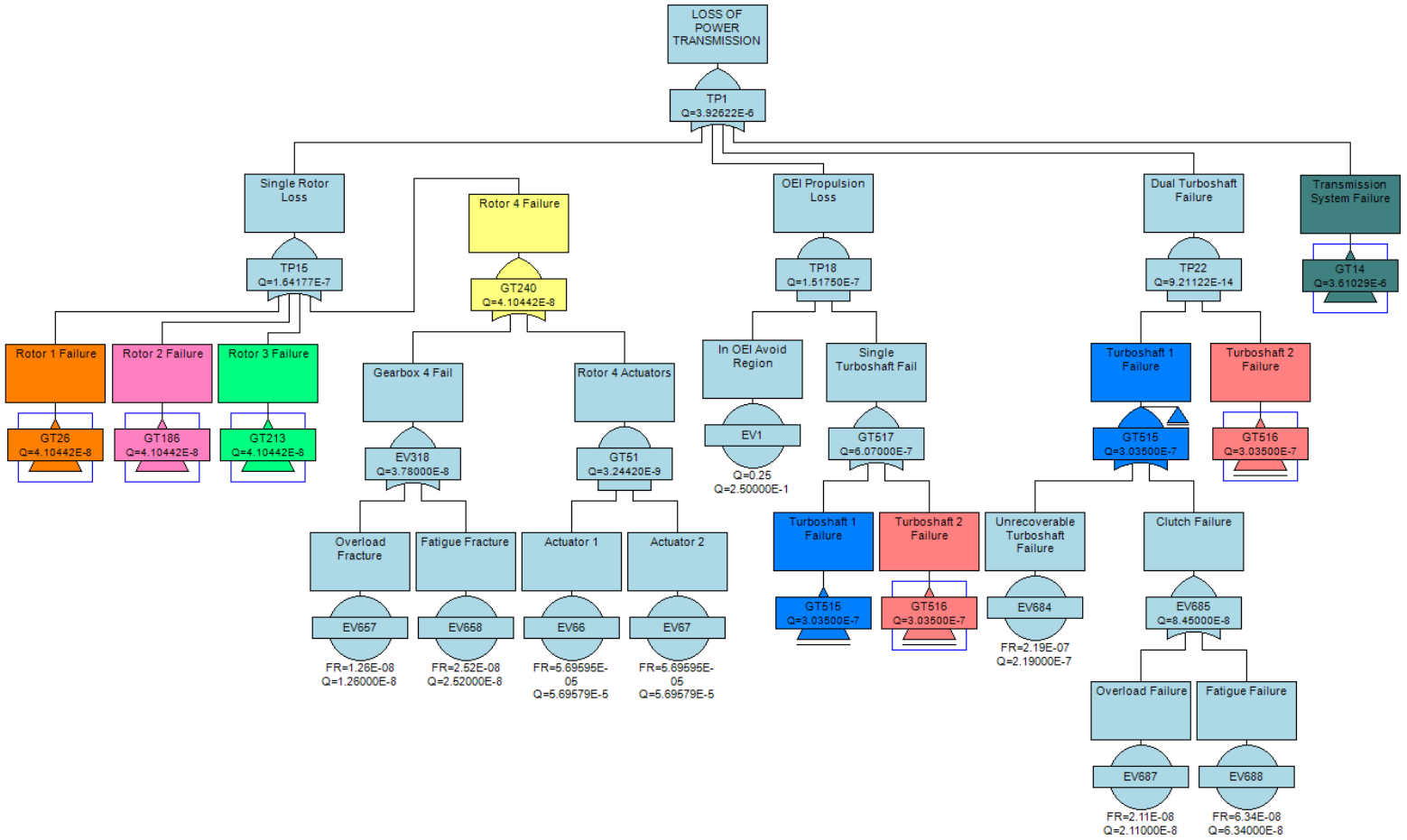

(Quadcopter Turboshaft FTA Continued)

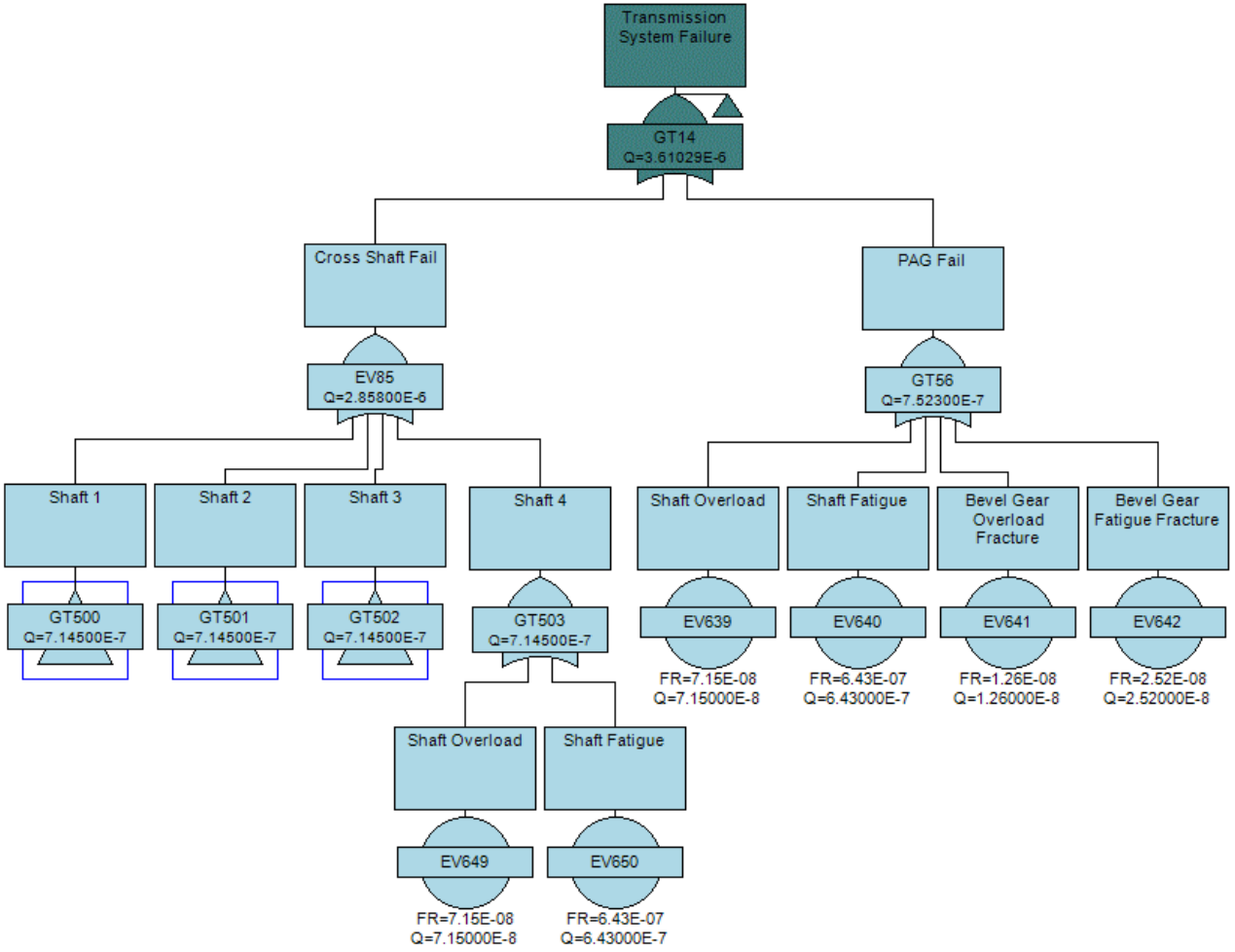

Appendix C - Figure 4: Hexacopter Collective FTA

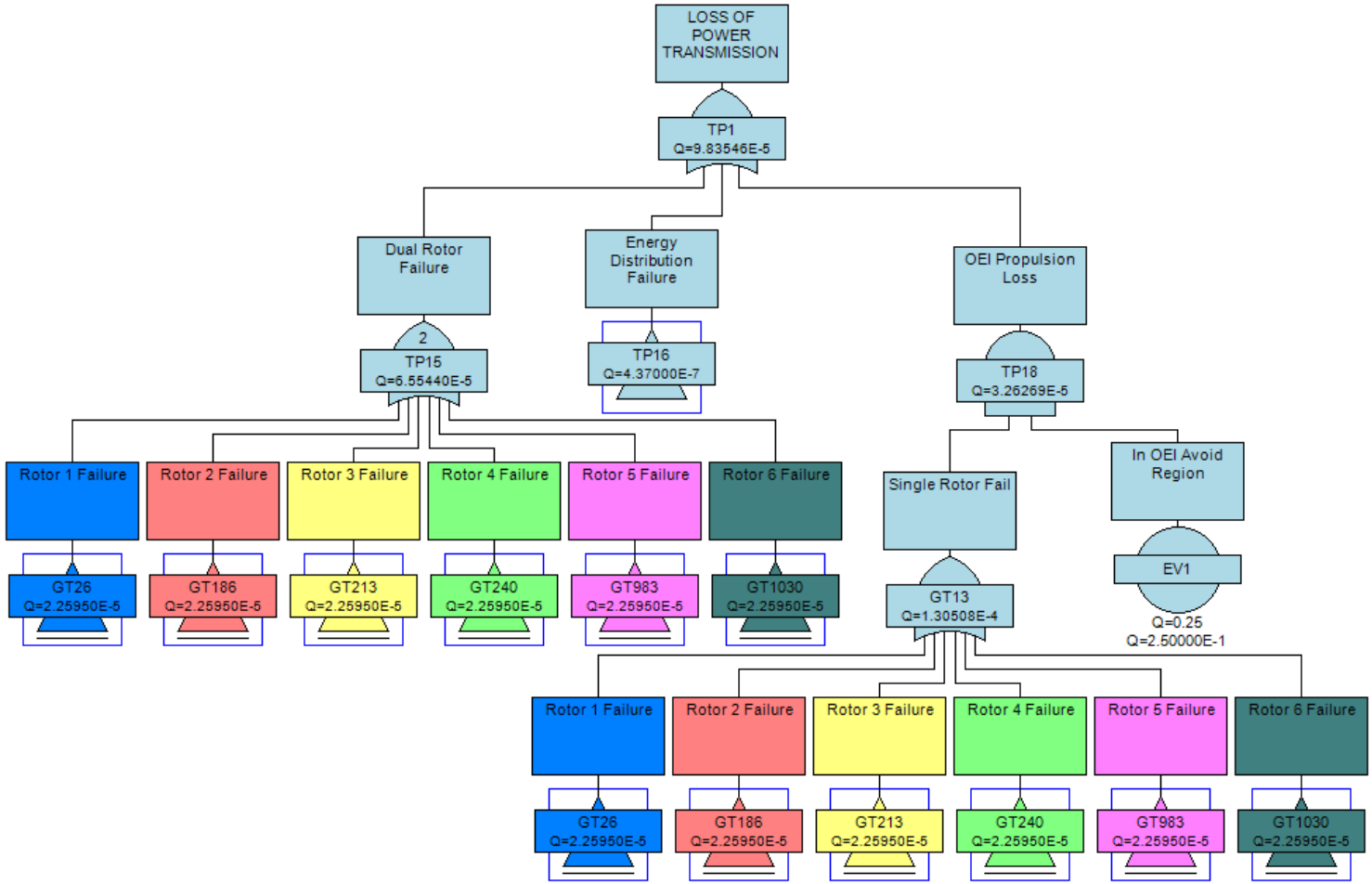

(Hexacopter Collective FTA Continued)

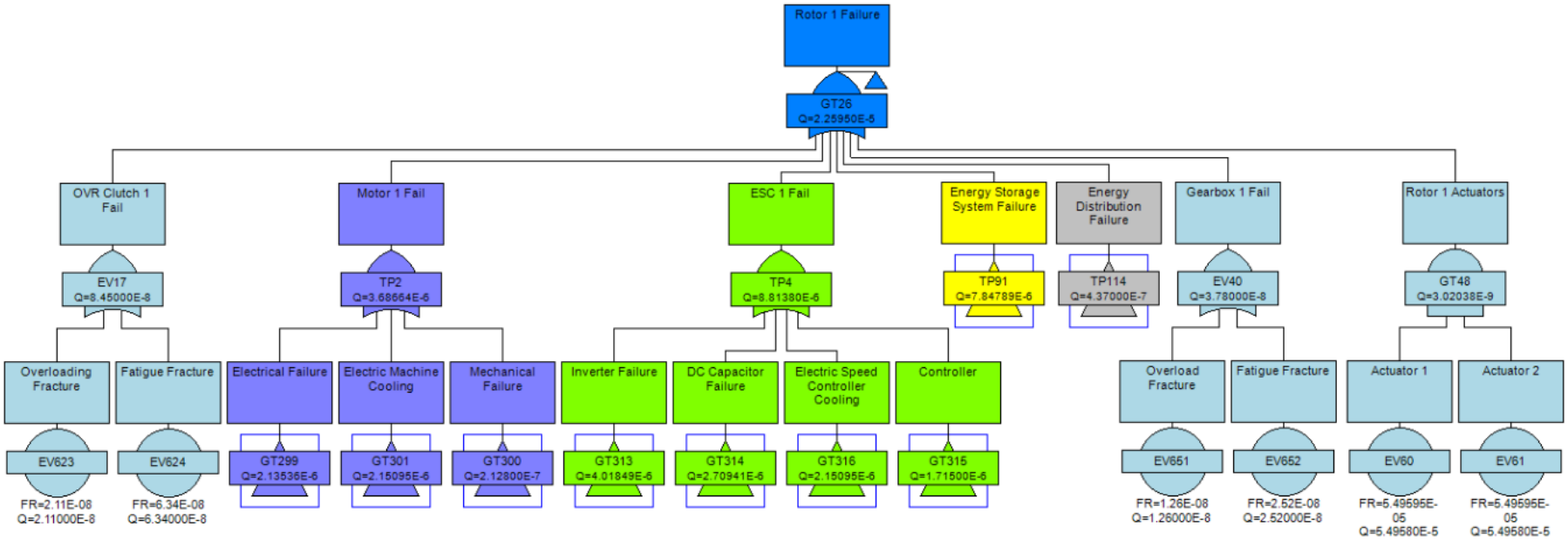

(Hexacopter Collective FTA Continued)

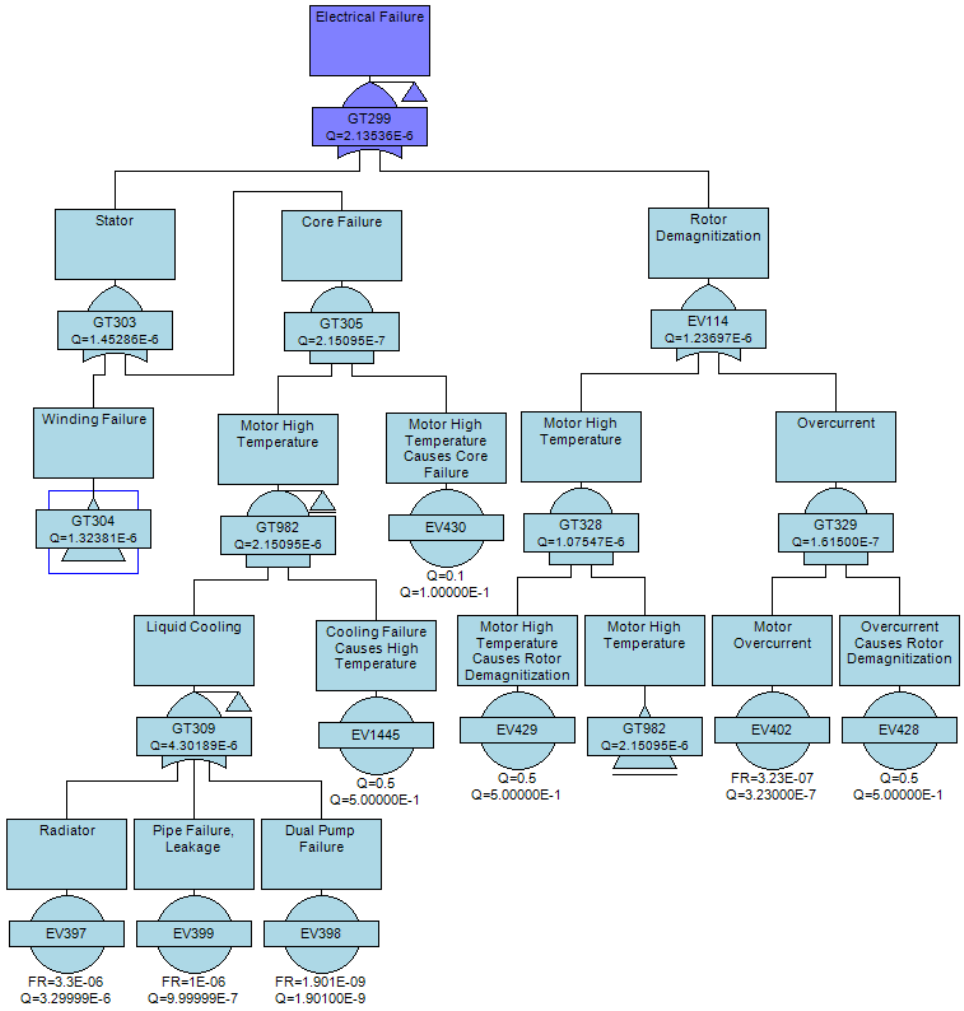

(Hexacopter Collective FTA Continued)

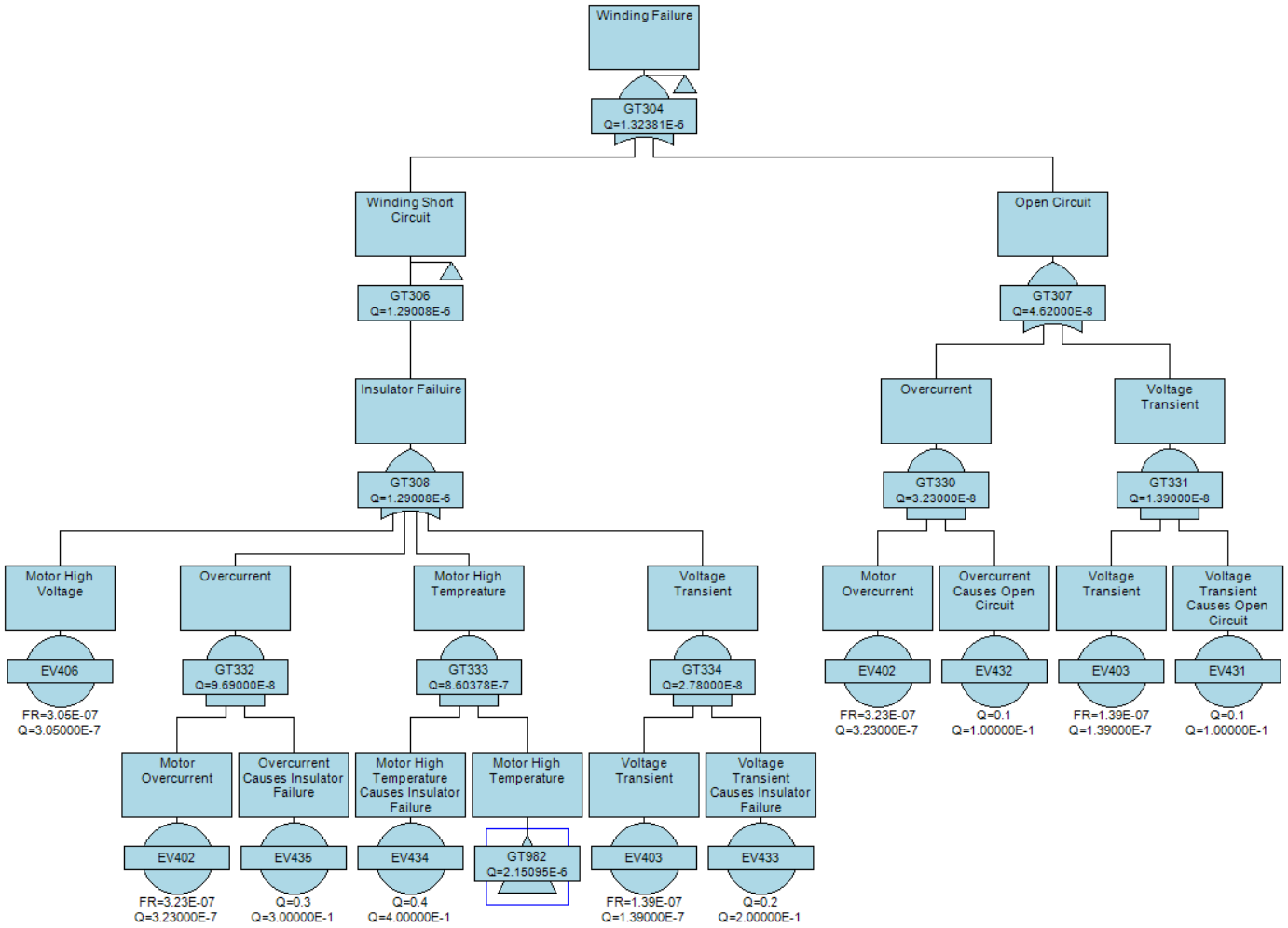

(Hexacopter Collective FTA Continued)

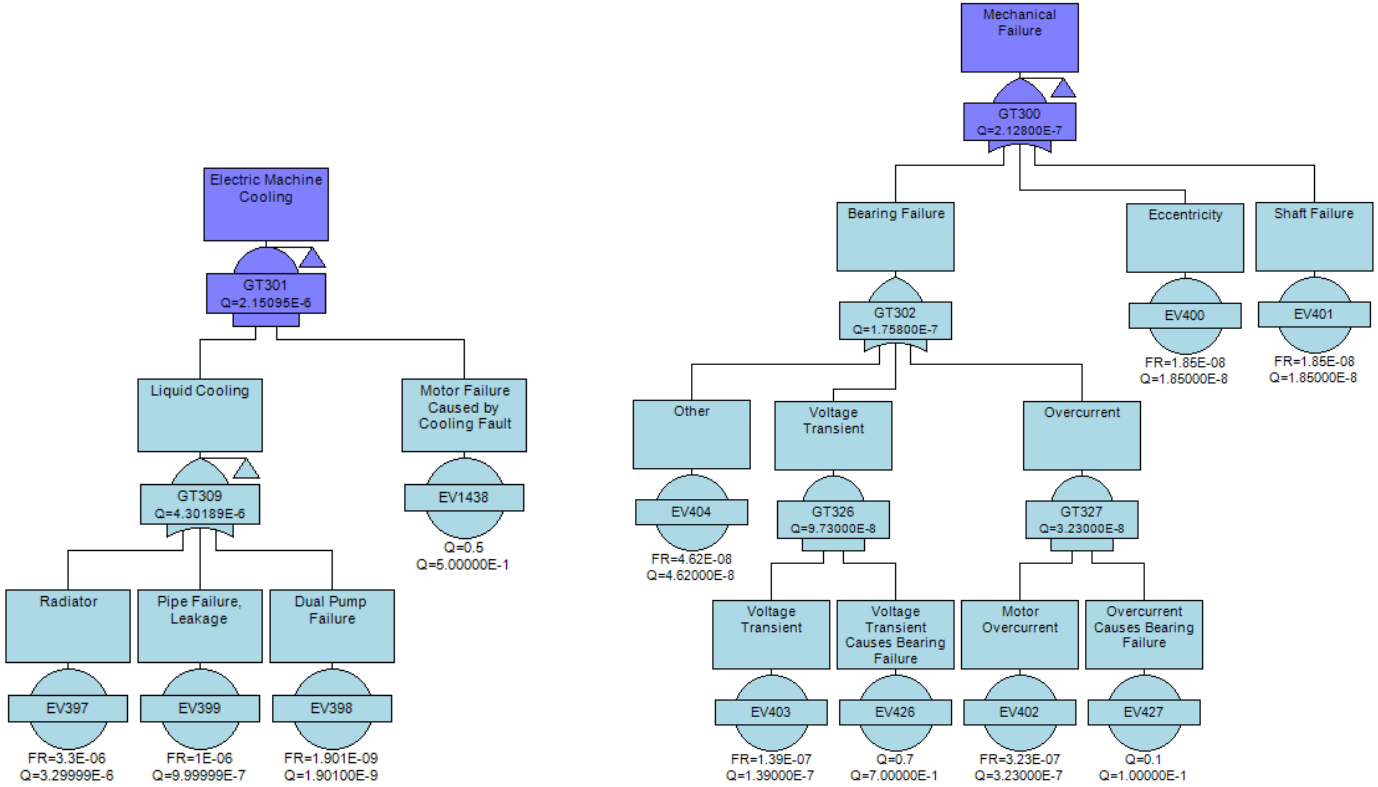

(Hexacopter Collective FTA Continued)

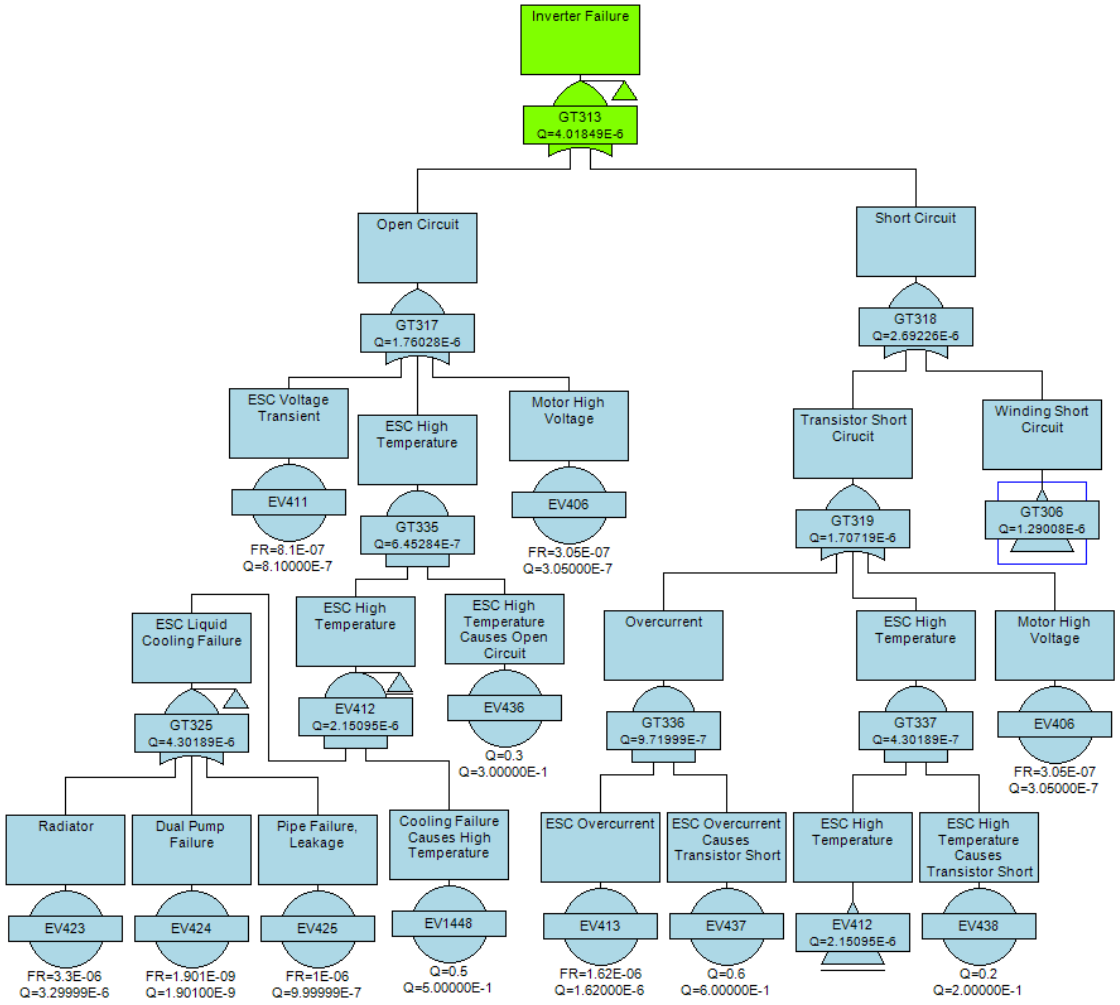

(Hexacopter Collective FTA Continued)

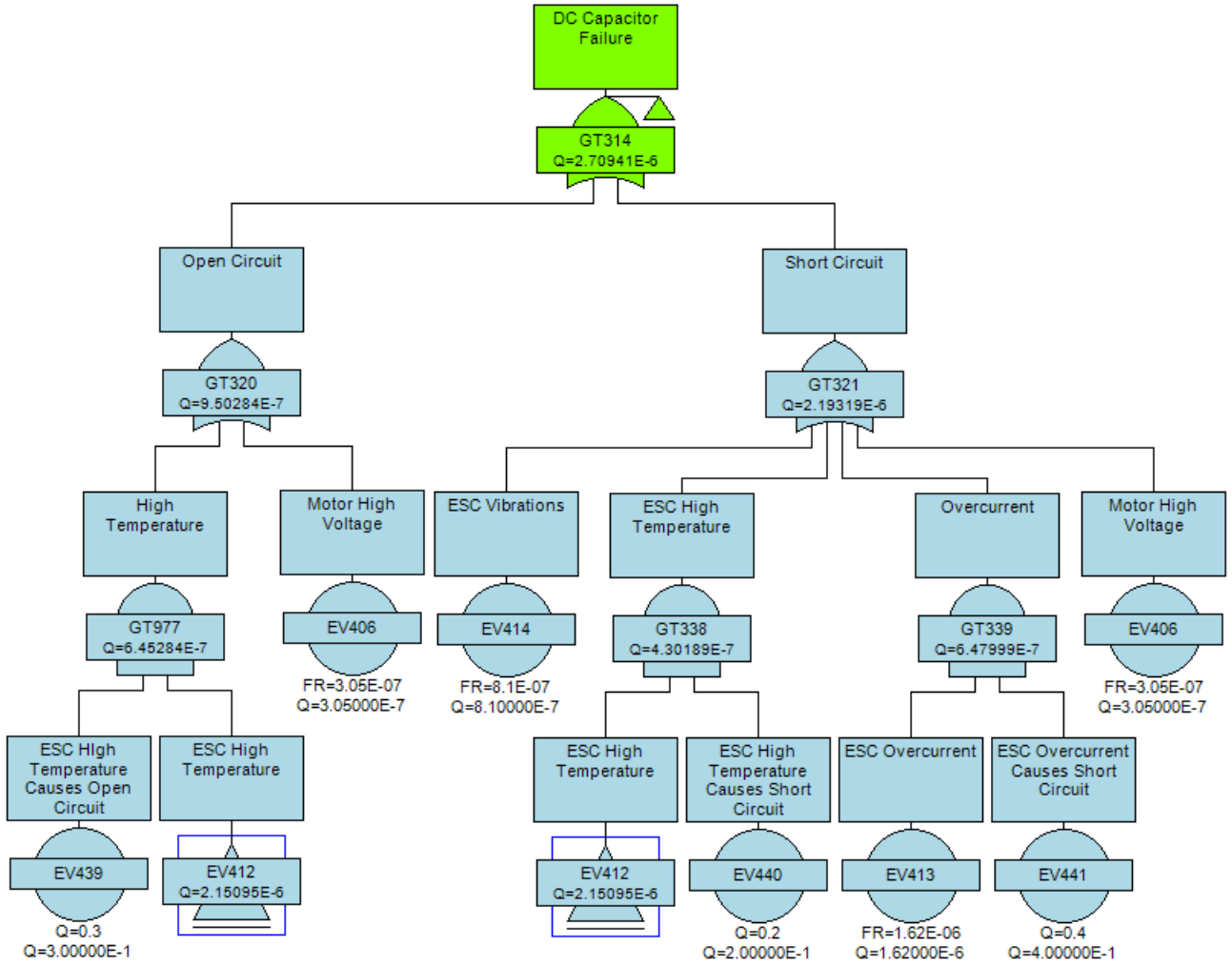

(Hexacopter Collective FTA Continued)

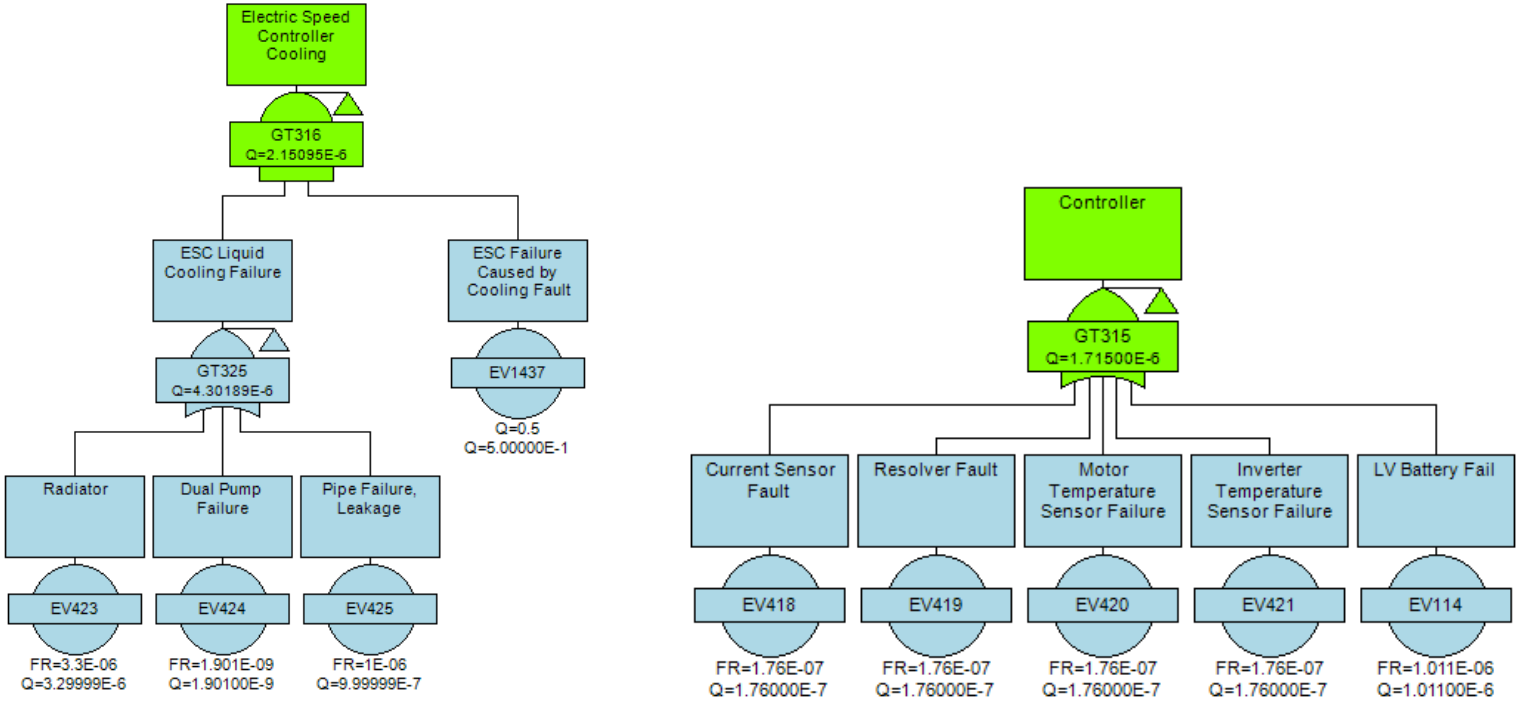

(Hexacopter Collective FTA Continued)

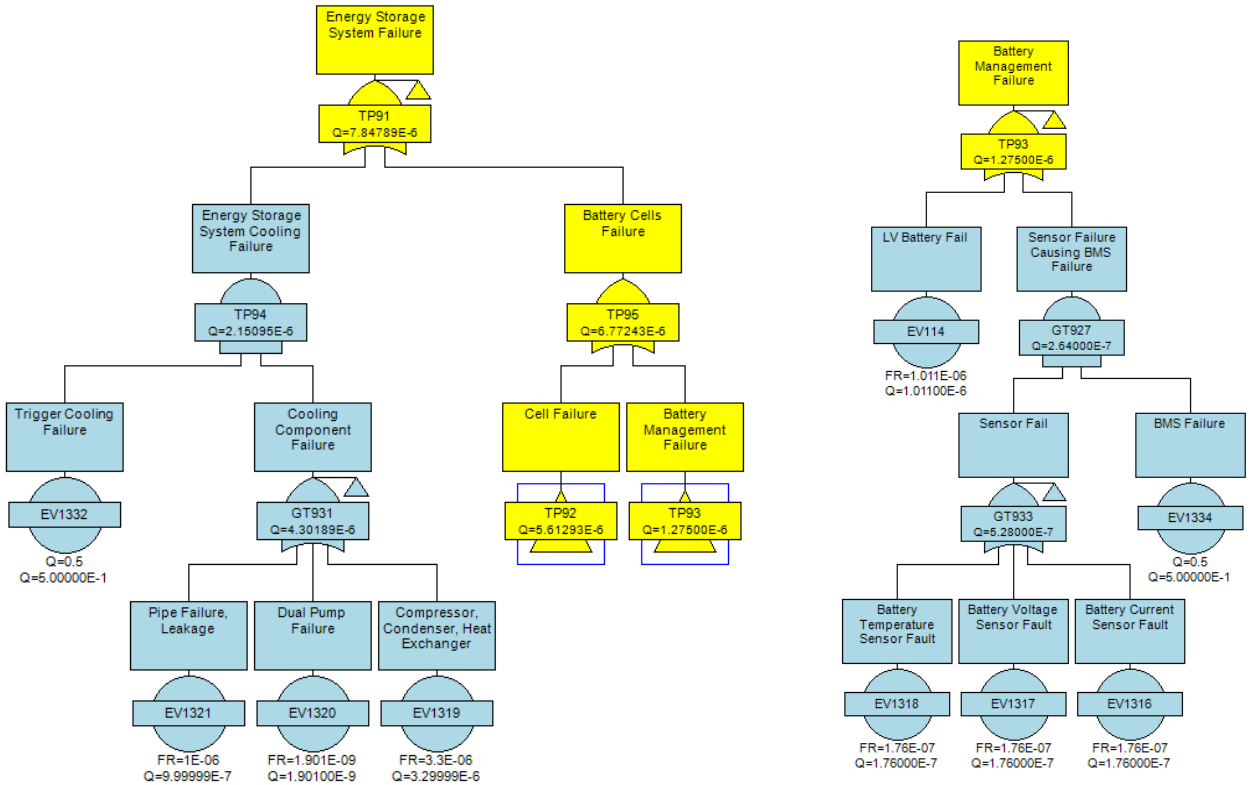

(Hexacopter Collective FTA Continued)

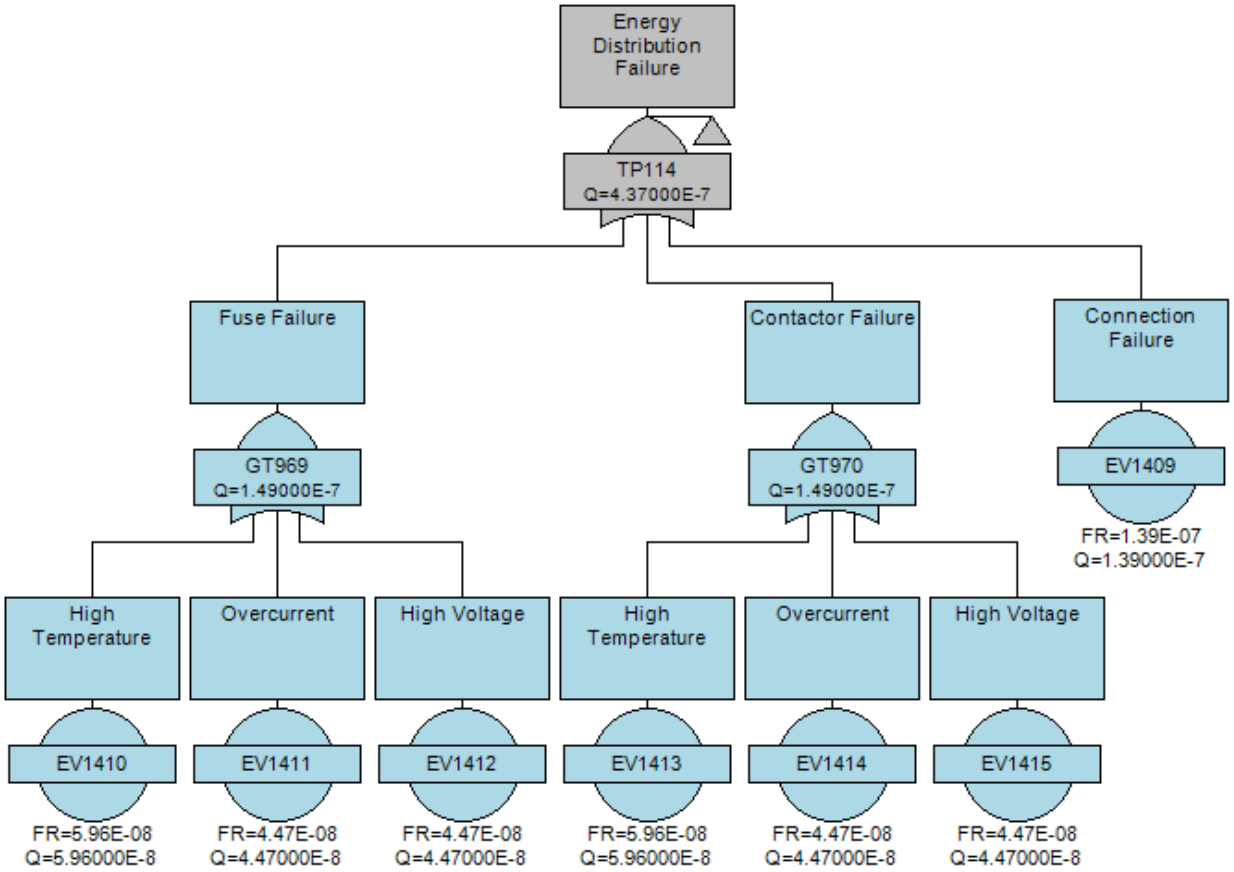

(Hexacopter Collective FTA Continued)

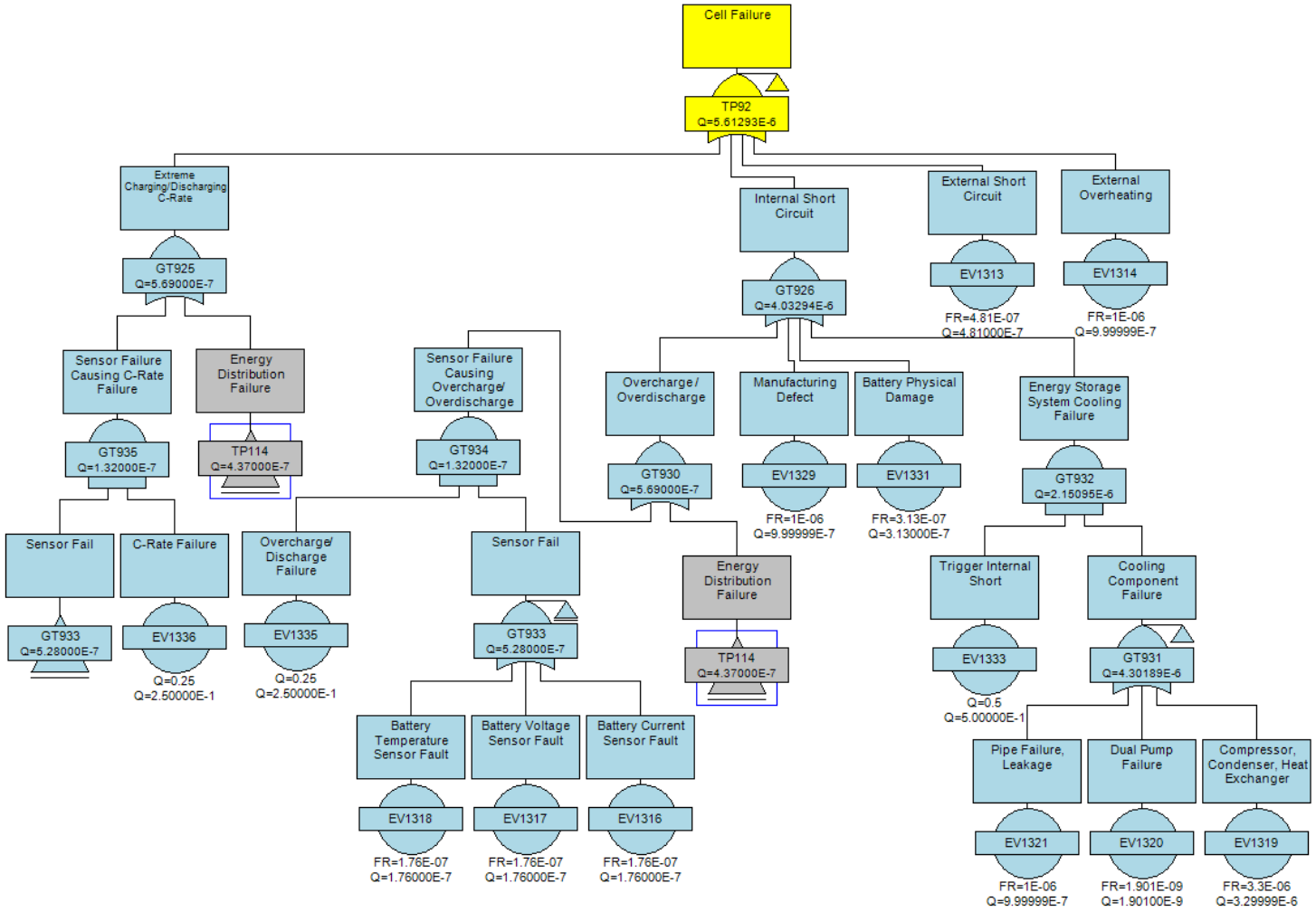

Appendix C - Figure 5: Hexacopter RPM FTA

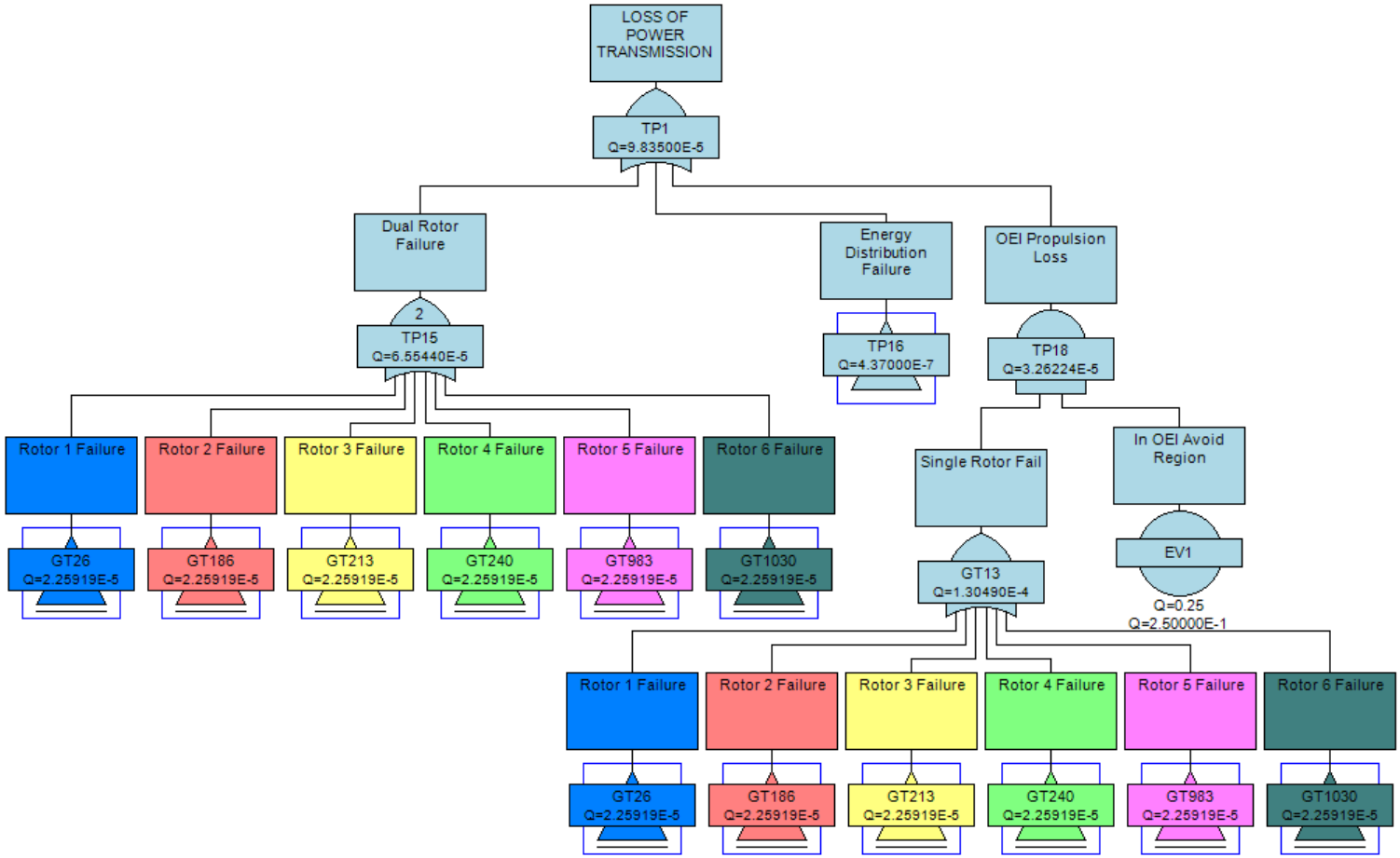

(Hexacopter RPM FTA Continued)

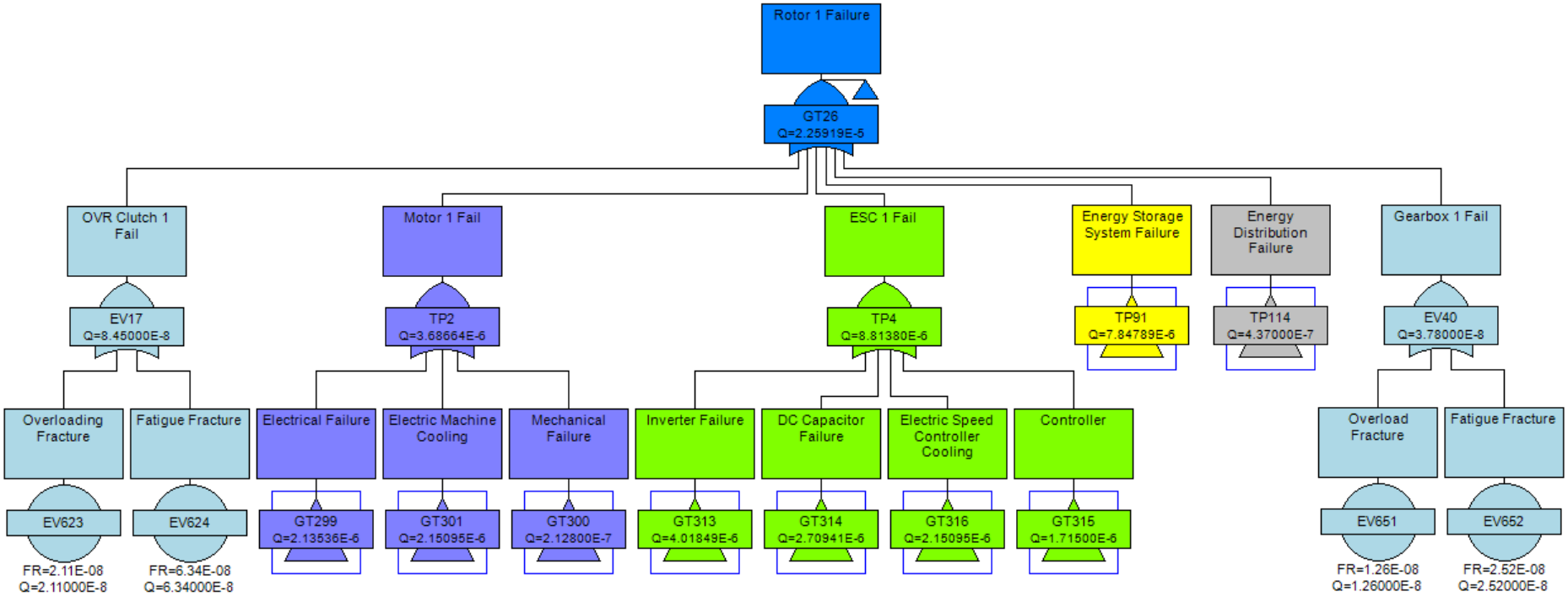

(Hexacopter RPM FTA Continued)

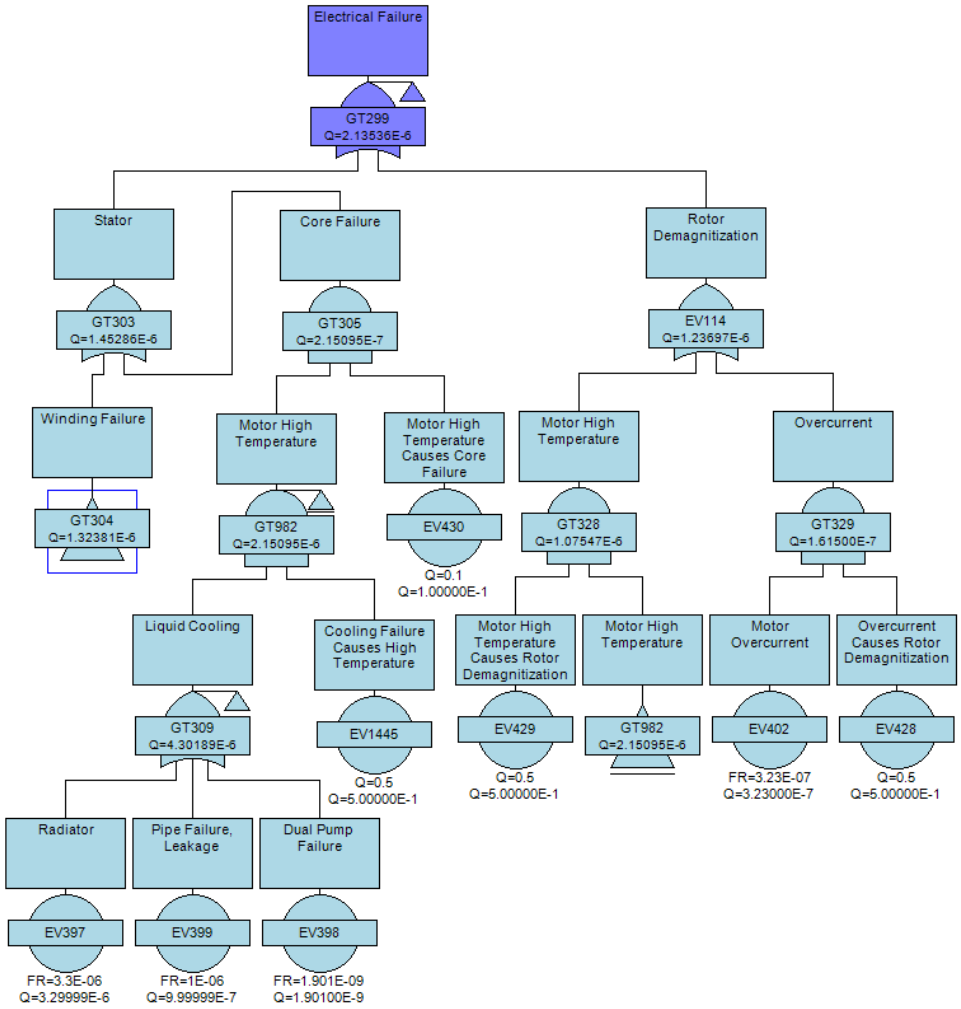

(Hexacopter RPM FTA Continued)

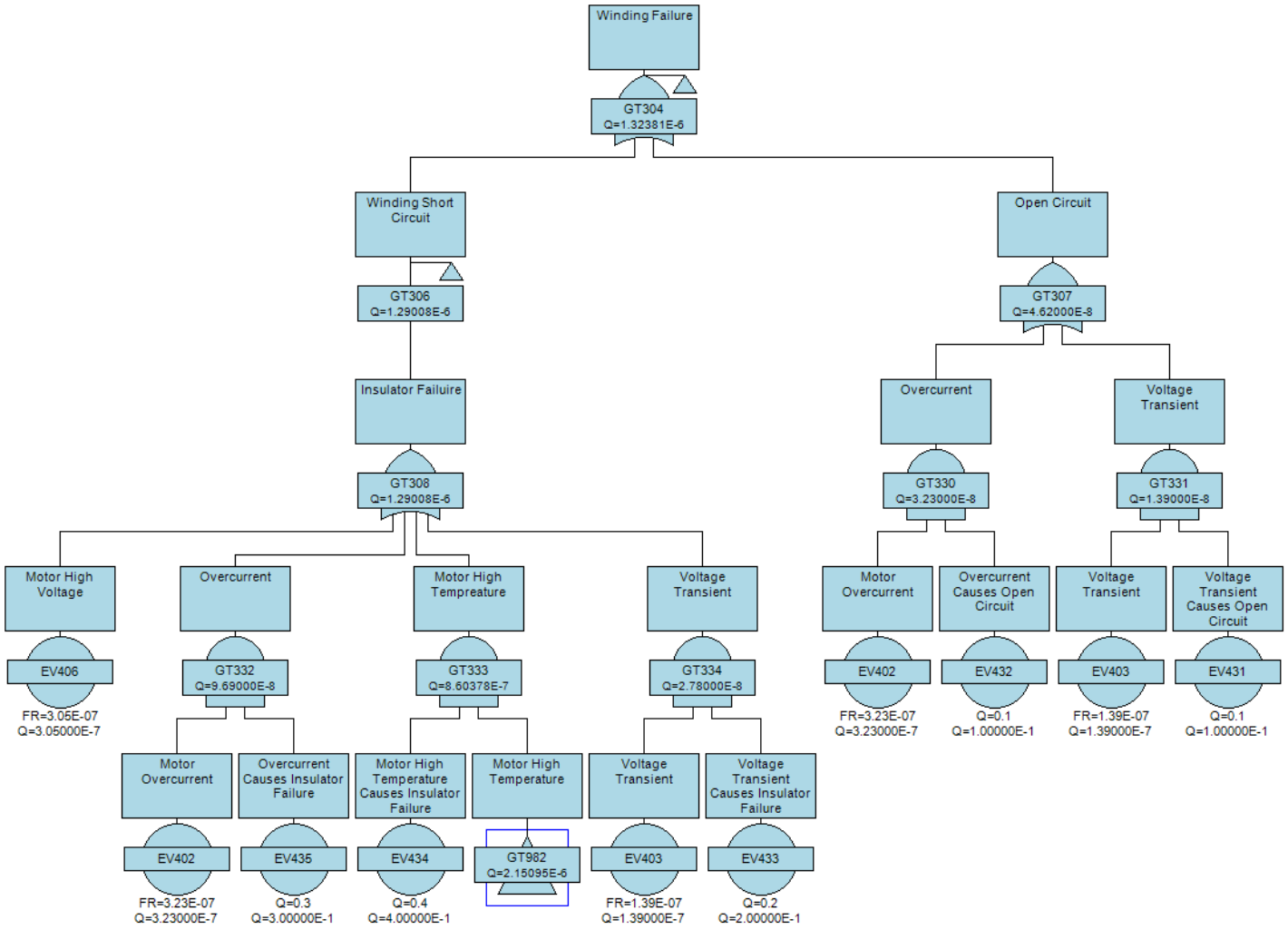

(Hexacopter RPM FTA Continued)

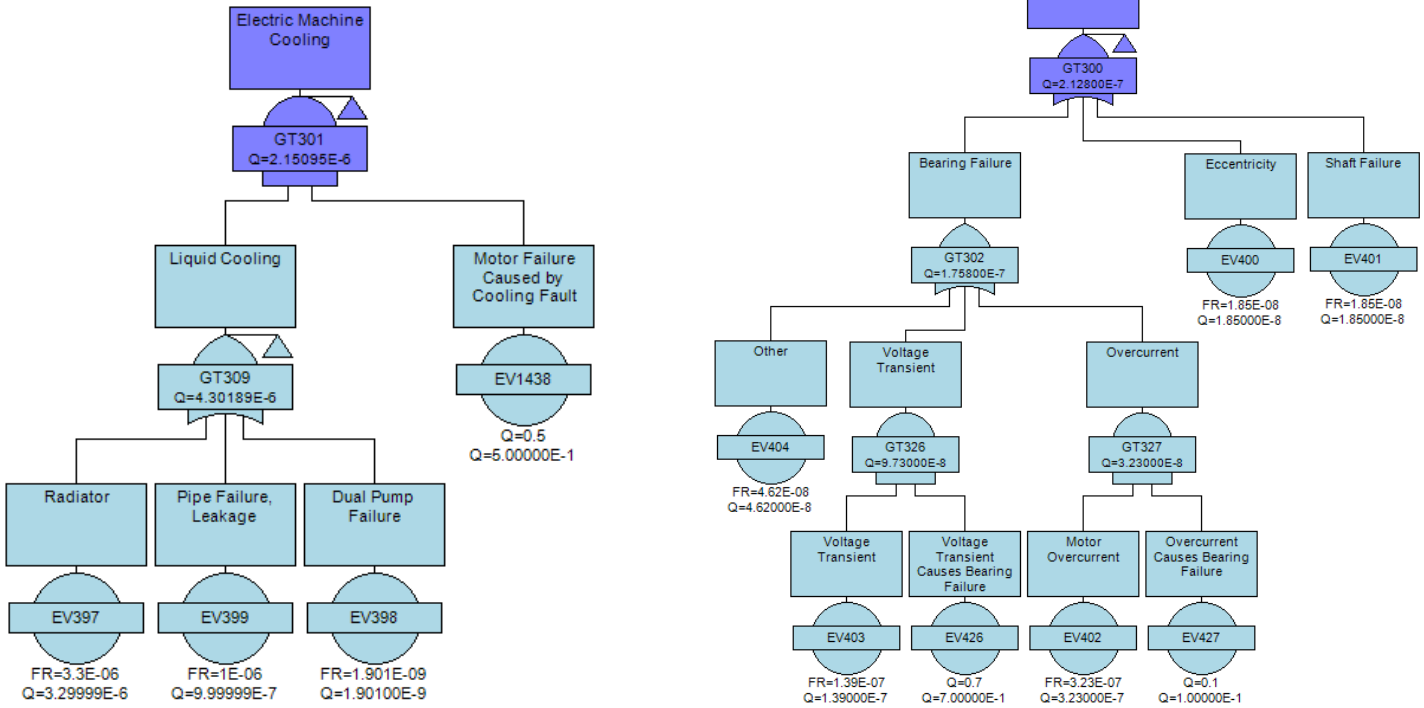

(Hexacopter RPM FTA Continued)

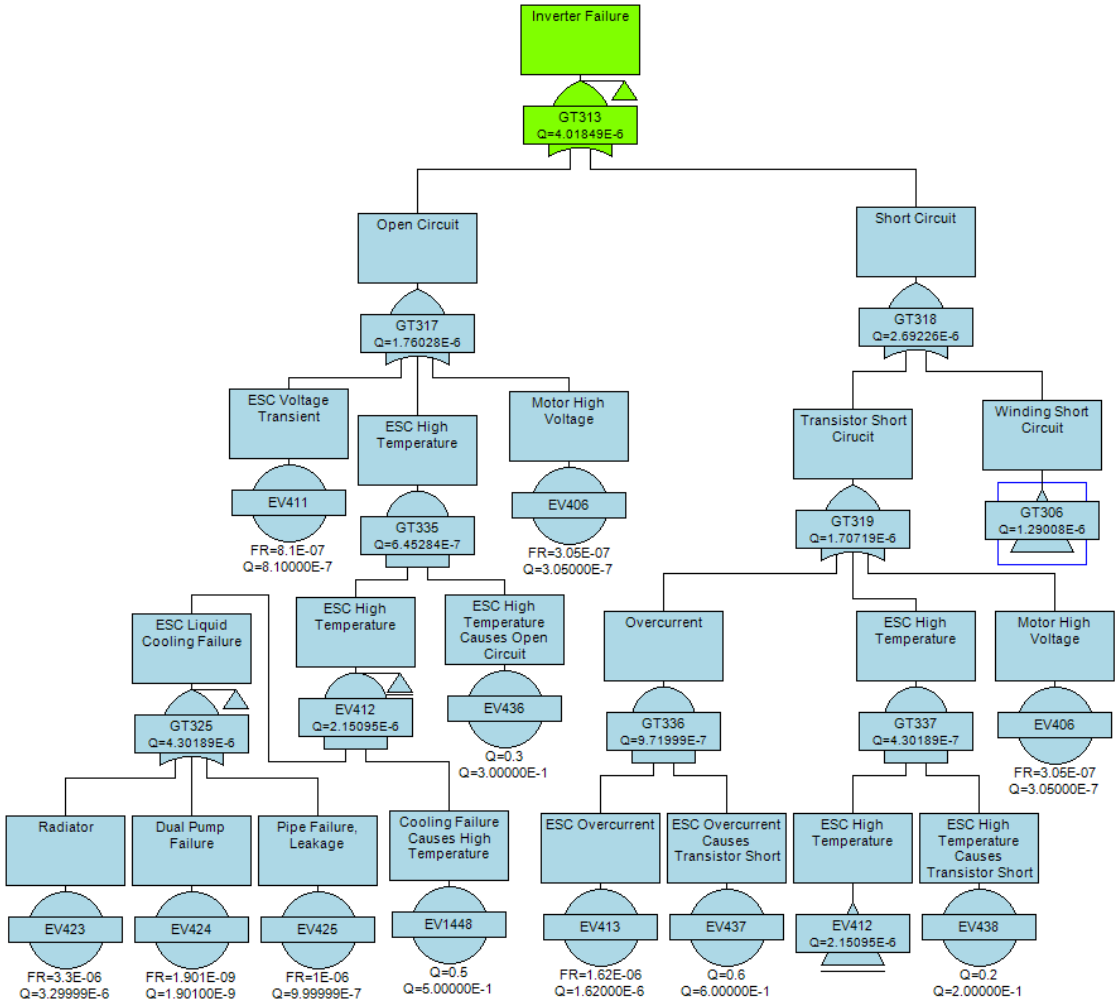

(Hexacopter RPM FTA Continued)

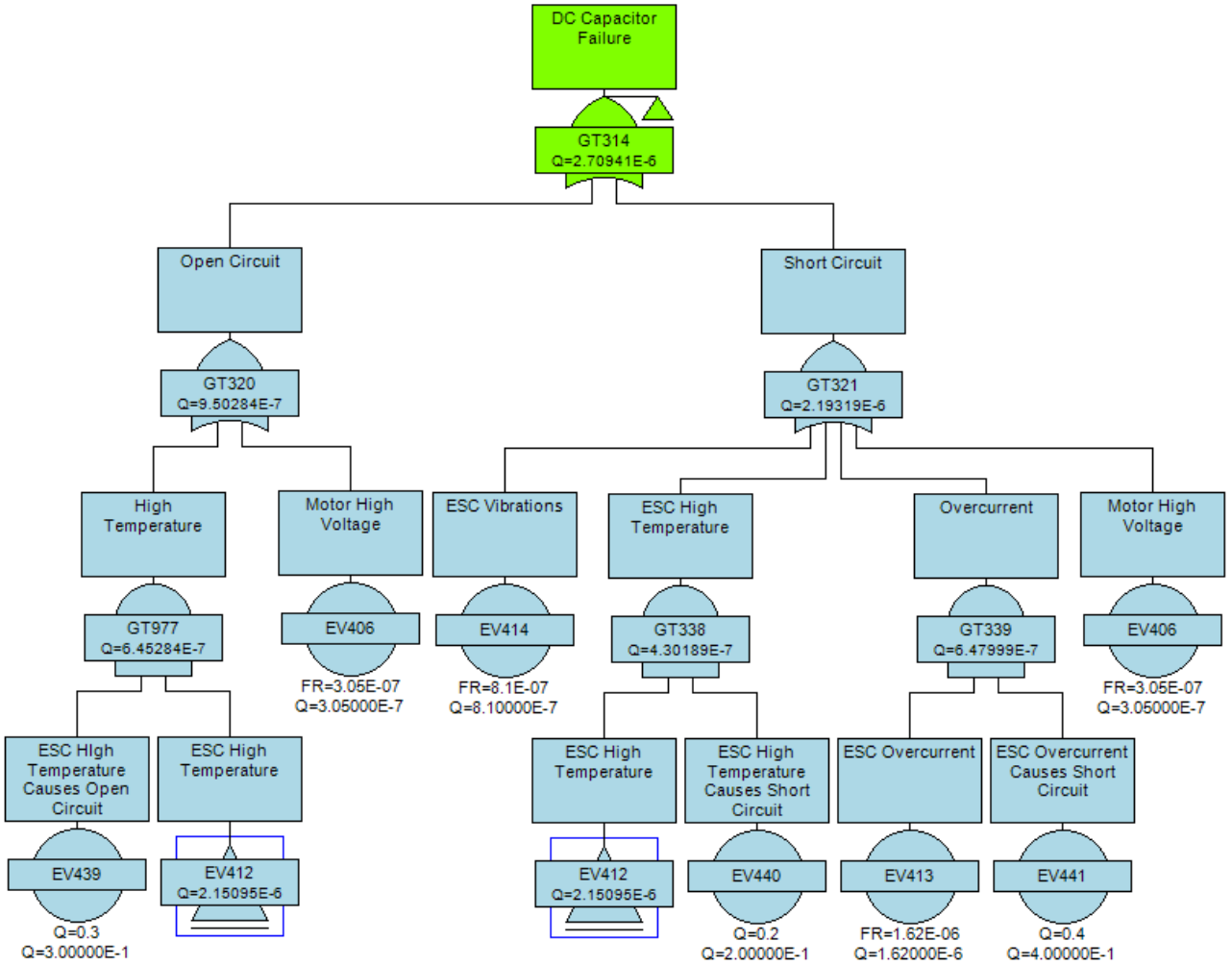

(Hexacopter RPM FTA Continued)

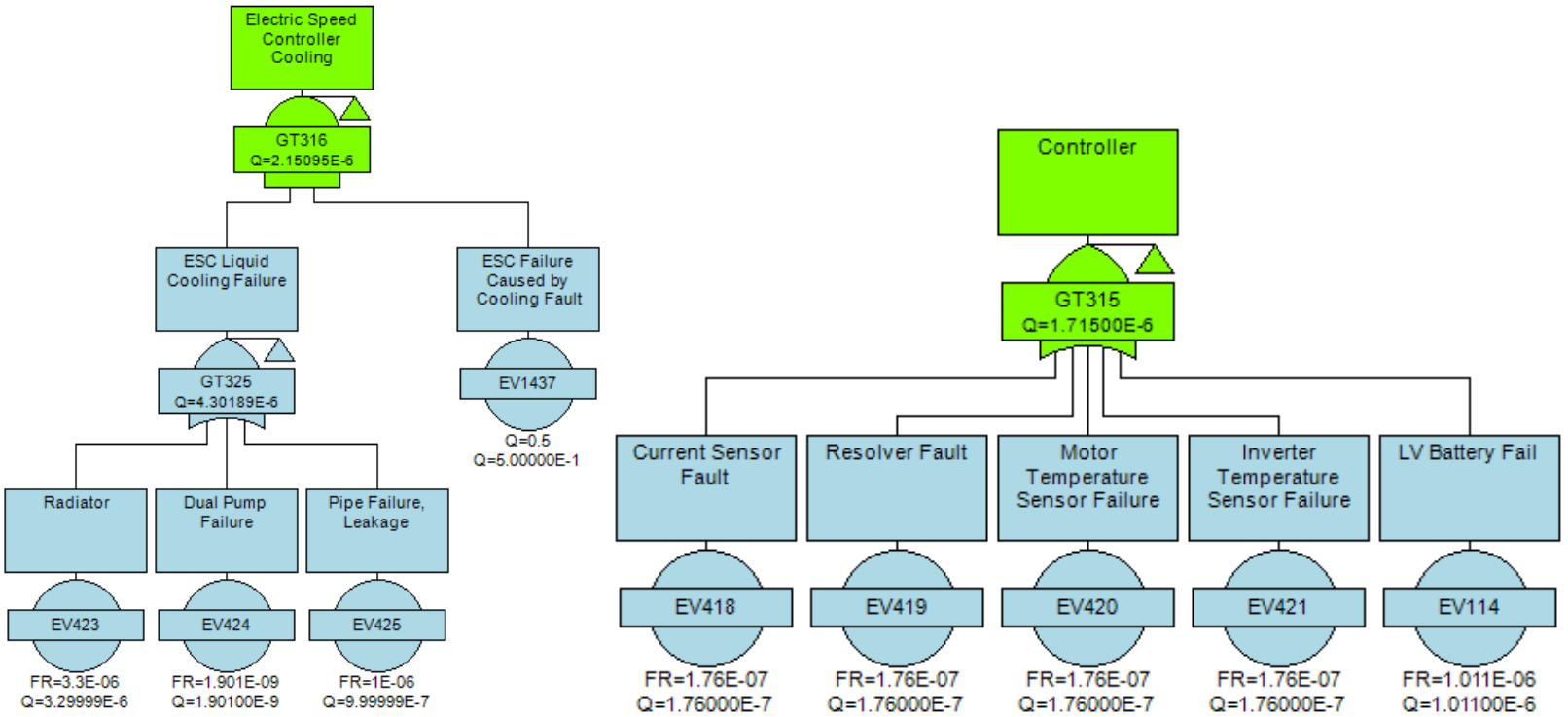

(Hexacopter RPM FTA Continued)

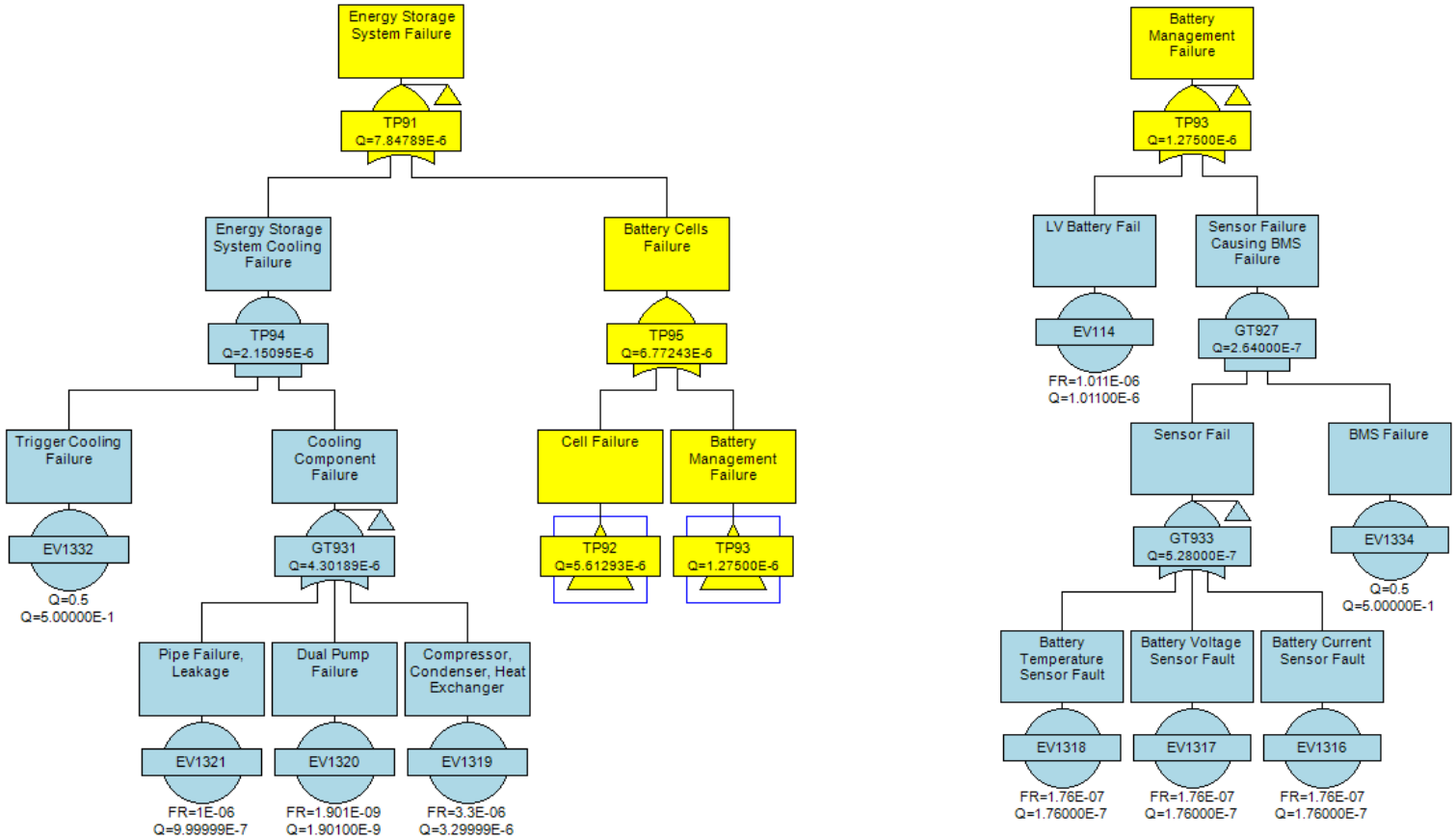

(Hexacopter RPM FTA Continued)

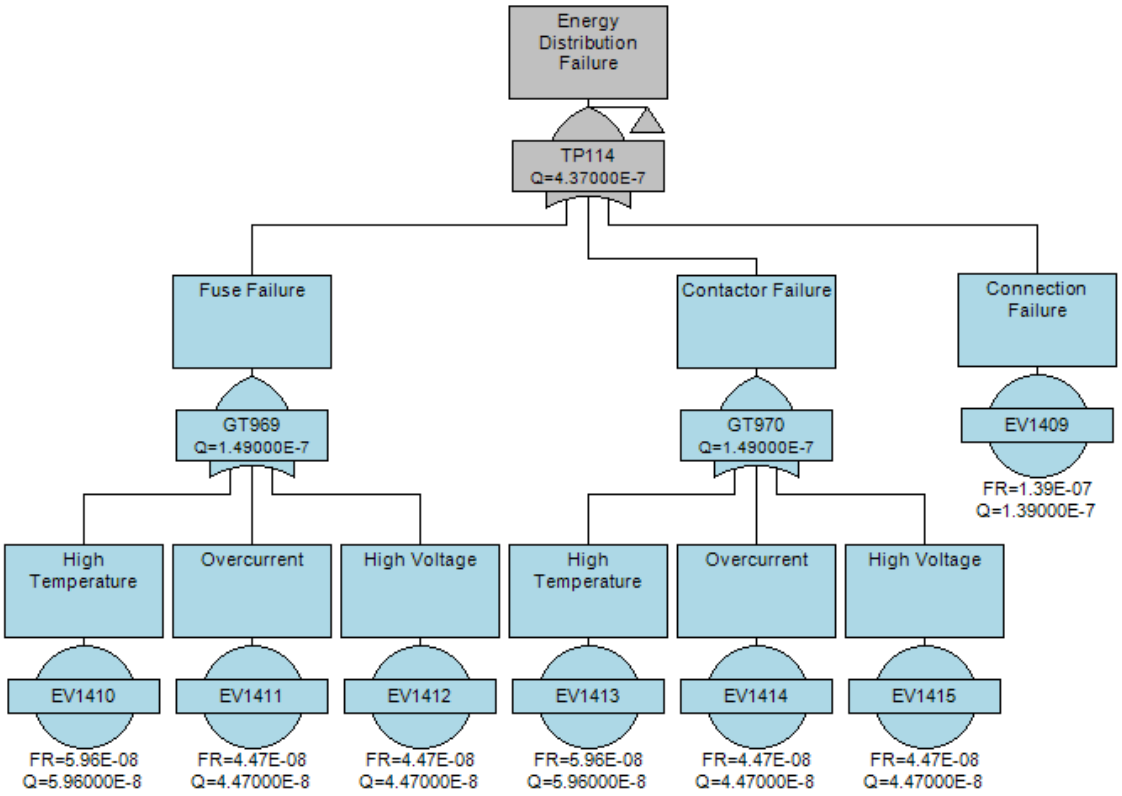

(Hexacopter RPM FTA Continued)

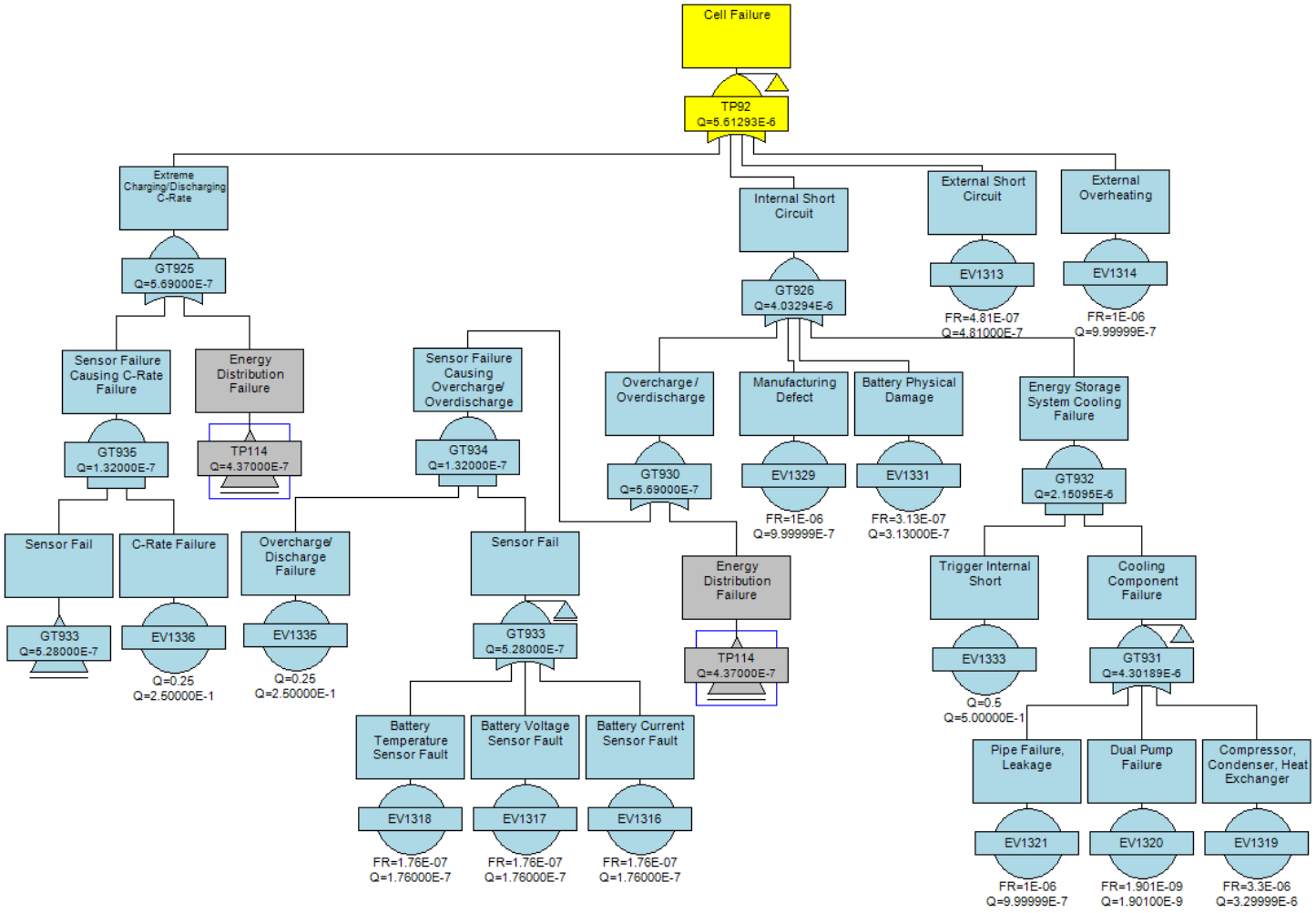

Appendix C - Figure 6: Octocopter RPM FTA

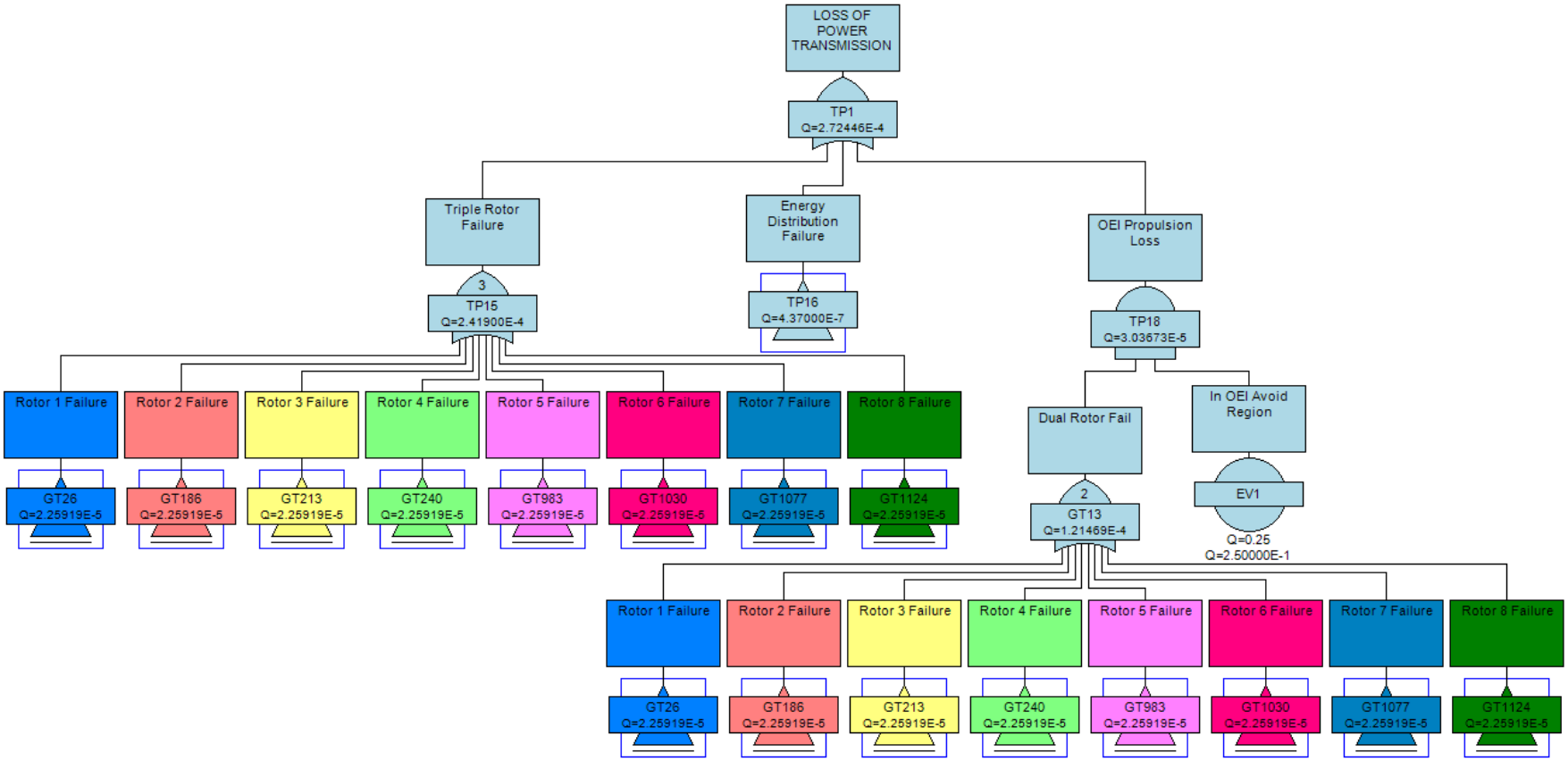

(Octocopter RPM FTA Continued)

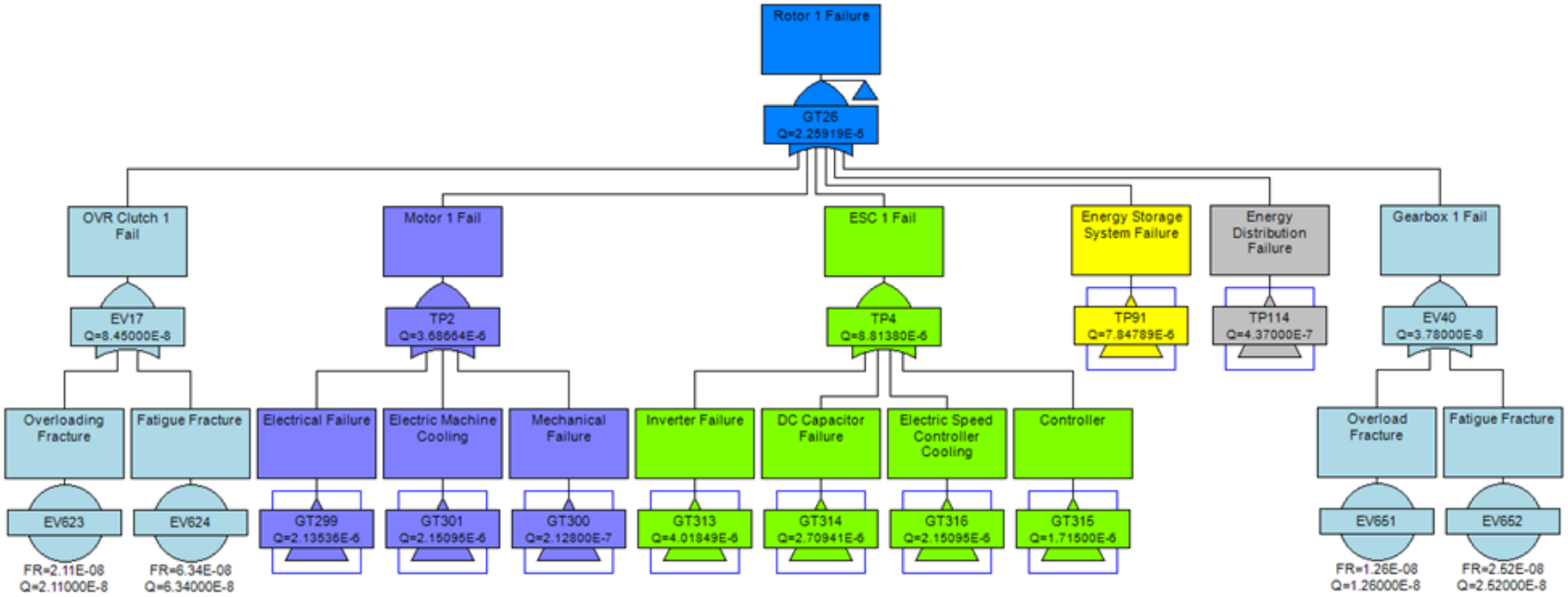

(Octocopter RPM FTA Continued)

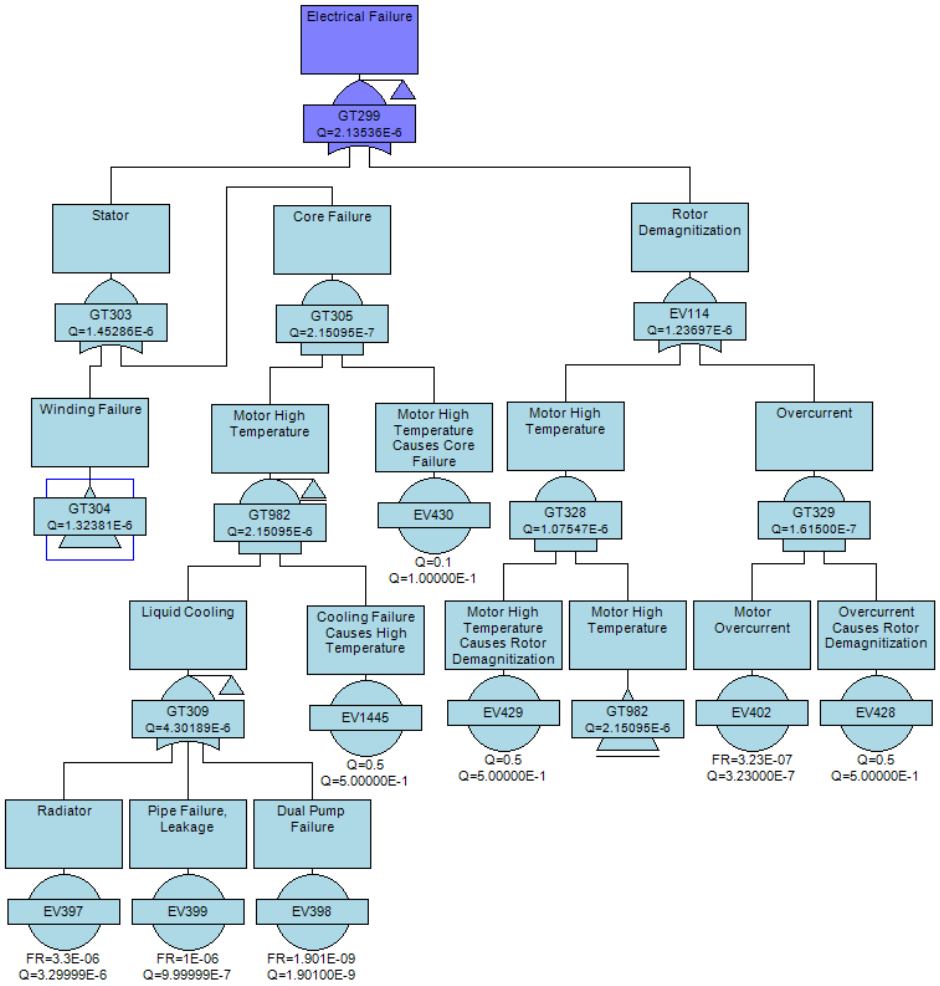

(Octocopter RPM FTA Continued)

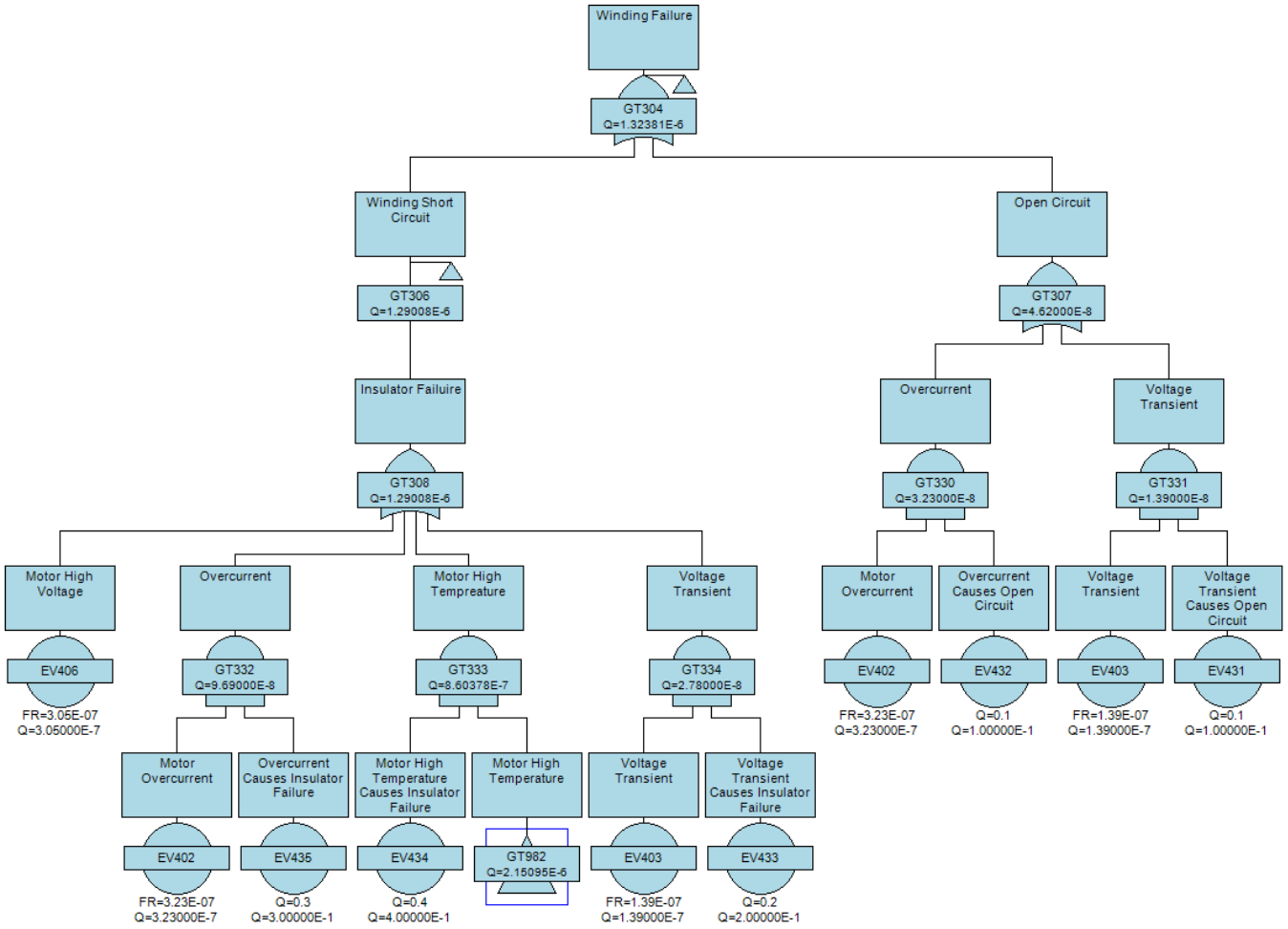

(Octocopter RPM FTA Continued)

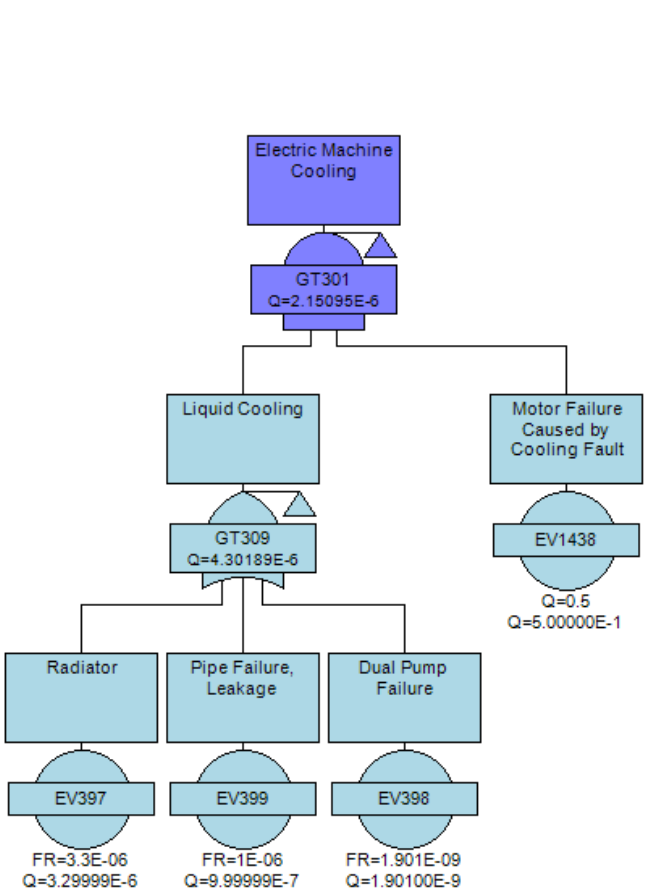

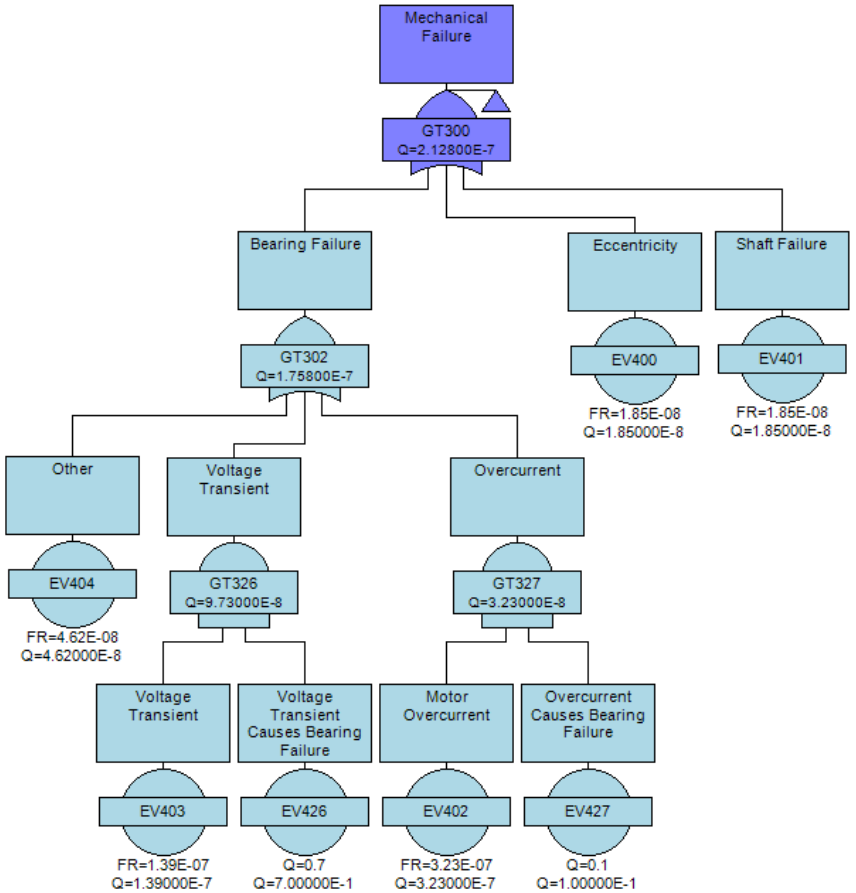

(Octocopter RPM FTA Continued)

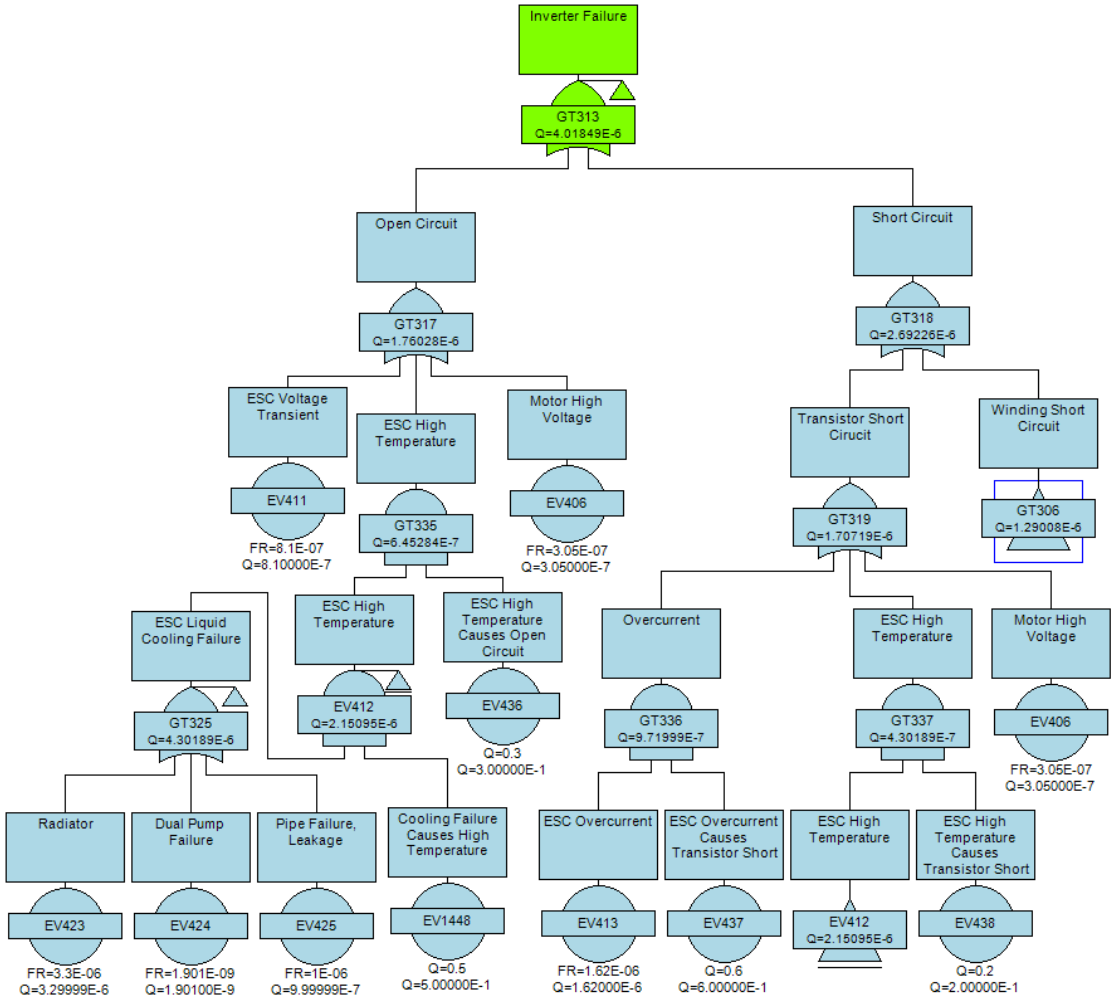

(Octocopter RPM FTA Continued)

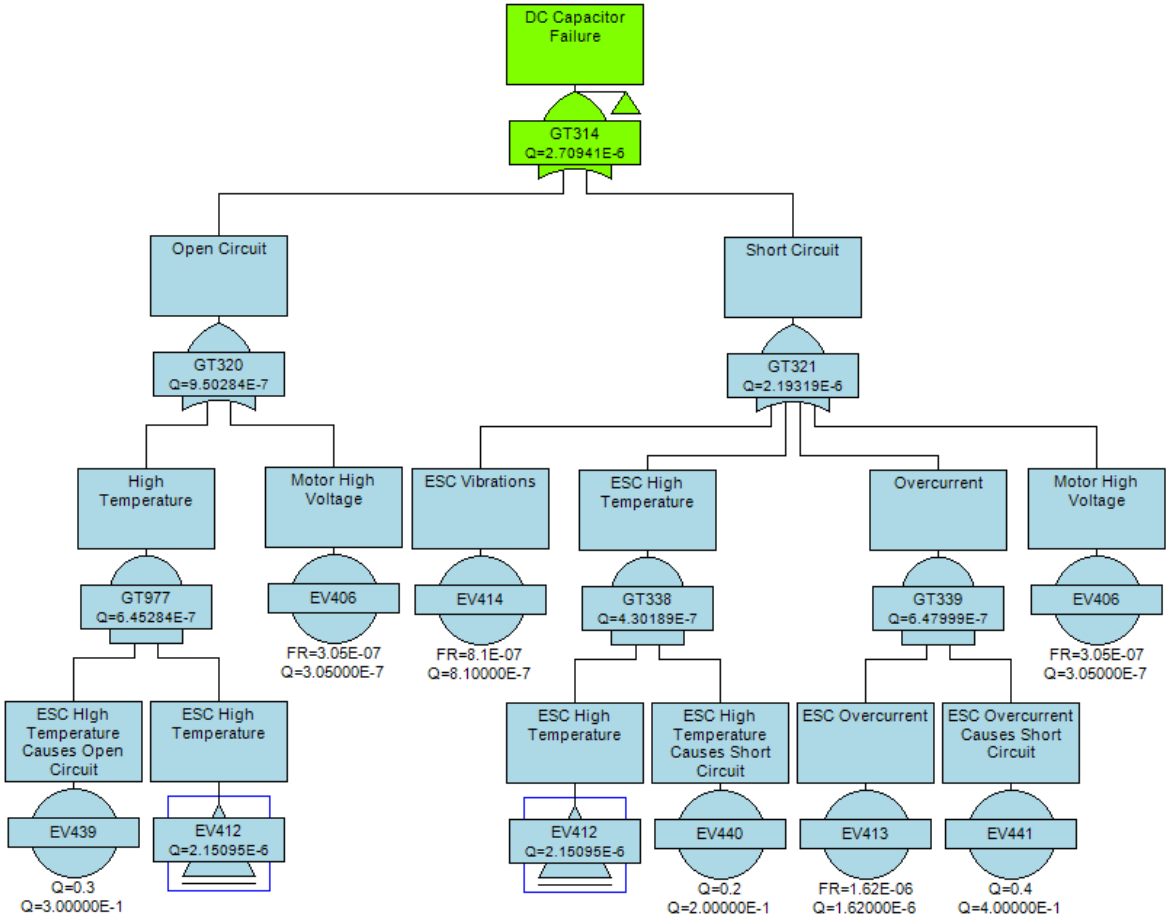

(Octocopter RPM FTA Continued)

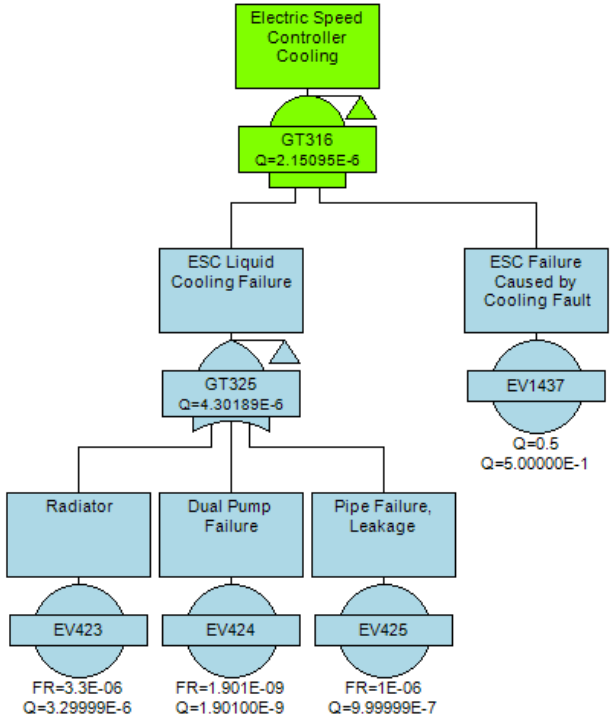

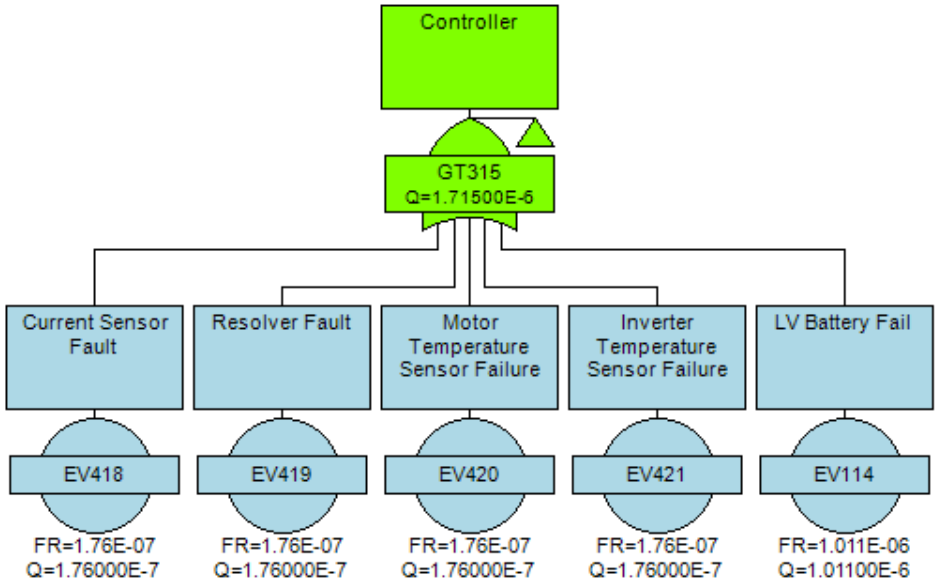

(Octocopter RPM FTA Continued)

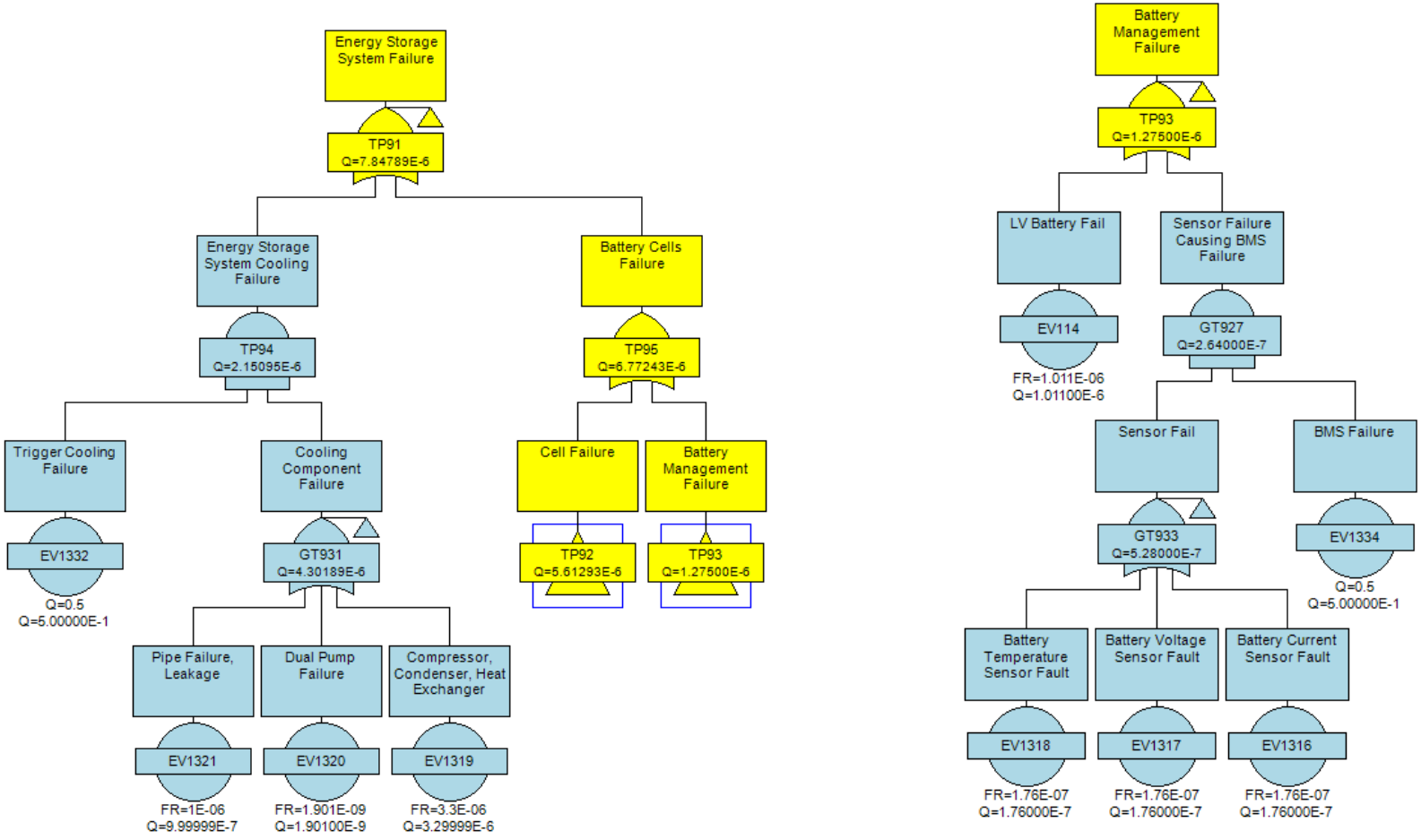

(Octocopter RPM FTA Continued)

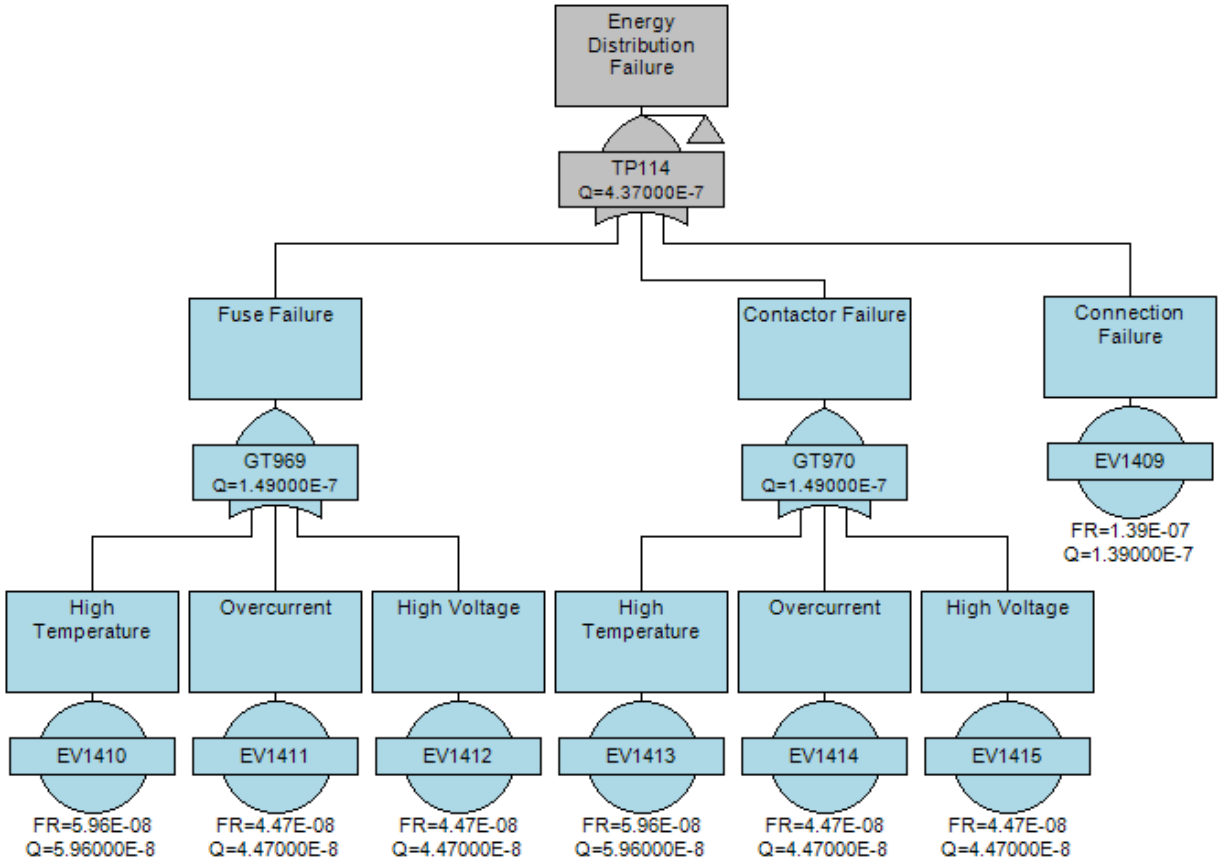

(Octocopter RPM FTA Continued)

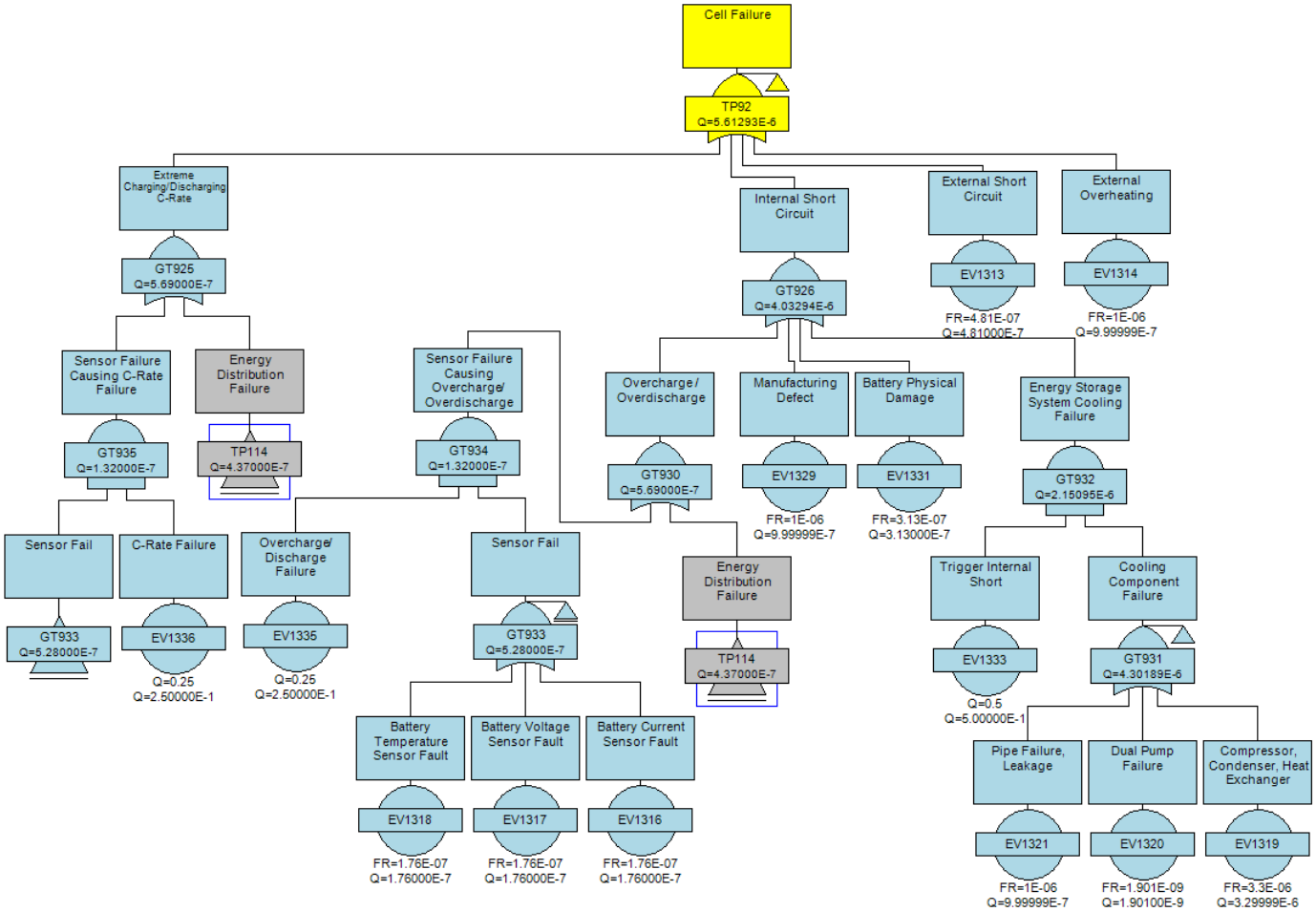

APPENDIX D **: DYNAMIC EVENT TREE (DET) RESULTS**

Table D1.1: Quadcopter Electric DET (Single Faults)

1st Injected Failure	Flight Phase	Minor	Major	Critical	Catastrophic
ED - No Torque	Takeoff	None	None	None	None
	Climb	None	None	None	None
	Cruise	None	None	None	None
	Landing	None	None	None	None
ED - Low Torque (SL-3)	Takeoff	None	None	None	None
	Climb	None	None	None	None
	Cruise	None	None	None	None
	Landing	None	None	None	None
ED - Low Torque (SL-2)	Takeoff	None	None	None	None
	Climb	None	None	None	None
	Cruise	None	None	None	None
	Landing	None	None	None	None
ED - Low Torque (SL-1)	Takeoff	None	None	None	None
	Climb	None	None	None	None
	Cruise	None	None	None	None
	Landing	None	None	None	None
ED - High Torque (SL-1)	Takeoff	None	Power limit state error	None	None
	Climb	None	Power limit state error	None	None
	Cruise	None	None	None	None
	Landing	None	None	None	None
ED - Torque Ripple (SL-1)	Takeoff	None	None	None	None
	Climb	None	None	None	None
	Cruise	None	None	None	None
	Landing	None	None	None	None
ED - Torque Ripple (SL-2)	Takeoff	None	None	None	None
	Climb	None	None	None	None
	Cruise	None	None	None	None
	Landing	None	None	None	None

SL = Severity Level

Table D1.1: Quadcopter Electric (Single Faults) (Continued)

1st Injected Failure	Flight Phase	Minor	Major	Critical	Catastrophic
ED - Torque Ripple (SL-3)	Takeoff	None	None	None	None
	Climb	None	None	None	None
	Cruise	None	None	None	None
	Landing	None	None	None	None
ED - Short Circuit 1	Takeoff	None	None	None	None
	Climb	None	None	None	None
	Cruise	None	None	None	None
	Landing	None	None	None	None
ED - Short Circuit 2	Takeoff	None	None	None	None
	Climb	None	None	None	None
	Cruise	None	None	None	None
	Landing	None	None	None	None
ED - Short Circuit 2	Takeoff	None	None	None	None
	Climb	None	None	None	None
	Cruise	None	None	None	None
	Landing	None	None	None	None
ED - Short Circuit 3	Takeoff	None	None	None	None
	Climb	None	None	None	None
	Cruise	None	None	None	None
	Landing	None	None	None	None
Actuator 1	Takeoff	None	None	None	None
	Climb	None	None	None	None
	Cruise	None	None	None	None
	Landing	None	None	None	None
Actuator 2	Takeoff	None	None	None	None
	Climb	None	None	None	None
	Cruise	None	None	None	None
	Landing	None	None	None	None
TS- Front left motor isolated	Takeoff	None	None	None	None
	Climb	None	None	None	None
	Cruise	None	None	None	None
	Landing	None	None	None	None

SL = Severity Level

Table D1.1: Quadcopter Electric DET (Single Faults) (Continued)

1st Injected Failure	Flight Phase	Minor	Major	Critical	Catastrophic
TS - Soft failure (SL-3)	**Takeoff**	None	None	None	**RPM too low for cross-shafted aircraft**
	Climb	None	None	None	**RPM too low for cross-shafted aircraft**
	Cruise	None	None	None	**RPM too low for cross-shafted aircraft**
	Landing	None	None	None	**RPM too low for cross-shafted aircraft**
TS - Soft failure (SL-2)	**Takeoff**	None	None	None	**Linear model velocity exceeded**
	Climb	None	None	None	**Linear model velocity exceeded**
	Cruise	None	None	None	None
	Landing	None	None	None	None
TS - Soft failure (SL-1)	Takeoff	None	None	None	None
	Climb	None	None	None	None
	Cruise	None	None	None	None
	Landing	None	None	None	None

SL = Severity Level

Bold red text signifies that case outcome crosses EASA threshold cutoff probability values: Catastrophic failures (10^{-9}) & Critical failures (10^{-7})

APPENDIX D: DYNAMIC EVENT TREE (DET) ANALYSIS

Table D1.2: Quadcopter Electric/Hybrid DET (ED-ED Faults) (Same Rotor)

1st Injected Failure	Mission Phase	2nd Injected Failure	Mission Phase	Minor	Major	Critical	Catastrophic
ED - No Torque	Takeoff	ED - No Torque	Takeoff	None	None	None	None
			Cruise	None	None	None	None
	Cruise	ED - No Torque	Landing	None	None	None	None
ED - No Torque	Takeoff	ED - Low Torque (SL-1)	Takeoff	None	None	None	None
			Cruise	None	None	None	None
	Cruise	ED - Low Torque (SL-1)	Landing	None	None	None	None
ED - No Torque	Cruise	ED - Torque Ripple (SL-3)	Landing	None	None	None	None
ED - No Torque	Cruise	ED - Short Circuit 1	Landing	None	None	None	None
		ED - Short Circuit 2		None	None	None	None
		ED - Short Circuit 3		None	None	None	None
ED - Low Torque (SL1)	Takeoff	ED - No Torque	Takeoff	None	None	None	None
			Cruise	None	None	None	None
	Cruise	ED - No Torque	Landing	None	None	None	None
ED - Low Torque (SL1)	Takeoff	ED - Low Torque (SL-1)	Takeoff	None	None	None	None
			Cruise	None	None	None	None
	Cruise	ED - Low Torque (SL-1)	Landing	None	None	None	None
ED - Torque Ripple (SL-3)	Cruise	ED - Low Torque (SL-1)	Landing	None	None	None	None

SL = Severity Level

Table D1.2: Quadcopter Electric/Hybrid DET (ED-ED Faults) (Same Rotor) (Continued)

1st Injected Failure	Mission Phase	2nd Injected Failure	Mission Phase	Minor	Major	Critical	Catastrophic
ED - Short Circuit 1	Cruise	No Torque	Landing	None	None	None	None
ED - Short Circuit 2				None	None	None	None
ED - Short Circuit 3				None	None	None	None

APPENDIX D: DYNAMIC EVENT TREE (DET) ANALYSIS

Table D1.3: Quadcopter Electric/Hybrid DET (ED-ACT Faults) (Two Rotors)

1st Injected Failure	Mission Phase	2nd Injected Failure	Mission Phase	Minor	Major	Critical	Catastrophic
ED - No torque	Takeoff	Actuator 1	Takeoff	None	None	None	None
			Cruise	None	None	None	None
	Cruise	Actuator 1	Landing	None	None	None	None
ED - Low torque	Takeoff	Actuator 1	Takeoff	None	None	None	None
			Cruise	None	None	None	None
	Cruise	Actuator 1	Landing	None	None	None	None
ED - Torque ripple	Takeoff	Actuator 1	Cruise	None	None	None	None
	Cruise		Landing	None	None	None	None
ED - Short circuit 1	Cruise	Actuator 1	Landing	None	None	None	None
ED - Short circuit 2				None	None	None	None
ED - Short circuit 3				None	None	None	None
Actuator 1	Takeoff	ED - No torque	Takeoff	None	None	None	None
			Cruise	None	None	None	None
	Cruise	ED - No torque	Landing	None	None	None	None
Actuator 1	Takeoff	ED - Low torque	Takeoff	None	None	None	None
			Cruise	None	None	None	None
	Cruise	ED - Low torque	Landing	None	None	None	None
Actuator 1	Takeoff	ED - Torque ripple	Cruise	None	None	None	None
	Cruise		Landing	None	None	None	None
Actuator 1	Cruise	ED - Short circuit 1	Landing	None	None	None	None
		ED - Short circuit 2		None	None	None	None
		ED - Short circuit 3		None	None	None	None

APPENDIX D: DYNAMIC EVENT TREE (DET) ANALYSIS

Table D1.4: Quadcopter Electric/Hybrid DET (ACT-TS Faults) (Same Rotor) (Continued)

1st Injected Failure	Flight Phase	2nd Injected Failure	Flight Phase	Minor	Major	Critical	Catastrophic
TS - Soft failure (SL-1)	Takeoff	Actuator 1	Takeoff	None	None	None	None
			Cruise	None	None	None	None
	Cruise	Actuator 1	Landing	None	None	None	None
TS - Soft failure (SL-2)	Takeoff	Actuator 1	Takeoff	None	None	None	Over-G
			Cruise	None	None	None	Over-G
	Cruise	Actuator 1	Landing	None	None	None	None
TS - Soft failure (SL-3)	Takeoff	Actuator 1	Takeoff	None	None	None	RPM too low for cross-shafted aircraft
			Cruise	None	None	None	RPM too low for cross-shafted aircraft
	Cruise	Actuator 1	Landing	None	None	None	RPM too low for cross-shafted aircraft
Actuator 1	Takeoff	TS - Soft failure (SL-1)	Takeoff	None	None	None	None
			Cruise	None	None	None	None
	Cruise	TS - Soft failure (SL-1)	Landing	None	None	None	None
Actuator 1	Takeoff	TS - Soft failure (SL-2)	Takeoff	None	None	None	Over-G
			Cruise	None	None	None	None
	Cruise	TS - Soft failure (SL-2)	Landing	None	None	None	None
Actuator 1	Takeoff	TS - Soft failure (SL-3)	Takeoff	None	None	None	RPM too low for cross-shafted aircraft
			Cruise	None	None	None	RPM too low for cross-shafted aircraft
	Cruise	TS - Soft failure (SL-3)	Landing	None	None	None	RPM too low for cross-shafted aircraft

SL = Severity Level

APPENDIX D: DYNAMIC EVENT TREE (DET) ANALYSIS

Table D1.5: Quadcopter Electric/Hybrid DET (ED-TS Faults) (Same Rotor)

1st Injected Failure	Flight Phase	2nd Injected Failure	Flight Phase	Minor	Major	Critical	Catastrophic
ED - No torque	Takeoff	TS - Soft failure (SL-1)	Takeoff	None	None	None	Linear model velocity exceeded
			Cruise	None	None	None	None
	Cruise	TS - Soft failure (SL-1)	Landing	None	None	None	None
ED - No torque	Takeoff	TS - Soft failure (SL-2)	Takeoff	None	None	None	RPM too low for cross-shafted aircraft
			Cruise	None	None	None	None
	Cruise	TS - Soft failure (SL-2)	Landing	None	None	None	None
ED - No torque	Takeoff	TS - Soft failure (SL-3)	Takeoff	None	None	None	RPM too low for cross-shafted aircraft
			Cruise	None	None	None	RPM too low for cross-shafted aircraft
	Cruise	TS - Soft failure (SL-3)	Landing	None	None	None	RPM too low for cross-shafted aircraft
ED - Low Torque (SL-1)	Takeoff	TS - Soft failure (SL-1)	Takeoff	None	None	None	None
			Cruise	None	None	None	None
	Cruise	TS - Soft failure (SL-1)	Landing	None	None	None	None
ED - Low Torque (SL-1)	Takeoff	TS - Soft failure (SL-2)	Takeoff	None	None	None	RPM too low for cross-shafted aircraft
			Cruise	None	None	None	None
	Cruise	TS - Soft failure (SL-2)	Landing	None	None	None	None

SL = Severity Level

Table D1.5: Quadcopter Electric/Hybrid DET (ED-TS Faults) (Same Rotor) (Continued)

1st Injected Failure	Flight Phase	2nd Injected Failure	Flight Phase	Minor	Major	Critical	Catastrophic
ED - Low Torque (SL-1)	Takeoff	TS - Soft failure (SL-3)	Takeoff	None	None	None	RPM too low for cross-shafted aircraft
			Cruise	None	None	None	RPM too low for cross-shafted aircraft
	Cruise	TS - Soft failure (SL-3)	Landing	None	None	None	RPM too low for cross-shafted aircraft
TS - Soft failure (SL-1)	Takeoff	ED - No torque	Takeoff	None	None	None	Linear Model Velocity Exceeded
			Cruise	None	None	None	None
	Cruise	ED - No torque	Landing	None	None	None	RPM too low for cross-shafted aircraft
TS - Soft failure (SL-2)	Takeoff	ED - No torque	Takeoff	None	None	None	RPM too low for cross-shafted aircraft
			Cruise	None	None	None	Linear Model Velocity exceeded; Motor temperature too hot
	Cruise	ED - No torque	Landing	None	None	None	RPM too low for cross-shafted aircraft
TS - Soft failure (SL-3)	Takeoff	ED - No torque	Takeoff	None	None	None	RPM too low for cross-shafted aircraft
			Cruise	None	None	None	RPM too low for cross-shafted aircraft
	Cruise	ED - No torque	Landing	None	None	None	RPM too low for cross-shafted aircraft
TS - Soft failure (SL-1)	Cruise	ED - Low Torque (SL-1)	Landing	None	None	None	None
TS - Soft failure (SL-2)			Landing	None	None	None	Motor temperature too hot
TS - Soft failure (SL-3)			Landing	None	None	None	RPM too low for cross-shafted aircraft

SL = Severity Level

APPENDIX D: DYNAMIC EVENT TREE (DET) ANALYSIS

Table D1.6: Quadcopter Electric/Hybrid DET (ED-ED Faults) (Two Rotors)

1st Injected Failure	Mission Phase	2nd Injected Failure	Mission Phase	Minor	Major	Critical	Catastrophic
ED - No Torque	Takeoff	ED - No Torque	Takeoff	None	None	None	RPM too low for cross-shafted aircraft
			Cruise	None	None	None	RPM too low for cross-shafted aircraft
	Cruise	ED - No Torque	Landing	None	None	None	RPM too low for cross-shafted aircraft
ED - No Torque	Takeoff	ED - Low Torque (SL-1)	Takeoff	None	None	None	RPM too low for cross-shafted aircraft
			Cruise	None	None	None	None
	Cruise	ED - Low Torque (SL-1)	Landing	None	None	None	None
ED - No Torque	Cruise	ED - Torque Ripple (SL-3)	Landing	None	None	None	None
ED - No Torque	Cruise	ED - Short Circuit 1 1.5	Landing	None	None	None	RPM too low for cross-shafted aircraft
		ED - Short Circuit 2 2.5		None	None	None	None
		ED - Short Circuit 3 1.5		None	None	None	RPM too low for cross-shafted aircraft
ED - Low Torque (SL-1)	Takeoff	ED - No Torque	Takeoff	None	None	None	RPM too low for cross-shafted aircraft
			Cruise	None	None	None	None
	Cruise	ED - No Torque	Landing	None	None	None	None
ED - Low Torque (SL-1)	Takeoff	ED - Low Torque (SL-1)	Takeoff	None	None	None	None
			Cruise	None	None	None	None
	Cruise	ED - Low Torque (SL-1)	Landing	None	None	None	None
ED - Torque Ripple (SL-3)	Cruise	ED - No Torque	Landing	None	None	None	None
Short Circuit 1 1.5	Cruise	ED - No Torque	Landing	None	None	None	RPM too low for cross-shafted aircraft
Short Circuit 2 2.5				None	None	None	None
Short Circuit 3 1.5				None	None	None	RPM too low for cross-shafted aircraft

SL = Severity Level

APPENDIX D: DYNAMIC EVENT TREE (DET) ANALYSIS

Table D2.1: Quadcopter Hybrid DET (Single Faults)

1st Injected Failure	Flight Phase	Minor	Major	Critical	Catastrophic
ED - No Torque	Takeoff	None	None	None	None
	Climb	None	None	None	None
	Cruise	None	None	None	None
	Landing	None	None	None	None
ED - Low Torque (SL-3)	Takeoff	None	None	None	None
	Climb	None	None	None	None
	Cruise	None	None	None	None
	Landing	None	None	None	None
ED - Low Torque (SL-2)	Takeoff	None	None	None	None
	Climb	None	None	None	None
	Cruise	None	None	None	None
	Landing	None	None	None	None
ED - Low Torque (SL-1)	Takeoff	None	None	None	None
	Climb	None	None	None	None
	Cruise	None	None	None	None
	Landing	None	None	None	None
ED - High Torque (SL-1)	Takeoff	None	None	None	None
	Climb	None	None	None	None
	Cruise	None	None	None	None
	Landing	None	None	None	None
ED - Torque Ripple (SL-1)	Takeoff	None	None	None	None
	Climb	None	None	None	None
	Cruise	None	None	None	None
	Landing	None	None	None	None
ED - Torque Ripple (SL-2)	Takeoff	None	None	None	None
	Climb	None	None	None	None
	Cruise	None	None	None	None
	Landing	None	None	None	None
ED - Torque Ripple (SL-3)	Takeoff	None	None	None	None
	Climb	None	None	None	None
	Cruise	None	None	None	None
	Landing	None	None	None	None

SL = Severity Level

Table D2.1: Quadcopter Hybrid DET (Single Faults) (Continued)

1st Injected Failure	Flight Phase	Minor	Major	Critical	Catastrophic
ED - Short Circuit 1	Takeoff	None	None	None	None
	Climb	None	None	None	None
	Cruise	None	None	None	None
	Landing	None	None	None	None
ED - Short Circuit 2	Takeoff	None	None	None	None
	Climb	None	None	None	None
	Cruise	None	None	None	None
	Landing	None	None	None	None
ED - Short Circuit 2	Takeoff	None	None	None	None
	Climb	None	None	None	None
	Cruise	None	None	None	None
	Landing	None	None	None	None
ED - Short Circuit 3	Takeoff	None	None	None	None
	Climb	None	None	None	None
	Cruise	None	None	None	None
	Landing	None	None	None	None
Actuator 1	Takeoff	None	None	None	None
	Climb	None	None	None	None
	Cruise	None	None	None	None
	Landing	None	None	None	None
Actuator 2	Takeoff	None	None	None	None
	Climb	None	None	None	None
	Cruise	None	None	None	None
	Landing	None	None	None	None
TS- Front left motor isolated	Takeoff	None	None	None	None
	Climb	None	None	None	None
	Cruise	None	None	None	None
	Landing	None	None	None	None
TS - Soft failure (SL-3)	**Takeoff**	None	None	None	**RPM too low for cross-shafted aircraft**
	Climb	None	None	None	**RPM too low for cross-shafted aircraft**
	Cruise	None	None	None	**RPM too low for cross-shafted aircraft**
	Landing	None	None	None	**RPM too low for cross-shafted aircraft**

SL = Severity Level

Bold red text signifies that case outcome crosses EASA threshold cutoff probability values: Catastrophic failures (10^{-9}) & Critical failures (10^{-7})

Table D2.1: Quadcopter Hybrid DET (Single Faults) (Continued)

1st Injected Failure	Flight Phase	Minor	Major	Critical	Catastrophic
TS - Soft failure (SL-2)	**Takeoff**	None	None	None	**Linear model velocity exceeded**
	Climb	None	None	None	**Linear model velocity exceeded**
	Cruise	None	None	None	None
	Landing	None	None	None	None
TS - Soft failure (SL-1)	Takeoff	None	None	None	None
	Climb	None	None	None	None
	Cruise	None	None	None	None
	Landing	None	None	None	None
Turbine-generator (SL-1)	Takeoff	None	None	None	None
	Climb	None	None	None	None
	Cruise	None	None	None	None
	Landing	None	None	None	None
Turbine-generator (SL-2)	Takeoff	None	None	None	None
	Climb	None	None	None	None
	Cruise	None	None	None	None
	Landing	None	None	None	None
Turbine-generator (SL-3)	**Takeoff**	Battery current too high	None	None	**Over-G**
	Climb	Battery current too high	None	None	**Over-G**
	Cruise	Battery current too high	None	Emergency Landing	None
	Landing	None	None	None	None

SL = Severity Level

Bold red text signifies that case outcome crosses EASA threshold cutoff probability values: Catastrophic failures (10^{-9}) & Critical failures (10^{-7})

APPENDIX D: DYNAMIC EVENT TREE (DET) ANALYSIS

Table D3.1: Quadcopter Turboshaft DET (Single Faults)

1st Injected Failure	Flight Phase	Minor	Major	Critical	Catastrophic
Turboshaft Engine - OEI	Takeoff	None	None	None	None
	Climb	None	None	None	None
	Cruise	None	None	None	None
	Landing	None	None	None	None
TS soft failure (SL-1)	Takeoff	None	None	None	None
	Climb	None	None	None	None
	Cruise	None	None	None	None
	Landing	None	None	None	None
TS soft failure (SL-2)	Takeoff	None	None	None	None
	Climb	None	None	None	None
	Cruise	None	None	None	None
	Landing	None	None	None	None
TS soft failure (SL-3)	Takeoff	None	None	None	None
	Climb	None	None	None	None
	Cruise	None	None	None	None
	Landing	None	None	None	None
Actuator 1	Takeoff	None	None	None	None
	Climb	None	None	None	None
	Cruise	None	None	None	None
	Landing	None	None	None	None
Actuator 2	Takeoff	None	None	None	None
	Climb	None	None	None	None
	Cruise	None	None	None	None
	Landing	None	None	None	None

SL = Severity Level

APPENDIX D: DYNAMIC EVENT TREE (DET) ANALYSIS

Table D3.2: Quadcopter Turboshaft DET (ACT-TS Faults) (Same Rotor)

1st Injected Failure	Flight Phase	2nd Injected Failure	Flight Phase	Minor	Major	Critical	Catastrophic
TS - Soft failure (SL-3)	Takeoff	Actuator 1	Climb	None	None	None	None
			Cruise	None	None	None	None
	Cruise	Actuator 1	Landing	None	None	None	None
Actuator 1	Takeoff	TS - Soft failure (SL-3)	Climb	None	None	None	None
			Cruise	None	None	None	None
	Cruise	TS - Soft failure (SL-3)	Landing	None	None	None	None

SL = Severity Level

APPENDIX D: DYNAMIC EVENT TREE (DET) ANALYSIS

Table D4.1: Hexacopter Collective Control DET (Single Faults)

SL = Severity Level

1st Injected Failure	Flight Phase	Minor	Major	Critical	Catastrophic
ED - No Torque	Takeoff	None	None	None	None
	Climb	None	None	None	None
	Cruise	None	None	None	None
	Landing	None	None	None	None
ED - Low Torque (SL-3)	Takeoff	None	None	None	None
	Climb	None	None	None	None
	Cruise	None	None	None	None
	Landing	None	None	None	None
ED - Low Torque (SL-2)	Takeoff	None	None	None	None
	Climb	None	None	None	None
	Cruise	None	None	None	None
	Landing	None	None	None	None
ED - Low Torque (SL-1)	**Takeoff**	None	None	**Motor temperature too hot**	None
	Climb	None	None	**Motor temperature too hot**	None
	Cruise	None	None	None	None
	Landing	None	None	None	None
ED - High Torque (SL-1)	Takeoff	None	None	None	None
	Climb	None	None	None	None
	Cruise	None	None	**Motor temperature too hot**	None
	Landing	None	None	None	None
ED - Torque Ripple (SL-1)	Takeoff	None	None	None	None
	Climb	None	None	None	None
	Cruise	None	None	None	None
	Landing	None	None	None	None
ED - Torque Ripple (SL-2)	Takeoff	None	None	None	None
	Climb	None	None	None	None
	Cruise	None	None	None	None
	Landing	None	None	None	None
ED - Torque Ripple (SL-3)	Takeoff	None	None	None	None
	Climb	None	None	None	None
	Cruise	None	None	None	None
	Landing	None	None	None	None

Bold red text signifies that case outcome crosses EASA threshold cutoff probability values: Catastrophic failures (10^{-9}) & Critical failures (10^{-7})

Table D4.1: Hexacopter Collective Control DET (Single Faults) (Continued)

SL = Severity Level

1st Injected Failure	Flight Phase	Minor	Major	Critical	Catastrophic
ED - Short Circuit 1	Takeoff	None	None	None	None
	Climb	None	None	None	None
	Cruise	None	None	None	None
	Landing	None	None	None	None
ED - Short Circuit 2	Takeoff	None	None	None	None
	Climb	None	None	None	None
	Cruise	None	None	None	None
	Landing	None	None	None	None
ED - Short Circuit 2	Takeoff	None	None	None	None
	Climb	None	None	None	None
	Cruise	None	None	None	None
	Landing	None	None	None	None
ED - Short Circuit 3	Takeoff	None	None	None	None
	Climb	None	None	None	None
	Cruise	None	None	None	None
	Landing	None	None	None	None
Actuator 1	Takeoff	None	None	None	None
	Climb	None	None	None	None
	Cruise	None	None	None	None
	Landing	None	None	None	None
Actuator 2	Takeoff	None	None	None	None
	Climb	None	None	None	None
	Cruise	None	None	None	None
	Landing	None	None	None	None
TS soft failure (SL-1)	Takeoff	None	None	None	None
	Climb	None	None	None	None
	Cruise	None	None	None	None
	Landing	None	None	None	None
TS soft failure (SL-2)	Takeoff	None	None	None	None
	Climb	None	None	None	None
	Cruise	None	None	None	None
	Landing	None	None	None	None
TS soft failure (SL-3)	Takeoff	None	None	None	None
	Climb	None	None	None	None
	Cruise	None	None	None	None
	Landing	None	None	None	None

APPENDIX D: DYNAMIC EVENT TREE (DET) ANALYSIS

Table D4.2: Hexacopter Collective Control DET (ED-ED Faults) (Same Rotor)

1st Injected Failure	Flight Phase	2nd Injected Failure	Flight Phase	Minor	Major	Critical	Catastrophic
ED - No Torque	Cruise	ED - Short circuit 1	Landing	None	None	None	None
		ED - Short circuit 2	Landing	None	None	None	None
		ED - Short circuit 3	Landing	None	None	None	None
ED - Low torque	Takeoff	ED - No Torque	Takeoff	None	None	None	None
			Cruise	None	None	None	None
	Cruise	ED - No Torque	Landing	None	None	None	None
ED - Short circuit 1	Cruise	ED - No Torque	Landing	None	None	None	None
ED - Short circuit 2				None	None	None	None
ED - Short circuit 3				None	None	None	None

APPENDIX D: DYNAMIC EVENT TREE (DET) ANALYSIS

Table D4.3: Hexacopter Collective Control DET (ED-ACT Faults) (Same Rotor)

1st Injected Failure	Mission Phase	2nd Injected Failure	Mission Phase	Minor	Major	Critical	Catastrophic
ED - No Torque	Takeoff	Actuator 1	Takeoff	None	None	None	None
			Cruise	None	None	None	None
	Cruise	Actuator 1	Landing	None	None	None	None
ED - Low torque	Takeoff	Actuator 1	Takeoff	None	None	Motor temperature too hot	None
			Cruise	None	None	Motor temperature too hot	None
	Cruise	Actuator 1	Landing	None	None	None	None
ED - Torque ripple	Takeoff	Actuator 1	Cruise	None	None	None	None
	Cruise		Landing	None	None	None	None
ED - Short circuit 1	Cruise	Actuator 1	Landing	None	None	None	None
ED - Short circuit 2				None	None	None	None
ED - Short circuit 3				None	None	None	None
Actuator 1	Takeoff	ED - No Torque	Takeoff	None	None	None	None
			Cruise	None	None	None	None
	Cruise	ED - No Torque	Landing	None	None	None	None
Actuator 1	Takeoff	ED - Low torque	Takeoff	None	None	Motor temperature too hot	None
			Cruise	None	None	None	None
	Cruise	ED - Low torque	Landing	None	None	None	None
Actuator 1	Takeoff	ED - Torque ripple	Cruise	None	None	None	None
	Cruise		Landing	None	None	None	None
Actuator 1	Cruise	ED - Short circuit 1	Landing	None	None	None	None
		Short circuit 2	Landing	None	None	None	None
		Short circuit 3	Landing	None	None	None	None

APPENDIX D: DYNAMIC EVENT TREE (DET) ANALYSIS

Table D5.1: Hexacopter RPM Control DET (Single Faults)

SL = Severity Level

1st Injected Failure	Flight Phase	Minor	Major	Critical	Catastrophic
ED - No Torque	**Takeoff**	None	None	None	**Inconclusive†**
	Climb	None	None	None	**Inconclusive†**
	Cruise	None	Inconclusive†	Inconclusive†	**Inconclusive†**
	Landing	Inconclusive†	None	Inconclusive†	**Inconclusive†**
ED - Low Torque (SL-3)	**Takeoff**	None	None	None	**Inconclusive†**
	Climb	None	None	None	**Inconclusive†**
	Cruise	None	Inconclusive†	Inconclusive†	**Inconclusive†**
	Landing	Inconclusive†	None	Inconclusive†	**Inconclusive†**
ED - Low Torque (SL-2)	**Takeoff**	None	None	None	**Inconclusive†**
	Climb	None	None	None	**Inconclusive†**
	Cruise	None	Inconclusive†	None	None
	Landing	Inconclusive†	None	Inconclusive†	**Inconclusive†**
ED - Low Torque (SL-1)	**Takeoff**	None	None	**Inconclusive†**	**Inconclusive†**
	Climb	None	Inconclusive†	Inconclusive†	**Inconclusive†**
	Cruise	Inconclusive†	None	None	None
	Landing	Inconclusive†	None	**Inconclusive†**	None

Bold red text signifies that case outcome crosses EASA threshold cutoff probability values: Catastrophic failures (10^{-9}) & Critical failures (10^{-7})

Table D5.1: Hexacopter RPM Control DET (Single Faults) (Continued)

SL = Severity Level

1st Injected Failure	Flight Phase	Minor	Major	Critical	Catastrophic
ED - High Torque (SL-1)	**Takeoff**	None	None	None	**Inconclusive†**
	Climb	None	None	None	**Inconclusive†**
	Cruise	None	None	**Inconclusive†**	None
	Landing	None	None	**Inconclusive†**	None
ED - Torque Ripple (SL-1)	Takeoff	None	None	None	None
	Climb	None	None	None	None
	Cruise	None	None	None	None
	Landing	None	None	None	None
ED - Torque Ripple (SL-2)	Takeoff	None	None	None	None
	Climb	None	None	None	None
	Cruise	None	None	None	None
	Landing	None	None	None	None
ED - Torque Ripple (SL-3)	Takeoff	None	None	None	None
	Climb	None	None	None	None
	Cruise	None	None	None	None
	Landing	None	None	None	None

Bold red text signifies that case outcome crosses EASA threshold cutoff probability values: Catastrophic failures (10^{-9}) & Critical failures (10^{-7})

Table D5.1: Hexacopter RPM Control DET (Single Faults) (Continued)

1st Injected Failure	Flight Phase	Minor	Major	Critical	Catastrophic
ED - Short Circuit 1 - 1.5	**Takeoff**	None	None	None	**Inconclusive†**
	Climb	None	None	None	**Inconclusive†**
	Cruise	None	Inconclusive†	Inconclusive†	**Inconclusive†**
	Landing	Inconclusive†	None	Inconclusive†	**Inconclusive†**
ED - Short Circuit 2	Takeoff	None	None	None	None
	Climb	None	None	None	**Inconclusive†**
	Cruise	None	None	None	None
	Landing	None	None	None	None
ED - Short Circuit 2	Takeoff	None	None	None	None
	Climb	None	None	None	None
	Cruise	None	None	None	None
	Landing	None	None	None	None
ED - Short Circuit 3	**Takeoff**	None	None	None	**Inconclusive†**
	Climb	None	None	None	**Inconclusive†**
	Cruise	None	Inconclusive†	Inconclusive†	**Inconclusive†**
	Landing	Inconclusive†	None	Inconclusive†	**Inconclusive†**

Bold red text signifies that case outcome crosses EASA threshold cutoff probability values: Catastrophic failures (10^{-9}) & Critical failures (10^{-7})

Table D5.1: Hexacopter RPM Control DET (Single Faults) (Continued)

1st Injected Failure	Flight Phase	Minor	Major	Critical	Catastrophic
TS - Lowest Efficiency (SL-1)	Takeoff	None	None	None	None
	Climb	None	None	None	None
	Cruise	None	None	None	None
	Landing	None	None	None	None
TS - Lower Efficiency (SL-2)	Takeoff	None	None	None	None
	Climb	None	None	None	None
	Cruise	None	None	None	None
	Landing	None	None	None	None
TS - Partial Efficiency (SL-3)	Takeoff	None	None	None	None
	Climb	None	None	None	None
	Cruise	None	None	None	None
	Landing	None	None	None	None

Table D6.1: Octocopter RPM Control DET (Single Faults)

SL = Severity Level

1st Injected Failure	Flight Phase	Minor	Major	Critical	Catastrophic
ED - No Torque	**Takeoff**	None	None	None	**Inconclusive†**
	Climb	None	None	None	**Inconclusive†**
	Cruise	None	Inconclusive†	Inconclusive†	**Inconclusive†**
	Landing	None	None	Inconclusive†	**Inconclusive†**
ED - Low Torque (SL-3)	Takeoff	None	None	None	**Inconclusive†**
	Climb	None	None	None	**Inconclusive†**
	Cruise	None	Inconclusive†	Inconclusive†	**Inconclusive†**
	Landing	None	None	Inconclusive†	**Inconclusive†**
ED - Low Torque (SL-2)	**Takeoff**	None	None	None	**Inconclusive†**
	Climb	None	None	None	**Inconclusive†**
	Cruise	None	Inconclusive†	Inconclusive†	**Inconclusive†**
	Landing	None	None	Inconclusive†	**Inconclusive†**
ED - Low Torque (SL-1)	**Takeoff**	None	None	**Inconclusive†**	None
	Climb	None	None	**Inconclusive†**	None
	Cruise	Inconclusive†	None	None	None
	Landing	None	None	Inconclusive†	**Inconclusive†**

Bold red text signifies that case outcome crosses EASA threshold cutoff probability values: Catastrophic failures (10^{-9}) & Critical failures (10^{-7})

Table D6.1: Octocopter RPM Control DET (Single Faults) (Continued)

SL = Severity Level

1st Injected Failure	Flight Phase	Minor	Major	Critical	Catastrophic
ED - High Torque (SL-1)	**Takeoff**	None	None	None	**Inconclusive†**
	Climb	None	Inconclusive†	**Inconclusive†**	**Inconclusive†**
	Cruise	None	None	**Inconclusive†**	None
	Landing	None	None	**Inconclusive†**	**Inconclusive†**
ED - Torque Ripple (SL-1)	Takeoff	None	None	None	None
	Climb	None	None	None	None
	Cruise	None	None	None	None
	Landing	None	None	None	None
ED - Torque Ripple (SL-2)	Takeoff	None	None	None	None
	Climb	None	None	None	None
	Cruise	None	None	None	None
	Landing	None	None	None	None
ED - Torque Ripple (SL-3)	Takeoff	None	None	None	None
	Climb	None	None	None	None
	Cruise	None	None	None	None
	Landing	None	None	None	None

Bold red text signifies that case outcome crosses EASA threshold cutoff probability values: Catastrophic failures (10^{-9}) & Critical failures (10^{-7})

Table D6.1: Octocopter RPM Control DET (Single Faults) (Continued)

1st Injected Failure	Flight Phase	Minor	Major	Critical	Catastrophic
ED - Short Circuit 1	**Takeoff**	None	None	None	**Inconclusive†**
	Climb	None	Inconclusive†	None	**Inconclusive†**
	Cruise	None	Inconclusive†	Inconclusive†	**Inconclusive†**
	Landing	None	None	Inconclusive†	**Inconclusive†**
ED - Short Circuit 2	Takeoff	None	None	None	None
	Climb	None	None	None	**Inconclusive†**
	Cruise	None	None	None	None
	Landing	None	None	None	None
ED - Short Circuit 2	Takeoff	None	None	None	None
	Climb	None	None	None	None
	Cruise	None	None	None	None
	Landing	None	None	None	None
ED - Short Circuit 3	**Takeoff**	None	None	None	**Inconclusive†**
	Climb	None	Inconclusive†	None	**Inconclusive†**
	Cruise	None	Inconclusive†	Inconclusive†	**Inconclusive†**
	Landing	None	None	Inconclusive†	**Inconclusive†**

Bold red text signifies that case outcome crosses EASA threshold cutoff probability values: Catastrophic failures (10^{-9}) & Critical failures (10^{-7})

Table D6.1: Octocopter RPM Control DET (Single Faults) (Continued)

1st Injected Failure	Flight Phase	Minor	Major	Critical	Catastrophic
TS - Lowest Efficiency (SL-1)	Takeoff	None	None	None	None
	Takeoff	None	None	None	None
	Cruise	None	None	None	None
	Landing	None	None	None	None
TS - Lower Efficiency (SL-2)	Takeoff	None	None	None	None
	Takeoff	None	None	None	None
	Cruise	None	None	None	None
	Landing	None	None	None	None
TS - Partial Efficiency (SL-3)	Takeoff	None	None	None	None
	Takeoff	None	None	None	None
	Cruise	None	None	None	None
	Landing	None	None	None	None

APPENDIX E **: DETAILED FMEA OF ELECTRIC DRIVES**

Table 43: FMEA summary for electric machines

Electric machine			
Cause	**Failure rate**		**Effect**
High Voltage	**Electrical + Mechanical 9.24 E-7**	33%	100% stator short circuit
Overcurrent		35%	30% stator short circuit 10% stator open circuit 50% rotor demagnetization 10% bearing failure
Voltage Transient		15%	10% stator short circuit 20% stator open circuit 70% bearing failure
Other Failure (oil, dust, …)		5%	100% bearing failure
Eccentricity		2%	100% mechanical
Shaft Failure		2%	100% mechanical
Vibration		3%	100% mechanical
Manufacturing Defect		5%	50% electrical 50% mechanical
Cooling Failure – Liquid	**4.30E-06**		50% complete failure of the machine
			50 % overtemperature (due to partial failure of the cooling system)
Over Temperature (due to partial failure of the cooling system)	**50% cooling failure**		40% stator short circuit 10% core failure 50% rotor demagnetization

Table 44: FMEA summary for electronic speed controller

Electronic Speed Controller			
Cause	**Failure rate**		**Effect**
High Voltage	**Inverter + DC capacitor 5.4 E-6**	30%	30% inverter open circuit 20% transistor short circuit 30% DC capacitor open circuit 20% DC capacitor short circuit
Overcurrent		30%	60% transistor short circuit 40% DC capacitor short circuit
Voltage Transient		15%	100% inverter open circuit
Vibration		15%	50% inverter fault 50% inverter fault
Manufacturing Defect		10%	50% inverter 50% DC capacitor
Sensor Failure	**4 x 1.76 E-7**		100% Controller failure
LV Battery Failure	**1.011E-06**		100% Controller failure
Cooling Failure – Liquid	**4.30E-06**		50% Complete failure of the machine
			50% overtemperature (due to partial failure of the cooling system)
Overtemperature (due to partial failure of the cooling system)	**50% cooling failure**		30% Inverter open circuit 20% transistor short circuit 30% DC capacitor open circuit 20% DC capacitor short circuit

Table 45: FMEA summary for electronic power distribution

Electronic power distribution			
Cause		**Failure rate**	**Effect**
fuse failure		**1.49 E-7**	100% failure of the electronic power distribution
	high temperature	40%	
	overcurrent	30%	
	high voltage	30%	
contactor failure		**1.49 E-7**	
	high temperature	40%	
	overcurrent	30%	
	voltage transient	30%	
connection failure		**1.39 E-7**	

Table 46: FMEA summary for energy storage system

Energy Storage System		
Cause	**Failure rate**	**Effect**
Sensor failure	**3 x 1.76 E-7**	50% BMS fault 25% Internal short circuit 25% Extreme Charging/Discharging
Electric Distribution	**4.37 E-7**	50% Internal short circuit 50% Extreme Charging/Discharging
Manufacturing Defect	**1.0 E-6**	100% Internal short circuit
Physical damage	**3.1 E-07**	100% Internal short circuit
External Overheating	**1.0 E-6**	30% Internal short circuit
LV battery failure	**1.01 E-06**	100% Controller failure
Cooling failure –Liquid	**4.30 E-6**	50% Complete failure of the battery 50% Internal short circuit

Table 47: Failure modes and causes defined for all the main components of the electric system. ESC: electronic speed controller; BMS: battery management system; EM: electric motor; BP: battery pack.

Failure Mode	***No torque***	***Low torque***	***Torque ripple***	***High torque***	***Short circuit modes 1,2,3***
Failure Cause	30% Rotor failure - total demagnetization 30% Mechanical failure [a] ESC, EM, or BP cooling failure - shutdown due to overtemperature 70% Electric distribution failure (open contactor, burn fuse, connections) [b] ESC controller failure except inverter or DC capacitor short circuit [b] BMS failure [c] 30% Cell external short circuit [d] 30% Cell internal short circuit [d]	70% Rotor failure - partial demagnetization [e] 70% Mechanical failure [f] DC capacitor open circuit EM, ESC, BP reach warning temperature – ESC derating 70% Cell internal failure [g] 70% Cell external failure [g]	Current sensor fault [h] Speed sensor fault [i] EM winding or Invert open phase fault [j]	30% Electric distribution failure (close contactor, short connection)	EM winding short circuit (single phase, bi-phase, three phase) and ESC short circuit (inverter or DC capacitor) [k] EM and ESC turn off due to vehicle supervisory controller request

APPENDIX E References

[a]	Rosero, J. A., Cusido, J., Garcia, A., Ortega, J. A., & Romeral, L. (2006, November). Broken bearings and eccentricity fault detection for a permanent magnet synchronous motor. In IECON 2006-32nd Annual Conference on IEEE Industrial Electronics (pp. 964-969). IEEE. Chen, Y., Liang, S., Li, W., Liang, H., & Wang, C. (2019). Faults and diagnosis methods of permanent magnet synchronous motors: A review. Applied Sciences, 9(10), 2116.
[b]	Bianchi, N., Bolognani, S., & Zigliotto, M. (1996, June). Analysis of PM synchronous motor drive failures during flux weakening operation. In PESC Record. 27th Annual IEEE Power Electronics Specialists Conference (Vol. 2, pp. 1542-1548). IEEE.
[c]	Shu, X., Yang, W., Guo, Y., Wei, K., Qin, B., & Zhu, G. (2020). A reliability study of electric vehicle battery from the perspective of power supply system. Journal of Power Sources, 451, 227805.

APPENDIX E References

[d]	Xiong, R., Yang, R., Chen, Z., Shen, W., & Sun, F. (2019). Online fault diagnosis of external short circuit for lithium-ion battery pack. IEEE Transactions on Industrial Electronics, 67(2), 1081-1091. Feng, X., Ouyang, M., Liu, X., Lu, L., Xia, Y., & He, X. (2018). Thermal runaway mechanism of lithium ion battery for electric vehicles: A review. Energy Storage Materials, 10, 246-267.
[e]	Bilgin, O., & Kazan, F. A. (2016, September). The effect of magnet temperature on speed, current and torque in PMSMs. In 2016 XXII International Conference on Electrical Machines (ICEM) (pp. 2080-2085). IEEE.
[f]	Rosero, J. A., Cusido, J., Garcia, A., Ortega, J. A., & Romeral, L. (2006, November). Broken bearings and eccentricity fault detection for a permanent magnet synchronous motor. In IECON 2006-32nd Annual Conference on IEEE Industrial Electronics (pp. 964-969). IEEE.
[g]	Redondo-Iglesias, E., Venet, P., & Pelissier, S. (2018). Efficiency degradation model of lithium-ion batteries for electric vehicles. IEEE Transactions on Industry Applications, 55(2), 1932-1940
[h]	El Khil, S. K., Jlassi, I., Cardoso, A. J. M., Estima, J. O., & Mrabet-Bellaaj, N. (2019). Diagnosis of open-switch and current sensor faults in PMSM drives through stator current analysis. IEEE Transactions on Industry Applications, 55(6), 5925-5937. Huang, G., Luo, Y. P., Zhang, C. F., He, J., & Huang, Y. S. (2016). Current sensor fault reconstruction for PMSM drives. Sensors, 16(2), 178.
[i]	Li, T., Ahmed, Q., Rizzoni, G., Meyer, J., Boesch, M., & Badreddine, B. (2017). Motor Resolver Fault Propagation Analysis for Electrified Powertrain. In ASME 2017 Dynamic Systems and Control Conference. American Society of Mechanical Engineers Digital Collection.
[j]	Bianchi, N., Bolognani, S., & Zigliotto, M. (1996, June). Analysis of PM synchronous motor drive failures during flux weakening operation. In PESC Record. 27th Annual IEEE Power Electronics Specialists Conference (Vol. 2, pp. 1542-1548). IEEE. El Khil, S. K., Jlassi, I., Cardoso, A. J. M., Estima, J. O., & Mrabet-Bellaaj, N. (2019). Diagnosis of open-switch and current sensor faults in PMSM drives through stator current analysis. IEEE Transactions on Industry Applications, 55(6), 5925-5937. Chen, Y., Liang, S., Li, W., Liang, H., & Wang, C. (2019). Faults and diagnosis methods of permanent magnet synchronous motors: A review. Applied Sciences, 9(10), 2116.
[k]	Chowdhury, M. H. (2016, June). Modeling of faults in permanent magnet synchronous machines. In 2016 IEEE Transportation Electrification Conference and Expo, Asia-Pacific (ITEC Asia-Pacific) (pp. 246-250). IEEE. Chen, Y., Liang, S., Li, W., Liang, H., & Wang, C. (2019). Faults and diagnosis methods of permanent magnet synchronous motors: A review. Applied Sciences, 9(10), 2116.

APPENDIX F **: DETAILED MODEL OF ELECTRIC DRIVE FAULT**

No Torque: $\boldsymbol{i_q^* = 0}$

Low Torque: $i_q^* = i_q^*(before\ fault) \cdot FaultVectorMotor$

$i_q^*(before\ fault)$ represents the q-axis current request one simulation step before the fault is injected.

$FaultVectorMotor$= amplitude of the fault]0,1[

High Torque: $i_q^* = \frac{i_q^*(before\ fault)}{FaultVectorMotor}$

$i_q^*(before\ fault)$ represents the q-axis current request one simulation step before the fault is injected.

Torque Ripple: $i_q^* = i_q^* + \frac{2}{3} \cdot bias_{max} \cdot FaultVectorMotor \cdot \sin(P \cdot \theta_m)$

$bias_{max} = \frac{100A}{number\ of\ rotors}$ θ_m= electric machine rotor angular position

Short circuit 1:

If time <= fault_time_intersection, $i_q^* = i_q^*(before\ fault) + 2i_q^*(before\ fault) \cdot (1 - e^{-50(i \cdot dt - FaultInjectTimeMotor)} + 1)$

If time > fault_time_intersection, $i_q^* = 3i_q^*(before\ fault) \cdot e^{-5(i - fault\_time\_intersection - \ln(2) + 1) \cdot dt}$

$$Fault_{time_{intersection}} = -\frac{\log\left(\frac{1/2}{I_q^*}\right)}{50} + \mathrm{Fault}_{\mathrm{injection}_{\mathrm{time}}} + \mathrm{dt}$$

Short circuit 2:

$i_q^* = i_q^* + 5((A - B) \cdot e^{\left(-2\left(i - \frac{FaultInjectTimeMotor}{dt}\right) \cdot dt\right) + B) \cdot \sin(40 \cdot i \cdot dt) \cdot FaultVectrMotor}$

FaultInjectTimeMotor represents the time instant when the fault is injected.

$A = FaultVectorMotor; B = \frac{A}{2}$

Short circuit 3:

If time <= fault_time_intersection, $i_q^* = i_q^*(before\ fault) + 2i_q^*(before\ fault) \cdot \left(1 - e^{-50(i \cdot dt - FaultInjectTimeMotor)} + 1\right) + 100((A - B) \cdot e^{\left(-2\left(i - \frac{FaultInjectTimeMotor}{dt}\right) \cdot dt\right) + B) \cdot \sin(40 \cdot i \cdot dt) \cdot FaultVectorMotor}$

If i > fault_time_intersection, $i_q^* = 3i_q^*(before\ fault) \cdot e^{-5(i - fault\_time\_intersection - \ln(2) + 1) \cdot dt} + 100((A - B) \cdot e^{\left(-2\left(i - \frac{FaultInjectTimeMotor}{dt}\right) \cdot dt\right) + B) \cdot \sin(40 \cdot i \cdot dt) \cdot FaultVectorMotor}$

$A = FaultVectorMotor; B = \frac{A}{2}$

APPENDIX G : CONVERSION FROM INDIVIDUAL ROTOR COLLECTIVE PITCH TO COCKPIT INPUT

The linear dynamic models include pitch effect in typical "cockpit" input: collective, cyclic (longitudinal and lateral) and pedal input. In order to include the effect of individual pitch actuators, there is a need to convert the input to individual rotor pitch $\boldsymbol{\theta_i}$.

$$[\theta_1,\ \theta_2, \ldots \theta_n]' = T_1[u_0, u_c, u_s, u_{ped}]' \quad (49)$$

$$[u_0, u_c, u_s, u_{ped}]' = T_2[\ \theta_1,\ \theta_2, \ldots \theta_n]' \quad (50)$$

The conversion matrices are formulated as follows derived from the NASA provided linear model by using the partial derivatives for angular velocity and control input, $\frac{\partial \Omega}{\partial u}$:

Quadrotors:

$$T_1 = \begin{bmatrix} 1 & -0.5 & -0.5 & 1 \\ 1 & 0.5 & -0.5 & -1 \\ 1 & -0.5 & 0.5 & -1 \\ 1 & 0.5 & 0.5 & 1 \end{bmatrix} \quad (51)$$

$$T_2 = \begin{bmatrix} 0.25 & 0.25 & 0.25 & 0.25 \\ -0.5 & 0.5 & -0.5 & 0.5 \\ -0.5 & -0.5 & 0.5 & 0.5 \\ 0.25 & -0.25 & -0.25 & 0.25 \end{bmatrix} \quad (52)$$

Hexacopter with pitch control:

$$T_1 = \begin{bmatrix} 1 & -0.5 & -0.5 & 1 \\ 1 & -0.5 & 0.5 & -1 \\ 1 & 0 & -0.5 & -1 \\ 1 & 0 & 0.5 & 1 \\ 1 & 0.5 & -0.5 & 1 \\ 1 & 0.5 & 0.5 & -1 \end{bmatrix} \quad (53)$$

$$T_2 = \begin{bmatrix} 0.16 & 0.16 & 0.16 & 0.16 & 0.16 & 0.16 \\ -0.5 & -0.5 & 0 & 0 & 0.5 & 0.5 \\ -0.25 & 0.25 & -0.5 & 0.5 & -0.25 & 0.25 \\ 0.13 & -0.13 & -0.25 & 0.25 & 0.13 & 0.13 \end{bmatrix} \quad (54)$$

It is understood that for the hexacopter, the transformation from 4 degrees of freedom to 6 and vice versa represents a projection, but is considered appropriate given that the dynamic model is a function of the cockpit input and not the individual rotor input.

APPENDIX H **: REDUCED ORDER DYNAMIC MODEL**

APPENDIX I

Firstly, the flapping coefficients, $\beta_{1s}, \beta_{1c}, \dots, \beta_{ns}, \beta_{nc}$ where n is the number of rotors, are considered unobservable states that therefore need to be ignored in the control synthesis. Additionally, the linear models currently model the motor angular velocity, $\Omega_1, \Omega_2, \dots, \Omega_n$ as states and not as input which will be required in order to model the variable RPM vehicles.

This section will present the adaptation of the linear dynamic models through reduced order model synthesis for the purpose of controller generation.

Angular velocity of the rotors

The model includes the angular velocity of the rotors $\Omega_1, \Omega_2, \dots, \Omega_n$ as states and the torque applied by the motors $\tau_1, \tau_2, \dots, \tau_n$ as control input.

For the pitch control vehicle, the angular velocity of the rotors is not part of the controller, and the motors will aim at keeping their velocities constant.

As an example, for the quadrotor vehicles, the state space model is:

$$\dot{x} = Ax + B_1 u + B_2 w \tag{55}$$

$$\text{With: } x = \begin{bmatrix} \beta_{1s}, \beta_{1c}, \beta_{2s}, \beta_{2c}, \beta_{3s}, \beta_{3c}, \beta_{4s}, \beta_{4c}, \\ \Omega_1, \Omega_2, \Omega_3, \Omega_4, u, v, w, p, q, r, \phi, \theta, \psi \end{bmatrix}^T \tag{56}$$

$$u = \left[u_0, u_c, u_s, u_{ped}, \tau_1, \tau_2, \tau_3, \tau_4\right]^T \tag{57}$$

$$w = [u_{wind}, v_{wind}, w_{wind}, p_{wind}, q_{wind}, r_{wind}]^T \tag{58}$$

Is restructured as follows:

$$\begin{matrix} \dot{x} \\ \dot{\Omega} \end{matrix} = \begin{bmatrix} A_{11} & A_{12} \\ A_{21} & A_{22} \end{bmatrix} \begin{matrix} x \\ \Omega \end{matrix} + \begin{bmatrix} B_{11} \\ B_{12} \end{bmatrix} u' + \begin{bmatrix} B_{tau_{11}} \\ B_{tau_{12}} \end{bmatrix} \tau + \begin{bmatrix} B_{21} \\ B_{22} \end{bmatrix} w \tag{59}$$

$$\text{With: } x = \begin{bmatrix} \beta_{1s}, \beta_{1c}, \beta_{2s}, \beta_{2c}, \beta_{3s}, \beta_{3c}, \beta_{4s}, \beta_{4c}, \\ u, v, w, p, q, r, \phi, \theta, \psi \end{bmatrix}^T \tag{60}$$

$$u' = \left[u_0, u_c, u_s, u_{ped},\right]^T \tag{61}$$

$$\tau' = [\tau_1, \tau_2, \tau_3, \tau_4]^T$$

$$w = [u_{wind}, v_{wind}, w_{wind}, p_{wind}, q_{wind}, r_{wind}]^T \tag{62}$$

With B_1 now split in B_u and B_τ.

The model reduction aims at removing the angular velocity dynamics, and imposing the torque required to keep the rotors spinning at the same velocity $\dot{\Omega} = 0$.

$$\dot{\Omega} = 0 = A_{21} x + A_{22} \Omega + B_{12} u' + B_{tau_{12}} \tau + B_{22} w \tag{63}$$

$$\tau = -B_{\tau_{12}}^{inv} (A_{21} x + A_{22} \Omega + B_{12} u' + B_{22} w) \tag{64}$$

This formulation allows to be fed back into equation (59) to express the dynamics without the angular velocity dynamics, as well as to formulate a linear expression for the additional torque required due to change in vehicle state, control input and wind disturbance.

The airframe dynamics without the angular velocity becomes:

$$\dot{x} = A_{11}x + B_{11}u' + B_{21}w - B_{tau_{11}}B_{tau_{12}}^{inv}(A_{21}x + A_{22}\Omega + B_{12}u' + B_{22}w) \quad (65)$$

Which can be simplified to:

$$\dot{x} = \left(A_{11} - B_{tau_{11}}B_{tau_{12}}^{inv}A_{21}\right)x + \left(B_{11} - B_{tau_{11}}B_{tau_{12}}^{inv}B_{21}\right)u' + (B_{21} - B_{tau_{11}}B_{tau_{12}}^{inv}B_{22})\mathrm{w} \quad (66)$$

In summary, this model reduction removed the angular velocity dynamics, allowed to create an expression for the torque required, as well as assigning directly the reaction torque due to the action of a control input. This is apparent for the pedal input, which increase the collective pitch and consequently the torque required on motors spinning in the positive direction, and vice versa on the motors spinning in the negative direction.

For the electric quadrotor vehicle in hover, the coefficient of the A matrix representing $\partial\dot{r}/\partial u_{pedal}$ in the nominal model of equation (67) was $\frac{\frac{3e^{-10}rad}{s^2}}{unit\ input}$, and after model reduction, following equation (68), becomes $\frac{2\frac{rad}{s^2}}{unit\ input}$.

It is important to note that Ω are still part of the state vector. For the aircraft with RPM control, the Ω states are assumed to be control input for controller generation. The disadvantage of this formulation is that the controller does not consider the transient effect of rotor ramp up and down on the aircraft dynamics.

Flapping angles

The flapping states of the rotors are assumed to have a fast response compared to the

In summary, the states that are to be kept for controller design are:

$$\boldsymbol{x_1} = [\boldsymbol{u}, \boldsymbol{v}, \boldsymbol{w}, \boldsymbol{p}, \boldsymbol{q}, \boldsymbol{r}, \boldsymbol{\phi}, \boldsymbol{\theta}, \boldsymbol{\psi}]^T \quad (69)$$

States with dynamics to be removed for controller design:

$$x_2 = [\beta_{1c}, \beta_{1s}, \beta_{2c}, \beta_{2s}, \dots, \beta_{nc}, \beta_{ns},]^T \quad (70)$$

Singular Perturbation method can be applied here to reduce the order of the linear models [1]. This is performed by imposing the flapping rate of the rotors to zero, that is $\dot{\beta_{1c}}, \dot{\beta_{1s}}, \dots, \dot{\beta_{nc}}, \dot{\beta_{ns}} = 0$.

The initial state-space model is reorganized as follows:

$$\begin{matrix} \dot{x_1} \\ \dot{x_2} \end{matrix} = \begin{bmatrix} A_{11} & A_{12} \\ A_{21} & A_{22} \end{bmatrix} \begin{matrix} x_1 \\ x_2 \end{matrix} + \begin{bmatrix} B_1 \\ B_2 \end{bmatrix} u \tag{71}$$

By removing $\dot{x_2}$, the dynamics of $\dot{x_1}$ can be expressed as follows:

$$\dot{x_1} = [A_{11} - A_{12}A_{22}^{-1}A_{21}]x_1 + [B_1 - A_{12}A_{22}^{-1}B_2]u \tag{72}$$

The dynamic modes of the aircraft before and after the model order reduction is presented on Figure 71. It can be seen that the higher frequency modes, dominated by flapping dynamics, are not present in the ROM. However, the other roots are located at a similar location, which points to the fact that the ROM might be appropriate for the controller generation.

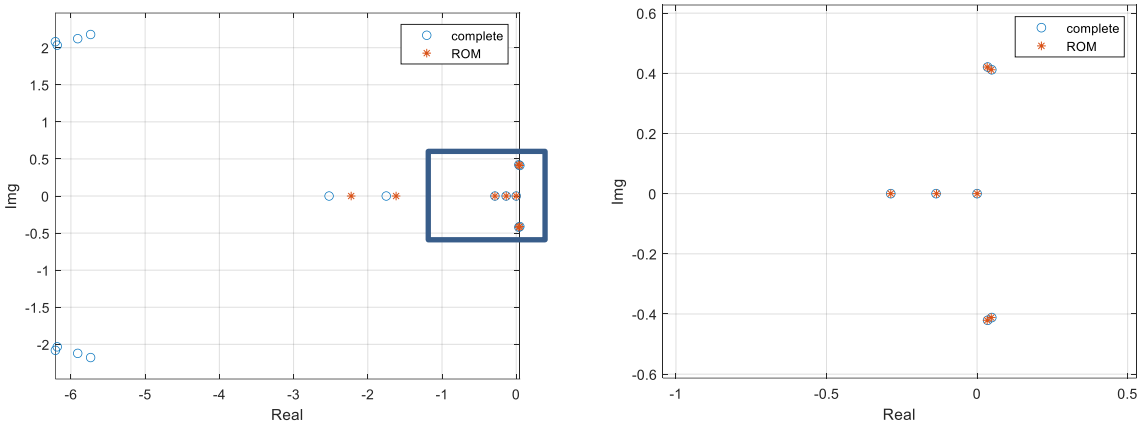

Figure 71: Roots of the linear dynamic model of the electric quadrotor in hover in the complex plane: complete dynamic system (circles) and reduced order model (asterix). On the right is a "zoom" on the origin of the complex plane where some of the roots are present.

APPENDIX J : TRIM AND CONTROL AUTHORITY ANALYSIS

Table 48: Trim and control authority of the Hexacopter Pitch

v (ft/s)	0	16.88	33.76	50.64	67.52	84.4	101.28	118.16	135.04	151.92	168.8
v knots	0	10	20	30	40	50	60	70	80	90	100
Torque required nominal (lb*ft)											
Rotor 1	852.1	774.0	620.7	496.8	428.3	399.3	397.5	416.8	454.6	507.2	578.3
Rotor 2	852.1	774.0	620.7	496.8	428.3	399.3	397.5	416.8	454.6	507.2	578.3
Rotor 3	802.7	750.5	641.4	550.0	495.1	469.8	468.0	486.5	523.7	579.5	653.5
Rotor 4	802.7	750.5	641.4	550.0	495.1	469.8	468.0	486.5	523.7	579.5	653.5
Rotor 5	755.0	727.0	659.4	599.0	558.2	538.1	537.9	557.1	595.3	656.4	734.8
Rotor 6	755.0	727.0	659.4	599.0	558.2	538.1	537.9	557.1	595.3	656.4	734.8
Pitch Nominal (deg)											
Rotor 1	10.2	9.7	8.9	8.2	7.8	7.7	7.8	8.0	8.5	9.0	9.7
Rotor 2	10.2	9.7	8.9	8.2	7.8	7.7	7.8	8.0	8.5	9.0	9.7
Rotor 3	10.0	9.6	8.9	8.3	8.0	7.9	8.0	8.3	8.8	9.3	10.0
Rotor 4	10.0	9.6	8.9	8.3	8.0	7.9	8.0	8.3	8.8	9.3	10.0
Rotor 5	9.8	9.5	9.0	8.5	8.2	8.2	8.3	8.6	9.1	9.6	10.4
Rotor 6	9.8	9.5	9.0	8.5	8.2	8.2	8.3	8.6	9.1	9.6	10.4
Control Authority MAX											
w (-) ft/s^2	-128	-128	-131	-136	-139	-144	-153.1	-159.4	-161.6	-159.4	-149
w (+) ft/s^3	92.3	89.9	86.6	87.3	87.4	90.3	96.6	102.7	107.5	110.1	108.9
p (-) rad/s^2	-22.4	-17.1	-14.5	-12.4	-11.1	-10.0	-9.2	-8.3	-7.7	-7.2	-6.9
p (+) rad/s^2	22.4	17.1	14.5	12.4	11.1	10.0	9.2	8.3	7.7	7.2	6.9
q (-) rad/s^2	-18.8	-18.5	-18.4	-19.3	-20.3	-21.2	-22.0	-22.5	-22.9	-23.0	-22.4
q (+) rad/s^2	18.6	18.4	18.5	19.5	20.6	21.6	22.4	22.9	23.4	23.5	22.9
r (-) rad/s^2	-0.6	-0.6	-0.6	-0.6	-0.6	-0.6	-0.6	-0.6	-0.6	-0.7	-0.8
r (+) rad/s^2	0.6	0.6	0.6	0.6	0.6	0.6	0.6	0.6	0.6	0.7	0.8

Table 49: Trim and control authority of the Hexacopter Pitch with motor 1 inoperative

v (ft/s)	0	16.88	33.76	50.64	67.52	84.4	101.28	118.16	135.04	151.92	168.8
v knots	0	10	20	30	40	50	60	70	80	90	100
Torque required with Motor 1 out (lb*ft)											
Rotor 1	627.8	634.3	505.9	385.3	309.8	274.7	234.7	281.8	379.3	480.4	604.5
Rotor 2	1195.5	1015.1	799.0	643.3	564.2	552.7	617.5	650.7	679.9	748.4	864.5
Rotor 3	1283.4	1051.3	860.8	749.3	678.4	700.2	845.5	881.2	885.4	951.4	1079.7
Rotor 4	706.2	804.0	718.3	611.7	536.2	450.6	299.1	308.5	402.4	478.0	540.9
Rotor 5	802.7	838.9	771.4	702.8	636.9	585.0	504.3	519.8	593.3	669.9	745.9
Rotor 6	524.7	442.5	395.8	378.4	374.3	395.3	466.8	479.5	465.2	481.7	495.4
Pitch with Motor 1 out (deg)											
Rotor 1 (imposed)	10.2	9.7	8.9	8.2	7.8	7.7	7.8	8.0	8.5	9.0	9.7
Rotor 2	14.9	14.0	12.7	11.8	11.2	11.2	12.1	14.0	12.2	12.1	15.3
Rotor 3	15.7	14.3	13.1	12.3	11.9	12.1	12.8	11.5	13.5	14.4	13.0
Rotor 4	11.6	12.5	12.0	11.0	10.4	9.4	7.2	5.9	9.3	10.7	9.3
Rotor 5	12.4	12.9	12.1	11.5	10.8	10.3	9.8	11.7	10.6	10.9	14.0
Rotor 6	3.5	2.4	2.1	2.2	2.6	3.3	4.9	5.1	4.8	4.9	5.3
Control Authority with one engine out											
w (-) ft/s^2	-72.8	-73.5	-76.2	-81.1	-86.7	-91.0	-96.5	-99.8	-101.6	-102.3	-98.9
w (+) ft/s^3	67.9	66.1	63.8	62.3	62.6	64.2	67.5	70.3	72.6	73.8	73.9
p (-) rad/s^2	-13.7	-16.0	-13.7	-11.6	-10.3	-9.2	-8.4	-7.4	-6.7	-6.1	-5.7
p (+) rad/s^2	21.6	18.2	15.4	13.2	11.8	10.8	10.1	9.2	8.6	8.2	8.1
q (-) rad/s^2	-12.9	-12.8	-12.8	-13.4	-14.0	-14.5	-14.8	-14.9	-14.8	-14.5	-13.7
q (+) rad/s^2	5.8	5.7	5.6	6.0	6.5	6.9	7.3	7.8	8.3	8.8	9.0
r (-) rad/s^2	-0.5	-0.5	-0.5	-0.5	-0.5	-0.5	-0.5	-0.5	-0.5	-0.5	-0.6
r (+) rad/s^2	0.4	0.4	0.4	0.4	0.4	0.4	0.4	0.4	0.5	0.5	0.6

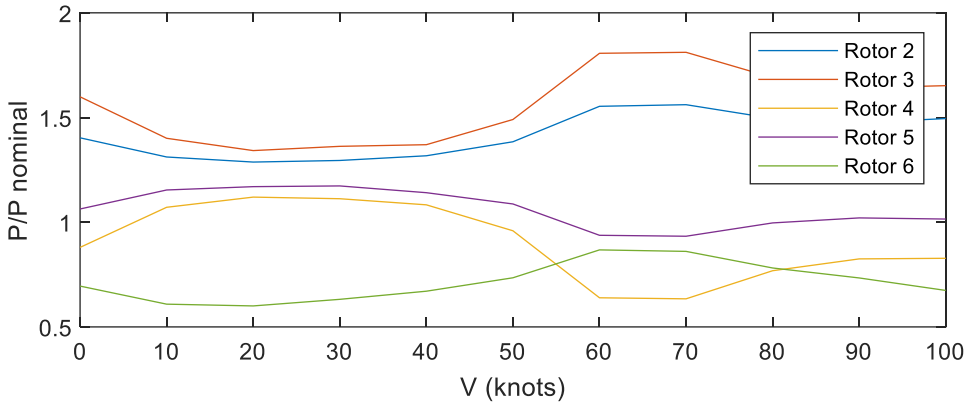

Figure 72 Power to operate with rotor 1 inoperative compared to nominal power

The same analysis was carried out on the RPM-control vehicles, as shown in Table 50 - Table 53. The different in the analysis is that the control input $[\boldsymbol{\theta_2} \dots \boldsymbol{\theta_n}]$ is replaced by the angular velocity of the rotors $[\boldsymbol{\Omega_2} \dots \boldsymbol{\Omega_n}]$.

Table 50: Trim and control authority of the Hexacopter RPM

v (ft/s)	0	16.88	33.76	50.64	67.52	84.4	101.28	118.16	135.04	151.92	168.8
v knots	0	10	20	30	40	50	60	70	80	90	100
Torque required nominal (lb*ft)	758.5	702.5	579.9	466.4	395.8	361.5	353.6	366.0	398.3	440.3	489.3
Rotor 1	758.5	702.5	579.9	466.4	395.8	361.5	353.6	366.0	398.3	440.3	489.3
Rotor 2	723.5	685.3	598.9	519.6	468.9	444.6	442.1	457.4	486.3	537.0	586.9
Rotor 3	723.5	685.3	598.9	519.6	468.9	444.6	442.1	457.4	486.3	537.0	586.9
Rotor 4	689.4	668.1	614.9	565.7	533.0	518.5	521.4	540.1	571.3	610.6	678.8
Rotor 5	689.4	668.1	614.9	565.7	533.0	518.5	521.4	540.1	571.3	610.6	678.8
Rotor 6											
Omega nominal (rad/s)											
Rotor 1	53.7	52.0	48.9	46.4	45.2	44.9	45.2	45.9	46.9	48.3	49.9
Rotor 2	53.7	52.0	48.9	46.4	45.2	44.9	45.2	45.9	46.9	48.3	49.9
Rotor 3	52.5	51.3	49.1	47.4	46.6	46.6	47.0	47.9	49.2	50.7	52.5
Rotor 4	52.5	51.3	49.1	47.4	46.6	46.6	47.0	47.9	49.2	50.7	52.5
Rotor 5	51.2	50.6	49.3	48.4	48.0	48.2	48.9	50.0	51.5	53.2	55.2
Rotor 6	51.2	50.6	49.3	48.4	48.0	48.2	48.9	50.0	51.5	53.2	55.2
Control Authority MAX											
w (-) ft/s^2	-29.9	-28.7	-26.8	-26.5	-26.8	-27.3	-28.8	-29.9	-30.7	-31.8	-33.5
w (+) ft/s^3	59.9	57.3	53.7	53.0	53.5	54.6	57.6	59.9	61.4	63.7	67.1
p (-) rad/s^2	-10.1	-9.8	-9.5	-9.4	-9.2	-9.5	-10.2	-10.7	-11.0	-11.4	-12.1
p (+) rad/s^2	10.1	9.8	9.5	9.4	9.2	9.5	10.2	10.7	11.0	11.4	12.1
q (-) rad/s^2	-8.1	-7.9	-7.8	-7.8	-7.8	-8.1	-8.4	-8.7	-9.1	-9.4	-9.9
q (+) rad/s^2	8.3	8.0	7.7	7.6	7.5	7.7	8.0	8.2	8.5	8.9	9.3
r (-) rad/s^2	-0.2	-0.2	-0.2	-0.2	-0.2	-0.2	-0.2	-0.2	-0.2	-0.2	-0.2
r (+) rad/s^2	0.2	0.2	0.2	0.2	0.2	0.2	0.2	0.2	0.2	0.2	0.2

Table 51: Trim and control authority of the Hexacopter RPM with motor 1 inoperative

v (ft/s)	0	16.9	33.8	50.6	67.5	84	101	118	135	152	169
v knots	0	10	20	30	40	50	60	70	80	90	100
Treq with Motor 1 out (lb*ft)											
	-11	-15	-38	-61	-76	-59	-25	14	60	103	105
	1169	1113	922	797	691	625	591	587	611	652	671
	1092	1021	936	816	731	664	648	654	684	750	741
	1092	985	839	642	589	559	541	549	576	633	887
	1100	1068	925	843	795	768	753	749	771	823	956
	-81	-47	10	85	89	105	129	185	230	247	185
Omega with Motor 1 out (rad/s)											
	26.9	26.0	24.4	23.2	22.0	21.7	22.0	22.7	23.7	25.1	24.9
	68.1	67.0	62.4	61.0	59.8	59.5	59.8	60.5	61.5	62.9	61.7
	65.6	63.7	62.2	59.8	59.1	59.0	59.5	60.4	61.6	63.2	61.1
	65.6	62.3	58.5	52.7	51.9	51.8	52.3	53.2	54.5	56.0	68.6
	66.2	65.5	61.5	59.9	59.5	59.8	60.4	61.5	63.0	64.7	68.9
	23.0	24.0	25.7	28.4	28.0	28.2	28.9	30.0	31.5	33.2	30.5
Control Authority with one engine out											
w (-) ft/s^2	-14.1	-13.8	####	####	####	###	-14.0	-14.6	-15.0	-15.5	####
w (+) ft/s^3	44.1	42.5	40.0	39.7	40.2	41.1	43.4	45.2	46.2	48.0	50.5
p (-) rad/s^2	-4.8	-4.7	-4.6	-4.7	-4.8	-5.0	-5.5	-5.8	-6.0	-6.3	-6.7
p (+) rad/s^2	5.0	4.9	4.8	4.7	4.5	4.6	5.0	5.3	5.4	5.6	5.8
q (-) rad/s^2	-4.2	-4.1	-3.9	-4.0	-4.1	-4.3	-4.4	-4.6	-4.9	-5.1	-5.4
q (+) rad/s^2	3.9	3.8	3.7	3.7	3.7	3.8	4.0	4.1	4.2	4.4	4.6
r (-) rad/s^2	-0.1	-0.1	-0.1	-0.1	-0.1	-0.1	-0.1	-0.1	-0.1	-0.1	-0.1
r (+) rad/s^2	0.1	0.1	0.1	0.1	0.1	0.1	0.1	0.1	0.1	0.1	0.1

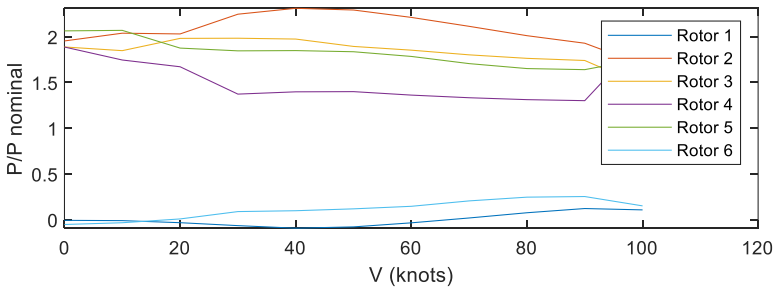

Figure 73 Power to operate with rotor 1 inoperative compared to nominal power

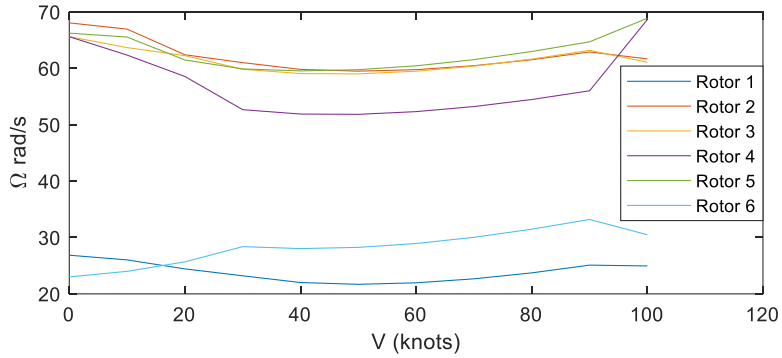

Figure 74 Rotor angular velocity for the hexacopter with rpm control to trim with rotor 1 inoperative

Table 52: Trim and control authority of the Octocopter RPM

v (ft/s)	0	16.88	33.76	50.64	67.52	84.4	101.28	118.16	135.04	151.92	168.8
v knots	0	10	20	30	40	50	60	70	80	90	100
Torque required nominal (lb*ft)											
Rotor 1	567.1	526.5	436.5	352.3	299.2	272.8	266.2	274.9	299.2	328.9	366.3
Rotor 2	567.1	526.5	436.5	352.3	299.2	272.8	266.2	274.9	299.2	328.9	366.3
Rotor 3	551.8	520.2	450.5	387.3	347.6	328.6	326.0	336.8	358.1	393.7	430.7
Rotor 4	551.8	520.2	450.5	387.3	347.6	328.6	326.0	336.8	358.1	393.7	430.7
Rotor 5	536.3	513.7	463.4	419.2	391.6	379.3	380.4	393.2	415.4	453.8	490.8
Rotor 6	536.3	513.7	463.4	419.2	391.6	379.3	380.4	393.2	415.4	453.8	490.8
Rotor 7	521.5	507.3	474.8	447.5	430.7	424.6	429.2	443.9	467.1	494.2	546.5
Rotor 8	521.5	507.3	474.8	447.5	430.7	424.6	429.2	443.9	467.1	494.2	546.5
Omega nominal (rad/s)											
Rotor 1	58.9	57.1	53.7	51.1	49.8	49.4	49.7	50.5	51.7	53.2	54.9
Rotor 2	58.9	57.1	53.7	51.1	49.8	49.4	49.7	50.5	51.7	53.2	54.9
Rotor 3	58.1	56.8	54.1	52.1	51.2	51.0	51.5	52.5	53.8	55.4	57.3
Rotor 4	58.1	56.8	54.1	52.1	51.2	51.0	51.5	52.5	53.8	55.4	57.3
Rotor 5	57.3	56.3	54.4	53.1	52.6	52.7	53.4	54.4	55.9	57.7	59.7
Rotor 6	57.3	56.3	54.4	53.1	52.6	52.7	53.4	54.4	55.9	57.7	59.7
Rotor 7	56.5	55.9	54.8	54.1	53.9	54.3	55.1	56.4	58.0	59.9	62.1
Rotor 8	56.5	55.9	54.8	54.1	53.9	54.3	55.1	56.4	58.0	59.9	62.1
Control Authority MAX											
w (-) ft/s^2	-29.4	-28.3	-26.6	-26.4	-26.0	-27.7	-29.0	-30.2	-31.5	-32.9	-34.5
w (+) ft/s^3	58.9	56.6	53.3	52.7	51.9	55.5	58.0	60.5	63.1	65.9	69.0
p (-) rad/s^2	-10.4	-10.1	-9.9	-9.7	-9.4	-10.2	-10.7	-11.3	-12.0	-12.7	-13.1
p (+) rad/s^2	10.4	10.1	9.9	9.7	9.4	10.2	10.7	11.3	12.0	12.7	13.1
q (-) rad/s^2	-6.7	-6.5	-6.3	-6.3	-6.4	-6.9	-7.1	-7.4	-7.7	-8.1	-8.5
q (+) rad/s^2	6.7	6.5	6.2	6.2	6.4	6.8	7.0	7.2	7.6	8.0	8.4
r (-) rad/s^2	-0.1	-0.1	-0.1	-0.1	-0.1	-0.1	-0.1	-0.1	-0.1	-0.1	-0.1
r (+) rad/s^2	0.1	0.1	0.1	0.1	0.1	0.1	0.1	0.1	0.1	0.1	0.1

Table 53 Trim and control authority of the Octocopter RPM with Motor 1 inoperative

v (ft/s)	0	16.88	33.76	50.64	67.52	84.4	101.28	118.16	135.04	151.92	168.8
v knots	0	10	20	30	40	50	60	70	80	90	100
Torque required with Motor 1 out (lb*ft)											
Rotor 1	-8.9	-11.0	-27.9	-43.6	-47.0	-43.7	-11.4	13.3	40.0	61.4	87.6
Rotor 2	891.2	1039.5	853.1	589.6	-46.7	413.3	283.1	390.2	556.4	113.8	294.9
Rotor 3	1461.4	209.3	184.4	1276.1	1191.3	-1256.0	608.7	549.2	929.5	768.0	784.0
Rotor 4	376.4	978.9	937.1	-941.4	1164.1	1231.2	423.1	412.9	-162.2	572.9	506.9
Rotor 5	655.0	936.2	771.2	1497.2	-110.7	1434.9	571.9	538.6	718.4	661.9	742.0
Rotor 6	-268.6	-128.6	-139	730.7	-114.2	1185.0	213.5	63.7	-3.8	583.5	479.0
Rotor 7	93.2	945.7	926.4	-1098	468.9	1243.9	232.9	354.0	-152.1	184.1	228.3
Rotor 8	1154.9	164.1	147.7	1223.2	496.6	-1368.3	474.0	538.4	1135.3	408.2	557.2
Omega with Motor 1 out (rad/s)											
Rotor 1 (imposed)	29.5	28.6	26.9	25.5	24.9	24.7	24.9	25.3	25.8	26.6	27.5
Rotor 2	75.5	84.4	77.8	66.7	24.9	60.7	51.4	61.7	77.3	31.9	48.0
Rotor 3	105.2	40.2	38.7	107.2	108.4	-69.4	76.8	73.4	110.5	91.2	88.8
Rotor 4	49.0	81.2	82.0	-30.5	106.6	119.8	59.8	59.5	2.1	72.5	64.0
Rotor 5	63.5	79.1	71.9	118.5	18.7	132.0	67.5	65.4	79.9	74.4	80.1
Rotor 6	15.1	21.8	20.3	71.9	18.5	109.6	40.3	28.9	22.7	68.0	58.6
Rotor 7	33.6	79.7	80.3	-37.6	57.1	110.1	41.0	49.1	6.4	34.4	37.9
Rotor 8	90.3	37.3	36.3	100.1	58.9	-70.4	58.5	64.3	113.7	52.8	62.9
Control Authority with one engine out											
w (-) ft/s^2	-13.2	-12.7	-12.1	-12.0	-11.7	-12.8	-13.6	-14.3	-15.1	-15.9	-16.6
w (+) ft/s^3	44.9	43.2	40.9	40.7	40.3	43.2	45.2	47.3	49.4	51.6	54.0
p (-) rad/s^2	-6.2	-6.1	-6.1	-6.1	-6.1	-6.7	-7.0	-7.5	-8.0	-8.6	-8.8
p (+) rad/s^2	9.0	8.8	8.7	8.5	8.3	9.1	9.5	10.0	10.7	11.3	11.7
q (-) rad/s^2	-4.3	-4.1	-4.1	-4.2	-4.4	-4.7	-4.9	-5.1	-5.4	-5.7	-5.9
q (+) rad/s^2	3.6	3.5	3.3	3.3	3.3	3.5	3.7	3.9	4.1	4.3	4.5
r (-) rad/s^2	-0.1	-0.1	-0.1	-0.1	-0.1	-0.1	-0.1	-0.1	-0.1	-0.1	-0.1
r (+) rad/s^2	0.1	0.1	0.1	0.1	0.1	0.1	0.1	0.1	0.1	0.1	0.1

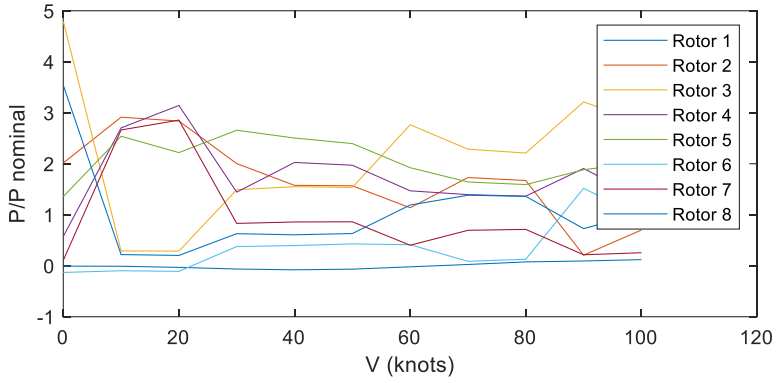

Figure 75 Power to operate with rotor 1 inoperative compared to nominal power

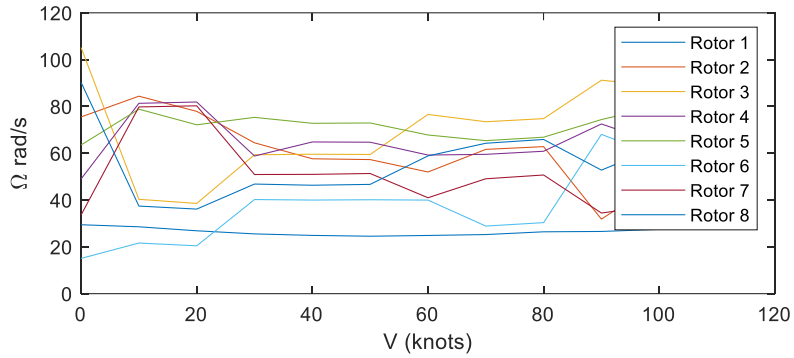

Figure 76 Rotor angular velocity for the octocopter with rpm control to trim with rotor 1 inoperative

APPENDIX K : NOMINAL FLIGHT FOR THE DIFFERENT AIRCRAFT

Quadcopter Electric

Figure 77 through Figure 80 show nominal mission characteristics for the quad electric vehicle. Figure 77 shows the translational velocity profile on the left and the translational displacement profile on the right. As can be seen, the vehicle follows the NDARC design mission closely with the desired vertical and horizontal velocities. The timed hover sections can be seen as well. Figure 78 shows the smooth angular velocity and displacement profiles. Figure 79 shows the rotor angular velocity and electric machine power profile where there can be seen that the angular velocities for the four rotors are equal to each other, as is expected due to the cross-shafting, and that the magnitude is constant outside some small magnitude excursions during transient flight phases. The electric machine power profile shows that the all four motors are well below the Intermediate Rated Power (IRP) and only cross the Maximum Continuous Power (MCP) during the take off and climb section. Figure 80 shows the heat map and the battery profile. Similar to Figure 79, the heat map shows that the torque limit approaches but doesn't cross the limit, and that the angular velocity of the motor stays constant throughout the nominal flight. The battery model shows a relatively linear discharge of the battery with the battery operation staying within the defined power limit.

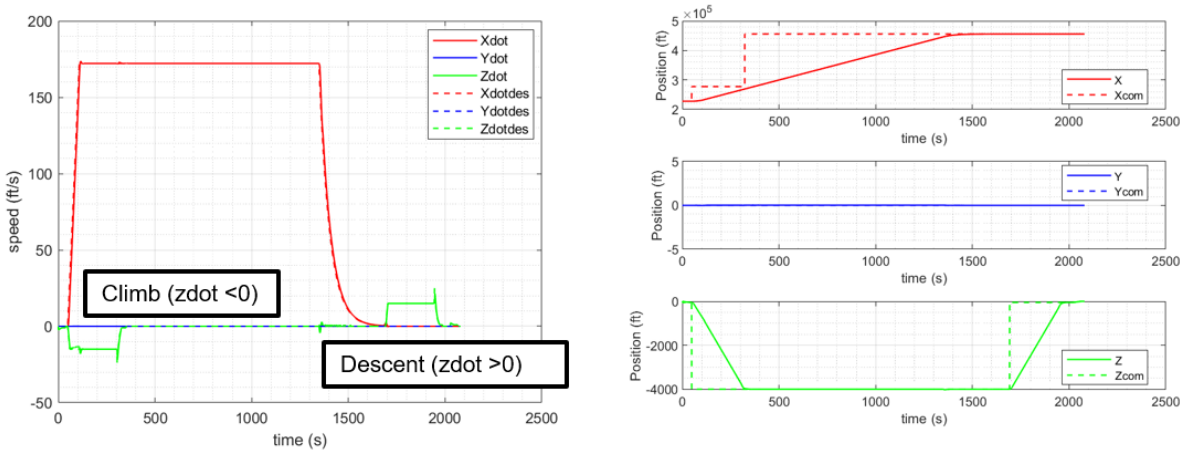

Figure 77 Quad Electric Nominal Translational Velocity Profile (LEFT) and Translational Displacement Profile (RIGHT)

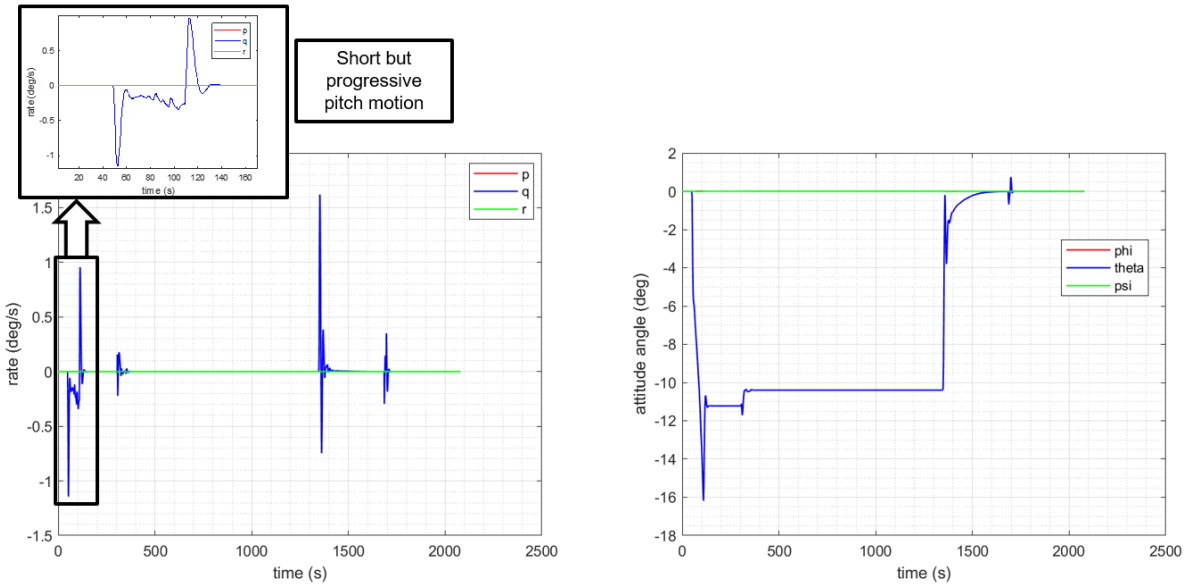

Figure 78 Quad Electric Nominal Angular Velocity Profile (LEFT) and Angular Displacement Profile (RIGHT)

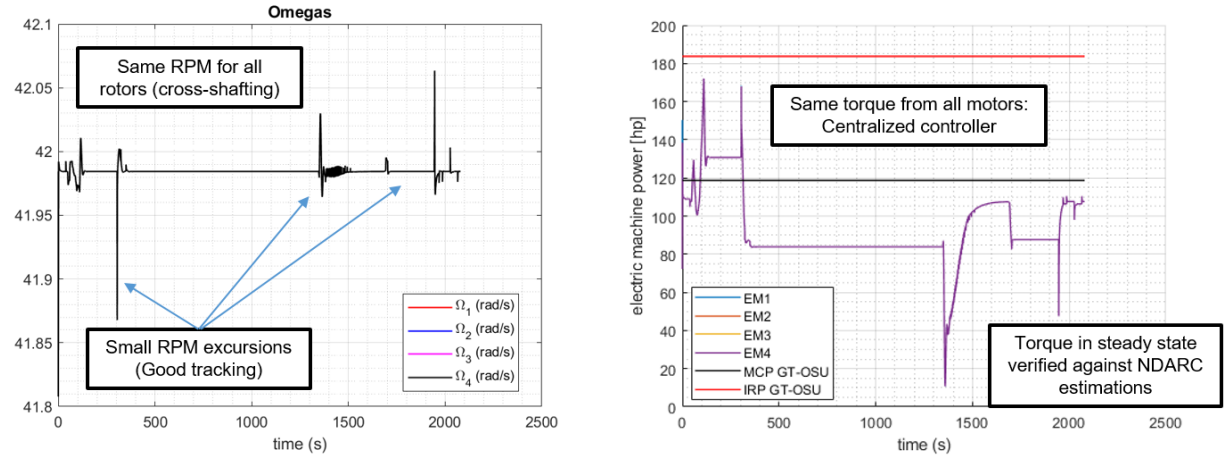

Figure 79 Quad Electric Nominal Rotor Angular Velocity (LEFT) and Electric Machine Power Profile (RIGHT)

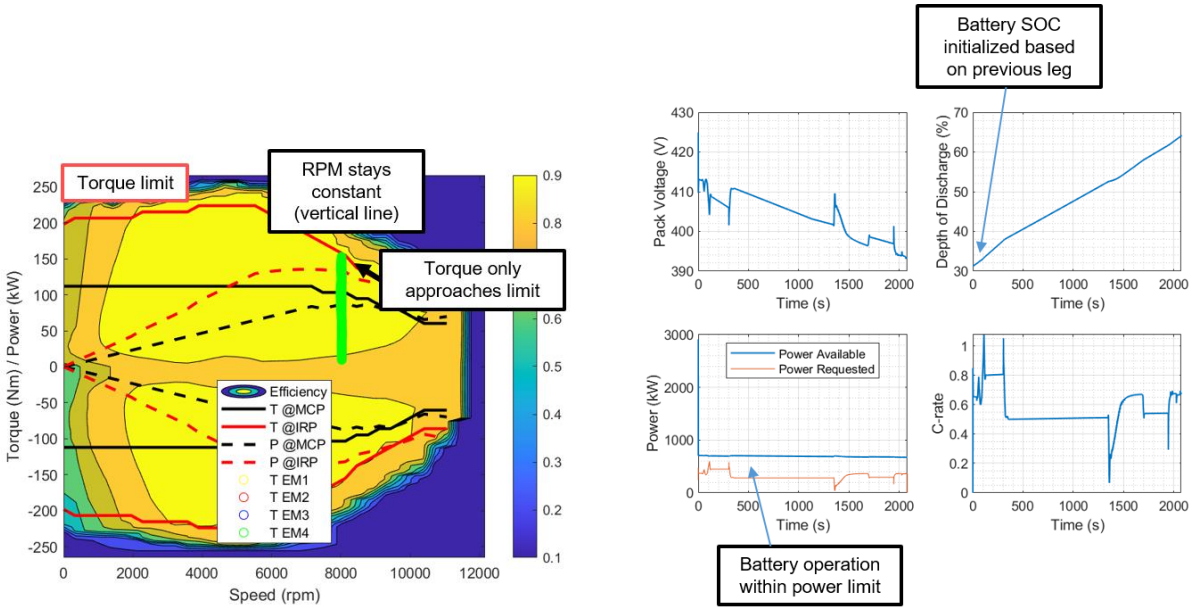

Figure 80 Quad Electric Heat Map (LEFT) and Battery Profile (RIGHT)

Quadcopter Turboshaft

Figure 81 to Figure 83 show the results of the nominal simulation for the quadrotor aircraft powered by the two turboshaft engines. The results are similar to the electric quadrotor, except for the results expressed in Figure 83 which are related to the turbine output. The low pressure and high pressure spool speeds and the power output of the turbine are expressed as a function of time. The low pressure spool, the spool from which the power is extracted stays relatively constant throughout the mission, while the high pressure spool velocity changes with the changes in power demands. It is important to note that the power output of the turbine is for one turbine only, and consequently, the power output of the combined turbines is twice as much. Given that the aircraft is performing only a longitudinal acceleration and that no wind is present, the lateral dynamic were omitted for the simulation.

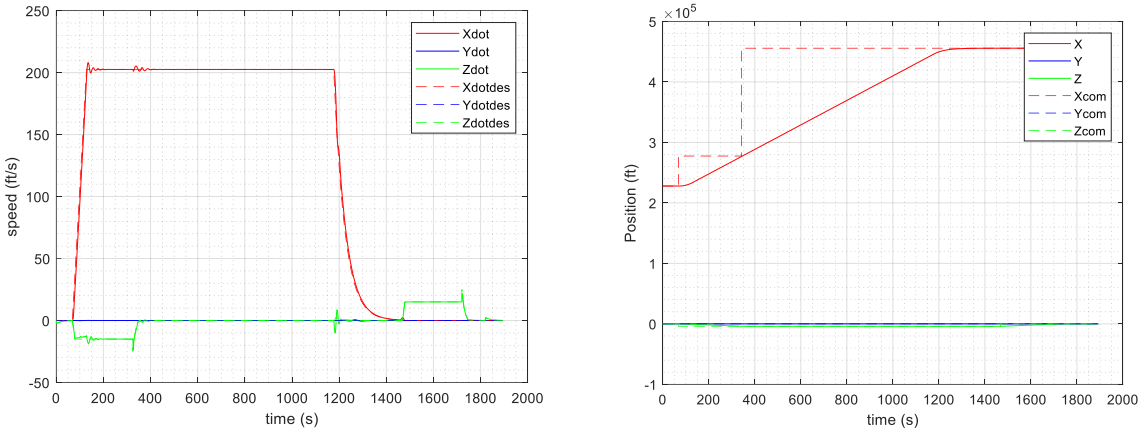

Figure 81 Quad with Turboshaft Nominal Translational Velocity Profile (LEFT) and Translational Displacement Profile (RIGHT)

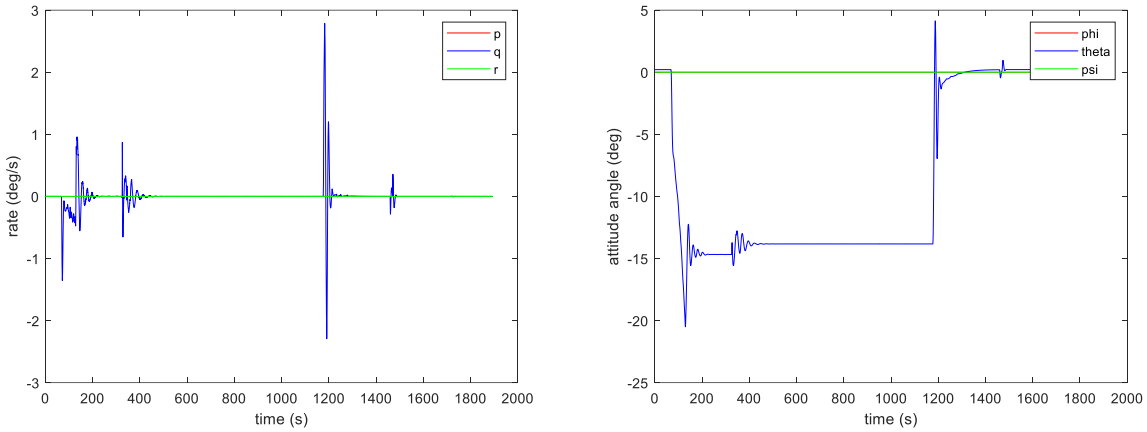

Figure 82 Quad with Turboshaft Nominal Angular Velocity Profile (LEFT) and Angular Displacement Profile (RIGHT)

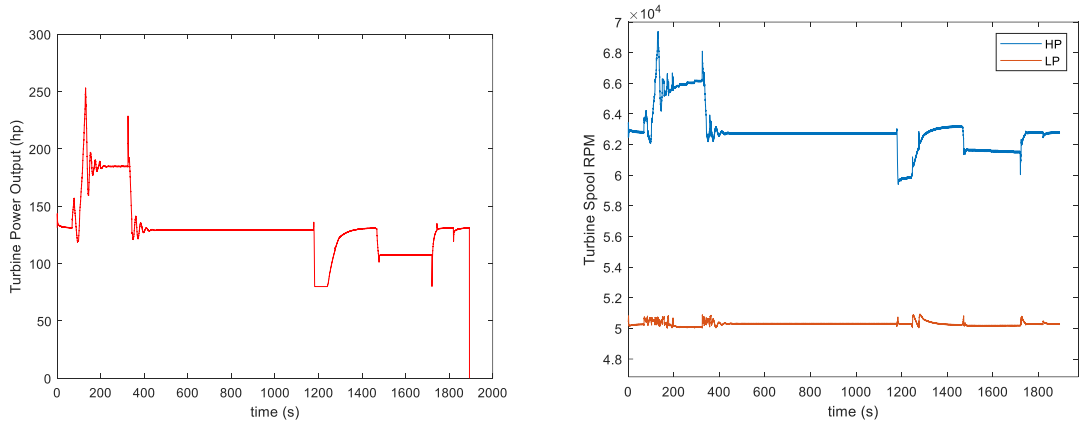

Figure 83 Quad with Turboshaft Turbine Power Output (LEFT) and Turbine Spool Speeds (RIGHT)

Quadcopter Hybrid

Figure 84 through Figure 88 show nominal mission characteristics for the quadcopter hybrid vehicle. Figure 84 shows the translation velocity and displacement profile. The profile looks very similar to the quad electric vehicle but the cruise speed is faster for this configuration. Figure 85 shows the angular velocity and displacement nominal profile. As for the quad electric, some oscillations can be seen during the transient periods which are nicely damped and contained. The results in Figure 87 and Figure 88 are very similar to the quad electric except for the battery model. Given that the aircraft is performing only a longitudinal acceleration and that no wind is present, the lateral dynamic were omitted for the simulation.

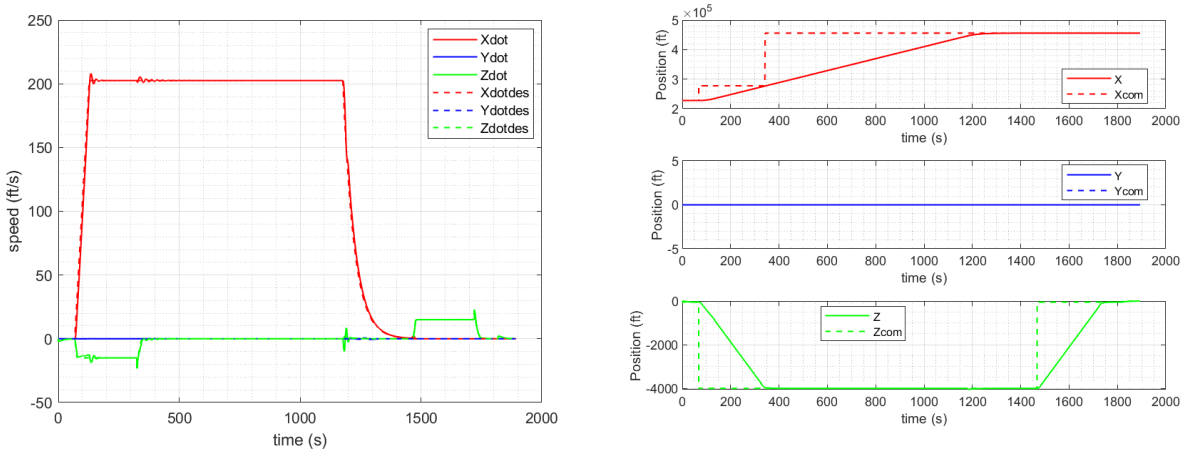

Figure 84 Quad Hybrid Nominal Translational Velocity Profile (LEFT) and Translational Displacement Profile (RIGHT)

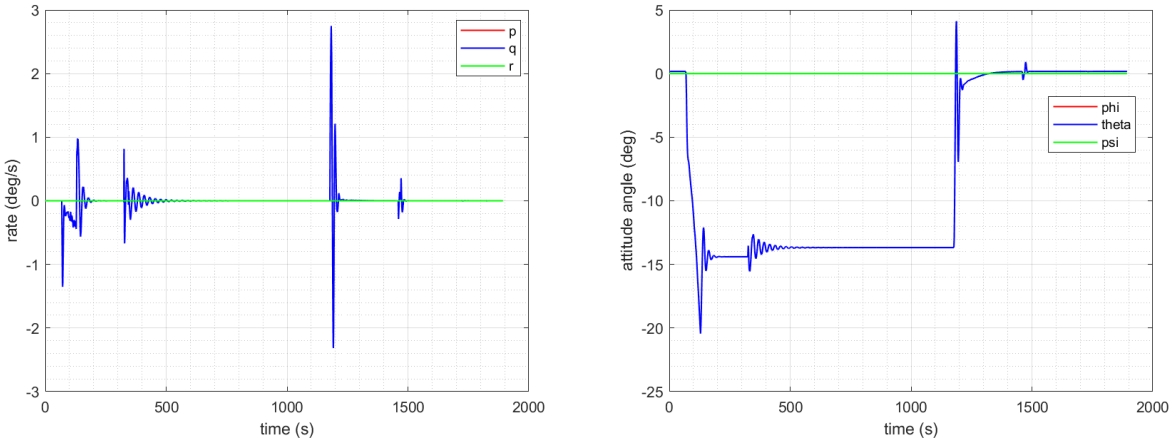

Figure 85 Quad Hybrid Nominal Angular Velocity Profile (LEFT) and Angular Displacement Profile (RIGHT)

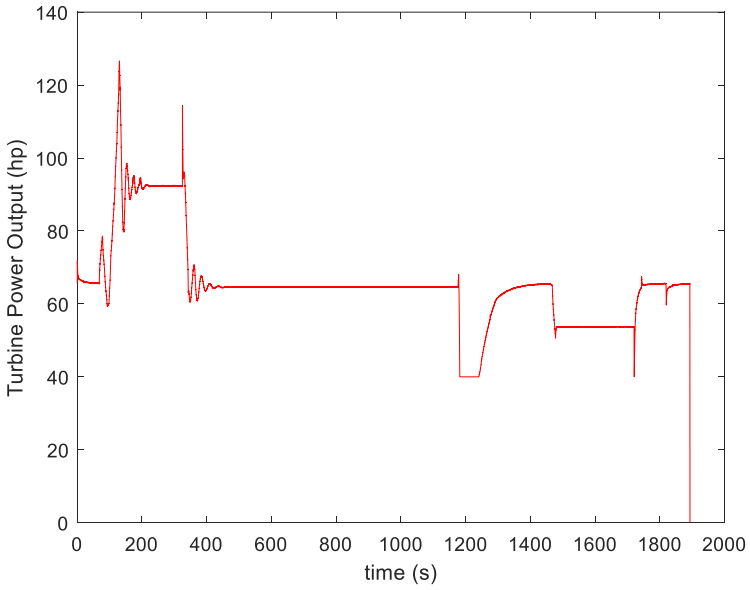

Figure 86 Turbine power output

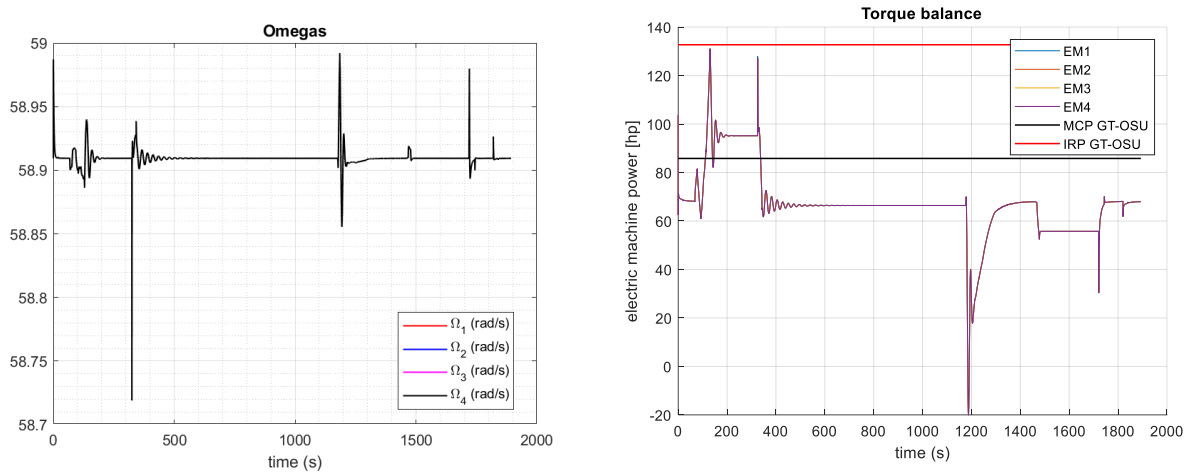

Figure 87 Quad Hybrid Nominal Rotor Angular Velocity (LEFT) and Electric Machine Power Profile (RIGHT)

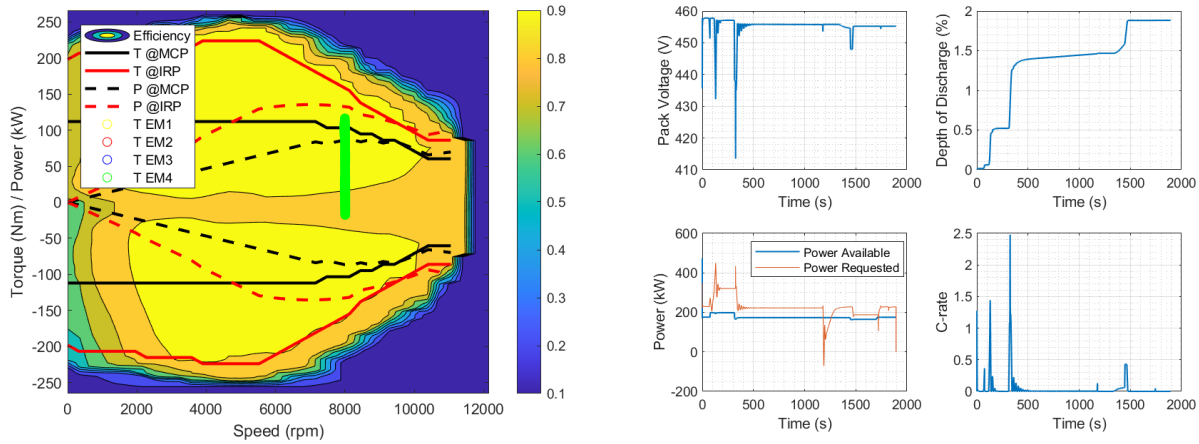

Figure 88 Quad Hybrid Heat Map (LEFT) and Battery Profile (RIGHT)

Hexacopter Variable Pitch

Figure 89 through Figure 92 show nominal mission characteristics for the hexacopter variable pitch vehicle. Figure 89 shows the translational velocity profile on the left and the translational displacement profile on the right which is identical to the quad electric flight. Figure 90 shows the smooth angular velocity and displacement profiles which is also very similar as the quad electric. Figure 91 shows the rotor angular velocity and electric machine power profile for the six motors. As can be seen, the angular velocities for the six rotors is kept nearly constant for the variable pitch configuration. The electric machine power profile shows that the all six motors are below the Intermediate Rated Power (IRP) and

cross the Maximum Continuous Power (MCP) during the take off and climb section. Figure 92 shows the heat map and the battery profile for the hexacopter variable pitch vehicle.

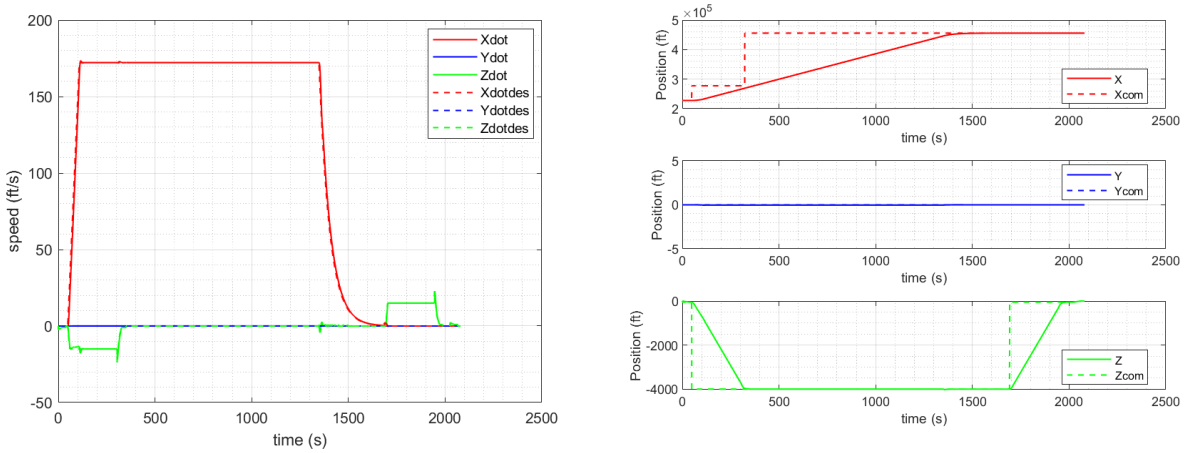

Figure 89 Hexacopter Variable Pitch Nominal Translational Velocity Profile (LEFT) and Translational Displacement Profile (RIGHT)

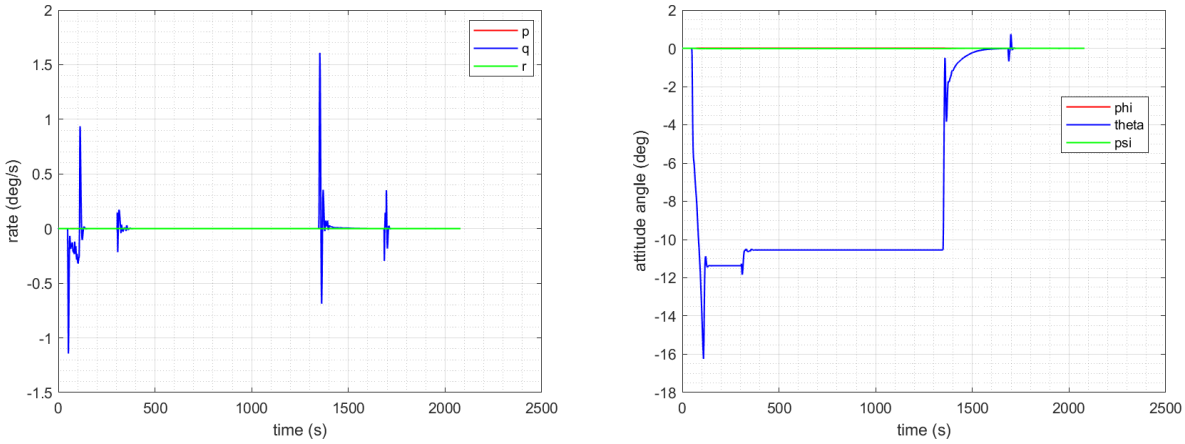

Figure 90 Hexacopter Variable Pitch Angular Velocity Profile (LEFT) and Angular Displacement Profile (RIGHT)

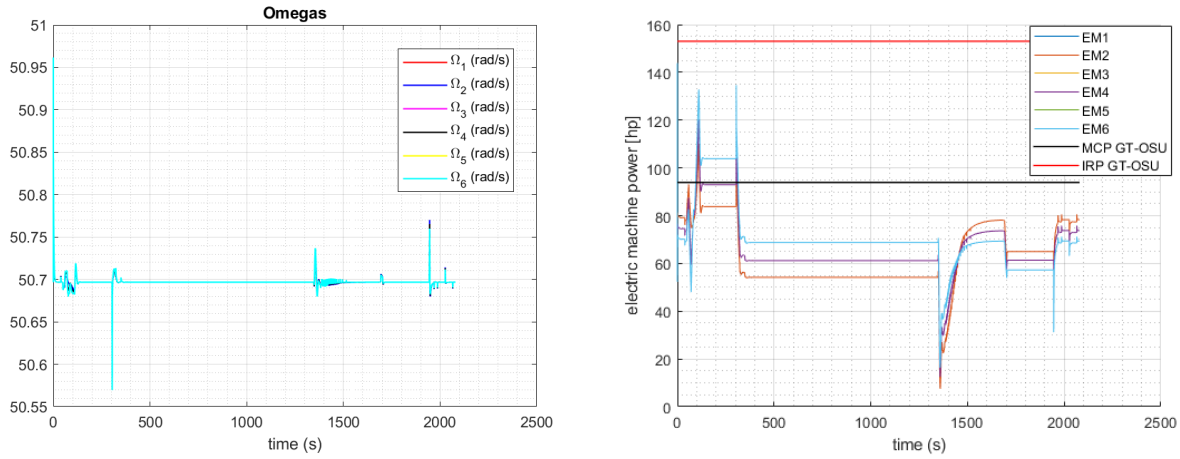

Figure 91 Hexacopter Variable Pitch Nominal Rotor Angular Velocity (LEFT) and Electric Machine Power Profile (RIGHT)

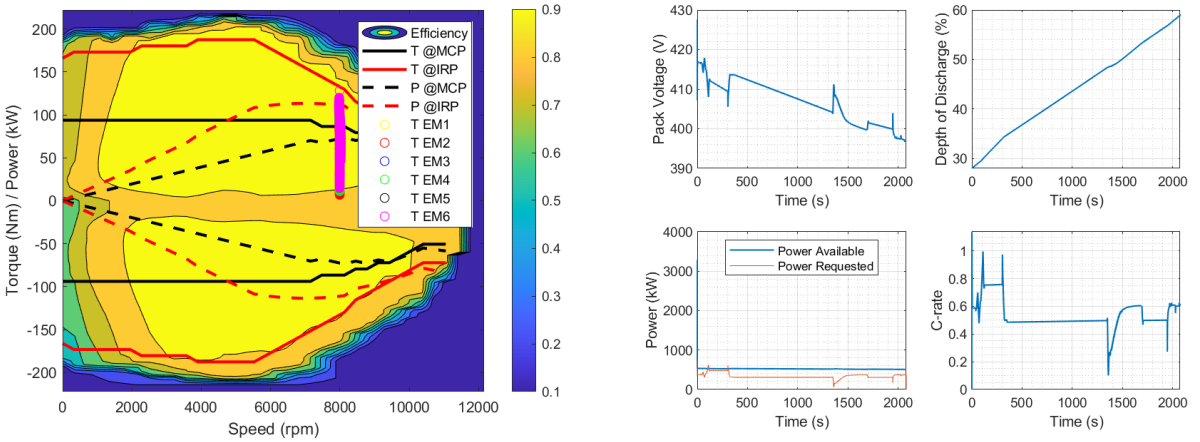

Figure 92 Hexacopter Variable Pitch Heat Map (LEFT) and Battery Profile (RIGHT)

Hexacopter Variable RPM

Figure 93 through Figure 96 show nominal mission characteristics for the hexacopter variable RPM vehicle. Figure 93 shows the translational velocity profile on the left and the translational displacement profile on the right. The flight profile is different to the hexacopter variable RPM in that the hexacopter variable RPM vehicle operates at a slower cruise velocity. Figure 94 shows angular velocity and displacement profile. Slightly more oscillations can be seen for the variable RPM vehicle as compared to the variable pitch hexacopter due to the tuning of the controller, yet the behavior is still satisfactory. Figure 95 shows the rotor angular velocity and electric machine power profile for the six motors. The time history for the angular velocities of the rotors show the differential between the motors required for vehicle control. Figure 96 shows the heat map and the battery profile.

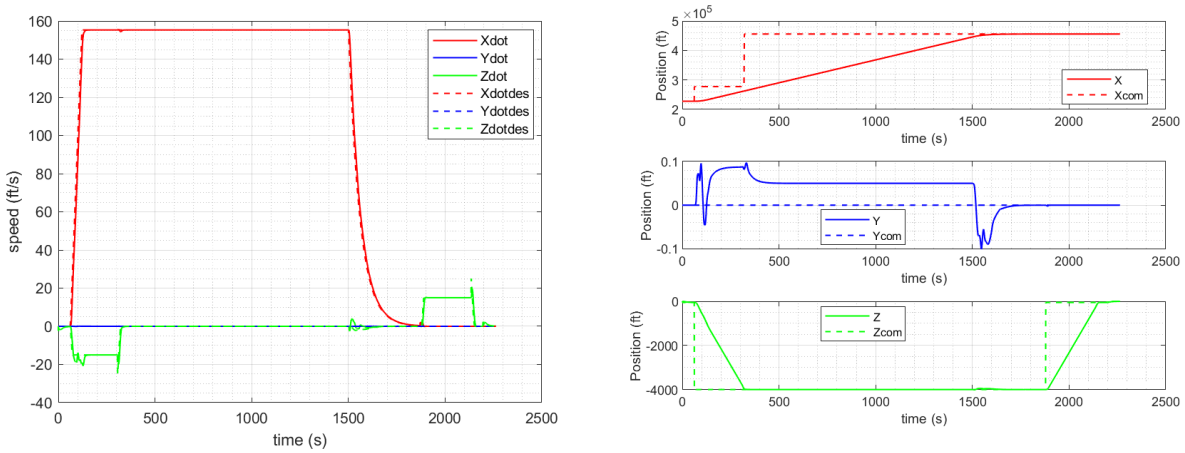

Figure 93 Hexacopter Variable RPM Nominal Translational Velocity Profile (LEFT) and Translational Displacement Profile (RIGHT)

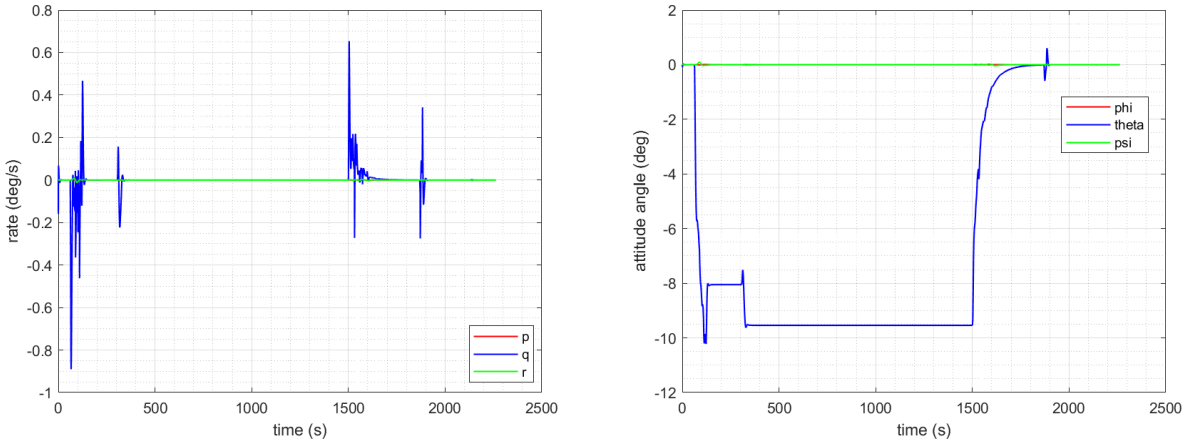

Figure 94 Hexacopter Variable RPM Angular Velocity Profile (LEFT) and Angular Displacement Profile (RIGHT)

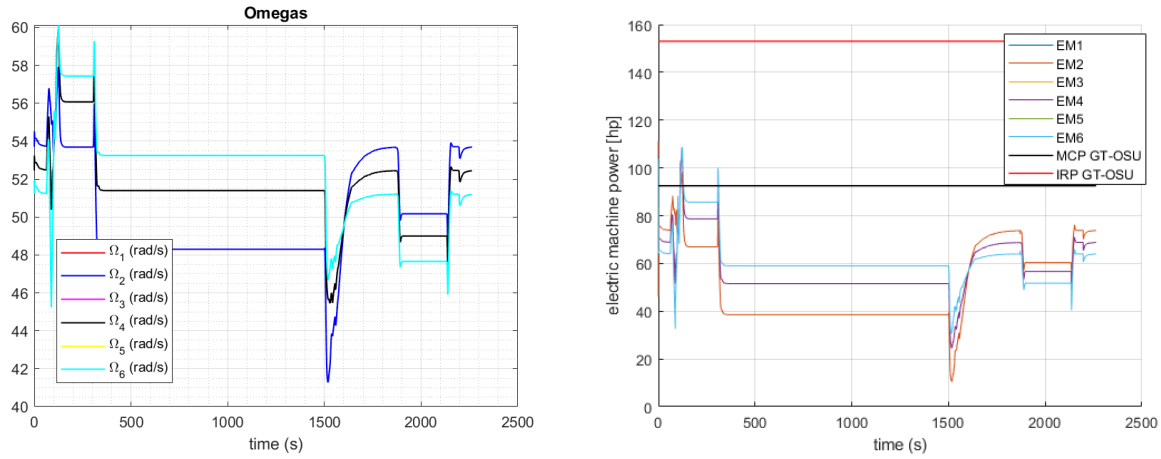

Figure 95 Hexacopter Variable RPM Nominal Rotor Angular Velocity (LEFT) and Electric Machine Power Profile (RIGHT)

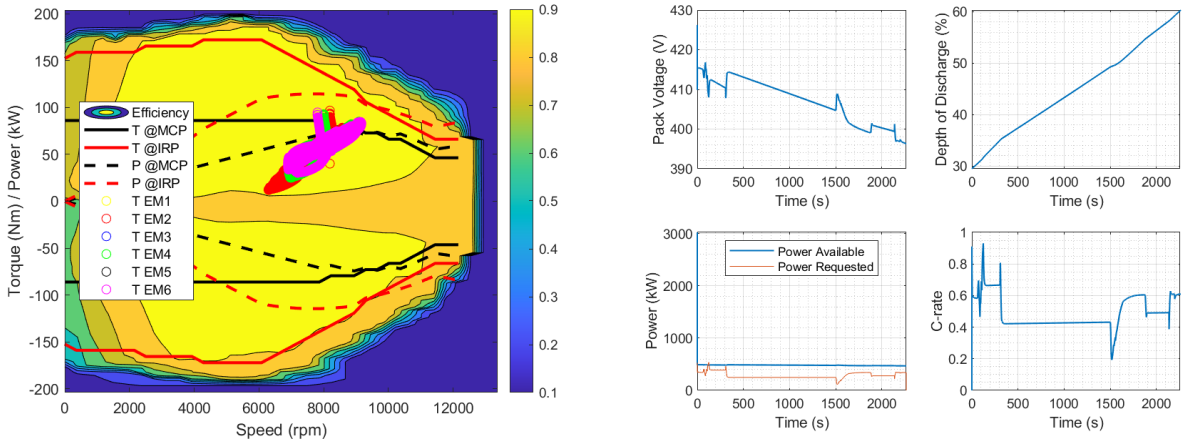

Figure 96 Hexacopter Variable RPM Heat Map (LEFT) and Battery Profile (RIGHT)

Octocopter Variable RPM

Figure 97 through Figure 100 show nominal mission characteristics for the octocopter variable RPM vehicle. The translational velocity profile and the translational displacement profile are very similar to the hexacopter variable RPM vehicle given that the cruise velocity is equal. Figure 98 shows angular velocity and displacement profile. Similar to the hexacopter variable RPM vehicle, some oscillations can be seen due to the tuning of the controller, yet the behavior is still satisfactory. Figure 99 shows the rotor angular velocity and electric machine power profile for the eight motors. Figure 100 shows the heat map and the battery profile.

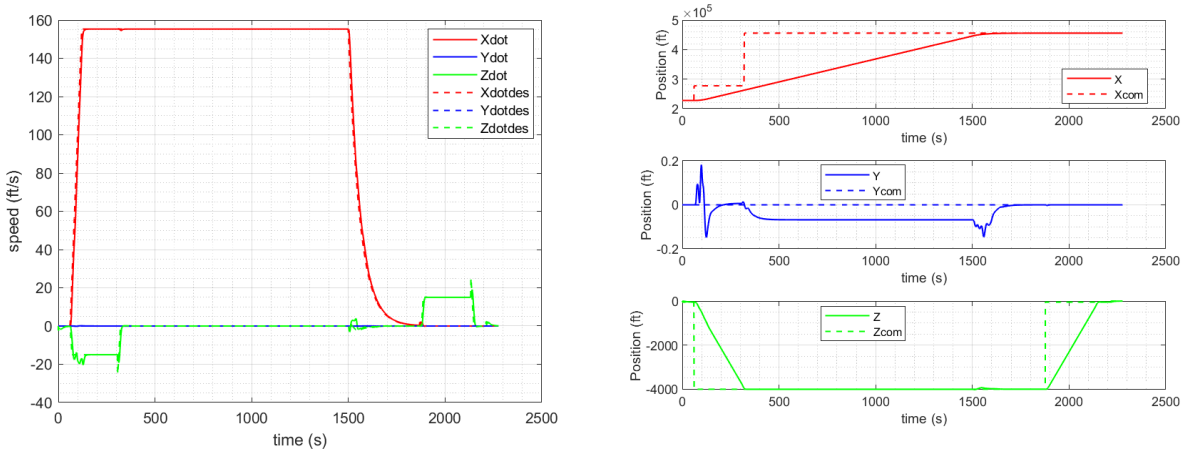

Figure 97 Octocopter Variable RPM Nominal Translational Velocity Profile (LEFT) and Translational Displacement Profile (RIGHT)

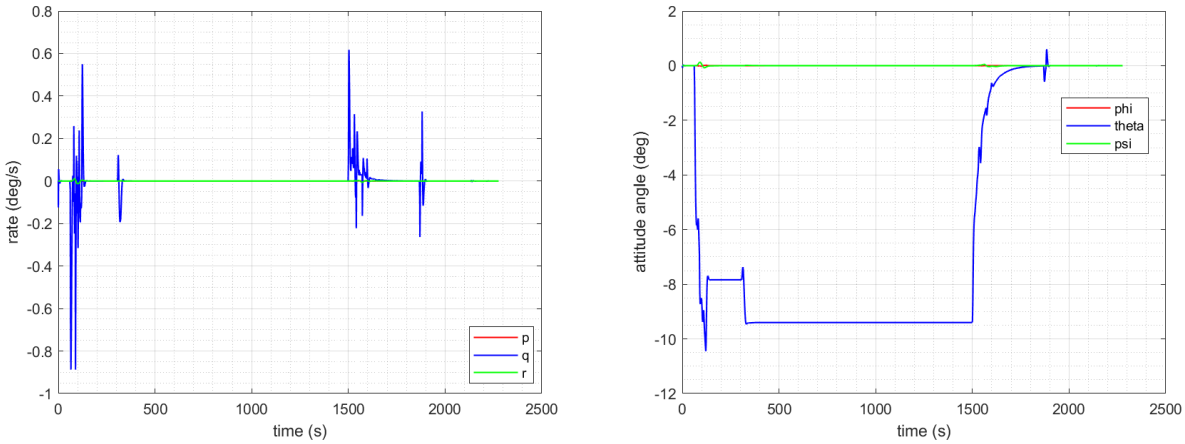

Figure 98 Octocopter Variable RPM Angular Velocity Profile (LEFT) and Angular Displacement Profile (RIGHT)

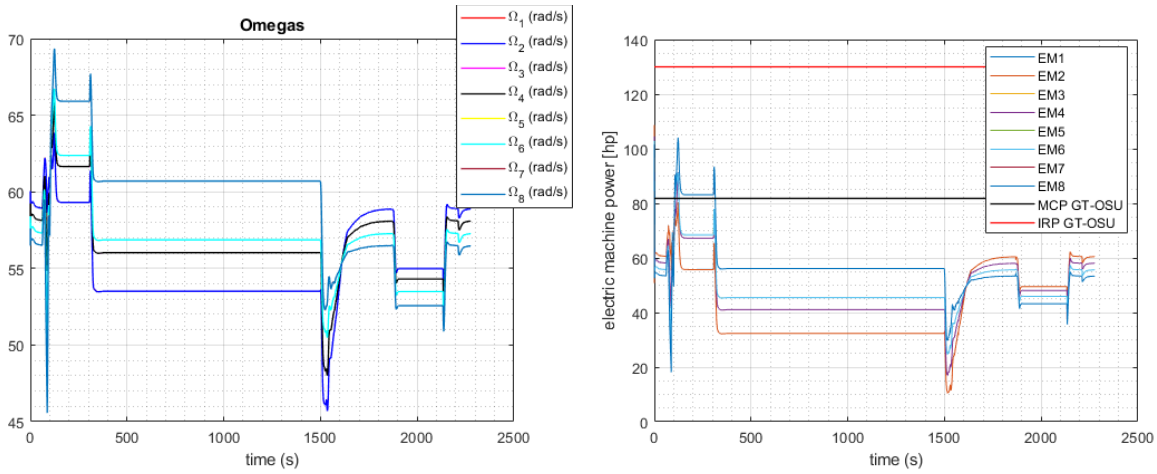

Figure 99 Octocopter Variable RPM Nominal Rotor Angular Velocity (LEFT) and Electric Machine Power Profile (RIGHT)

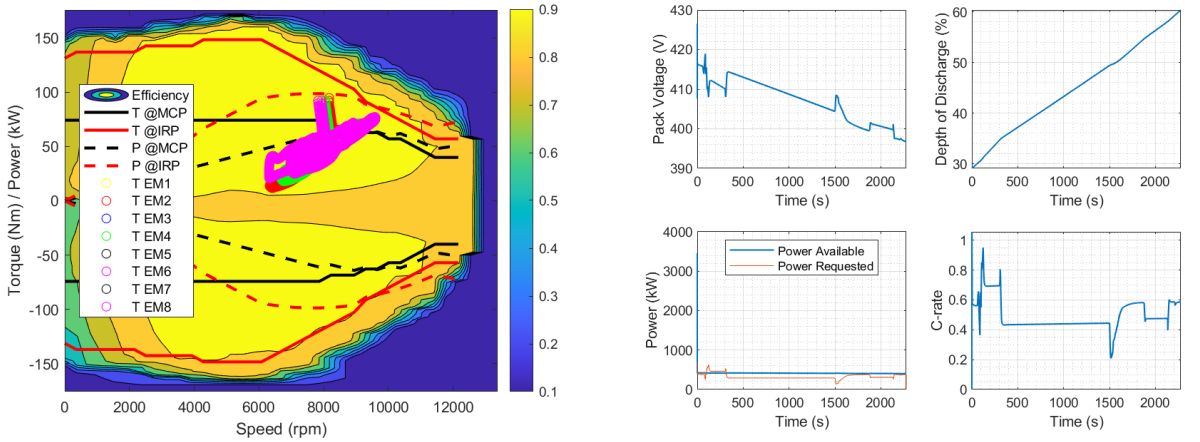

Figure 100 Octocopter Variable RPM Heat Map (LEFT) and Battery Profile (RIGHT)

APPENDIX L **: EMERGENCY MANEUVER**

As discussed in Section 1.4, an emergency maneuver is triggered when certain threshold conditions are met in the simulation. A simulated emergency maneuver for the quad electric vehicle starting at 200 seconds into the simulation can be seen in Figure 101 through Figure 104. As can be seen in Figure 101, once the emergency maneuver is started the guidance and navigation module commands to simultaneously slow the aircraft down and decrease its altitude such that zero horizontal velocity is achieved when the altitude is zero. The rate of descend is 15 ft/s for the remainder of the maneuver. Although Figure 102 shows a larger pitch response of the vehicle during the maneuver, stability is maintained throughout. Figure 103 shows that the motors practically idle for a short duration when the vehicle is slowing down and descending simultaneously.

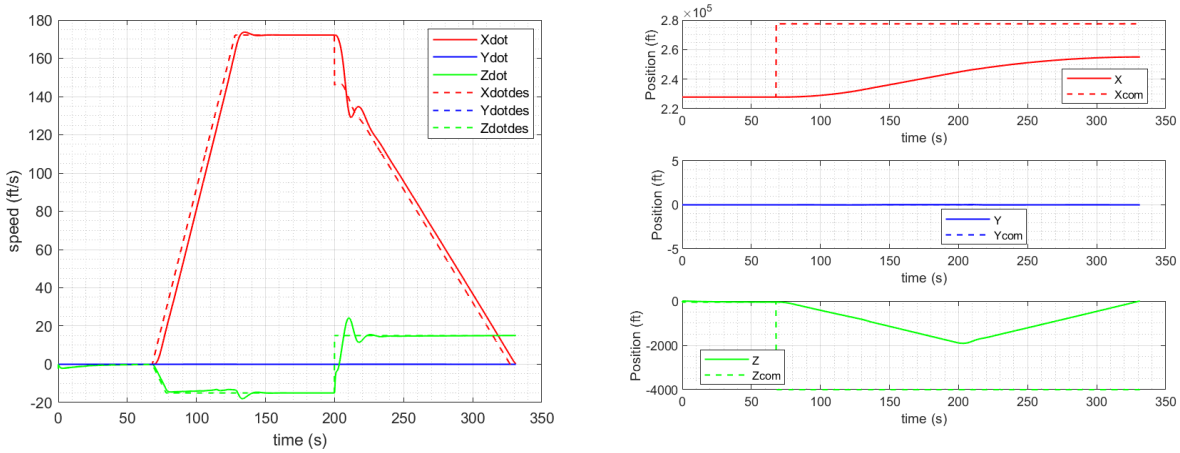

Figure 101 Quad Electric Emergency Maneuver Translational Velocity Profile (LEFT) and Translational Displacement Profile (RIGHT)

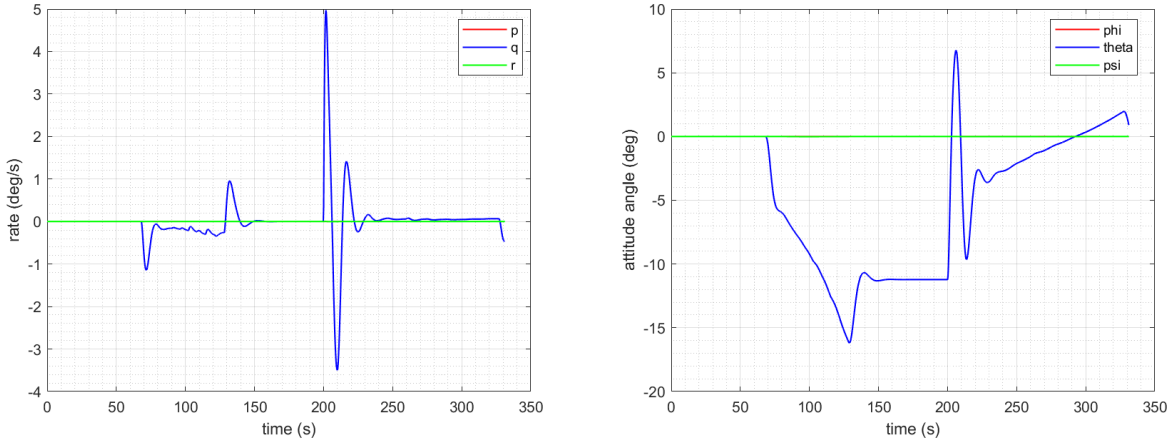

Figure 102 Quad Electric Emergency Maneuver Angular Velocity Profile (LEFT) and Angular Displacement Profile (RIGHT)

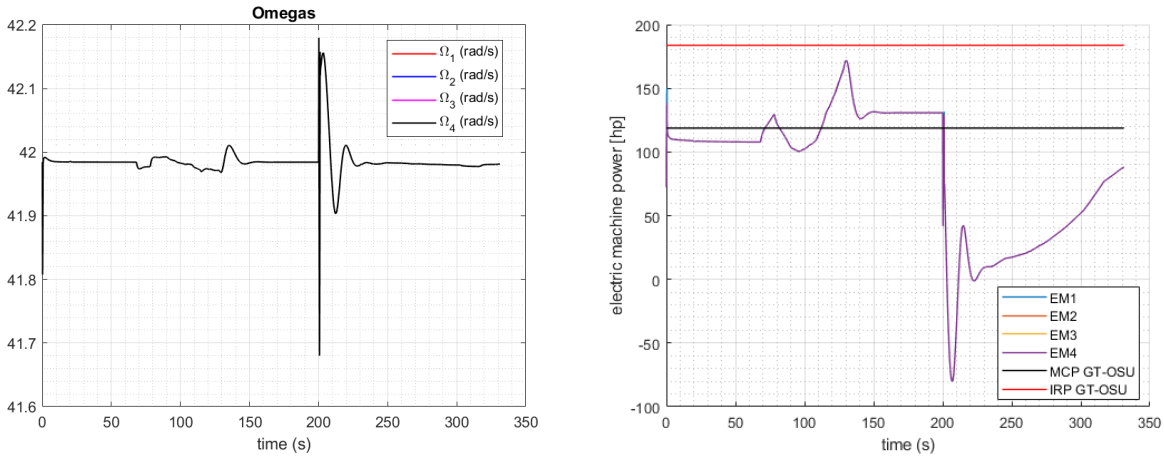

Figure 103 Quad Electric Emergency Maneuver Rotor Angular Velocity (LEFT) and Electric Machine Power Profile (RIGHT)

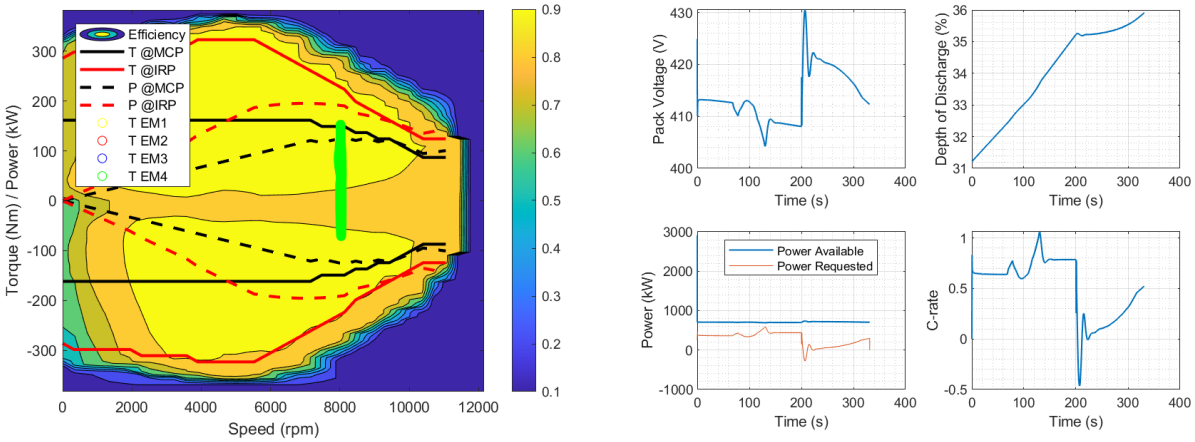

Figure 104 Quad Electric Emergency Maneuver Heat Map (LEFT) and Battery Profile (RIGHT)

APPENDIX M **: OEI/OMI DEMONSTRATION**

This section shows for each configuration verification plots for the OEI/OMI fault injection at 200 seconds in motor/engine 1.

Quadrotor Electric OMI

Figure 105 through Figure 108 show time histories for relevant parameters for an OMI condition in motor 1 after 200 sec for the quadcopter electric configuration. As can be seen, the vehicle sees minimal impact thanks to the cross-shafting architecture and is able to continue the mission. The electric machine power approaches the IRP rating of the motors during the continuation of the climb but settles back around MCP during the cruise.

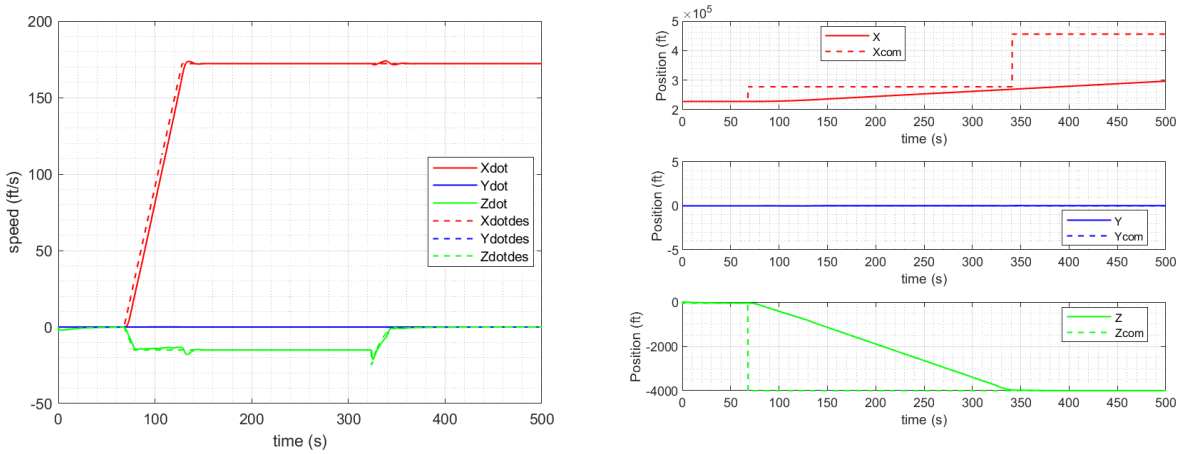

Figure 105 Quadrotor Electric OMI Translational Velocity Profile (LEFT) and Translational Displacement Profile (RIGHT)

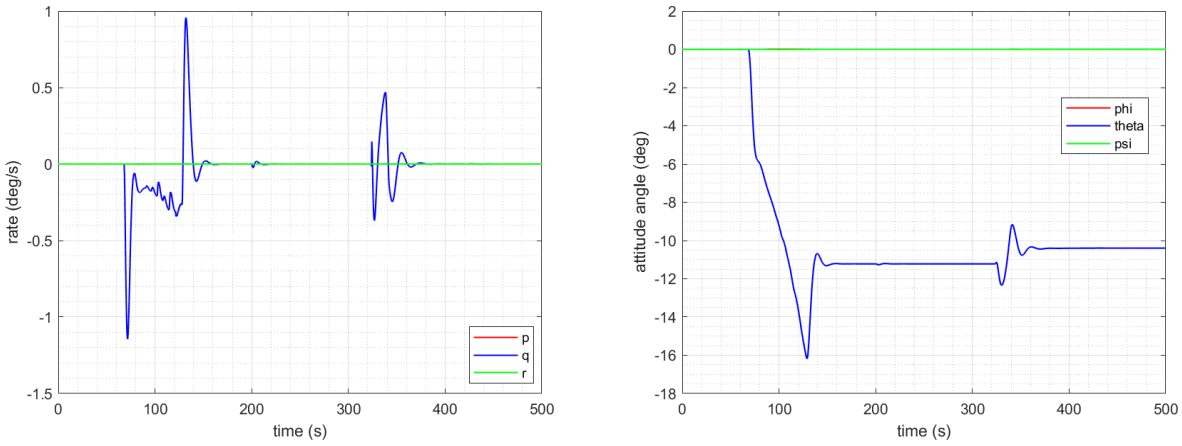

Figure 106 Quad Electric OMI Angular Velocity Profile (LEFT) and Angular Displacement Profile (RIGHT)

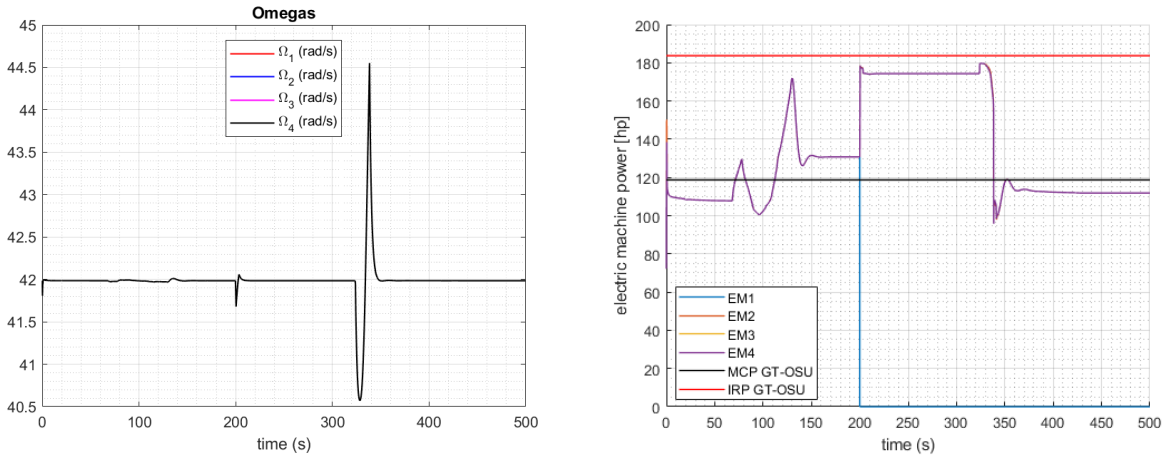

Figure 107 Quad Electric OMI Rotor Angular Velocity (LEFT) and Electric Machine Power Profile (RIGHT)

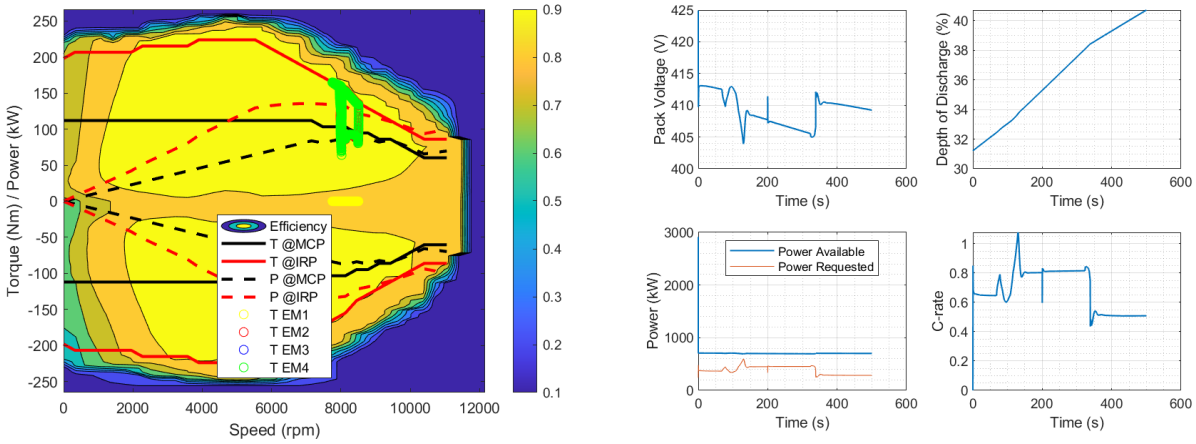

Figure 108 Quad Electric OMI Heat Map (LEFT) and Battery Profile (RIGHT)

Quadrotor Hybrid OEI

No OEI condition is included for the quadrotor hybrid configuration. Due to the inherent configuration of the quadrotor hybrid, a loss of one motor would results in a loss of the one and only turboshaft engine. The exercise at this point becomes a measure of how well the emergency landing can be achieved using the flight battery.

It was noted during the simulation that for the operation with a failed turbogenerator, that the battery discharge rate was too high. Consequently, the battery was upsized by a factor of 2 to be able to operate with a realistic discharge rate.

Quadrotor Turboshaft OEI

The turboshaft with one engine inoperative operates in a similar way as the nominal configuration, except that the full power required is transferred to a single turbine after the fault. The high pressure turbine spool goes up after the fault, as shown in Figure 109.

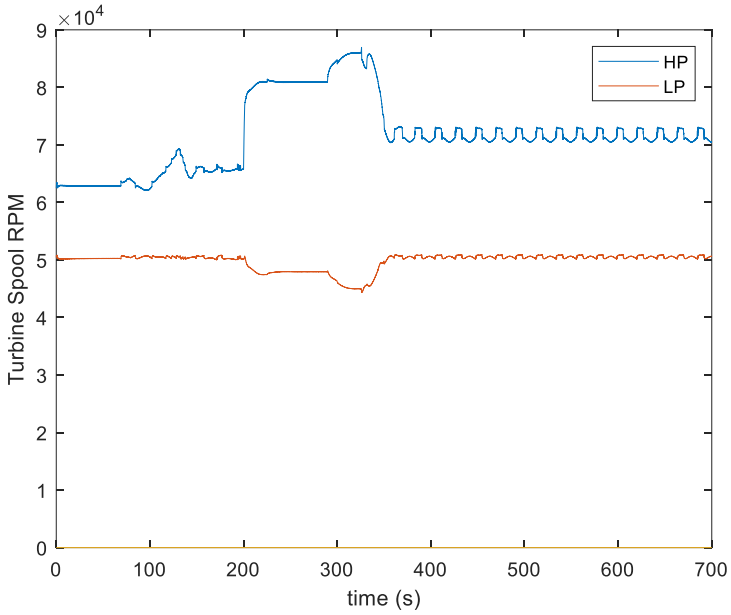

Figure 109 Spool dynamics after engine fault at t=200s

Hexacopter Variable Pitch OMI

Figure 110 through Figure 113 show time histories for relevant parameters for an OMI condition in motor 1 after 200 sec for the hexacopter variable pitch vehicle. As can be seen, the vehicle attitude attains a stable condition after the fault occurs and the vehicle is able to continue the mission. The results show that motor 3 approaches the IRP limit for the continuation of the climb but then settles back around the MCP limit.

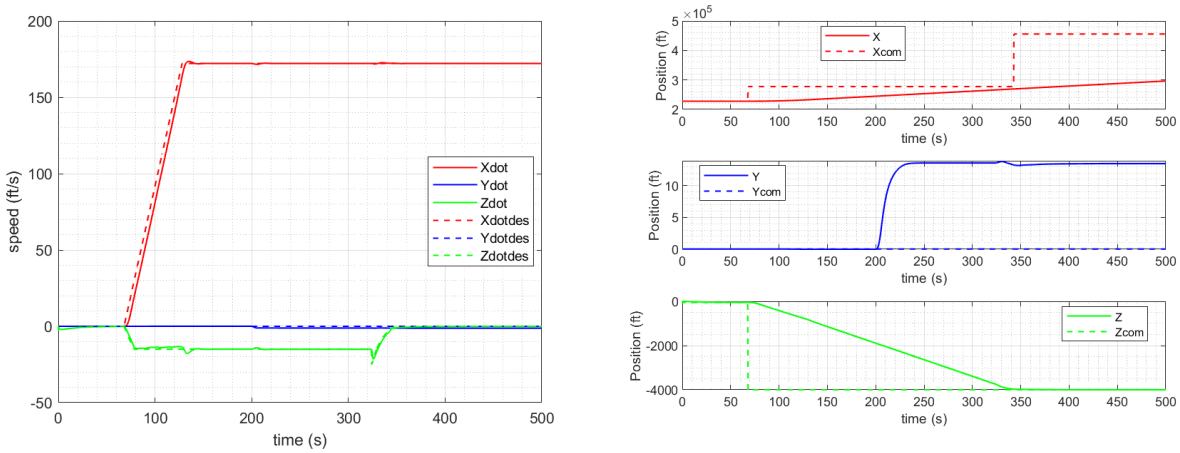

Figure 110 Hexacopter Variable Pitch OMI Translational Velocity Profile (LEFT) and Translational Displacement Profile (RIGHT)

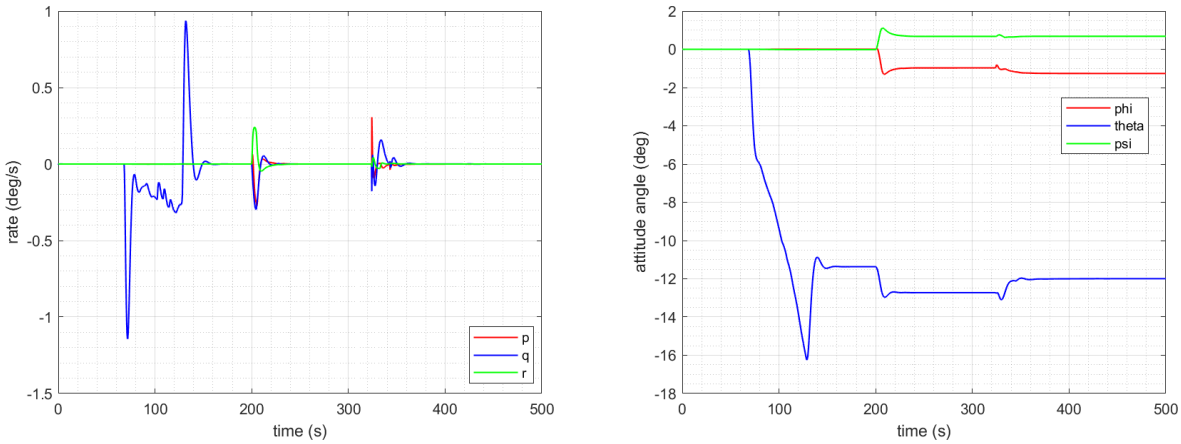

Figure 111 Hexacopter Variable Pitch OMI Angular Velocity Profile (LEFT) and Angular Displacement Profile (RIGHT)

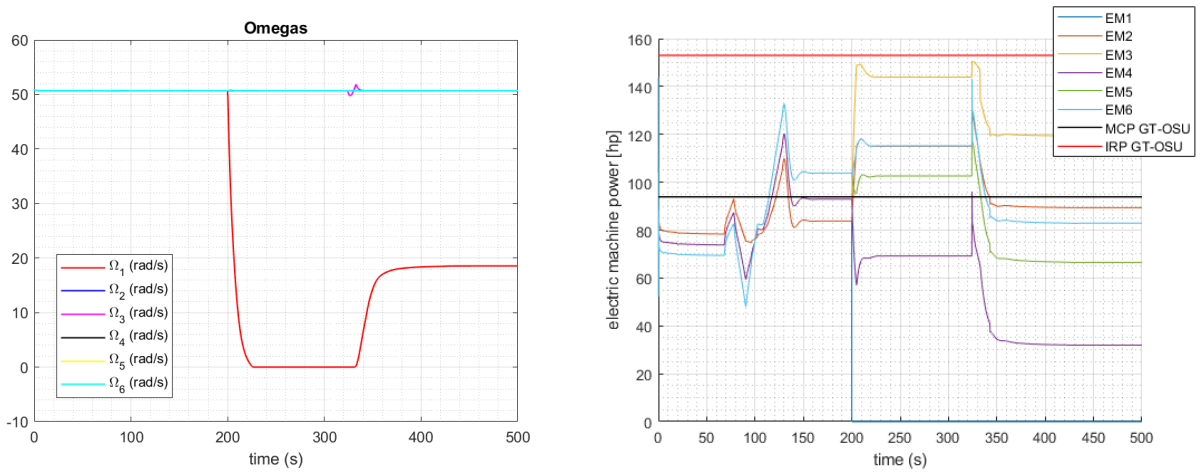

Figure 112 Hexacopter Variable Pitch OMI Rotor Angular Velocity (LEFT) and Electric Machine Power Profile (RIGHT)

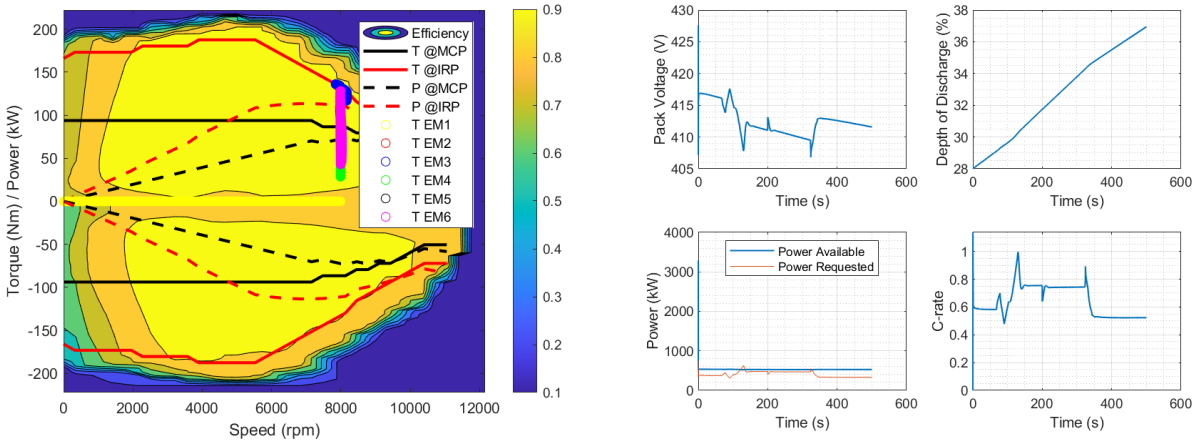

Figure 113 Hexacopter Variable Pitch OMI Heat Map (LEFT) and Battery Profile (RIGHT)

Hexacopter Variable RPM OMI

Figure 110 through Figure 113 show time histories for relevant parameters for an OMI condition in motor 1 after 200 sec for the hexacopter variable RPM vehicle. As can be seen, the vehicle response sees more transient as compared to the hexacopter variable pitch configuration and stable flight can't be achieved after the fault. One interesting observation is that a fault in motor 1 results in motor 6 approaching idle which is the diagonal opposite motor. The hexacopter variable RPM vehicle effectively becomes a quadrotor configuration.

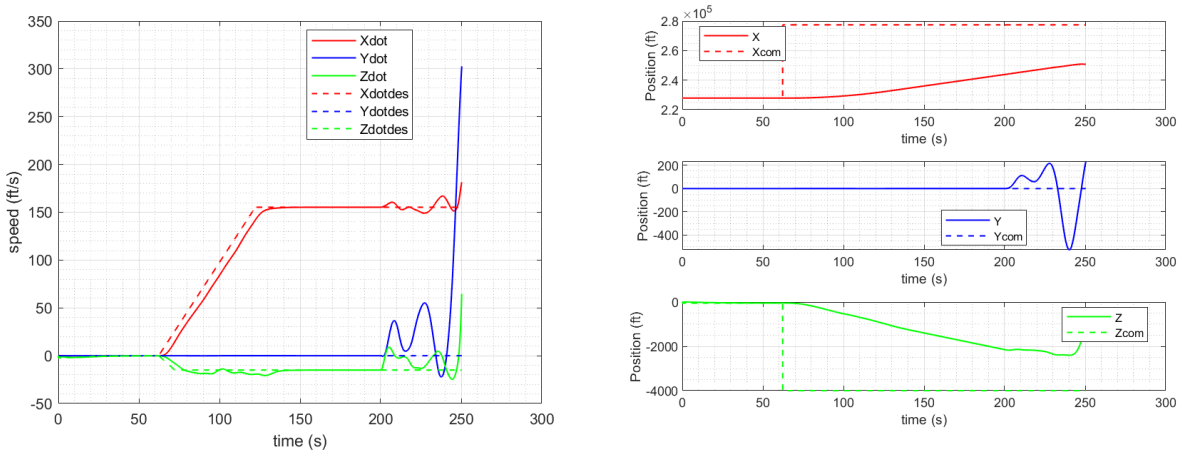

Figure 114 Hexacopter Variable RPM OMI Translational Velocity Profile (LEFT) and Translational Displacement Profile (RIGHT)

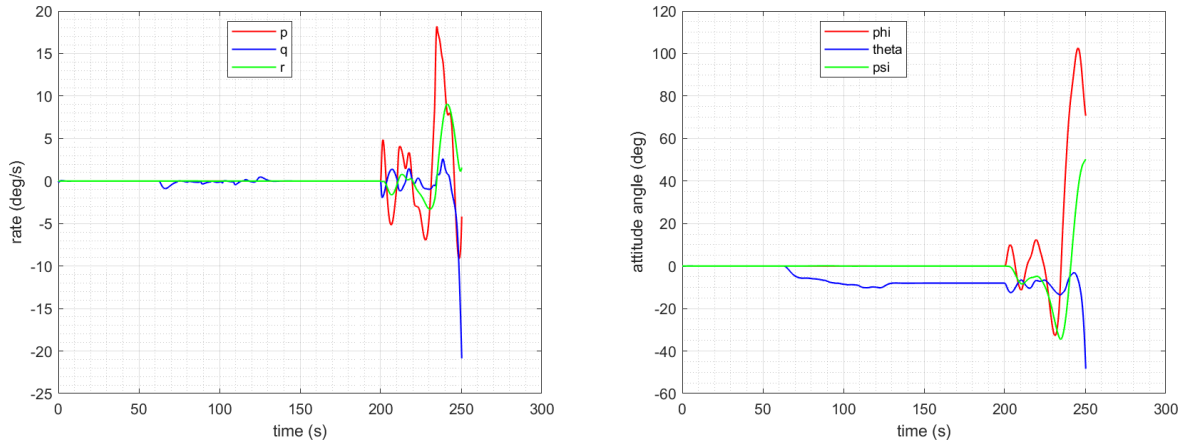

Figure 115 Hexacopter Variable RPM OMI Angular Velocity Profile (LEFT) and Angular Displacement Profile (RIGHT)

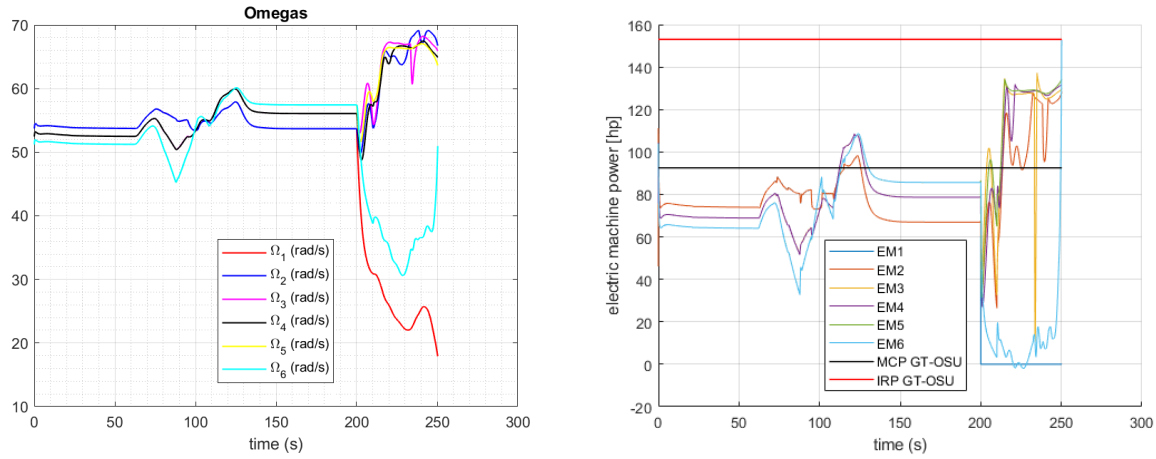

Figure 116 Hexacopter Variable RPM OMI Rotor Angular Velocity (LEFT) and Electric Machine Power Profile (RIGHT)

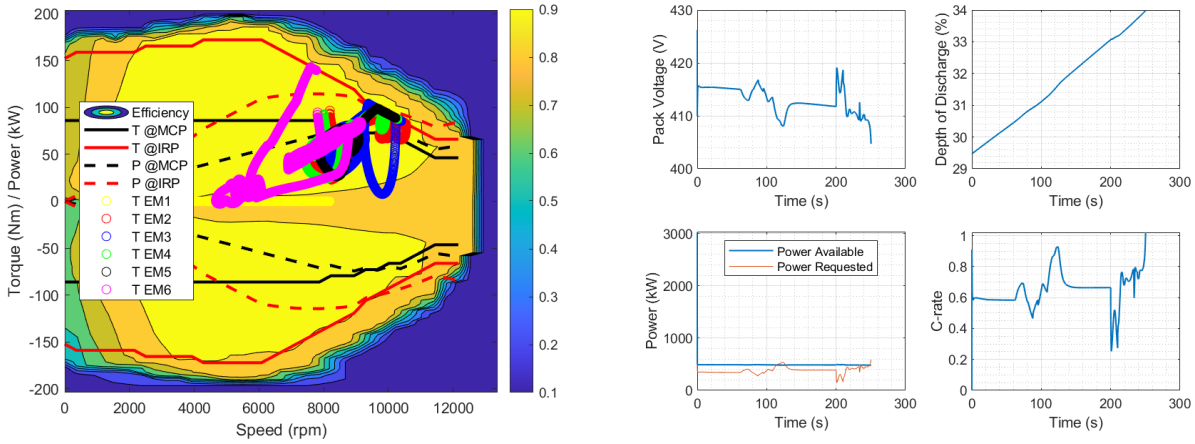

Figure 117 Hexacopter Variable RPM OMI Heat Map (LEFT) and Battery Profile (RIGHT)

Octocopter Variable RPM OMI

Figure 118 through Figure 121 show time histories for relevant parameters for an OMI condition in motor 1 after 200 sec for the octocopter variable RPM vehicle. As can be seen, the vehicle response contains similar transients as the hexacopter variable RPM configuration and stable flight can't be achieved after the fault. As can be seen, the loss of power in motor 1 redistributes the necessary increase in power of the remaining engines more evenly than the hexacopter variable RPM vehicle.

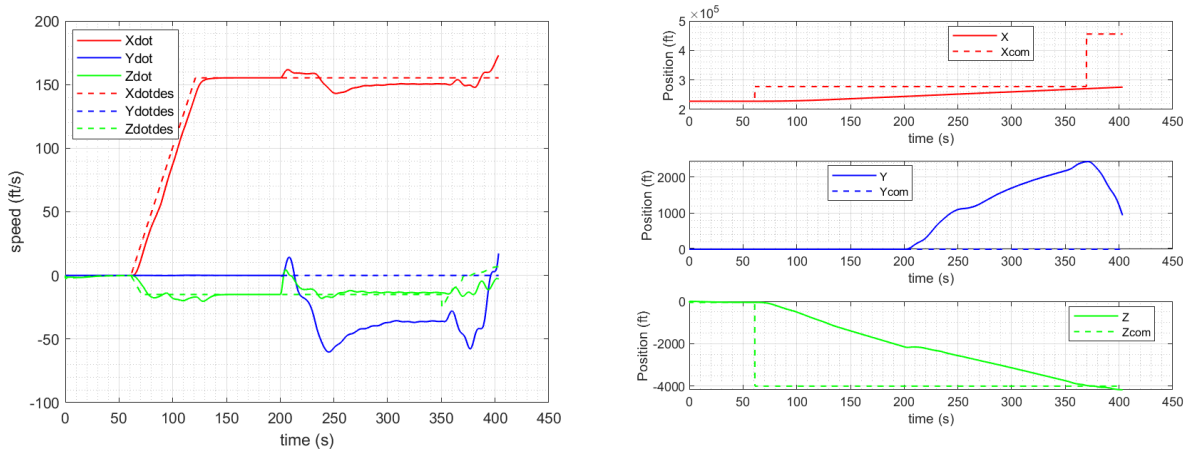

Figure 118 Octocopter Variable RPM OMI Translational Velocity Profile (LEFT) and Translational Displacement Profile (RIGHT)

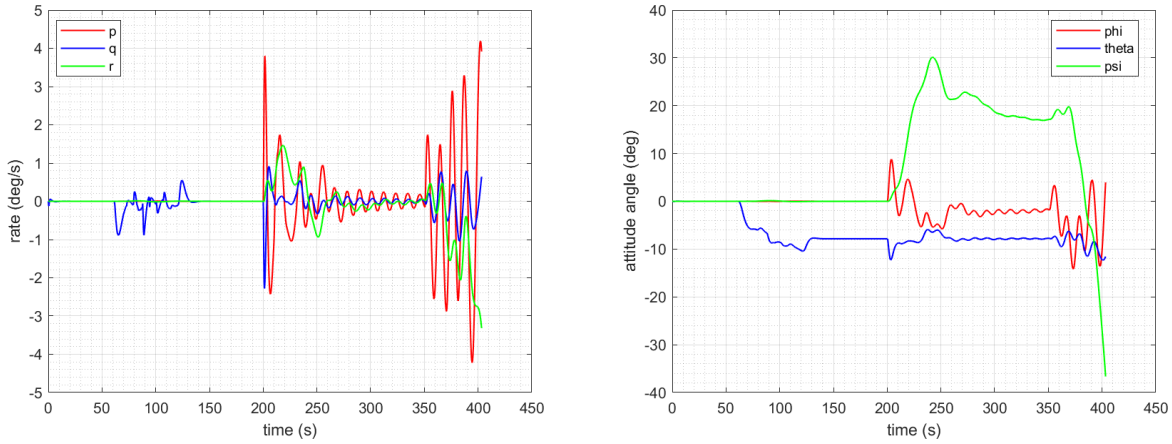

Figure 119: Octocopter Variable RPM OMI Angular Velocity Profile (LEFT) and Angular Displacement Profile (RIGHT)

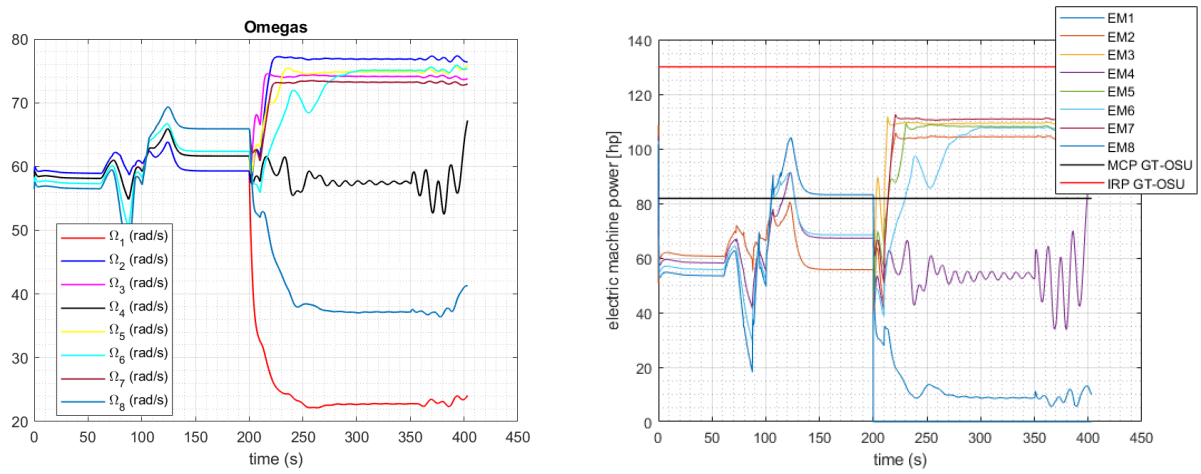

Figure 120: Octocopter Variable RPM OMI Rotor Angular Velocity (LEFT) and Electric Machine Power Profile (RIGHT)

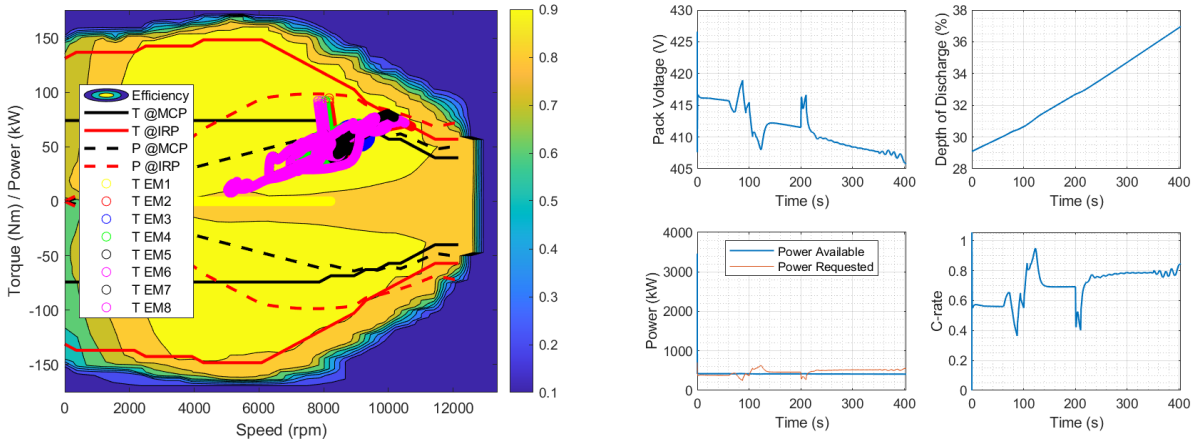

Figure 121: Octocopter Variable RPM OMI Heat Map (LEFT) and Battery Profile (RIGHT)

APPENDIX N: **POWER ASSESSMENT OF THE DIFFERENT AIRCRAFT**

This appendix presents the simulation results for hexacopter with pitch control, hexacopter with rpm control and octocopter with rpm control for the following cases: nominal operation, wind operation, and operation with a no-torque condition during the initial phase of flight.

In order to simulate the whole mission for the cases with one engine inoperative, there is a need to have a system that can successfully complete the whole mission. Consequently, the motors for the RPM-control are upsized, according to the GT-OSU OMI guidelines (see Section X).

Hexacopter Pitch Control

Nominal Operation

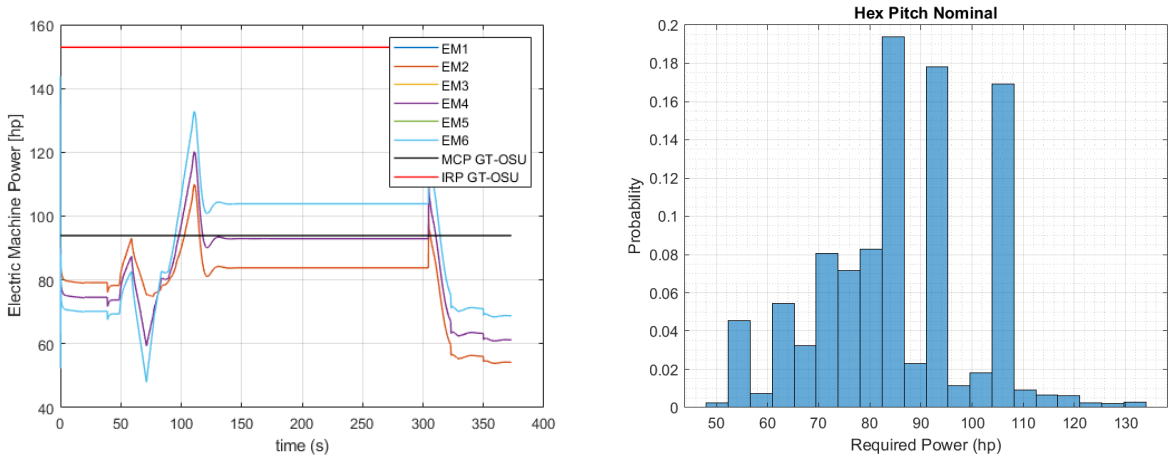

Figure 122: Hexacopter with pitch control during takeoff, acceleration and climb: Power as a function of time and power bucket distribution

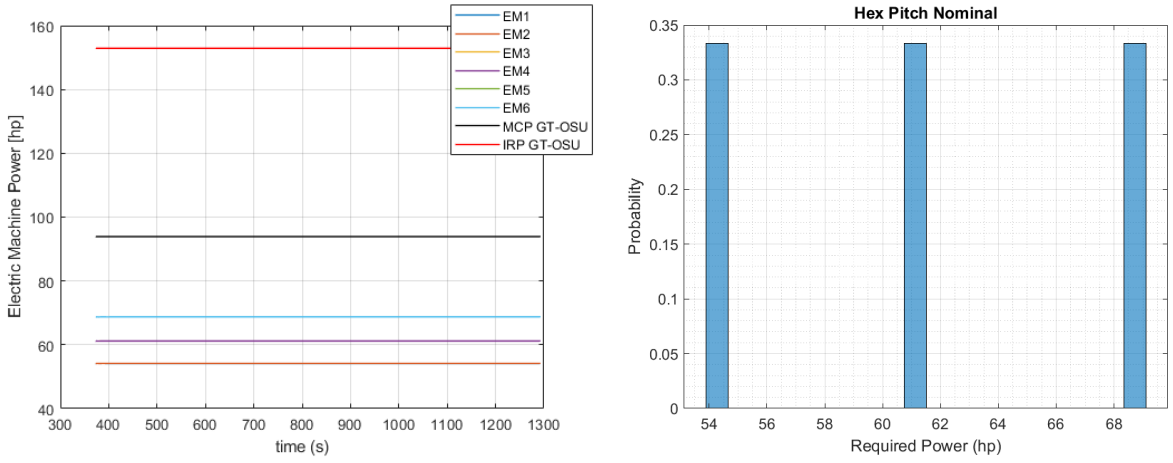

Figure 123: Hexacopter with pitch control during cruise: Power as a function of time and power bucket distribution

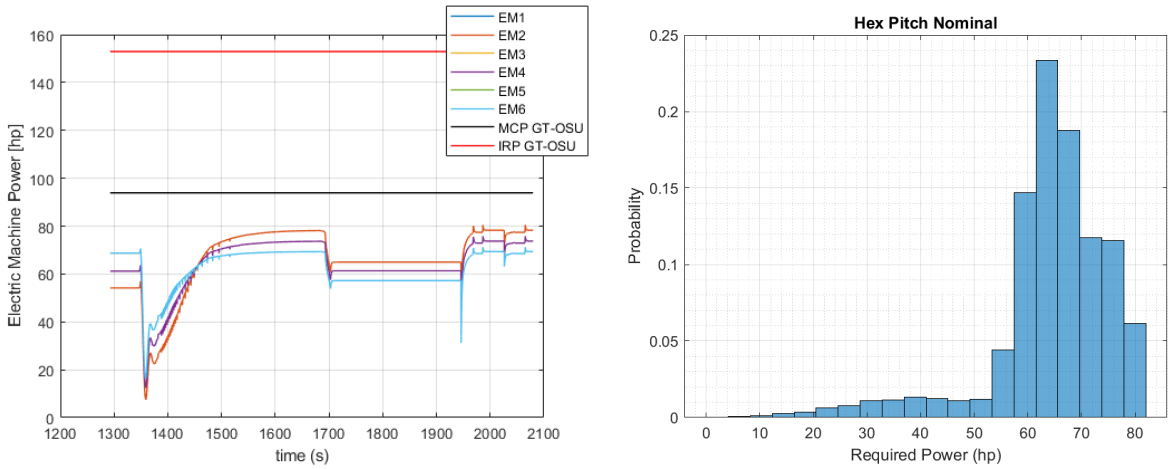

Figure 124: Hexacopter with pitch control descent and landing: Power as a function of time and power bucket distribution

Operations with wind disturbances

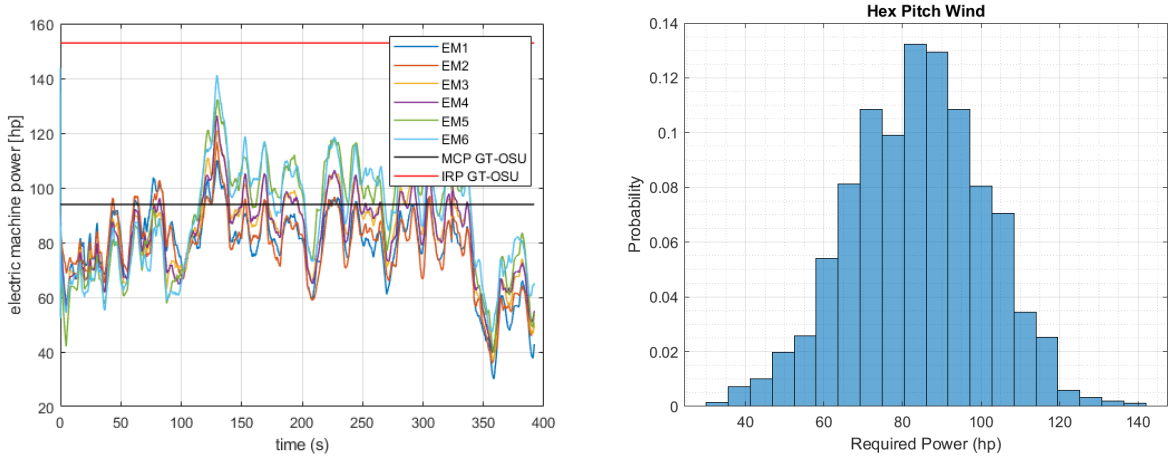

Figure 125: Hexacopter with pitch control during takeoff, acceleration and climb: Power as a function of time and power bucket distribution

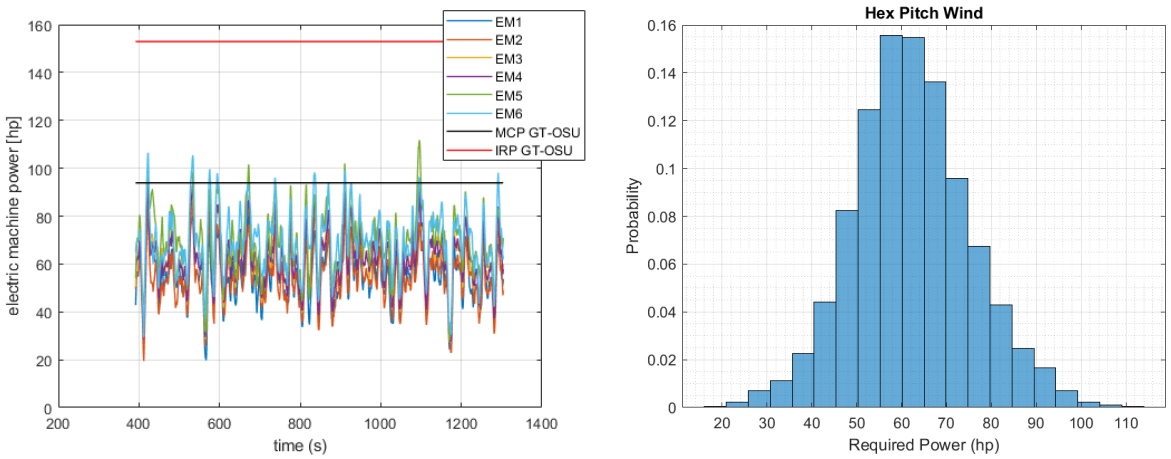

Figure 126: Hexacopter with pitch control during cruise: Power as a function of time and power bucket distribution

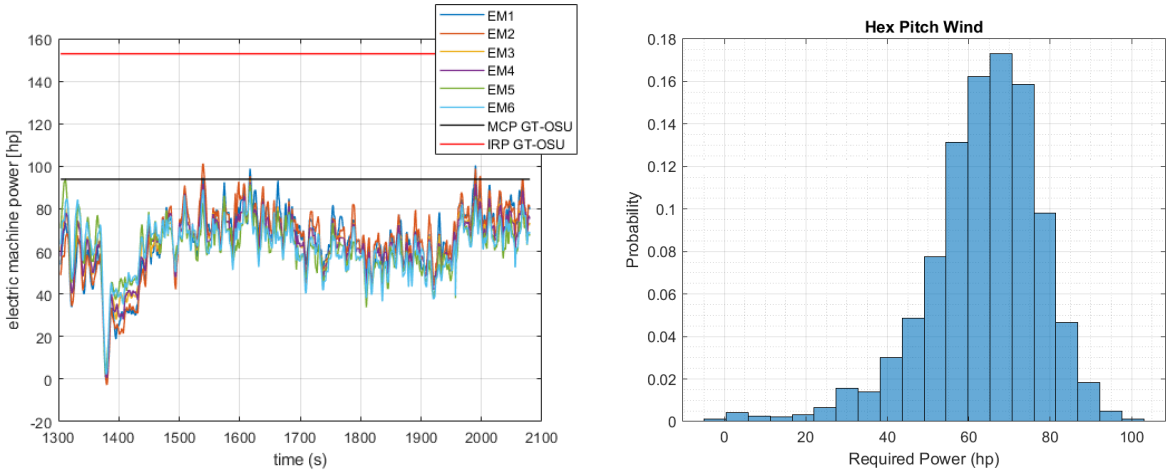

Figure 127: Hexacopter with pitch control descent and landing: Power as a function of time and power bucket distribution

Operation with one engine inoperative

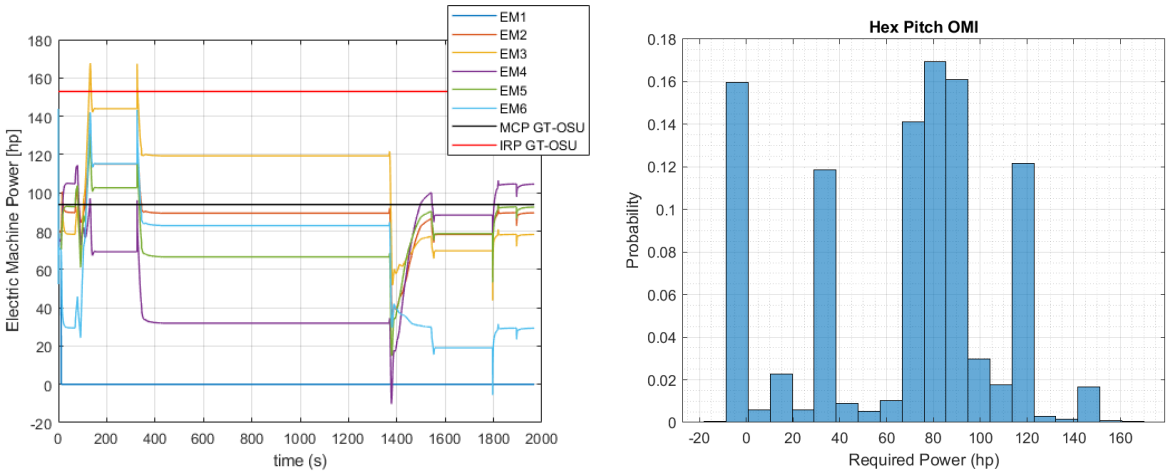

Figure 128: Hexacopter with pitch control: Power as a function of time and power bucket distribution

Hexacopter with RPM Control

Nominal Operation

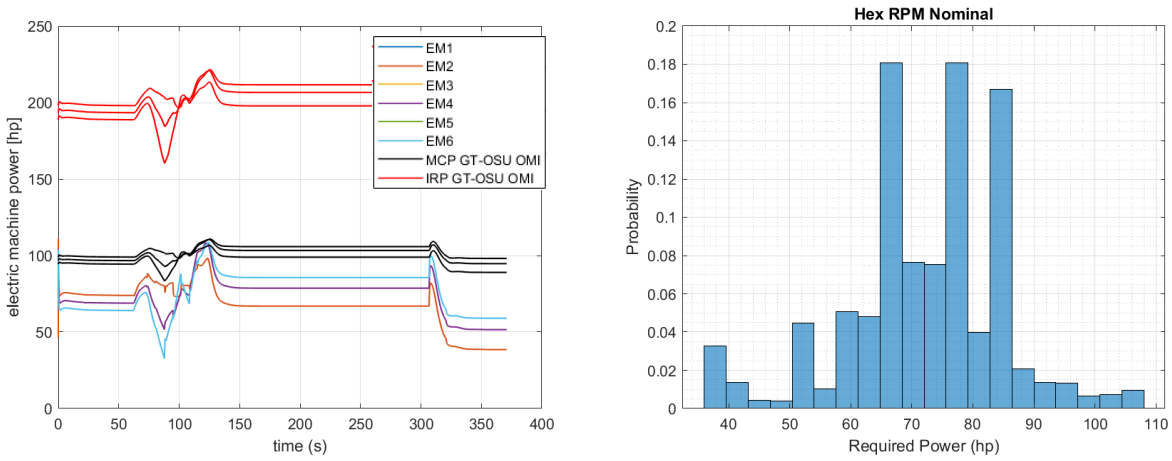

Figure 129: Hexacopter with RPM control during takeoff, acceleration and climb: Power as a function of time and power bucket distribution

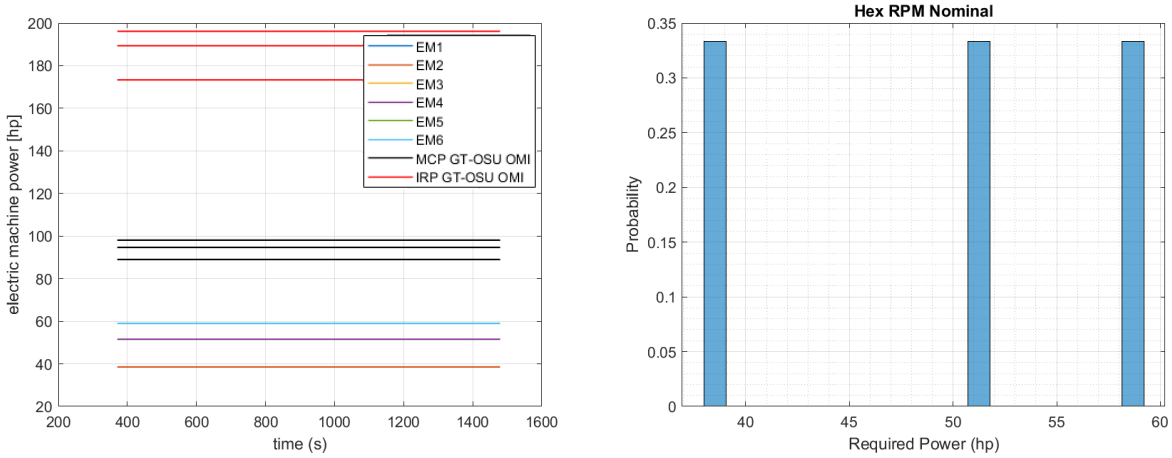

Figure 130: Hexacopter with RPM control during cruise: Power as a function of time and power bucket distribution

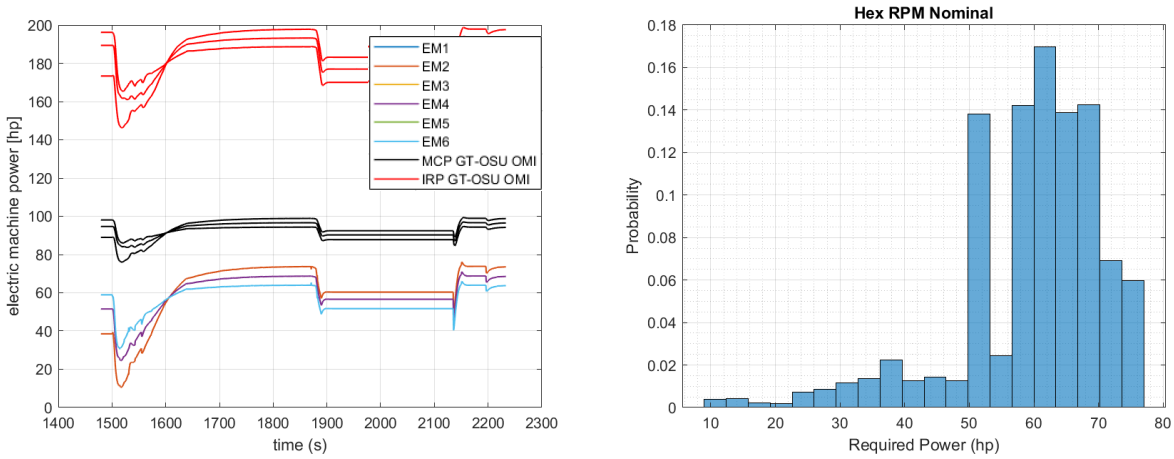

Figure 131: Hexacopter with RPM control descent and landing: Power as a function of time and power bucket distribution

Operations with wind disturbances

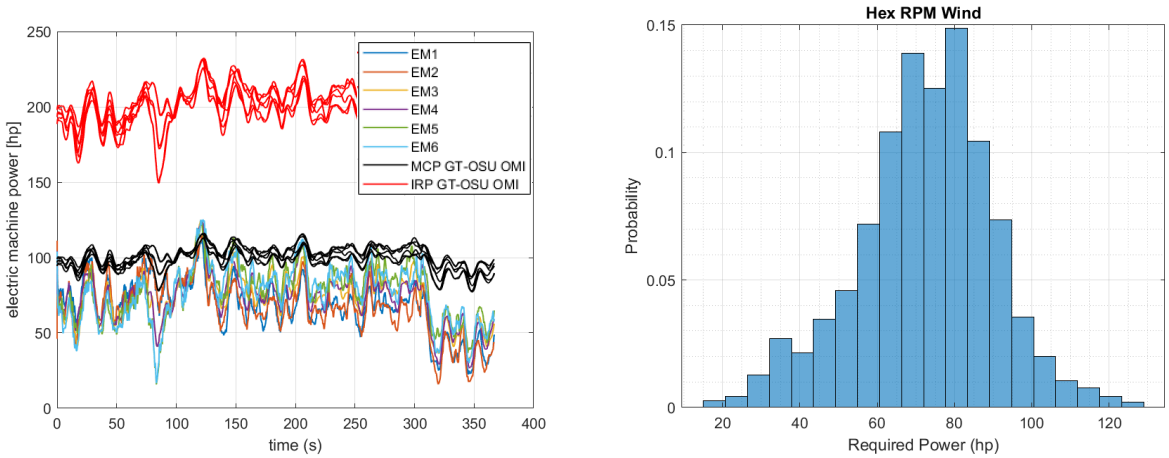

Figure 132: Hexacopter with RPM control during takeoff, acceleration and climb: Power as a function of time and power bucket distribution

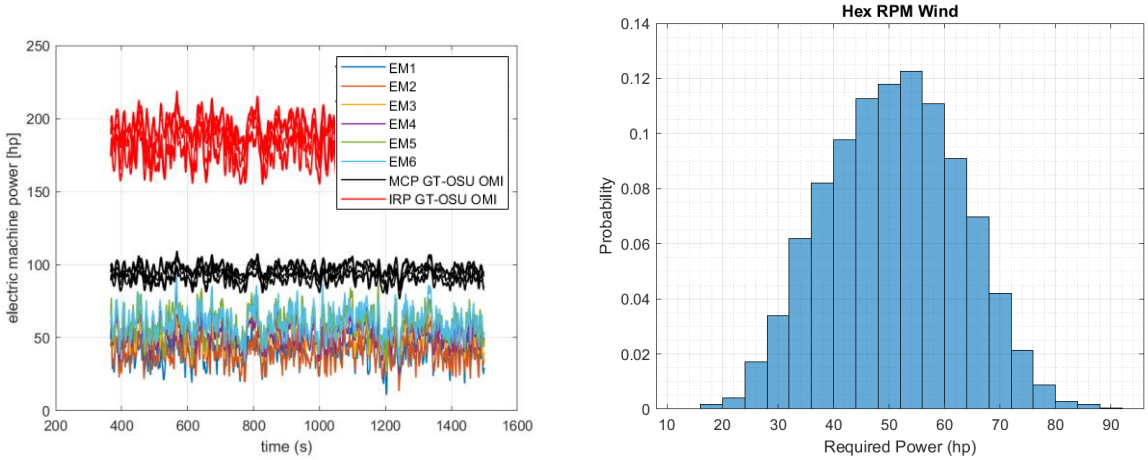

Figure 133: Hexacopter with RPM control during cruise: Power as a function of time and power bucket distribution

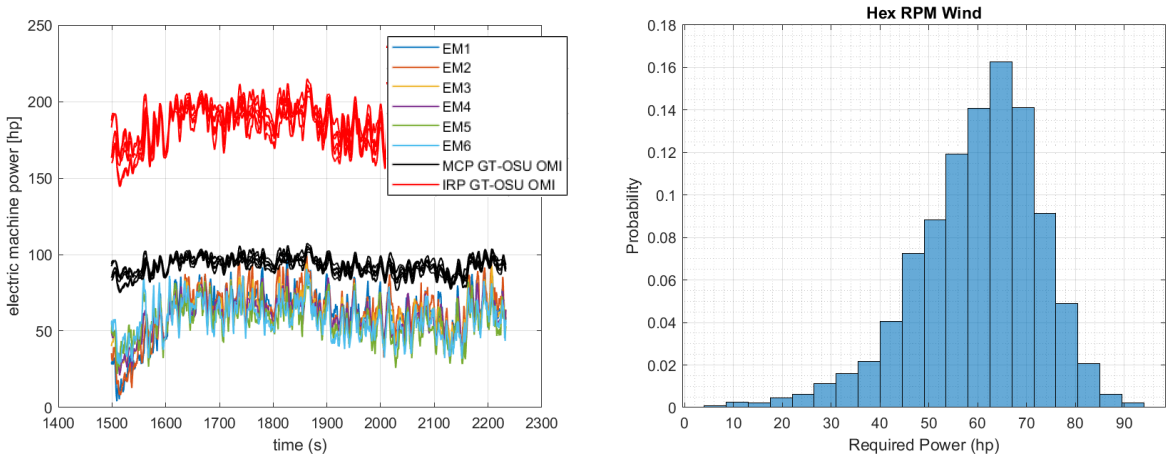

Figure 134: Hexacopter with RPM control descent and landing: Power as a function of time and power bucket distribution

Operation with one motor inoperative

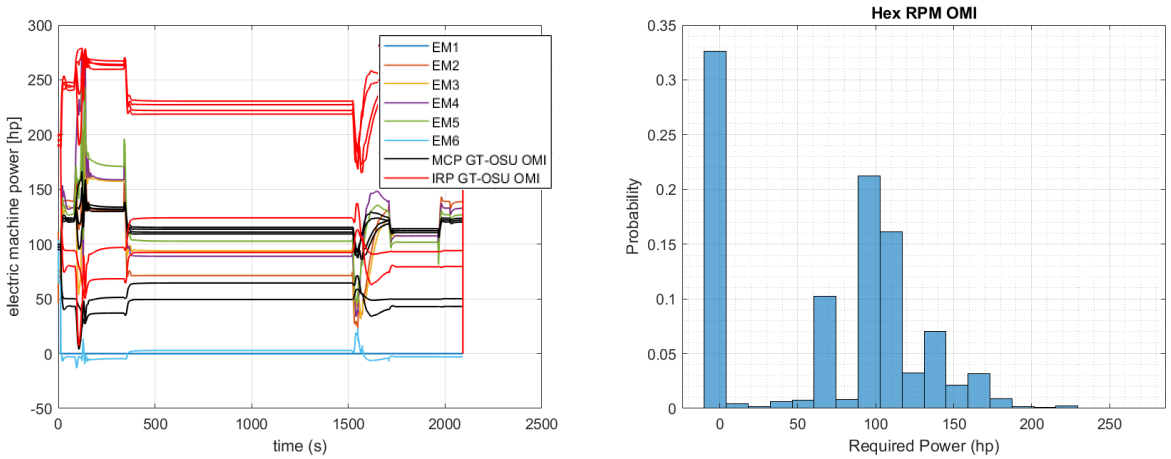

Figure 135: Hexacopter with RPM control: Power as a function of time and power bucket distribution

Octocopter with RPM Control

Nominal Operation

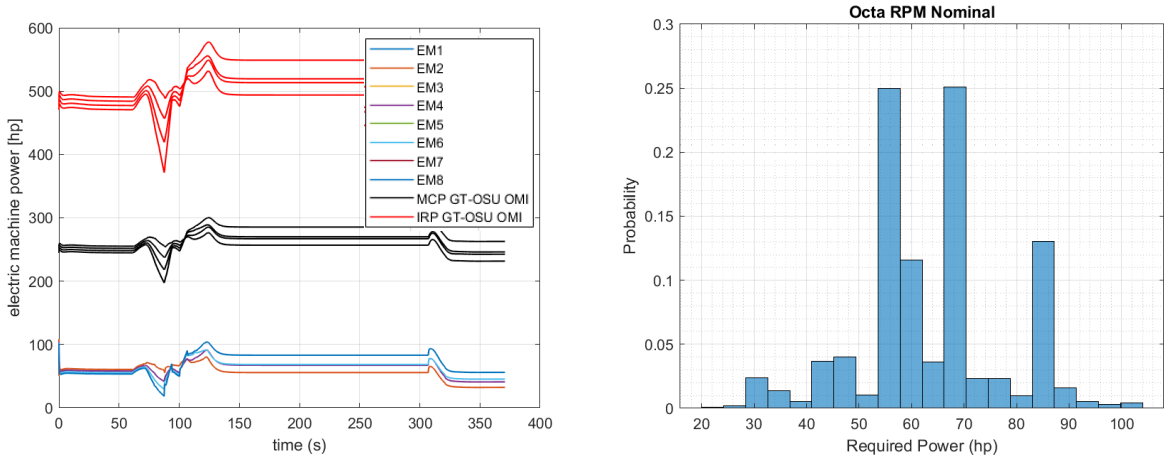

Figure 136: Octocopter with RPM control during takeoff, acceleration and climb: Power as a function of time and power bucket distribution

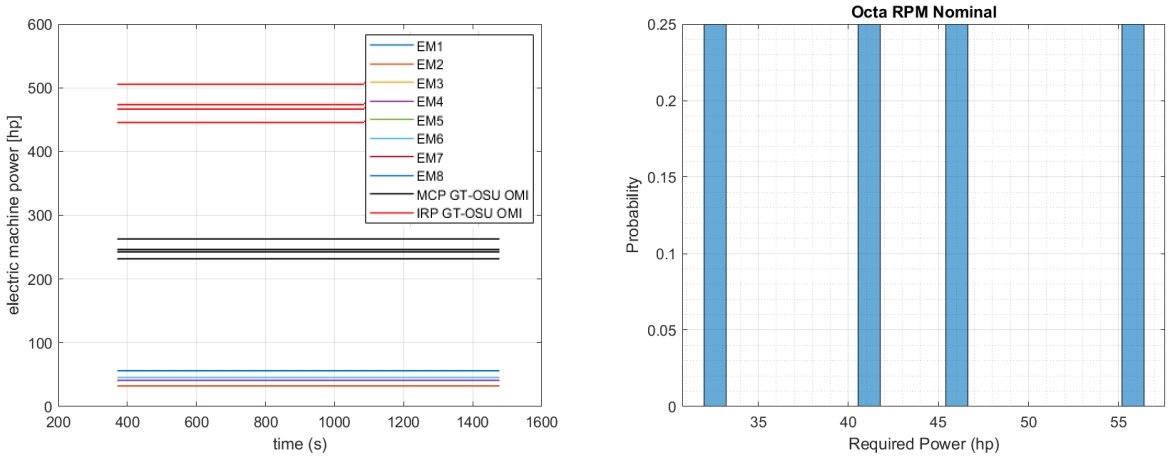

Figure 137: Octocopter with RPM control during cruise: Power as a function of time and power bucket distribution

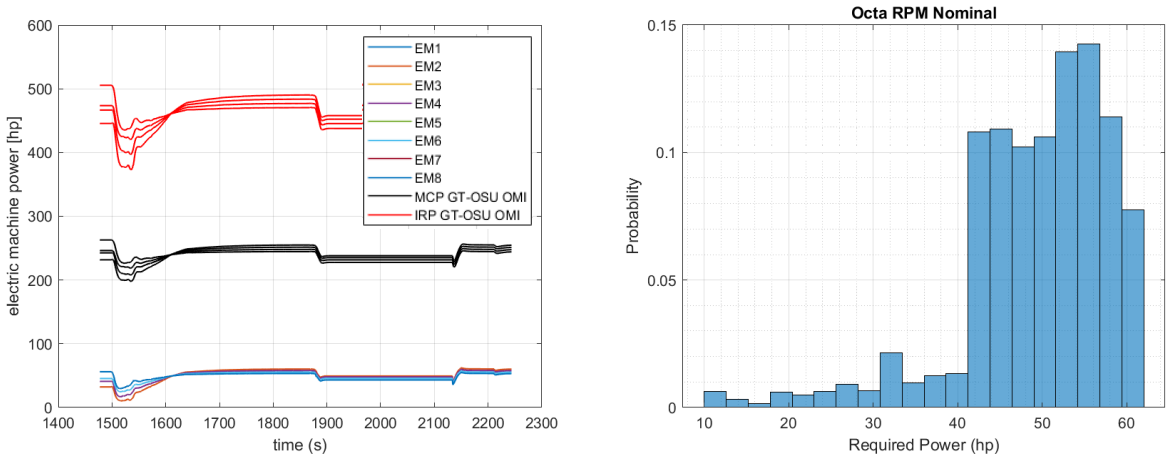

Figure 138: Octocopter with RPM control descent and landing: Power as a function of time and power bucket distribution

Operation under wind disturbances

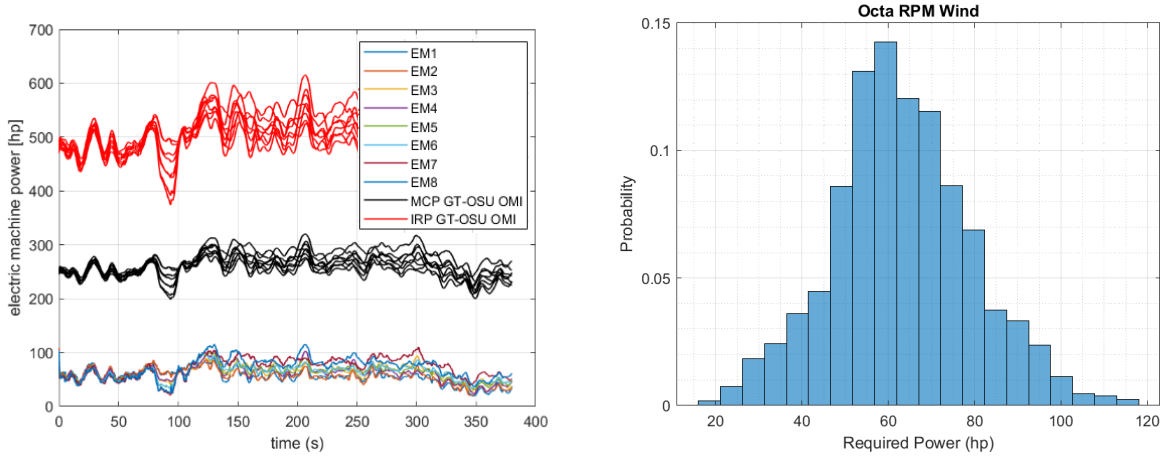

Figure 139: Octocopter with RPM control during takeoff, acceleration and climb: Power as a function of time and power bucket distribution

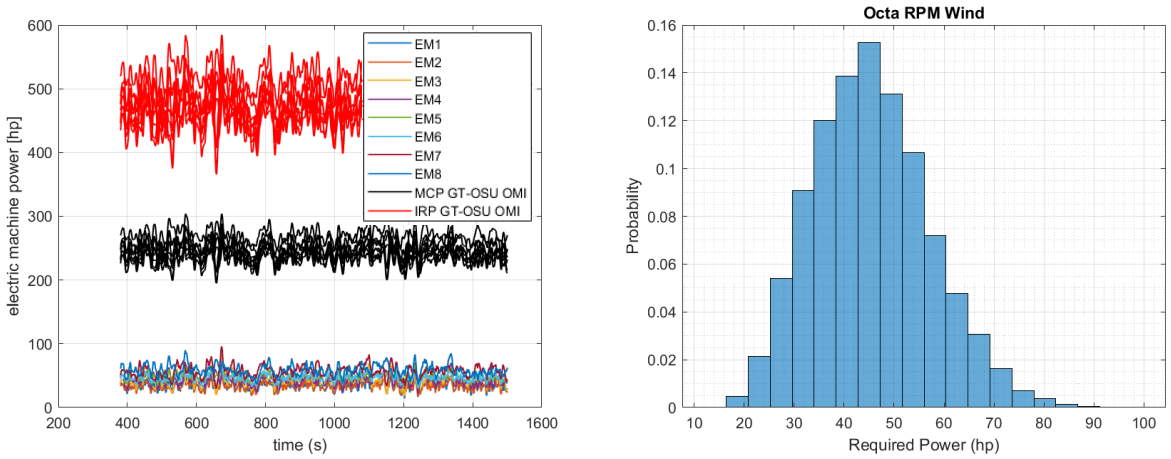

Figure 140: Octocopter with RPM control during cruise: Power as a function of time and power bucket distribution

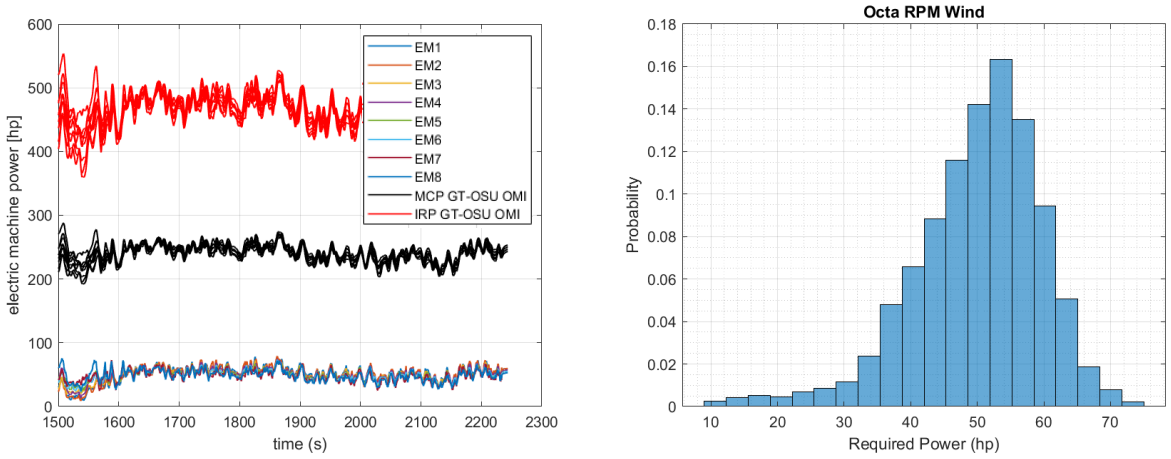

Figure 141: Octocopter with RPM control descent and landing: Power as a function of time and power bucket distribution

Operation with one engine inoperative

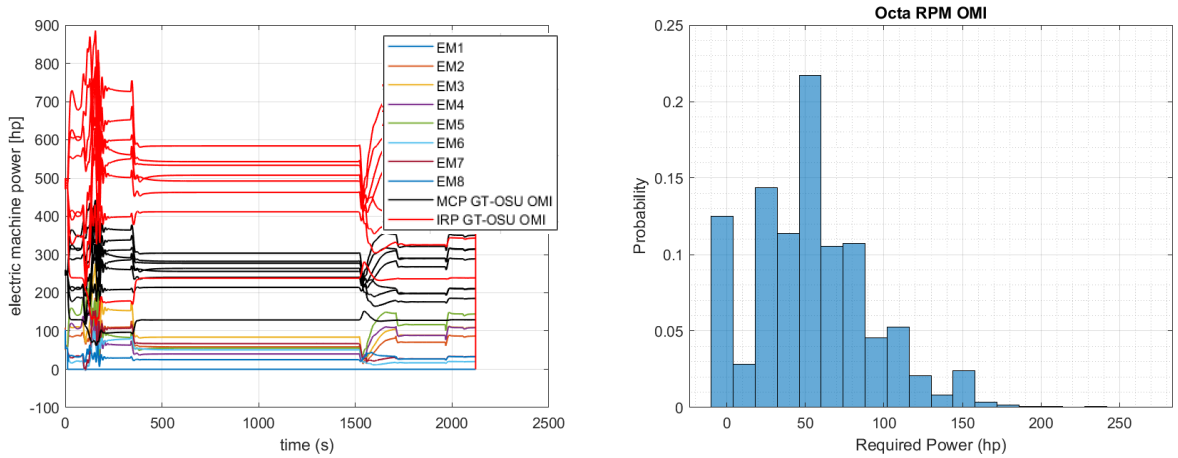

Figure 142: Hexacopter with RPM control: Power as a function of time and power bucket distribution

Summary Tables

Table M1: Hexacopter Variable Pitch Nominal Power Analysis

	Mean (hp)			Max (hp)			95% Upper Power Bandwidth (hp)		
	Takeoff	Cruise	Landing	Takeoff	Cruise	Landing	Takeoff	Cruise	Landing
Motor 1	79.7	54.3	66.0	110.3	54.4	80.7	92.0	54.3	78.5
Motor 2	79.7	54.3	66.0	110.3	54.4	80.7	92.0	54.3	78.5
Motor 3	85.0	61.4	64.3	120.6	61.4	76.0	99.5	61.4	74.0
Motor 4	85.0	61.4	64.3	120.6	61.4	76.0	99.5	61.4	74.0
Motor 5	91.6	69.0	62.3	133.2	69.0	71.4	110.5	69.0	69.6
Motor 6	91.6	69.0	62.3	133.2	69.0	71.4	110.5	69.0	69.6

Table M2: Hexacopter Variable Pitch Wind Power Analysis

	Mean (hp)			Max (hp)			95% Upper Power Bandwidth (hp)		
	Takeoff	Cruise	Landing	Takeoff	Cruise	Landing	Takeoff	Cruise	Landing
Motor 1	78.8	54.9	65.2	110.4	88.2	100.7	99.2	73.4	87.0
Motor 2	78.8	55.0	65.5	117.2	87.9	101.5	97.0	74.4	87.3
Motor 3	83.4	62.0	63.7	121.3	94.9	93.6	105.3	82.3	81.3
Motor 4	83.4	62.0	63.7	126.8	94.6	92.8	104.8	82.6	81.4
Motor 5	89.4	69.7	61.8	132.7	112.1	94.6	117.1	91.2	79.2
Motor 6	89.4	69.7	62.0	141.6	106.8	89.2	116.5	92.9	79.5

Table M3: Hexacopter Variable Pitch OMI Power Analysis

	Mean (hp)	Max (hp)	95% Upper Power Bandwidth (hp)
	Mission	Mission	Mission
Motor 1	Motor 1 out	Motor 1 out	Motor 1 out
Motor 2	89.1	138.8	115.4
Motor 3	106.0	168.2	144.4
Motor 4	56.5	114.8	104.9
Motor 5	76.0	130.2	103.0
Motor 6	67.3	142.5	115.6

Table M4: Hexacopter Variable RPM Nominal Power Analysis

	Mean (hp)			Max (hp)			95% Upper Power Bandwidth (hp)		
	Takeoff	Cruise	Landing	Takeoff	Cruise	Landing	Takeoff	Cruise	Landing
Motor 1	67.9	38.7	61.3	96.2	38.7	75.1	85.9	38.7	74.1
Motor 2	67.9	38.7	61.3	96.2	38.7	75.1	85.9	38.7	74.1
Motor 3	73.7	51.7	59.5	106.9	51.7	69.9	90.1	51.7	69.0
Motor 4	73.7	51.7	59.5	106.9	51.7	69.9	90.1	51.7	69.0
Motor 5	76.7	59.2	56.8	106.9	59.2	65.0	94.4	59.2	64.2
Motor 6	76.7	59.2	56.8	106.9	59.2	65.0	94.4	59.2	64.2

Table M5: Hexacopter Variable RPM Wind Power Analysis

	Mean (hp)			Max (hp)			95% Upper Power Bandwidth (hp)		
	Takeoff	Cruise	Landing	Takeoff	Cruise	Landing	Takeoff	Cruise	Landing
Motor 1	68.2	39.2	62.1	107.0	65.6	90.3	92.7	51.2	80.7
Motor 2	67.0	39.9	63.1	117.0	65.1	93.9	92.2	53.1	82.5
Motor 3	73.4	52.5	60.7	124.8	79.1	88.6	97.8	65.8	77.3
Motor 4	73.4	53.1	60.0	120.0	78.5	83.4	100.9	67.1	74.9
Motor 5	76.9	60.0	56.9	119.1	86.2	79.8	105.1	73.8	72.0
Motor 6	75.8	60.7	57.8	128.9	91.4	84.0	103.8	75.2	73.3

Table M6: Hexacopter Variable RPM OMI Power Analysis

	Mean (hp)	Max (hp)	95% Upper Power Bandwidth (hp)
	Mission	Mission	Mission
Motor 1	Motor 1 out	Motor 1 out	Motor 1 out
Motor 2	92.1	181.8	139.7
Motor 3	105.3	211.3	158.8
Motor 4	108.5	271.1	161.6
Motor 5	114.6	232.1	173.2
Motor 6	0.7	67.1	2.9

Table M7: Octocopter Variable RPM Nominal Power Analysis

	Mean (hp)			Max (hp)			95% Upper Power Bandwidth (hp)		
	Takeoff	Cruise	Landing	Takeoff	Cruise	Landing	Takeoff	Cruise	Landing
Motor 1	56.4	32.5	50.5	78.3	32.5	61.7	72.9	32.5	60.8
Motor 2	56.4	32.5	50.5	78.3	32.5	61.7	72.9	32.5	60.8
Motor 3	62.6	41.2	50.1	90.0	41.2	59.2	76.8	41.2	58.3
Motor 4	62.6	41.2	50.1	90.0	41.2	59.2	76.8	41.2	58.3
Motor 5	63.1	45.6	49.1	90.4	45.6	56.7	82.6	45.6	55.9
Motor 6	63.1	45.6	49.1	90.4	45.6	56.7	82.7	45.6	55.9
Motor 7	71.8	56.3	48.2	103.1	56.3	56.3	91.3	56.3	53.8
Motor 8	71.8	56.3	48.2	103.1	56.3	56.3	91.3	56.3	53.8

Table M8: Octocopter Variable RPM Wind Power Analysis

	Mean (hp)			Max (hp)			95% Upper Power Bandwidth (hp)		
	Takeoff	Cruise	Landing	Takeoff	Cruise	Landing	Takeoff	Cruise	Landing
Motor 1	56.1	34.1	51.2	88.0	56.0	72.8	78.5	45.2	65.4
Motor 2	56.4	33.6	51.3	89.8	66.1	74.8	75.6	44.8	66.0
Motor 3	63.0	42.2	50.3	95.7	83.2	70.8	82.8	56.2	62.9
Motor 4	61.7	43.5	51.0	103.8	72.8	70.9	91.4	57.4	62.9
Motor 5	62.7	47.4	49.6	99.6	67.6	67.6	89.5	58.2	61.1
Motor 6	63.2	46.7	49.6	101.8	76.6	69.7	84.1	57.0	61.0
Motor 7	72.2	57.3	48.1	111.2	98.5	67.0	98.4	72.4	59.9

Motor 8	70.5	58.7	48.8	117.5	89.1	70.3	106.0	75.1	61.3

Table M9: Octocopter Variable RPM OMI Power Analysis

	Mean (hp)	**Max (hp)**	**95% Upper Power Bandwidth (hp)**
	Mission	**Mission**	**Mission**
Motor 1	Motor 1 out	Motor 1 out	Motor 1 out
Motor 2	69.1	183.3	110.3
Motor 3	95.1	269.7	155.2
Motor 4	62.7	158.2	110.9
Motor 5	84.9	241.0	149.4
Motor 6	42.4	96.6	77.9
Motor 7	58.6	150.1	107.3
Motor 8	28.2	59.0	38.4

APPENDIX O **: RPM VEHICLE MOTOR SIZE ANALYSIS**

The DET evaluation for the hexacopter RPM vehicle and octocopter RPM vehicle shows that with the GT-OSU motors for the majority of the faults either critical or catastrophic outcomes are achieved. A natural subsequent question that arises is if this is due to motor sizing. Figure 143 through Figure 145 show the outcome for the hexacopter RPM vehicle with GT-OSU sized motors when a low torque (SL2) is injected in the takeoff section. As can be seen, the vehicle is not able to recover and a catastrophic outcome is achieved. Using upsized motors developed by GT-OSUOMI, the outcome shows favorable and the vehicle is able to recover as can be seen in Figure 146 through Figure 148. This shows that including more powerful motors can help in the recovery capability of the vehicle after a fault occurred.

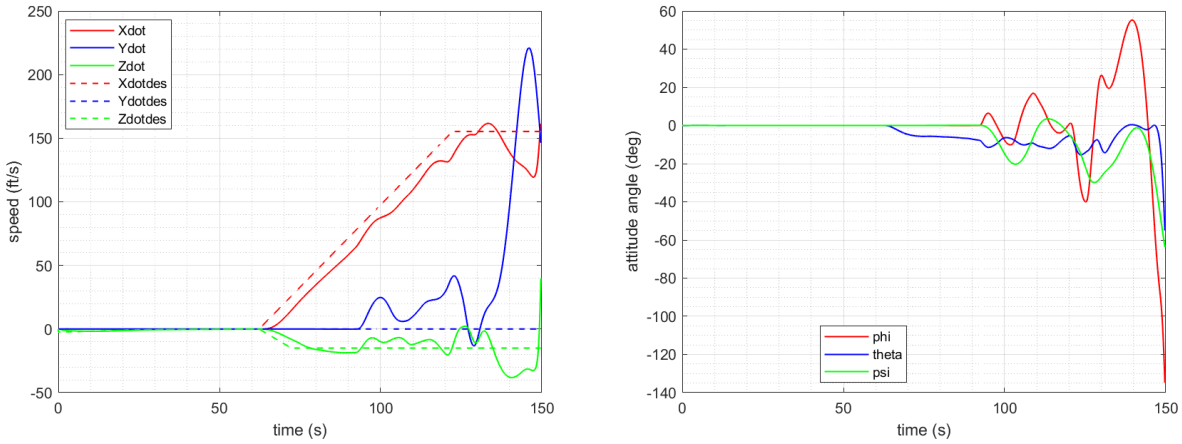

Figure 143 Hexacopter RPM Low Torque (SL2) GT-OSU Motors Translational Velocity Profile (LEFT) and Attitude Angle Profile (RIGHT)

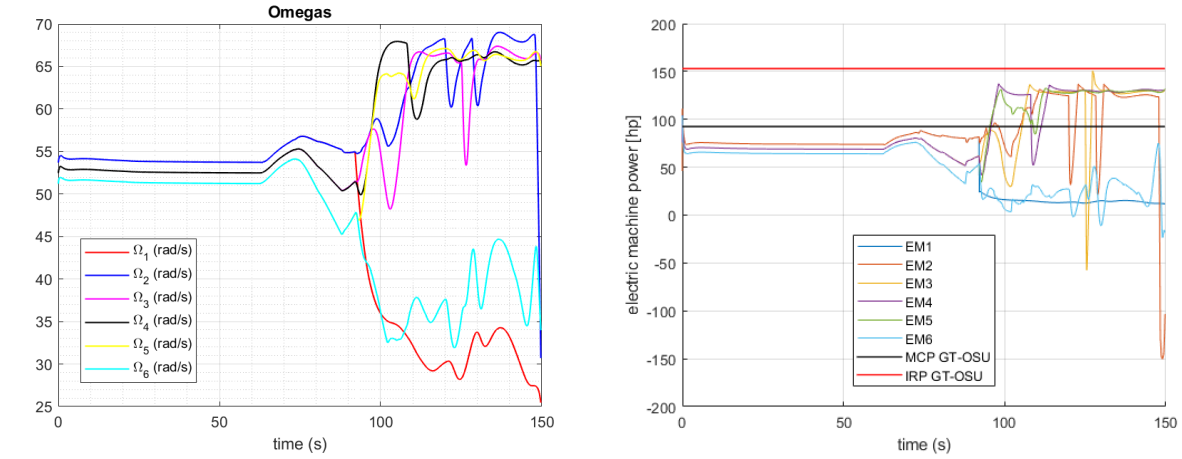

Figure 144 Hexacopter RPM Low Torque (SL2) GT-OSU Motors RPM Profile (LEFT) and Electric Machine Profile (RIGHT)

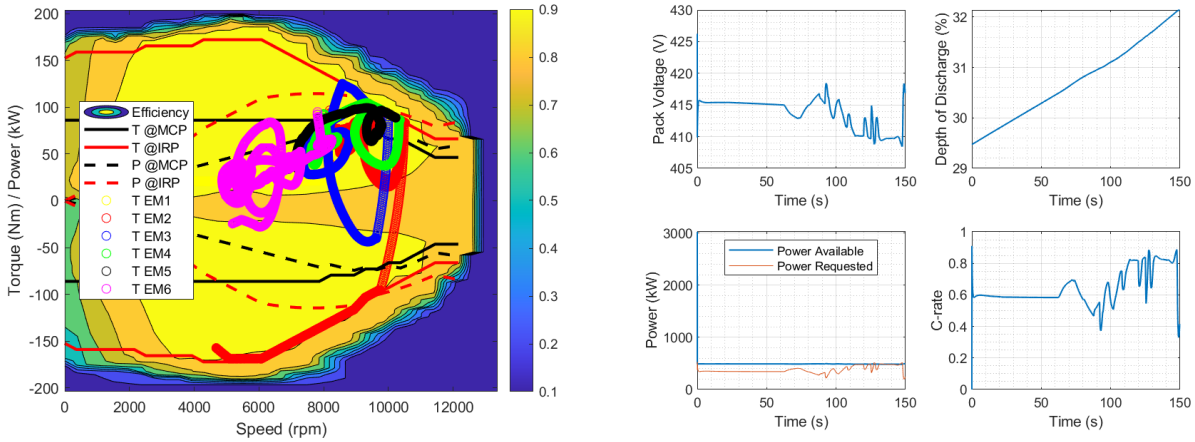

Figure 145 Hexacopter RPM Low Torque (SL2) GT-OSU Motors Heat Map (LEFT) and Battery Profile (RIGHT)

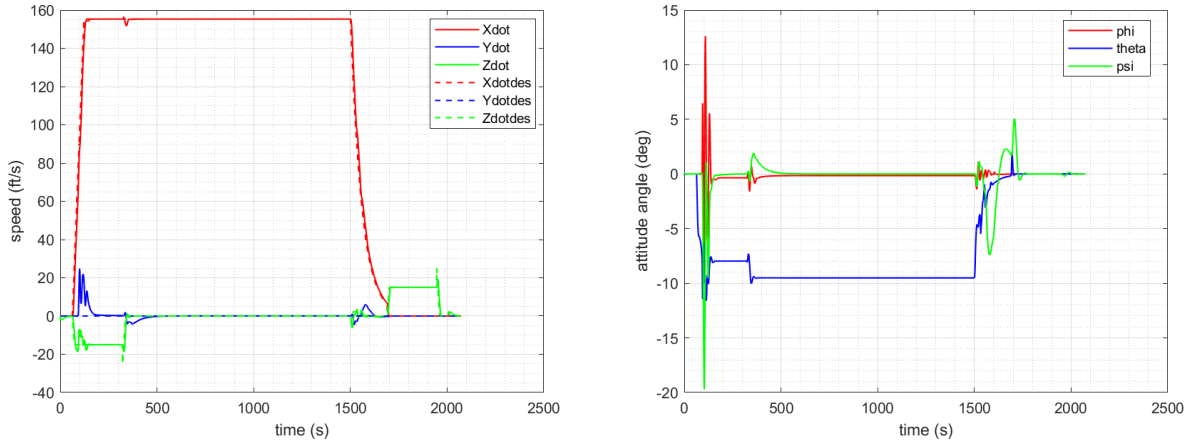

Figure 146 Hexacopter RPM Low Torque (SL2) GT-OSU OMI Motors Translational Velocity Profile (LEFT) and Attitude Angle Profile (RIGHT)

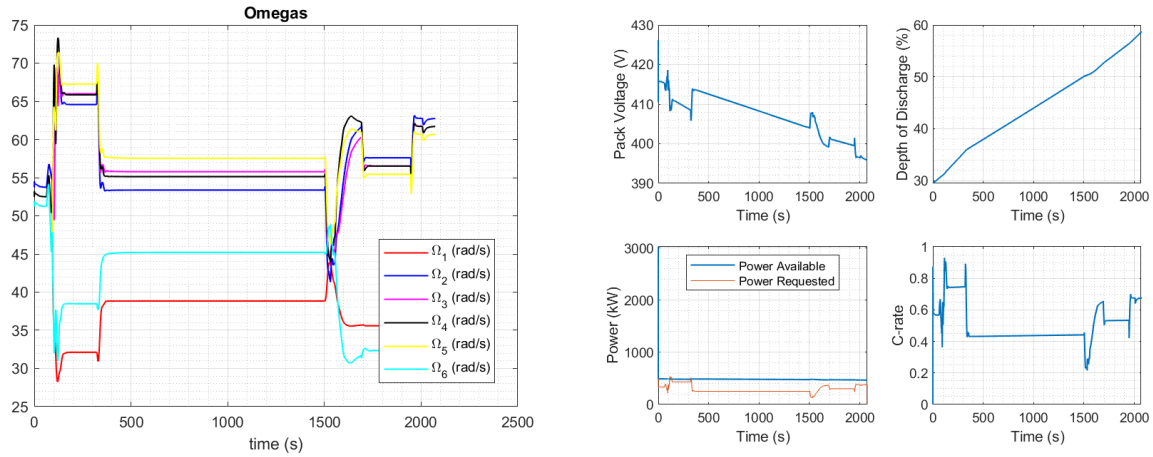

Figure 147 Hexacopter RPM Low Torque (SL2) GT-OSU OMI Motors RPM Profile (LEFT) and Electric Machine Profile (RIGHT)

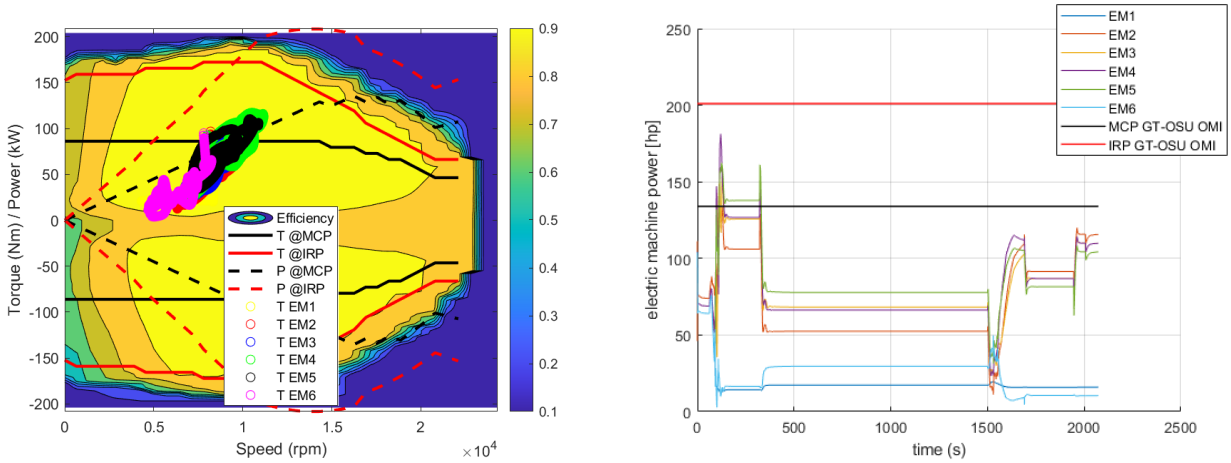

Figure 148 Hexacopter RPM Low Torque (SL2) GT-OSU OMI Motors Heat Map (LEFT) and Battery Profile (RIGHT)

Similarly for the Octocopter RPM, Figure 149 through Figure 151 show the outcome for the octocopter RPM vehicle with GT-OSU sized motors when a low torque (SL3) is injected in the takeoff section. As can be seen, the vehicle is not able to recover and a catastrophic outcome is achieved. Figure 152 through Figure 154 show the same fault simulated with upsized motors developed by GT-OSU OMI, the outcome shows favorable and the vehicle is able to recover as can be seen. Therefore, upsizing the motors could potentially help with the recovery of the vehicle.

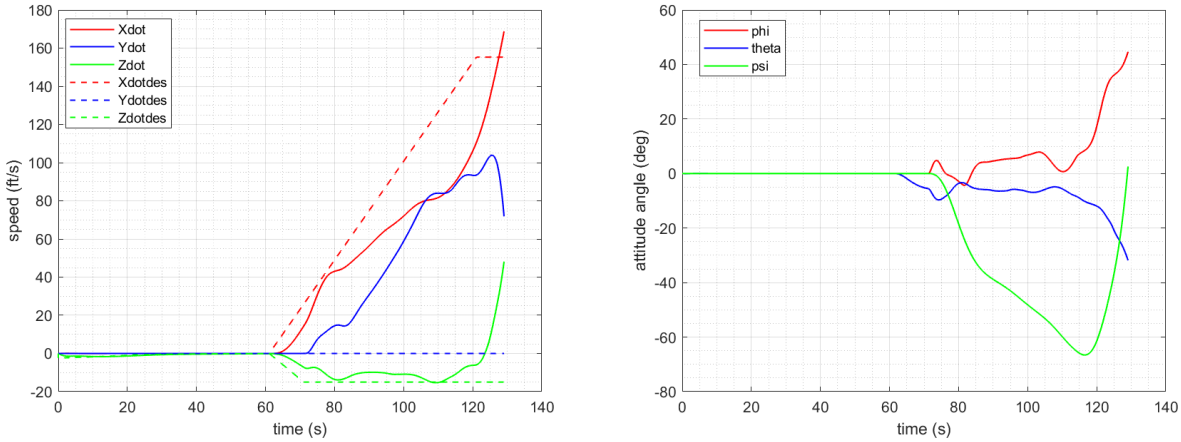

Figure 149 Octocopter RPM Low Torque (SL3) GT-OSU Motors Translational Velocity Profile (LEFT) and Attitude Angle Profile (RIGHT)

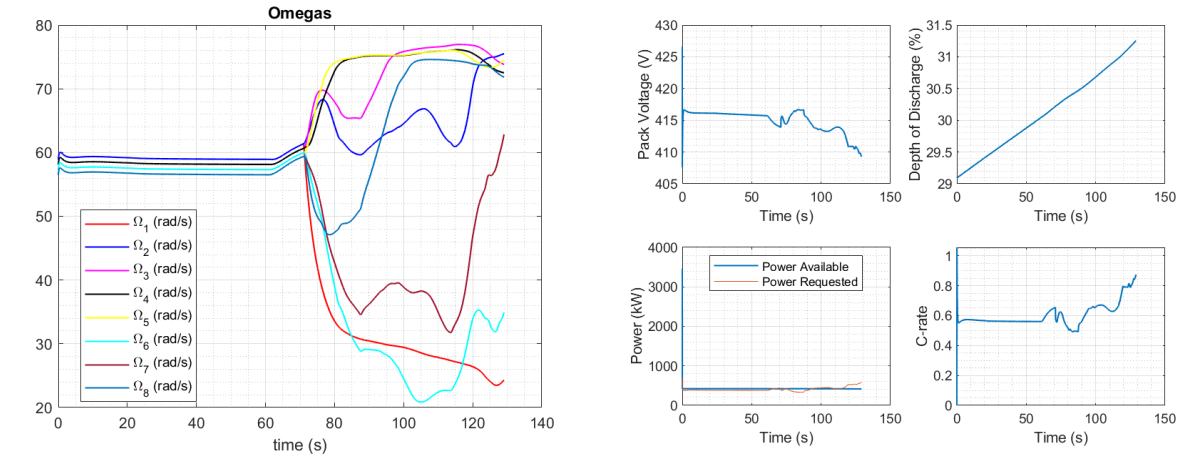

Figure 150 Octocopter RPM Low Torque (SL3) GT-OSU Motors RPM Profile (LEFT) and Electric Machine Profile (RIGHT)

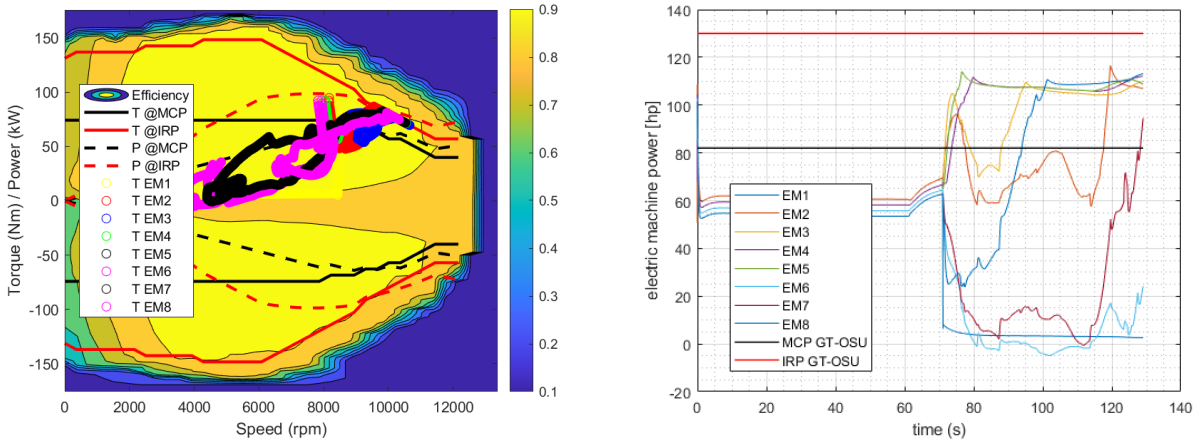

Figure 151 Octocopter RPM Low Torque (SL3) GT-OSU Motors Heat Map (LEFT) and Battery Profile (RIGHT)

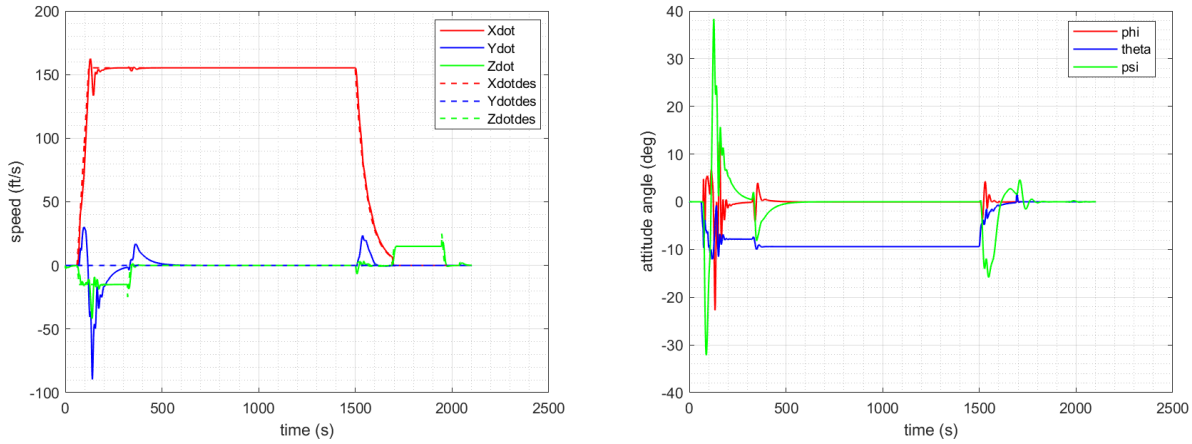

Figure 152 Octocopter RPM Low Torque (SL3) GT-OSU OMI Motors Translational Velocity Profile (LEFT) and Attitude Angle Profile (RIGHT)

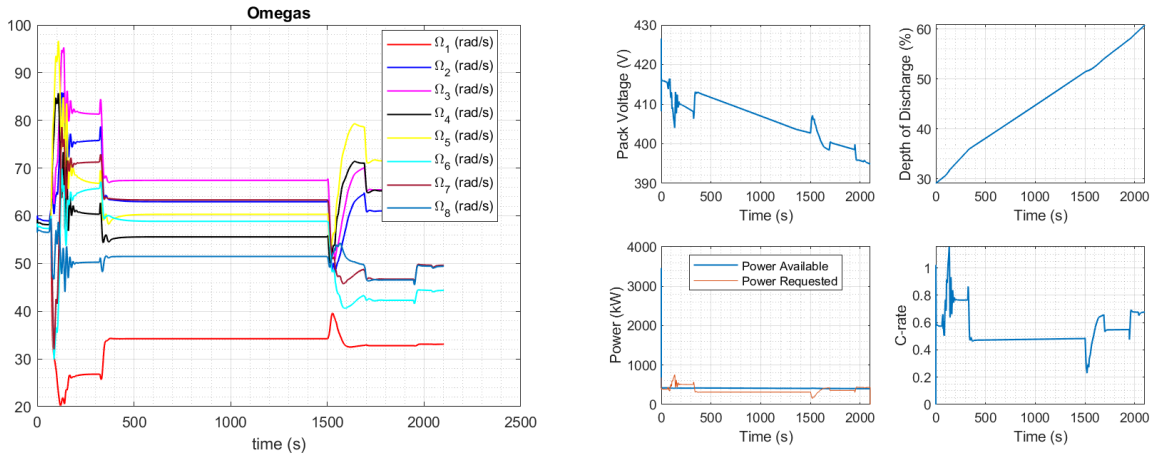

Figure 153 Octocopter RPM Low Torque (SL3) GT-OSU OMI Motors RPM Profile (LEFT) and Electric Machine Profile (RIGHT)

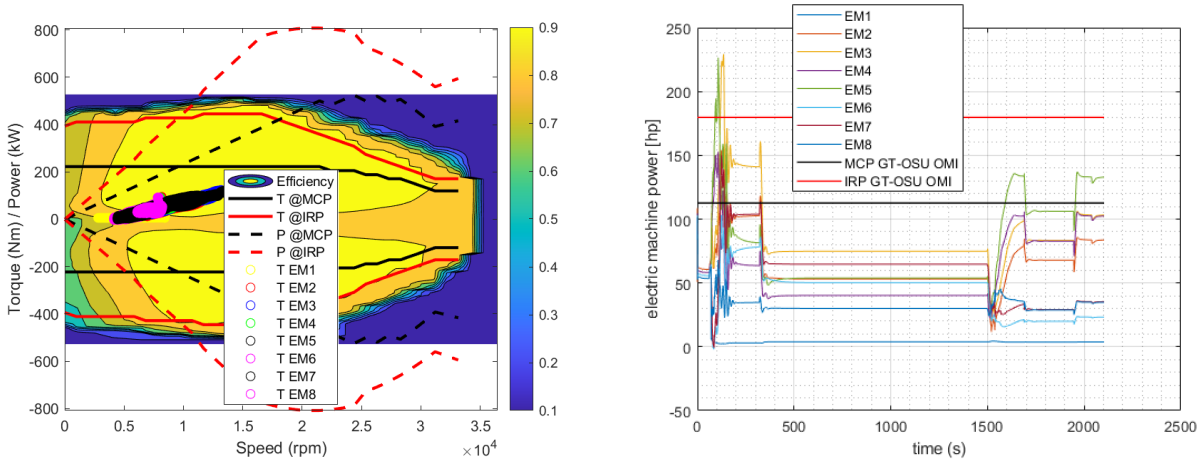

Figure 154 Octocopter RPM Low Torque (SL3) GT-OSU OMI Motors Heat Map (LEFT) and Battery Profile (RIGHT)

APPENDIX P **: DYNAMIC EVENT TREE HAZARD CONDITIONS**

March 2021 Final Report, Reliability and Safety Assessment of Urban Air Mobility Concept Vehicles, Contract No. 80ARC020F0055, GTRI Document No. D9015A001R2, April 2021

During the Dynamic Event Tree (DET) simulation, the DET will continuously monitor the aircraft state and if any of the specified hazard conditions are met, the DET simulation will stop the simulation and declare branch outcome event one of the four severity levels: Catastrophic/Critical/Marginal/Minor, as classified in MIL-STD-1629A [20]. This analysis will provide us quantitative estimates of the worst likelihood Catastrophic outcomes (see Section 2.2.1).

Following are all the hazard conditions that are defined for the Dynamic Event Tree simulation:

1. Failure to Maintain Altitude (*Cruise*)

Short Summary: Aircraft not maintaining assigned altitude. Could lead to emergency landing or collision with other aircraft/terrain.

Description: From the air transport pilot flight testing standards for helicopters, a pilot must be able to maintain the specified altitude within 100 feet during inflight maneuvers (Section IV) including steep turns, powerplant failure. Failure to remain at the correct altitude is a hazard due to possible collision with terrain or other aircraft. FAR 91 prescribes VFR cruising altitudes at any thousand foot + 500 feet and IFR cruising altitudes at any thousand foot. Altitude deviation greater than 500 feet therefore poses serious collision hazards to other aircraft at another cruising altitude.

Failure to Maintain Altitude: Altitude Deviation > 100ft for > 10s – (Minor) – Flag 1.1

Failure to Maintain Altitude: Altitude Deviation > 100ft for > 20s– (Marginal) – Flag 1.2

Failure to Maintain Altitude: Altitude Deviation > 100ft for > 30s – (Critical) – Flag 1.3

Failure to Maintain Altitude: Altitude Deviation > 500ft for > 30s – (Catastrophic) – Flag 1.4

2. Failure to Climb (***Takeoff/Climb***)

Short Summary: Unable to climb to cruise altitude. Collision hazard to other aircraft/terrain.

Description: FAR 29.67 (2) specifies “The steady rate of climb without ground effect, 1000 feet above the takeoff surface, must be at least 150 feet per minute, for each weight, altitude, and temperature for which takeoff data are to be scheduled…” Failure to climb at an adequate rate leads to possible collision with terrain or other aircraft.

Failure to Climb: Climb rate <150 ft/min for > 10s (Critical) – Flag 2.1

Failure to Climb: Climb rate <150 ft/min for > 30s (Catastrophic) – Flag 2.2

3. Emergency Landing (All Phases)

Short Summary: Landing before end of mission due to failure.

Description: FAR 29.562 specifies Emergency Landing Dynamic Conditions for transport category rotorcraft.

(a) The rotorcraft, although it may be damaged in a crash landing, must be designed to reasonably protect each occupant when—

March 2021 Final Report, Reliability and Safety Assessment of Urban Air Mobility Concept Vehicles, Contract No. 80ARC020F0055, GTRI Document No. D9015A001R2, April 2021

(1) A change in downward velocity of not less than 30 feet per second when the seat or other seating device is oriented in its nominal position with respect to the rotorcraft's reference system, the rotorcraft's longitudinal axis is canted upward 60° with respect to the impact velocity vector, and the rotorcraft's lateral axis is perpendicular to a vertical plane containing the impact velocity vector and the rotorcraft's longitudinal axis. Peak floor deceleration must occur in not more than 0.031 seconds after impact and must reach a minimum of 30g's.
(2) A change in forward velocity of not less than 42 feet per second when the seat or other seating device is oriented in its nominal position with respect to the rotorcraft's reference system, the rotorcraft's longitudinal axis is yawed 10° either right or left of the impact velocity vector (whichever would cause the greatest load on the shoulder harness), the rotorcraft's lateral axis is contained in a horizontal plane containing the impact velocity vector, and the rotorcraft's vertical axis is perpendicular to a horizontal plane containing the impact velocity vector. Peak floor deceleration must occur in not more than 0.071 seconds after impact and must reach a minimum of 18.4g's.

If an emergency landing occurs within the certification limits, there is a reasonable expectation that occupants will be well protected and escape serious injury, however there may still be partial or total loss of the vehicle, so the event is considered as Critical. For an emergency landing beyond the certification limits, the occupants are likely to be seriously injured.

Emergency Landing (Survivable): Altitude = 0; Final descent rate < 1800 ft/min; Final horizontal velocity < 42 ft/s; 0<Pitch < 60 deg; (Critical) – Flag 3.1

Emergency Landing (Fatal): Altitude = 0; Final descent rate > 1800 ft/min; Final horizontal velocity > 42 ft/s; Pitch > 60 deg; (Catastrophic) – Flag 3.2

4. Unsafe Attitude (All Phases)

Short summary: Attitude is outside envelope of normal operation.

Description: From the air transport pilot testing standards Section IV A, a steep turn must not exceed 30 degrees of bank. An excessively large roll or pitch angle is likely to result in loss of control. In addition, the pilot may also become disoriented and fail to recover.

Unsafe Attitude: Roll, Pitch >45 deg (Marginal) – Flag 4.1

Unsafe Attitude: Roll, Pitch> 75 (Critical) – Flag 4.2

5. Loss of Control *(Takeoff/Climb/Approach/Landing)*

Short summary: Unable to control aircraft attitude. Collision hazard to other aircraft/terrain.

Description: The testing standards for helicopter air transport pilot requires pilots to maintain the desired heading within 10 degrees during rejected takeoff (Section III Task D), powerplant failure (Section IV Task B), Instrument Procedures (Section V). Failure to follow the flightpath results in a potential hazard for collision with other aircraft and terrain.

Loss of Control: Heading deviation > 10 degrees for > 10s. (Catastrophic) – Flag 5

March 2021 Final Report, Reliability and Safety Assessment of Urban Air Mobility Concept Vehicles, Contract No. 80ARC020F0055, GTRI Document No. D9015A001R2, April 2021

6. Loss of Control *(Cruise)*

Short summary: Unable to control aircraft heading.

Description: The testing standards for helicopter air transport pilot requires pilots to maintain the desired heading within 10 degrees during rejected takeoff (Section III Task D), powerplant failure (Section IV Task B), Instrument Procedures (Section V). Failure to follow the flightpath results in a potential hazard for collision with other aircraft and terrain.

Loss of Control: Heading deviation > 10 degrees for > 10s. (Critical) – Flag 6

7. Control Saturation (All Phases)

Short summary: Maximum control effort. Unable to reject disturbances from this state.

Description: This failure describes a scenario where the aircraft is accurately tracking the prescribed flightpath however one or more of the controls (roll, pitch, yaw) are at the maximum value. In this condition the aircraft would be unable to make certain maneuvers in order to reject wind gust disturbance or to avoid collision with other aircraft.

Control Saturation: Actuator command at or beyond limit for >10s (Critical) – Flag 7.1

Control Saturation: RPM command at or beyond limit for >10s (Critical) – Flag 7.2

8. Unsafe Maneuvering (All Phases)

Short summary: Extreme maneuvering rate. Disorienting to pilot and crew. May exceed structural limits.

Description: The air transport pilot testing standards require “smooth, stabilized flight” for all maneuvers as well as “positive controls”. This is difficult to define and monitor as a multicopter requires stability augmentation which is constantly making adjustments. Monitoring the aircraft angular rates is simple and an excessive angular rate can be interpreted as clearly not “smooth, stabilized flight”.

Unsafe Maneuvering: Roll, Pitch, Yaw Rate > 100 deg/s (Catastrophic) – Flag 8

9. Over-G (All Phases)

Short summary: Aircraft exceeds design load limits

Description: Although load limits are established for each aircraft individually, FAR29.337 requires a rotorcraft to be designed for a limit maneuvering load factor ranging from positive limit of 3.5 to negative limit of -1.0.

Over-G: Aircraft load factor exceeds 3.5 or -1.0 (Catastrophic) – Flag 13

10. Linear Model Velocity Exceeded (All Phases)

Short summary: Aircraft exceeds velocity allowed by linear models in simulation

March 2021 Final Report, Reliability and Safety Assessment of Urban Air Mobility Concept Vehicles, Contract No. 80ARC020F0055, GTRI Document No. D9015A001R2, April 2021

Description: Aircraft exceeds velocity allowed by linear models in simulation, although the states will go NaN in the simulation, the simulation keeps running. This is a method to catch that.

Exceeding of Linear Model: First state in state vector Xairframe is NaN (Catastrophic) - Flag 14

11. RPM too low for cross-shafted aircraft (All Phases)

Short summary: For the quadrotor configurations, any rotor speed that goes below 20 rad/s will terminate the code.

Description: This is a simulation flag that is necessary due to limitations with the linearized NDARC models since there is a decoupling between RPM and collective control. Since we understand that a quadrotor won't be able to fly with one rotor out, we flag this condition and terminate the code.

Motor out: One of the rotor RPM will decrease below 20 rad/s (Catastrophic) - Flag 15

12. RPM too low for non-cross-shafted aircraft (All Phases)

Short summary: For the non-quadrotor configurations, if all rotor speeds go below 20 rad/s, the code will be terminated.

Description: This is a simulation flag that is necessary due to limitations with the linearized NDARC models since there is a decoupling between RPM and collective control. Since we understand that a vehicle won't be able to fly with all rotors out, we flag this condition and terminate the code.

All motors out: All of the rotor RPM will decrease below 20 rad/s (Catastrophic) - Flag 16

13. Motor temperature too hot (All Phases)

Short summary: Electric machine or electronic speed controller temperature too hot.

Description: If components become too hot in the powertrain, either an emergency landing or catastrophic failure is triggered.

Temperature too high: T_em (electric machine temperature) > 130 Celsius or T_esp (esc temperature) > 80 Celsius for > 10 sec (Critical) – Flag 17.1

Temperature too high: T_em (electric machine temperature) > 160 Celsius or T_esp (esc temperature) > 100 Celsius for > 10 sec (Catastrophic) – Flag 17.2

14. Battery depth of discharge too high (All Phases)

Short summary: Battery is energy is low and can cause loss of power.

Description: In case of the excess energy drawing event, the battery depth of discharge may overcome the critical limit of 80%. In such case, the depth of discharge goes over 90% an emergency landing is required since the residual energy is low and the battery pack becomes unreliable.

Discharge rate too high: d_curr (depth of discharge) > 0.8 (Critical) – Flag 18.1

Current too high: d_curr (depth of discharge) > 0.9 (Catastrophic) – Flag 18.2

15. Power_limit_state error (All Phases)

Short summary: power_limit_state variable becomes 1 for either one or all motors.

Description: The power_limit_state parameter is used to asses current power status of the powertrain. In nominal conditions the power_limit_state parameter is equal to zero. The power_limit_state variable becomes "1" when an electric motor power is saturated to the IRP or MCP limits. In detail IRP can be sustained for max 30 minutes, then MCP limit is enabled. This situation can occur in real flight when the power demand from an individual motor is larger than for which it is designed, for example in OMI conditions. The power_limit_state variable becomes "2" when the rate of change of the desired current for the electric motor exceeds 200 A/s indicating an upper limit for rate of change of current of the electric motor. This situation can occur when the desired transient of electric motor current is larger than the maximum designed rate of change for example in the case for a change in RPM required to stabilize the vehicle in a wind turbulence field. Finally, the power_limit_state variable becomes "3" when the desired current from the electric motor has exceeded the current limit from the battery pack. This indicates that the battery size is not sufficient to support the desired current draw of the electric motors. This could indicate an overall sizing issue of the battery pack for the relevant flight operating conditions.

Error in one motor: power_limit_state = 1 for one motor (Marginal) – **Flag 19.1**

Error in all motor: power_limit_state = 1 for all motors (Marginal) – **Flag 19.2**